**DOCTOR OF PHILOSOPHY**

# Unraveling the multifunctionality of human Spindly

Conte, Claudia

*Award date:*
2015


# Unravelling the multifunctionality of human Spindly

**Claudia Conte**

*Supervisor Dr. Eric Griffis*

Submission for the degree of
Doctor of Philosophy

**September 2015**

# Declaration

This thesis, submitted for the degree of Doctor in Philosophy at the University of Dundee, has been performed in the laboratory of Dr. Eric Griffis at the Centre for Gene Regulation & Expression within the College of Life Sciences, Dundee. The presented work was performed under the guidance of Dr Eric Griffis and contains no material which has been accepted for the award of any degree in any university.

Claudia Conte

---

I declare that Claudia Conte has spent the equivalent of at least nine terms in the research department of the College of Life Sciences at the University of Dundee and that she has fulfilled the conditions of Ordinance General No. 39 of the University of Dundee and is qualified to submit the accompanying thesis in application for the degree of Doctor of Philosophy.

Dr. Eric Griffis

*Supervisor*

---

## Acknowledgements

Firstly, I would like to express my gratitude to my supervisor Dr. Eric Griffis for its guidance and support during these years in carrying out this project. I am grateful for all the constructive discussions and the advices and for helping me to find a positive side of things when I could not see it.

My gratitude goes to Dr. Arno Müller and Dr. Simon Bullock for taking the time to read the thesis and examining my PhD.

I would like to acknowledge my thesis committee members Prof. Inke Näthke and Prof. Tom Owen-Huges for the insightful comments and advices during our meetings.

A thank to College of Life Sciences, GRE, all the staff members and all the facilities members for all the support and the technical assistance.

Thanks to the Dundee Cancer Centre for accepting me in the PhD program and to Cancer Research-UK for providing the funding to pursue my PhD project.

A big thanks to my labmates: dear Taciana, thanks for the invaluable help and all the chatting in the office…it has always been an interesting time! Dear Sara, thanks for all the support and all the stimulating discussions we had over these years, scientific and not… always much appreciated!

A special thanks goes to my "Dundonian Family" that provided me with unconditional friendship and enriched my time in Dundee. Dear Giuli, thanks for all our hilarious moments and continuous chats about everything and anything! Thanks for the "limbo"…it has been a huge privilege and a big pleasure to work with you. Thanks also for our nights discovering Dundee…always a lot of fun! Dear Blondie, thanks for all the long "listening session" and questions (Marzullona!!) … they have always been really helpful! Thanks for all your positive energy and your love, you taught me so much and you should be seriously proud of it! Thanks for all the nice moments spent together…you are unique! A special thanks to my dear Tuzza; thanks for your patience

and support … it has not been an easy time for you! Thanks for all the nice food and the movies you provided and thanks for all the help with technology…you are officially my reference point! Dear little Kasiu, thanks for your friendship and all the funny moments spent together. Thanks for making the big effort to "follow" our "Italian mentality" sacrificing sometimes your English…this meant a lot (please, please do not lose your lovely accent!)! In once guys, thanks for all the moments we spent together, all the laughter and tears that I will always remember as the greatest moments in Dundee. Knowing you was the best gift that this experience could give me!.

I would like to thank my family, my lovely parents and my sister, for all their love and encouragement during all these years.

Last, but not least, a huge thanks to my big love and best friend Alessio, who always encouraged and supported me even from the other side of the world. Thanks for all the joyful times spent together and for always listening to me and to all my madness with extreme patient and "interest". You helped me to believe in myself even in the darkest moments, you were always the first to believe in me, thanks so much!

# Abstract

Spindly was discovered in 2007 as a protein crucial for cells to progress through mitosis. It was shown to be required for recruitment of the dynein/dynactin motor complex to kinetochores thus to promote chromosome alignment and mitotic progression. Kinetochore recruitment of the dynein/dynactin motor complex is crucial for maturation of kinetochore-microtubule attachments and for silencing the spindle assembly checkpoint (SAC), the surveillance pathway that monitors bi-orientation and inhibits anaphase onset until chromosomes are attached to opposing spindle poles.
In human cells, Spindly depletion produces strong chromosome alignment defects with cells arrested in mitosis. Conversely expression of a single point mutant form allows for separation of these two functions of Spindly: it rescues chromosome alignment but inhibits SAC silencing and the recruitment of the motor complex.

In this work the interaction of Spindly with the dynein/dynactin motor complex was examined, untangling the subunits specifically involved in the binding. It was demonstrated that the single point mutation specifically impairs the interaction with dynactin, potentially affecting the capacity of the motor to strip proteins away and suggesting a role for Spindly as an adaptor of the complex, involved in enhancing its processivity.

Previous reports have shown that the constant presence of Spindly at kinetochore impedes SAC inhibition, whereas its depletion allows for an alternative mechanism dynein- independent to silence the SAC on aligned kinetochores. In the present thesis the interaction of Spindly with the proteins involved in the SAC pathway was described, hinting at a further role of Spindly in the SAC signalling related to activation/ maintenance.

It has been earlier described that depletion of *Drosophila melanogaster* Spindly generates defects also in cytoskeletal organisation. Here was identified a pool of human Spindly in interphase cells localising at microtubule plus-ends. It was proved that Spindly plays a direct role in cell migration and that it localises at the leading edge of migrating cells, specifically at focal adhesion sites, together with actin filaments and dynein/dynactin.

With this work we present the discovery of new functions of human Spindly as a novel promoter of dynein/dynactin processivity in different biochemical processes where Spindly could represent a key scaffold protein necessary to link this motor complex to multiple cargos/sites.

# Table of contests

# List of Tables

# List of figures

# List of abbreviations

| | |
|---|---|
| 3AT: | 3-amino-1, 2, 4-triazole |
| 6AAA ATPase: | ATPases Associated with diverse cellular Activities |
| A280: | absorbance at 280nm |
| ACN: | acetonitrile |
| APC/C: | Anaphase-Promoting complex/Cyclosome |
| ARP1: | actin related protein |
| Arp2/3: | actin-related protein-2/3 |
| ATP: | adenosine triphosphate |
| BFP: | blue fluorescent proteins |
| BicD/ BicD2: | protein Bicaudal D |
| BNIP1: | BLC2/Adenovirus E1B 19 kDa Interacting Protein 1 |
| BrdU: | bromodeoxyuridine |
| BSA: | bovine serum albumin |
| Bub: | budding uninhibited by benzimidazoles |
| cDNA: | complementary DNA |
| C-Mad2: | closed Mad2 |
| *C*-terminus: | carboxyl-terminus |
| CAP-Gly: | cytoskeleton-associated protein glycin rich |
| Cdc20: | cell division cycle 20 |
| CCAN: | Constitutive Centromere Associated Network |
| CDK: | cyclin-dependent kinases |
| CENP-E: | centromere *protein* E |
| CENP-F: | centromere protein E |
| CHAPS: | 3-[(3-cholamidopropyl)dimethylammonio]-1-propanesulfonate |
| CLIP170: | cytoplasmic linker protein 170 |
| CPC: | chromosome passenger complex |
| CTRL: | control |
| DAPI: | 2-(4-amidinophenyl)-1H -indole-6-carboxamidine |
| DSBs: | double-strand breaks |
| DHC: | dynein heavy chain |
| DIC: | dynein intermediate chain |
| *D. mel*.: | Drosophila melanogaster |
| DMF: | dimethylformamide |
| DMSO: | dimethyl sulfoxide |
| Spindly: | *Drosophila melanogaster* Spindly |
| DNA: | deoxyribonucleic acid |
| DOA: | drop out amino-acid |
| DTT: | dithiothreitol |
| EB1: | end binding 1 |
| ECL: | enhanced chemiluminescence |
| ECM: | extracellular matrix |
| EDTA: | ethylenediaminetetraacetic acid |
| EGTA: | ethylene glycol tetraacetic acid |
| EM: | electron microscopy |
| ER: | endoplasmic reticulum |
| FAK: | focal adhesion kinase |
| FB: | human fibroblast |
| Fig: | figure |
| FLAG IP: | FLAG- Immunoprecipitation |
| FKBP: | FK506 binding protein |
| FRB: | FKBP12-rapamycin binding |
| FTI: | farnesyl transferase inhibitor |
| Fwd: | forward |

| | |
|---|---|
| GAPDH: | Glyceraldehyde 3-phosphate dehydrogenase |
| GDI: | Guanosine nucleotide dissociation inhibitor |
| GEF: | Guanine nucleotide exchange factors |
| GFP: | green fluorescent protein |
| GM130: | *cis*-Golgi matrix 130 |
| GTP: | Guanosine-5'-triphosphate |
| HI-FBS: | heat-inactivated fetal bovine serum |
| HIS: | histidine |
| HRP: | horseradish peroxidase |
| HSpindly: | *Homo Sapiens* Spindly |
| HU: | hydroxyurea |
| IFT: | intraflagellar transport |
| IgG: | immunoglobulin |
| IF: | intermediate filaments |
| IFT: | intraflagellar transport |
| IPTG: | Isopropyl β-D-1-thiogalactopyranoside |
| IP: | immunoprecipitation |
| JAS: | jasplakinolide |
| kDa: | kilo dalton |
| KT: | kinetochore |
| JMY: | Junction-mediating and -regulatory protein |
| LAT A: | latrunculin A |
| LC: | light chain |
| LEU: | leucine |
| LiAC: | lithium acetate |
| LIC: | light intermediate chain |
| Lis1: | lissencephaly-1 |
| LPC: | lysophosphatidylcholine |
| mSpindly: | *Mus musculus* Spindly |
| MACF: | microtubule actin cross-linking factor |
| Mad: | mitotic arrest deficient |
| MAP: | microtubule associating protein |
| MAPK: | Mitogen-activated protein kinases |
| MCC: | mitotic checkpoint complex |
| MEF: | mouse embryonic fibroblast |
| MLC: | Myosin light chain |
| MLCK: | Myosin light chain kinase |
| mM: | millimolar |
| μM: | micrometer |
| Mps1: | MonoPolar Spindle 1 |
| mRNA: | messenger ribonucleic acid |
| MS: | mass spectrometry |
| MT: | microtubule |
| MTOC: | microtubule organising centre |
| NAG: | neuroblastoma-amplified protein |
| NSF: | N-ethylmaleimide sensitive fusion protein |
| NudE: | nuclear distribution protein E |
| NudEL: | Nuclear distribution protein nudE-like |
| NEM: | N-Ethylmaleimide |
| $NH_4HCO_3$: | ammonium bicarbonate |
| nm: | nanometer |
| nM: | nanomolar |
| NOC: | nocodazole |
| *N*-terminus: | amino-terminus |
| O-Mad2: | open Mad2 |
| PAFAH: | platelet-activating factor acetyl-hydrolase |
| PBS: | phosphate-buffered saline |

| | |
|---|---|
| PCNA: | proliferating cell nuclear antigen |
| PEG: | Polyethylene glycol |
| PFA: | Paraformaldehyde |
| p-Myosin: | phospho-Myosin |
| PMSF: | Phenylmethylsulfonyl Fluoride |
| PP1: | protein phosphatase 1 |
| PP2A: | protein phosphatase 2 A |
| Rab: | Ras-related protein in brain |
| RanBP2: | Ran binding protein 2 |
| RanGAP: | Ran GTPase-activating protein |
| Rb IgG: | rabbit Immunoglobulin |
| Rev: | reverse |
| RFP: | red fluorescent protein |
| RILP: | Rab-interacting lysosomal protein |
| RINT-1: | Rad50-interacting protein 1 |
| RNA: | ribonucleic acid |
| RNAi: | RNA interference |
| ROCK: | Rho associated protein kinase |
| RPM: | revolution per minute |
| RZZ: | Rod-Zwilch-ZW10 complex |
| SAC: | spindle assembly checkpoint |
| SDS-PAGE: | sodium dodecyl sulfate polyacrylamide gel electrophoresis |
| SEC: | size exclusion chromatography |
| siCTRL: | silencing control |
| siRNA: | small interfering RNA |
| siSpin: | silencing Spindly |
| SNAP: | soluble NSF attachment protein |
| SPDL-1: | *Caenorhabditis elegans* Spindly |
| Spindly IP: | Spindly immunoprecipitation |
| Src: | sarcoma-family kinase |
| ssDNA: | single strand DNA |
| STLC: | S-trityl-L-cystein |
| TBS: | Tris-buffered saline |
| TE: | tris-EDTA |
| TFA: | trifluoracetic acid |
| TIRF: | total internal reflection fluorescence |
| TRP: | Tryptophan |
| UT: | untreated |
| WASP: | Wiskott–Aldrich syndrome protein |
| WAVE: | WASP-family verprolin-homologous protein |
| WASH: | Wiskott–Aldrich syndrome protein and SCAR homologue |
| X-Gal: | 5-bromo-4-chloro-3-indolyl-β-D-galactopyranoside |
| Y2H: | yeast-two hybrid |
| YFP: | yellow fluorescent protein |
| YPAD: | Yeast-peptone- adenine-dextrose |
| ZW10: | zeste-white 10 |

# 1 . Introduction

## 1.1 Preamble

Animal cells possess a cytoskeletal structure that allows them to grow, divide and move, facilitating considerable changes in the cell shape. To accomplish all these functions the cytoskeleton relies on the constant interplay of three major filament systems, actin, intermediate filaments and microtubules, that have to be coordinated in order to accommodate different physiological needs. The close interplay between these cytoskeletal structures is possible thanks to different proteins, motors and cross-linkers; moreover, the strong coupling is mediated via biochemical signalling and gene regulation that allows the cytoskeletal network to cover a wide range of functions. Therefore, understanding how these pathways are organised and what are the proteins involved could help to get new insights in cell functioning.

Many cellular processes rely on the cytoskeleton network, such as cell migration and cell division. To regulate cell migration the three cytoskeletal components are highly coordinated to ensure cell polarisation and interactions with the cell matrix. Microtubules and actin filaments collaborate at the cell front to drive protrusion formation and to mediate the delivery of different components. Also, they closely interplay in cell adhesion; while the actin cytoskeleton generates traction forces to drag the cell body, microtubules control the dynamics of adhesion complexes. In a similar way, actin filaments and microtubules work together in cell division, mainly in centrosome separation and in cytokinesis, ensuring generation of two daughter cells. Central for this process is the formation of the mitotic spindle, a microtubule-based structure that allows capture and alignment of chromosomes and in turn faithful segregation.

Spindly was identified as an important molecular player of the cell division, critical to ensure proper chromosome alignment and correct transmission of the genomic material. However, its depletion was shown to affect also cytoskeletal structures in interphase cells, indicating a potential general role in the maintenance of the cytoskeleton network activities.

Work in this thesis aims to untangle different aspects of the functioning of Spindly in both mitosis and interphase, focusing on its capacity to regulate the cytoskeleton network.

## 1.2 Cell division

Prokaryotes and eukaryotes have common strategies for cell division. Although the cell organisation is much different, in both cases cells first grow and duplicate the DNA in each chromosome and then chromosomes are segregated in equal number to each daughter cell ensuring fidelity of the transmission of genome and cytoplasm.

Since prokaryotes are much simpler, cell division is faster and easier; they contain only a single circular chromosome and replication and segregation are often coupled. Chromosomes are bound to the cell membrane and thus when a cell separates each daughter will inherit the new chromosome. This process is called Binary Fission and it generates genetically identical daughter cells (Reyes-Lamothe *et al.*, 2012). In eukaryotes, the process is much more intricate, due to the higher complexity of the cell organisation. It is possible to distinguish an INTERPHASE, when the DNA duplication occurs, and a MITOTIC PHASE, when the chromosome segregation process happens. Interphase can in turn be divided in three different phases required to prepare the cell to properly transmit its genetic material once in mitosis. There are three GAP phases: **$G_1$** (or Gap phase 1), important for the cell to grow in size and synthesise mRNA, protein and ribosomes; **$G_2$** (or Gap phase 2), for protein synthesis and organelles replication before mitosis; **$G_0$** (or Gap phase 0) that occurs after mitosis, in lieu of or within $G_1$ and frequently takes place as cells terminally differentiate and most probably will never divide again. Between $G_1$ and $G_2$ is the synthesis phase (or **S phase**) during which chromosomes are replicated to generate two sister chromatids so to double the amount of DNA. All these steps are crucial for proper initiation of the cell division process, the mitotic phase (or M phase). This can be divided into five steps:

1) **Prophase**: the DNA condensate into chromosomes and the MT cytoskeleton is reorganised; the centrosomes (the main microtubule organising centre in animal cells)

are replicated and move to the opposite poles thanks to the activity of motor proteins; the mitotic spindle starts to form outside the nucleus.

2) **Prometaphase**: the nuclear envelope (the physical barrier that encloses the nucleus) breaks down and sister chromatids are released from the nucleus. Sister chromatids are bound to each other at the centre thanks to the kinetochore (a multiprotein structure formed around the centromere), which allows microtubules to capture chromosomes. Microtubules generated from either end of the cell and attached to the kinetochores are now called kinetochore microtubules (k-fibres).

3) **Metaphase**: microtubules and kinetochores bind to each other to position chromosomes aligned at the centre of the cell and to generate the 'so-called' metaphase plate.

4) **Anaphase**: sister chromatids are separated and pulled by the spindle to the opposite poles of the cell while the spindle simultaneously elongate and move towards opposite poles. In doing so, anaphase ensures that each daughter cell receives an equal set of chromosomes.

5) **Telophase**: the nuclear envelope re-forms around each set of chromosomes, thus separating the nuclear DNA from the cytoplasm, and the chromosomes begin to decondense.

The final step of cell division is cytokinesis, characterised by the separation of the parental cytoplasm following the generation of a cleavage furrow by invagination of the plasma membrane (Fig. 1.1.) (Alberts *et al.*, 2007).

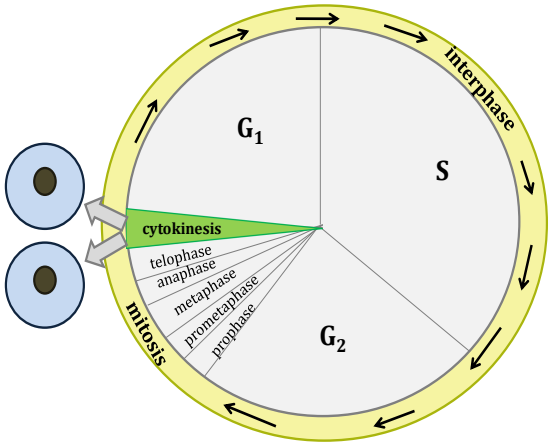


**Figure 1. 1. Schematic representation of cell division cycle.**

Cell division relies on many different steps that have to properly occur to ensure fidelity to the process: microtubules have to form a stable bipolar spindle and correct attachments have to be generated with the kinetochore site, to then allow correct alignment and separation. These steps are strictly controlled by the cell that presents an error correction mechanism to disrupt mis-attachments and a surveillance mechanism to prevent anaphase until correct inter-kinetochore tension is generated. Errors in these processes are indeed highly correlated with aneuploidy and tumorigenesis (Holland and Cleveland, 2012). Correct chromosome alignment is therefore coordinated with the silencing of the mitotic checkpoint to allow anaphase onset only upon bi-orientation. How these steps are so finely synchronised has not been fully elucidated yet. The identification of Spindly, a protein essential for both chromosome alignment and checkpoint silencing, indicates the possible presence of a 'molecular sensor' able to coordinate these two processes (Griffis *et al.*, 2007) (Chan *et al.*, 2009) (Barisic *et al.*, 2010) (Gassmann *et al.*, 2010).

### 1.2.1 The mitotic spindle

The whole cell division process relies on the proper movement of chromosomes; it is powered by a macromolecular machine known as the mitotic spindle apparatus, made up of centrosomes, chromosomes, microtubules (MT), cross-linkers, and microtubule motors.

The mitotic spindle assembly begins in early prophase, while the nuclear envelope is still intact. The core of the mitotic spindle is represented by microtubules, 13 parallel protofilaments of heterodimers of α- and β- tubulin that are arranged in a hollow tube and are generated by polymerisation of tubulin subunits from a microtubule nucleating structure (or microtubule organising centre (MTOC)), which in many cells is the centrosome (Alberts *et al.*, 2007). Centrosomes are composed of two centrioles surrounded by an amorphous mass of protein called pericentriolar material (or matrix) that regulates microtubule behaviour (Woodruff *et al.*, 2014). To ensure equality in the formation of the spindle, centrosomes have to duplicate in S phase and then separate at the onset of mitosis. It is crucial for a cell to avoid the over-duplication of centrosomes, which could generate multipolar spindles and abnormal cell division. The separation of centrosomes and their migration towards the poles of the cell is mediated by microtubule forces and motor proteins like dynein and kinesin Eg5 that slide anti-parallel MTs attached to centrosomes (Hinchcliffe and Sluder, 2001).

Microtubules grow outwards from their site of polymerisation at centrosomes, extending outwards with their plus-ends polymerising to facilitate spindle organisation while the minus-end is normally bound to the MTOC. An interesting feature of microtubule growth is ‘dynamic instability’: an alternate period of slow polymerisation (elongation) followed by rapid depolymerisation (shortening). When microtubules go from growing to shortening, it is called ‘catastrophe’; conversely when the opposite occurs it is referred as ‘rescue’ (Mitchison and Kirschner, 1984).

MT dynamic is governed by the rate of GTP hydrolysis, the concentration of soluble tubulin dimers within the cell, and microtubule nucleating proteins that bind to plus-ends. Tubulin subunits bind the nucleotide GTP and only the GTP-bound tubulin can polymerise into MTs; then GTP hydrolyses to GDP rapidly after polymerisation (Desai and Mitchison, 1997). Growing microtubules contain a cap of GTP-tubulin, and the loss of this cap leads to catastrophe (Alberts *et al.*, 2007). The tubulin nucleotide exchange rate differs according to the phase the cell is in: it requires minutes in interphase, while only seconds in mitosis. During the $G_2$/M transition the frequency of catastrophe is higher, thus microtubules are shorter and more dynamic as spindles form (Belmont *et al.*, 1990).

#### *1.2.1.1 Mitotic spindle formation*

To date, two different theories of spindle assembly have been proposed.

The first postulated theory is based on the "search and capture" model and was described for the first time by Mitchison and Kirschner and then furtherly visualised and validated by other researchers (Mitchison and Kirschner, 1984) (Hayden J. H., 1990) (Rieder and Alexander, 1990). This model is based on centrosomal MT nucleation followed by cycles of growth, shrinkage, and regrowth to explore the cytoplasm; eventually microtubules will make contact with (or 'capture') the kinetochore of a chromosome, arresting its dynamics (O'Connell and Khodjakov, 2007). Further studies demonstrated that the capture timing of KT-MT is not based on a random search for a single target but there is a signal based on a Ran-GTPase gradient present around mitotic chromosomes that facilitates the capture (Wollman *et al.*, 2005). This gradient induces microtubule nucleation and stabilisation by increasing the microtubule rescue frequency and reducing the microtubule catastrophe frequency when it is located proximal to chromosomes (Carazo-Salas *et al.*, 2001). It derives from the activity of the

chromosome-associated guanine-nucleotide-exchange (GEF) factor RCC1 that binds to chromosomes and generates a high local concentration of Ran-GTP, which in turn binds to Importin-β inducing the release of the MT stabilizing factors that it normally sequesters (Carazo-Salas *et al.*, 1999). Then RanGTP diffuses away from chromosomes before the GTP becomes hydrolysed into GDP, therefore generating a gradient that sharply decreases with distance from the chromosomes (Kalab *et al.*, 2002). In addition to stabilising microtubules to promote kinetochore capture, chromatin bound RCC1 has been shown to directly stimulate microtubule nucleation around chromatin (Carazo-Salas *et al.*, 1999). The discovery of the GTPase gradient allowed scientists to postulate the second theory for the spindle formation, useful to explain this process in those cells that do not present centrosomes, such as oocytes and *Xenopus* egg extracts (Carazo-Salas *et al.*, 2001). More precisely, this theory is based on acentrosomal nucleation of microtubules near chromosomes and their subsequent assembly into anti-parallel bundles that will adopt a spindle-like structure. It has indeed been demonstrated that microtubules can be nucleated from the kinetochores just as from the centrosomes, through a MT plus ends polymerisation process (Kitamura *et al.*, 2010). Data collected from Kitamura and colleagues also demonstrated that microtubules derived from KTs can interact with microtubules nucleated from spindle poles along their length, facilitating the loading of chromosomes onto the lateral surface of microtubules.

These two mechanisms are not mutually exclusive, but instead they look to be interconnected; indeed the 'search and capture' model can be applied also to those microtubules nucleated from chromosomes (Wadsworth and Khodjakov, 2004). Moreover, a common structure exists that can combine microtubules nucleated from kinetochores and microtubules nucleated from centrosomes; astral microtubules can be captured by k-fibres and the distal ends of k-fibres can then be transported poleward along astral microtubules by dynein motors (Khodjakov *et al.*, 2003). The motor

complex dynein/dynactin, as well as the Nuclear Mitotic apparatus (NuMA) protein, are involved in establishing and maintaining the standard spindle width and in crosslinking microtubules to generate sliding forces (Merdes *et al.*, 1996).

What is hence clear is that cells rely on multiple mechanisms to rapidly assemble the mitotic spindle.

### 1.2.2 The kinetochore

Proper chromosome segregation requires correct attachments between microtubules and the kinetochore sites on chromosomes. After nuclear envelope breakdown has occurred, kinetochores start to interact with the spindle microtubules; attachments are predominantly made 'side-on' along the microtubule lattice and then replaced by ''end-on'' attachment. Only if these connections are properly generated chromosomes can bi-orient and become aligned on the metaphase plate.

Kinetochore proteins are directly involved not only in the association with microtubules but also in the translocation of chromosomes along microtubule polymers thanks to two main motor proteins that localise at KTs: CENP-E and dynein (Kapoor *et al.*, 2006). CENP-E allows for plus-end motility along k-fibres, moving chromosome from the poles towards the equator (MT plus-ends) whereas dynein moves chromosomes towards the minus-ends of microtubules (Sharp *et al.*, 2000)

Moreover, kinetochores are central in the regulation of microtubules dynamics; kinetochore microtubules keep growing upon attachments by adding tubulin subunits at the KT-MT interface to maintain spindle length and to promote chromosome movements prior to anaphase. Cycles of depolymerisation and polymerisation at kinetochore pairs lead to the oscillations of chromosomes at the metaphase plate (Rieder and Salmon, 1998).

#### *1.2.2.1 Kinetochore structure*

Over the years researchers have been able to describe the ultrastructure of kinetochores, identifying three distinct regions: the inner kinetochore (which interfaces with chromatin); the outer kinetochore (which interacts with microtubules); and the central kinetochore, in between the first two (McEwen *et al.*, 1998). From the outer kinetochore the fibrous corona, a dense array of fibres, extends outwards. Each kinetochore can bind several spindle microtubules (Cheeseman, 2014).

The assembly of the kinetochore relies on the presence at the centromere of CENP-A nucleosomes, a variant of histone H3, with which associate those proteins that constitutively bind to centromeres generating the so-called 'constitutive centromere-associated network', or CCAN. This network of proteins helps to define the 'kinetochore-restriction site' where MT attachments are made (McAinsh and Meraldi, 2011). All the other proteins that assemble in the kinetochore are recruited between the end of $G_2$ phase and the beginning of M phase. Some of them are quite dynamic and so are depleted following microtubule attachments; others persist longer, until the end of mitosis or even until $G_1$ phase (Liu *et al.*, 2006).

Cheesesman and co-workers identified ten proteins central for the kinetochore-microtubule interaction; they constitute the KMN network that in vertebrates is made up of the Knl1 complex (Knl1 and Zwint), the Mis12 complex (Nnf1, Mis12, Dsn1 and Nsl1) and the Ndc80 complex (Ndc80 (Hec1), Nuf2, Spc24 and Spc25) (Cheeseman *et al.*, 2006). The KMN network serves as an important kinetochore 'hub' for both microtubule attachments and spindle checkpoint assembly and signalling. The Ndc80 complex and the Knl1 complex are crucial respectively to bind microtubules and stabilise KT-MT associations.

Moreover they can mediate the targeting of spindle assembly checkpoint proteins onto kinetochores (Varma *et al.*, 2013): by recruiting Bub1, BubR1, Bub3, PP1, Mps1 and the Rod-Zwilch-ZW10 (RZZ) complex via the Knl1 complex (Vleugel *et al.*, 2013) (Espeut *et al.*, 2012) (London *et al.*, 2012) (Starr *et al.*, 2000), and by mediating the association of Mps1 and of the Mad1-Mad2 complex through the Ndc80 complex (Zhu *et al.*, 2013) (Martin-Lluesma *et al.*, 2002). Additionally, Ndc80 links the CCAN with the outer kinetochore plate by binding CENP-T (Nishino *et al.*, 2013). The third component of the KMN complex is the Mis12 complex that interacts with CENP-C on one side and with the Ndc80 complex and the Knl1 complex on the other side bridging in this way the outer kinetochore region and the inner centromeric DNA (Screpanti *et al.*, 2011) (Kline *et al.*, 2006) (Fig. 1.2).

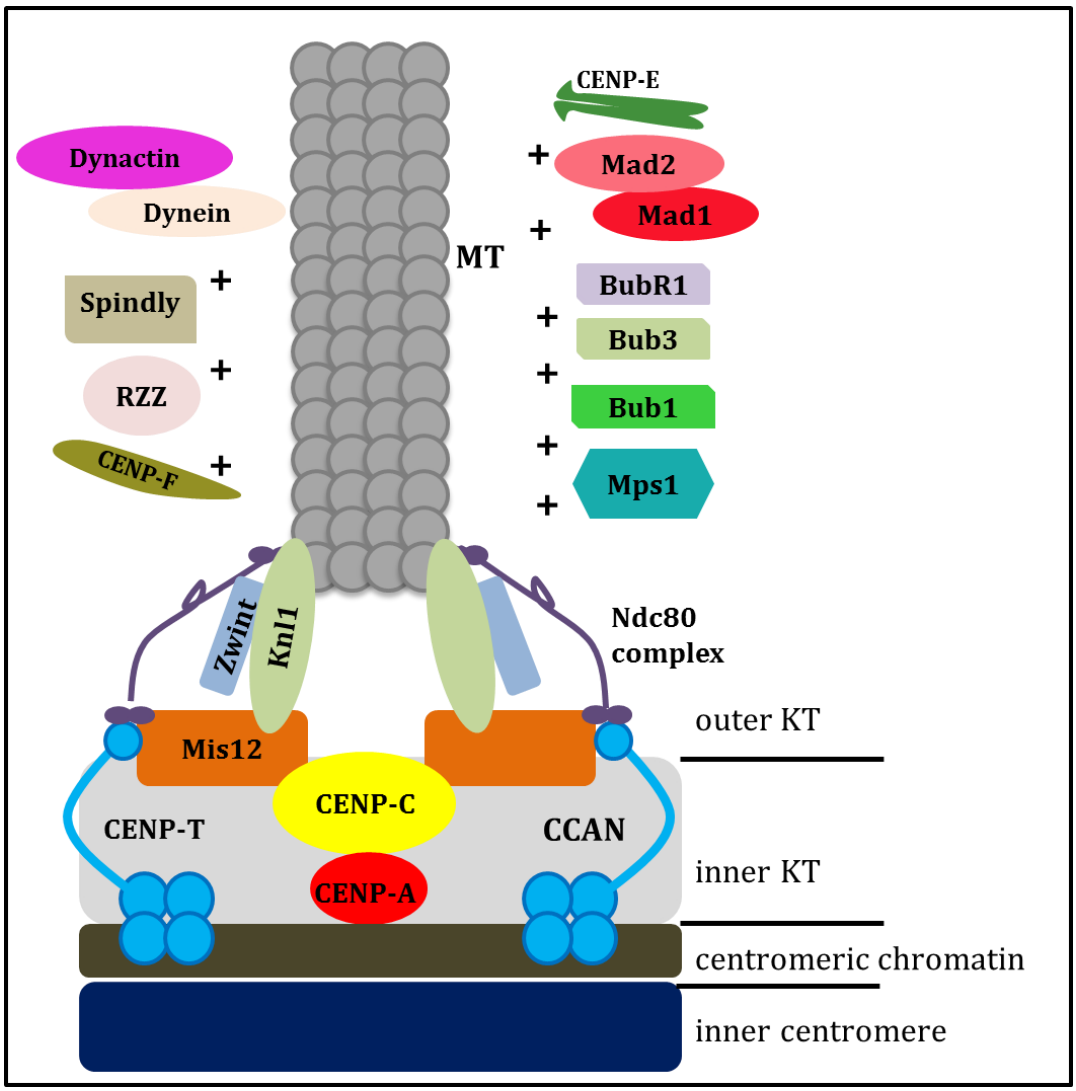


**Figure 1. 2.Schematic representation of the kinetochore structure.**
Molecular architecture of a kinetochore showing (from the bottom to the top): the inner centromere, the centromeric chromatin, on which assembles the CCAN network of proteins forming, the inner KT, and the outer KT. The CCAN recruits then the KMN network (Knl1/Mis12/Ndc80 complexes) that operate in the formation of outer KT plate, thus to recruit other molecular players for execution of mitosis: Bub1, Bub3, BubR1, Mad1/Mad2, Mps1, RZZ, Spindly, dynein/dynactin (Suzuki *et al.*, 2015) (Petrovic *et al.*, 2010) (Vos *et al.*, 2011) (Zhang *et al.*, 2015) (Kim *et al.*, 2012) (Vleugel *et al.*, 2013) (Moyle *et al.*, 2014).

### *1.2.2.2 Chromosome-microtubule attachment*

Errors in the chromosome partitioning process generate chromosome aberrations and formation of malignancies (Holland and Cleveland, 2012). These defects can be related to different aspects of cell division: a weak mitotic checkpoint (which allows anaphase onset before all chromosomes are properly aligned on the metaphase plate), overexpression of Separase or Securin (two regulators of chromosome cohesion),

formation of multipolar spindles (which often originates from supernumerary centrosomes), and/or failure in the specification of the kinetochore formation site (Weaver and Cleveland, 2005). This latter is quite critical; failure in the specification process will impair attachments on the mitotic spindle, while definition of multiple sites will gives rise to inappropriate attachments.

Several kinetochore binding proteins are involved in the regulation of KT-MT attachments. The whole KMN complex is essential for the microtubule interaction: the Ndc80/Nuf2 dimer, within the Ndc80 complex, and the Knl1 protein, within the Knl1 complex, present microtubule-binding sites (one each) (Cheeseman *et al.*, 2006).
These attachments are regulated by Aurora B kinase that phosphorylates microtubule binding sites, inducing detachment when improper interactions have occurred (DeLuca *et al.*, 2006). Other kinetochore proteins are involved in the generation and stabilisation of stable KT-MT attachments. The RZZ complex, recruited at KTs by Zwint (in the inner kinetochore plate), is directly involved in the association of the dynein/dynactin motor complex and it can delay microtubules 'end-on' attachments by binding the Ndc80 tail and consequently affecting the microtubule interaction (Kops *et al.*, 2005) (Gassmann *et al.*, 2008) (Cheerambathur *et al.*, 2013). In a similar way, inhibition of Spindly, another important player in the kinetochore recruitment of the dynein/dynactin motor complex, has been shown to generate defects in chromosome segregation resembling the lack of 'end-on' attachments (Gassmann *et al.*, 2008) (Gassmann *et al.*, 2010).

Dynein is a promoter of load-bearing attachments; only once associated with KTs, it can accelerate their formation and at the same time it can avoid the generation of improper attachments providing a force that orients the KT toward the spindle pole at which the particular microtubule originates (Yang *et al.*, 2007). By doing so, dynein

reduces the possibility that the same kinetochore captures a microtubule from the opposite pole (Varma *et al.*, 2008).

Although many proteins control the process of attachments, chromosomes can engage in a variety of erroneous bindings besides the correct amphitelic (bi-oriented) one. Three major types of mis-attachment can occur: **merotelic attachments**, where one kinetochore binds to microtubules from both poles; **syntelic attachments**, in which both kinetochores have bound microtubules from the same pole; **monotelic attachment**, where one kinetochore attaches to microtubules from one spindle pole and the other kinetochore is not bound (Fig. 1.3) (Tanaka, 2008).

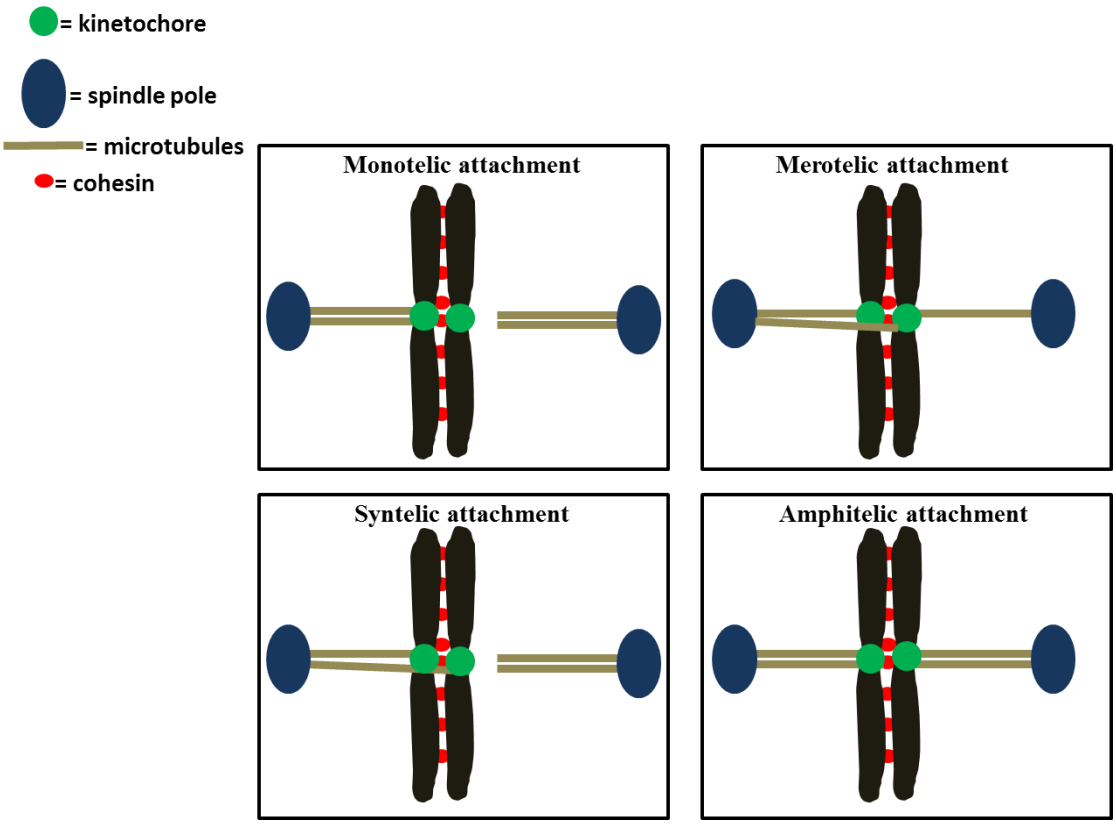


**Figure 1. 3. Kinetochore-microtubules interactions.**
Schematic representation of the possible attachments that can occur in mitosis between KTs and MTs. Monotelic and syntelic attachments generate mono-orientated mitotic spindles (that is connected to only one spindle pole) while merotelic and amphitelic attachments give rise to bi-orientated mitotic spindle (connected to both poles) (for full description see the main text).

The frequency of mis-attachments can be high within a cell; therefore they have to be either prevented or corrected. Cells possess an error-correction pathway that allows faithful chromosome segregation to occur even when mis-attachments have been made. This signalling is mediated by Aurora B kinase and detects and corrects mono-oriented attachments (Lampson et al., 2004). Aurora B localises between the sister kinetochores where it can phosphorylate the Ndc80 complex and consequently reduce its microtubule binding affinity (Ciferri *et al.*, 2008). Therefore, Aurora B keeps up the phosphorylation status of Ndc80 until proper tension is not generated (upon correct attachments). Once bi-orientation has occurred, tension is produced and kinetochores are pulled apart, physically separating Ndc80 from centromeric Aurora B.

Two important binding partners of Aurora B are Survivin and INCENP, which are positioned between microtubules and kinetochores and so are able to sense the tension generated upon bi-orientation (Lampson and Cheeseman, 2011). These four proteins (Aurora B, Borealin, Survivin and INCENP) function together in the same complex, the chromosome passenger complex (CPC) that is involved not only in the error-corrections process but also in the regulation of bipolar spindle stability and completion of cytokinesis (Carmena *et al.*, 2012). The CPC re-localises throughout mitosis to ensure phosphorylation of different substrates and so the regulation of different pathways during cell division. The CPC is essential also for spindle checkpoint activation and maintenance promoting the recruitment of Mps1 to KTs (Saurin *et al.*, 2011). Consequently Aurora B kinetochore substrates are de-phosphorylated to allow mitotic progression; its counteracting phosphatases are protein phosphatase 1 (PP1), at the outer kinetochore, and protein phosphatase 2 A (PP2A) B56 subunit, at the inner centromere (Funabiki and Wynne, 2013).

### 1.2.3 The spindle assembly checkpoint

Cells utilise a surveillance and signalling system that monitors MT-KT interactions and delays anaphase onset until all chromosomes are properly attached to the spindle. This checkpoint, called the Spindle Assembly Checkpoint (SAC), has to guard against the degradation of Cyclin B and the cleavage of the cohesin rings that keep duplicated chromosomes (sister chromatids) linked from the moment they are replicated until anaphase onset (Nasmyth and Haering, 2009). Once anaphase starts, the cohesin-ring is physically cleaved by Separase and by spindle forces that pull chromatids towards the spindle poles. This means that until the last kinetochore is correctly attached sister chromatids have to be linked to resist pulling forces from the spindle and to prevent early chromosome segregation. Additionally, for complete exit from mitosis, cells have to degrade Cyclin B as well (Sivakumar and Gorbsky, 2015). Therefore the mitotic checkpoint sets the time when mitotic exit and anaphase onset can occur (Musacchio, 2011) (Lara-Gonzalez *et al.*, 2012).

The molecular players involved in this signalling were identified in 1991 in a genetic screen in *Saccharomyces cerevisiae* that looked for mutants that failed to arrest in mitosis after microtubule destabilisation. The screens identified Mad1, Mad2, Mad3 (mitotic arrest-deficient), Bub1, and Bub3 (binding uninhibited by benzimidazole) (Hoyt *et al.*, 1991) (Li and Murray, 1991). Subsequently homologues were described in higher eukaryotes and the kinetochore kinase Mps1 (monopolar spindle) with a dominant effect on the checkpoint was described (Weiss and Winey, 1996). Initially, how the complex was functioning was not clear; to fully understand the mechanism more complicated cell biology experiments were performed utilising laser ablation and physical manipulation of chromosomes. These experiments guided researchers attention first to kinetochores and hence to the importance of tension generation upon MT-KT attachment (Rieder *et al.*, 1995).

SAC proteins are recruited on unattached KTs and are removed only upon kinetochore stretching that indicates correct bi-orientation (Uchida *et al.*, 2009) (Maresca and Salmon, 2010). The core SAC effector is the mitotic-checkpoint complex (MCC), made up of Mad2-Cdc20 and BubR1-Bub3 (Chao *et al.*, 2012) (Fig. 1.4, **(i)**). Additional proteins involved in this signalling are the RZZ complex, $p31^{comet}$ , kinases including Aurora B, Mps1, MAPKs, Cdk1-Cyclin B and Plk1, the motor proteins CENP-E and dynein, and dynein-accessory factors (dynactin, NudE/L, Lis1, Spindly) (Karess, 2005) (Eytan *et al.*, 2013) (Takenaka *et al.*, 1998) (D'Angiolella *et al.*, 2003) (Mao *et al.*, 2003) (Silva *et al.*, 2014).

The SAC functions generating a "wait anaphase" signal that inhibits the E3 ubiquitin ligase APC/C (anaphase-promoting complex/cyclosome) impairing proteasomal degradation of two crucial substrates, Cyclin B, the mitotic Cdk1 cofactor, and Securin, the protein that protects sister chromatid Cohesin from Separase (Peters, 2006). Inhibition of APC/C is directly mediated by the MCC complex that binds Cdc20 through Mad2 blocking APC/C-Cdc20 (Fang *et al.*, 1998); association of BubR1 also potentiate the inhibitory signal Mad2-mediated, reinforcing the idea that is the whole MCC complex necessary to prevent anaphase onset (Fang, 2002), (Fig. 1.4).

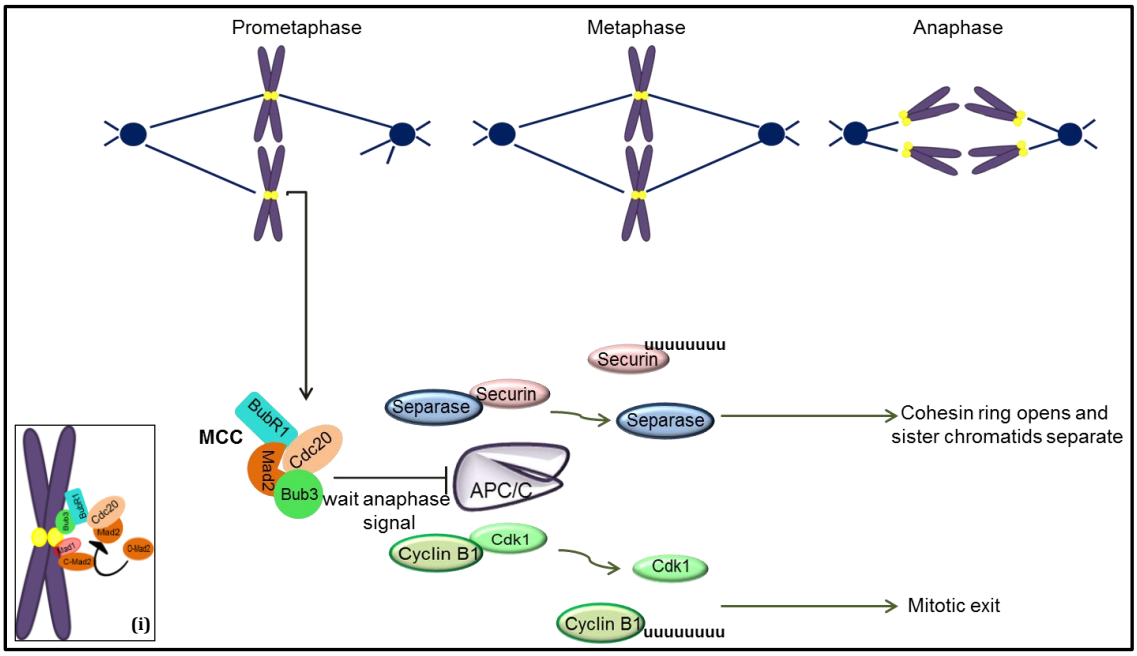


**Figure 1. 4. Schematic representation of the regulation of the spindle assembly checkpoint.** In prometaphase is catalysed the assembly of the mitotic checkpoint complex (MCC; made up of Bub3/BubR1/Mad2/Cdc20) onto unattached kinetochores. This complex inhibits the APC/C ubiquitin ligase. Once bi-orientation has been achieved (metaphase), the MCC is not assembled any longer and the APC/C is activated and promotes the degradation of Securin and Cyclin B1 and in turn sister chromatids separation and inactivation of Cdk1 (anaphase). These steps will allow for mitotic exit. **(i)** Model of SAC effectors assembly onto unattached KTs.

### *1.2.3.1 Spindle Assembly Checkpoint formation*

SAC molecular players get associated to kinetochores in prometaphase through Bub1, a fundamental SAC kinase recruited at first via the Knl1 complex (Sharp-Baker and Chen, 2001) (Johnson *et al.*, 2004). Knl1 specifically interacts with Bub1 upon Mps1 phosphorylation of its *N*-terminus (Kiyomitsu *et al.*, 2011) (London *et al.*, 2012). Phospho-Knl1 also allows the localisation of BubR1, a pseudo-kinase important for chromosome bi-orientation, and of Bub3, a further component of the MCC. While Bub1 kinetochore localisation depends on Bub3 interaction with Knl1, BubR1 localisation relies on Bub1, suggesting a dimerisation between these two proteins (Taylor *et al.*, 1998) (Vleugel *et al.*, 2015) (Fig. 1.5).

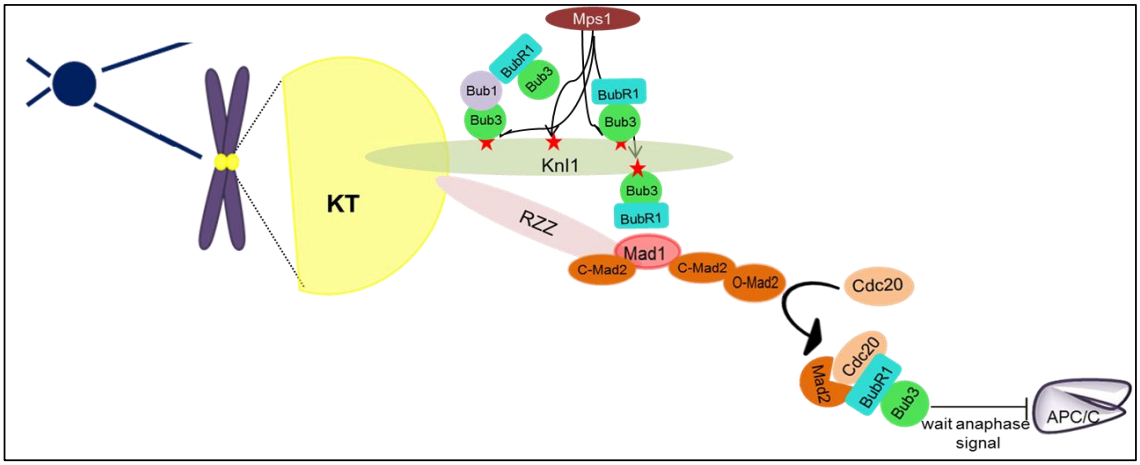


**Figure 1. 5. Diagram representing spindle assembly checkpoint formation pathway.** Mps1 phosphorylates multiple sites on Knl1 (red stars) allowing the subsequent association of Bub3 and binding of Bub1 and BubR1. This first step is critical to then promote recruitment of other SAC components to activate the "wait anaphase signal" and inhibits APC/C (for detail see main text).

Bub1 is also central for the sequential localisation of Mad1 at KTs, which then remains stably associated with KTs until microtubules have attached (Howell *et al.*, 2004). The recruitment of Mad1 to kinetochore occurs at the beginning of prometaphase and it allows for further association of Mad2 to site. It has been demonstrated that Mad2 exists in two conformations: a closed conformation (C-Mad2) that is bound to Mad1, and an open conformation (O-Mad2) that is present in the cytoplasm and that is transiently engaged with the kinetochore (Vink *et al.*, 2006) (De Antoni *et al.*, 2005). Precisely, O-Mad2 dimerises with C-Mad2 already presents at KT and is then converted into C-Mad2 that binds to Cdc20, making up a complex that will allow for subsequent assembly and functioning of the MCC (De Antoni *et al.*, 2005). Stable kinetochore localisation of Mad1 required also the RZZ complex that is first engaged at KTs upon Aurora B-mediated phosphorylation of Zwint, a constitutive binding protein of the Knl1 complex (Fig. 1.5) (Kasuboski *et al.*, 2011) (Varma *et al.*, 2013).

### *1.2.3.2 Spindle Assembly Checkpoint silencing*

The correct chromosome alignment and thus the correct attachments between KTs and MTs induce the inactivation of the SAC. There are different theories that try to explain this silencing process; they seem to be all somehow coordinated and therefore strictly related to one another.

The stripping model

The physical removal, or "stripping", of checkpoint proteins away from the kinetochore is essential for silencing the SAC. It has indeed been shown that when Mad1 is artificially tethered to kinetochores (via the KMN component Mis12), Mad2 is continuously captured and cells are arrested in metaphase; moreover, by increasing the levels of Mad1 at bioriented KTs upon SAC silencing it is possible to reactivate the signalling indicating that all the SAC molecular players have to be removed from KTs to allow progression through mitosis (Ballister *et al.*, 2014).

The transport of the SAC components towards spindle poles depends on lateral interaction of KTs with non-kinetochore microtubules as well as with kinetochore microtubules and it is quite rapid (Howell *et al.*, 2001). This process relies on the minus-end motor complex dynein/dynactin: experiments based on ATP depletion or inhibition of dynein/dynactin by microinjection of antibodies, either anti-p50 (or dynamitin, a dynactin subunit) antibody or anti-DIC (dynein intermediate chain), have demonstrated to block this transport process and to arrest cells in metaphase accumulating Mad2 at metaphase kinetochores (Howell *et al.*, 2001). Furthermore, inhibition of the motor complex reduces generation of tension at kinetochores upon chromosome alignment, suggesting a crucial role for the motor in the process of tension generation linked as well to the activation of the SAC-silencing process (Yang *et al.*, 2007). Kinetochore recruitment of dynein/dynactin relies on the presence of the RZZ

complex and Spindly at KTs. It has been shown that depletion of Spindly not only impairs dynein recruitment at KTs but also halt cells in metaphase retaining Mad2 at high levels (Griffis *et al.*, 2007). In human cells depleted of Spindly, Mad2 can still be removed from the few aligned KTs, suggesting the presence of an alternative dynein-independent mechanism and proposing that KT-dynein-mediated removal is required only upon association of Spindly with KTs (Chan *et al.*, 2009) (Gassmann *et al.*, 2010).

The phosphatase-based model

The recruitment of SAC proteins to kinetochores is promoted by phosphorylation of Knl1 mediated by two kinases: Mps1 and Aurora B (Yamagishi *et al.*, 2012). Vice versa, the silencing of the mitotic checkpoint requires de-phosphorylation of those kinetochore proteins to allow removal from this site (Funabiki and Wynne, 2013). As Mps1 and Aurora B are involved in both chromosome alignment and SAC activation, kinetochore phosphatases can interplay for stabilisation of the attachments and SAC silencing. On one side stabilisation of the attachments is achieved by physical separation of Aurora B from its substrates, as a result of inter- and intra-kinetochore tension and by Mps1 phosphorylation that promotes the formation of stable 'end-on' attachments upon a conformational change that releases Ndc80 (Liu *et al.*, 2009) (Dou *et al.*, 2015); on the other side, phosphatases have to be recruited to KTs to ensure the stabilisation of KT-MT binding and de-phosphorylation (and subsequent release) of spindle assembly checkpoint proteins (Funabiki and Wynne, 2013). Therefore, spatial separation upon tension is not sufficient to allow prometaphase-metaphase transition.

Kinetochore phosphatases recruited for mitotic transition are protein phosphatase 1 (PP1) and protein phosphatase 2 A (PP2A). In yeast it has been shown that PP1 antagonises both Mps1 and Aurora B, while in mammalian cells this function requires kinetochore localisation of PP2A phosphatase (London *et al.*, 2012) (Kruse *et al.*, 2013)

(Espert *et al.*, 2014) (Nijenhuis *et al.*, 2014). PP1 is a serine/threonine phosphatase that controls many pathways within a cell with high specificity for each function thanks to precise interactions between the different regulatory subunits and the catalytic subunit (Korrodi-Gregorio *et al.*, 2014). Most interactions between PP1 and its binding partners occur via a RVxF site (K/R/H/N/S-V/I/L-x-F/W/Y, where x is any residue other than Phe, Ile, Met, Tyr, Asp or Pro), which allows PP1 to come close to the interactor protein to then make additional bindings. The association of PP1 with kinetochores occurs via a RVSF site present on Knl1 and once there PP1 promotes the removal of phosphate groups from Aurora B-kinetochore substrates (such as H3, Sds22, Knl1 and CENP-E) and it stabilises microtubule attachments (Liu *et al.*, 2010). However, Knl1 is also phosphorylated by Mps1 in order to recruit Bub1, Bub3 and BubR1 onto unattached KTs. It has been shown that in yeast overexpression of Mps1 enhances this binding while overexpression of PP1 directly inhibits it (London *et al.*, 2012). Thus PP1 is a key player in the mitotic exit process and it is required for inactivation of the spindle checkpoint,

Conversely, in mammalian cells there exists another process to change the phosphorylation status of kinetochores. Previous works have described a role for PP2A (specifically the B56 subunit) in the de-phosphorylation process of Aurora B-kinetochore substrates upon BubR1 recruitment (Kruse *et al.*, 2013). PP2A holoenzymes consist of a catalytic subunit (C), a scaffold subunit (A) and a regulatory subunits B (for which exists four different families). B55 and B56 are the most relevant regulatory subunits that play a role in mitosis progression (Kiely and Kiely, 2015). PP2A-B56 has been proved to be involved in different mitotic functions: sister chromatid cohesion, KT-MT attachments and chromosome movements (Kiely and Kiely, 2015). Recently its potential role in SAC silencing has been investigated and it has been shown that it is strategic for the de-phosphorylation of the Knl1 sites involved

in the kinetochore recruitment of Bub1, Bub3 and BubR1 counteracting both kinases. In this way it controls SAC silencing as well as MT-KT attachments (Espert *et al.*, 2014). In mammals is believed that these two phosphatases play a coordinated role: PP2A B56 is responsible for the initial removal of Bub proteins from KTs and then PP1 takes over to finish up the de-phosphorylation process (Espert *et al.*, 2014). Therefore, it is hypothesised a first weak inhibition signal PP2A-B56 mediated that rapidly silences the checkpoint by de-phosphorylation of Knl1 (at this point SAC can still rapidly reactivate if attachments are lost upon re-localisation of Aurora B and subsequent re-phosphorylation of Knl1), and then a complete switch off mediated by PP1 that de-phosphorylates further Knl1, bringing the kinetochore back to the initial status.

The disassembly model

As previously stated, the core complex of the mitotic checkpoint is represented by the MCC complex (Sudakin *et al.*, 2001). Its disassembly is key for SAC silencing. The process is mediated by $p31^{comet}$, a binding partner of C-Mad2 that co-expresses with Mad2 during the cell cycle and it is needed for efficient progression through mitosis (Habu *et al.*, 2002). $p31^{comet}$ recognises the same binding site as O-Mad2 and reduces the interaction between Cdc20 and Mad2 dissociating the MCC complex and preventing its re-formation (Teichner *et al.*, 2011). Such a process requires energy that is provided by the TRIP13 ATPase, a binding partner of $p31^{comet}$, able to mediate the disassembly and the release of Mad2 from the MCC (Eytan *et al.*, 2014). TRIP13 also promotes the release of Cdc20 from BubR1 but the mechanism behind this process is still uncertain (Eytan *et al.*, 2014). During SAC silencing APC15 is activated as well to mediate Cdc20-auto-ubiquitination promoting the disassembly of the MCC complex (Foster and Morgan, 2012). CEUDC2, a mitotic substrate of CDK, can also bind to phospho-Cdc20 promoting Mad2 release and consequent activation of $APC/C^{Cdc20}$ (Gao *et al.*, 2011).

Therefore there are multiple mechanisms that induce SAC silencing; the three models just described are not mutually exclusive but they closely collaborate to drive rapid SAC inactivation and anaphase onset (Wang *et al.*, 2014).

## 1.3 Spindly

The inactivation of the SAC requires interplay of different proteins once bi-orientation has been achieved. Recruitment of the dynein motor is one of the most important steps. In this process there are different proteins involved, such as dynactin, the RZZ complex, Lis1/NudE/NudEL and Spindly (Schroer, 2004) (Starr *et al.*, 1998) (Karess, 2005) (Li *et al.*, 2005) (Griffis *et al.*, 2007).

Spindly was identified in *Drosophila melanogaster (D. mel.)* S2 cells (Spindly) through two RNAi screens, which looked at the mitotic index and at the spreading and morphology of these cells (Griffis *et al.*, 2007). From the interphase screening it was reported an alteration in the normal shape of S2 cells: they were not round but showed spiky and elongated microtubule-rich projections (Griffis *et al.*, 2007). The phenotype registered at mitosis was much stronger. Spindly depleted cells could not progress through mitosis but they arrested in metaphase, retaining Mad2 and Rod on aligned KTs and exhibiting chromosome scattering phenotypes (Griffis *et al.*, 2007) (Gassmann *et al.*, 2010). This phenotype is perfectly in line with defects observed upon depletion of dynein (or inhibition of other previously identified dynein co-factors) (Yang *et al.*, 2007) (Varma *et al.*, 2008). After its initial description in *D.mel.*, homologues of Spindly were identified also in *C. elegans* (SPDL-1) (Gassmann *et al.*, 2008) (Yamamoto *et al.*, 2008), *H. sapiens* (hSpindly) (Griffis *et al.*, 2007) (Chan *et al.*, 2009) and *M. musculus* (mSpindly) (Zhang *et al.*, 2010), with each protein showing equivalent phenotypes when inhibited.

In mitosis, Spindly behaves as a classical KT protein: it localises to kinetochores in prometaphase and then, once attachments have been made, it is transported down the mitotic spindle to the spindle poles (Griffis *et al.*, 2007) (Chan *et al.*, 2009) (Gassmann *et al.*, 2010). The KT-shedding of Spindly was reported to be dynein-dependent;

depletion of the motor protein led to accumulation of Spindly on aligned kinetochores (Griffis *et al.*, 2007) (Chan *et al.*, 2009) (Barisic *et al.*, 2010). These data confirmed the interdependence between Spindly and dynein, a behaviour resembling other SAC components (Howell *et al.*, 2001).

Regarding Spindly recruitment at KTs, immunofluorescence and live imaging experiments have revealed a close relation with the RZZ complex; depletion of this complex was proved to prevent Spindly targeting to KTs, demonstrating the recruitment-dependency of Spindly for the RZZ complex and suggesting to be part of the same complex (Griffis *et al.*, 2007) (Gassmann *et al.*, 2008) (Chan *et al.*, 2009). As registered for RZZ depleted cells, Spindly depleted cells spend more time in mitosis (longer times between nuclear envelope breakdown and anaphase onset) compared to control cells. These cells show great difficulty in aligning their chromosomes, indicating that Spindly, besides its role as a kinetochore-recruitment factor for dynein/dynactin, plays a role in regulating the chromosome alignment process. Normally, indeed, the RZZ complex inhibits chromosome alignment by impairing the Ndc80 binding affinity for 'end-on' interactions; the presence of Spindly helps therefore to relieve this impairment by bridging RZZ with dynein and releasing Ndc80 to generate stable attachments between KTs and MTs (Gassmann *et al.*, 2008). Additionally, inhibition of Spindly expression was reported to regulate the steady state of a component of the RZZ complex, ZW10, controlling its turnover at kinetochores (Barisic *et al.*, 2010). Thus, Spindly functions as an important adaptor between the RZZ complex and the dynein/dynactin motor complex.

The human Spindly (hSpindly) gene encodes for a 605-amino acid protein consisting of two coiled coil domains separated by a short conserved stretch of amino acids, called the 'Spindly box' (251-KGNSLFAEV-260) (important for the recruitment

of dynein/dynactin motor complex at KTs (Gassmann *et al.*, 2010)). The *C*-terminus of Spindly is a highly unstructured and basic domain with a farnesylation site that allows for kinetochore localisation (Moudgil *et al.*, 2015) (Fig. 1.6).

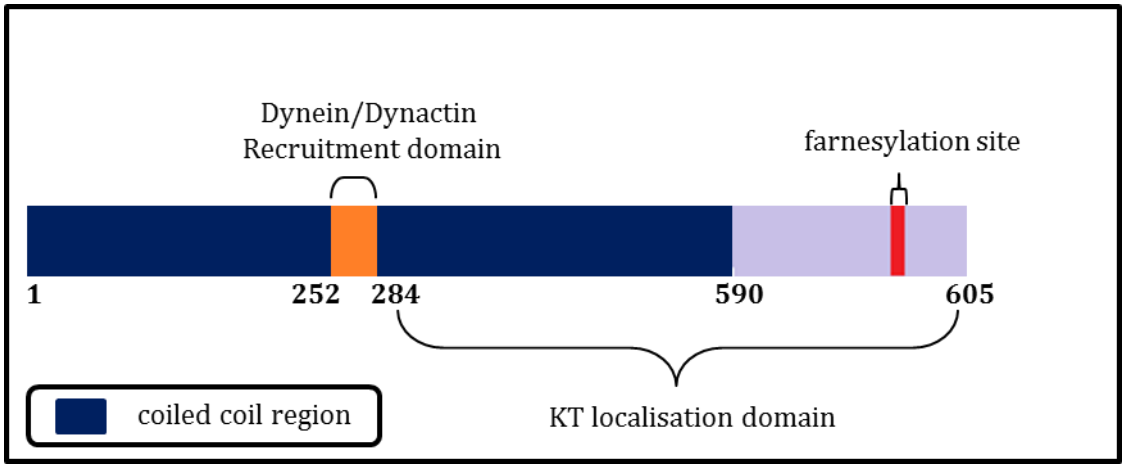


**Figure 1. 6. Schematic representation of human Spindly domains.**

Studies revealed that a single point mutation within the 'Spindly box' region (either a serine or a phenylalanine into alanine: S256A or F258A for human Spindly) forms a protein that can still localise to KTs and promotes chromosome alignment but that cannot recruit the dynein/dynactin motor complex, inhibiting poleward transport of SAC proteins (Gassmann *et al.*, 2010). Curiously, cells exclusively expressing Spindly mutants have high levels of Mad1, Mad2 and CENP-E on aligned KTs, very different from what registered in Spindly-depleted cells, where SAC proteins can leave KTs in a dynein-independent manner. This suggests on one side the presence of a dynein-independent mechanism that allows for removal of SAC components from KTs and that is active only when Spindly does not localise to KTs; on the other side, the previous result indicates that if Spindly is retained at kinetochores the checkpoint is kept active (Chan *et al.*, 2009) (Gassmann *et al.*, 2010).

A further proof of this relationship between Spindly and the SAC activity came from studies conducted from Barisic and co-workers; they showed that expression of Spindly mutant constructs (lacking either the whole 'Spindly-box' or the first 253

amino acid of the protein) blocked SAC inactivation upon microtubule attachment and bi-orientation. Expression of these Spindly mutants also impaired the recruitment of dynein/dynactin at KTs and consequently the streaming of SAC proteins (Barisic *et al.*, 2010).

Recently, Spindly-kinetochore localisation has been deeply analysed; it has been reported that it directly depends on a sequence in the *C*-terminal portion of the protein that contains a variant of the CAAX box (-CPQQ-) needed for farnesylation (Moudgil *et al.*, 2015) (Holland *et al.*, 2015). In the farnesylation modification the *C*-terminal cysteine accepts a farnesyl group becoming more hydrophobic and increasing therefore its binding affinity for plasma membranes and proteins (Zhang and Casey, 1996). Inhibition of farnesylation (by a specific farnesyl transferase inhibitor, FTI) or mutation in the *C*-terminus of Spindly, showed similar reduction of Spindly kinetochore-levels and consequently a decrease in the kinetochore levels of both dynein and dynactin with an additional chromosome misalignment (Holland *et al.*, 2015). This indicates that farnesylation is involved in the interaction between Spindly and the RZZ complex (its kinetochore binding partner); to confirm this, samples pre-treated with a FTI showed reduction in the association between Spindly and ZW10 or Rod (Moudgil *et al.*, 2015). This suggests that farnesylation induces a conformational change in Spindly that promotes the interaction with the RZZ complex. Interestingly, Spindly depletion causes cells to spend much more time in metaphase when compared with FTI-treated cells, suggesting that either there is another way to silence the checkpoint that does not requires the kinetochore localisation of Spindly or that there is a compensatory mechanism that is activated in cells treated with FTI (Holland *et al.*, 2015).

Finally, Spindly has also been studied in meiosis. In mouse oocytes Spindly was shown to have the same kinetochore localisation as in mitosis (aggregating in

prometaphase) and to translocate to microtubules and to the spindle poles upon attachments. Mouse oocytes depleted of Spindly show a similar phenotype to mitotic Spindly-depleted cells, with metaphase stage arrest, indicating that Spindly participates in SAC silencing, chromosome alignment and spindle formation in meiosis as well (Zhang *et al.*, 2010).

## 1.4 Dynein

In eukaryotic cells, transport of cellular components along the cytoskeletal tracks is carried out by motor proteins, myosins, which walk along or slide on actin filaments, and kinesins and dyneins that walk on microtubules (Wickstead and Gull, 2011). Microtubule motors can be distinguished in metazoans since kinesins move towards the plus-ends (generally arrayed at the cell periphery) and dynein moves towards the minus-ends (mostly towards the MTOC). For all of these motor proteins, ATP hydrolysis is fundamental to power movement along their tracks although they have different modes of coupling ATP hydrolysis to stepping (Vale, 2000).

In vertebrates there are nine dynein subfamilies; most of them are axonemal and slide microtubules past each other to generate the beating motion of cilia and flagella, whereas only two are cytoplasmic and transport cargos along microtubules: intraflagellar transport (IFT) dynein or dynein 2, and cytoplasmic dynein or dynein 1 (Allan, 2011). Dynein 2 expression is limited to ciliated cells and within the Golgi apparatus (Mikami *et al.*, 2002); conversely dynein 1 has many different functions for all the minus-end directed transport throughout the cytoplasm in all phases of the cell cycle. Transport of organelles, mRNA and proteins, mitotic spindle orientation, nuclear and cellular migration, and chromosome movements are all dynein-dependent processes (Allan, 2011). The capacity of dynein 1 to carry out all these different functions is surprising and it implies the presence of a tight regulation system to couple the right cargo and to exert the specific function.

Structurally, all forms of dynein consist of the same subunits: two heavy chains (HC), two intermediate chains (IC), two light intermediate chains (LIC) and a variable number of light chains (LC). The motor activity relies on the heavy chain polypeptide that contains 6 AAA ATPase domains arranged into a ring in the *C*-terminus. ATP hydrolysis by AAA1 and AAA3 are needed for motility, while ATP hydrolysis by

AAA2 and AAA4 seems to have regulatory role. Between AAA4 and AAA5 projects outwards the 'stalk', which contains the microtubule-binding site (Burgess *et al.*, 2003). The *N*-terminus domain of dynein mediates homo-dimerisation of the heavy chain and contains the cargo-binding domain (the 'stem'). Within the 'stem' is the linker, a motile element that joins the tail and the AAA1 domain and changes position in response to nucleotide generating force (Burgess *et al.*, 2003). Moreover, the stem interacts with dimers of the accessory non-catalytic subunits that are also important for cargo binding.

The ICs are the largest accessory subunits and mediate interactions with different dynein adaptor proteins, such as the $p150^{Glued}$ (referred to herein as p150) subunit of dynactin and the ZW10 subunit of the RZZ complex allowing association with kinetochores (Vaughan and Vallee, 1995) (Whyte *et al.*, 2008). The LIC1 subunit, instead, interacts with pericentrin, facilitating dynein binding with centrosomes (Tynan *et al.*, 2000). Lastly, there are three classes of LCs that mediate binding with transmembrane receptors, ion channels and viruses (Allan, 2011)).

#### *1.4.1.1 Dynein Processivity*

Motor processivity is defined by the number of steps the motor can take before detaching from the microtubule. Yeast cytoplasmic dynein has been described as processive on its own, with a run length of 1/2 μm, whereas mammalian cytoplasmic dynein can produce movements only when attached to a solid surface (Reck-Peterson *et al.*, 2006) (Toba *et al.*, 2006). Over the years it was discovered that different species of dynein can travel at different velocities: yeast dynein is much slower than *Dyctyostelium* dynein and metazoan dynein and they show irregular stepping behaviour (Reck-Peterson *et al.*, 2006) (Nishiura *et al.*, 2004) (Trokter *et al.*, 2012). It is possible to record not only 8 nm forward steps (the typical step size of kinesins), but also backward and lateral stepping (Reck-Peterson *et al.*, 2006) with mammalian dynein

showing even higher variability in the stepping size (from 8 to 32 nm) (Toba *et al.*, 2006). Dynein processivity requires not only intact linkers and dimerisation (Reck-Peterson *et al.*, 2006) but also purified dynactin, which has been shown to double the processivity of the motor (King *et al.*, 2003) (Culver-Hanlon *et al.*, 2006). Although, dynactin is a crucial activator of motor processivity, it has a weak affinity for dynein, suggesting the presence of another layer of regulation (King *et al.*, 2003) (McKenney *et al.*, 2014). It has been shown that dynein can engage different partners to modulate its functions, in terms of both processivity and cargo-specificity (Kardon and Vale, 2009) (McKenney *et al.*, 2014) (Fig. 1.7).

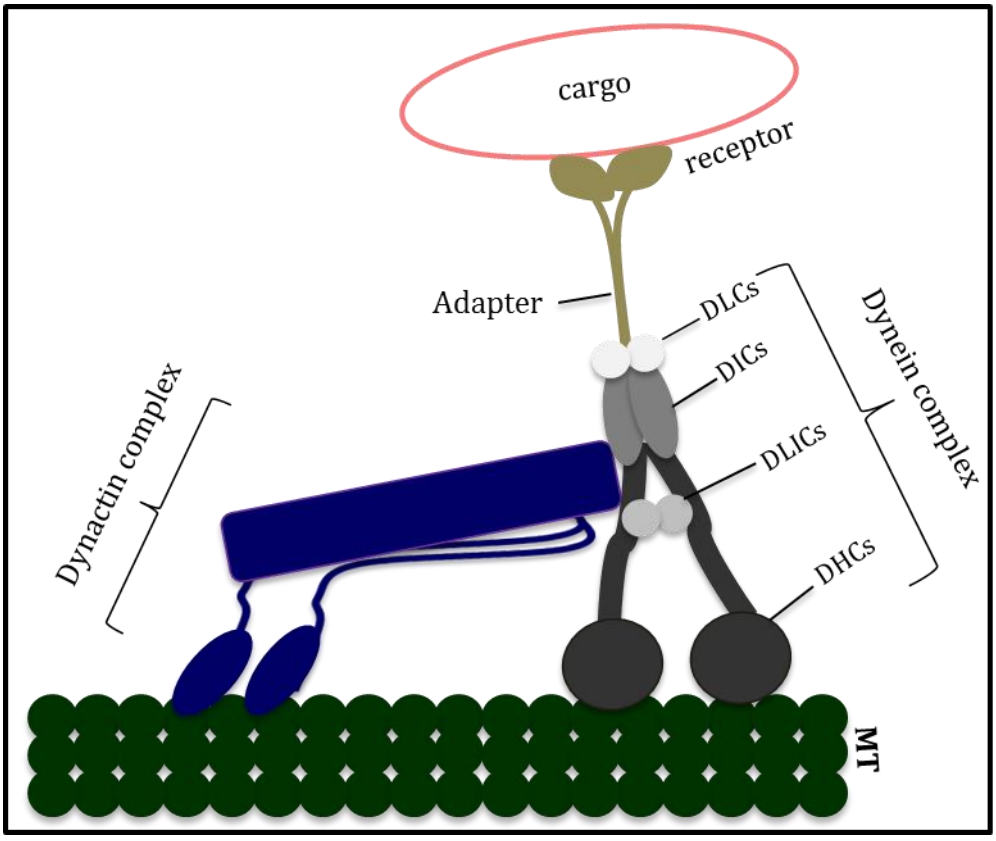


**Figure 1. 7. Cartoon of the tripartite-dynein motor complex.**
Dynein is not processive on its own; it requires interaction with adapter molecules (such as BicD2 or Spindly) and the dynactin complex. The adaptors mediate the link with the cargo, while dynactin enhance the microtubule binding. DHC: dynein heavy chain; DLIC: dynein light intermediate chain; DIC: dynein intermediate chain; DLC: dynein light chain.

### *1.4.1.2 Dynein regulatory factors*

The way in which dynein interacts with the innumerable cargos that it can transport towards the microtubule minus-end has not been properly elucidated yet. Only with complex regulation of processivity and targeting can dynein move the many specific cargos and execute all of the functions for which it is responsible. One hypothesis is that the specificity is defined by expressing splice variants of the different subunits of dynein; expression of different isoforms of ICs or LICs mediates association with different proteins (Kuta *et al.*, 2010). Additionally, binding different dynein adaptors allows loading of diverse cargos and execution of different functions (Kardon and Vale, 2009). The key adaptors of dynein are discussed in more details in the next paragraphs.

Dynactin

Dynactin is itself a multi-subunit complex shown to be involved in most, if not all, dynein activities (Schroer, 2004). It was reported as crucial for enhancing the processivity of the motor via its p150 subunit that interacts with the IC of dynein (King and Schroer, 2000) (Echeverri *et al.*, 1996). The p150 subunit binds to microtubules via the CAP-Gly (cytoskeleton-associated protein glycine rich) domain (Culver-Hanlon *et al.*, 2006), and it also associates with microtubule plus-end proteins, like EB1 (ending binding 1) and CLIP170 (CAP-Gly domain-containing linker protein 170) (Duellberg *et al.*, 2014). The microtubule plus-end binding seems to be related with the cargo loading and initiation of transport (Vaughan *et al.*, 2002). However, alterations in the microtubule binding site of dynactin do not affect the processivity of the motor (Kim *et al.*, 2007). To date, many studies have shown that the association between dynein and dynactin is not sufficient to activate motor processivity and cargo transport (Schlager *et al.*, 2014) (Zhang *et al.*, 2011). BicD, Spindly, Rab11-FIP3 and Hook3 have been

identified as important additional players in the activation of the processivity in the presence of the dynein/dynactin complex (McKenney *et al.*, 2014).

The p150 subunit links dynein to GTPases that mediate the trafficking from the endoplasmic reticulum (ER) to the Golgi apparatus: it interacts with the Rab-interacting lysosomal protein (RILP), a RAB7 GTPase associated with late endosomes (Johansson *et al.*, 2007). Other subunits of dynactin are likewise involved in the cargo-linking process: the p50/dynamitin subunit associates with Bicaudal D for intracellular trafficking and the ARP1 subunit associates with βIII spectrin, a protein found on cytosolic surface of the Golgi apparatus and on other cellular membranes (Hoogenraad *et al.*, 2001) (Holleran *et al.*, 2001).

Bicaudal D

Bicaudal D (BicD in flies or Bicaudal D1/D2 in mammals (BicD1/2)) has been widely described for its role for dynein-mediated transport, specifically for mRNA localisation in flies and for Golgi-vesicle transport in mammalian cells (Swan and Suter, 1996) (Hoogenraad *et al.*, 2001). Moreover, BicD functions in nuclear positioning via interaction with the nucleoporin RanBP2 in mammals, in lipid droplet transport and microtubule organisation in association with dynein (Splinter *et al.*, 2010) (Larsen *et al.*, 2008) (Fumoto *et al.*, 2006).

The interaction with the dynein/dynactin motor complex occurs at the *N*-terminus of the coiled coil of BicD and it dramatically increases the processivity of the motor (Urnavicius *et al.*, 2015) (Schlager *et al.*, 2014) (McKenney *et al.*, 2014); the *C*-terminus coiled coil instead mediates the interaction with specific cargos (Hoogenraad *et al.*, 2003). Interestingly it has been demonstrated that overexpression of BICD2-N (BICD2 *N*-terminus) prevents both the dynein cargo-binding and the MT association, suggesting that interaction with cargos is needed to induce a conformational change that

activates the triple complex (BICD2N-dynein-dynactin) and allows for MT binding to occur (Splinter *et al.*, 2012).

Lis1

Lis1 was identified as the target of sporadic mutations causing human type I lissencephaly, a brain developmental disease resulting from defects in neuronal division and migration (Reiner *et al.*, 1993). Subsequently, Lis1 has been shown to localise in non-neuronal cells as a regulator of cytoplasmic dynein, being required for several dynein-dependent processes, such as mitotic spindle orientation, kinetochore activity, centrosome positioning, and mRNA and organelle transport (Smith *et al.*, 2000) (Faulkner *et al.*, 2000) (Kardon and Vale, 2009). Lis1 interferes with the coupling between ATPase activity and microtubule binding of dynein (Huang *et al.*, 2012). When Lis1 is bound to dynein, the motor stays attached to microtubules even upon several ATP hydrolysis cycles (Huang *et al.*, 2012). Alterations of Lis1 expression lead to massive defects in the functions of dynein at KTs: it delays anaphase onset and interferes with chromosome congression to the metaphase plate. Moreover, overexpression of Lis1 displaces dynactin from MT plus-ends in interphase cells (Faulkner *et al.*, 2000).

Lis1 can work on its own or in close collaboration with NudE (or NudEL), which promotes the tight binding of Lis1 to dynein mediating the force generation process (Efimov and Morris, 2000) (McKenney *et al.*, 2010). The Lis1/NudE/NudEL complex is required to target dynein to the microtubule plus-ends and is involved in many dynein-mediated activities such as cell migration, targeting of dynein onto cortical microtubules and correct functioning of the mitotic spindle (Dujardin *et al.*, 2003) (Lee *et al.*, 2003) (Faulkner *et al.*, 2000).

It is still unclear whether Lis1 associates with dynein on moving cargo *in vivo*.

NudE/NudEL

Besides their role in association with Lis1, NudE and NudEL are also needed for several other activities of dynein on their own associating with the motor via three binding sites (Liang *et al.*, 2004) (McKenney *et al.*, 2011). NudE/NudEL localise at centrosomes and at kinetochores (Feng *et al.*, 2000) (Stehman *et al.*, 2007), where they arrive earlier than dynein, Lis1 and dynactin, and their inhibition prevents dynein localisation and arrests cells in metaphase (Stehman *et al.*, 2007). NudE does not interact with dynactin, suggesting that NudE/NudEL play a primary role in kinetochore assembly and microtubule attachment functions of dynein, while the dynein pool that interacts with dynactin appears to be mainly responsible for mediating the SAC stripping function (Stehman *et al.*, 2007).

Outside mitosis, NudE and NudEL are further implicated in mediating dynein binding to cellular membranes for organelle positioning; depletion of either NudE or NudEL generates loss of dynein from those membranes (Lam *et al.*, 2010).

The RZZ complex

The RZZ complex is made up of three different proteins: Rod, Zwilch and ZW10 (Karess, 2005). It has been reported as a main player in the recruitment of the dynein/dynactin complex to kinetochores (Starr *et al.*, 1998) (Whyte *et al.*, 2008); it can physically link dynein to KTs and induce dynein-mediated kinetochore-movements (Varma *et al.*, 2013). ZW10 (or Zeste white 10) binds to the motor complex directly, upon phosphorylation of the IC of dynein, and indirectly, through interaction with the p50 (/dynamitin) subunit of dynactin (Starr *et al.*, 1998) (Whyte *et al.*, 2008). The RZZ complex is important for two kinetochore functions mediated by dynein: chromosomes alignment and silencing of the SAC signalling. Both functions rely upon the recruitment of Spindly, a binding partner of the complex in mitosis. By promoting the association of

the dynein/dynactin motor complex to KTs, the RZZ complex induces its own removal, together with the SAC proteins, stimulating the inactivation of the checkpoint (Howell *et al.*, 2001) (Karess, 2005). This process of removal allows also the stabilisation of stable 'end-on' attachments since it increases the binding affinity of Ndc80 for MTs by relieving the inhibition due to the presence of RZZ at KT (Barisic and Geley, 2011). However, RZZ and dynein/dynactin have different dwell times at KTs; RZZ exchanges on and off of kinetochores much slower than the motor (Famulski *et al.*, 2008).

Besides the role in mitosis, ZW10 plays an alternative role in a dynein-mediated process in interphase. It localises to the Golgi apparatus and it promotes dynein-association with it inducing minus-end-directed movements of the Golgi itself, endosomes and lysosomes (Hirose *et al.*, 2004) (Varma *et al.*, 2006) (Civril *et al.*, 2010).

Spindly

Spindly has been widely described as a dynein co-factor at kinetochores during mitosis (Griffis *et al.*, 2007) (Gassmann *et al.*, 2008) (Chan *et al.*, 2009; Cheerambathur *et al.*, 2013; Holland *et al.*, 2015). It has been reviewed earlier in this chapter (see paragraph **1.3**), so it will not be analysed again in this paragraph.

## 1.5 Mitotic proteins in interphase

Over the years researchers have widely demonstrated that many proteins are able to play alternative roles in several pathways different from those where they were initially identified. It is believed that proteins have evolved to carry out second/additional function(s) that can differ according to cell cycle state, cellular localisation, cell type, oligomeric state or different proportion of a ligand/substrate ratio. There could be several inputs that work together to switch a protein function. Jeffery denominated those proteins with multiple roles as 'moonlighting protein' in 1999 (Jeffery, 1999).

To date have been identified several mitotic proteins that are able to play additional roles in interphase.

Dynein is an important "moonlighting protein". It can mediate a wide range of functions, including virus transport, mitotic division, cell migration, lysosome and late endosomes transport and nuclear migration (Vallee *et al.*, 2012). Dynein can interact with many regulatory factors (some of them already described) that seem to facilitate its capacity to play several functions and to load different cargos according to the phase of the cycle the cell is in and to the cellular compartment where dynein is expressed (Kardon and Vale, 2009). As already stated there are numerous dynein interactors that could mediate the linking to cargos suggesting the presence of potential diverse cargo recruitment mechanisms (Akhmanova and Hammer, 2010). This fine regulation of dynein depicts it as maybe the best "moonlighting protein" identified to date. In this context, different dynein adaptors have been proved to behave as "multifunctional" proteins on their selves. For instance, Lis1 plays a role in brain development (Reiner *et al.*, 1993) as well as in cell division, cell migration and nuclear migration (Faulkner *et al.*, 2000) (Smith *et al.*, 2000) (Dujardin *et al.*, 2003)

NudEL, a close binding partner of Lis1 and dynein implied in regulation of some dynein/Lis1-mediated functions, is also described playing a role in organelles

trafficking. It interacts with ER/Golgi membrane, synaptosomal membrane and synaptic vesicle and it possesses a Lis1-binding site and a dynein-binding site that have to be intact to allow proper functioning of the protein and correct mediation of the motor activity. Mutations on one or both of these binding sites generate fragmentations/dispersions of the Golgi cisternae, lysosomes and endosomes (Liang *et al.*, 2004).

Furthermore, ZW10, a component of the RZZ complex originally identified as a *D. mel.* mutant involved in kinetochore function (Chan *et al.*, 2000), is involved in membrane trafficking between the ER and the Golgi apparatus, being associated with ER membranes via an interphase specific interaction with RINT-1(Hirose et al., 2004). These proteins, associated with a third one called NAG, make up the NRZ complex (NAG/RINT-1/ZW10) that is associated to the ER through the ER SNAP-receptors syntaxin 18 and BNIP1 (Civril *et al.*, 2010). ZW10 was shown also interacting with the Golgi apparatus as a consequence of its movements to the minus-end of microtubules, in association with dynactin through which it could be assisting dynein-mediated endocytosis (Starr *et al.*, 1998) (Varma *et al.*, 2006). Furthermore, ZW10 was recorded to localise at the leading edge of migrating cells potentially involved, also in this case, in the recruitment of dynein at the cortex of lamellipodia (Varma *et al.*, 2006).

Zwint, an important kinetochore protein in mitosis, has been described as a player in membrane trafficking as well via its interaction with Rab3c (van Vlijmen *et al.*, 2008).

Mad1, an important SAC molecular player, possesses also an alternative role in interphase, binding to the Golgi apparatus and co-localising with Rab6A in both *trans*-Golgi network and endosomes (Wan *et al.*, 2014). Moreover, Mad1 depletion was

shown to decrease the migratory capacity of cells: indeed, the presence of Mad1 at the Golgi apparatus promotes α5-integrin secretion that in turn stimulates cellular adhesion, spreading and motility, which ties the interphase localisation and functioning of Mad1 to cell migration (Wan *et al.*, 2014). For this interphase function Mad1 does not require Mad2 interaction; conversely, for its interphase localisation at the nuclear pore complex, it strictly depends on Mad2 presence, even though their function in that context has not been elucidated yet (Campbell *et al.*, 2001).

## 1.6 Cell migration

An important process regulated by the cytoskeleton network in cells is represented by migration, a vital mechanism in many biological contexts, in both normal physiology as well as in pathological conditions. It is central for tissue development during embryogenesis, but also for wound healing, tumour metastasis and inflammatory responses (Lauffenburger and Horwitz, 1996). The activation of this process requires specific signals, represented by growth factors, chemokines or extracellular matrix molecules, which activate specific receptors and signalling cascades (Fig. 1.8) (Ridley *et al.*, 2003).

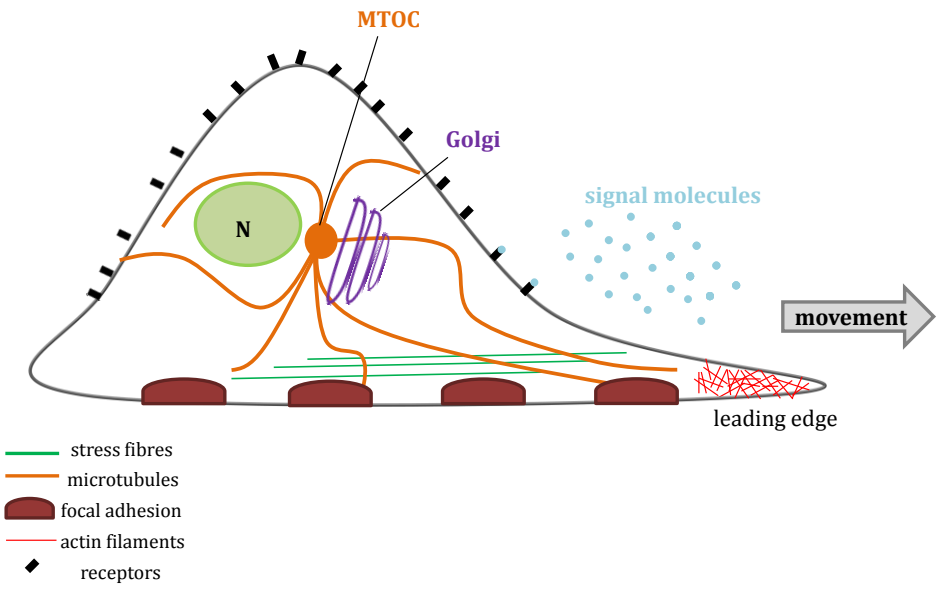


**Figure 1. 8. Schematic representation of a migrating cell.**
Signal molecules bind to receptors and promote cell polarisation with subsequent activation of Rho GTPases and formation of protrusions (leading edge) towards the direction of migration and adhesions with ECM and surrounding cells. N: nucleus.

### 1.6.1 Cell polarisation and protrusions formation

To migrate, cells must polarise defining a protruding front (the side closest to the direction of migration) and a retracting rear (opposite side to the front) to promote translocation of the cell body. Polarisation is often dictated by the extracellular

environment and it requires modifications in the actin cytoskeleton distribution and asymmetric activation of cell-membrane receptors. The assembly and polymerisation of actin at the cell front stimulates the extension of flat membrane protrusions to initiate the migration cycle. Actin dynamically polymerises to generate filaments that represent the basal structure for cell movement; polymerisation occurs at the plus end and is usually correlated with the disassembly at the minus end (Alberts *et al.*, 2007). The process is divided in three phases: nucleation (three actin monomers generally interact), elongation (monomers are rapidly added to the filament at the plus (or barbed) end) and steady state (monomers disassembly from the minus end and at the same time polymerisation is maintained at the plus end by monomers present in the cytosol) (Alberts *et al.*, 2007).

There are different types of protrusion according to the organisation of actin filaments (Yamaguchi and Condeelis, 2007) (Krause and Gautreau, 2014) (Ridley, 2015):

- Lamellipodia: broad, flat protrusions at the leading edge that contain a branched network of actin filaments and elongate when cells migrate along the extracellular matrix; these protrusions require Rac GTPase activation for actin polymerisation and Integrin-mediated adhesion that also maintains Rac GTPase activity in a positive feedback loop. Lamellipodia are transient structures that protrude and retract.
- Filopodia: thin finger-like protrusions that extend from the cellular membrane and are made of long, unbranched actin bundles. Filopodia can support residual slow migration in the absence of lamellipodia and they consent the cell to probe the surrounding environment. Cdc42 is the best GTPase involved in filopodia formation, acting through formins to stimulate actin polymerisation (Kuhn and Geyer, 2014).
- Invadopodia: often generated in cancer cell migration and specialised to invade through the basement membrane by releasing several molecules and most importantly matrix

metalloproteases that allow for degradation of the ECM. Rho GTPases are well studied to play a role in invadopodia formation: Cdc42 has been reported to act through N-WASP for this process as well as other Cdc42 GEFs proteins (Beaty and Condeelis, 2014).

- Podosomes: conical, actin rich structures localised at the substrate-attached part of the cell that present an F-actin-rich core surrounded by a ring structure characterised by adhesion and scaffolding protein. These protrusions are highly dynamic and actively engaged in matrix remodelling and tissue invasion.
- Blebs: outward bulges in the plasma membrane driven by hydrostatic pressure from inside the cell. In this case the actin-Myosin cytoskeleton is involved: while Myosin 2 generates contraction, providing the contractility necessary for the extension of the blebs, actin assembly provides them stability. To activate this type of migration cells need to upregulate the RhoA/ROCK pathway (Sanz-Moreno *et al.*, 2008).

Several proteins regulate the rate and organisation of actin polymerisation in protrusions by affecting the pool of available monomers and free ends. The Arp2/3 complex, for example, is expressed in lamellipodia where it binds to the side of an existing actin filament promoting the branching of a new filament by stimulating actin nucleation via activation of the Wiskott-Aldrich syndrome family proteins (WASP, N-WASP, WAVE and WASH proteins) (Skoble *et al.*, 2000). This family of proteins mediate the interaction between Arp2/3 and the actin so to constitute the nucleation core (Pollard, 2007). Many other actin-nucleating proteins are involved in this process, regulating the rate and the organisation of actin polymerisation and orchestrating the availability of actin monomers and free ends and controlling the architecture of the leading edge (dos Remedios *et al.*, 2003). Spire for instance binds to the rear-facing pointed ends of filaments and prevents depolymerisation of actin (Quinlan *et al.*, 2005);

Formins instead, bound to the rapidly growing barbed end of nascent actin filaments, mediate nucleation of linear unbranched actin filaments, leading to the formation of actin cables, filopodia or stress fibres (Goode and Eck, 2007).

### 1.6.2 Focal adhesions

Protrusions are stabilised by interactions with adjacent cells or with the extracellular matrix (ECM) (Le Clainche and Carlier, 2008). Interactions with the ECM, a complex network of polysaccharides (such as glycosaminoglycan or cellulose) and proteins (such as collagen and fibronectin) secreted by cells, are mediated by Integrins, migration-promoting receptors that recognise particular motifs in the ECM component fibronectin and support both adhesion and intracellular signalling. Integrins form clusters, or 'focal complexes', which recruit focal adhesion kinase (FAK), Rho and Myosin 2 to allow assembly of actin and generation of traction forces on filaments (by mediating association with structural proteins such as Vinculin, α-actinin, Paxillin and Talin (Kanchanawong *et al.*, 2010)) and at the same time the maturation of a 'focal complex' into a 'focal adhesion' (Miyamoto *et al.*, 1995).

Movements rely on traction forces generation upon connection between actin stress fibres and the ECM. Focal adhesion sites in this context act as molecular clutch that tethers to the ECM and impedes the retrograde movement of actin, allowing for generation of traction forces at the site of adhesion. However proper movement requires not only constant formation of focal adhesion sites but also their disassembly at the rear, to promote retraction of the cell tail and detachment to allow forward movement of the cell body (Crowley and Horwitz, 1995).

Adhesions close to the leading edge normally are highly dynamic and rapidly form and turn over (Webb *et al.*, 2002). This process is mediated by reorganisation of actin filaments and recruitment of several molecules, such as FAK, Src and calpain; also

microtubules play a role by modulating their contraction forces (Webb *et al.*, 2002) (Ren *et al.*, 2000). The probability that a nascent adhesion in the lamellipodium matures, rather than disassembles, seems to depend on the level of active Myosin 2, which is involved in their elongation and growth by mediation of actin bundling process (Choi *et al.*, 2008). The role of Myosin 2 as a regulator of protrusion is related with its capacity to generate forces on adhesions without interacting with them but by attaching to the actin bundles with which adhesions are associated (Vicente-Manzanares *et al.*, 2007). Indeed, increased levels of active Myosin 2 results in large actin bundles and stable adhesions, leading to decrease of signalling to Rac GTPase at the front of the cell and protrusion formation. On the other side, low levels of active Myosin 2 lead to less actin bundling and increased protrusion formation (Vicente-Manzanares *et al.*, 2009). The recruitment of Myosin 2 is itself related with the stretch of actin filaments; at the rear of the cell, actin filaments interact with the intracellular portion of focal adhesions resulting in being more stretched compared with those at the front of the cell that instead interact with the plasma membrane. This results in higher levels of Myosin 2 associated with filaments at the rear of the migrating cell, generating an unequal distribution of tension (Chi *et al.*, 2014). Myosin 2 is activated upon phosphorylation of the regulatory light chain (RLC) that increases its activity in the presence of actin. Phosphorylation is mainly dependent on two kinases: the Rho kinase (ROCK), activated by Rho GTPase, and the Myosin light chain kinase (MLCK) that regulates the activity of Myosin 2 and actin, driving cell contractility (Etienne-Manneville and Hall, 2002) (Riento and Ridley, 2003). Rho/ROCK signalling mediates the retraction of the trailing edge of cells and it has been implicated in adhesion disassembly during cell detachment; indeed inhibition of ROCK or MLCK induces an elongated morphology with impaired rear-end detachment (Worthylake *et al.*, 2001). Eventually, this process is inactivated by the Myosin phosphatase that mediates the de-phosphorylation process.

### 1.6.3 Rho GTPases

Key regulators of cell shape changes and protrusion formation are proteins from the Rho family of small guanosine triphosphate (GTP)-binding proteins (GTPases), like Rac, Rho and Cdc42. Such proteins are active only when bound to GTP and in this conformation they can activate the downstream pathways. In their inactive state, so when they are bound to GDP, Rho GTPases are free in the cytoplasm and associate to the guanine nucleotide displacement inhibitor (GDI); growth factors can then bind and activate their receptors to turn on specific membrane-bound regulatory proteins called guanine nucleotide exchange factors (GEFs) to activate Rho proteins at the membrane by releasing them from GDI and promoting the exchange of GDP for GTP (Ridley, 2015). The GTP-bound Rho protein can in turn associate with the plasma membrane and bind downstream effector proteins to initiate the biological response. Therefore, according to the amount of small G proteins active the expression of Rho GTPases can be locally regulated in different regions of the cell.

Rac is generally active at the front of the cell where it stimulates formation of protrusions regulating actin polymerisation and branching of actin filaments by inducing the activation of Arp2/3 complex by WAVE family proteins. Rac also inhibits the disassembly of actin filaments by inactivation of actin depolymerising factors, such as ADF/Cofilin (Hall, 1998).

Rho is required to regulate the contraction and retraction forces in the cell body and at the rear; at these regions it is also needed for maturation of existing contacts (Raftopoulou and Hall, 2004). Rho is involved in the bundling process that involve actin and Myosin 2 in order to generate contractile actin-myosin bundles, like stress fibres, and to make up new focal adhesion sites through the activation of the Formin Diaphanous (Dia) and ROCK.

Rho and Rac also interplay with each other by antagonising each other to maintain cells polarity by preventing the formation of Rac-mediated protrusion in sites that are not the front of the cell (Raftopoulou and Hall, 2004).

Important in cell migration is also the Rho GTPase Cdc42, active at the front of the cell, that, together with dynein, mediates the re-localisation of the MTOC and of the Golgi apparatus in front of the nucleus towards the leading edge to polarise cell migration and guide vesicle transport towards the leading edge (Palazzo *et al.*, 2001) (Magdalena *et al.*, 2003). Additionally, Cdc42 is required for polymerisation of F-actin during protrusion formation by activation of the Arp2/3 complex through WASP family proteins (Hall, 1998) (Etienne-Manneville and Hall, 2002).

### 1.6.4 Microtubules in cell migration

Microtubules are also involved in establishing polarity and re-orienting the MTOC and therefore are essential for cell migration (Watanabe *et al.*, 2005).

Depolymerisation of microtubules promotes formation of focal adhesions whereas their polymerisation induces lamellipodia formation. The assembly state of microtubules is directly related with cell migration since it can modulate the activity of Rho GTPases: at the leading edge of fibroblasts the concentration of RhoA is increased upon MT depolymerisation (Ren *et al.*, 1999), while instead MT polymerisation activates Rac1 (Waterman-Storer *et al.*, 1999). Many microtubule associating proteins (MAPs) are implicated in microtubule stabilisation at the leading edge, tethering microtubules to actin filaments and crosslinking these two cytoskeleton structures (Rodriguez *et al.*, 2003). For instance, CLIP170 plays a role in cell polarity by associating with IQGAP, an actin-binding protein that binds on one side with Rac and Cdc42 and on the other side with CLIP170 behaving as a cross-linker (Fukata *et al.*, 2002). MACF 1/Spectraplakin also mediates this cross-interaction since it co-localises

with and binds to microtubules and actin cytoskeleton (Leung *et al.*, 1999). Cytoplasmic dynein and dynactin seem to play a similar function; they co-localise with F-actin at the leading edge of fibroblasts and participate in MTOC re-distribution for cell polarisation; defects in dynein expression interferes with directed cell movements and with centrosome re-organisation (Etienne-Manneville, 2001) (Palazzo *et al.*, 2001) (Dujardin *et al.*, 2003).

Actin filaments and microtubules can associate to one another *in vivo* affecting their organisation and dynamics. A retrograde flux of actin filaments (toward the cell centre) generates a backward force on microtubules that actively pushes them away from the direction of migration (Salmon *et al.*, 2002). Dynein and other cross-linkers can either resist this retrograde flow to link the actin network and MTs to the leading edge or they can act as a membrane anchor for MTs to allow the invasion of the actin network at the front of the cell (Salmon *et al.*, 2002).

Microtubules interact with focal adhesions as well promoting their turnover (Kaverina *et al.*, 1998).

Hence, microtubules influence cell motility by controlling actin assembly, adhesion turnover and cell polarity; many different factors are involved in this crosstalk that is critical to allow communication and interplay between these two cytoskeleton networks generating also cooperatives effects and feedback loops that stimulate both sides (Etienne-Manneville, 2013).

### 1.6.5 Vesicle transport

As stated earlier, cell migration requires polarisation of the cell, a process that allows identifying a leading edge and a trailing end. For this, a plethora of proteins have to be spatially segregated and confined within the cell. The intracellular localisation of proteins that are membrane associated - either due to a membrane anchor or via binding of a membrane-associated protein - depends predominantly on vesicular trafficking.

Therefore cells possess an active 'polarysed' endo-exocytic process that mediates the targeting of such proteins, for instance Integrins, to specific regions of the cell surface (Maritzen *et al.*, 2015). Many studies indicate an increase in the rate of internalisation of endocytosis at the leading edge of migrating cells; receptors are internalised into early endosomes and then either targeted for degradation or recycled to the plasma membrane (Jones *et al.*, 2006). The major route for internalisation is through clathrin-mediated endocytosis, which is initiated upon chemokine binding to the receptor and its subsequent phosphorylation. Once internalised, these receptors can either proceed to late endosomes/lysosomes to be degraded or can dissociate from the ligand and enter the recycling compartment to traffic back to the plasma membrane.

Small GTPases of the Rab family are responsible for the regulation of the intracellular trafficking steps; importantly they undergo post-translational modification by isoprenylation, generating hydrophobic moieties that facilitate membrane association. Rabs are inactive when bound to GDP and in this state are distributed to the cytosol complexing with GDI that interacts with the isoprenylated *C*-terminus of the Rabs and blocks their dissociation from GDP. Subsequently, once on appropriate membrane, the GEFs promote the exchange of GDP to GTP activating the Rab that in turn recruits downstream 'effector' proteins, such as tethering factors, kinases, phosphatases, scaffold proteins and actin/microtubule-based motor proteins (Somsel Rodman and Wandinger-Ness, 2000). An example of a crucial endocytic trafficking for cell migration is represented by the internalisation of Integrins. This process is triggered by the removal of active, GTP-bound, Rac from the membrane, which leads to turning off of Rac and of the protrusive activity of cells (del Pozo *et al.*, 2004). The Integrin-trafficking can occur via two potential pathways: one under the control of Rab4 GTPase (called 'short-loop') and one under the control of Rab11 GTPase (called 'long-loop') (Maritzen *et al.*, 2015). The 'long loop' is characterised by endosomes that pass through

the perinuclear recycling compartment before reaching the plasma membrane and it is mediated as well by the ARF subfamily of GTPases that also control the actin cytoskeleton, integrating vesicular transport with actin polymerisation (Jones *et al.*, 2006). As well as Integrins, also other cell surface adhesions proteins are recycled from the plasma membrane by endocytosis regulating the cell migration process (like syndecans or E-cadherin) (Jacquemet *et al.*, 2013).

An interesting feature of Rabs is their capacity to regulate microtubules motors and their capacity to attach membranous cargo to the microtubule cytoskeleton. For example, Rab14 was demonstrated to interact with KIF16B (kinesin-3 subunit) regulating in this way Golgi-to-endosome trafficking of the FGFR (fibroblast growth factor receptor). Although Rabs can associate directly with kinesin motor proteins, often they can bind to adaptor proteins first and only subsequently to different kinesin complexes. Moreover, some Rabs can interact with multiple kinesins and regulate distinct trafficking processes: for example Rab6 associates with kinesin-1 and 3 via BICD and BICDR-1 (BICD-related protein 1) respectively regulating trafficking processes (Grigoriev *et al.*, 2007).

On the other side, Rab GTPases can interact with the minus end microtubule-based motor protein dynein as well, directing a wide range of intracellular trafficking steps. Rab7, for instance, associates with dynein through the binding of RILP (Rab interacting lysosomal protein) to dynactin (p150) to control endosomal transport (Jordens *et al.*, 2001) Rab11A interacts with dynein light chain subunits controlling the endosomes sorting process (Horgan *et al.*, 2010). Also Rab6, already shown to interact with kinesin, can associate with dynein as well via binding dynactin (p150 and p50 subunits) and regulating in this way the trafficking steps in the biosynthetic pathway (Hoogenraad *et al.*, 2001).

## 1.7 Aims and objectives

Since its discovery Spindly has been described as an important mitotic player, in close relation with the dynein/dynactin motor complex and with the spindle assembly checkpoint (SAC). Previous studies have clearly shown that the silencing of the SAC requires the recruitment of the dynein/dynactin motor complex onto kinetochores and that this loading is highly dependent on Spindly presence (Griffis *et al.*, 2007) (Gassmann *et al.*, 2008) (Chan *et al.*, 2009).

Even though this model is widely accepted, direct interaction between Spindly and dynein/dynactin has been inadequately studied and the function of Spindly in the SAC has not been fully addressed. Paradoxically it has been demonstrated that Spindly-depleted cells can somehow remove SAC components from kinetochores without recruiting dynein/dynactin, while the presence of Spindly mutants on attached kinetochores prevents SAC silencing, suggesting a much more direct role for Spindly in SAC activation/maintenance (Gassmann *et al.*, 2010).

This thesis aims to closely dissect the interaction between Spindly and the dynein/dynactin motor complex and to understand the contribution of Spindly within the spindle assembly checkpoint pathway.

Additionally, to date, little is known regarding human Spindly outside mitosis either on its own or in relation with other proteins/cellular activities. Previously it was shown that depletion of *Drosophila* Spindly can generate defects in cytoskeletal organisation (Griffis *et al.*, 2007). Therefore, this work seeks to unravel the role of Spindly in interphase, with a close look at its function in relation to cytoskeleton (and cell migration).

It is true that many proteins have been shown to play two or more additional functions within a cell beside the one for which they were initially described; so with this thesis we plan to understand whether this is the case for Spindly, believing that it

could represent a versatile scaffold protein able to bring together multiple complexes in different biochemical processes.

# 2 . Material and methods

## 2.1 Cell lines and growth conditions

Human embryonic kidney cells HEK293 (kindly gifted by Prof. D. R. Alessi, University of Dundee), human osteosarcoma U2OS cells (kindly gifted by Dr. S. Rocha, University of Dundee) human cervix carcinoma cells HeLa (ATCC), human keratinocyte cells HaCaT (kindly gifted by Dr. L. Unterholzner, University of Dundee), mouse embryonic fibroblast (MEF) cells (kindly gifted by Dr. V. Cowling, University of Dundee) and human foreskin fibroblast (FB) cells (kindly gifted by prof. A. Huebner, Dresden) were maintained in Opti-MEM (Gibco) supplemented with 10% heat-inactivated fetal bovine serum (HI-FBS) (Gibco), 1% Penicillin, Streptomycin and Glutamine (Gibco) for no more than 30 passages.

Cell lines were grown at 37°C with 5% $CO_2$ in a humidified incubator.

When the experiment required mitotic enrichment, cells were treated with the indicated drug for the specified period of time before being collected

## 2.2 Generation of stable cell lines

U2OS cells with an integrated FRT site and a Tet Repressor (kindly gifted by Prof. A. Lamond, University of Dundee), were kept in medium with Zeocin (100µg/mL; Invitrogen) and Blasticidin (15µg/mL; Calbiochem). 48 hours prior to transfection, Zeocin and Blasticidin were removed from the culture medium. The pOG44 vector (a kind gift from Prof. J. R. Swedlow, University of Dundee) and the wild type or the mutant (F258A and S256A) version of the pCDNA5/FRT/TO LAP-Spindly constructs (Gassmann *et al.*, 2010) were co-transfected in a ratio of 9:1 pOG44: pgLAP vector into U2OS cells. After 48 hours from transfection stable integrating cell lines were drug selected by using 150 µg/mL of Hygromycin (Calbiochem) and 15 µg/mL of Blasticidin, and clonally isolated (see **Chapter 7**. Appendix- Fig. 7.1).

Similarly, human cervical carcinoma cells (HeLa) with the same integrated FRT and TetRepressor system as well as an expression vector containing the GFP-Spindly constructs (either wild type or mutants) were generated in Dr. A. Saurin's laboratory (University of Dundee) and donated to us.

All cells were grown in MEM (Gibco) supplemented with 10% HI-FBS, 1% Penicillin, Streptomycin and Glutamine (Gibco) for no more than 30 passages. Expression of the GFP construct was induced by administration of doxycycline (0.1-1μg/mL) (Calbiochem).

## 2.3 Small Interfering RNA (siRNA) Transfection

Small interfering RNA oligonucleotides were synthesized by SIGMA and transfected into cells using Lipofectamine RNAiMax (Invitrogen) according to manufacturer's instructions. The oligonucleotide sequences used for siRNA knockdown are as follows: a GC-matched non-targeting control (MISSION Negative Control, SIGMA) diluted to a final concentration of 20nM; Spindly Endo1 (GAAAGGGUCUCAAACAGAA) and Spindly-UTR-66 (CUUGAUCUGACAUAUAUCA) (neither of which target the expressed Spindly constructs) combined together to a final concentration of 20nM. Cells were seeded and directly treated. Treatment was left on for 96 hours and then cells were fixed, harvested or seeded again for subsequent analysis.

## 2.4 Overexpression transfection

DNA transfection procedure was carried out using FuGene HD (Promega) according to manufacturer's instructions. Cells were transfected 24 hours after being seeded with FuGene/DNA in a ratio of 3:1 incubated in 200μL of serum-free media. The mix was dropped onto cells growing in MEM supplemented with 10% FBS and plates were incubated at 37°C for at least 24 hours before experiment was conducted.

All the DNA plasmids used in this study were purified using the QIAprep Spin Miniprep Kit (QIAGEN), following manufacturer's instructions.

## 2.5 Protein Lysis

Cells were lysed using the following lysis buffer: 50mM Tris/HCl pH 7.5, 150 mM NaCl, 100mM N-Ethylmaleimide (NEM), 0.3% CHAPS, 1mM EGTA, 1mM EDTA, 10mM Na-β-glycerophosphate, 1mM Na-orthovanadate, 50mM Na-Fluoride, 10mM Na-pyrophosphate, 270mM sucrose, 0.1mM PMSF, 1mM Benzamidine, 0.1% β-mercaptoethanol, 1 protease inhibitor cocktail tablet (Roche) for 10 mL of buffer. Cells were then transferred into Eppendorf tubes and put under constant agitation for 10 minutes at 4°C. Samples were subsequently spun down for 15 minutes at 13,000 rpm at 4°C. Supernatants were collected and stored at -80°C.

## 2.6 Western blot

Protein concentration was measured using Bradford dye (BioRad), accordingly to manufacturer's instructions. Samples were prepared in 2x loading buffer (LDS sample buffer, Novex-Life Technologies) and boiled at 95°C for 5 minutes. Soluble fractions were resolved on Tris-glycine SDS-PAGE gels (4-12% gradient gel; Novex NuPAGE SDS-PAGE Precast Gels, Life Technologies) run at 120-150 volts. Running buffer used was 50mM MOPS, 50mM Tris Base, 0.1% SDS, 1mM EDTA.

The gels were then transferred to nitrocellulose membrane (Amersham Protran 0.2 NC, GE Healthcare) for 2 hours at 100 volts in transfer buffer (25mM Tris Base, 192mM glycine, 0.1% SDS, 10% Methanol). The membrane was blocked in 5% milk dissolved in Tris-buffered saline [TBS]-0.2% Tween 20 for 1 hour and subsequently probed with primary antibodies overnight. Antibodies used are showed in **Table 2.1**.

Membranes were subsequently washed three times in TBS-Tween buffer and incubated with HRP–conjugated secondary antibodies (Cell Signalling) for 1 hour. Membranes were subsequently washed with TBS-Tween buffer and developed using ECL solution (Pierce) onto X ray film (Konica Minolta).

**Table 2. 1.List of antibodies used.**

| ANTIBODY | MANUFACTURE | SPECIES | DILUTION |
|---|---|---|---|
| Spindly | (Griffis *et al.*, 2007) | Rabbit | 1:5000 |
| DIC | (Vaughan and Vallee, 1995) | Rabbit | 1:1000 |
| ZW10 | AbCam | Rabbit | 1:1000 |
| Mad2 | ThermoScientific | Rabbit | 1:1000 |
| Mad1 | Bethyl Laboratories | Rabbit | 1:1000 |
| Bub1 | Bethyl Laboratories | Rabbit | 1:1000 |
| BubR1 | Bethyl Laboratories | Rabbit | 1:1000 |
| GFP | Novus Biological | Sheep | 1:5000 |
| p50 | BD Biosciences | Mouse | 1:1000 |
| p150 | SantaCruz | Mouse | 1:1000 |
| DHC | SantaCruz | Rabbit | 1:1000 |
| FLAG | Sigma | Mouse | 1:2000 |
| PCNA | SantaCruz | Mouse | 1:200 |
| Geminin | SantaCruz | Rabbit | 1:200 |
| pHistoneH3 | Novus Biological | Rabbit | 1:500 |
| GAPDH | SantaCruz | Mouse | 1:1000 |
| CENP-E | SantaCruz | Goat | 1:1000 |
| CENP-F | SantaCruz | Goat | 1:1000 |

## 2.7 Immunoprecipitation

200 µg of protein from whole cell lysate were incubated overnight at 4 °C under constant agitation with 1 µg of antibody in buffer D (20nM HEPES pH 7.9, 1mM DTT, 0.1% NP40, 20% glycerol, 1mM PMSF, 5mM NaF, 500 µM $Na_3VO_4$ and 1 protease inhibitor cocktail tablet (Roche) per 10 mL of final volume).

Normal IgG was always used as negative control. Protein G Sepharose beads (Generon) or Protein A magnetic beads (Invitrogen) were added for 2 hours at 4°C under constant agitation. Precipitates were subsequently washed twice with lysis buffer and twice with PBS 1X. Washes were carried out under constant agitation at 4°C (10 minutes incubation for each wash). Loading buffer (2x) was then added to the beads that were boiled for 5 minutes and resolved by Western Blot analysis (see **2.6**).

## 2.8 Gel filtration

### 2.8.1 Superose 6 column

HEK293 cells were collected and lysed as previously described (see **2.5**). Cells were then transferred into Eppendorf tubes and put under constant agitation for 10 minutes at 4°C. Samples were subsequently spun down for 15 minutes at 13,000 rpm at 4°C and supernatants were collected. 200 µL of samples were then loaded into the Superose 6 column (10x300mm, 13µm particles, 40nm pores, GE Healthcare) equilibrated in lysis buffer. Prior to running our samples we calibrated the column by loading the standards (100 µL injection) diluted as follow: IgG (0.5mg/mL); BSA (1mg/mL); trypsin inhibitor (1mg/mL). Experiments were conducted at 4°C.

Fractions were collected in a 96-well plate (Eppendorf, Deepwell plate 96/1000 µL) and resolved in 2x LDS sample buffer. Western Blot was then carried out to identify elution profile of our proteins of interest. Antibodies dilution as previously stated (see **Table 1**).

### 2.8.2 SEC-1000 column

HEK293 cells were collected and lysed (see **2.5**), sonicated for 30 minutes (30'' pulse on/ 30'' pulse off) at 4°C and spun down for 10 minutes at 4°C at 13,000 rpm. Supernatant was collected and filtered using ultrafree-MC centrifugal filter units (pore size 0.45 microns, Millipore). Samples were then injected into the column (200 µL

injection). Column used was BioBasic SEC-1000 (7.8x300mm, 5µm particles, 1000Å pores, ThermoScientific) equilibrated in lysis buffer. Prior running our samples column was calibrated by loading the standards (100 µL injection), diluted as follow: IgG (0.5mg/mL); BSA (1mg/mL); trypsin inhibitor (1mg/mL). Experiments were conducted at room temperature.

Fractions were collected in a 96-well plate (Eppendorf, Deepwell plate 96/1000 µL) and resolved in 2x LDS sample buffer. Western Blot was then carried out to identify elution profile of our proteins of interest. Antibodies dilution as previously stated (see **Table 2.1**).

### 2.8.3 Double thymidine block

Cells were mitotically enriched by double thymidine block. First incubation with thymidine (2mM, Sigma) was carried on for 18 hours, and then cells were washed in PBS and released in complete media for 9 hours. Subsequently cells were incubated again with thymidine for 12 hours, washed with PBS and released in complete media for 6 hours. Nocodazole (40ng/mL, Calbiochem) was added for 16 hours and cells were finally harvested by mitotic shake-off, lysed and ran through the column.

## 2.9 Mass spectrometry analysis

HEK293 cells were seeded into 15cm petri dishes and once confluent treated overnight either with Nocodazole (40ng/mL) or S-trytil-L-cysteine (STLC, 5µM; Enzo, Life Sciences) to enrich the mitotic population. Asynchronous cells were used as control. After treatment cells were collected by mitotic shake-off, pelleted down and immunoprecipitation was performed by incubation with anti-Spindly antibody (see **2.7**) overnight at 4°C. Normal rabbit IgG were used as negative control. Samples were eluted in sample buffer and boiled at 95°C for 5 minutes.

Soluble fractions were resolved on Tris-glycine SDS-PAGE gels as previously described (see **2.6**) and they were subsequently stained with Coomassie Instant Blue (Expedeon) for at least one hour. Bands were cut and the gel pieces were washed twice with 100µL 100mM Ammonium bicarbonate ($NH_4HCO_3$): 100% Acetonitrile (ACN) for 10 minutes at room temperature on a shaker. Subsequently de-staining was performed by addition of 50µL of 100% ACN. Then, 100mM $NH_4HCO_3$ was added to make 100mM $NH_4HCO_3$: 100% ACN and samples were incubated at 37$^{o}$C for 30 minutes on a shaker.

Samples were reduced by adding 10mM of DTT and consequent boiling for 30 minutes at 50°C. For the alkylation step iodoacetamide (IAA) (Sigma) (50mM) was added following incubation in the dark at room temperature for 45 minutes. Gel pieces were dried completely in a vacuum centrifuge (maximum temperature: 45°C). The digestion was performed with 10µl of 1µg/µl trypsin in 490µl of 50mM $NH_4HCO_3$. 10-20µL of diluted trypsin solution was added to dry gel pieces and tubes were incubated overnight at 37$^{o}$C. 10-20µL of trypsin was then added again and incubation was carried on for a further 4 hours. An equal volume of 100% ACN was supplemented to the samples and sonication was carried out for 15 minutes in a sonication bath. Supernatant was placed in a new tube and 100µL 70%ACN: 0.1% trifluoroacetic acid (TFA) was added. Sonication was carried out as before. Pooled supernatant volume was reduced to approximately 60-100µL in a vacuum centrifuge at 60°C. Excess of salt and polymers were removed from the samples by cleaning through a 'home-made' C18 "Ziptip" column (POROS R2 Applied biosystems 1-1129-06, method: http://greproteomics.lifesci.dundee.ac.uk/webpage%20front%20page/dreamweaver%20webpage/Ziptip%20Protocol1.pdf). Activation of the columns was carried out by washes with 20 µl of a ACN: TFA solution (50% ACN:0.1% TFA).

The excess of 50% ACN: 0.1% TFA was washed off using 0.1% TFA and columns were loaded with the sample. The peptide solution was then loaded onto the column, and excess salt and contaminants washed away with ~40 µl 0.1% TFA. Bound peptides were eluted in a new Eppendorf tube with 40 µl of 50% ACN: 0.1% TFA. The elution step was repeated for a final volume of 80 µl. Samples were dried in a vacuum centrifuge system at 60°C to a final volume of 10 µl. This volume was then reconstituted to 30 µl with 0.1%TFA.

Peptide samples were analysed on an Orbitrap Velos (Thermo Scientific) mass spectrometer with a gradient of 2-40% Buffer A (0.1 % formic acid): Buffer B (80 % acetonitrile, 0.1 % formic acid) over 156 minutes with a flow rate of 0.3µl/min. The parent ion scan was set at a resolution of 60,000 (units) while the MS/MS was set at 'Normal scan' with a peak width of 0.6. Scans were undertaken at 335-1800 *m/z* range and the MS/MS had a minimum signal of 5000 ions. The mass window tolerances were set to 10 ppm for all data dependant acquisition. For the mass spectrometry analysis the top abundant 15 precursor ions were selected for following MS/MS, using collision induced dissociation (CID), on ions 2+ and over (1+ ions excluded) with a collision energy of 35% and an activation time of 10 milliseconds.

A 10 ml fraction of the 30 ml peptide solution was loaded on to the instrument for each run. Mass spectrometry .raw files were processed using MaxQuant 1.5.1.2.8 (Cox and Mann, 2008), and then using a Uniprot Human Database (January 2015) to identify peptides. The fixed search parameters were Carbamidomethyl (C), with variable modifications set to Oxidation (M), Phospho (STY) Sites, Acetyl (Protein N-term). Peptide spectral matching FDR (False Discovery Rate), Protein FDR and site FDR were all set to 0.01. Minimum peptide length was 7 amino acids. The data were culled using the reversed and probable contaminants indicators in the output of MaxQuant.

## 2.10 Immunofluorescence

PFA 4% solution was obtained by diluting Paraformaldehyde 32% Solution (VWR) in PHEM 1X (60mM PIPES, pH 6.9; 25 mM HEPES; 10 mM EDTA; 2mM MgCl 2x $6H_2O$).

Cells were seeded onto sterilised glass coverslips (Menzel-Glaser). When confluent, cells were fixed in 4% PFA for 10 minutes at room temperature, washed in PHEM-wash (PHEM + 0.1% Triton X-100), permeabilized in PHEM-T (PHEM + 0.5% Triton X-100) for 5 minutes and fixed again in 4% PFA for 10 minutes. After three washes in PHEM-wash they were blocked in Abdil (TBS-0.1% Tween, 0.1% Azide, 2% BSA) for 1 hour. At this point slides were incubated with primary antibodies for one hour at room temperature or overnight at 4°C. The antibodies were diluted in AbDil and diluted as indicated in **Table 2.2**.

**Table 2. 2. List of antibodies used.**

| ANTIBODY | MANUFACTURE | SPECIES | DILUTION |
|---|---|---|---|
| Spindly | (Griffis *et al.*, 2007) | Rabbit | 1:1000 |
| DIC | (Vaughan and Vallee, 1995) | Rabbit | 1:100 |
| GFP | Novus Biological | Sheep | 1:500 |
| p50 | BD Biosciences | Mouse | 1:100 |
| p150 | SantaCruz | Mouse | 1:100 |
| DHC | SantaCruz | Rabbit | 1:100 |
| Tubulin | Sigma | Rat | 1:500 |
| PhalloidinAtto488 | Sigma | | 1:500 |
| pMyosin LightChain2 | Cell Signalling | Rabbit | 1:200 |

After four washes in PHEM-wash, the coverslips were incubated for one hour with secondary (either Alexa or Jackson) antibodies diluted in Abdil (1:500) and the DNA was stained with DAPI (Sigma) (1:500). Coverslips were washed three times in PHEM-wash and once in PHEM 1X prior to be mounted onto VWR SuperPremium Microscope Slides. As mounting media we used DAKO (Agilent Technologies). Slides were nail polished and let dry before imaging was performed.

High-resolution images were collected with an imaging system (DeltaVision Restoration; Applied Precision) using a 20X/0.75, 40X/1.42 oil, 60X/1.42 oil or a 100X/1.35 oil (Olympus) objective lens. Images were then processed using OMERO software or FiJi software.

## 2.11 Rapamycin mis-localisation assay

HeLa or U2OS cells were transiently transfected with three different plasmids: one FRB-, one FKBP- and one YFP- tagged. The FKBP tag was expressed in the mCherry-Spindly plasmid while the FRB tag was expressed in the Lin11 one (a plasma membrane marker) (plasmid kindly gifted from Dr. A. Saurin, University of Dundee). The YFP tag was expressed in the plasmid for the protein that we wanted to check as Spindly interactor (plasmids donated by Dr. A. Saurin, University of Dundee). After 24 hours from transfection, we administrated rapamycin (Cayman Chemical) 4μM and incubate for a time between 30 minutes up to 4 hours. The rapamycin induces dimerisation of the FRB-FKBP constructs (Putyrski and Schultz, 2012) mis-localising in this case mCherry-Spindly to the plasma membrane. Subsequently we fixed cells and performed immunostaining as previously described (see **2.10**). Images were analysed using the Fiji Software. Measurements were conducted by drawing a line across the two edges of a cell and measuring the fluorescence intensity for both channels (green (YFP) and red (mCherry)).

### 2.11.1 Molecular cloning

Protocol performed by Dr. Eric Griffis.

The FKBP coding sequence was inserted before the stop codon of the Spindly gene using the In-Fusion cloning method (Clontech). The mCherry-Spindly plasmid (from the DSTT service) was linearized with the following primers: TAAGCGGCCGCTCGAGTCTAGAGG and CTGTTGAGGGCACTGGGTCTCTGG; the FKBP fragment (a gift from Dr. A. Saurin, University of Dundee) was amplified with the following primers: CAGTGCCCTCAACAGGGAGTGCAGGTGGAGACTATCTCC and TCGAGCGGCCGCTTATTCCAGTTTTAGAAGCTCCACATCG in which the

underlined regions are homologous to the breakpoints in the linearized mCherry-Spindly plasmid. After the ligation reaction, colonies were screened by PCR and confirmed by sequencing, which was performed by the Sequencing Service (College of Life Sciences, University of Dundee, http://www.dnaseq.co.uk).

## 2.12 Wound-Healing cell based assay

U2OS cells (~ $7x10^5$ cells), previously treated for 96 hours with oligonucleotides for siRNA knockdown (see **2.3**) either negative control or against Spindly, were seeded into the Silicone Culture-Insert (IBIDI) and left grow for at least 24 hours. Once cells were confluent, the insert was removed and cells were washed once with fresh media before beginning the imaging. A sample of the cell population was collected for Western Blot experiment to confirm the silencing of Spindly.

For the synchronised experiments, cells were treated with hydroxyurea (HU) (1mM, Sigma) for 24 hours prior being imaged. A sample of the cell population was collected for Western Blotting to confirm silencing of Spindly and S phase synchronisation.

For the rescue experiments stable U2OS cells expressing either GFP-Spindly WT or S256A were treated with siRNA for Spindly or a non-targeting control. Subsequently doxycycline (0.1-1 μg/mL) was administrated overnight to induce expression of the GFP construct. Then wound closure was followed over the time. A small portion of the cell population was harvested for Western Blot experiment to control silencing and GFP expression.

Video (or images) were recorded at different time points (as indicated) using a 20X/0.45 air objective (Nikon Eclipse Ti microscope system). Images were then processed using the Fiji software. Measurements were conducted by drawing a line and measuring the distance between the two edges of the wound at the indicated time points.

Kymograph analyses were conducted using Volocity software to measure the velocity of movement over the time.

## 2.13 Scratch assay

MEF, FB or HaCaT cells were seeded onto glass coverslip and left to grow until confluence. Then we mechanically generated a scratch by using a 200µL tip and we fixed the slides at different time to check for protein recruitment at the leading edge. Staining protocol used was the same aforementioned (see **2.10**).

### 2.13.1 TIRF imaging

Imaging was performed by Dr. Eric Griffis (University of Dundee).

For visualising Spindly and microtubules cells were co-transfected with mCherry-Spindly and TagBFP2-Tubulin (a gift from Mike Davidson, Florida State University, Tallahassee, FL). Conversely, for visualising Spindly and Zyxin (for focal adhesion formation), cells were co-transfected with GFP-Spindly and RFP-Zyxin (a gift from Trina Schroer, John Hopkins, Baltimore, MD). In both experiments total internal reflection fluorescence (TIRF) imaging was performed with a Nikon Ti-Eclipse with a motorized TIRF-PAU slider, a 100X/1.45 N.A. objective, a PerfectFocus 2 focusing system (Nikon Instruments), a Neos ATOF, 100mW 561nm DPSS and 100mW 405nm and 150mW 488nm diode lasers (Coherent Inc. and Solamere Technology Group), a quad dichroic (Chroma Technology), an Evolve Delta camera (Photometrics), and appropriate emission filters mounted in a filter wheel (Chroma Technology and Nikon Imaging). Images were acquired with µ-Manager.

## 2.14 Cell fractionation experiment

U2OS cells were grown to confluence in a 150mm petri dish, washed with chilled PBS 1X and lysed in 200µL of Buffer A (10 mM HEPES, pH7.9, 10 mM KCl, 1.5 mM $MgCl_2$, 1 mM DTT, 0.5 µg/µL Leupeptin, 0.5 µg/µL Aprotinin, 0.5 µg/µL Pepstatin, 0.1 mM PMSF, 0.34 M sucrose, 10 % Glycerol, 0.1 % Triton X-100, 1µL DTT, 1µL LPC), swirled and placed on ice for 20 minutes. Cells were then scraped, transferred to Eppendorf tube and spun down at 13,000 rpm for 10 minutes at 4°C. Supernatant was removed and collected into a new Eppendorf tube as "cytoplasmic" fraction. To the remaining pellet we added 50µL of Buffer A combined with 0.2 µL benzonase nuclease (SIGMA) and 10 µL 0.1M $CaCl_2$ and incubate at 37°C for 1 minute. Sample was then placed back on ice and supplemented with 0.2µL of EGTA 0.5M and incubated in ice for 5 minutes. We then spun down at 13,000 rpm for 5 minutes at 4°C. Supernatant was removed and collected into a new Eppendorf tube as "nuclear" fraction. To the remaining pellet we added 50 µL of Buffer B (3 mM EDTA, 0.2 mM EGTA, 1 mM DTT, 0.5 µg/µL Leupeptin, 0.5 µg/µL Aprotinin, 0.5 µg/µL Pepstatin, 1µL LPC) and incubated at room temperature for 1 minute. We finally spun down at 15,000 rpm for 5 minutes at 4°C. Supernatant was removed and collected into a new Eppendorf tube as "chromatin" fraction.

## 2.15 Yeast-Two Hybrid assay

The yeast strain used was AH109 (Invitrogen) that contains a HIS3 gene and a LacZ gene regulated by Gal4-binding sites. We grew the yeast in 5mL of YPAD media overnight at 30°C under constant agitation and the following morning we inoculated 50mL of YPAD with the overnight culture and let it grow until optical density (OD660nm) reached 0.6-0.8. At this point, we spun down the yeast for 3 minutes at 5000 rpm and washed the pellet with sterilised water (10mL); we spun them again (3

minutes 5000 rpm) and then re-suspended the cells in 500µL TE/LiAC buffer (TE 10X: Tris-HCl 100mM and 10mM EDTA; LiAC (Litium acetate) 1M). Yeast cells were transformed with a pAS2.6 plasmid (Invitrogen) encoding Spindly fused to the DNA binding domain of Gal4 (containing a TRP1 selectable marker) and with a pACT2.6 plasmid (Invitrogen) encoding p150 or p50 to the Gal4 activation domain (containing also a LEU2 selectable marker). For the reverse experiment we transformed the yeast with Spindly fused to the Gal4 activation domain and p150/p50 fused to the DNA-binding domain of Gal4. Empty vectors were used as control. All constructs were synthesised from the Division of Signal Transduction Therapy Unit (DSTT, University of Dundee).

Competent cells were transformed with 1 µg of DNA, 10 µg of ssDNA salmon sperm (Invitrogen), 600 µL of PEG/LiAc solution (polyethylene glycol/lithium acetate: 40% PEG, 1X TE, 1X LiAc) and incubated at 28°C for 30 minutes under constant agitation. We then added 70 µL of DMSO and incubated again for 15 minutes at 42°C under constant agitation. After 10 minutes on ice and a spin down, we plated cells onto minimal medium lacking leucine (LEU), tryptophan (TRP) and histidine (HIS) and incubated at 30°C. Single colony from each transformant was grown in 5mL of minimal media (DOA, lacking histidine (HIS), leucine (LEU) and tryptophan (TRP)) overnight. The following day cells were seeded onto plates containing different concentrations of 3-amino-1,2,4-triazole (3AT) to assay reporter gene activation. 3AT is a competitive inhibitor of the product of HIS3 gene that catalyses the production of histidine. Under this condition the yeast survives only if can produce histidine, so upon binding between the bait and the prey.

To further validate positive interaction, we screened as well with 5-bromo-4-chloro-3-indolyl-β-D-galactopyranoside (X-Gal) that can be cleaved only in presence of an active β-galactosidase, producing characteristic blue colonies. We seeded cells onto

nitrocellulose membrane placed on a YPAD plate for 24 hours and then we froze the membrane in liquid nitrogen and placed it on a filter paper impregnated with XGal dissolved in DMF (Dimethylformamide) and in Z buffer ($Na_2HPO_4$ $7H_2O$, $NaH_2PO_4$ $H_2O$, KCl, $MgSO_4$ $7H_2O$, adjusted at pH=7) supplemented with β-mercaptoethanol. The plate was incubated at 37°C and blue colony formation was assessed for a period of 24 hours.

### 2.15.1 Site-direct mutagenesis

The vectors encoding for Spindly (both the activating, pACT2.6, and the binding, pAS2.6, plasmids) were mutated in the S256 site using Phusion Hot Start DNA polymerase (ThermoScientific). Primers used were: fwd: GTAATAGGCAACGCTTTGTTTGCAGAGGTGGGAAGATCGAAGG; rev: GGAAACAAAGCGCTTGCCTTTACTATTGGGATCCAAGGCTTGC. DNA constructs were verified by DNA sequencing performed by the Sequencing Service (College of Life Sciences, University of Dundee, http://www.dnaseq.co.uk).

## 2.16 *In vitro* binding assay

This experiment was carried out in the R. Vale Lab (University of California, San Francisco) using our constructs to express hSpindly WT or S256A mutated. hSpindly constructs were expressed in bacteria and protein expression was induced with 1 mM IPTG while dynein and dynactin complexes were isolated from fresh pig brains. Protein purification was carried out as described in (McKenney *et al.*, 2014) as well as the binding assay.

# 3 . Spindly plays a role in the recruitment of the dynein/dynactin motor complex to kinetochores

## 3.1 Introduction

When a cell enters mitosis, a high-fidelity machinery is activated to ensure proper distribution of the genomic material to the new daughter cells and also to avoid chromosome mis-segregation, which would lead to developmental disorders or cancer generation. For accurate cell division the machinery that aligns and separates the genomic material must be able to physically interact with chromosomes. One way in which this occurs is thanks to a large multiprotein structure present on chromosomes, the kinetochore (KT), that associates with spindle microtubules and allows for chromosome capture, oscillations, alignment and eventual segregation (Cheeseman, 2014).

Recruitment of the motor dynein to KTs is a critical step for proper cell division; it is central for both chromosome alignment and mitotic checkpoint (or SAC) silencing (King and Schroer, 2000) (Yang *et al.*, 2007) (Howell *et al.*, 2001). As widely described earlier (see **1.4**), dynein is the sole processive minus-end directed microtubule motor in many eukaryotes, so it mediates a wide array of functions: the streaming of SAC components from KTs towards poles, the sliding of kinetochores towards the microtubule minus-ends and the proper KT-MT interactions (Allan, 2011) (Howell *et al.*, 2001) (Yang *et al.*, 2007). Upon KT-MT initial lateral interaction, dynein generates a critical pulling force that allows chromosome poleward movement; inhibition of dynein expression upon injection of anti-dynein antibodies represses chromosome movement and delays mitosis (Yang *et al.*, 2007).

The process through which the motor complex gets recruited to KTs is still under investigation, but it has been clearly proven that several kinetochore proteins can promote it. It was demonstrated that the recruitment of Spindly to kinetochores is critical as well as the presence of the RZZ complex (Barisic *et al.*, 2010) (Gassmann *et al.*, 2008) (Chan *et al.*, 2009). Initially it was hypothesised that the recruitment occurred

via the dynactin subunit p50/dynamitin, which was shown to interact with ZW10 (Starr *et al.*, 1998); however further research called this conclusion into question. Former studies have demonstrated that Spindly-depleted cells are not able to recruit the dynein/dynactin motor complex to KTs even in presence of the RZZ complex, with a consequent delay in mitosis progression due to errors in chromosome alignment and SAC silencing (Griffis *et al.*, 2007) (Gassmann *et al.*, 2008) (Chan *et al.*, 2009) (Gassmann *et al.*, 2010) (Barisic *et al.*, 2010) (Cheerambathur *et al.*, 2013). Additionally, the analysis of Spindly protein sequences identified an interesting conserved region of primary amino acid sequence lying in a break between N-terminal coiled-coil domains (called the 'Spindly box', in recognition of this new protein domain (Griffis *et al.*, 2007)). It was shown that a single mutation within this sequence could separate these two functions generating a protein retained onto kinetochores and unable to recruit dynein/dynactin, but still able to promote chromosome alignment (Gassmann *et al.*, 2010). In Spindly-mutant cells, the SAC was shown to be hyper-activated and SAC proteins retained on aligned kinetochores, suggesting that the removal of Spindly is essential for SAC silencing (Gassmann *et al.*, 2010).

In this chapter we demonstrate that Spindly can bind the dynein/dynactin motor complex, precisely via interaction with a component of the multi-subunit dynactin sub-complex (named p150). This interaction could be needed to enhance the processivity of the motor, in line with recent publications that demonstrated that to be active and processive *in vitro* dynein requires other regulatory factors besides dynactin (McKenney *et al.*, 2014) (Schlager *et al.*, 2014). Furthermore, here we show that the mutation within the 'Spindly box' specifically prevents the binding of Spindly to the p150 subunit of dynactin, and, in turns, impedes the streaming of SAC effectors towards spindle poles inhibiting therefore the silencing of the checkpoint.

Overall, the results collected in this chapter describe Spindly as a novel adaptor of the minus-end dynein/dynactin motor complex important for the transport of specific mitotic cargos.

## 3.2 Spindly localises with dynactin at kinetochores

Only a few proteins are constitutively localised at centromeres throughout the cell cycle (the constitutive centromere-associated network or CCAN). Most kinetochore proteins are recruited to the centromere when mitosis begins and/or throughout mitosis. For example, the Ndc80 complex and the chromosome passenger complex (CPC) complex accumulate at centromeres in prophase, while the checkpoint effectors and the minus-end directed motor dynein localise there only in early prometaphase (Liu *et al.*, 2006). Once a cell has entered metaphase the levels of some proteins diminish (like for the SAC proteins), while instead other proteins will only then associate with kinetochores (such as EB1, APC and RanGAPs), reflecting correct KT-MT interactions and showing how MT-binding alters KT composition (Tirnauer *et al.*, 2002) (Kaplan *et al.*, 2001) (Joseph *et al.*, 2004). Therefore, proteins that compose this structure can be highly dynamic, and they show diverse residence times according to the stage of mitosis in which they play a role. It was previously shown that the minus-end directed motor dynein and its adaptor dynactin are among those proteins that are enriched at kinetochores only in prometaphase, and that they move to spindle poles once bi-orientation is achieved (Pfarr *et al.*, 1990) (Echeverri *et al.*, 1996). Figure 3.1 shows that Spindly has a similar distribution profile in mitosis: it gets recruited to kinetochores in early prometaphase and then, in metaphase, it starts to stream along k-fibres to reach the spindle poles. As expected, in anaphase and telophase Spindly is no longer detectable at kinetochores.

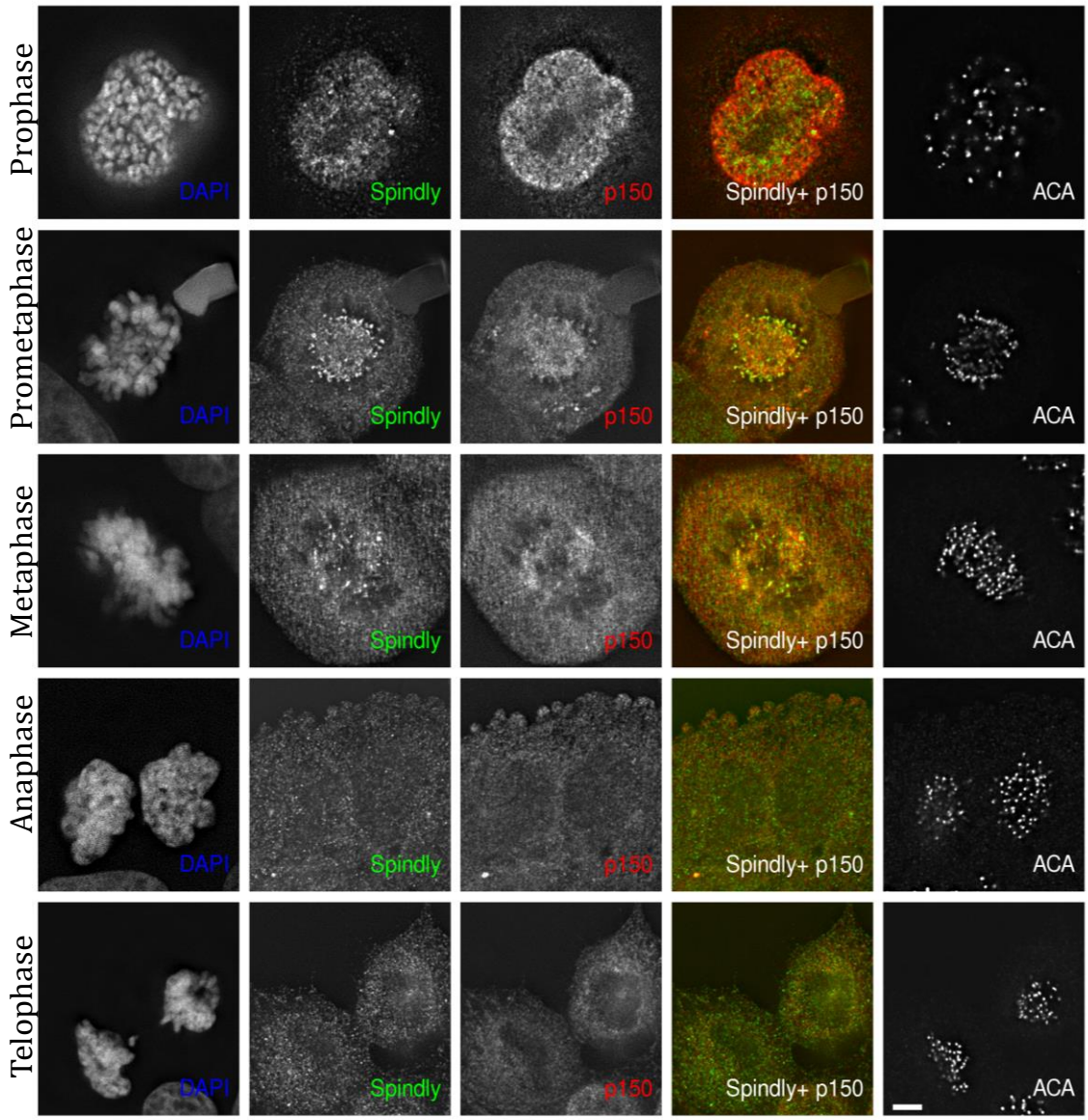


**Figure 3. 1. Mitotic distribution of Spindly**
U2OS cells were stained with anti-Spindly (green), anti-ACA (anti-centromere antibody, white) and anti-p150 (red) antibodies. Spindly localises to kinetochores during prometaphase, mainly at the spindle poles and along k-fibres in metaphase and it is no longer detectable in anaphase and telophase; similar distribution profile is reported for dynactin (p150 staining), with which Spindly co-localise Chromosomes were stained with DAPI (blue). 100X magnification. Scale bar: 5µm. Double channel representation of either Spindly+ACA or p150+ACA is presented in the appendix, to show their kinetochore localisation (**Chapter 8- Fig. 8.2**).

## 3.3 Spindly interacts with the dynein/dynactin motor complex

Spindly was first identified as a crucial player for proper completion of mitosis; S2 *Drosophila melanogaster* cells lacking Spindly arrest in metaphase and cannot recruit the dynein/dynactin motor complex to promote the removal of the checkpoint effectors and anaphase onset (Griffis *et al.*, 2007). To date, the importance of Spindly in this process has been clearly underlined, but evidence of direct interaction between Spindly and the motor complex is still missing. With the aim to investigate this relationship more closely, we decided to perform immunoprecipitation of endogenous Spindly from HEK293 cell extracts to analyse the presence of either dynein or dynactin subunits. Figure 3.2 shows Spindly association with the p150 subunit of dynactin as well as with the dynein intermediate chain (DIC).

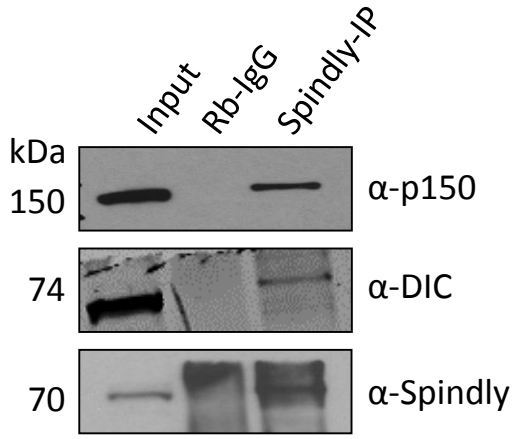


**Figure 3. 2. Spindly immunoprecipitates both dynein and dynactin.**
Immunoprecipitation of endogenous Spindly from HEK293 cell lysates. 200/400 µg of total cell extract were used to immunoprecipitate Spindly with anti-Spindly antibody. Rabbit IgG was used as negative control. Immunoprecipitated complexes were analysed by Western blot using the indicated antibodies. Input corresponds to whole cell extract. Anti-Spindly antibody specificity was validated by testing samples treated with control siRNA or siRNA against Spindly that confirm the molecular weight band predicted for the protein (see Fig. 3.6, this chapter). (DIC: dynein intermediate chain)

Since dynein and dynactin associate closely (Vaughan and Vallee, 1995) (Echeverri *et al.*, 1996), the result obtained in Fig. 3.2 suggested that either Spindly interacts with both complexes independently, or it binds to only one of the two but

indirectly it pulls down both complexes due to their own interaction. Hence, we sought to study the elution profile of these three proteins taking advantage of size exclusion chromatography technique, with the aim of delineating the potential complex.

We performed gel filtration experiments fractionating lysates from HEK293 cells on a Superose 6 column (Fig. 3.3). Western blot analysis of the fractions revealed the presence of Spindly, as well as dynactin (p150 subunit), at the beginning of the elution profile, immediately after the void volume (Fig. 3.3, (a)), indicating the presence of a large complex that is likely to include many other proteins besides Spindly and dynactin. Indeed Tubulin had a similar elution profile (Fig. 3.3, (b)).

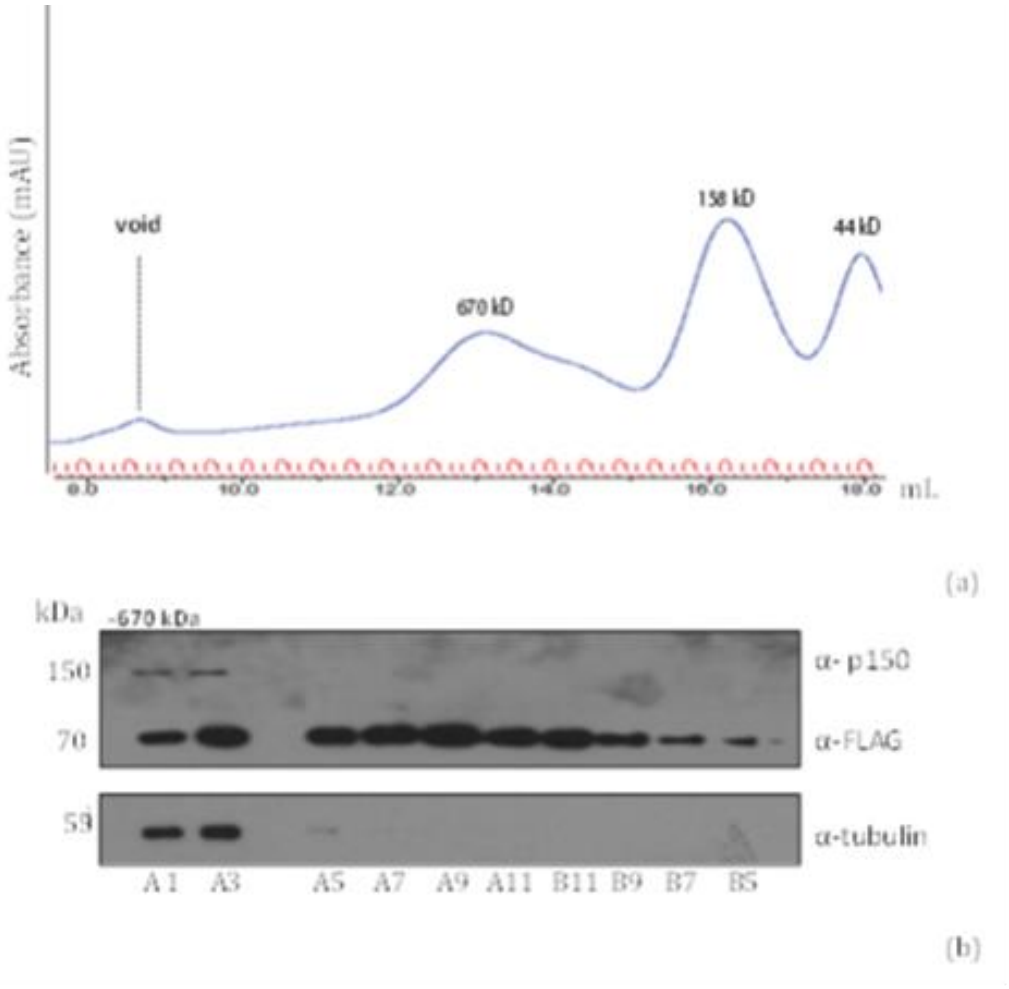


**Figure 3. 3. Spindly co-elutes with dynactin.**
Extracts of HEK293 cells expressing FLAG-Spindly were analysed by gel filtration on a Superose 6 column and resolved by Western blot. (a) Elution profile ($A^{280}$) of the total cell lysate; (b) Western blot analysis of collected fractions. Antibodies as indicated.

Data in figure 3.3 indicates that with the column used we could not separate properly the complex. Indeed Tubulin is the core component of microtubules and its presence in the same fractions with Spindly and dynactin indicates the possibility that we did not isolate the different single components of the complex from the microtubules in our lysate. Therefore, we decided to carry out size-exclusion chromatography of the extracts using a SEC-1000 gel filtration column that provides greater separation of the higher molecular weight species. Cell lysates from either asynchronous (Figure 3.4, (b)) or mitotically enriched (Figure 3.4, (c)) HEK293 cells were passed through the column and then analysed by Western blot. Figure 3.4 shows the dynactin complex (p150 and p50 subunits) enriched in B fractions (~450 kDa), while Spindly elutes preferentially in the later fractions ( C fractions (~250/200 kDa); Fig. 3.4. (b) and (c)).

It is worth to point out that the two diverse SEC experiments (Fig. 3.3 and Fig. 3.4) differed not only in the type of SEC column used but also in the protocol used for the lysate preparation (see **2.8**); samples analysed by size-exclusion chromatography on a SEC-1000 were sonicated and the fractionation step was conducted at room temperature.

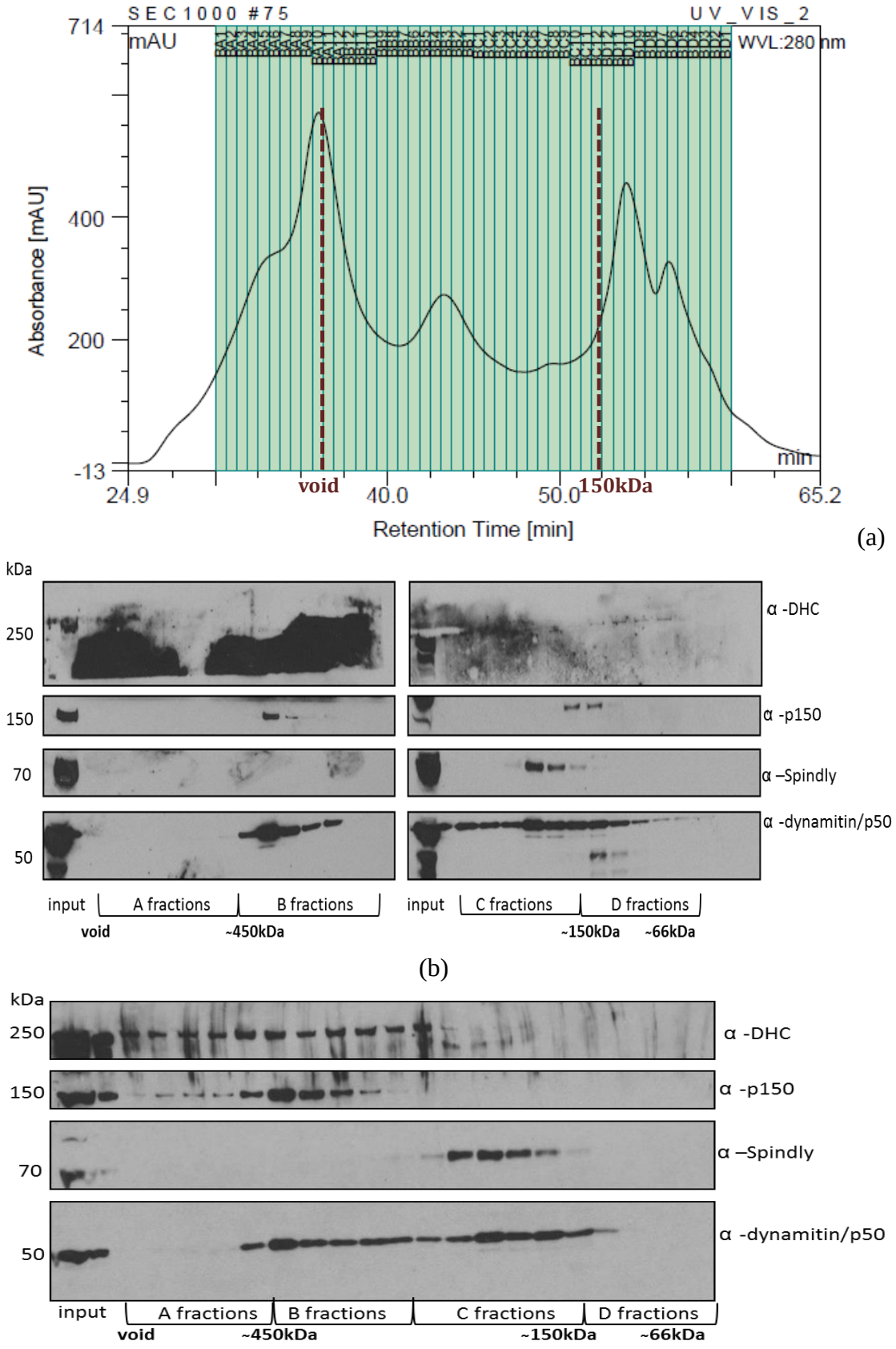


**Figure 3. 4. Spindly elution profile.**
Extracts of HEK293 cells were analysed by size exclusion chromatography on a SEC-1000 gel filtration column. Elution profile of the total cell lysate for both experiments (a); Fractions were resolved by Western blot: asynchronous cells (b), or mitotically enriched cells (c). Antibodies as indicated. Inputs represent the whole cell lysate. (DHC: dynein heavy chain)

This result pointed out that Spindly can be a part of two different complexes: one with the dynactin complex (a heavier complex eluting after the void volume, see Fig. 3.3) and another one with other potential partners that would need to be further explored (Fig. 3.4). Also it is important to mention that Spindly is a very elongated molecule and that we have seen, from the purification of recombinant proteins, which it does not run according to its molecular weight in size-exclusion chromatography experiments (data not shown). Both the rod-like shape of Spindly structure together with the high presence of coiled-coil regions could be affecting its running properties, suggesting possible presence of dimers instead of monomers of the protein.

## 3.4 Spindly associates directly with the p150 subunit of dynactin

Data collected so far led us to believe that there could be an interaction between Spindly and dynactin, but one that is not stable enough to last through gel filtration. To confirm this, we decided to carry out a yeast-two hybrid assay using two dynactin subunits, p150 and p50 as baits and Spindly as a prey (or vice versa). To this aim, bait/prey constructs were generated (from the DSTT unit, University of Dundee) containing either a GAL4 DNA-binding domain or GAL4 DNA-activating domain. Transformed cells were then plated onto minimal medium lacking leucine (LEU), histidine (HIS) and tryptophan (TRP) to assay reporter gene activation. Selective media contained different concentrations of 3 AT (3-amino-1,2,4-triazole), a competitive inhibitor of the product of HIS3 gene. Under this condition the yeast will survive only if it can produce histidine, therefore only upon binding between the bait and the prey that will activate the transcription of the reporter gene. Moreover, to test positive interaction, cells were plated onto nitrocellulose filter paper that was frozen in liquid nitrogen and then placed onto a piece of filter paper impregnated with X-Gal (5-bromo-4-chloro-3-indolyl-β-D-galactopyranoside) to test for activity of β-galactosidase in cleaving its substrate lacZ to generate blue colonies (Fig. 3.5).

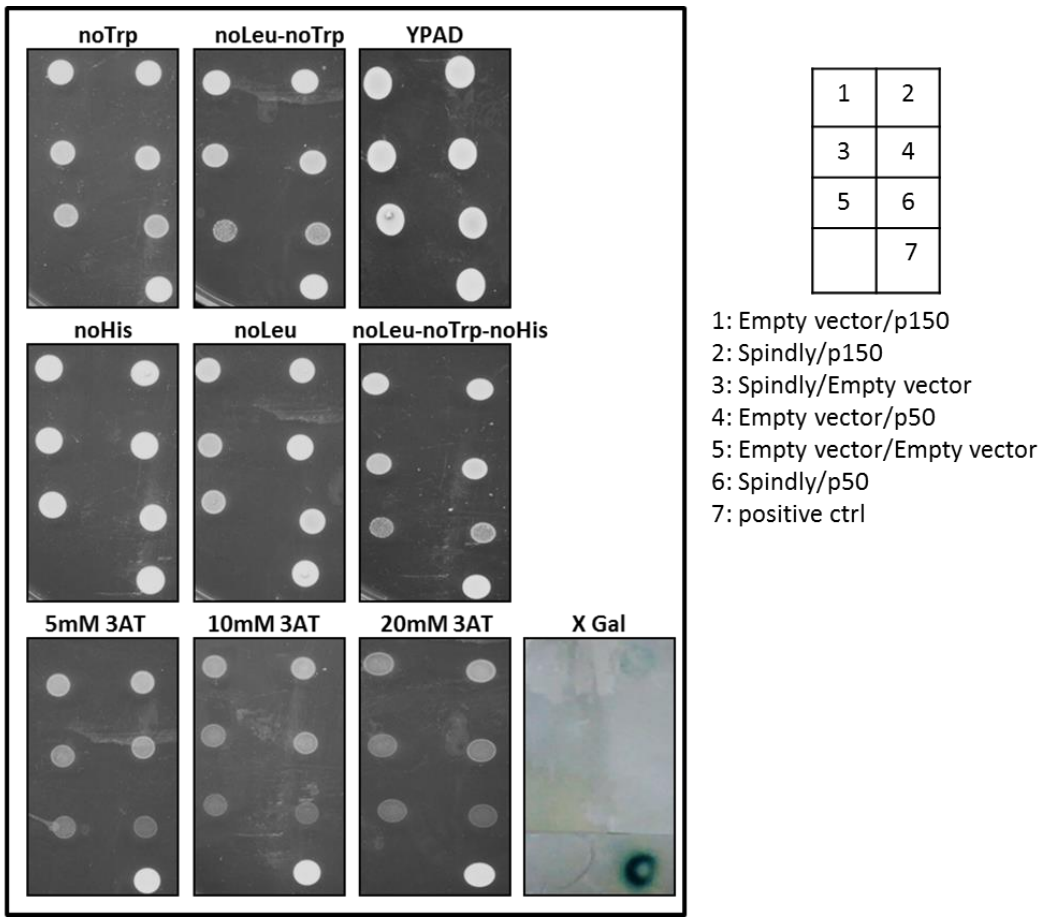


**Figure 3. 5. Spindly interacts with the p150 subunit of dynactin.**
Yeast two-hybrid assays were performed with a GAL4 DNA-binding domain fusion (or activation domain fusion) for each protein as indicated in the table on the right hand-side of the panel. Cells were grown on media lacking LEU, TRP and HIS and selected for histidine production by adding different concentrations of 3-AT or tested for lacZ reporter gene activity (XGal). Empty vectors were used as control. Positive control used were SLX4 (activating domain) and XPF (binding domain).

Experiment in figure 3.5 revealed that only when the Spindly construct was mixed with the p150 construct, cells grew on the selective media and promote LacZ activity; they instead did not show the same ability when Spindly and p50 constructs were mixed. Since Spindly is absent from yeast and the p150 construct was not active by itself, we can conclude that there is likely a direct association between Spindly and p150. However, it is important to point out that, although Spindly/p150 colony seemed to be the densest one, in the data presented the empty vector controls did show potential

cross-activation (basal growth visible), requiring further validation to prove the specificity of the interaction.

## 3.5 The interaction with dynactin relies on a specific region within Spindly

### 3.5.1 Substitution in the Spindly box affects kinetochore recruitment of p150

Spindly was identified in *D. mel.* as a critical recruiting factor of dynein but not of dynactin at KTs (Griffis *et al.*, 2007). Conversely, human Spindly was described as crucial for the recruitment of the whole motor complex and therefore it was proposed that it could be binding either of the multi-subunits of the complex. Subsequently, Gassmann and colleagues identified two single point mutations within the 'Spindly box', the conserved region present in all Spindly proteins, that could affect the capacity of Spindly to recruit dynein/dynactin to kinetochores (Gassmann *et al.*, 2010) (Fig. 3.6 (d)). Substitution of Serine 256 (or Phenylalanine 258) with Alanine produces a Spindly protein that, even if still able to bind to KTs, totally prevents the silencing of the checkpoint and leads to metaphase-arrest of cells (Gassmann *et al.*, 2010).

We therefore wondered if this single point mutation could disturb the direct binding of Spindly to the motor complex and, more precisely, the association with p150, which we described above. Hence, we decided to analyse the recruitment of dynactin to kinetochores upon expression of Spindly mutant. To this end, we performed immunostaining of HeLa cells depleted of the endogenous Spindly, but expressing GFP Spindly WT or S256A under stimulation with doxycycline (Fig. 3.6 (a) (b)).

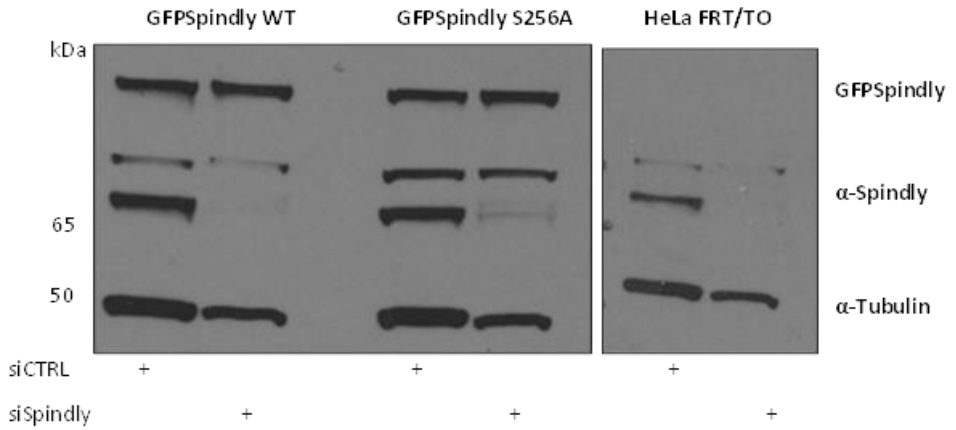
GFPSpindly WT
GFPSpindly S256A
HeLa FRT/TO
kDa
65
50
GFPSpindly
α-Spindly
α-Tubulin
siCTRL
siSpindly

(a)

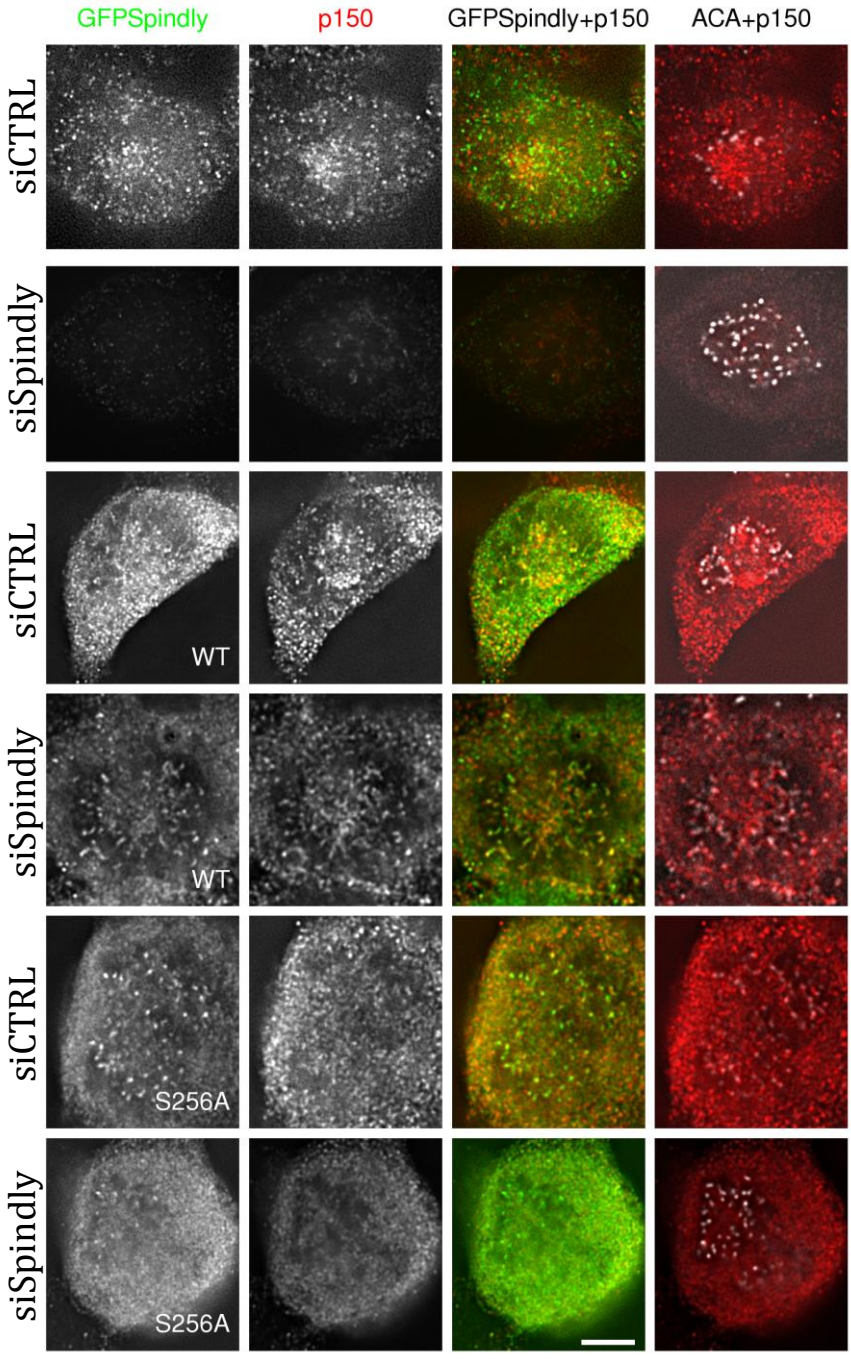
GFPSpindly
p150
GFPSpindly+p150
ACA+p150
siCTRL
siSpindly
siCTRL
WT
siSpindly
WT
siCTRL
S256A
siSpindly
S256A

(b)

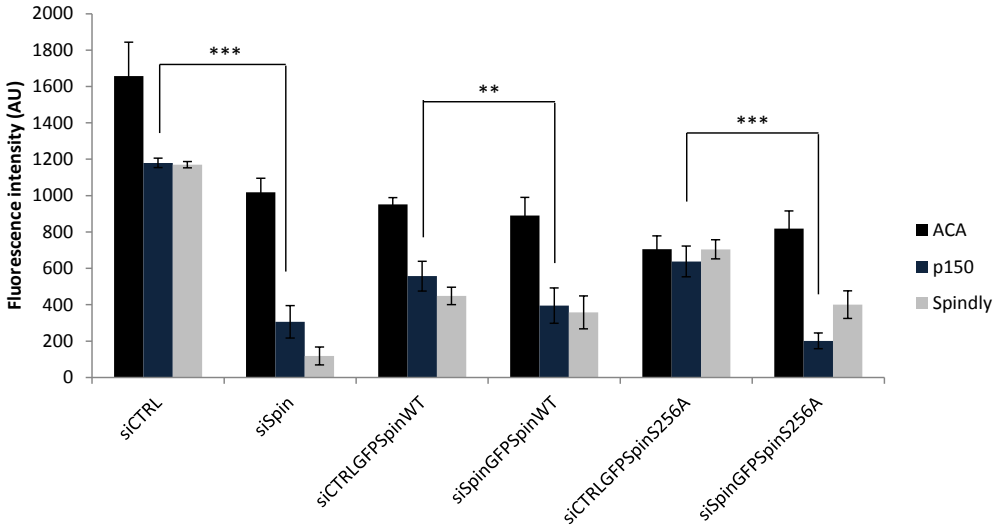


(c)

A

| | | | |
|---|---|---|---|
| *H. sapiens* 1-605 | 251 | NSK**GNSLFAEVED**RRAA | 267 |
| *M. Musculus* 1-608 | 251 | NSK**GNSLFAEVED**RRVA | 267 |
| *G. gallus* 1-608 | 251 | TSK**GNSLFAEVED**RRAE | 267 |
| *X. laevis* 1-610 | 252 | NSK**GNSLFAEVED**RRSE | 269 |
| *D. rerio* 1-590 | 253 | NSK**GNSLFSEVED**KRAA | 269 |
| *S. purpuratus* 1-564 | 206 | NKK**GNSLFAEVED**KRQA | 222 |
| *D. melanogaster* 1-807 | 229 | DRK**GNSLFAEVDD**QRQA | 245 |
| *C. elegans* 1-479 | 193 | AAR**GNSMFSEVID**AERK | 208 |

(d)

**Figure 3. 6. Single point mutation affects the recruitment of the motor complex.**
HeLa cells expressing indicated GFP-Spindly constructs were incubated for 96 hours with siRNA to deplete endogenous Spindly expression. To drive the expression of GFP-Spindly, doxycycline was administrated to a final concentration of 1µg/mL for a minimum 24 hours. (a) Western Blot confirmed Spindly silencing and GFP expression upon administration of doxycycline (1 µg/mL). (b) Immunofluorescence of HeLa cells expressing different Spindly constructs; staining shows: nuclei (DAPI, blue), Spindly (either endogenous or GFP tagged, green); dynactin (p150, red); kinetochore (ACA, white). 100X magnification. Scale bars: 5µm. (c) Graph shows relative fluorescence intensity levels of kinetochore recruitment of p150, Spindly and ACA. Fluorescence intensity at kinetochores was measured for different channels using the FiJi software (n ≥ 100). Mean ± standard deviation (represented by error bars) were determined from at least three independent experiments. Statistical analysis was performed with Excel and data were analysed by Student's *t-test* with significance defined by *: **= p< 0.005; ***= p<0.001. (d) Sequence alignment of the conserved motif in the Spindly protein family. Red arrow indicates the conserved Serine (S) that was mutated to Alanine (A) for the experiment.

Quantifications of immunofluorescence images (Fig. 3.6 (b) and (c)) confirmed defects in the kinetochore enrichment of dynactin (p150 subunit staining) when Spindly was

mutated within the 'Spindly box' (S256A) (Fig. 3.6 (c)), corroborating our hypothesis of a defective binding with dynactin upon mutation. Defects in p150 KT-association was highly specific for dynactin; indeed when we tested dynein recruitment we did not registered any defect upon Spindly depletion (data not shown).

### 3.5.2 Expression of Spindly mutants shows defective binding only with dynactin

To shed light on this relationship we collaborated with the Vale lab (namely with Dr. Richard McKenney, University of California, San Francisco) in order to test, by an *in vitro* binding assay, the capacity of Spindly, either WT or S256A, to bind dynein and dynactin. Spindly was purified from bacteria and dynein/dynactin complexes from fresh pig brains. The proteins were mixed together and Spindly and interactors were pulled down with StrepTactin agarose beads (as described in (McKenney *et al.*, 2014). Figure 3.7 reveals that Spindly S256A can bind only with dynein (DIC) but not with dynactin (p50 subunit). This result is in line with the underlined defects in p150 kinetochore-recruitment presented in figure 3.6 (b) and (c).

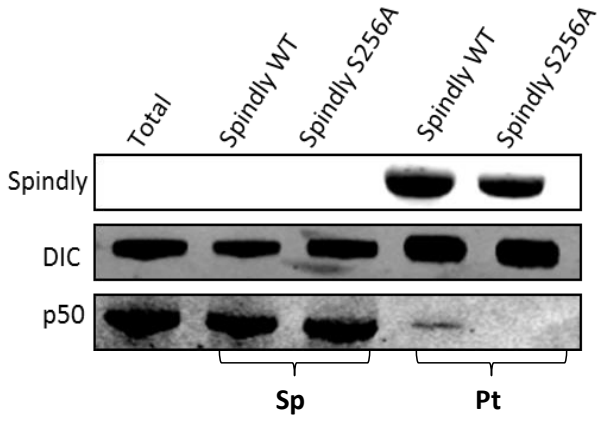


**Figure 3. 7. SpindlyS256A expression impairs the binding to dynactin.**
Recombinant full length human Spindly, WT or S256A were expressed and purified from bacteria. Dynein (DIC: dynein intermediate chain) and dynactin (p50/dynamitin subunit) complexes were separately purified from pig brains and mixed with the tagged Spindly attached to beads. The binding assay was performed as indicated in (McKenney *et al.*, 2014). Sp: supernatant; Pt: pellet. Experiment conducted in the Vale Lab by Dr. R.J. McKenney (University of California, San Francisco).

### 3.5.3 The Spindly box plays a crucial role in Spindly-dynactin association

Results above described led us to think that the mutation directly impaired the association of Spindly with dynactin. To corroborate this hypothesis, we decided to test the interaction in cells. To this aim we generated FLAG-Spindly constructs (WT or S256A) and expressed them in HEK293 cells. Using an anti-FLAG antibody we carried out a FLAG pull down. Data reported in figure 3.8 (a) confirms that the S256A mutation specifically affects the interaction between Spindly and dynactin, but it does not perturb the interaction with dynein. Furthermore, the yeast-two-hybrid assay using a Spindly S256A construct (either as a prey or as a bait), corroborate the impairment of the binding as a result of the mutation; it was possible to record positive interaction only when the yeast was transformed with the Spindly WT construct (Figure 3.8, (b)).

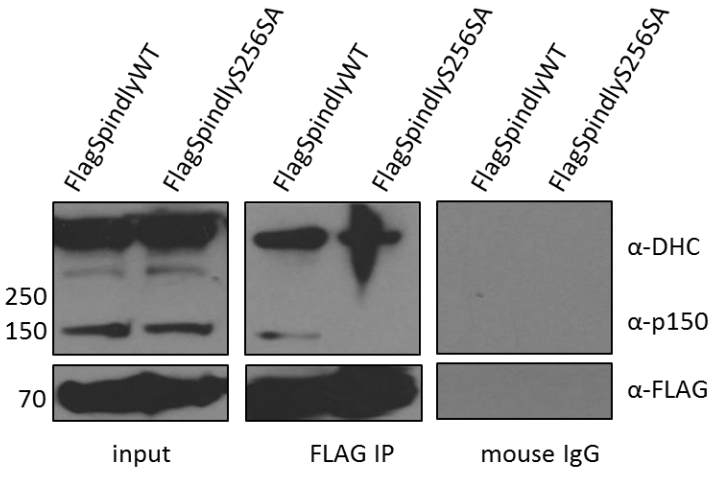


(a)

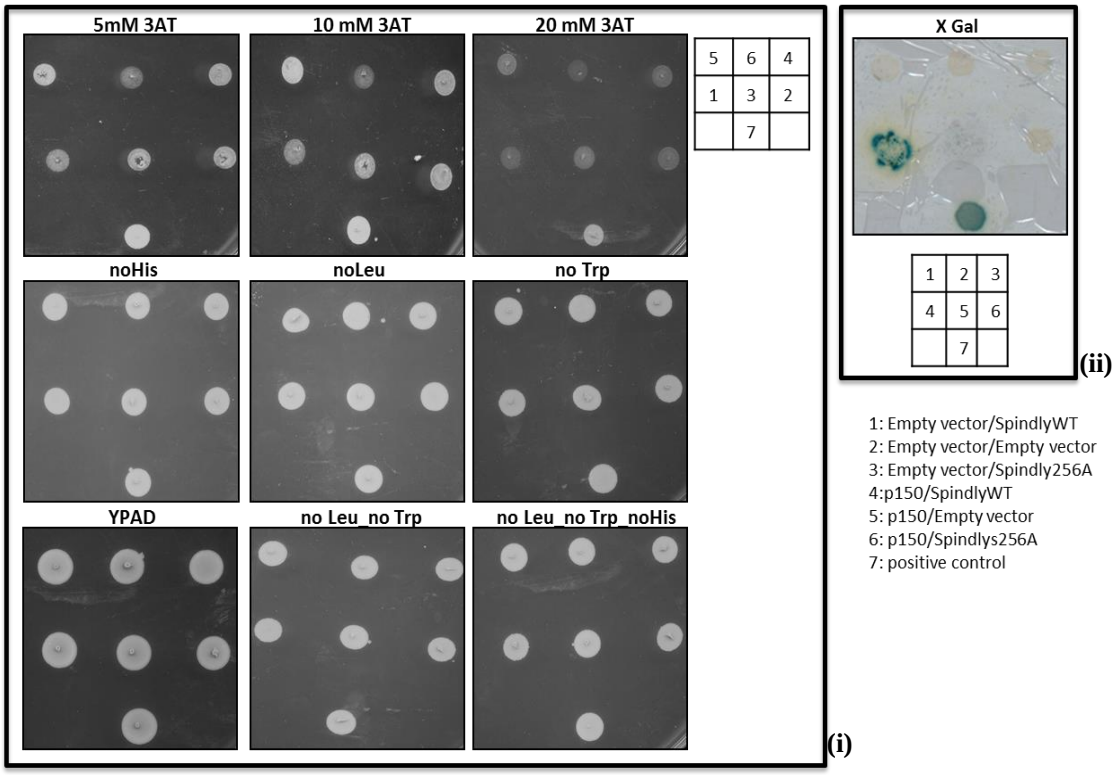


(b)

**Figure 3. 8. The serine 256 is crucial for Spindly association with dynactin.**
(a) HEK293 cells were transfected with the indicated constructs. 200/400 µg of total protein was used to immunoprecipitate FLAG-Spindly from the cells. Mouse IgG was used as negative control. Immunoprecipitated complexes were analysed by Western blot using the indicated antibodies. Inputs correspond to whole cell extracts. (b) Yeast two-hybrid assays were performed with a GAL4 DNA-binding domain fusion (or activation domain fusion) for each protein as indicated in the table on the top right corner of **(i)** and on the bottom side of **(ii)**. Cells were grown on media lacking LEU, TRP and HIS and selected for histidine production by adding different concentrations of 3-AT **(i)** or tested for lacZ reporter gene activity **(ii)**. Empty vectors were used as control.

Putting together our data we conclude that Spindly recruits the minus-end motor complex dynein/dynactin to kinetochores by binding the p150 subunit of the dynein-activator dynactin. This association requires the ‘Spindly box’ region. Our data also revealed that Spindly S256A can still pull down dynein (Fig. 3.8 (a)), hinting to an association that in this case does not go through the ‘Spindly box’ region and that is possibly dynactin-independent.

## 3.6 Discussion

The capacity of dynein to be processive is different in diverse species; *S.cerevisiae* dynein has to dimerise in order to be processive (Nishiura *et al.*, 2004) (Reck-Peterson *et al.*, 2006), while mammalian dynein has been reported to make a step 8nm long (as in the other species) only when multiple molecules of dynein interact with a microtubule, showing mainly diffusive movements when expressed by itself (Mallik *et al.*, 2004). Dynein utilises ATP hydrolysis to walk along microtubules, but it requires co-activators to promote active processive movements to reach the minus-end of a microtubule and to load cargos (Carter, 2013) (Schlager *et al.*, 2014).

Many studies have underlined the importance of dynactin for the execution of the different functions of dynein within cells (King and Schroer, 2000) (Culver-Hanlon *et al.*, 2006), but it has also been shown that it is not sufficient to change the movement rates of dynein along microtubules (Schlager *et al.*, 2014) (McKenney *et al.*, 2014). Over the years, many different adaptors that help dynein to bind specific cargos have been identified and more recent studies have pointed out how one of these, Bicaudal-D2 (BICD2), can work together with dynactin in order to promote the processivity of the motor (Kardon and Vale, 2009) (Vallee *et al.*, 2012) (Schlager *et al.*, 2014) (McKenney *et al.*, 2014). To date, dynein is the only processive minus end directed motor described in cells outside of plants, and thus the need of adaptors that promote the binding and the loading of specific cargos is of critical importance and strictly related with its high versatility.

Analysing our results we conclude that Spindly is a novel adaptor for the dynein/dynactin motor complex and hence it might help the motility of the motor along microtubules and potentially the direct loading of specific cargos. Figure 3.9 represents a schematic model of what we think could be happening: when Spindly is expressed in its endogenous wild-type form, it promotes the recruitment of the motor complex to the

kinetochore (KT); in turn the cargo is loaded onto the motor that subsequently moves along the microtubule (MT) (Fig. 3.9, (a)). Conversely, when Spindly is mutated within the 'Spindly box' (Spindly box*), the binding via p150 is defective, the cargo loading is impaired and the processivity of the motor along the MT is not enhanced (Fig. 3.9, (b)). So the motor still localises at KTs but it cannot be activated.

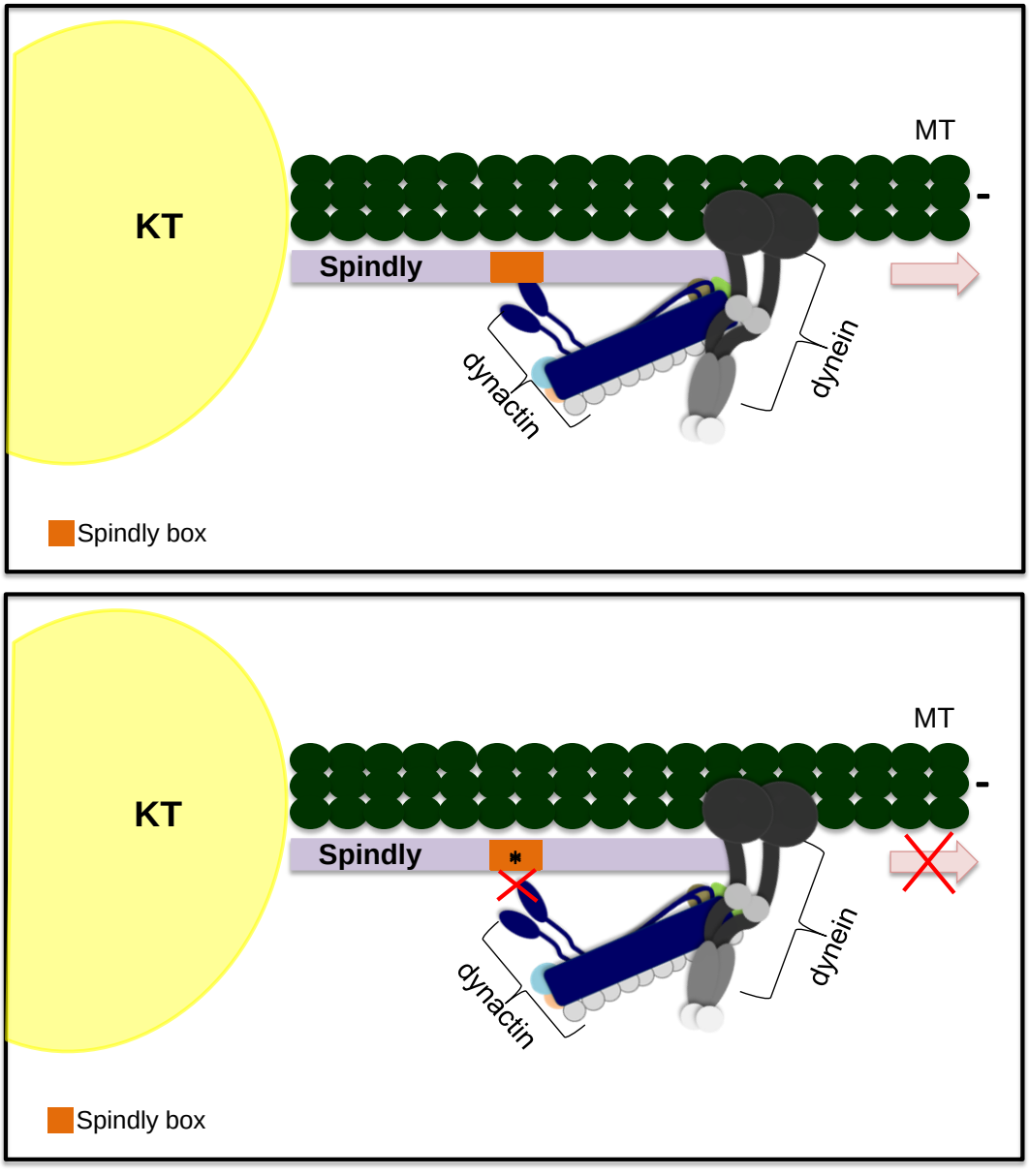


**Figure 3. 9. Schematic model of the ternary complex.**
(a) The presence of Spindly WT enhances the binding between dynein and dynactin, promoting the cargo loading and the movement towards the minus-end of a microtubule (MT); (b) on the other hand, when Spindly is mutated within the Spindly box (Spindly*), the binding with dynactin is impaired with consequent defects in the motor processivity and in the cargo.

It is important to notice that in our study we demonstrated how Spindly S256A can still bind to dynein (Fig. 3.7; Fig. 3.8); this is in line with previous studies that described Spindly mutants still able to sustain correct chromosome alignment (Gassmann *et al.*, 2010) and allow for normal dynein streaming process from kinetochores (Dr. K. Vaughan personal communication). However, it has been revealed how instead the same mutation on Spindly abrogates dynein-kinetochore recruitment leading to chromosome segregation defects similarly to Spindly depletion phenotypes (Cheerambathur *et al.*, 2013). Consequently, to date, the mechanism through which dynein gets recruited to kinetochore is still not entirely defined. The initial model proposed, by which dynein is localised to KTs via the RZZ complex and Spindly seems to be incomplete; it appears to be not comprehensive for all of the interactions identified up to the present time. Indeed, conflicting reports have stated that either dynein requires dynactin-mediated interaction with the RZZ complex to be localised, or, in a totally opposite direction, dynein can be assembled at kinetochores in absence of the RZZ complex, binding via the factor NudE/NudEL (Starr *et al.*, 1998) (Stehman *et al.*, 2007). Obviously clarity needs to be gained, but it is definitely conceivable that there is a handoff between different recruitment factors that allows for the targeting of dynein and consequently for the execution of all its functions at the kinetochore. It also raises the possibility that some of the actions of dynein at the KT do not require processivity (namely overcoming the RZZ-dependent inhibition of KT-MT binding) and hence do not require association with dynactin, while other activities (such as SAC streaming or KT gliding) are processive and dependent upon dynactin binding. Future experiments will be needed to sort out these possibilities.

# 4 . Spindly is an active player of the Spindle Assembly Checkpoint

## 4.1 Introduction

The Spindle Assembly Checkpoint (SAC) is the mitotic checkpoint necessary to ensure that chromosome alignment proceeds towards anaphase onset with the right timing; it senses the status of kinetochore-microtubule attachments (or tension) and generates a signal that prevents anaphase until all chromosomes are correctly aligned on the spindle (Musacchio, 2011) (Lara-Gonzalez *et al.*, 2012).

As already described (see **1.2.3**), the activation and the perpetuation of the signal are based on the presence on kinetochores of the SAC components: Mps1, Bub1, Bub3, Mad1, Mad2, Mad3/BubR1 and Cdc20 (Foley and Kapoor, 2013). The mitotic checkpoint complex (MCC: Mad2-Cdc20 plus BubR1-Bub3) prevents mitosis progression by inhibiting the ubiquitin ligase activity of the APC/C complex and preventing the degradation of Cyclin B and Securin, which respectively establish and maintain the mitotic phospho-environment and inhibit Separase to prevent the cleavage of the cohesin molecules that link sister chromatids (Musacchio, 2011) (Lara-Gonzalez *et al.*, 2012). Once bi-orientation is achieved, the SAC is silenced and the activity of the APC/C can drive anaphase onset. Several processes contribute to the silencing: disassembly of the MCC, recruitment of phosphatases to KTs and physical removal of the SAC components from KTs (Wang *et al.*, 2014). This latter step is mediated by the minus-end directed motor dynein and, as discussed in the previous chapter, its localisation is directly dependent upon Spindly recruitment at KTs (Griffis *et al.*, 2007). Indeed, any treatment that affects dynein localisation at kinetochores (such as dynein inhibition or expression of the SpindlyS256A mutant) causes retention of Spindly and checkpoint proteins at KTs (Griffis *et al.*, 2007) (Gassmann *et al.*, 2010). Conversely, elimination of Spindly function (by depletion of either Spindly itself or a component of the RZZ complex) allows for SAC silencing even without dynein recruitment to KTs

(Gassmann *et al.*, 2008). All together these previous reports indicate that Spindly could play a function in SAC activation and/or maintenance.

In this chapter a crosstalk between Spindly and some of the components of the mitotic checkpoint is shown. We identified novel mitotic binding partners of Spindly directly involved in SAC signalling or assembly (Mps1, BubR1, CENP-E and CENP-F). We also described an interaction between Spindly and PP2A, a phosphatase recently demonstrated to be a key player in the checkpoint silencing process that could suggest how the cell coordinate the SAC inactivation step (Espert *et al.*, 2014) (Nijenhuis *et al.*, 2014).

Overall, data here presented indicate that Spindly, apart from a function in mitotic checkpoint silencing, acts in maintaining the checkpoint signalling mostly via its association with BubR1.

## 4.2 Spindly binds kinetochore via the RZZ complex

The assembly of the spindle checkpoint relies on kinetochores (Foley and Kapoor, 2013). As described in the introduction (see **1.2.2**), the kinetochore contains an outer plate on which several proteins are rapidly assembled at the beginning of mitosis, where the mitotic checkpoint effectors are recruited (Joglekar *et al.*, 2006) and the RZZ (Rod-Zwilch-Zw10) complex ((Karess, 2005), and Spindly exert their function (Griffis *et al.*, 2007).

A recent paper from Varma and co-workers has depicted Spindly as a long rod-shaped protein that binds kinetochores via its *C*-terminal region by interacting with the RZZ complex (Varma *et al.*, 2013). To confirm this idea, we performed immunoprecipitation experiments using HEK293 cells, mitotically enriched by overnight treatment with S-trityl-L-cysteine (STLC; a specific inhibitor of the kinesin Eg5 that induces monopolar spindles and arrests cells in M phase (Skoufias *et al.*, 2006)) and then released for two hours into Colchicine (an inhibitor of microtubule polymerisation (Taylor, 1965)). Mitotic cells were collected by shake-off and immunoprecipitation was then carried out by incubating cell lysates with an anti-Spindly antibody overnight (Fig. 4.1). Results from this pull-down corroborate the hypothesis that Spindly binds to the RZZ complex (Fig. 4.1).

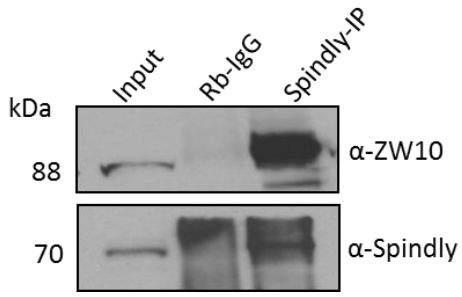


**Figure 4. 1. Spindly interacts with the RZZ complex.**
HEK293 cells were enriched in mitosis and immunoprecipitation was performed with anti-Spindly antibody. Rabbit IgG (Rb- IgG) were used as negative control. Samples were blotted with indicated antibodies. Input represents the whole cell lysate.
Samples used in this experiment have already been presented in this thesis (see Fig. 3.2).

## 4.3 Crosstalk between Spindly and the SAC molecular players

The RZZ complex plays a role in the recruitment of Mad1/Mad2 complex and consequently also in SAC activation (Buffin *et al.*, 2005) (Kops *et al.*, 2005). Given the interaction between Spindly and ZW10, we wondered whether KT recruitment of Spindly could be involved as well in the assembly or amplification of the whole checkpoint signalling. Hence, it was decided to study the interaction between Spindly and different SAC effectors. To this end, HEK293 cells were transfected with BubR1, Bub1, Mad1 or Mps1 - YFP expression vectors, or an empty vector (YFP-E) and, after 40 hours from transfection, we mitotically enriched the cell population by adding Nocodazole (an inhibitor of microtubules polymerisation (Spurck *et al.*, 1986)) overnight. Cells were subsequently harvested by mitotic shake-off and immunoprecipitation was performed with anti-Spindly antibody (Fig 4.2).

Figure 4.2 indicates that there is an association of Spindly with BubR1 and Mps1, while results were not very convincing for interactions with Mad1 and Bub1. Data obtained substantiates the starting hypothesis that Spindly is involved within the spindle assembly checkpoint pathway.

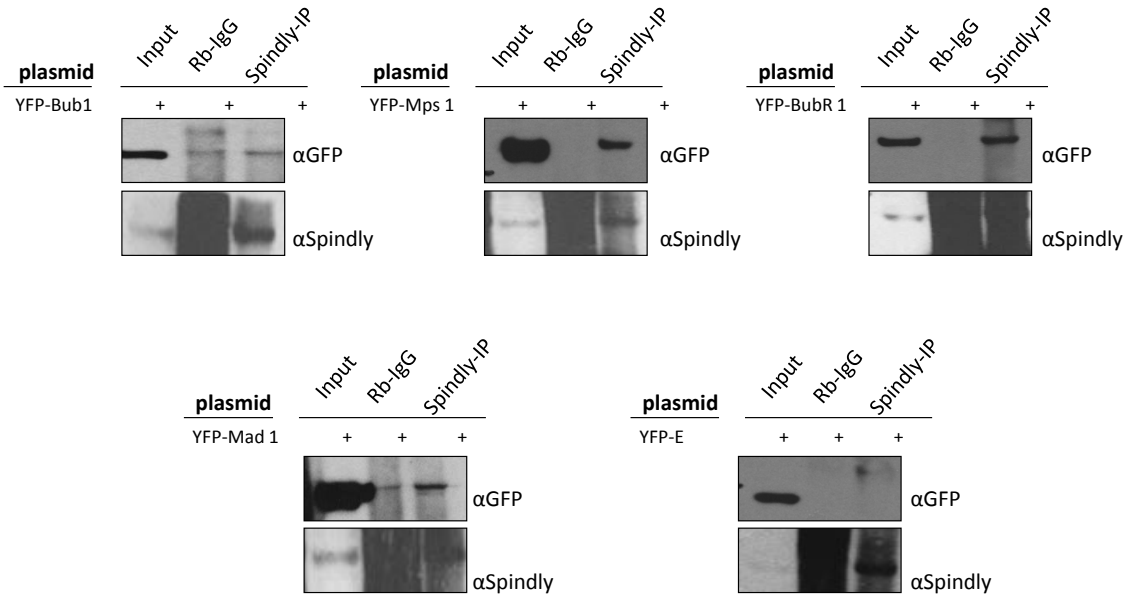


**Figure 4. 2. Spindly interacts with SAC components.**
HEK293 cells were transfected with YPF-SAC proteins (as indicated in the figure) and enriched in mitosis (Nocodazole 40ng/mL). Immunoprecipitation was performed with anti-Spindly antibody and samples were analysed by Western blot. Rabbit IgG were used as negative control for all the samples. Antibodies as indicated. Input represents the whole cell lysate. YPF-E: YFP-empty vector.

Bearing in mind that data in figure 4.2 were obtained under the conditions where SAC proteins were over-expressed, we decided to use size-exclusion chromatography to further study the association between Spindly and the SAC components at endogenous levels. To this end, HEK293 cells were mitotically enriched by double Thymidine block and release in Nocodazole for 12 hours. Thymidine inhibits DNA synthesis synchronising cells in S phase (Thomas and Lingwood, 1975), so then the release in Nocodazole allows cells to proceed to M phase where they will be halt again, since the lack of MTs will trigger SAC activation (Spurck *et al.*, 1986).

Fractionation was performed on a SEC-1000 column and fractions were probed for different SAC components by Western blot (Fig. 4.3).

Figure 4.3 reveals that Spindly and BubR1 partially co-elute (panel (b), C fractions (~ 250 kDa)) suggesting that these two proteins could be within the same complex.

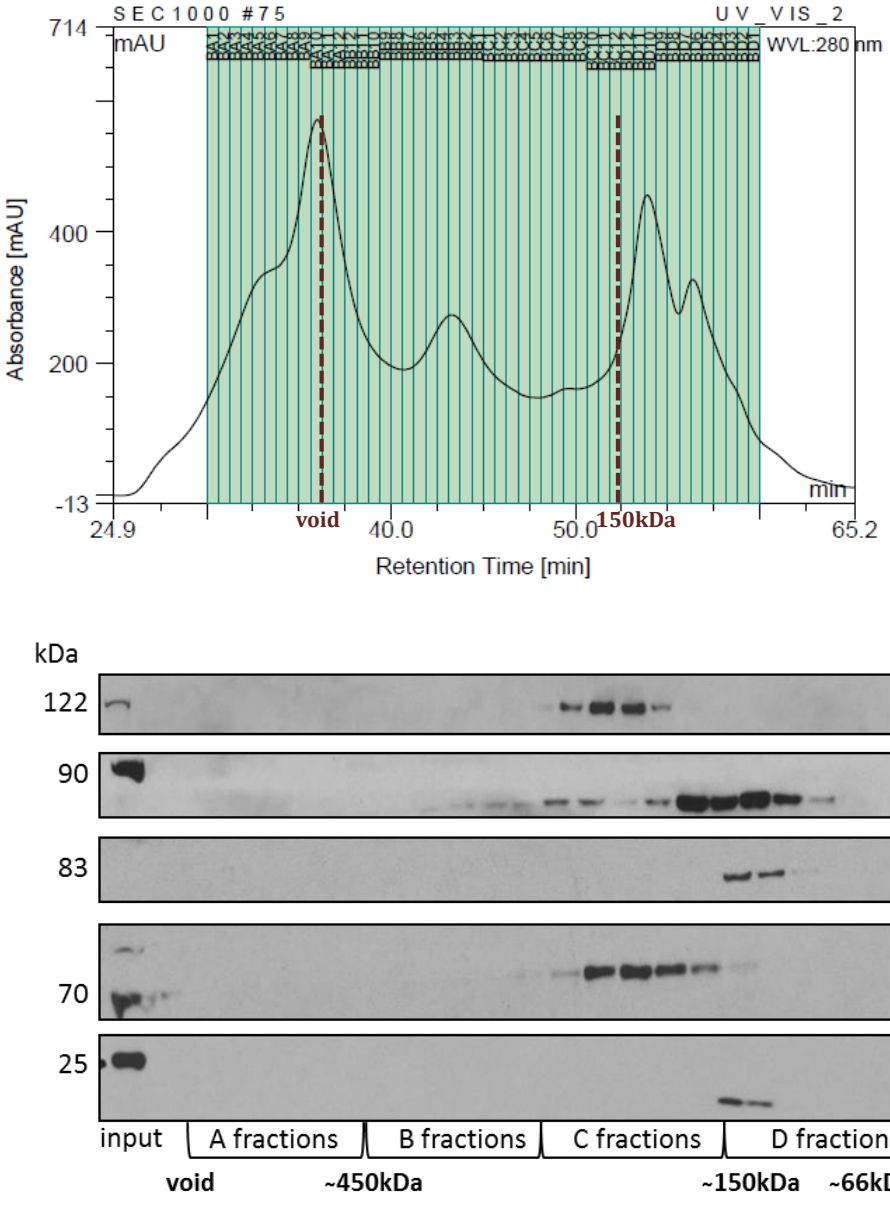


**Figure 4. 3. Spindly co-elutes with BubR1.**
HEK293 cell lysates mitotically enriched by double Thymidine (2mM) block and released in Nocodazole (40 ng/mL) for 12 hours, were fractionated through a SEC-1000 column. (a) Elution profile of the total cell lysate; (b) Western blot analysis for the indicated antibodies. Input represents the whole cell lysate.

Interestingly, Mad1 and Mad2 co-elute with ZW10, which indicates therefore a presence of two separate complexes containing SAC components at kinetochores (Fig. 4.3, panel (b), D fractions (~150 kDa)).

This is in line with data from other laboratories that have already identified the association of different proteins of the SAC with different kinetochore proteins: whereas Mad1/Mad2 associate with kinetochores thanks to the RZZ complex (Buffin *et al.*, 2005), BubR1-Bub3 bind through Bub1/Knl1 (Sharp-Baker and Chen, 2001).

To further validate this result we immunoprecipitated Spindly from C and D fractions (see Fig. 4.3) and confirmed the interaction with BubR1 (Fig. 4.4).

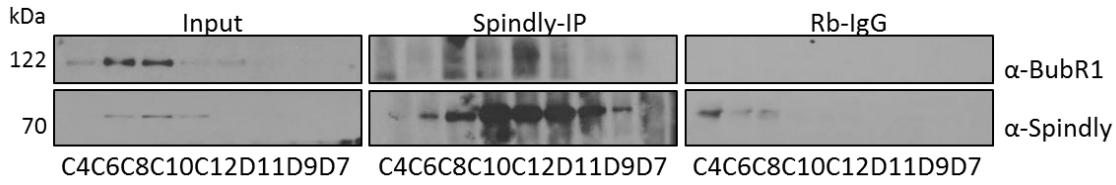


**Figure 4. 4. Spindly immunoprecipitates BubR1.**
Immunoprecipitation of endogenous Spindly from SEC- fractions (Cs and Ds) was performed using anti-Spindly antibodies. 200 µl of the original fraction were used to immunoprecipitate Spindly. Rabbit IgG were used as negative control. Samples were analysed by Western blot with the indicated antibodies. Input represents the starting material.

Data collected from these assays support our hypothesis of a physical crosstalk between Spindly and the SAC, likely to be mediated via BubR1. In fact, although BubR1 is loaded onto kinetochores earlier (in prophase) it could be an adaptor partly responsible for targeting Spindly to or stabilising it onto kinetochores.

## 4.4 Spindly and SAC checkpoint proteins interact "*in vivo*"

Rapamycin is a small molecule that can induce dimerisation of the proteins FKBP12 (or FKBP) and mTOR (or mTOR's minimal rapamycin binding fragment FRB). This dimerisation capacity has been established as a technique that allows controlling the association of two proteins (expressing FKBP and FRB tags) in living cells (Putyrski and Schultz, 2012).

To corroborate our previous results, we sought to analyse the interaction between Spindly and different SAC components "*in vivo*", taking advantage of this method. We thus generated a mCherry-Spindly-FKBP tagged construct that will bind to any protein containing a FRB domain upon addition of rapamycin. We have chosen to use a Lin11-FRB to drive the mis-localisation of mCherry-Spindly-FKBP to the plasma membrane, so we will be able to screen for positive interaction upon co-localisation of mCherry and YFP proteins at the plasma membrane (Fig. 4.5).

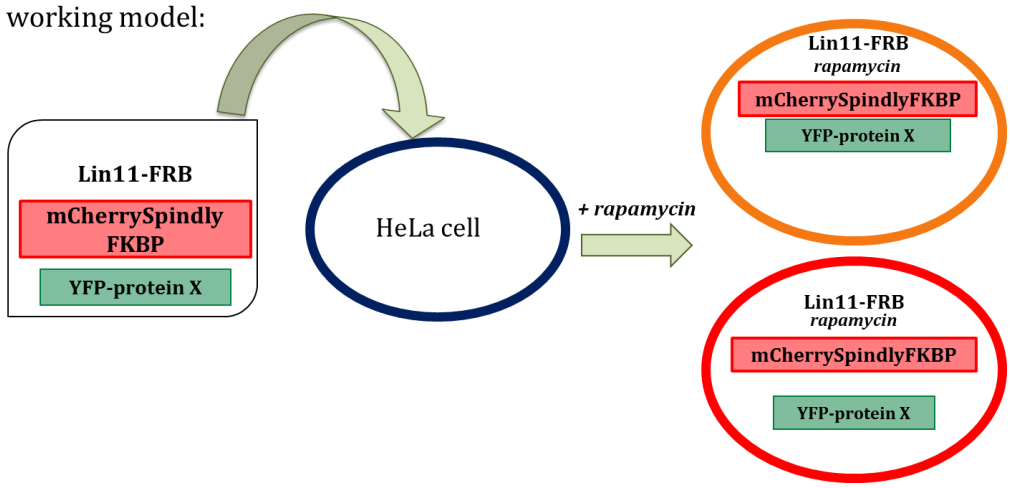


**Figure 4. 5. The FRB-FKBP system.**
Schematic representation of the work flow for cell transfection and subsequent rapamycin mis-localisation assay. Screening was carried out by looking for either red plasma membrane (= interaction does not occur) or orange plasma membrane (= interaction does occur).

We tri-transfected HeLa cells with the YFP tagged protein of interest (the different SAC effectors to test), Lin11-FRB and mCherry-Spindly-FKBP. After about 40 hours from the transfection, we treated cells with rapamycin (4 μM for 1 hour at 37°C), then fixed with PFA and visualised protein localisation.

Figure 4.6 (a) demonstrates the mis-localisation of BubR1, Mad2 and Mps1 to the plasma membrane upon rapamycin administration (left-hand side panel). Conversely, Mad1 and Bub1did not mis-localise to the plasma membrane upon treatment. Also, we observed only a weak interaction of Spindly with ZW10, suggesting that their association could be mitotic specific. Panel (b) in figure 4.6 indicates neither membrane localisation for the FKBP construct when transfected on its own nor background YFP-fluorescence.

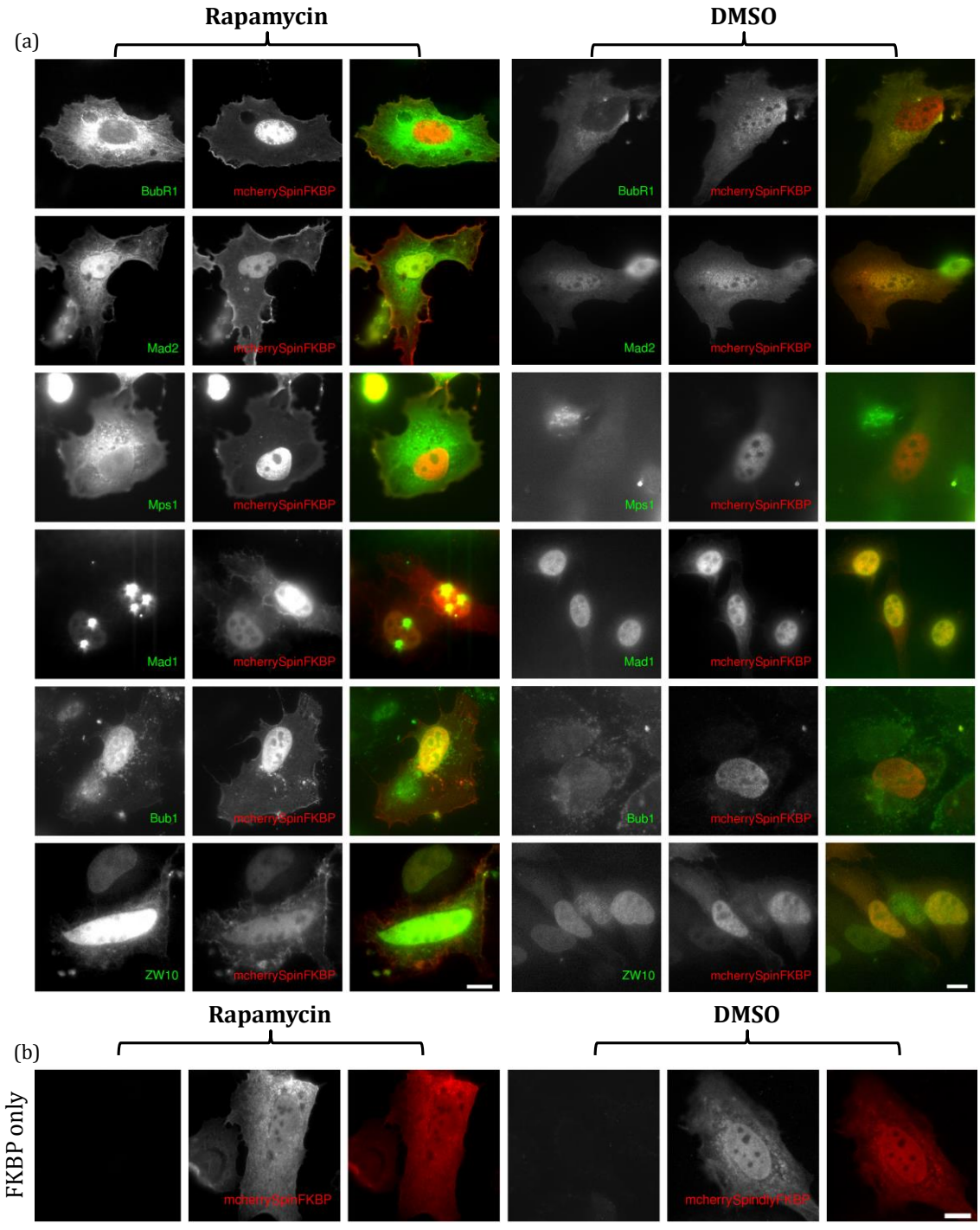
Rapamycin
DMSO
(a)
BubR1
mcherrySpinFKBP
Mad2
Mps1
Mad1
Bub1
ZW10
(b)
FKBP only
mcherrySpindlyFKBP

(c)

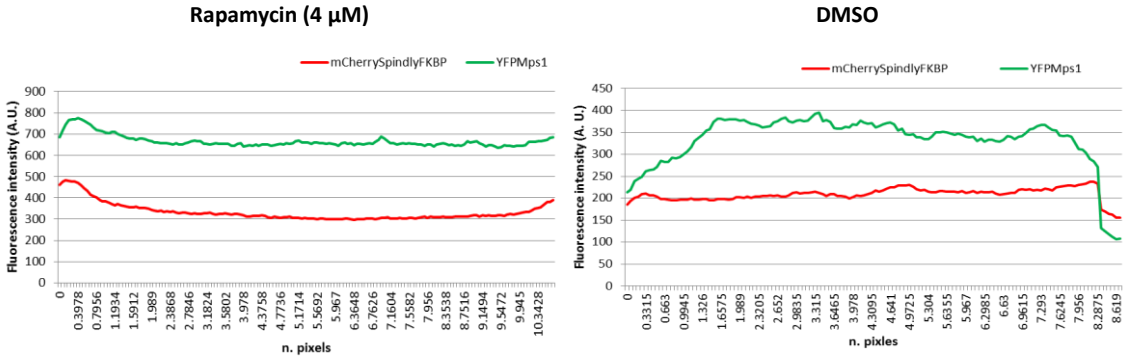


**Figure 4. 6. Mis-localisation of Spindly reveals interaction with SAC components.**
(a) HeLa cells were transfected with the indicated SAC component (YFP tagged), mCherrySpindly-FKBP and Lin11-FRB for 40 hrs. Rapamycin (4 µM) was administered for 1 hour (at 37 °C) and then cells were visualised: SAC protein (green), Spindly (red). (b) Cells were transfected only with the FKBP construct and treated with rapamycin as negative control. Left-hand side panel Rapamycin treated samples; right-hand side DMSO treated samples. 60X magnification. Scale bar 10µm.
(c) Measurements conducted for Mps1 mis-localisation recruitment at the plasma membrane; values were obtained by drawing a line between the two edges of the cell (excluding carefully the nucleus, where often an over-expression was registered) and then the fluorescence intensity was measured using a plug-in in FiJi (multichannel plug-in) and plotted with Excel. Similar measurements were conducted for all the SAC components tested. For each experiment 50 cells were measured and then the average values for each channel were plotted.

It has been reported that the recruitment of Spindly at KTs is dependent on the RZZ complex, since defects in ZW10 expression abrogate this process and also that the Spindly *C*-terminus is important for its KT localisation (Griffis *et al.*, 2007) (Gassmann *et al.*, 2008) (Barisic *et al.*, 2010). We therefore hypothesise that Spindly associates to KTs via its *C*-terminus in relation with the RZZ complex. To validate this hypothesis, we generated a mCherrySpindly-FKBP construct truncated of the C-terminal region (1-520 amino acids) and repeated the rapamycin mis-localisation experiment (Fig. 4.7).

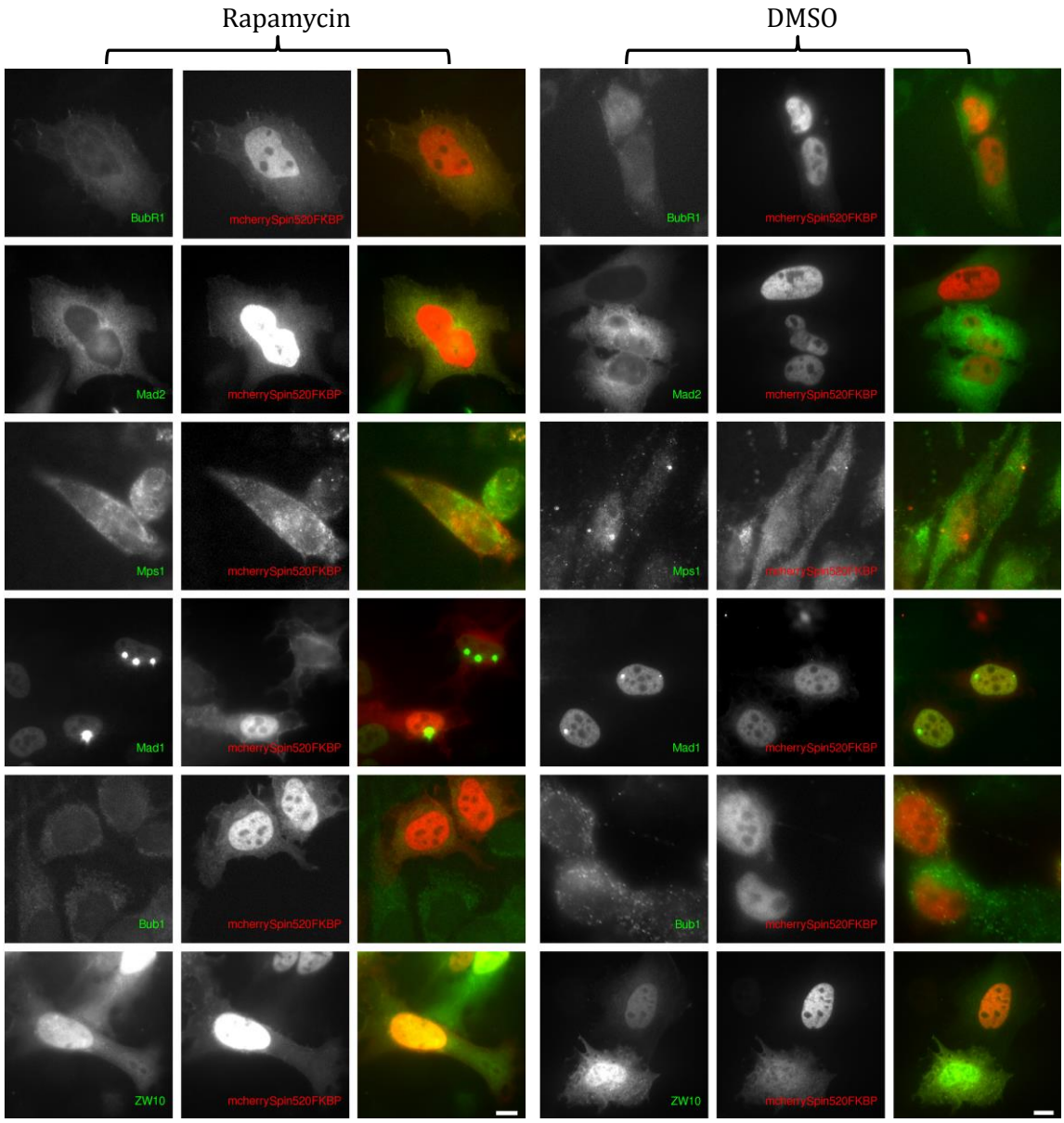


**Figure 4. 7. mCherry-Spindly520-FKBP can still interact with ZW10 and with the SAC components.**
HeLa cells were transfected with different YFP-tagged proteins, mCherry-Spindly520-FKBP and Lin11-FRB for 40 hrs. Rapamycin (4 μM) was administered for 1 hour (at 37 C) and then cells were fixed and visualised: SAC protein (green), Spindly (red). Left-hand side panel Rapamycin-treated samples; right-hand side DMSO-treated samples. 60X magnification. Scale bar 10μm.

Figure 4.7 reveals that all the proteins tested are still able to associate with Spindly at the plasma membrane as in the WT experiment (Fig. 4.6), suggesting that the *C*-terminus is not the site required for binding or at least it is not the only site involved (Fig. 4.7) (for measurements analysis see graphs in **Chapter 8.** Appendix- Fig. 8.2).

Previous reports have already revealed that Spindly possesses different sites for KT-binding within its structure besides those present in the *C*-terminus (Barisic *et al.*, 2010) (Moudgil *et al.*, 2015); our data therefore confirm that the *C*-terminus of Spindly is dispensable for association with kinetochore/SAC components.

## 4.5 Identification of novel binding partners for Spindly in mitosis

To identify novel mitotic proteins interacting with Spindly, it was decided to exploit the mass spectrometry (MS) technique to gain insights into the prometaphase complex of which Spindly could be a component.

HEK293 cells were mitotically enriched and harvested by mitotic shake-off upon overnight treatment with either STLC or Nocodazole. Cells without mitotic drug treatment were also collected as control. We used these two treatments with the aim to analyse two different statuses of KT-MT attachments that we think could give us different interactors of Spindly. Nocodazole is a drug that arrests cells in M phase; it inhibits MTs polymerisation and therefore the formation of the metaphase spindle, blocking the cells in prometaphase and leaving KTs unattached (Spurck *et al.*, 1986). On the other side, STLC is a potent inhibitor of kinesin Eg5 that arrests cells similarly in M phase, but in this case they are able to make a dense microtubule network since this drug does not affect microtubules polymerisation (Skoufias *et al.*, 2006). STLC treated cells halt in mitosis with a monopolar spindle; so in this case KT-MT attachments occur and therefore the interactions between proteins at KTs are different.

Cells were lysed and immunoprecipitation was performed by incubation with anti-Spindly or control Rabbit IgG antibodies overnight (Fig. 4.8, (a)). Subsequently, samples were fractionated by SDS-PAGE and the gels were stained. The lanes were split into three horizontal sections (as indicated from red lines in Fig. 4.8, (b)) and into eight vertical sections (as indicated from black lines in Fig. 4.8, (b)) and the gel pieces were processed for mass spectrometry analysis (see **2.9**). In parallel, samples were run to confirm positive pull-down of endogenous Spindly from all the samples (Fig. 4.8 (a)).

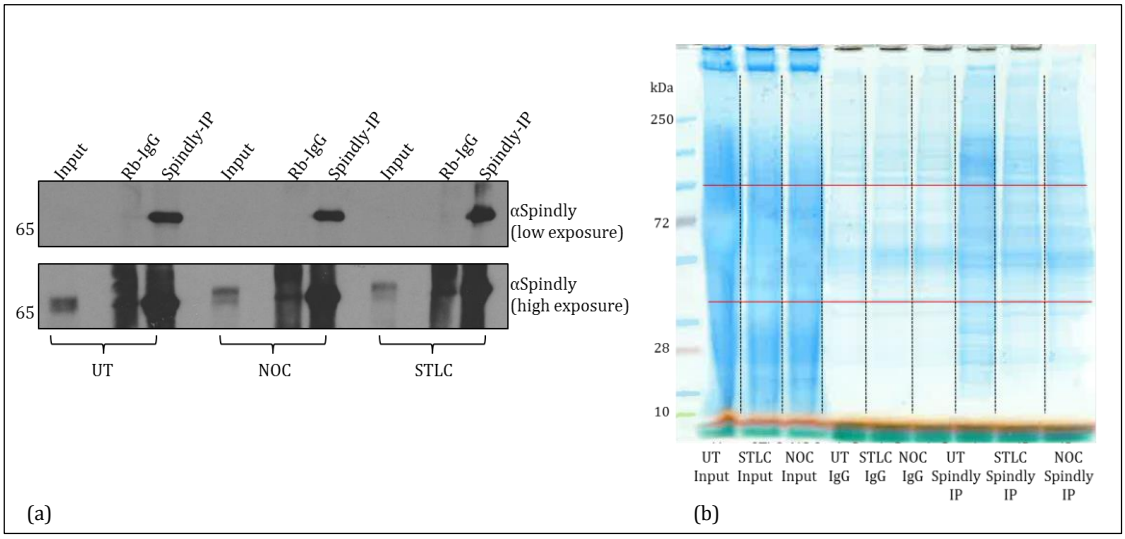


**Figure 4. 8. Spindly-IP for mass spectrometry analysis.**
(a) HEK293 cells were enriched in mitosis and immunoprecipitation was performed with anti-Spindly antibody. Rabbit IgG was used as negative control. Samples were then blotted with indicated antibodies Input represents the whole cell lysate. (b) The immunoprecipitates were resolved on a SDS-polyacrylamide gel and stained with Instant Blue. Gels were divided into the indicated sections (black and red lines) and processed for mass spectrometry analysis. UT: untreated samples; NOC: nocodazole-treated samples; STLC: s-tritryl-L-cysteine treated samples.

Analysis of the datasets obtained was conducted with the MaxQuant software (Cox and Mann, 2008), aimed to identify proteins enriched in the Spindly immunoprecipitation samples. This software allows us to run the .raw data against a contaminant database, to eliminate possible contaminants (like keratins) present in our datasets, as well as against a Human reverse database, to eliminate all the false positive hits (those that will align with this database will be discarded). After this initial analysis, we subsequently screened our datasets for mitotic and kinetochore enriched proteins that could be part of the 'Spindly-mitotic complex'. Specifically we took into account the number of peptides identified for each protein and the intensity value at which they were identified. We compared the list obtained for the "Spindly IP" dataset with the "IgG" dataset (our negative control) and proceeded with the analysis only for those proteins that gave an intensity value equal to zero in the "IgG" dataset.

Figure 4.9 summarises the data from the mass spectrometry analysis. In the left hand-side (**(i)**) of panel 1 are tables highlighting all the mitotic related proteins enriched in the Spindly-IP datasets under different conditions: untreated cells (UT) (a), Nocodazole treated cells (NOC) (b), and STLC treated cells (c); in the right hand-side (**(ii)**) of panel 1 instead is represented a network analysis performed using the String-bd software (Jensen *et al.*, 2009) for all the conditions tested. This analysis allows to link proteins according to the information already available on physical and functional protein-protein interactions, proved either by experimental data or computationally prediction (see legend underneath each network analysis, Fig. 4.9, panel (1), **(ii)**). Panel 2 is a summary of the identified protein functions obtained from the UniProt Human Database.

**(1)**

| KT BINDING PROTEINS | PEPTIDE | INTENSITY SpindlyIP | INTENSITY IgG |
|---|---|---|---|
| CENP-F | 81 | 12206621 | 0 |
| CENP-E | 35 | 6929300 | 0 |
| KNTC1 (ROD) | 6 | 3418200 | 0 |
| Spc25 | 3 | 1033200 | 0 |
| SAC RELATED PROTEINS | | | |
| BUB1B | 9 | 1931000 | 0 |
| CDC23 | 10 | 3002890 | 0 |
| CDC16 | 5 | 3429220 | 0 |
| PHOSPHATASES | | | |
| PP2A B56 | 6 | 1171100 | 0 |
| CENTROSOME ASSOCIATED PROTEINS | | | |
| NUMA1 | 12 | 2083500 | 0 |
| DYNEIN/DYNACTIN | | | |
| DYNEIN 2 HEAVY CHAIN | 4 | 1241200 | 0 |
| DYNACTIN subunit 5 (p25) | 1 | 568240 | 0 |

**(i)**

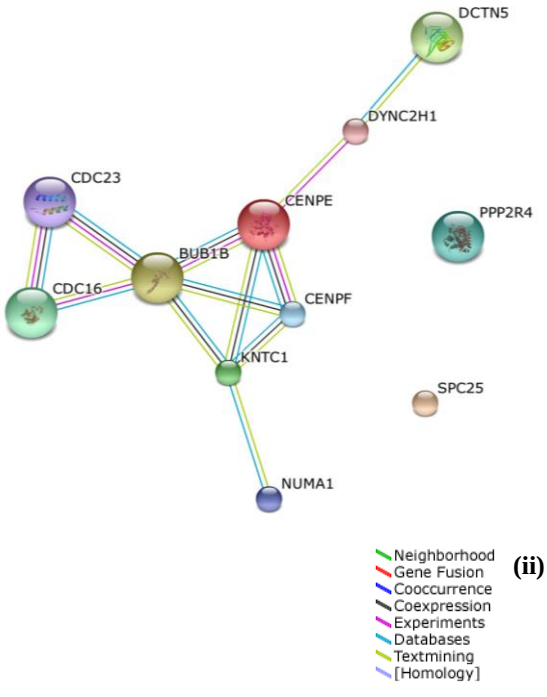


**(ii)**

(a)

| KT BINDING PROTEINS | PEPTIDE | INTENSITY SpindlyIP | INTENSITY IgG |
|---|---|---|---|
| CENP-F | 81 | 81830590 | 0 |
| CENP-E | 35 | 16080000 | 0 |
| KNTC1 (ROD) | 6 | 600330 | 0 |
| SAC RELATED PROTEINS | | | |
| BUB1B | 9 | 1185600 | 0 |
| MAD2 | 11 | 411520 | 0 |
| CDC16 | 5 | 407640 | 0 |
| PHOSPHATASES | | | |
| PP2A B56 iso delta | 6 | 524270 | 0 |
| PP2A B55 | 3 | 126810 | 0 |
| PP1 subunit 12 | 7 | 1393539 | 0 |
| PP1 subunit 8 | 4 | 919300 | 0 |
| CENTROSOME ASSOCIATED PROTEINS | | | |
| PERICENTRIN | 36 | 15200000 | 0 |
| DYNEIN/DYNACTIN | | | |
| DYNEIN 2 HEAVY CHAIN | 4 | 1421100 | 0 |
| DYNACTIN subunit 5 (p25) | 1 | 52795 | 0 |

**(i)**

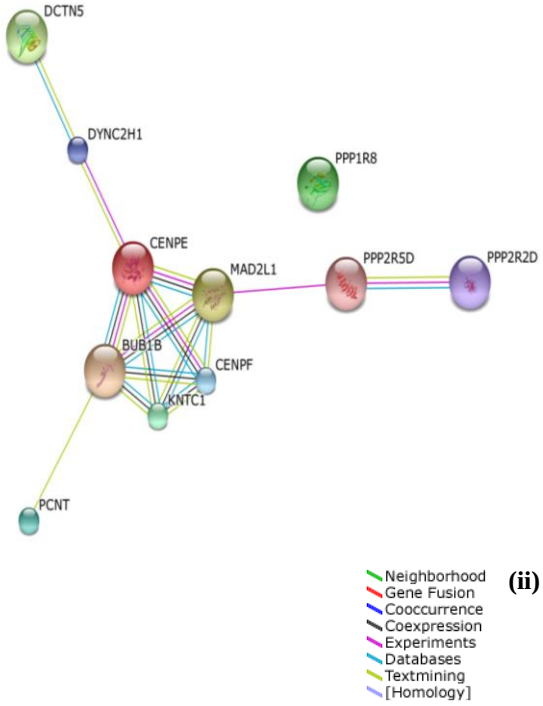


**(ii)**

(b)

| KT BINDING PROTEINS | PEPTIDE | INTENSITY SpindlyIP | INTENSITY IgG |
|---|---|---|---|
| CENP-F | 81 | 16028542 | 0 |
| CENP-E | 35 | 4829500 | 0 |
| SAC RELATED PROTEINS | | | |
| BUB1B | 9 | 1547660 | 0 |
| CDC23 | 10 | 1700900 | 0 |
| CDC27 | 10 | 2491600 | 0 |
| PHOSPHATASES | | | |
| PP2A B56 | 6 | 299880 | 0 |
| PP2A B55 | 6 | 381080 | 0 |
| PP1 subunit 12 | 7 | 1036300 | 0 |
| PP1 subunit 8 | 4 | 2551900 | 0 |
| CENTROSOME ASSOCIATED PROTEINS | | | |
| PERICENTRIN | 36 | 6738100 | 0 |
| NUMA1 | 12 | 737414 | 0 |
| DYNEIN/DYNACTIN | | | |
| DYNEIN LIGHT CHAIN | 3 | 2190800 | 0 |
| DYNEIN 2 HEAVY CHAIN | 4 | 3356541 | 0 |
| DYNACTIN subunit 5 (p25) | 1 | 52795 | 0 |
| MITOTIC KINASES | | | |
| Cyclin B1 | 7 | 1049800 | 0 |
| PLK1 | 3 | 835290 | 0 |

**(i)**

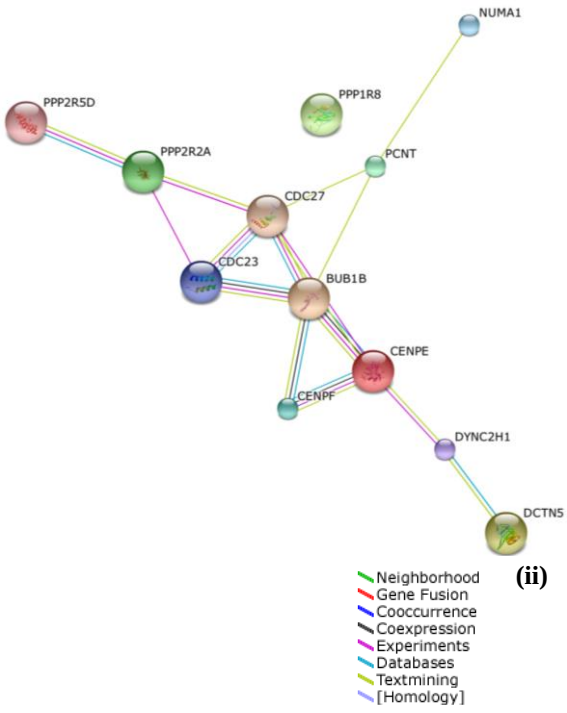


**(ii)**

(c)

**(2)**

| PROTEIN NAME | PROTEIN FUNCTION |
|---|---|
| **CENP-E** | centromere protein E. Essential for the maintenance of chromosomal stability through efficient stabilization of microtubule capture at kinetochores. Plays a key role in the movement of chromosomes toward the metaphase plate during mitosis. |
| **CENP-F** | centromere protein F (mitosin). Required for kinetochore function and chromosome segregation in mitosis. Required for kinetochore localization of dynein, LIS1, NDE1 and NDEL1. |
| **BUB1B** | Essential component of the mitotic checkpoint. Required for normal mitotic progression. Required also to monitor kinetochore motor CENP- E and its kinetochore localisation. |
| **DCTN5** | Subunit 5 of dynactin. It is a component of the pointed-end subcomplex and is thought to bind membranous cargo. (p25) |
| **DLIC** | Cytoplasmic dynein 1 light intermediate chain 1. Acts as one of several non-catalytic accessory components of the cytoplasmic dynein 1 complex. |
| **DYNC2H1** | dynein, cytoplasmic 2, heavy chain 1. Involved in the retrograde transport in the cilium. |
| **KNTC1** | kinetochore associated 1. Required for the assembly of the dynein-dynactin and MAD1-MAD2 complexes onto kinetochores. |
| **SPC25** | SPC25, NDC80 kinetochore complex component, homolog. Is required for chromosome segregation and spindle checkpoint activity. |
| **PCTN** | Pericentrin. Plays a role, together with DISC1, in the microtubule network formation. Is an integral component of the pericentriolar material (PCM). |
| **MAD2L1** | MAD2 mitotic arrest deficient-like 1. Required for the execution of the mitotic checkpoint which monitors the process of kinetochore- spindle attachment and inhibits the activity of the APC/C. |
| **NUMA1** | nuclear mitotic apparatus protein 1. Required for maintenance and establishment of the mitotic spindle poles. |
| **PPP1R8** | protein phosphatase 1, regulatory subunit 8; Inhibitor subunit of the major nuclear protein phosphatase-1 (PP-1). |
| **PPP2R4D** | protein phosphatase 2A activator, regulatory subunit 4. |
| **PPP2R2D** | protein phosphatase 2, regulatory subunit B, delta of protein phosphatase 2A (PP2A) that plays a key role in cell cycle by controlling mitosis entry and exit. |
| **PPP2R5D** | protein phosphatase 2, regulatory subunit B, delta. |
| **CDC23** | cell division cycle 23 homolog; component of the anaphase promoting complex/cyclosome (APC/C). |
| **CDC27** | cell division cycle 27 homolog. |
| **CDC16** | cell division cycle 16 homolog. |
| **CYCLIN B1** | G2/mitotic-specific cyclin B1. Essential for the control of the cell cycle at the G2/M transition. |
| **PLK1** | Serine/threonine-protein kinase that performs several important functions throughout M phase of the cell cycle. |

**Figure 4. 9. Identification of novel Spindly binding partners in mitotic cells.**
**Panel 1: (i)** Table summarising molecular candidates enriched in Spindly IP samples and that scored zero for the intensity value in the IgG IP samples. (a) Untreated cells; (b) Nocodazole treated cells; (c) STLC treated cells. **(ii)** STRING network diagram representing the network for the Spindly-IP enriched proteins. This "evidence view" was obtained from String-bd.org, a database of known and predicted protein interactions derived from different sources. Colour legend is reported to explain the different connection lines. Single lines mean confidence of interaction, whereas double lines indicate evidence for interaction. Each protein is represented by a node. (a) Untreated cells; (b) nocodazole treated cells; (c) STLC treated cells.
**Panel 2**: Summary of the functions of enriched proteins (adapted from information obtained from Uniprot.org) .

The three sets of data gathered from the mass spectrometry analysis revealed some similarities among the proteins enriched in the three different conditions tested, with consistency in the intensity and peptide counting registered (Fig. 4.9): the kinetochore binding proteins CENP-E and CENP-F; the SAC component BubR1 (BUB1B); the phosphatase PP2A (various subunits) and the subunit 5 (p25) of dynactin. The presence of different subunits of dynactin in the MS data is a further confirmation of the association between Spindly and dynactin (as already proved in **Chapter 3**), no matter what phase the cell is in. Moreover, it is worth to point out that we also found other subunits of both dynein and dynactin in the MS data; these proteins were not included in our lists since their IgG values were not equal to zero. Similarly, the recurrence of BubR1 (BUB1B) in all the datasets strongly supports our former results about an association between Spindly and this SAC effector (see Fig. 4.4. and 4.6). Likewise, the presence of Rod (KNTC-1) corroborates our information, previously gained (see Fig. 4.1), about a connection between Spindly and the RZZ complex.

Interestingly, we could identify specific mitotic proteins in the mitotically synchronised samples: Mad1, a specific SAC component normally recruited at the beginning of mitosis, was highly enriched in both STLC and NOC treated samples, according to the fact that it is a specific mitotic kinetochore protein that does not present fast turnover KT-MT attachment (and consequently it gets retained at KTs upon STLC treatment). Conversely, Mad2 levels were higher in the NOC samples, in line with the fast turnover of this SAC component upon KT-MT attachment. In our data it was also recorded the presence of the SAC protein Bub3, which, as Mad2, was highly enriched upon NOC treatment. For all these interactors the IgG values were not equal to zero, so we did not proceed with further analysis. It is worth to point out as well that other mitotic kinetochore proteins were recorded at high levels of intensity in the mitotic samples (however also in this case IgG values were not equal to zero). We identified NudE and

Lis1 in the UT data set as well as in the STLC data set (with intensity values, in the latter condition, definitely higher); these proteins have been reported as binding partner of dynein at KTs in mitosis, so it would be interesting in the future to further validate the data analysing the potential pathway of interaction that could involve Spindly and dynein at kinetochore in the mitotic division.

Looking at the whole set of data gathered from the mass spectrometry experiment (reported in **Chapter 8. Appendix- Paragraph 8.5**), it is possible to notice that, even though there were several kinetochore proteins highly enriched in the Spindly IP samples, this "category" of proteins was not the most abundant one. We did register the presence of cytoskeleton proteins, RNA factors, proteins involved in intracellular trafficking, actin binding proteins and centrosome proteins that could be new binding partners of Spindly. Since the initial aim of this study was not to study the whole interactome of Spindly but to identify specifically new mitotic binding partners in relation with Spindly-kinetochore localisation and functioning, we did not analyse the other potential interactors reported. However, it would be interesting to follow up this initial analysis and carry out a more comprehensive examination to identify Spindly's binding partner in different cellular contexts.

### 4.5.1 Validation of Mass Spectrometry data

For some of the new kinetochore potential binding partners of Spindly identified in these analyses, we carried out further validation experiments to assess the interaction. HEK293 cells were cultured and treated as previously described for the MS analysis, and subsequently Spindly immunoprecipitation was performed (Fig. 4.10).

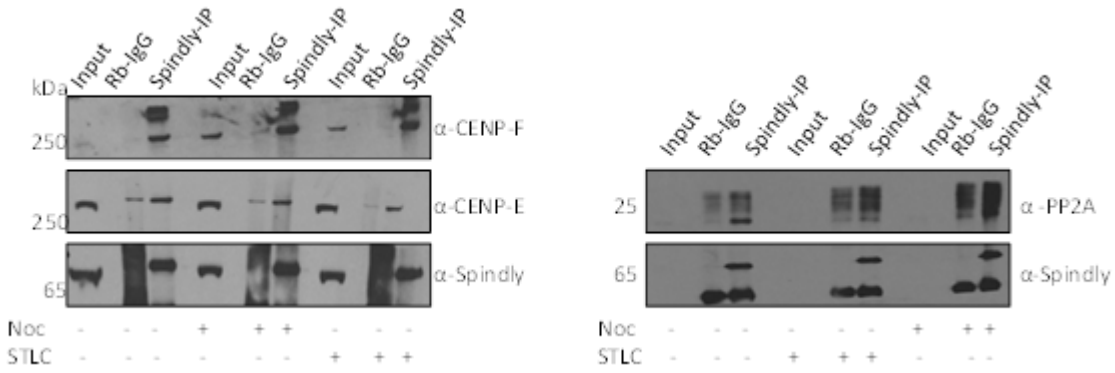


**Figure 4. 10. Spindly-IP validates the mass spectrometry results.**
HEK293 cells, either synchronised in mitosis (NOC or STLC) or untreated (UT), were harvested and 200/400 µg of the total protein was used to immunoprecipitate Spindly. Rabbit IgG was used as a negative control. Immunoprecipitated complexes were analysed by Western blot using the indicated antibodies. Inputs correspond to the whole cell extracts.

Results presented in figure 4.10 established the interaction between Spindly and the kinetochore proteins CENP-E and CENP-F, as well as the phosphatase PP2A. We noticed the presence of shifting bands in the blots for PP2A and CENP-F (Fig. 4.10); this could indicate post translational modifications for both proteins. The band presents in the CENP-F blot was particularly enriched after the pull-down, suggesting that it could bind to Spindly with high affinity; it could also be that it is not CENP-F related but it is something else that interacts with Spindly and it would need to be further investigated. PP2A has been demonstrated to undergo carboxy-methylation and phosphorylation (Kiely and Kiely, 2015), but the case reported in the above figure suggests that it could also potentially be subjected to ubiquitination. Surely this possibility would need to be deeply studied, but the previously proved high degree of regulation that is used to control this phosphatase (Kiely and Kiely, 2015), opens the possibility to different possible post translational modifications that have not been discovered yet.

## 4.6 Discussion

Proper interactions between kinetochores and spindle microtubules are crucial to ensure fidelity in chromosome segregation, and the mitotic checkpoint is required to monitor this process. The removal of checkpoint proteins from KTs has to occur to promote the SAC silencing, and it has been shown to rely on the dynein/dynactin motor complex (Howell *et al.*, 2001). Together with the RZZ complex, Spindly is involved in the recruitment of the dynein/dynactin to KTs to allow the silencing process.

In this chapter we have shown an interaction between Spindly and the RZZ complex (see Fig. 4.1). Moreover, new associations between Spindly and the SAC components have been established. Spindly was demonstrated to associate with BubR1 and Mps1 when overexpressed (see Fig. 4.2 and Fig. 4.6). The association with BubR1 was further confirmed by SEC first and by co-immunoprecipitation of Spindly from fractions after. BubR1 was found to be the only SAC component tested that remains associated with Spindly throughout IP or SEC from cells arrested in early prometaphase (see Fig. 4.4) suggesting phase-specificity for this interaction. BubR1 is a component of the MCC, together with Bub3, Mad2 and Cdc20 (Sudakin *et al.*, 2001), and it associates with unattached/incorrectly attached kinetochores, playing an important role in kinetochore-microtubule interactions (Elowe, 2011). It gets localised to the kinetochore by binding to Bub1, which is recruited earlier by Mps1-mediated Knl1 phosphorylation (Vleugel *et al.*, 2013). BubR1 can therefore represent the link between Spindly and the SAC pathway. Moreover we corroborated the involvement of Spindly with the mitotic checkpoint "*in vivo*", by using a system to mis-localise proteins at the plasma membrane and look for the specificity of the interaction (see Fig. 4.6). Exploiting the same system we additionally showed that the *C*-terminus of Spindly, although necessary for KT binding *in vivo*, is neither crucial for the interaction with the SAC components nor for that with the RZZ complex (see Fig. 4.7).

With the aim to detect novel mitotic binding partners of Spindly a mass spectrometry analysis was performed upon synchronisation of cells in mitosis, using different drugs to study different KT-MT attachment status. Kinetochore proteins behave differently in mitosis, associating to sites with different timing and showing different dynamics upon binding; indeed the pool of proteins that can be registered prior to MT attachment to KT is different from those present already right after their binding (see **Chapter 1- Paragraph 1.2.2.1**). Therefore, our goal with the mass spectrometry analysis was to identify binding partners of Spindly at the KT according to the diverse population of proteins present (prometaphase- no KT/MT attachment (NOC treatment) or prometaphase- KT/MT attachment (STLC treatment)). The wide approach of the mass spectrometry analysis allows in fact for a more comprehensive characterisation of the mitotic-interactome of Spindly in synchronised cells.

From the list of proteins obtained we identified new interesting Spindly interactors, such as CENP-E and CENP-F. During mitosis these CENP-E and CENP-F are kinetochore localised, but they possess different recruitment timing and they exert different functions. CENP-F is recruited from the nucleus at the beginning of mitosis and it is a stable kinetochore protein that stays until metaphase/anaphase transition (Zhu *et al.*, 1995). CENP-E, however, is recruited onto kinetochores in late prometaphase and is a 'sensor' factor for KT-MT attachments (Yao *et al.*, 2000). CENP-E is involved in checkpoint assembly: it interacts with BubR1 establishing a feedback signalling for activation/inactivation of the SAC (Mao *et al.*, 2003), which in turns promotes kinetochore localisation of Mad2 (Johnson *et al.*, 2004). Conversely, CENP-F has not been described as an active player of the spindle assembly checkpoint, but it directly binds to CENP-E promoting its kinetochore stabilisation (Chan *et al.*, 1998) . Defects in CENP-E expression also affect kinetochore CENP-F localisation, indicating a reciprocal

control between these two proteins (Johnson *et al.*, 2004). Both these proteins were identified in our mass spectrometry analysis (see Fig. 4.9) as novel kinetochore binding partners of Spindly, and for both of them we could validated the interaction by immunoprecipitation (see Fig. 4.10). We therefore think that CENP-F could represent the stable kinetochore binding partner of Spindly, to which it could anchor from the beginning of prometaphase. Recent publications have demonstrated that Spindly has to undergo farnesylation at its *C*-terminus to get recruited to KTs (Holland *et al.*, 2015) (Moudgil *et al.*, 2015); both CENP-F and CENP-E have been shown to be farnesylated in mitosis (Ashar *et al.*, 2000). So, Spindly immunoprecipitations after treatment with farnesyl-transferase inhibitors should be repeated to confirm that the interactions seen in our results are specific and not due only to the presence of the farnesyl group.

Curiously, Spindly cannot interact with kinetochores in the absence of RZZ, which suggests that RZZ is essential to promote the interaction between Spindly and CENP-E and/or CENP-F. Additionally, since CENP-E is a known binding partner of BubR1, it is possible that the Spindly-BubR1 interaction is mediated by CENP-E. Further experiments will be needed to better understand the associations between Spindly and CENP-E and/or CENP-F. However the massive size of CENP-E and CENP-F and a dearth of full-length cDNAs complicate dissecting these interactions.

Generally, it is possible to separate kinetochore proteins into two large groups according to their kinetochore dynamics: (1) those that stably interact with unattached kinetochores and (2) those that transiently associate. Spindle checkpoint proteins show a rapid capacity of recovery at kinetochores after photo-bleaching (Mps1, Bub3, Cdc20 and Mad2), while the constitutive proteins (such as CENPs and KMN components) do not (Howell *et al.*, 2004) (Vink *et al.*, 2006) (Hori *et al.*, 2003). For example, BubR1, that is constantly incorporated into the MCC and released into the cytosol, turns over

rapidly; conversely, Bub1, acting as a recruitment platform, is firmly associated with KTs (Howell *et al.*, 2004). When we tested GFP-Spindly for fluorescence recovery after photo-bleaching (FRAP) we registered a quite slow turnover and a very high immobile fraction of this protein (preliminary data, not shown). Publications have revealed that GFP-tagged RZZ components are not dynamic either (Famulski *et al.*, 2008), but recover slowly in FRAP experiments, similar to components of the KMN complex indicating that this complex is stably bound to prophase kinetochore (Hori *et al.*, 2003). Worth noticing is that in Spindly depleted cells the turnover of ZW10 was even further reduced (Barisic *et al.*, 2010), suggesting that Spindly promotes the turnover of the RZZ complex on KTs. The RZZ complex binds to kinetochores via Zwint, an outer plate kinetochore protein that ensures proper localisation of the complex in mitosis (Starr *et al.*, 2000). Similarly Spindly, by binding to CENP-F, could be stably tethered to kinetochores until MTs attach and dynein drives its dissociation.

In our MS data, we also found the phosphatase protein 2A (various subunits, see Fig. 4.9), recently identified as an essential player in the checkpoint silencing process (Nijenhuis *et al.*, 2014). Indeed, once the checkpoint has been satisfied, its effectors have not only to be removed, but also different substrates have to be de-phosphorylated to prevent re-/continued activation. Mps1-mediated phosphorylation of Knl1 promotes BubR1 recruitment (through Bub1), which, in turn, recruits PP2A to antagonise the action of the kinases that provide the signal to recruit SAC proteins (Espert *et al.*, 2014) (Nijenhuis *et al.*, 2014).

Here we observed the presence of an interaction between Spindly and PP2A, both of which are potentially playing a role in the silencing process: Spindly, by recruiting the dynein/dynactin motor complex and therefore promoting the stripping process, and PP2A, by de-phosphorylating Knl1 and therefore promoting the dissociation of the Bub1 and BubR1. The stripping and de-phosphorylation processes could happen

concurrently so to synchronise the SAC signalling at each kinetochore. Interestingly, in our MS data we found also protein phosphatase 1 (PP1) being pulled down with Spindly. Recently a PP2A and PP1 activation loop essential for faithful cell division was identified (Grallert *et al.*, 2015). Therefore, it would be interesting to understand whether Spindly could have a part in the regulation of this system.

In the scheme in Fig. 4.11, we propose a model for the functioning of Spindly in the mitotic checkpoint signalling. When mitosis starts, unattached kinetochores assemble hierarchically; transient kinetochore proteins get recruited and the SAC gets assembled activating the 'wait anaphase signal' (Fig. 4.11, (a)). Spindly is recruited as well and it binds to CENP-F, the RZZ complex and BubR1 (Fig. 4.11, (a), right hand-side). Attachment between microtubules and kinetochores occurs (Fig. 4.11, (b), left hand-side) and the checkpoint signalling senses the tension generated. Now the "wait anaphase signal" can be silenced. Therefore phosphatases become active and the dynein/dynactin motor complex is recruited to KTs (Fig. 4.11, (b), right hand-side). In turn, SAC components (as well as Spindly and the RZZ complex) are loaded and stripped away thanks to the motor complex dynein/dynactin (Fig. 4.11, (c)). Anaphase can now begin.

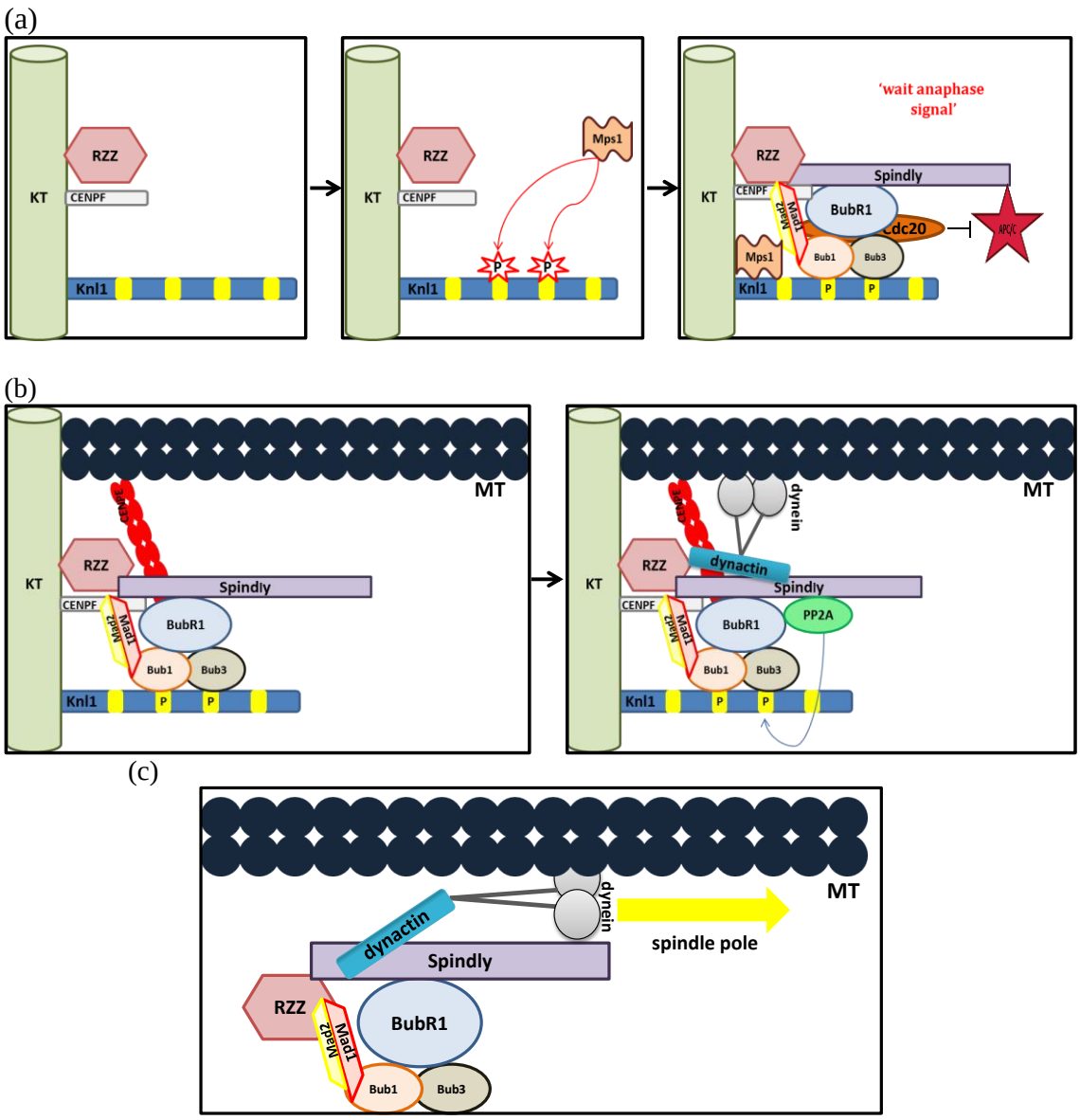


**Figure 4. 11. Proposed model for checkpoint assembly in mitosis.**
When a cell enters mitosis, kinetochore proteins are recruited to allow proper functioning throughout the process. In the 'unattached kinetochore' state (a), the spindle assembly checkpoint assembles to prevent anaphase onset. Mps1 phosphorylates Knl1 (a, middle panel) and allows the subsequent recruitment of Bub1, Bub3 and BubR1. Bub1 drives the localisation of Mad1 and Mad2, in cooperation with the RZZ complex. Spindly gets recruited as well (a, right-hand side panel). In the 'attached kinetochore' situation (b), CENP-E get localised via BubR1 (left-hand side panel) and the checkpoint can be silenced: PP2A dephosphorylates Knl1 allowing the release of Bub1, Bub3 and BubR1 and Spindly promotes binding of the motor complex dynein/dynactin to the SAC proteins (right-hand side panel). Finally, for anaphase to start, SAC components, Spindly and RZZ are stripped towards spindle poles (c).

Previous data showed that maintaining Spindly on KTs keeps the SAC active, whereas the lack of Spindly on KTs allows SAC silencing without the need to recruit dynein, but the mechanism by which the kinetochore presence of Spindly persistently activates the SAC has so far been unclear (Gassmann *et al.*, 2010). Our data that show interactions with two major SAC effectors (BubR1 and PP2A) allow us to form three hypotheses for the behaviour of Spindly: 1) Spindly could be creating aberrant phosphatase signalling that could affect the regulation of the phospho-equilibrium at KTs important for SAC activation/inactivation; 2) Spindly interaction with BubR1 could be critical to allow the silencing, thus it has to be removed to progress though mitosis; 3) Spindly presence on KTs could be sufficient for maintaining SAC activity retaining proteins at site.

Experiments to test these hypotheses will be essential for unravelling the real role of Spindly in SAC signalling.

# 5 . A new role for human Spindly in interphase

## 5.1 Introduction

Spindly was identified through two RNAi screens in *Drosophila melanogaster* S2 cells in which mitotic and interphase phenotypes were analysed. In interphase cells, Spindly depletion generated alterations in cytoskeletal architecture with spiky and elongated microtubule-rich projections in contrast to the normal smooth rounded S2 cells. Moreover, expression of GFP-Spindly in live cells produced a pattern of continuously moving punctae of the protein, similar to how a microtubule plus-end binding protein would behave (Griffis *et al.*, 2007). Indeed, Spindly was shown to localise at the plus-tips of microtubules, when expressed at low levels together with EB1, a microtubule-associated protein present at growing ends in interphase cells (Griffis *et al.*, 2007) (Morrison *et al.*, 1998).

After the initial study in 2007, all of the subsequent publications on Spindly have been focused on describing its role during mitosis in human cells and worms (Gassmann *et al.*, 2008) (Yamamoto *et al.*, 2008) (Gassmann *et al.*, 2010) (Barisic *et al.*, 2010) (Cheerambathur *et al.*, 2013); thus there is no evidence on whether Spindly in other organisms plays a role similar to the one described for Spindly in interphase cells. We therefore sought to study the role of human Spindly in interphase, with a close look at microtubule localisation and cytoskeleton function.

It was previously demonstrated that the minus-end motor protein dynein is targeted to the microtubule growing ends via the p150 subunit of dynactin, which is itself recruited by EB1 and CLIP-170, proteins that bind to the plus-end of microtubules and regulate their dynamics (Folker *et al.*, 2005) (Duellberg *et al.*, 2014). This cytoplasmic motor complex dynein/dynactin was also described to be involved in cytoskeleton reorganisation upon wounding and, more precisely, in directed cell movement (Palazzo *et al.*, 2001) (Faulkner *et al.*, 2000) (Smith *et al.*, 2000). Furthermore, dynein was

recorded helping neural progenitor cells to migrate from the ventricular zone during early brain development via an interaction with Lis1 (Reiner et al., 1993).

Given our previous results underlying the role of human Spindly as a dynein/dynactin molecular adaptor in mitotic cells (see **Chapter 3**), we hypothesised a similar function for Spindly in interphase cells.

In this chapter an important new function for Spindly in cell migration is described. We identified a direct role of human Spindly in wound healing and cell movement, with its specific localisation at focal adhesion tips upon wounding. These results delineate for the first time an interphase role for Spindly, corroborating our initial idea that places Spindly as a new adaptor for the dynein/dynactin motor complex in multiple cellular processes and in different cell cycle phases.

## 5.2 Localisation of human Spindly in non-mitotic cells

To date, there has been no data on human Spindly in non-mitotic cells and nothing is known about its localisation and function outside mitosis. To shed the light on this topic, we started analysing its distribution throughout the cell cycle using an antibody against the proliferating cell nuclear antigene (PCNA) as a cell cycle marker. PCNA is involved in DNA replication, clamping the DNA polymerase δ in S phase; this allows visualising changes that occur during cell cycle on the genome duplicating machinery and therefore identify the different cell cycle stages (Easwaran *et al.*, 2005). Co-staining of U2OS cells with anti-Spindly and anti-PCNA antibodies has revealed that, even though Spindly is mainly a nuclear protein, is possible to identify a pool within the cytoplasm (Fig. 5.1, (a) and (b)). However there was no difference in the amount of Spindly seen in the cytoplasm regardless of the cell cycle stage as revealed by PCNA distribution (Fig. 5.1, (a)**)**. Furthermore, fractionation of cell lysates and analysis of the different fractions (nuclear, cytoplasmic and chromatin) by Western blot has demonstrated the presence of Spindly not only in the expected nuclear fraction (Fig. 5.1, (c), **(i)**) but also in the chromatin (Fig. 5.1, (c), **(ii)**) and in the cytoplasmic ones (Fig. 5.1, (c) **(iii)**). The discovery of Spindly in these two other cell compartments indicates that Spindly might play additional functions besides its role in mitosis.

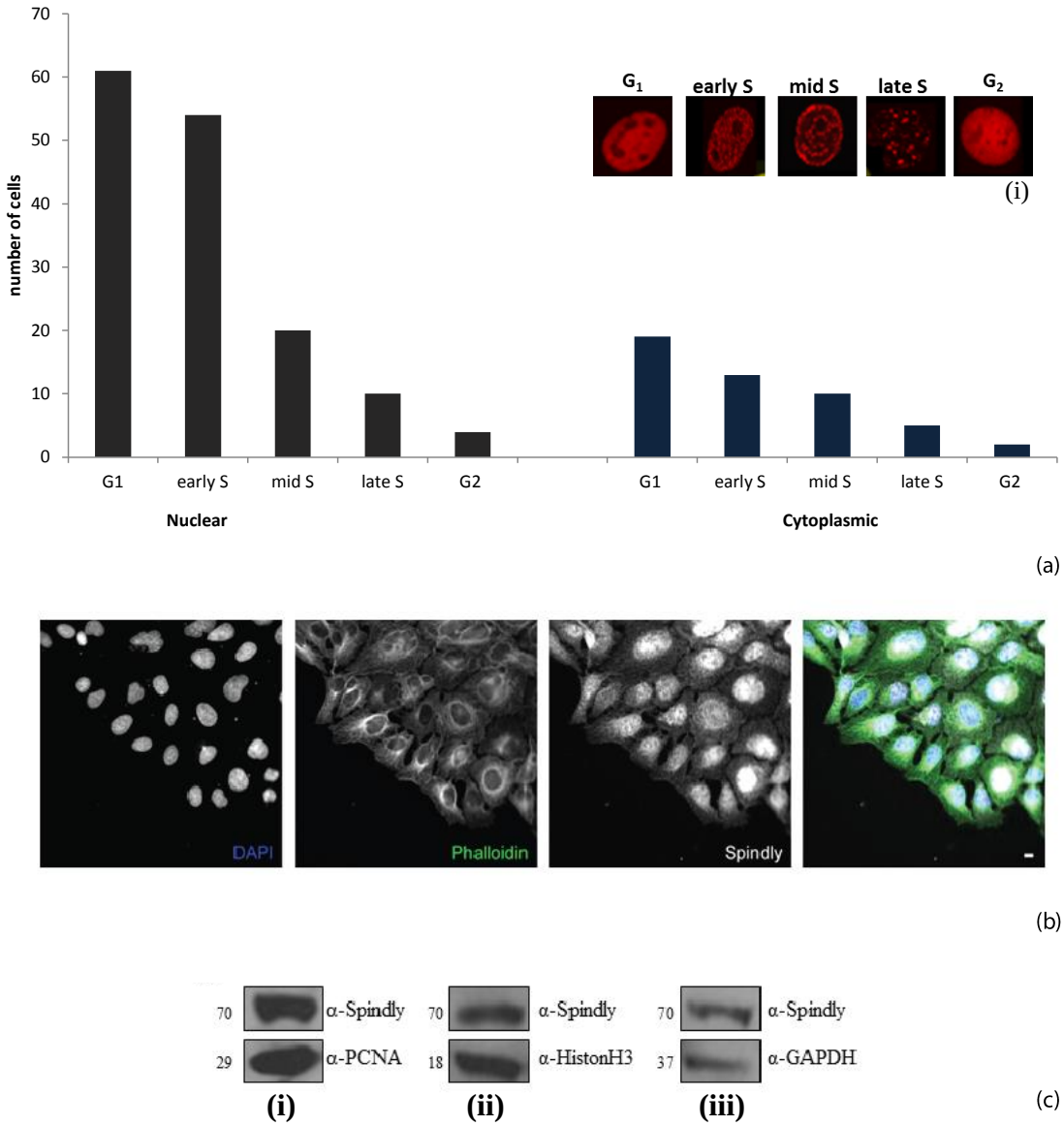


**Figure 5. 1. Spindly is not exclusively a nuclear protein.**
Examination of Spindly localisation within interphase cells. (a) Analysis of Spindly distribution profile throughout the cell cycle using the PCNA cell cycle marker; cells in different phases were manually counted using as mask the characteristic PCNA staining reported in (i) (image adopted from Cardoso-lab.org) and then plotted using Excel. (b) Immunostaining of U2OS cells showing nuclei (DAPI, blue), actin (Phalloidin, green) and Spindly (white). 40X magnification. Scale bar 10µm. (c) Fractionation experiment of U2OS cell lysate **(i)** nuclear fraction, **(ii)** chromatin fraction and **(iii)** cytoplasmic fraction. Cross check analysis of the fractions was performed and results are reported in the appendix (see **Chapter 8- Fig. 8.3**).

To explore further the role of Spindly in interphase we asked whether the localisation seen in S2 cells was conserved in human cells. To this end we co-transfected U2OS cells with GFP-Spindly and BFP-Tubulin to study the potential association of Spindly with microtubules.

A live imaging experiment was carried out using total internal reflection fluorescence (TIRF) microscopy, a technique that allows better imaging of microtubules present at the basal cortex of the cell (Toomre and Manstein, 2001). Imaging was performed by Dr. Eric Griffis (University of Dundee).

Figure 5.2 shows a microtubule plus-end localisation for GFP-Spindly, which stays associated during a shrinkage and growth event.

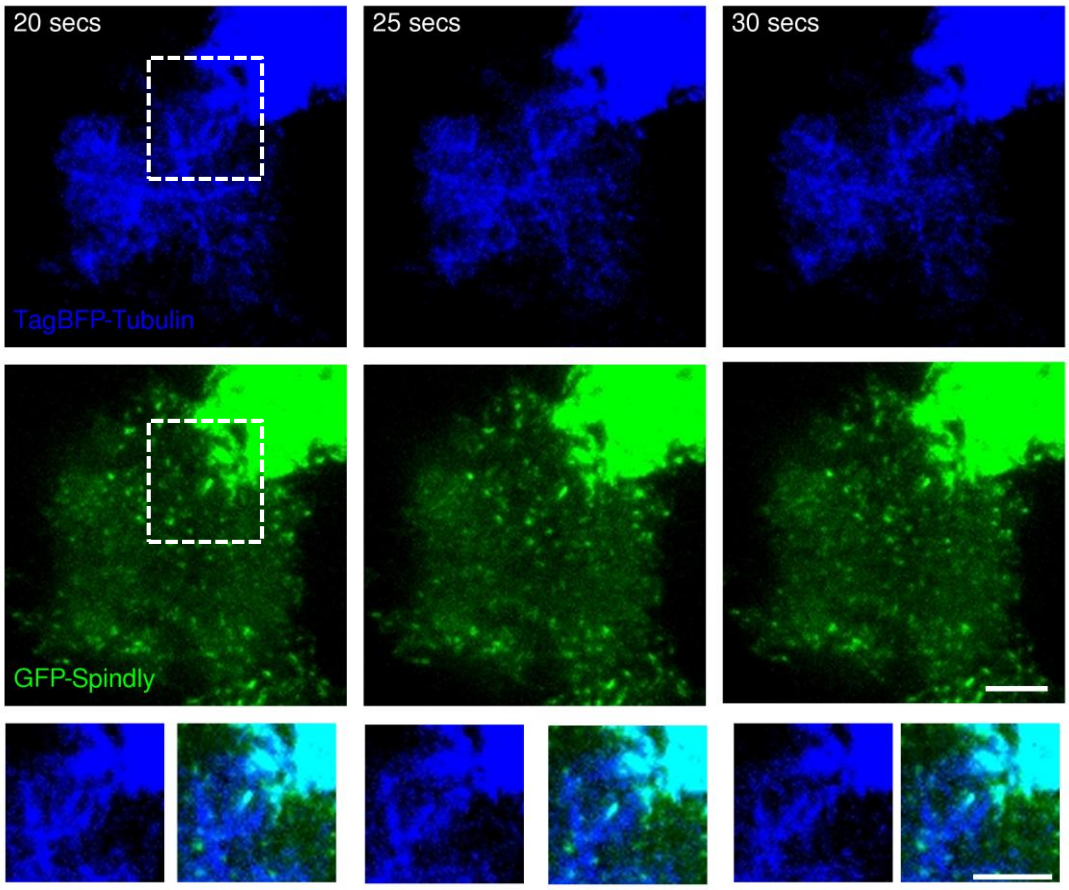


**Figure 5. 2. Spindly localises at microtubule tips.**
Still images from TIRF time-lapse analysis of U2OS cells transiently co-expressing GFP-Spindly (green) and BFP-Tubulin (blue). Scale bar 5 µm. Bottom of the panel shows magnified images derived from the boxed areas (dashed white box) followed over the time for both channels (green, Spindly; blue, Tubulin). Imaging performed by Dr. E. Griffis (University of Dundee).

The visualisation of human Spindly at microtubule tips together with the identification of new pools of Spindly in interphase cells bring up the possibility of a novel function for this protein in relation to the microtubule cytoskeleton, a function different from the already described mitotic one.

## 5.3 Human Spindly depletion affects cell migration

Given previous data that described Spindly in the cytoplasm of interphase cells (Fig. 5.1) and its presence at microtubules ends (Fig. 5.2), we sought to describe what cellular process (/es) Spindly might be involved with in non-mitotic cells.

It has already been demonstrated that microtubules are directly involved in cell migration and in the organization of cell polarity; many microtubule-associated proteins localising at their growing ends play parts in this process as well as the centrosome, the microtubule nucleating structure that directs the polymerisation of tubulin subunits (Schuyler and Pellman, 2001). The centrosome has to be repositioned between the leading edge and the nucleus upon wounding in order to set the direction of cell migration a critical step to allow wound closure (Palazzo *et al.*, 2001) (Magdalena *et al.*, 2003). Inhibition or overexpression of dynein and/or dynactin has been shown to disturb centrosome reorientation, but not to interfere with microtubule stabilisation (Palazzo *et al.*, 2001). Also, a separate pool of cytoplasmic dynein associating with actin-rich cortical cytoskeleton has been identified, together with its regulatory proteins dynactin and Lis1 (Faulkner *et al.*, 2000) (Dujardin *et al.*, 2003). It was proposed that, upon binding to microtubules, cortical dynein is involved in the generation of pulling forces, which in turns influences actin-based motility.

Localisation of Spindly at microtubule tips and its close interaction with the dynein/dynactin motor complex (see **Chapter 3**), led us to hypothesise that Spindly could also be involved in cell movement and in cytoskeleton re-organisation upon cells receiving the correct stimulus to begin directed movement. Thus, we carried out a scratch assay to study cell migration *in vitro* in Spindly-depleted cells in order to verify our hypothesis. This method is based on the generation of an artificial gap ("scratch") on a monolayer of cells that will lead to movement of the cells on the edge toward the opening until contacting cells on the other edge, thus to close the "scratch".

We silenced Spindly expression in U2OS cells by treatment with specific siRNAs for 96 hours and then seeded cells into two small wells separated by a silicon wall (IBIDI silicon inserts). Once confluence was reached, the insert was removed automatically generating a gap in the monolayer of cells thanks to the silicon wall. We followed the movement of the cells on the edge by live imaging for at least 24 hours and then analysed the movies by measuring the width of "scratch" over time. Cells depleted of Spindly showed slow closure rate with incapacity to close the gap after 24 hours; we recorded a much slower rate of cell migration into the "scratch" when compared with control cells (Figure 5.3 (panel 1)). Measurements were conducted by drawing lines from one edge toward the other (several measurements were performed for each image collected drawing lines from the top to the bottom of the "scratch") and then values were averaged for each time point analysed. Results were further validated by scratching the monolayer of cells with a 200µL tip so to corroborate the data using a different technique and measurements were conducted in the same way (data not shown).

To confirm that this phenotype was strictly due to lack of Spindly expression, we then depleted the endogenous Spindly from U2OS cells expressing siRNA-resistant GFP-Spindly upon administration of doxycycline and performed the scratch assay again. Figure 5.3 (panel 2) shows that re-expressing an exogenous copy of Spindly rescued the migration phenotype; cells expressing GFP-Spindly showed a rate of closure similar to control cells.

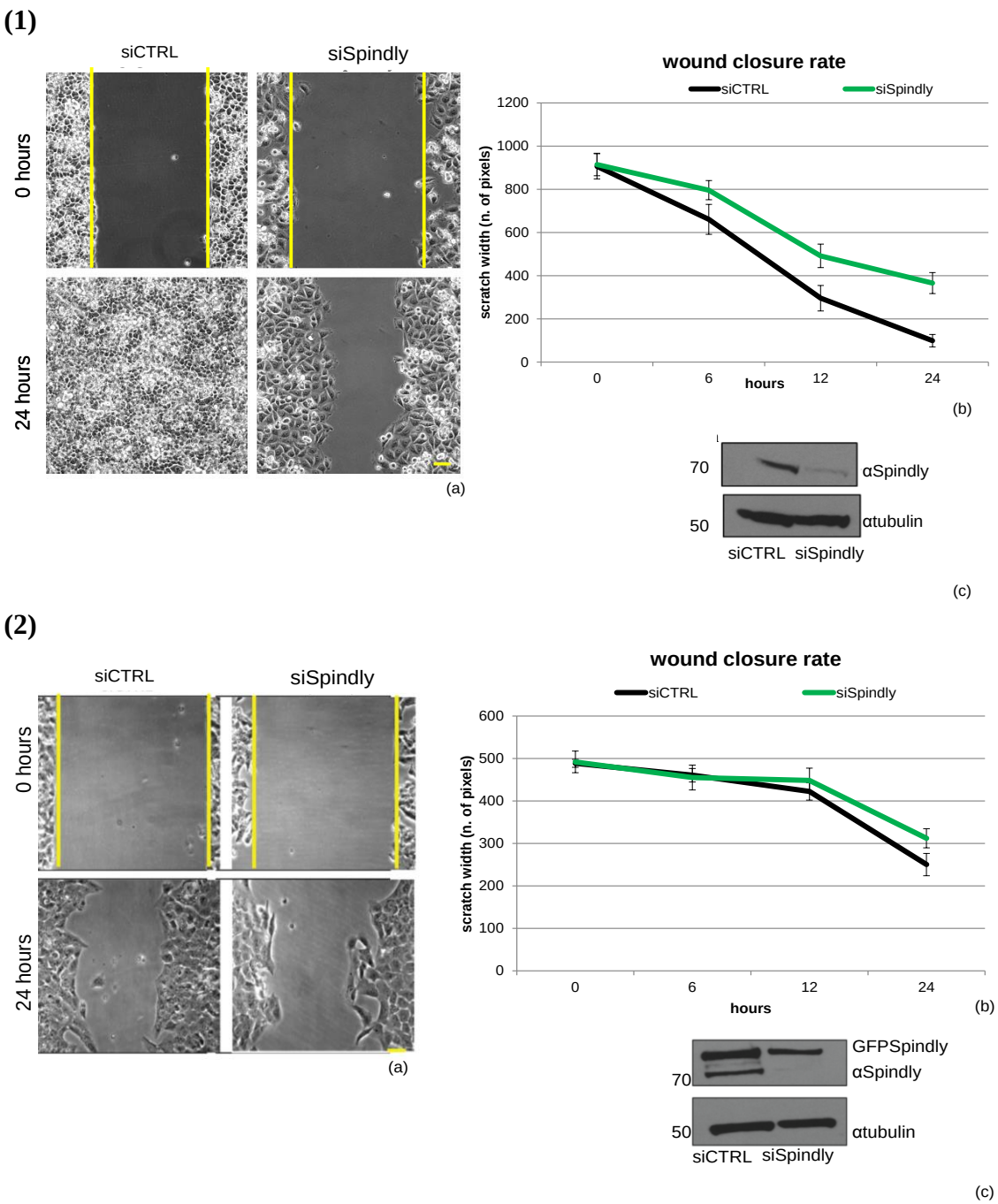


**Figure 5. 3.Spindly plays a direct role in cell migration.**
**(1) Silencing of Spindly specifically affects cell migration.** (a) Still images from time-lapse analysis showing a delay in cell movement in U2OS Spindly depleted cells compared to control cells. Scale bar 50 µm. (b) Quantification of the width of the scratch in control and Spindly depleted U2OS cells over time. Data indicate the mean± standard deviation (represented by error bars) from at least 3 independent experiments. (c) Western blot of same population of cells confirms the silencing; Tubulin was used as loading control.
**(2) Expression of GFP-Spindly rescues migration defects.** (a) Still images from time-lapse analysis showing rescued cell movement in U2OS GFP-Spindly depleted cells compared to U2OS GFP-Spindly control cells. Scale bar 50 µm. (b) Quantification of the width of the scratch in U2OS GFP-Spindly control and depleted cells over time. Data indicate the mean data indicate the mean± standard deviation (error bars) from at least 3 independent experiments (c) Western blotting of same population of cells confirms the silencing and the GFP-Spindly expression; Tubulin was used as loading control. [This figure represents experiments conducted with commercial inserts; anyway similar results were obtained scratching with a 200µL tip (data not shown)].

In parallel, we analysed U2OS cells depleted of dynactin subunits, either p150 or p50, and compared them with control cells. Dynactin has been observed at microtubules growing ends and at the cell cortex where it has been proposed to exert pulling forces on microtubules to promote cell migration (Busson *et al.*, 1998) (Vaughan *et al.*, 1999). We observed that dynactin depleted cells presented much slower migration rate compared to control cells (Fig. 5.4). The phenotype documented was comparable to the one described for Spindly depleted cells (see Fig. 5.3, (panel 1)).

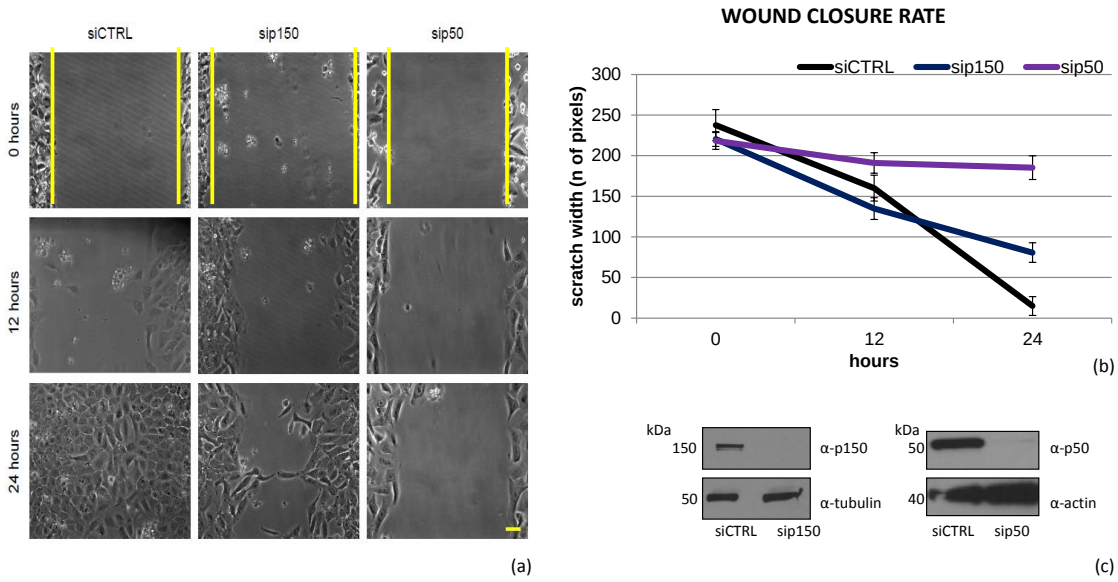


**Figure 5. 4. Depletion of dynactin prevents cell movement.**
(a) Still images from time-lapse analysis showing delayed cell movement in U2OS cells lacking dynactin (p150 or p50) subunits. 20X magnification. Scale bar 50 µm. (b) Quantification of the width of the scratch in control and dynactin depleted U2OS cells over time. Data indicate the mean± standard deviation (represented by error bars) from at least 3 independent experiments. (c) Western blot of same population of cells confirms the silencing; Tubulin (or Actin) was used as loading control.

As previously mentioned, Spindly depleted cells are defective in division and proliferation processes, due to the role of Spindly in mitosis. Therefore, to exclude the possibility that the phenotype defined above was related to defects in cell proliferation, we synchronised cells in S phase by administrating Hydroxyurea (HU) (1mM) for 24 hours and repeated the scratch assay. The treatment allowed us to study cell migration in cells that are neither dividing nor proliferating.

In those cells the lack of Spindly would generate a phenotype strictly related with its non-mitotic function. Control or HU treated cells were imaged for 24 hours (Fig. 5.5, (a)) and then kymographic analysis of the movies were carried out to extract velocities values from the linear movement of the cells (Fig. 5.5, (c)). The synchronisation and the silencing of Spindly were confirmed by Western blot analysis (Fig. 5.5, (b)).

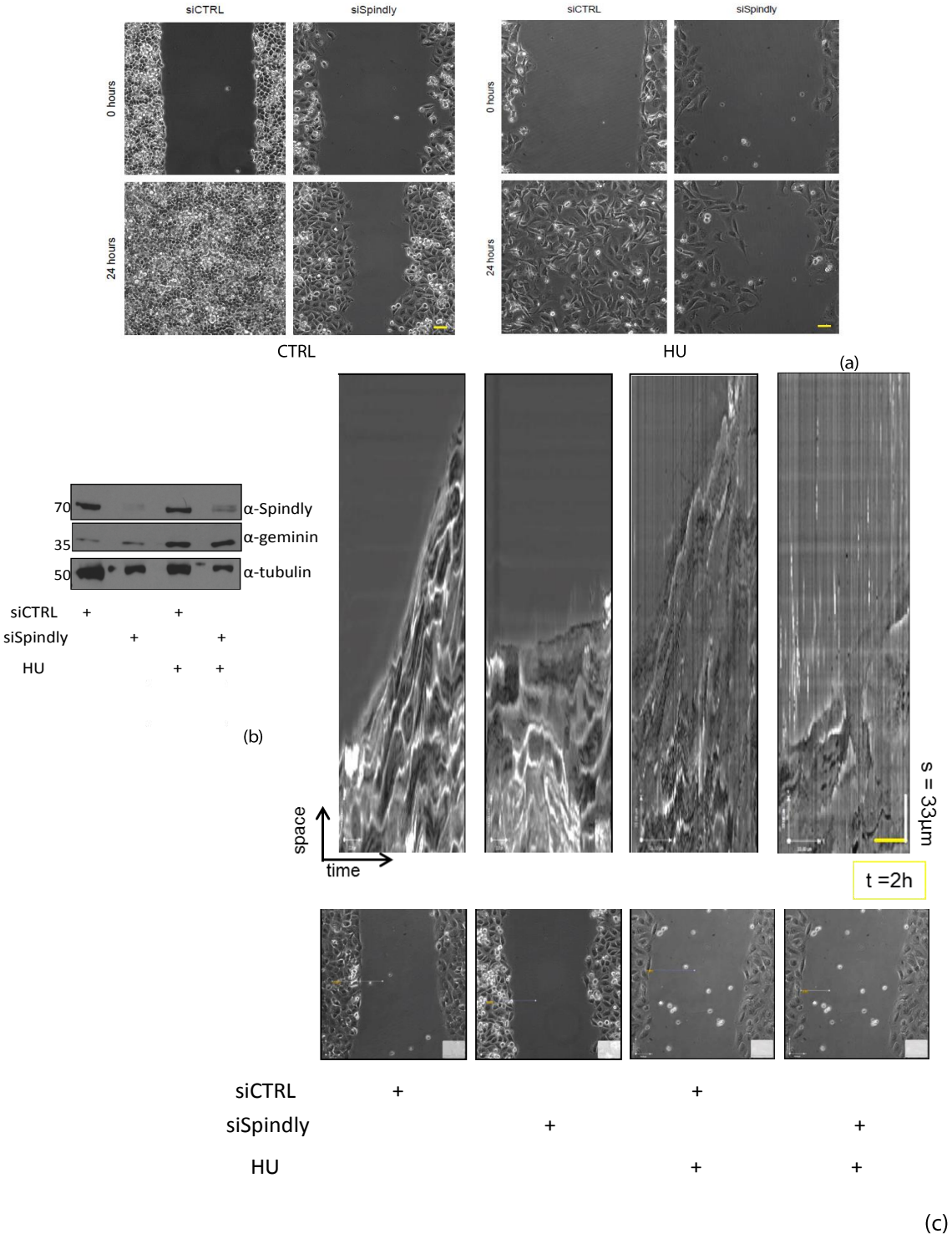


**Figure 5. 5. S phase synchronisation confirms lower migration speeds in Spindly depleted cells.**

(a) Still images of time-lapse analysis comparing control cells (either siCTRL or siSpindly; left hand-side) and hydroxyurea (HU, 1mM) treated cells (either siCTRL or siSpindly; right hand-side). 20X magnification. Scale bar 50 µm. (b) Western blot of U2OS control or Spindly depleted cells upon either control or HU treatment (1mM) to confirm S phase synchronisation. Geminin was used as S phase marker. Tubulin was used as loading control. (c) Kymograph analysis of the time-lapse experiments obtained using the Volocity software. Scale bar = space (s): 33µm; time (t): 2 hours.

This experiment provides further evidence that Spindly depleted cells are intrinsically defective in cell migration, and that the defects we measure are not produced by errors in cell division created by Spindly depletion. Interestingly, we did not register differences in the slope obtained from the kymograph analysis of control and HU treated cells (Fig. 5.5, (c)), suggesting that cell divisions and/or density do not contribute greatly to the speed of cell migration. We therefore can confirm that Spindly plays a role in the cell migration process, a totally new function never described to date. This non-mitotic function could be due to its association with the motor complex dynein/dynactin to help the motor exerts its function in cell movement; however, our data cannot necessarily connect Spindly to dynein/dynactin in this context. Nevertheless, is important to notice that, when we tried to rescue the migration defects expressing the GFP-Spindly mutant construct, which impairs the binding of Spindly to dynactin (S256A; see **Chapter 3**), we were not able to rescue the cell movement rate to control levels. Cells expressing only the exogenous copy of the mutant protein were still slower compared to control cells (Fig. 5.6).

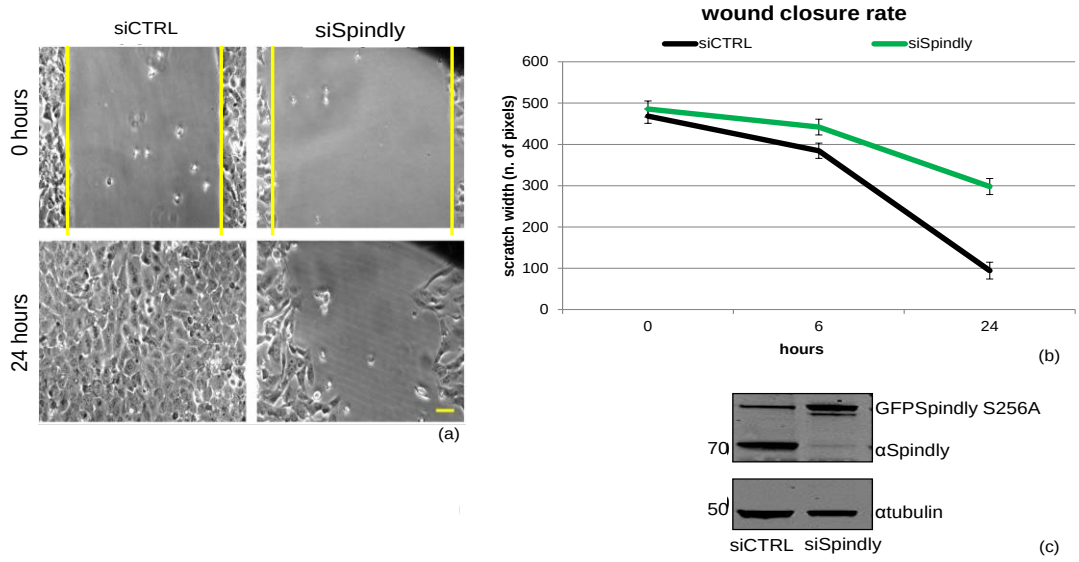


**Figure 5. 6. Expression of GFP-Spindly S256A does not rescues migration defects.**
(a) Still images from time-lapse analysis showing cell migration experiment in U2OS GFP-Spindly S256A Spindly-depleted cells compared to U2OS GFP-Spindly S256A siRNA control cells. Scale bar 50 µm. (b) Quantification of the width of the scratch in U2OS GFP-Spindly S256A control and depleted cells over time. Data indicate the mean± standard deviation (represented by error bars) from at least 3 independent experiments. (c) Western blot of same

populations of cells confirms the silencing and the GFP expression; Tubulin was used as loading control.

According to this data we can confirm that Spindly is playing a role in cell migration that could be associated with the dynein/dynactin motor complex; this interplay is likely to occur through a mechanism similar to that one previously shown for the SAC stripping process in mitosis.

## 5.4 Spindly depletion does not affect MTOC reorientation

A well-studied step in the wound repair process is the reorientation of centrosomes (or MTOC) to a position between the leading edge and the nucleus (Gundersen and Bulinski, 1988), a crucial activity that sets the direction of migration. Defects in dynein or dynactin expression block the MTOC reorientation process completely (Palazzo *et al.*, 2001). Given that our previous studies have revealed high similarity in cell migration defects between Spindly depleted cells and dynactin depleted cells, we wanted to verify whether Spindly was also required for reorientation of the centrosome. Reorientation normally occurs within the first two hours upon wounding (Palazzo *et al.*, 2001), so we scratched a monolayer of U2OS cells, fixed and stained with Pericentrin to visualise centrosomes (Fig. 5.7).

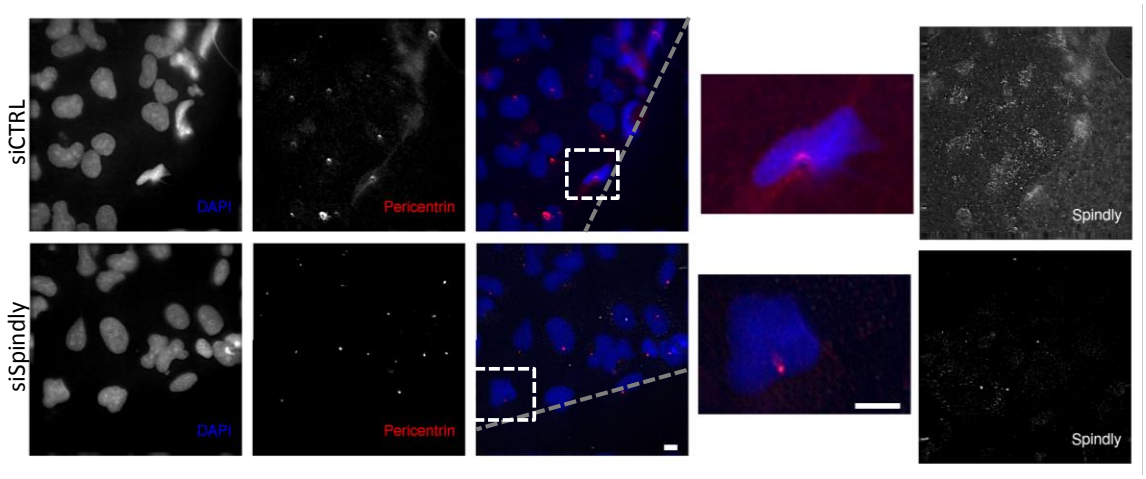


**Figure 5. 7. Spindly depletion does not affect centrosome positioning.**
Immunostaining of U2OS cells fixed four hours upon wounding (edge indicated by dotted grey line): nuclei (DAPI, blue), centrosomes (anti-Pericentrin, red). Grey dotted line indicates the cell front. Details represent magnified images derived from the boxed areas (dashed white box) for two channels (DAPI and Pericentrin). 40X magnification. Scale bar 10µm. Right hand side of the panel is anti-Spindly staining to show the effectiveness of the silencing (anti-Spindly, white).

This assay did not reveal any striking defective phenotype or differences in centrosome positioning upon Spindly depletion (measurements were performed to confirm the absence of defects in cells lacking Spindly ($n \geq 35$), graphs not shown). This suggests that Spindly is not involved in the polarisation of the cell to set the axis to direct the migration process. It could instead be recruited at the leading edge in a secondary step to facilitate other processes (as discussed further in this chapter).

## 5.5 Localisation of Spindly during cell migration

To study the behaviour of cytoplasmic Spindly during cell migration in more detail, we immunostained migrating cells: human fibroblasts, HaCaT cells, or mouse embryonic fibroblasts (MEFs) (Fig. 5.8; (a)/ (b), (c) and (d) respectively).

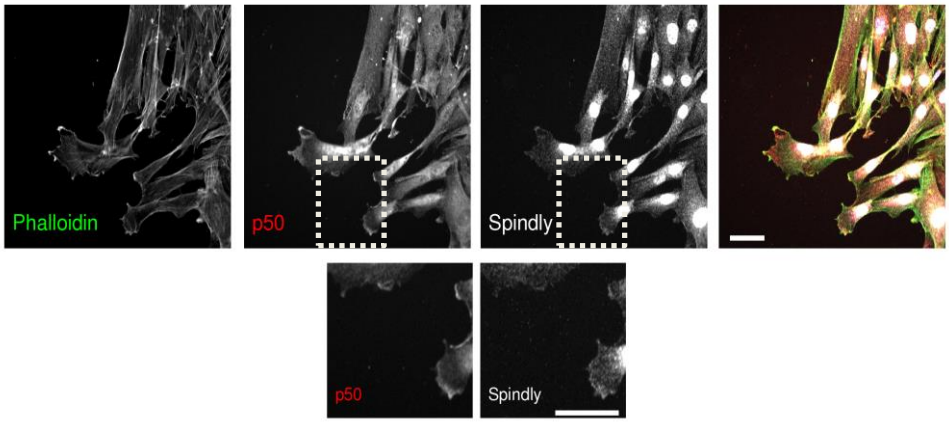


(a)

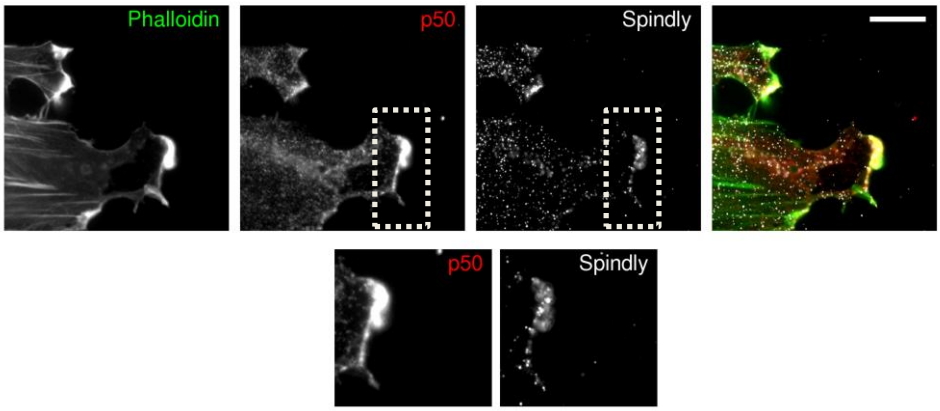


(b)

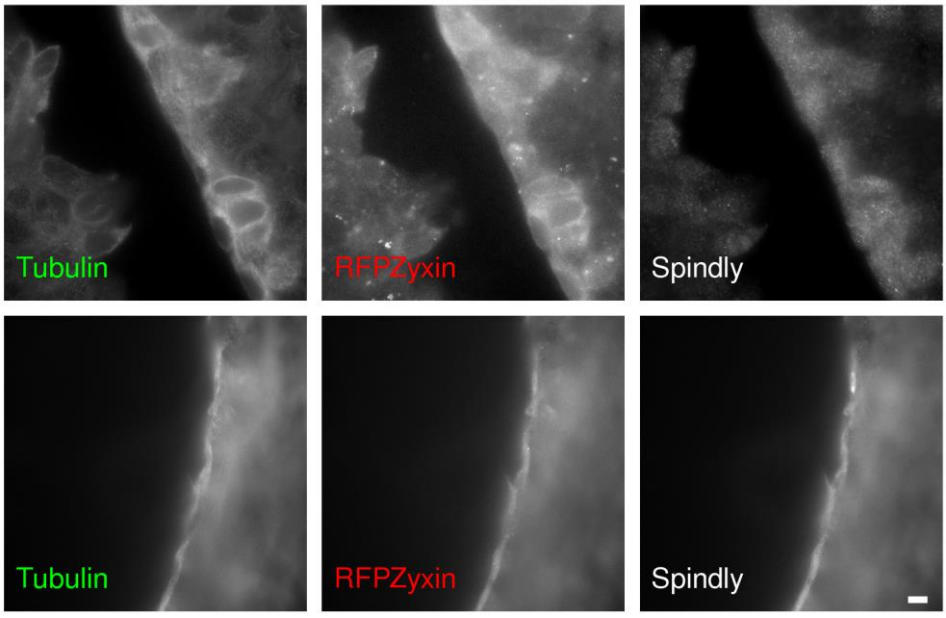


(c)

(d)

**Figure 5. 8. Spindly is recruited to the leading edge and to focal adhesions upon scratching.**

(a) Immunofluorescence of Human fibroblasts wounded for at least eight hours before fixation showing: actin (Phalloidin, green), dynactin (anti-p50, red) and Spindly (anti-Spindly, white). 20X magnification. Scale bar 10 µm. (b) 60X magnification of cells as (a). Scale bar 10 µm. Details underneath each panel ((a) and (b)) represent magnified images derived from the boxed areas (dashed white box). HaCAT cells (c) or primary Mouse embryonic fibroblasts (d) were

scratched and fixed after eight hours. 20X magnification. Staining shows: Tubulin (anti-Tubulin, green), RFP-Zyxin (red), Spindly (anti-Spindly, white). Scale bar 10 μm.

We detected a clear enrichment of Spindly at the leading edges (within lamellipodial protrusions, as highlighted from the boxed areas in figure 5.8 (a) and (b)) of moving human fibroblast migrating towards the other edge of the wound. Dynactin (p50 subunit) co-localised with Spindly at these sites, an enrichment of the dynein-complex consistent with previous results showing a direct role for this motor in cell movement (Dujardin *et al.*, 2003). Furthermore, Spindly was enriched also at the leading edge MEFs (Fig. 5.8 (d)), co-localising with RFP-Zyxin, a specific marker of focal adhesions (Reinhard *et al.*, 1999). For HaCAT cells instead we could not registered a clear enrichment at the leading edge but only an upregulation in the leading edge (Fig. 5.8 (c)).

To further analyse leading edge localisation of Spindly and its dynamics, we co-transfected both U2OS cells and human fibroblasts with GFP-Spindly and RFP-Zyxin constructs. Upon scratch wounding, we followed the cells by TIRF microscopy (Fig. 5.9). Imaging was performed by Dr. Eric Griffis (University of Dundee).

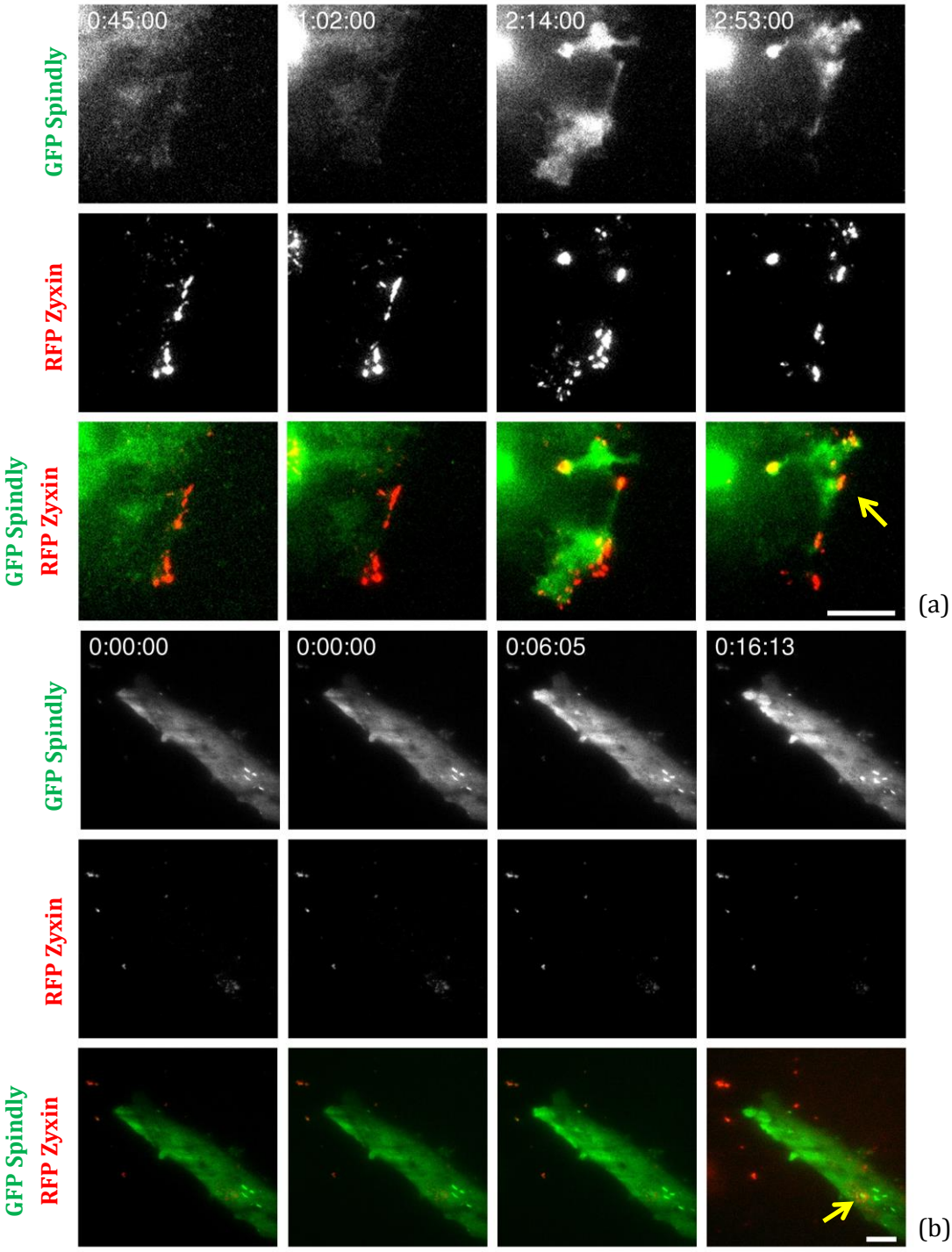


**Figure 5. 9. Localisation of Spindly at the leading edge during wound healing.**
(a) U2OS cells or (b) human fibroblasts were transiently co-transfected with GFP-Spindly (green) and RFP-Zyxin (red). Cells were followed over time under a TIRF microscope. Yellow arrows indicate co-localisation of Spindly with Zyxin. Scale bar 10 µm. Imaging performed by Dr. E. Griffis (University of Dundee).

Imaging in figure 5.9 confirmed the recruitment of Spindly to the leading edge in actively moving cells where it co-localises with the focal adhesion marker Zyxin. We have noticed that Spindly co-localised with Zyxin only significantly after migration and Zyxin redistribution had begun; this indicates that Spindly could be involved in the later stages of focal adhesion maturation or turnover (Nagano *et al.*, 2012).

## 5.6 Spindly recruitment at the cell front is based on the presence of actin filaments

The actin cytoskeleton is directly and dynamically involved in cell migration (Le Clainche and Carlier, 2008). Polarization of actin filaments and their re-organisation at the leading edge are two crucial steps promoting cell movement and thus are highly organised (Le Clainche and Carlier, 2008). Several proteins assemble at the leading edge in order to promote membrane protrusion, adhesion formation and contact with the extracellular-matrix (Sastry and Burridge, 2000). As well as actin filaments, microtubules are also involved in the internal organisation of the cell, playing a direct role in cell shaping and mechanics. Their capacity to regulate cell polarity relies on the presence of microtubule-associated proteins that control microtubule nucleation and dynamics (Etienne-Manneville, 2013). Given the high importance of both systems in cell migration and polarisation, a common belief is that there is a functional crosstalk between microtubules and actin filaments (Rodriguez *et al.*, 2003).

To investigate the specificity of Spindly recruitment to the leading edge and how it gets localised there, we perturbed either microtubules, by administrating Nocodazole (as MT depolymerising agent), or actin filaments, by adding either Latrunculin A (LAT A) or Jasplakinolide (JAS), and looked at Spindly localisation (Fig. 5.10). Latrunculin A blocks actin polymerisation causing depolymerisation (Coue *et al.*, 1987)) while treatment with Jasplakinolide *in vivo* disrupts actin filaments inducing polymerisation of monomeric actin into amorphous masses (Bubb *et al.*, 2000)

(a)

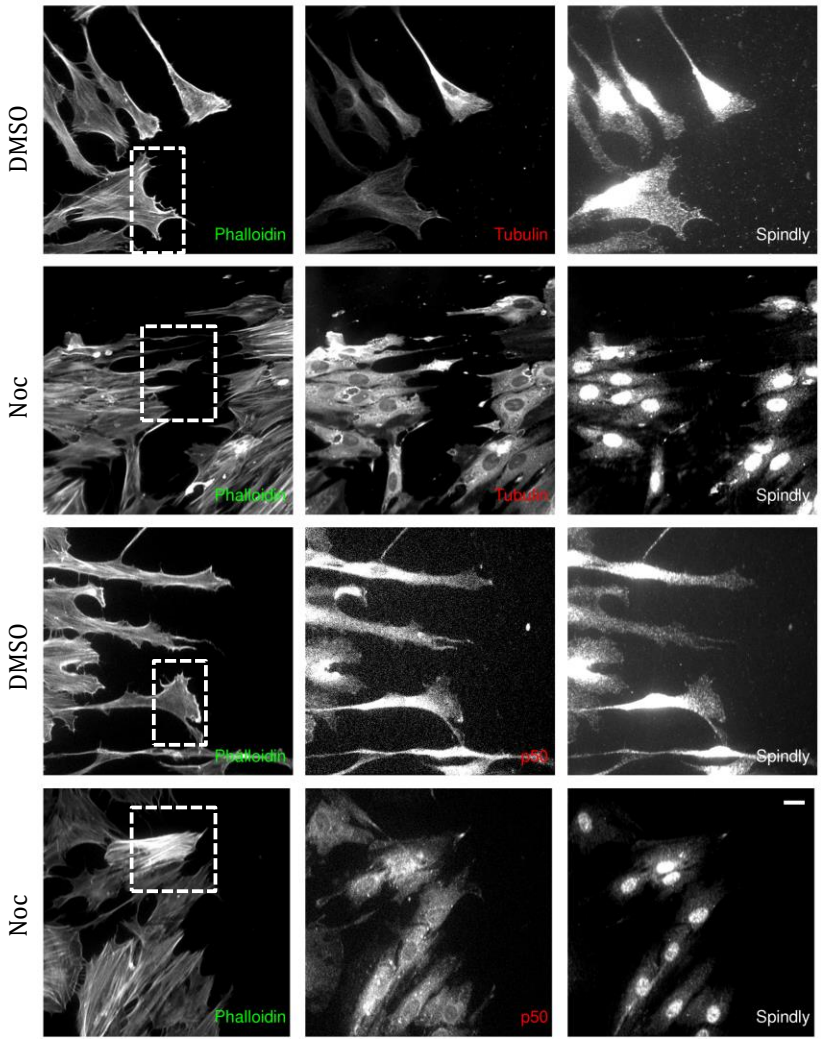
DMSO
Noc
DMSO
Noc
Phalloidin
Tubulin
Spindly
Phalloidin
Tubulin
Spindly
Phalloidin
p50
Spindly
Phalloidin
p50
Spindly

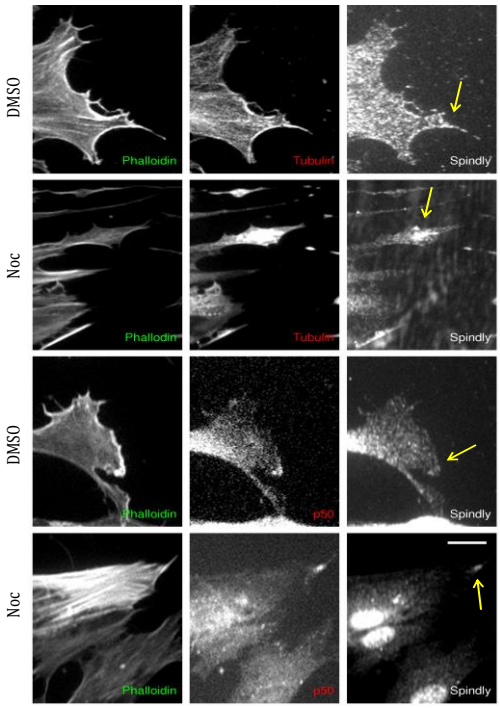
DMSO
Noc
DMSO
Noc
Phalloidin
Tubulin
Spindly
Phalloidin
Tubulin
Spindly
Phalloidin
p50
Spindly
Phalloidin
p50
Spindly

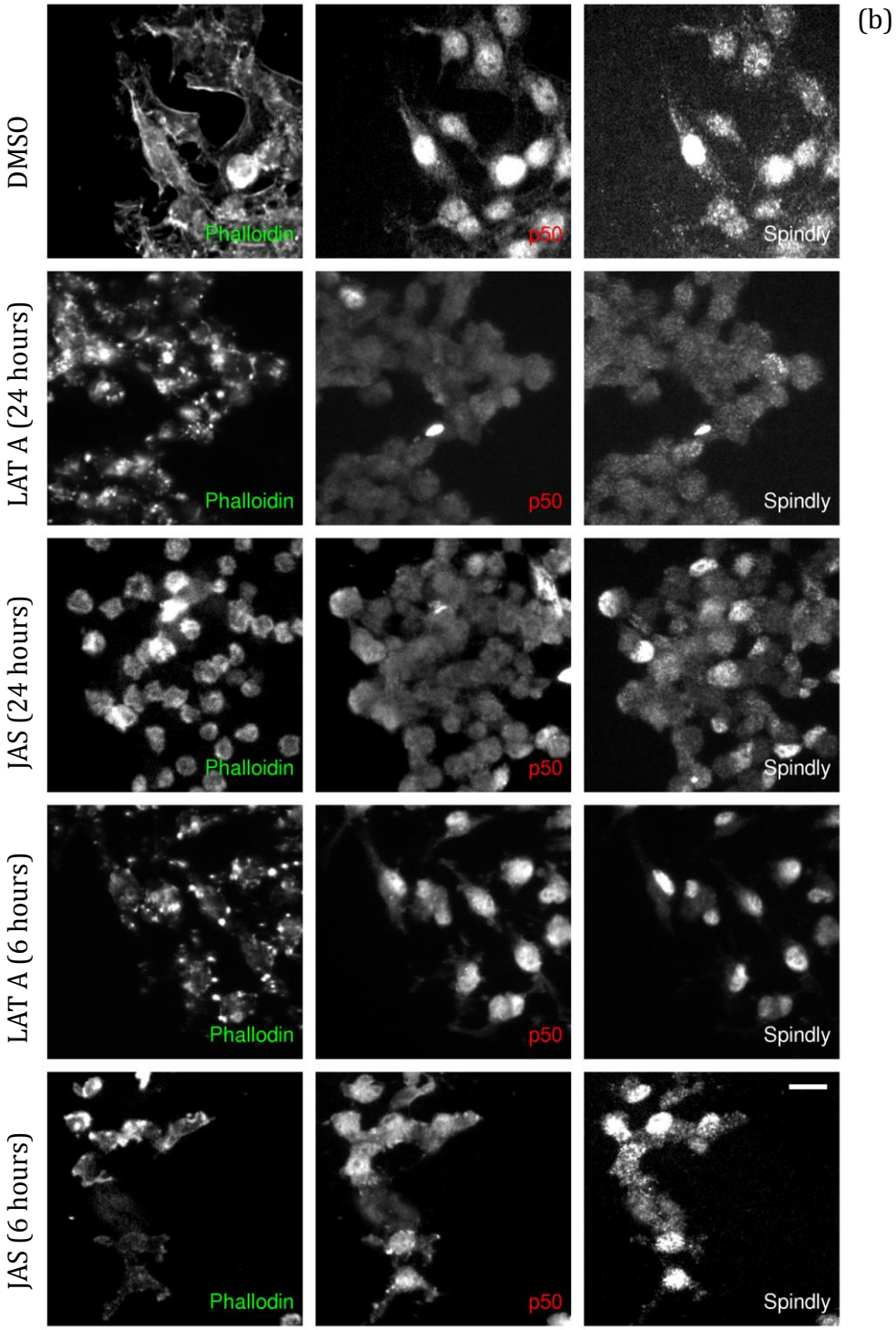


**Figure 5. 10. Spindly and dynactin localisation at the leading edge is not dependent from microtubules.**
Immunofluorescence of human fibroblasts treated with (a) Nocodazole (Noc, 100 nM) for 10 hours, or with (b) Latrunculin (LAT A) or Jasplakinolide (JAS) (100nM) for either 6 or 24 hours prior to fixation. DMSO was used as negative control (both panels (a) and (b)). **Panel (a)**: actin filaments (Phalloidin, green); microtubules (anti-Tubulin, red) or dynactin (anti-p50, red); Spindly (anti-Spindly, white). The bottom side of **panel (a)** shows magnified images derived from the boxed areas (dashed white box). Yellow arrows indicate accumulation of actin, p50 and Spindly at focal adhesion sites **Panel (b)**: actin filaments (Phalloidin, green); dynactin (anti-p50, red); Spindly (anti-Spindly, white). 20X magnification. Scale bar 20 µm.

Overnight treatment of U2OS cells with Nocodazole did not affect Spindly recruitment to actin-rich sites at the cell periphery (Fig. 5.10, (a), yellow arrows). On the other hand, when we affected the actin filament network by administrating either LAT A or JAS, we registered defects in localisation (Fig. 5.10, (b)). In this scenario however it is important to point out that these actin inhibitors dramatically affect the cell morphology so the defects registered could be related to side effects due to the treatment. Therefore there is the possibility that the defects registered in our experiments could be not specific. Thus, it would be worth to repeat this study using a new cocktail of actin drugs recently developed that allow to arrest actin dynamics without affecting the cell structure (by pre-incubating cells with Y27632 (ROCK inhibitor) and then adding LAT A and JAS for short period of time (Peng *et al.*, 2011)). On the other side, to analyse deeper the interplay between actin and Spindly in cell migration we could also study actin dynamics upon Spindly depletion. For instance it would be interesting to overexpress Rho GTPase and look at stress fibres formation and dynamics upon siRNA of Spindly.

## 5.7 Spindly depletion affects actin and phospho-Myosin distribution in migrating cells

The cell migration cycle includes protrusion, adhesion, contraction and retraction, and all of the steps are tightly coordinated. After protrusion, translocation of the cell body occurs thanks to a coordinated contraction of the actomyosin cytoskeleton, more specifically thanks to phosphorylation of Myosin 2 mediated by Myosin regulatory light chain kinases (MLCKs), a kinase that allow for separation of the diverse Myosin 2 functions by phosphorylating distinct Myosin contractile modules (Lauffenburger and Horwitz, 1996). At the lamellipodium, MLC kinases together with Rho kinase (ROCK) have been demonstrated to regulate the extension of the region and the formation of focal complexes by phosphorylating Myosin 2 inducing in this way its activation and subsequent regulation of stress fibres and focal adhesions formation (Totsukawa *et al.*, 2004). Given the defects observed in cell migration upon Spindly depletion, we decided to analyse localisation of actin and phospho-Myosin (pMyosin) in U2OS cells depleted of Spindly at the edge of a wound (Fig. 5.11).

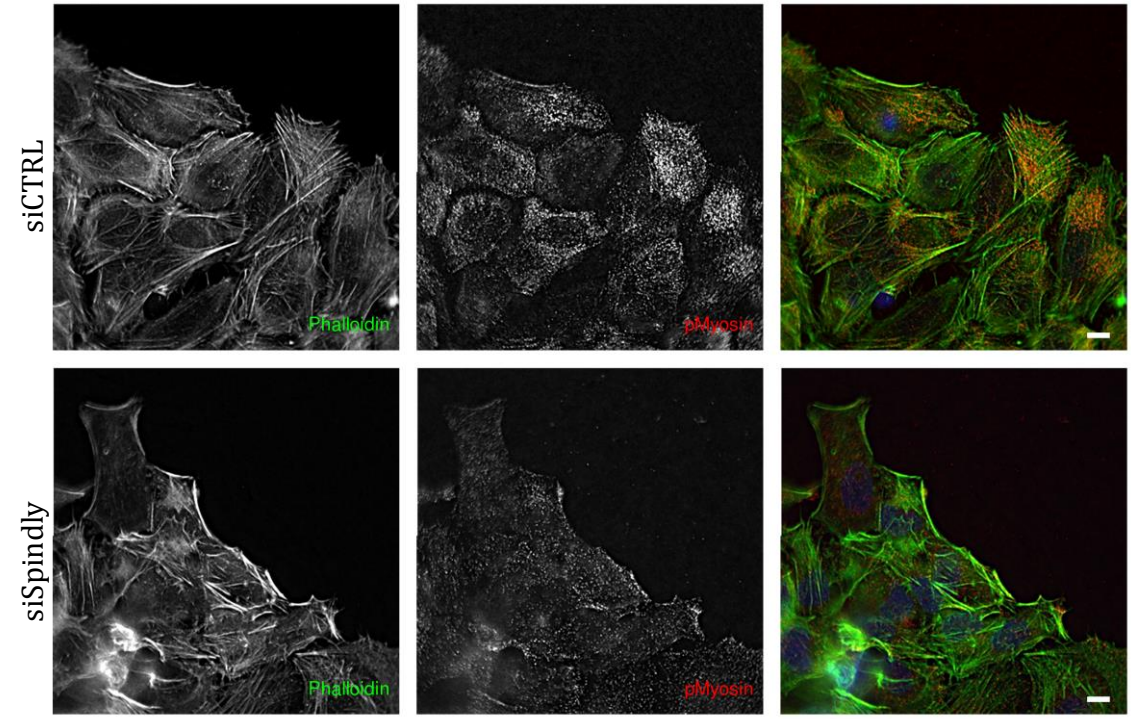


(a)

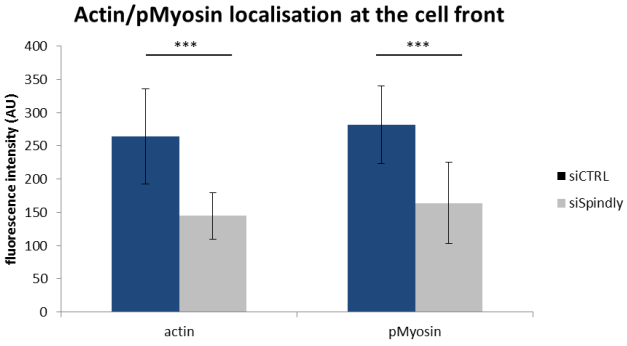


(b)

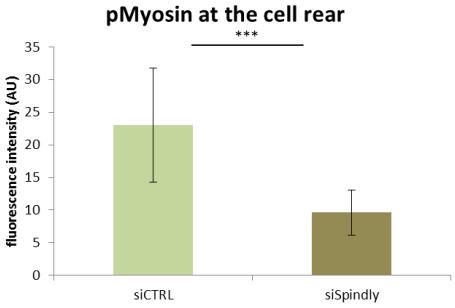


(c)

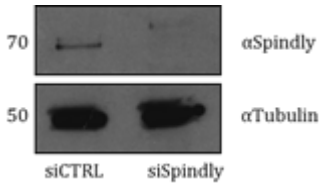


(d)

**Figure 5. 11. Spindly depleted cells present lower amount of actin and pMyosin.**
U2OS cells were treated with either siRNA for Spindly or control (CTRL) for 96 hours. Wound was performed and after 3 hours cells were fixed and stained. (a) Staining shows: actin filaments (Phalloidin, green); phospho-Myosin (pMyosin, red); Spindly (anti-Spindly, white). Scale bar 10 µm. (b) Quantification of the fluorescence intensity of either actin or pMyosin at the cell front in control or Spindly depleted cells. (c) Quantification of the fluorescence intensity of pMyosin at the cell rear in control or Spindly depleted cells. Measurements were performed with the FiJi software (n ≥ 50) and statistical analysis was performed with Excel. Data indicate the mean ± standard deviation (represented by error bars) from at least three experiments and were analysed by Student's *t-test* with significance defined by *: ***= p<0.001. (d) A sample of the same cell population was harvested and analysed by Western Blotting to confirm the silencing.

Figure 5.11 reveals that upon Spindly depletion both actin polymer and phospho-Myosin levels are reduced. We registered a significant reduction of about 40% in the amount of both markers at the cell front (5.11, (b)) and of about 58% in the level of phospho-Myosin at the cell rear (Fig. 5.11, (c)). This data corroborate our hypothesis that Spindly plays a critical role in cell migration, and it suggests that there is a function for Spindly in the formation of actin polymers and regulation of Myosin activity.

## 5.8 New potential interactors for human Spindly in interphase

As stated earlier, human Spindly has never been studied in non-mitotic cells, so there are no clues on how its recruitment to cytoplasmic foci could be facilitated and what binding partners it might have at the leading edge. Consequently, it was decided to investigate potential interactors, taking advantage of mass spectrometry technique.

We exploited the untreated HEK293 cells already processed for the former described MS study (reported in Chapter 4- Paragraph **4.5** / Fig. **4.8**). We screened the dataset for actin-related proteins that could explain the presence of Spindly at the cell front and therefore could give us new potential interactors. Specifically we took into account the number of peptides identified for each protein and the intensity value at which they were identified. We compared the list obtained for the "Spindly IP" dataset with the "IgG" dataset (our negative control) and proceeded with the analysis only for those proteins that gave an intensity value equal to zero in the "IgG" dataset.

A summary of candidates that could be implicated in the recruitment and/or in the functioning of Spindly in the cell movement process is presented in figure 5.12. Functions of the proteins reported in the table (Fig. 5.12 (a)) were confirmed from the UniProt Human Database (Fig. 5.12 (b)) and a network analysis was performed using the String-bd software (Fig. 5.12 (c)) to link those proteins according to the information already available on physical and functional protein-protein interactions, proved either by experimental data or computationally prediction (Jensen *et al.*, 2009).

| ACTIN ASSOCIATED PROTEINS | PEPTIDES | INTENSITY Spindly-IP | INTENSITY Rb IgG |
|---|---|---|---|
| MACF1 | 32 | 1045200 | 0 |
| Myosin IC | 21 | 1787900 | 0 |
| ANILLIN like protein | 11 | 3305500 | 0 |
| Arp 2/3 | 6 | 6866880 | 0 |
| FAK | 3 | 4026500 | 0 |
| Rab GAP 1 | 3 | 2278500 | 0 |
| HOOK3 | 3 | 1070200 | 0 |
| Formin BP4 | 2 | 1368800 | 0 |
| Arp 2/3 subunit 5 | 2 | 561970 | 0 |
| EMERIN | 2 | 555000 | 0 |

(a)

| Protein name | Protein function |
|---|---|
| **ANLN** | anillin, actin binding protein; Required for cytokinesis. Essential for the structural integrity of the cleavage furrow and for completion of cleavage furrow ingression. |
| **HOOK3** | hook homolog 3 (Drosophila); May regulate clearance of endocytosed receptors such as MSR1. Participates in defining the architecture and localization of the Golgi complex. |
| **MYO1C** | myosin IC; Myosins are actin-based motor molecules with ATPase activity. Unconventional myosins serve in intracellular movements. Their highly divergent tails are presumed to bind to membranous compartments, which would be moved relative to actin filaments. |
| **MACF1** | microtubule-actin crosslinking factor 1. |
| **EMD** | emerin. Stabilizes and promotes the formation of a nuclear actin cortical network. Stimulates actin polymerization in vitro by binding and stabilizing the pointed end of growing filaments. Inhibits beta-catenin activity by preventing its accumulation in the nucleus. Links centrosomes to the nuclear envelope via a microtubule association. |
| **RABGAP1** | RAB GTPase activating protein 1. May act as a GTPase-activating protein of RAB6A. May play a role in microtubule nucleation by centrosome. May participate in a RAB6A-mediated pathway involved in the metaphase- anaphase transition. |
| **ACTR2** | ARP2 actin-related protein 2 homolog. Functions as ATP-binding component of the Arp2/3 complex which is involved in regulation of actin polymerization and together with an activating nucleation-promoting factor (NPF) mediates the formation of branched actin networks. |
| **ARPC5** | actin related protein 2/3 complex, subunit 5. Functions as component of the Arp2/3 complex which is involved in regulation of actin polymerization and together with an activating nucleation-promoting factor (NPF) mediates the formation of branched actin networks. |
| **FAK** | PTK2 protein tyrosine kinase 2. Non-receptor protein-tyrosine kinase that plays an essential role in regulating cell migration, adhesion, spreading, reorganization of the actin cytoskeleton, formation and disassembly of focal adhesions and cell protrusions, cell cycle progression, cell proliferation and apoptosis. |
| **FNBP1** | Formin-binding protein. It may act as a link between RND2 signaling and regulation of actin cytoskeleton. Required to coordinate membrane tubulation with reorganisation of the actin cytoskeleton during the late stage of clathrin-mediated endocytosis. Also it enhances actin polymerisation via the recruitment of WASL/N-WASP, which in turns activates the Arp2/3 complex. |

(b)

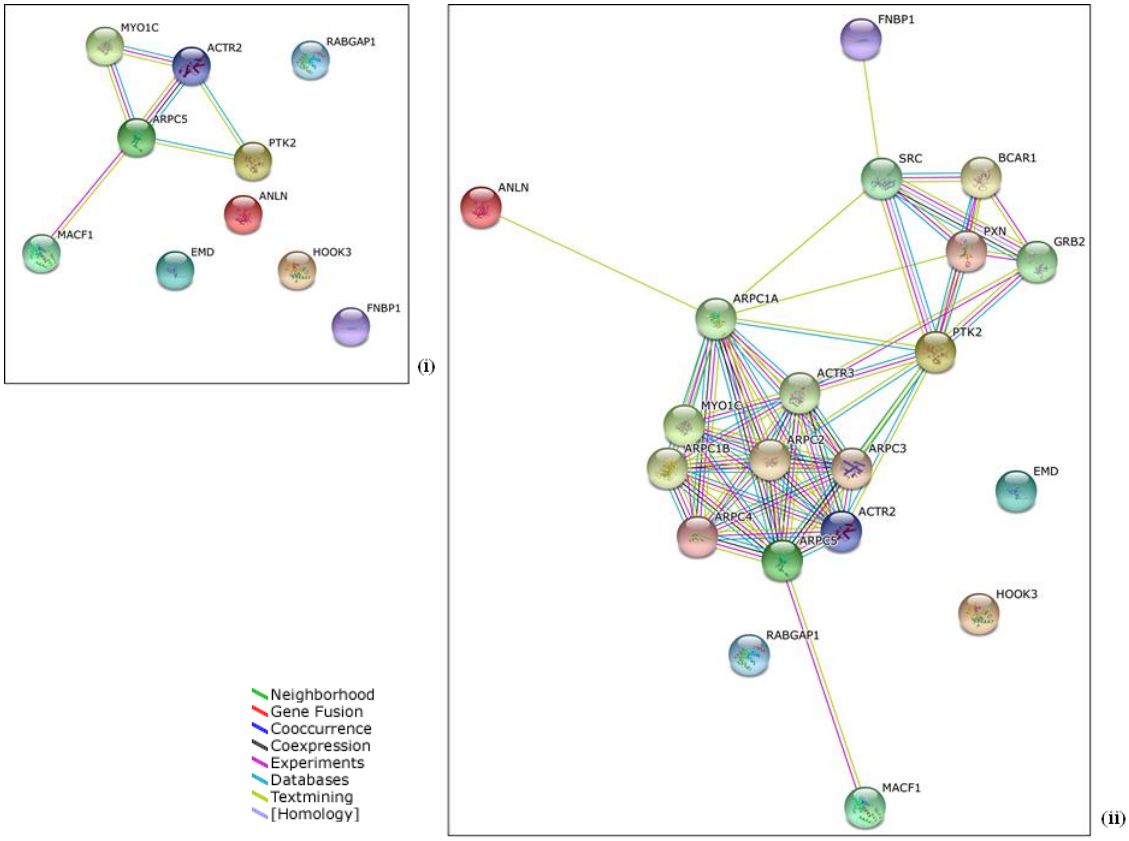


(c)

**Figure 5. 12. Identification of novel Spindly binding partners in interphase cells.**
(a) Table reporting molecular candidates enriched in samples immunoprecipitated with anti-Spindly antibody Rabbit IgG was used as a negative control. (b) Summary of the functions of the enriched proteins (adapted from information obtained from UniProt Database, www.uniprot.com). (c) STRING network Diagram representing the network for either only the Spindly-IP enriched proteins **(i)** or for the Spindly-IP enriched proteins plus their previously reported binding partners **(ii)**. This "evidence view" was obtained from String-bd.org, a database of known and predicted protein interactions derived from different sources. Colour legend is reported in the left hand-side of the panel to explain the different connection lines. Single lines mean confidence of interaction, whereas double lines indicate evidence for interaction. Each protein is represented by a node.

The sub-set of proteins obtained from the mass spectrometry analysis includes several known regulators of the actin and microtubule cytoskeleton (as reported in the table in figure 5.11, (b)). Additionally, in the list of enriched proteins for the Spindly-IP dataset, we also found other interesting proteins involved in cell migration but we did not consider them in our analysis since their IgG value was not equal to zero.

The presence of proteins already described involved in directed cell movement, cell polarisation or adhesion formation/turnover, reinforces the hypothesis that Spindly can play a role in this process in association with actin and/or microtubules, as was already suggested from results obtained earlier in this chapter.

## 5.9 Discussion

The cytoskeleton is made up of three different networks: microtubules (MTs), actin filaments and intermediate filaments (IFs). These three structures cooperate in many different cellular processes, allowing a cell to respond properly to a wide range of stimuli (Wickstead and Gull, 2011). Among these processes, cell migration directly involves the whole network to ensure first a change in the cell morphology, in response to specific signals, and then actin assembly at the leading edge, to promote extension of the membrane. Finally, the disassembly of adhesions and actomyosin contraction at the trailing edge allows for the forward movement of the cell body (Le Clainche and Carlier, 2008). Actin polymerisation dynamics are closely regulated by many different signalling molecules and a legion of binding proteins (Pollard and Borisy, 2003). Dynamic microtubules have also been shown to associate with focal adhesions in migrating cells as well as to be directly involved in cell movement (Vasiliev *et al.*, 1970) (Kaverina *et al.*, 1998). They perform an important role in controlling focal adhesion turnover and localise to the areas near these adhesion sites as direct players in the microtubule organisation or stabilisation at the leading edge (Stehbens and Wittmann, 2012). Even though actin has a main role in the organisation of the leading edge of the cell, microtubules are likewise required to maintain polarisation; the actomyosin network pushes microtubules rearwards in the lamella of motile cells where microtubule tips can be loaded with factors that regulate actomyosin activity (Salmon *et al.*, 2002) (Rogers *et al.*, 2004).

In this chapter we defined a striking role for human Spindly in cell migration; we proved an involvement of the protein in directed cell movement, describing a phenotype highly similar with those already delineated for dynein, dynactin and Lis1 (Faulkner *et al.*, 2000) (Dujardin *et al.*, 2003). Spindly depleted cells showed a reduction in the rate

of cell migration upon wounding and staining of migrating cells revealed the protein specifically recruited at the leading edge in an actin-dependent manner.
Also, we registered a reduction in both actin polymer and phospho-Myosin levels upon depletion of Spindly that suggests a role for Spindly in the formation of actin polymers and in the regulation of Myosin activity in cell migration.

As already pointed out in **Chapter 3**, Spindly is a novel adaptor for the minus-end motor complex dynein/dynactin; here we showed that this could be true not only in mitotic cells but also in interphase cells. Our results led us to propose a model where Spindly is involved in the enhancement of the dynein/dynactin targeting or motor processivity in order to promote cargo loading and/or tension generation at focal adhesion sites. The fact that we did not see centrosome positioning defects in our studies (as previously reported for dynein depleted cells (Palazzo *et al.*, 2001) (Levy and Holzbaur, 2008)) and that Spindly was enriched at focal adhesions late in their formation could suggest that the association of Spindly with the leading edge happens downstream of MTOC reorganisation and that is involved in regulation of focal adhesion maturation and turnover. According to this view, we see Spindly as a potential MT/actin filament cross-linker, crucial for proper cytoskeleton interplay during cell migration. The importance of MT/actin filament crosstalk is related to the capacity to deliver molecules or membrane components to the leading edge (Watanabe *et al.*, 2005); this mechanism has been described based on cell polarisation, more precisely on MTOC reorganisation that requires Cdc42 (a small Rho GTPase) and dynein (Palazzo *et al.*, 2001). Dynein and dynactin are recruited to the cell front from where they could generate pulling forces to move the centrosome toward the leading edge, this would allow placing the Golgi apparatus and the endocytic recycling compartment in front of the nucleus to polarise membrane trafficking toward the leading edge. Moreover, dynein

has been demonstrated to be involved in Golgi dynamics and structure maintaining in association with dynactin (that associates with spectrin (Holleran *et al.*, 2001)) suggesting a role for it in the trafficking of cargos at the front of the cell (Etienne-Manneville, 2013). Therefore Spindly could either help the recruitment of dynein at the leading edge or promote the process of cargo loading and enhancing the processivity of the motor.

From our mass spectrometry analysis we identified a list of potential binding partners of high interest. Several of them are cytoskeletal regulatory proteins also involved in focal adhesion formation, assembly and dynamics; they contribute to the reorganisation of the cytoskeleton network upon wounding corroborating our hypothesis that Spindly can exert a role in cell motility. Interesting was, for instance, the presence of MACF1 (microtubule actin cross-linking factor 1, also called ACF7), a protein that plays a role in stabilisation of microtubules at the leading edge and also controls focal adhesion assembly and dynamics (Kodama *et al.*, 2003). In the same way, Anillin attracted our attention since it has been described in the regulation of actin cytoskeleton dynamics as well as in the cross-talk between actomyosin cytoskeleton and microtubules (Tian *et al.*, 2015). Spindly could also immunoprecipitate other proteins directly involved in the focal adhesion assembly process. Focal adhesion kinase (FAK) is crucial for the turnover of cell contacts. It is typically located at focal adhesions and phosphorylated upon integrin engagement (Burridge *et al.*, 1992) (Arold *et al.*, 2002); it mediates the link between the extracellular matrix (ECM) and the cytoplasmic cytoskeleton as does Emerin, (in our Spindly-IP as well) by interacting with the nuclear lamins (Clements *et al.*, 2000) (Chang *et al.*, 2013). Curiously, we identified two subunits of the Arp2/3 complex, a major player in the regulation of actin cytoskeleton since it stimulates polymerisation of new actin filaments (Pollard, 2007). The Arp2/3 complex has been found at the leading edge of motile cells (precisely within

lamellipodia, where we also observe Spindly) and it is involved in the establishment of cell polarity (Magdalena *et al.*, 2003). Finally, it was intriguing to find RABGAP1, the GTPase activating protein of Rab6, a marker for vesicle trafficking that promotes microtubule-mediated transport to the cell periphery together with kinesin-1 or dynein via BicD (Grigoriev *et al.*, 2007) (Hoogenraad *et al.*, 2003).

It remains to be determined what exactly its function is; Spindly could be operating through its regulation of dynein/dynactin, it could have a direct role in regulating actin polymerisation or focal adhesion function, or it could play a combination of these activities.

Although experiments conducted in this study suggest a new role for Spindly in cell migration in interphase cells in relation with the motor complex dynein/dynactin, further analyses are still needed to fully understand the mechanism behind its recruitment at the leading edge and its mechanism of action. Our data support different potential functions of Spindly in cell migration. On one side, cortical Spindly could be directly modifying actomyosin activities to promote protrusion or focal adhesion maturation and/or turnover (as hinted from its specific localisation and recruitment at sites, potentially by an association with FAK) (Fig. 5.13 (a)). On the other side, Spindly could be playing a function in association with the dynein/dynactin motor complex at the leading edge, potentially mediating the intracellular trafficking of actin filaments from the front to the rear to support actin turnover (as suggested from the interaction with Arp2/3, Anillin and Formin Binding Protein) (Fig. 5.13 (b)). Finally, the localisation of Spindly at the leading edge and at the MT-plus ends suggests a potential role in the stabilisation of MTs at the leading edge and/or in the physical linking of the two cytoskeleton networks, MTs and actin filaments (as suggested also from the interactors MACF1) (Fig. 5.13 (c)).

These hypotheses are not mutually exclusive and they would need to be tested to understand the dynamics of these interactions.

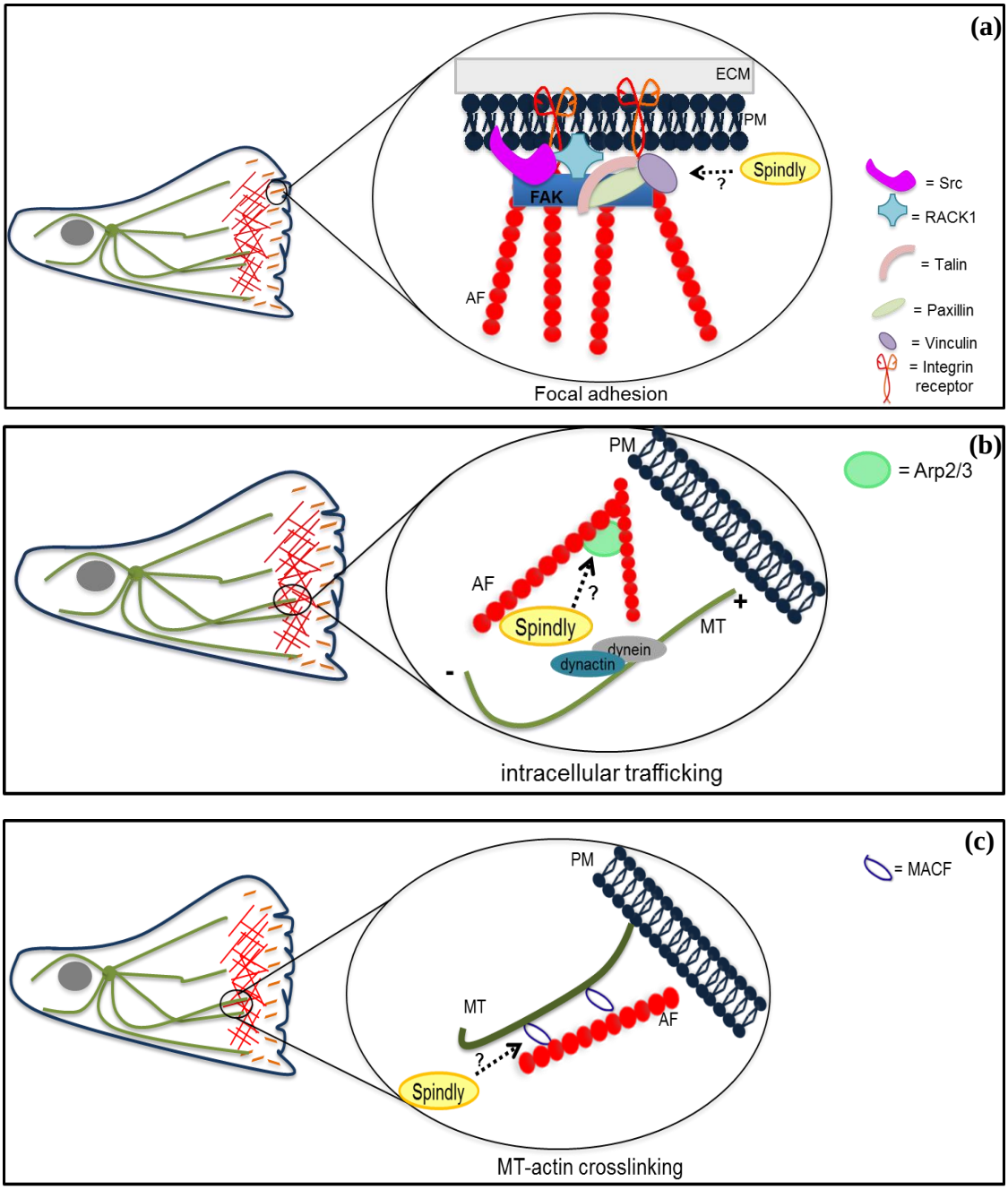


**Figure 5. 13. Schematic model for potential functioning of Spindly in cell migration.** Spindly could be: (a) involved in focal adhesion maturation and/or turnover; (b) interacting directly with actin filaments and maybe mediating their trafficking in association with dynein/dynactin; (c) mediating the crosslinking between actin filaments and microtubules, potentially in relation with MACF1. PM: plasma membrane; MT: microtubules; AF: actin filaments.

# 6 . Discussions and future perspective

## 6.1 Spindly in mitosis

Spindly was discovered due to its role in mitotic progression. Cells depleted of this protein were incapable of proceeding through cell division but were arrested in metaphase and were eventually undergoing either apoptosis or mitotic slippage with progression into anaphase and poor outcomes for the daughter cells. The studies that followed the initial discovery of Spindly shed light on other important details about its function in mitosis, pointing out why the lack of Spindly induced such a strong mitotic phenotype, in relation with its role in the regulation of chromosome alignment and spindle assembly checkpoint silencing and also identifying a critical region involved in these functions (see **Chapter 1- Paragraph 1.3**) (Griffis *et al.*, 2007) (Gassmann *et al.*, 2008) (Chan *et al.*, 2009) (Gassmann *et al.*, 2010) (Barisic *et al.*, 2010). Therefore the emergent model places Spindly as central in the progression of mitosis and in the coordination of KT-MT binding with SAC silencing process.

The aim of this thesis was to investigate in depth the role of Spindly in mitosis. We focused on the interaction with the dynein/dynactin motor complex and on the functioning of Spindly in relation with the mitotic checkpoint, following the idea that Spindly could play a part not only in its silencing but in establishing or maintaining the signalling of the SAC until bi-orientation has been achieved.

### 6.1.1 The interaction between Spindly and the dynein/dynactin motor complex

Kinetochore localisation of dynein is needed for poleward movement of chromosomes in early mitosis upon interaction with microtubules (Yang *et al.*, 2007); then once bi-orientation is achieved dynein leaves the kinetochore and streams along microtubules to the spindle poles stripping away the components of the SAC to silence the signalling and promote anaphase onset (Howell *et al.*, 2001). The presence of

Spindly at kinetochores is fundamental for the correct localisation of the dynein/dynactin motor complex (Griffis *et al.*, 2007) (Gassmann *et al.*, 2008) (Chan *et al.*, 2009) (Gassmann *et al.*, 2010) (Barisic *et al.*, 2010) (Cheerambathur *et al.*, 2013).

In this work, we have shown for the first time an interaction between Spindly and the dynein/dynactin motor complex. Results obtained revealed that Spindly can pull-down both dynein and dynactin (see **Fig. 3.2** / **Fig. 3.8**). Interestingly, it has been demonstrated a specific binding between Spindly and the p150 subunit dependent on the "Spindly box" region (see **Fig. 3.5** / **Fig. 3.8**); thus this subunit is likely to be a link between Spindly and the motor complex.

Recent publications pointed out that dynactin is not sufficient to activate the processivity of dynein, but instead motility requires an adaptor protein that can link both complexes (Schlager *et al.*, 2014). Among the proteins tested, Spindly was described to have the capacity to promote dynein/dynactin processivity (McKenney *et al.*, 2014). Putting together results from these publications and those gathered in this thesis, the hypothesis that Spindly is an important adaptor of the dynein/dynactin motor complex becomes stronger. It is likely that dynein/dynactin and Spindly generate a ternary complex active only in specific sites within the cell and for selective cellular processes. To dissect this association and the assembly process of the complex, additional experiments will follow this thesis. We have begun experiments in collaboration with the Carter lab (LMB, Cambridge), which previously solved the crystal structure of dynein (Carter *et al.*, 2011) and the EM (electron microscopy) structure of the dynein/dynactin complex (Urnavicius *et al.*, 2015), to look at this potential ternary complex. The Carter lab has managed to solve the EM structure of Spindly (although not with a level of resolution where we can identify amino acids), but we have not been able to reconstitute the ternary complex yet (as judged by SEC experiments (data not shown)) using recombinant human Spindly (produced in bacteria or in insect cells), pig

brain dynactin and a recombinant dynein tail complex, suggesting that there has to be an additional layer of regulation. We are currently exploring whether dimerisation/multimerisation of Spindly influences complex assembly (we see binding of dynein/dynactin when Spindly is present at high concentrations on beads, but not in solution). It is also possible that the farnesylation site at the *C*-terminus drives the protein to locally concentrate on the kinetochore and to promote clustering and subsequently the dynein/dynactin binding, similar to how kinesin Unc104 membrane association promotes its dimerisation and activation (Tomishige *et al.*, 2002). We are therefore making an MBP-Spindly expression construct with a C-terminal leucine zipper from GCN4 to make a dimerised protein that the Carter lab can test.
If we can assemble the Spindly-dynein-dynactin complex, the Carter lab will solve the structure by cryo-EM.

As reported in the Introduction (see **Chapter 1- Paragraph 1.3**), the structure of Spindly is characterised by two coiled-coil regions interspersed with a highly conserved sequence, the 'Spindly-box', present in all the species among which Spindly has been identified (Gassmann *et al.*, 2010) (Barisic *et al.*, 2010). The work presented in this thesis showed that single mutation within this region (S256A) specifically impairs the association between Spindly and the p150 subunit of dynactin, but it does not seem to affect the interaction with dynein. This hints that Spindly interacts also with dynein, but independently of dynactin to allow for chromosome alignment to occur properly (Gassmann *et al.*, 2010). Moreover, our collaborators in the Vaughan lab have found that dynein can still stream from kinetochores when the Spindly S256A mutant is expressed, whereas it does not when Spindly is depleted. This result suggests that in the S256A mutant expressing cells dynein reaches the kinetochores and streams away without loading/stripping cargos and it could explain why cells expressing the mutant can still align chromosome properly. These data also show that Spindly interacts with

dynein/dynactin in a manner that is different from BicD, which only interacts with the holo-complex but cannot bind to either complex separately.

Previous data have reported how dynein can play two functions at KTs, regulating chromosome alignment and stripping proteins from KTs to allow anaphase onset (Howell *et al.*, 2001) (Yang *et al.*, 2007). It has been demonstrated that dynein is present at KTs in two states, a phosphorylated one (on the intermediate chain), which interacts with the RZZ complex, and a non-phosphorylated one, which associates with dynactin (Whyte *et al.*, 2008). Therefore, it might be that phospho-dynein binds to KTs prior to microtubule attachments and that KT-MT interactions then induce the de-phosphorylation (upon generation of tension) to promote association with dynactin and activation of the stripping process. In this scenario, Spindly could behave as an activator of the motor complex and/or as an anchor for the motor to the RZZ complex. The registered interaction between Spindly and dynein in both immunoprecipitation experiments and in direct *in vitro* binding assays indicate that there is a strong association that is not affected by the S256A mutation. We therefore hypothesise that while phospho-dynein interacts with the RZZ complex through Spindly it is inhibited from streaming but capable of relieving the RZZ-mediated inhibition of forming proper 'end-on' KT-MT attachment. Once dynactin associates with Spindly and the dynein that it is bound, the motor becomes processive and can promote stripping of SAC components.

Further studies will allow us to shed the light on this mechanism. It would be interesting to look at the processivity of the dynein/dynactin motor complex when the Spindly mutant is substituted with the wild-type protein. The Vale lab revealed that this complex is processive on microtubules, but in personal communications with Dr. McKenney, we did find out that Spindly was not as efficient at promoting processivity of dynein/dynactin as BicD. Our IP and Y2H results showed that the S256A mutant

cannot bind to the p150 dynactin subunit, suggesting that this mutant may not be able to support processive motility on microtubules. If we can find conditions that promote the formation of a stable ternary Spindly/dynein/dynactin complex (as previously explained), the Vale lab will retest the WT and S256A Spindly proteins for their ability to promote motor processivity.

### 6.1.2 A role for Spindly in SAC signalling

As previously stated, *Drosophila* Spindly plays a role in SAC silencing; indeed its depletion causes Mad2 accumulation on aligned kinetochores (Griffis *et al.*, 2007). Curiously, in human cells depletion of Spindly did not have the same effect. This indicated that in the absence of Spindly, dynein (which is never brought to the kinetochore under this condition) is not needed to silence the SAC, suggesting that Spindly may reinforce or help to maintain the checkpoint. The goal of this thesis was therefore to investigate a possible active role for Spindly in checkpoint signalling.

Data collected in the present study identified an interaction between Spindly and proteins of the SAC pathway. Spindly was demonstrated to pull down BubR1 and Mps1, two important players of the mitotic checkpoint. BubR1 is part of the MCC complex, the core player of the SAC involved in the direct inactivation of the APC/C (Lara-Gonzalez *et al.*, 2012) (interactions with APC/C components were also observed in our MS analysis). BubR1 also plays a role in the inactivation of the SAC (see **Chapter 1- Paragraph 1.2**), thus the interaction between Spindly and BubR1 could be important either for the activation/signalling of the checkpoint and/or for its inactivation. If the interaction between Spindly and BubR1 is essential, and if we can find a subtle mutation that alters the binding, then we would be able to make a double mutant that will fail to arrest cells in mitosis in spite of its continued presence on kinetochores.

The association with BubR1 was confirmed also by the MS analysis of mitotic cells and by a 'mis-localisation' system that allowed us to verify the binding in cells. Upon mis-localisation to the plasma membrane Spindly was still able to interact with BubR1 as well as with Mps1 and Mad2. The fact that the association with Mps1 and Mad2 was seen only when the SAC proteins were overexpressed suggests that it might be indirect or of low affinity. Further investigations will be carried out in order to verify the potential presence of a complex and the mechanisms behind its assembly, to understand when Spindly starts its association in the SAC pathway. It would be interesting to repeat the size-exclusion chromatography experiment, comparing lysates made from cells treated with Nocodazole or STLC to enrich for cells with different kinetochore statuses (+/- MT attachments) and potentially get different population of interactors.

In the future, the exact nature of the role of Spindly in the SAC signalling pathway needs to be determined; looking at our results we can propose some potential models. Spindly could be a scaffold protein that, after KT-MT attachment, mediates the loading of the SAC components onto a large dynein/dynactin transport complex; so, when Spindly is not removed from kinetochores, it keeps SAC proteins present and the checkpoint active. Alternatively, Spindly could be inhibiting the crucial de-phosphorylation of Knl1 that facilitates SAC silencing. Finding that Spindly co-immunoprecipitates with key phosphatases PP2A and PP1 and the kinase Mps1 suggests that it could have a role in regulating KT phospho-signalling. If this was the case, then the regulation of well-characterised kinetochore phosphosites, which are involved in SAC activation/inactivation, would be altered in cells expressing solely the unstrippable Spindly mutant (S256A).

Finally it could also be that the mere presence of Spindly on the kinetochore is sufficient for maintaining SAC activity. Then we should be able to recapitulate the 'Spindly box' mutant effect by using the FRB-FKBP system, where we use Spindly-

FKBP and a KT protein-FRB. This technique has already been exploited to show that the retention of Mad1 and/or Mps1 is sufficient to arrest cells in metaphase (Jelluma *et al.*, 2010) (Kuijt *et al.*, 2014). We could also use this system to determine which proteins are aberrantly retained on KTs when Spindly is irreversibly targeted, and we can use the Spindly truncation mutants to determine which domains of Spindly are required for the arrest.

Our work further illuminated the interactions between Spindly and the kinetochore. First of all, we observed an association with the RZZ complex; Spindly was observed able to pull down the ZW10 component in IP experiments and Rod was identified in the MS results, confirming the already proposed interaction of Spindly with this complex (Chan *et al.*, 2009) (Barisic *et al.*, 2010). The RZZ complex is important to mediate the localisation of Spindly at the KT, and the *C*-terminus of Spindly (which is essential for correct KT targeting) has been found to locate close to Zwilch, ZW10 and the *N*-terminus of Rod (Varma *et al.*, 2013) Moreover, this domain of Spindly has recently been shown to be farnesylated to allow for kinetochore binding (Holland *et al.*, 2015) (Moudgil *et al.*, 2015); this post-translational modification could be required for the interaction with the RZZ complex as well as with the two kinetochore proteins, CENP-E and CENP-F, which were identified in our study as novel binding partners of Spindly.

CENP-E and CENP-F are proteins that require farnesylation to allow correct progression through mitosis (Ashar *et al.*, 2000) (Hussein, 2002) (Schafer-Hales *et al.*, 2007), hence these three fibrous corona proteins, crucial for correct microtubule attachments, are all farnesylated to either interact with each other or with some common farnesyl-binding anchor. Curiously, the interactions with CENP-E and/or -F are insufficient to anchor Spindly at KTs. In the absence of RZZ, CENP-E and -F are present, but Spindly does not reach kinetochores (Barisic and Geley, 2011). Spindly

could therefore require an initial interaction with RZZ to then bind to these CENP proteins and/or a common anchor. FRET experiments could help to elucidate how these kinetochore complexes are interacting with Spindly in the presence and absence of MT attachments. Studies of the dynamics of Spindly in the absence of CENP-E/F can also determine whether these proteins mediate the anchoring of Spindly to kinetochores.

## 6.2 Spindly in interphase

Previous reports on Spindly have looked at it mainly as a mitotic protein, localised within the nucleus before entry into mitosis and then degraded upon exit from mitosis (see **Chapter 1- Paragraph 1.3**). Our aim in this thesis was therefore to untangle the function of human Spindly in non-mitotic cells and more precisely its role in interphase in relation with the cytoskeleton network.

### 6.2.1 Spindly in cell migration

In this work, a novel role for human Spindly in interphase was described, in line with what was already proposed for *D.mel.* Spindly. We identified a pool of the protein within the cytoplasm and on chromatin (see **Fig. 5.1**) and we reported presence of GFP-Spindly at the plus-ends of growing microtubules (see **Fig. 5.2**), validating former data obtained in a different organism (Griffis *et al.*, 2007). Moreover, size-exclusion chromatography analysis of asynchronous cells revealed a fractionation profile that suggested the formation of a complex between Spindly and dynactin not exclusive for mitosis and consequently indicates a possible role for Spindly as an adaptor of the motor complex for different cellular processes (see **Chapter 3**).

Dynein and dynactin have been shown to be active players in the cell migration process; they have been demonstrated to be involved in cytoskeleton reorganisation upon monolayer wounding and in directed cell movement (Palazzo *et al.*, 2001) (Faulkner *et al.*, 2000) (Dujardin *et al.*, 2003). Dynein has also been proved to be crucial for anchoring microtubules at the cell front (precisely at the cell cortex) to then generate forces needed for centrosome repositioning to direct cell migration (Dujardin *et al.*, 2003) (Manneville *et al.*, 2010).

In this thesis, we analysed cell migration in Spindly-depleted cells, revealing slow rates of cell movement in cell-culture based wound-healing assays. We demonstrated

the tight dependency of this phenotype on Spindly expression, since a GFP-Spindly construct could rescue the migration rate up to control levels and independently from mitosis.

We reported an enrichment of hSpindly at the leading edge of fibroblasts and, more precisely, a co-localisation with Zyxin at focal adhesion sites within lamellipodia. Spindly was observed at focal adhesions significantly after Zyxin redistribution had begun, consistent with a role in later stages of cell migration (potentially in relation to focal adhesions maturation or turnover). The similar defects were registered in dynactin depleted cells with a comparable localisation within the lamellipodia in migrating fibroblasts, let us hypothesise a non-mitotic function of Spindly mediated by an association with the dynein/dynactin motor complex, potentially using a similar mechanism as in mitosis.

To validate our hypothesis of a close relation between Spindly and dynein/dynactin in cell migration, it would be useful to look carefully at the two main functions of dynein in this process: cellular trafficking and centrosome positioning. A preliminary analysis was conducted to examine MTOC re-organisation upon wounding in Spindly-depleted cells, but no obvious defects were observed suggesting that Spindly is not crucial for this process to occur. Live imaging experiments tracking centrosome positioning in Spindly-depleted cells would help to rule out this supposition and so to determine if the process happens with the same timing in cells lacking Spindly. On the other side, Spindly could also be involved in the dynein-mediated membrane trafficking process (Schmoranzer *et al.*, 2003) (Manneville *et al.*, 2010). Following this idea, it could be that Spindly plays a role in cell migration similar to the one we showed it plays in mitosis, as a modulator of the targeting and/or processivity of the dynein/dynactin motor complex in order to promote streaming of cargos to the delivery site. Thus,

Spindly could work with dynein/dynactin in different cell cycle phases as a cargo-specific adaptor of the motor complex in different cellular processes.

Future studies will investigate this possibility, looking closely at membrane trafficking in Spindly-depleted cells. Nevertheless, we think that Spindly is not involved with all interphase functions of the dynein/dynactin complex; in fact, lack of Spindly expression does not affect dynein/dynactin-dependent endosome positioning in S2 cells (Griffis *et al.*, 2007) or the morphology of the Golgi apparatus in HeLa cells (data not shown).

The presence of Spindly at focal adhesion sites (within lamellipodia) and its capacity to bind to other proteins important for focal adhesions and/or lamellipodia formation, together with its essential requirement for cell migration, strongly suggest that Spindly is involved with cytoskeletal activity at the leading edge. Future work will be needed to establish if Spindly is directly involved in maturation/turnover of focal adhesions and/or if it can act more as a cross-linker between microtubules and actin filaments near the membrane. To make progress towards this goal, a better understanding of binding partners of Spindly in this molecular process is crucial. In our work we started analysing the network of proteins to which Spindly could be associating to promote cell migration, we gained different interesting insights that would be interesting to study further in the future.

Data collected in this thesis did not allow us to determine the specific pathway in which Spindly acts; however, they did reveal a novel function for Spindly in interphase that surely will need to be deeply explored in the future. It would be interesting to define whether the role of Spindly in this cellular process is solely through dynein/dynactin or whether it has other functions on its own. Both possibilities are plausible and not exclusive; Spindly could, on one side, regulate the motor complex at

the cell front and/or at focal adhesions, and, on the other side, it could interact with actin and/or microtubule filaments and mediate protrusion formation or dynamics.

## 6.3 Final remarks

Most tumours arise from aneuploidy due to chromosome mis-segregation or over-replication and so show chromosomal instability (CIN). CIN can originate from errors during cell division that lead to the total gain/loss or fractionation of chromosomes; CIN occurs often from deletions, amplifications or translocations that arise from breaks in the DNA (Geigl *et al.*, 2008). Over the years it has been shown that SAC impairment is a major cause of CIN; this impairment has been registered with high frequency in many cancer cells and it is associated with either deletions/mutations/truncations within SAC genes (Weaver and Cleveland, 2005). To date, many SAC components have been described playing a role in aneuploidy generation and consequently in carcinogenesis (Barbosa *et al.*, 2011). For example, inherited mutations in the BUB1B gene result in chromosomal mis-segregation and increased tumour incidence in humans (Hanks *et al.*, 2004). Additionally, Mad2 knock out has been widely proven to lead to premature anaphase onset, with subsequent mitotic catastrophe and apoptosis, while the down regulation of Mad1 is associated respectively with SAC inactivation and aneuploidy (Wang *et al.*, 2010) (Bargiela-Iparraguirre *et al.*, 2014) (Kienitz *et al.*, 2005). Similar behaviour has been reported for Bub1 and Mps1 where either down regulation or overexpression is associated with weakening of the SAC and tumour formation (Jeganathan *et al.*, 2007) (Ling *et al.*, 2014). Thus, a debilitated SAC contributes to oncogenesis in many types of cancer confirming that the expression levels of SAC components is crucial to ensure correct cell division (Barbosa *et al.*, 2011).

Intriguingly, the role of dynein has been recently elucidated in some tumours too. Precisely, studies on the light chain LC7 (km23-1) showed that the overexpression of this subunit causes accumulation of cells in prometaphase, retention of BubR1 at KTs and in turn suppression of cell growth, suggesting that high levels of the protein disrupt its functioning in SAC proteins streaming and putting LC7 as a critical cell growth

regulator (Pulipati *et al.*, 2011). Targeting the SAC and chromosome alignment simultaneously has been reported able to kill tumour cells (Janssen *et al.*, 2009). Specific targeting of mitotic- dynein/dynactin can therefore effectively inhibit growth of rapidly dividing cancer cells, and a better understanding of its regulation can identify new targets that can be exploited to inhibit tumour growth.

In this thesis we identified new interactions that can show how Spindly is involved in the regulation of the spindle assembly checkpoint and therefore in the transition between metaphase and anaphase during mitosis. Mapping its capacity to interact with the dynein/dynactin motor complex and its association with some of the SAC components, we shed light on novel mechanisms that, upon further studies, would allow us to much better dissect the key inflection point that lies at the heart of the cell division process. Our findings propose Spindly as a multifunctional protein in mitosis; it indeed is involved in the SAC pathway (where it could be an active player of the signalling), in the dynein/dynactin stripping process (where it is critical for timing the silencing of the SAC) and in the 'sensing' of correct KT-MT associations (where, interacting with CENP-E, could behave as a coordinator between the SAC signalling and the KT-MT attachments). For all the different functions that it plays, it could be essential that it is not mutated or over/under-expressed as this would deeply alter cell division and potentially induce carcinogenesis. However, to date there is not much known about Spindly and cancer generation (information obtained from www.oncomine.org), but its critical role in cell division indicates that understanding its mechanism of action could represent an important target for future cancer drug development.

In the present work, we depicted a new role for Spindly in cell migration. Surely this function has to be explored in detail, but cell migration is core to the process of metastasis and many factors that regulate cell migration have been shown to be mutated and/or upregulated in metastatic cells. Actin, actin-regulatory proteins, adhesion molecules and membrane signalling proteins are often overexpressed in solid tumours being involved either in the formation of protrusions (like lamellipodia or invadopodia) or in setting the direction of motility (Stevenson *et al.*, 2012). Researchers are therefore trying to identify pathways that are activated in the processes of metastasis and invasions. So, also in this case, further exploring the role of Spindly in cell migration, including identifying the specific molecular pathways that are disrupted in Spindly depleted cells, the cell types and the type of migration (1D, 2D or 3D) that are affected and defining its binding partners would help to understand how the machinery works. The fact that Spindly localises at lamellipodia suggests that it could be involved in their regulation and dynamics, important process also in cancer cells. Of note is that BubR1 and Mad2 have recently been reported to play a second role in cancer cell migration; their inhibition was shown to slow down the migration process, while their overexpression could promote migration and invasion (Bargiela-Iparraguirre *et al.*, 2014). Thus, it could be that there are other ways in which SAC activity affects the capacity of cancer cells to migrate and to invade surrounding areas. We already demonstrated defects in cell migration velocities upon depletion of Spindly, and so it would be interesting to determine whether over/under-expression of Spindly in cancer cells could affect migration and invasiveness as well.

Finally, we have recently also discovered a further role for Spindly in interphase cells that we think is related with the DNA damage response. We found that Spindly is recruited at double-strand breaks (DSBs) sites upon damage (UV-A irradiation upon Bromodeoxyuridine (BrdU) sensitisation) and that Spindly-depleted cells are more sensitive to DNA damaging agent treatment (preliminary data, not shown). As reported in **Chapter 5**, when we analyse the expression of Spindly in different subcellular compartments, we found a pool of the protein on chromatin, consistent with the possibility that it has an undiscovered function in processes associated with chromatin. We already tested the possibility that this role is dynein-dependent too, but we did not observe the recruitment of dynein at sites of damage. Of note is that a recent paper has pointed at microtubule protein trafficking to the site of damage as the strategy used by microtubule-targeting agents to delay DNA damage repair response in cancer treatments (Poruchynsky *et al.*, 2015). The proteins involved in the DNA damage response tested in the aforementioned publication were demonstrated to interact with dynein, proposing an important role for the motor in this process (Poruchynsky *et al.*, 2015). Thus, it could be that Spindly helps dynein/dynactin to drive the trafficking of DNA repair proteins towards the damaged sites, but then Spindly can localise at sites of DNA DSBs as well. In our analyses, we also recorded recruitment at DSBs of Bub1 and BubR1 (preliminary data, not shown), in line with a recent report that has shown involvement of Bub1 in non-homologous end joining repair pathway in human cells (Jessulat *et al.*, 2015). Many reports have also highlighted the role of phosphatases in the DNA damage response (Freeman and Monteiro, 2010). So, our working hypothesis is that Spindly is bound by or recruits BubR1 (and/or Bub1) at sites of damage, and, once there, it helps to resolve the damage, potentially by recruiting phosphatases. Data collected so far represent a good starting point to move further in studying the roles of Spindly in DNA damage-repair and understanding how mitotic signalling cascades could be repurposed

to guard the genome during interphase. We know that defects in DNA damage response induce genomic instability and eventually carcinogenesis (Hosoya and Miyagawa, 2014); once again alterations in Spindly function could play a role in the cancer generation process. Defects in its expression could impair the DNA damage response and consequently allow tumour formation.

Overall, Spindly, as an extended (70nm) protein with distinct binding surfaces, could behave as a scaffold protein involved in the assembly of several large molecular machines where different proteins have to be brought together to orchestrate a particular cellular activity. The finding that Spindly is fundamental in several cellular processes let us to hypothesise that its expression, localisation, and post-translational modifications have to be carefully modulated to promote all of its varied functions (Fig. 6.1). Therefore, it is plausible that, if mis-regulated, Spindly leads to generation of defective cell divisions, altered cell migration and inefficient DNA damage repair, pathways that, when inhibited or altered, precede tumorigenesis.

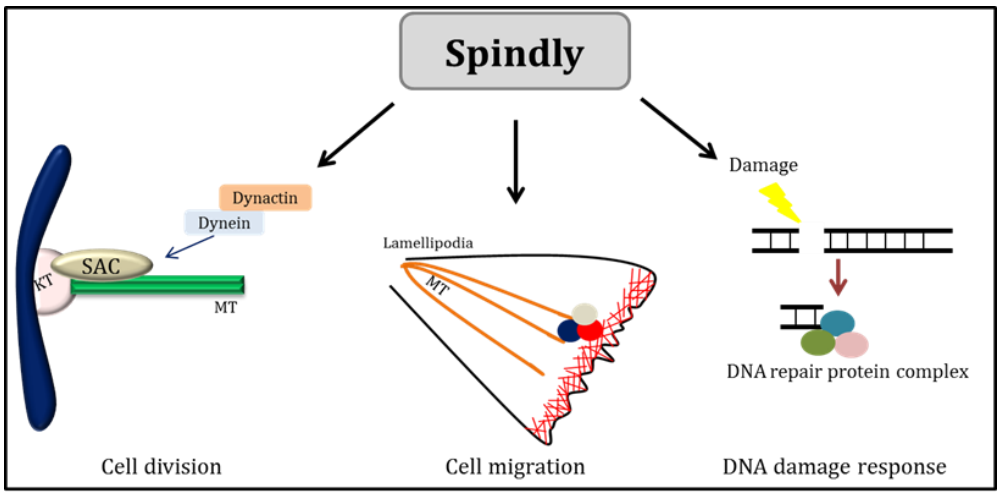


**Figure 6. 1.Overall diagram summarising the different functions of human Spindly.**

# 7 . Bibliography

Akhmanova, A. and Hammer, J. A., 3rd (2010) Linking molecular motors to membrane cargo. Curr Opin Cell Biol, 22, 479-487.

Alberts, B., Johnson, A., Lewis, J., Raff, M., Roberts, K. and Walter, P. (2007) Molecular Biology of the Cell. Garland Science, New York, 5th ed.

Allan, V. J. (2011) Cytoplasmic dynein. Biochem Soc Trans, 39, 1169-1178.

Arold, S. T., Hoellerer, M. K. and Noble, M. E. M. (2002) The structural basis of localization and signaling by the focal adhesion targeting domain. Structure, 10, 319–327.

Ashar, H. R., James, L., Gray, K., Carr, D., Black, S., Armstrong, L., Bishop, W. R. and Kirschmeier, P. (2000) Farnesyl transferase inhibitors block the farnesylation of CENP-E and CENP-F and alter the association of CENP-E with the microtubules. J Biol Chem, 275, 30451-30457.

Ballister, E. R., Riegman, M. and Lampson, M. A. (2014) Recruitment of Mad1 to metaphase kinetochores is sufficient to reactivate the mitotic checkpoint. J Cell Biol, 204, 901-908.

Barbosa, J., Nascimento, A. V., Faria, J., Silva, P. and Bousbaa, H. (2011) The spindle assembly checkpoint: perspectives in tumorigenesis and cancer therapy. Frontiers in Biology, 6, 147-155.

Bargiela-Iparraguirre, J., Prado-Marchal, L., Pajuelo-Lozano, N., Jimenez, B., Perona, R. and Sanchez-Perez, I. (2014) Mad2 and BubR1 modulates tumourigenesis and paclitaxel response in MKN45 gastric cancer cells. Cell Cycle, 13, 3590-3601.

Barisic, M. and Geley, S. (2011) Spindly switch controls anaphase: spindly and RZZ functions in chromosome attachment and mitotic checkpoint control. Cell Cycle, 10, 449-456.

Barisic, M., Sohm, B., Mikolcevic, P., Wandke, C., Rauch, V., Ringer, T., Hess, M., Bonn, G. and Geley, S. (2010) Spindly/CCDC99 is required for efficient chromosome congression and mitotic checkpoint regulation. Mol Biol Cell, 21, 1968-1981.

Beaty, B. T. and Condeelis, J. (2014) Digging a little deeper: the stages of invadopodium formation and maturation. Eur J Cell Biol, 93, 438-444.

Belmont, L. D., Hyman, A. A., Sawin, K. E. and Mitchison, T. J. (1990) Real-time visualization of cell cycle-dependent changes in microtubule dynamics in cytoplasmic extracts. Cell, 62, 579-589.

Bubb, M. R., Spector, I., Beyer, B. B. and Fosen, K. M. (2000) Effects of jasplakinolide on the kinetics of actin polymerization. An explanation for certain in vivo observations. J Biol Chem, 275, 5163-5170.

Buffin, E., Lefebvre, C., Huang, J., Gagou, M. E. and Karess, R. E. (2005) Recruitment of Mad2 to the kinetochore requires the Rod/Zw10 complex. Curr Biol, 15, 856-861.

Burgess, S. A., Walker, M. L., Sakakibara, H., Knight, P. J. and Oiwa, K. (2003) Dynein structure and power stroke. Nature, 421, 715-718.

Burridge, K., Turner, C. E. and Romer, L. H. (1992) Tyrosine phosphorylation of paxillin and pp125FAK accompanies cell adhesion to extracellular matrix: a role in cytoskeletal assembly. J Cell Biol, 119, 893-903.

Busson, S., Dujardin, D., Moreau, A., Dompierre, J. and De Mey, J. R. (1998) Dynein and dynactin are localized to astral microtubules and at cortical sites in mitotic epithelial cells. Curr Biol, 8, 541-544.

Campbell, M. S., Chan, G. K. and Yen, T. J. (2001) Mitotic checkpoint proteins HsMAD1 and HsMAD2 are associated with nuclear pore complexes in interphase. J Cell Sci, 114, 953-963.

Carazo-Salas, R. E., Gruss, O. J., Mattaj, I. W. and Karsenti, E. (2001) Ran-GTP coordinates regulation of microtubule nucleation and dynamics during mitotic-spindle assembly. Nat Cell Biol, 3, 228-234.

Carazo-Salas, R. E., Guarguaglini, G., Gruss, O. J., Segref, A., Karsenti, E. and Mattaj, I. W. (1999) Generation of GTP-bound Ran by RCC1 is required for chromatin-induced mitotic spindle formation. Nature, 400, 178-181.

Carmena, M., Wheelock, M., Funabiki, H. and Earnshaw, W. C. (2012) The chromosomal passenger complex (CPC): from easy rider to the godfather of mitosis. Nat Rev Mol Cell Biol, 13, 789-803.

Carter, A. P. (2013) Crystal clear insights into how the dynein motor moves. J Cell Sci, 126, 705-713.

Carter, A. P., Cho, C., Jin, L. and Vale, R. D. (2011) Crystal structure of the dynein motor domain. Science, 331, 1159-1165.

Chan, G. K., Jablonski, S. A., Starr, D. A., Goldberg, M. L. and Yen, T. J. (2000) Human Zw10 and ROD are mitotic checkpoint proteins that bind to kinetochores. Nat Cell Biol, 2, 944-947.

Chan, G. K., Schaar, B. T. and Yen, T. J. (1998) Characterization of the kinetochore binding domain of CENP-E reveals interactions with the kinetochore proteins CENP-F and hBUBR1. J Cell Biol, 143, 49-63.

Chan, Y. W., Fava, L. L., Uldschmid, A., Schmitz, M. H., Gerlich, D. W., Nigg, E. A. and Santamaria, A. (2009) Mitotic control of kinetochore-associated dynein and spindle orientation by human Spindly. J Cell Biol, 185, 859-874.

Chang, W., Folker, E. S., Worman, H. J. and Gundersen, G. G. (2013) Emerin organizes actin flow for nuclear movement and centrosome orientation in migrating fibroblasts. Mol Biol Cell, 24, 3869-3880.

Chao, W. C., Kulkarni, K., Zhang, Z., Kong, E. H. and Barford, D. (2012) Structure of the mitotic checkpoint complex. Nature, 484, 208-213.

Cheerambathur, D. K., Gassmann, R., Cook, B., Oegema, K. and Desai, A. (2013) Crosstalk between microtubule attachment complexes ensures accurate chromosome segregation. Science, 342, 1239-1242.

Cheeseman, I. M. (2014) The kinetochore. Cold Spring Harb Perspect Biol, 6, a015826.

Cheeseman, I. M., Chappie, J. S., Wilson-Kubalek, E. M. and Desai, A. (2006) The conserved KMN network constitutes the core microtubule-binding site of the kinetochore. Cell, 127, 983-997.

Chi, Q., Yin, T., Gregersen, H., Deng, X., Fan, Y., Zhao, J., Liao, D. and Wang, G. (2014) Rear actomyosin contractility-driven directional cell migration in three-dimensional matrices: a mechano-chemical coupling mechanism. J R Soc Interface, 11, 6.

Choi, C. K., Vicente-Manzanares, M., Zareno, J., Whitmore, L. A., Mogilner, A. and Horwitz, A. R. (2008) Actin and alpha-actinin orchestrate the assembly and maturation of nascent adhesions in a myosin II motor-independent manner. Nat Cell Biol, 10, 1039-1050.

Ciferri, C., Pasqualato, S., Screpanti, E., Varetti, G., Santaguida, S., Dos Reis, G., Maiolica, A., Polka, J., De Luca, J. G., De Wulf, P., Salek, M., Rappsilber, J., Moores, C. A., Salmon, E. D. and Musacchio, A. (2008) Implications for

kinetochore-microtubule attachment from the structure of an engineered Ndc80 complex. Cell, 133, 427-439.

Civril, F., Wehenkel, A., Giorgi, F. M., Santaguida, S., Di Fonzo, A., Grigorean, G., Ciccarelli, F. D. and Musacchio, A. (2010) Structural analysis of the RZZ complex reveals common ancestry with multisubunit vesicle tethering machinery. Structure, 18, 616-626.

Clements, L., Manilal, S., Love, D. R. and Morris, G. E. (2000) Direct interaction between emerin and lamin A. Biochem Biophys Res Commun, 267, 709-714.

Coue, M., Brenner, S. L., Spector, I. and Korn, E. D. (1987) Inhibition of actin polymerization by latrunculin A. FEBS Lett, 213, 316-318.

Cox, J. and Mann, M. (2008) MaxQuant enables high peptide identification rates, individualized p.p.b.-range mass accuracies and proteome-wide protein quantification. Nat Biotechnol, 26, 1367-1372.

Crowley, E. and Horwitz, A. F. (1995) Tyrosine phosphorylation and cytoskeletal tension regulate the release of fibroblast adhesions. J Cell Biol, 131, 525-537.

Culver-Hanlon, T. L., Lex, S. A., Stephens, A. D., Quintyne, N. J. and King, S. J. (2006) A microtubule-binding domain in dynactin increases dynein processivity by skating along microtubules. Nat Cell Biol, 8, 264-270.

D'Angiolella, V., Mari, C., Nocera, D., Rametti, L. and Grieco, D. (2003) The spindle checkpoint requires cyclin-dependent kinase activity. Genes Dev, 17, 2520-2525.

De Antoni, A., Pearson, C. G., Cimini, D., Canman, J. C., Sala, V., Nezi, L., Mapelli, M., Sironi, L., Faretta, M., Salmon, E. D. and Musacchio, A. (2005) The Mad1/Mad2 complex as a template for Mad2 activation in the spindle assembly checkpoint. Curr Biol, 15, 214-225.

del Pozo, M. A., Alderson, N. B., Kiosses, W. B., Chiang, H. H., Anderson, R. G. and Schwartz, M. A. (2004) Integrins regulate Rac targeting by internalization of membrane domains. Science, 303, 839-842.

DeLuca, J. G., Gall, W. E., Ciferri, C., Cimini, D., Musacchio, A. and Salmon, E. D. (2006) Kinetochore microtubule dynamics and attachment stability are regulated by Hec1. Cell, 127, 969-982.

Desai, A. and Mitchison, T. J. (1997) Microtubule polymerization dynamics. Annu Rev Cell Dev Biol, 13, 83-117.

dos Remedios, C. G., Chhabra, D., Kekic, M., Dedova, I. V., Tsubakihara, M., Berry, D. A. and Nosworthy, N. J. (2003) Actin binding proteins: regulation of cytoskeletal microfilaments. Physiol Rev, 83, 433-473.

Dou, Z., Liu, X., Wang, W., Zhu, T., Wang, X., Xu, L., Abrieu, A., Fu, C., Hill, D. L. and Yao, X. (2015) Dynamic localization of Mps1 kinase to kinetochores is essential for accurate spindle microtubule attachment. Proc Natl Acad Sci U S A, 3, 201508791.

Duellberg, C., Trokter, M., Jha, R., Sen, I., Steinmetz, M. O. and Surrey, T. (2014) Reconstitution of a hierarchical +TIP interaction network controlling microtubule end tracking of dynein. Nat Cell Biol, 16, 804-811.

Dujardin, D. L., Barnhart, L. E., Stehman, S. A., Gomes, E. R., Gundersen, G. G. and Vallee, R. B. (2003) A role for cytoplasmic dynein and LIS1 in directed cell movement. J Cell Biol, 163, 1205-1211.

Easwaran, H. P., Leonhardt, H. and Cardoso, M. C. (2005) Cell cycle markers for live cell analyses. Cell Cycle, 4, 453-455.

Echeverri, C. J., Paschal, B. M., Vaughan, K. T. and Vallee, R. B. (1996) Molecular characterization of the 50-kD subunit of dynactin reveals function for the complex in chromosome alignment and spindle organization during mitosis. J Cell Biol, 132, 617-633.

Efimov, V. P. and Morris, N. R. (2000) The LIS1-related NUDF protein of Aspergillus nidulans interacts with the coiled-coil domain of the NUDE/RO11 protein. J Cell Biol, 150, 681-688.

Elowe, S. (2011) Bub1 and BubR1: at the interface between chromosome attachment and the spindle checkpoint. Mol Cell Biol, 31, 3085-3093.

Espert, A., Uluocak, P., Bastos, R. N., Mangat, D., Graab, P. and Gruneberg, U. (2014) PP2A-B56 opposes Mps1 phosphorylation of Knl1 and thereby promotes spindle assembly checkpoint silencing. J Cell Biol, 206, 833-842.

Espeut, J., Cheerambathur, D. K., Krenning, L., Oegema, K. and Desai, A. (2012) Microtubule binding by KNL-1 contributes to spindle checkpoint silencing at the kinetochore. J Cell Biol, 196, 469-482.

Etienne-Manneville, S. (2013) Microtubules in cell migration. Annu Rev Cell Dev Biol, 29, 471-499.

Etienne-Manneville, S. and Hall, A. (2002) Rho GTPases in cell biology. Nature, 420, 629-635.

Etienne-Manneville, S. a. H., A. (2001) Integrin-Mediated Activation of Cdc42 Controls Cell Polarity in Migrating Astrocytes through PKC . Cell, 106, 489-498.

Eytan, E., Sitry-Shevah, D., Teichner, A. and Hershko, A. (2013) Roles of different pools of the mitotic checkpoint complex and the mechanisms of their disassembly. Proc Natl Acad Sci U S A, 110, 10568-10573.

Eytan, E., Wang, K., Miniowitz-Shemtov, S., Sitry-Shevah, D., Kaisari, S., Yen, T. J., Liu, S. T. and Hershko, A. (2014) Disassembly of mitotic checkpoint complexes by the joint action of the AAA-ATPase TRIP13 and p31(comet). Proc Natl Acad Sci U S A, 111, 12019-12024.

Famulski, J. K., Vos, L., Sun, X. and Chan, G. (2008) Stable hZW10 kinetochore residency, mediated by hZwint-1 interaction, is essential for the mitotic checkpoint. J Cell Biol, 180, 507-520.

Fang, G. (2002) Checkpoint protein BubR1 acts synergistically with Mad2 to inhibit anaphase-promoting complex. Mol Biol Cell, 13, 755-766.

Fang, G., Yu, H. and Kirschner, M. W. (1998) The checkpoint protein MAD2 and the mitotic regulator CDC20 form a ternary complex with the anaphase-promoting complex to control anaphase initiation. Genes Dev, 12, 1871-1883.

Faulkner, N. E., Dujardin, D. L., Tai, C. Y., Vaughan, K. T., O'Connell, C. B., Wang, Y. and Vallee, R. B. (2000) A role for the lissencephaly gene LIS1 in mitosis and cytoplasmic dynein function. Nat Cell Biol, 2, 784-791.

Feng, Y., Olson, E. C., Stukenberg, P. T., Flanagan, L. A., Kirschner, M. W. and Walsh, C. A. (2000) LIS1 regulates CNS lamination by interacting with mNudE, a central component of the centrosome. Neuron, 28, 665-679.

Foley, E. A. and Kapoor, T. M. (2013) Microtubule attachment and spindle assembly checkpoint signalling at the kinetochore. Nat Rev Mol Cell Biol, 14, 25-37.

Folker, E. S., Baker, B. M. and Goodson, H. V. (2005) Interactions between CLIP-170, tubulin, and microtubules: implications for the mechanism of Clip-170 plus-end tracking behavior. Mol Biol Cell, 16, 5373-5384.

Foster, S. A. and Morgan, D. O. (2012) The APC/C subunit Mnd2/Apc15 promotes Cdc20 autoubiquitination and spindle assembly checkpoint inactivation. Mol Cell, 47, 921-932.

Freeman, A. K. and Monteiro, A. N. (2010) Phosphatases in the cellular response to DNA damage. Cell Communication and Signalling, 8, 1-12.

Fukata, M., Watanabe, T., Noritake, J., Nakagawa, M., Yamaga, M., Kuroda, S., Matsuura, Y., Iwamatsu, A., Perez, F. and Kaibuchi, K. (2002) Rac1 and Cdc42 capture microtubules through IQGAP1 and CLIP-170. Cell, 109, 873-885.

Fumoto, K., Hoogenraad, C. C. and Kikuchi, A. (2006) GSK-3beta-regulated interaction of BICD with dynein is involved in microtubule anchorage at centrosome. Embo J, 25, 5670-5682.

Funabiki, H. and Wynne, D. J. (2013) Making an effective switch at the kinetochore by phosphorylation and dephosphorylation. Chromosoma, 122, 135-158.

Gao, Y. F., Li, T., Chang, Y., Wang, Y. B., Zhang, W. N., Li, W. H., He, K., Mu, R., Zhen, C., Man, J. H., Pan, X., Chen, L., Yu, M., Liang, B., Chen, Y., Xia, Q., Zhou, T., Gong, W. L., Li, A. L., Li, H. Y. and Zhang, X. M. (2011) Cdk1-phosphorylated CUEDC2 promotes spindle checkpoint inactivation and chromosomal instability. Nat Cell Biol, 13, 924-933.

Gassmann, R., Essex, A., Hu, J. S., Maddox, P. S., Motegi, F., Sugimoto, A., O'Rourke, S. M., Bowerman, B., McLeod, I., Yates, J. R., 3rd, Oegema, K., Cheeseman, I. M. and Desai, A. (2008) A new mechanism controlling kinetochore-microtubule interactions revealed by comparison of two dynein-targeting components: SPDL-1 and the Rod/Zwilch/Zw10 complex. Genes Dev, 22, 2385-2399.

Gassmann, R., Holland, A. J., Varma, D., Wan, X., Civril, F., Cleveland, D. W., Oegema, K., Salmon, E. D. and Desai, A. (2010) Removal of Spindly from microtubule-attached kinetochores controls spindle checkpoint silencing in human cells. Genes Dev, 24, 957-971.

Geigl, J. B., Obenauf, A. C., Schwarzbraun, T. and Speicher, M. R. (2008) Defining 'chromosomal instability'. Trends Genet, 24, 64-69.

Goode, B. L. and Eck, M. J. (2007) Mechanism and function of formins in the control of actin assembly. Annu Rev Biochem, 76, 593-627.

Grallert, A., Boke, E., Hagting, A., Hodgson, B., Connolly, Y., Griffiths, J. R., Smith, D. L., Pines, J. and Hagan, I. M. (2015) A PP1-PP2A phosphatase relay controls mitotic progression. Nature, 517, 94-98.

Griffis, E. R., Stuurman, N. and Vale, R. D. (2007) Spindly, a novel protein essential for silencing the spindle assembly checkpoint, recruits dynein to the kinetochore. J Cell Biol, 177, 1005-1015.

Grigoriev, I., Splinter, D., Keijzer, N., Wulf, P. S., Demmers, J., Ohtsuka, T., Modesti, M., Maly, I. V., Grosveld, F., Hoogenraad, C. C. and Akhmanova, A. (2007) Rab6 regulates transport and targeting of exocytotic carriers. Dev Cell, 13, 305-314.

Gundersen, G. G. and Bulinski, J. C. (1988) Selective stabilization of microtubules oriented toward the direction of cell migration. Proc Natl Acad Sci U S A, 85, 5946-5950.

Habu, T., Kim, S. H., Weinstein, J. and Matsumoto, T. (2002) Identification of a MAD2-binding protein, CMT2, and its role in mitosis. Embo J, 21, 6419-6428.

Hall, A. (1998) G proteins and small GTPases: distant relatives keep in touch. Science, 280, 2074-2075.

Hanks, S., Coleman, K., Reid, S., Plaja, A., Firth, H., Fitzpatrick, D., Kidd, A., Mehes, K., Nash, R., Robin, N., Shannon, N., Tolmie, J., Swansbury, J., Irrthum, A., Douglas,

J. and Rahman, N. (2004) Constitutional aneuploidy and cancer predisposition caused by biallelic mutations in BUB1B. Nat Genet, 36, 1159-1161.

Hayden J. H., B. S. S. a. R. C. L. (1990) Kinetochores Capture Astral Microtubules during Chromosome Attachment to the Mitotic Spindle: Direct Visualization in Live Newt Lung Cells. J Cell Biol, 111, 1039-1045.

Hinchcliffe, E. H. and Sluder, G. (2001) "It takes two to tango": understanding how centrosome duplication is regulated throughout the cell cycle. Genes Dev, 15, 1167-1181.

Hirose, H., Arasaki, K., Dohmae, N., Takio, K., Hatsuzawa, K., Nagahama, M., Tani, K., Yamamoto, A., Tohyama, M. and Tagaya, M. (2004) Implication of ZW10 in membrane trafficking between the endoplasmic reticulum and Golgi. Embo J, 23, 1267-1278.

Holland, A. J. and Cleveland, D. W. (2012) Losing balance: the origin and impact of aneuploidy in cancer. EMBO Rep, 13, 501-514.

Holland, A. J., Reis, R. M., Niessen, S., Pereira, C., Andres, D. A., Spielmann, H. P., Cleveland, D. W., Desai, A. and Gassmann, R. (2015) Preventing farnesylation of the dynein adaptor Spindly contributes to the mitotic defects caused by farnesyltransferase inhibitors. Mol Biol Cell, 26, 1845-1856.

Holleran, E. A., Ligon, L. A., Tokito, M., Stankewich, M. C., Morrow, J. S. and Holzbaur, E. L. (2001) beta III spectrin binds to the Arp1 subunit of dynactin. J Biol Chem, 276, 36598-36605.

Hoogenraad, C. C., Akhmanova, A., Howell, S. A., Dortland, B. R., De Zeeuw, C. I., Willemsen, R., Visser, P., Grosveld, F. and Galjart, N. (2001) Mammalian Golgi-associated Bicaudal-D2 functions in the dynein-dynactin pathway by interacting with these complexes. Embo J, 20, 4041-4054.

Hoogenraad, C. C., Wulf, P., Schiefermeier, N., Stepanova, T., Galjart, N., Small, J. V., Grosveld, F., de Zeeuw, C. I. and Akhmanova, A. (2003) Bicaudal D induces selective dynein-mediated microtubule minus end-directed transport. Embo J, 22, 6004-6015.

Horgan, C. P., Hanscom, S. R., Jolly, R. S., Futter, C. E. and McCaffrey, M. W. (2010) Rab11-FIP3 binds dynein light intermediate chain 2 and its overexpression fragments the Golgi complex. Biochem Biophys Res Commun, 394, 387-392.

Hori, T., Haraguchi, T., Hiraoka, Y., Kimura, H. and Fukagawa, T. (2003) Dynamic behavior of Nuf2-Hec1 complex that localizes to the centrosome and centromere and is essential for mitotic progression in vertebrate cells. J Cell Sci, 116, 3347-3362.

Hosoya, N. and Miyagawa, K. (2014) Targeting DNA damage response in cancer therapy. Cancer Sci, 105, 370-388.

Howell, B. J., McEwen, B. F., Canman, J. C., Hoffman, D. B., Farrar, E. M., Rieder, C. L. and Salmon, E. D. (2001) Cytoplasmic dynein/dynactin drives kinetochore protein transport to the spindle poles and has a role in mitotic spindle checkpoint inactivation. J Cell Biol, 155, 1159-1172.

Howell, B. J., Moree, B., Farrar, E. M., Stewart, S., Fang, G. and Salmon, E. D. (2004) Spindle checkpoint protein dynamics at kinetochores in living cells. Curr Biol, 14, 953-964.

Hoyt, M. A., Totis, L. and Roberts, B. T. (1991) S. cerevisiae genes required for cell cycle arrest in response to loss of microtubule function. Cell, 66, 507-517.

Huang, J., Roberts, A. J., Leschziner, A. E. and Reck-Peterson, S. L. (2012) Lis1 acts as a "clutch" between the ATPase and microtubule-binding domains of the dynein motor. Cell, 150, 975-986.

Hussein, D. a. T., S.S. (2002) Farnesylation of Cenp-F is required for G2/M progression and degradation after mitosis. J Cell Sci, 115, 3403-3414.

Jacquemet, G., Humphries, M. J. and Caswell, P. T. (2013) Role of adhesion receptor trafficking in 3D cell migration. Curr Opin Cell Biol, 25, 627-632.

Janssen, A., Kops, G. J. and Medema, R. H. (2009) Elevating the frequency of chromosome mis-segregation as a strategy to kill tumor cells. Proc Natl Acad Sci U S A, 106, 19108-19113.

Jeffery, C. J. (1999) Moonlighting proteins. Trends Biochem Sci, 24, 8-11.

Jeganathan, K., Malureanu, L., Baker, D. J., Abraham, S. C. and van Deursen, J. M. (2007) Bub1 mediates cell death in response to chromosome missegregation and acts to suppress spontaneous tumorigenesis. J Cell Biol, 179, 255-267.

Jelluma, N., Dansen, T. B., Sliedrecht, T., Kwiatkowski, N. P. and Kops, G. J. (2010) Release of Mps1 from kinetochores is crucial for timely anaphase onset. J Cell Biol, 191, 281-290.

Jensen, L. J., Kuhn, M., Stark, M., Chaffron, S., Creevey, C., Muller, J., Doerks, T., Julien, P., Roth, A., Simonovic, M., Bork, P. and von Mering, C. (2009) STRING 8--a global view on proteins and their functional interactions in 630 organisms. Nucleic Acids Res, 37, 21.

Jessulat, M., Malty, R. H., Nguyen-Tran, D. H., Deineko, V., Aoki, H., Vlasblom, J., Omidi, K., Jin, K., Minic, Z., Hooshyar, M., Burnside, D., Samanfar, B., Phanse, S., Freywald, T., Prasad, B., Zhang, Z., Vizeacoumar, F., Krogan, N. J., Freywald, A., Golshani, A. and Babu, M. (2015) Spindle Checkpoint Factors Bub1 and Bub2 Promote DNA Double-Strand Break Repair by Nonhomologous End Joining. Mol Cell Biol, 35, 2448-2463.

Joglekar, A. P., Bouck, D. C., Molk, J. N., Bloom, K. S. and Salmon, E. D. (2006) Molecular architecture of a kinetochore-microtubule attachment site. Nat Cell Biol, 8, 581-585.

Johansson, M., Rocha, N., Zwart, W., Jordens, I., Janssen, L., Kuijl, C., Olkkonen, V. M. and Neefjes, J. (2007) Activation of endosomal dynein motors by stepwise assembly of Rab7-RILP-p150Glued, ORP1L, and the receptor betalll spectrin. J Cell Biol, 176, 459-471.

Johnson, V. L., Scott, M. I., Holt, S. V., Hussein, D. and Taylor, S. S. (2004) Bub1 is required for kinetochore localization of BubR1, Cenp-E, Cenp-F and Mad2, and chromosome congression. J Cell Sci, 117, 1577-1589.

Jones, M. C., Caswell, P. T. and Norman, J. C. (2006) Endocytic recycling pathways: emerging regulators of cell migration. Curr Opin Cell Biol, 18, 549-557.

Jordens, I., Fernandez-Borja, M., Marsman, M., Dusseljee, S., Janssen, L., Calafat, J., Janssen, H., Wubbolts, R. and Neefjes, J. (2001) The Rab7 effector protein RILP controls lysosomal transport by inducing the recruitment of dynein-dynactin motors. Curr Biol, 11, 1680-1685.

Joseph, J., Liu, S. T., Jablonski, S. A., Yen, T. J. and Dasso, M. (2004) The RanGAP1-RanBP2 complex is essential for microtubule-kinetochore interactions in vivo. Curr Biol, 14, 611-617.

Kalab, P., Weis, K. and Heald, R. (2002) Visualization of a Ran-GTP gradient in interphase and mitotic Xenopus egg extracts. Science, 295, 2452-2456.

Kanchanawong, P., Shtengel, G., Pasapera, A. M., Ramko, E. B., Davidson, M. W., Hess, H. F. and Waterman, C. M. (2010) Nanoscale architecture of integrin-based cell adhesions. Nature, 468, 580-584.

Kaplan, K. B., Burds, A. A., Swedlow, J. R., Bekir, S. S., Sorger, P. K. and Nathke, I. S. (2001) A role for the Adenomatous Polyposis Coli protein in chromosome segregation. Nat Cell Biol, 3, 429-432.

Kapoor, T. M., Lampson, M. A., Hergert, P., Cameron, L., Cimini, D., Salmon, E. D., McEwen, B. F. and Khodjakov, A. (2006) Chromosomes can congress to the metaphase plate before biorientation. Science, 311, 388-391.

Kardon, J. R. and Vale, R. D. (2009) Regulators of the cytoplasmic dynein motor. Nat Rev Mol Cell Biol, 10, 854-865.

Karess, R. (2005) Rod-Zw10-Zwilch: a key player in the spindle checkpoint. Trends Cell Biol, 15, 386-392.

Kasuboski, J. M., Bader, J. R., Vaughan, P. S., Tauhata, S. B., Winding, M., Morrissey, M. A., Joyce, M. V., Boggess, W., Vos, L., Chan, G. K., Hinchcliffe, E. H. and Vaughan, K. T. (2011) Zwint-1 is a novel Aurora B substrate required for the assembly of a dynein-binding platform on kinetochores. Mol Biol Cell, 22, 3318-3330.

Kaverina, I., Rottner, K. and Small, J. V. (1998) Targeting, capture, and stabilization of microtubules at early focal adhesions. J Cell Biol, 142, 181-190.

Khodjakov, A., Copenagle, L., Gordon, M. B., Compton, D. A. and Kapoor, T. M. (2003) Minus-end capture of preformed kinetochore fibers contributes to spindle morphogenesis. J Cell Biol, 160, 671-683.

Kiely, M. and Kiely, P. A. (2015) PP2A: The Wolf in Sheep's Clothing? Cancers, 7, 648-669.

Kienitz, A., Vogel, C., Morales, I., Muller, R. and Bastians, H. (2005) Partial downregulation of MAD1 causes spindle checkpoint inactivation and aneuploidy, but does not confer resistance towards taxol. Oncogene, 24, 4301-4310.

Kim, H., Ling, S. C., Rogers, G. C., Kural, C., Selvin, P. R., Rogers, S. L. and Gelfand, V. I. (2007) Microtubule binding by dynactin is required for microtubule organization but not cargo transport. J Cell Biol, 176, 641-651.

Kim, S., Sun, H., Tomchick, D. R., Yu, H. and Luo, X. (2012) Structure of human Mad1 C-terminal domain reveals its involvement in kinetochore targeting. Proc Natl Acad Sci U S A, 109, 6549-6554.

King, S. J., Brown, C. L., Maier, K. C., Quintyne, N. J. and Schroer, T. A. (2003) Analysis of the dynein-dynactin interaction in vitro and in vivo. Mol Biol Cell, 14, 5089-5097.

King, S. J. and Schroer, T. A. (2000) Dynactin increases the processivity of the cytoplasmic dynein motor. Nat Cell Biol, 2, 20-24.

Kitamura, E., Tanaka, K., Komoto, S., Kitamura, Y., Antony, C. and Tanaka, T. U. (2010) Kinetochores generate microtubules with distal plus ends: their roles and limited lifetime in mitosis. Dev Cell, 18, 248-259.

Kiyomitsu, T., Murakami, H. and Yanagida, M. (2011) Protein interaction domain mapping of human kinetochore protein Blinkin reveals a consensus motif for binding of spindle assembly checkpoint proteins Bub1 and BubR1. Mol Cell Biol, 31, 998-1011.

Kline, S. L., Cheeseman, I. M., Hori, T., Fukagawa, T. and Desai, A. (2006) The human Mis12 complex is required for kinetochore assembly and proper chromosome segregation. J Cell Biol, 173, 9-17.

Kodama, A., Karakesisoglou, I., Wong, E., Vaezi, A. and Fuchs, E. (2003) ACF7: an essential integrator of microtubule dynamics. Cell, 115, 343-354.

Kops, G. J., Kim, Y., Weaver, B. A., Mao, Y., McLeod, I., Yates, J. R., 3rd, Tagaya, M. and Cleveland, D. W. (2005) ZW10 links mitotic checkpoint signaling to the structural kinetochore. J Cell Biol, 169, 49-60.

Korrodi-Gregorio, L., Esteves, S. L. and Fardilha, M. (2014) Protein phosphatase 1 catalytic isoforms: specificity toward interacting proteins. Transl Res, 164, 366-391.

Krause, M. and Gautreau, A. (2014) Steering cell migration: lamellipodium dynamics and the regulation of directional persistence. Nat Rev Mol Cell Biol, 15, 577-590.

Kruse, T., Zhang, G., Larsen, M. S., Lischetti, T., Streicher, W., Kragh Nielsen, T., Bjorn, S. P. and Nilsson, J. (2013) Direct binding between BubR1 and B56-PP2A phosphatase complexes regulate mitotic progression. J Cell Sci, 126, 1086-1092.

Kuhn, S. and Geyer, M. (2014) Formins as effector proteins of Rho GTPases. Small GTPases, 5, 10.

Kuijt, T. E., Omerzu, M., Saurin, A. T. and Kops, G. J. (2014) Conditional targeting of MAD1 to kinetochores is sufficient to reactivate the spindle assembly checkpoint in metaphase. Chromosoma, 123, 471-480.

Kuta, A., Deng, W., Morsi El-Kadi, A., Banks, G. T., Hafezparast, M., Pfister, K. K. and Fisher, E. M. (2010) Mouse cytoplasmic dynein intermediate chains: identification of new isoforms, alternative splicing and tissue distribution of transcripts. PLoS One, 5, 0011682.

Lam, C., Vergnolle, M. A., Thorpe, L., Woodman, P. G. and Allan, V. J. (2010) Functional interplay between LIS1, NDE1 and NDEL1 in dynein-dependent organelle positioning. J Cell Sci, 123, 202-212.

Lampson, M. A. and Cheeseman, I. M. (2011) Sensing centromere tension: Aurora B and the regulation of kinetochore function. Trends Cell Biol, 21, 133-140.

Lara-Gonzalez, P., Westhorpe, F. G. and Taylor, S. S. (2012) The spindle assembly checkpoint. Curr Biol, 22, R966-980.

Larsen, K. S., Xu, J., Cermelli, S., Shu, Z. and Gross, S. P. (2008) BicaudalD actively regulates microtubule motor activity in lipid droplet transport. PLoS One, 3, 19.

Lauffenburger, D. A. and Horwitz, A. F. (1996) Cell migration: a physically integrated molecular process. Cell, 84, 359-369.

Le Clainche, C. and Carlier, M. F. (2008) Regulation of actin assembly associated with protrusion and adhesion in cell migration. Physiol Rev, 88, 489-513.

Lee, W. L., Oberle, J. R. and Cooper, J. A. (2003) The role of the lissencephaly protein Pac1 during nuclear migration in budding yeast. J Cell Biol, 160, 355-364.

Leung, C. L., Sun, D., Zheng, M., Knowles, D. R. and Liem, R. K. (1999) Microtubule actin cross-linking factor (MACF): a hybrid of dystonin and dystrophin that can interact with the actin and microtubule cytoskeletons. J Cell Biol, 147, 1275-1286.

Levy, J. R. and Holzbaur, E. L. F. (2008) Dynein drives nuclear rotation during forward progression of motile fibroblasts. 121, Journal of cell science, 3187-3195.

Li, J., Lee, W. L. and Cooper, J. A. (2005) NudEL targets dynein to microtubule ends through LIS1. Nat Cell Biol, 7, 686-690.
Li, R. and Murray, A. W. (1991) Feedback control of mitosis in budding yeast. Cell, 66, 519-531.
Liang, Y., Yu, W., Li, Y., Yang, Z., Yan, X., Huang, Q. and Zhu, X. (2004) Nudel functions in membrane traffic mainly through association with Lis1 and cytoplasmic dynein. J Cell Biol, 164, 557-566.
Ling, Y., Zhang, X., Bai, Y., Li, P., Wei, C., Song, T., Zheng, Z., Guan, K., Zhang, Y., Zhang, B., Liu, X., Ma, R. Z., Cao, C., Zhong, H. and Xu, Q. (2014) Overexpression of Mps1 in colon cancer cells attenuates the spindle assembly checkpoint and increases aneuploidy. Biochem Biophys Res Commun, 450, 1690-1695.
Liu, D., Vader, G., Vromans, M. J. M., Lampson, M. A. and Lens, S. M. A. (2009) Sensing Chromosome Bi-Orientation by Spatial Separation of Aurora B Kinase from Kinetochore Substrates. Science, 323, 1350-1353.
Liu, D., Vleugel, M., Backer, C. B., Hori, T., Fukagawa, T., Cheeseman, I. M. and Lampson, M. A. (2010) Regulated targeting of protein phosphatase 1 to the outer kinetochore by KNL1 opposes Aurora B kinase. J Cell Biol, 188, 809-820.
Liu, S. T., Rattner, J. B., Jablonski, S. A. and Yen, T. J. (2006) Mapping the assembly pathways that specify formation of the trilaminar kinetochore plates in human cells. J Cell Biol, 175, 41-53.
London, N., Ceto, S., Ranish, J. A. and Biggins, S. (2012) Phosphoregulation of Spc105 by Mps1 and PP1 regulates Bub1 localization to kinetochores. Curr Biol, 22, 900-906.
Magdalena, J., Millard, T. H. and Machesky, L. M. (2003) Microtubule involvement in NIH 3T3 Golgi and MTOC polarity establishment. J Cell Sci, 116, 743-756.
Mallik, R., Carter, B. C., Lex, S. A., King, S. J. and Gross, S. P. (2004) Cytoplasmic dynein functions as a gear in response to load. Nature, 427, 649-652.
Manneville, J. B., Jehanno, M. and Etienne-Manneville, S. (2010) Dlg1 binds GKAP to control dynein association with microtubules, centrosome positioning, and cell polarity. J Cell Biol, 191, 585-598.
Mao, Y., Abrieu, A. and Cleveland, D. W. (2003) Activating and Silencing the Mitotic Checkpoint through CENP-E-Dependent Activation/Inactivation of BubR1. Cell, 114, 87-98.
Maresca, T. J. and Salmon, E. D. (2010) Welcome to a new kind of tension: translating kinetochore mechanics into a wait-anaphase signal. J Cell Sci, 123, 825-835.
Maritzen, T., Schachtner, H. and Legler, D. F. (2015) On the move: endocytic trafficking in cell migration. Cell Mol Life Sci, 72, 2119-2134.
Martin-Lluesma, S., Stucke, V. M. and Nigg, E. A. (2002) Role of Hec1 in spindle checkpoint signaling and kinetochore recruitment of Mad1/Mad2. Science, 297, 2267-2270.
McAinsh, A. D. and Meraldi, P. (2011) The CCAN complex: linking centromere specification to control of kinetochore-microtubule dynamics. Semin Cell Dev Biol, 22, 946-952.
McEwen, B. F., Hsieh, C. E., Mattheyses, A. L. and Rieder, C. L. (1998) A new look at kinetochore structure in vertebrate somatic cells using high-pressure freezing and freeze substitution. Chromosoma, 107, 366-375.
McKenney, R. J., Huynh, W., Tanenbaum, M. E., Bhabha, G. and Vale, R. D. (2014) Activation of cytoplasmic dynein motility by dynactin-cargo adapter complexes. Science, 345, 337-341.

McKenney, R. J., Vershinin, M., Kunwar, A., Vallee, R. B. and Gross, S. P. (2010) LIS1 and NudE induce a persistent dynein force-producing state. Cell, 141, 304-314.

McKenney, R. J., Weil, S. J., Scherer, J. and Vallee, R. B. (2011) Mutually exclusive cytoplasmic dynein regulation by NudE-Lis1 and dynactin. J Biol Chem, 286, 39615-39622.

Merdes, A., Ramyar, K., Vechio, J. D. and Cleveland, D. W. (1996) A complex of NuMA and cytoplasmic dynein is essential for mitotic spindle assembly. Cell, 87, 447-458.

Mikami, A., Tynan, S. H., Hama, T., Luby-Phelps, K., Saito, T., Crandall, J. E., Besharse, J. C. and Vallee, R. B. (2002) Molecular structure of cytoplasmic dynein 2 and its distribution in neuronal and ciliated cells. J Cell Sci, 115, 4801-4808.

Mitchison, T. and Kirschner, M. (1984) Dynamic instability of microtubule growth. Nature, 312, 237-242.

Miyamoto, S., Teramoto, H., Coso, O. A., Gutkind, J. S., Burbelo, P. D., Akiyama, S. K. and Yamada, K. M. (1995) Integrin function: molecular hierarchies of cytoskeletal and signaling molecules. J Cell Biol, 131, 791-805.

Morrison, E. E., Wardleworth, B. N., Askham, J. M., Markham, A. F. and Meredith, D. M. (1998) EB1, a protein which interacts with the APC tumour suppressor, is associated with the microtubule cytoskeleton throughout the cell cycle. Oncogene, 17, 3471-3477.

Moudgil, D. K., Westcott, N., Famulski, J. K., Patel, K., Macdonald, D., Hang, H. and Chan, G. K. (2015) A novel role of farnesylation in targeting a mitotic checkpoint protein, human Spindly, to kinetochores. J Cell Biol, 208, 881-896.

Moyle, M. W., Kim, T., Hattersley, N., Espeut, J., Cheerambathur, D. K., Oegema, K. and Desai, A. (2014) A Bub1-Mad1 interaction targets the Mad1-Mad2 complex to unattached kinetochores to initiate the spindle checkpoint. J Cell Biol, 204, 647-657.

Musacchio, A. (2011) Spindle assembly checkpoint: the third decade. Philos Trans R Soc Lond B Biol Sci, 366, 3595-3604.

Nagano, M., Hoshino, D., Koshikawa, N., Akizawa, T. and Seiki, M. (2012) Turnover of focal adhesions and cancer cell migration. Int J Cell Biol, 310616, 26.

Nasmyth, K. and Haering, C. H. (2009) Cohesin: its roles and mechanisms. Annu Rev Genet, 43, 525-558.

Nijenhuis, W., Vallardi, G., Teixeira, A., Kops, G. J. and Saurin, A. T. (2014) Negative feedback at kinetochores underlies a responsive spindle checkpoint signal. Nat Cell Biol, 16, 1257-1264.

Nishino, T., Rago, F., Hori, T., Tomii, K., Cheeseman, I. M. and Fukagawa, T. (2013) CENP-T provides a structural platform for outer kinetochore assembly. Embo J, 32, 424-436.

Nishiura, M., Kon, T., Shiroguchi, K., Ohkura, R., Shima, T., Toyoshima, Y. Y. and Sutoh, K. (2004) A single-headed recombinant fragment of Dictyostelium cytoplasmic dynein can drive the robust sliding of microtubules. J Biol Chem, 279, 22799-22802.

O'Connell, C. B. and Khodjakov, A. L. (2007) Cooperative mechanisms of mitotic spindle formation. J Cell Sci, 120, 1717-1722.

Palazzo, A. F., Joseph, H. L., Chen, Y. J., Dujardin, D. L., Alberts, A. S., Pfister, K. K., Vallee, R. B. and Gundersen, G. G. (2001) Cdc42, dynein, and dynactin regulate MTOC reorientation independent of Rho-regulated microtubule stabilization. Curr Biol, 11, 1536-1541.

Peng, G. E., Wilson, S. R. and Weiner, O. D. (2011) A pharmacological cocktail for arresting actin dynamics in living cells. Mol Biol Cell, 22, 3986-3994.
Peters, J. M. (2006) The anaphase promoting complex/cyclosome: a machine designed to destroy. Nat Rev Mol Cell Biol, 7, 644-656.
Petrovic, A., Pasqualato, S., Dube, P., Krenn, V., Santaguida, S., Cittaro, D., Monzani, S., Massimiliano, L., Keller, J., Tarricone, A., Maiolica, A., Stark, H. and Musacchio, A. (2010) The MIS12 complex is a protein interaction hub for outer kinetochore assembly. J Cell Biol, 190, 835-852.
Pfarr, C. M., Coue, M., Grissom, P. M., Hays, T. S., Porter, M. E. and McIntosh, J. R. (1990) Cytoplasmic dynein is localized to kinetochores during mitosis. Nature, 345, 263-265.
Pollard, T. D. (2007) Regulation of actin filament assembly by Arp2/3 complex and formins. Annu Rev Biophys Biomol Struct, 36, 451-477.
Pollard, T. D. and Borisy, G. G. (2003) Cellular Motility Driven by Assembly and Disassembly of Actin Filaments. Cell, 112, 453–465.
Poruchynsky, M. S., Komlodi-Pasztor, E., Trostel, S., Wilkerson, J., Regairaz, M., Pommier, Y., Zhang, X., Kumar Maity, T., Robey, R., Burotto, M., Sackett, D., Guha, U. and Fojo, A. T. (2015) Microtubule-targeting agents augment the toxicity of DNA-damaging agents by disrupting intracellular trafficking of DNA repair proteins. Proc Natl Acad Sci U S A, 112, 1571-1576.
Pulipati, N. R., Jin, Q., Liu, X., Sun, B., Pandey, M. K., Huber, J. P., Ding, W. and Mulder, K. M. (2011) Overexpression of the dynein light chain km23-1 in human ovarian carcinoma cells inhibits tumor formation in vivo and causes mitotic delay at prometaphase/metaphase. Int J Cancer, 129, 553-564.
Putyrski, M. and Schultz, C. (2012) Protein translocation as a tool: The current rapamycin story. FEBS Lett, 586, 2097-2105.
Quinlan, M. E., Heuser, J. E., Kerkhoff, E. and Mullins, R. D. (2005) Drosophila Spire is an actin nucleation factor. Nature, 433, 382-388.
Raftopoulou, M. and Hall, A. (2004) Cell migration: Rho GTPases lead the way. Dev Biol, 265, 23-32.
Reck-Peterson, S. L., Yildiz, A., Carter, A. P., Gennerich, A., Zhang, N. and Vale, R. D. (2006) Single-molecule analysis of dynein processivity and stepping behavior. Cell, 126, 335-348.
Reiner, O., Carrozzo, R., Shen, Y., Wehnert, M., Faustinella, F., Dobyns, W. B., Caskey, C. T. and Ledbetter, D. H. (1993) Isolation of a Miller-Dieker lissencephaly gene containing G protein beta-subunit-like repeats. Nature, 364, 717-721.
Reinhard, M., Zumbrunn, J., Jaquemar, D., Kuhn, M., Walter, U. and Trueb, B. (1999) An alpha-actinin binding site of zyxin is essential for subcellular zyxin localization and alpha-actinin recruitment. J Biol Chem, 274, 13410-13418.
Ren, X. D., Kiosses, W. B. and Schwartz, M. A. (1999) Regulation of the small GTP-binding protein Rho by cell adhesion and the cytoskeleton. Embo J, 18, 578-585.
Ren, X. D., Kiosses, W. B., Sieg, D. J., Otey, C. A., Schlaepfer, D. D. and Schwartz, M. A. (2000) Focal adhesion kinase suppresses Rho activity to promote focal adhesion turnover. J Cell Sci, 113, 3673-3678.
Reyes-Lamothe, R., Nicolas, E. and Sherratt, D. J. (2012) Chromosome replication and segregation in bacteria. Annu Rev Genet, 46, 121-143.
Ridley, A. J. (2015) Rho GTPase signalling in cell migration. Curr Opin Cell Biol, 36, 103-112.

Ridley, A. J., Schwartz, M. A., Burridge, K., Firtel, R. A., Ginsberg, M. H., Borisy, G., Parsons, J. T. and Horwitz, A. R. (2003) Cell migration: integrating signals from front to back. Science, 302, 1704-1709.

Rieder, C. L. and Alexander, S. P. (1990) Kinetochores are transported poleward along a single astral microtubule during chromosome attachment to the spindle in newt lung cells. J Cell Biol, 110, 81-95.

Rieder, C. L., Cole, R. W., Khodjakov, A. and Sluder, G. (1995) The checkpoint delaying anaphase in response to chromosome monoorientation is mediated by an inhibitory signal produced by unattached kinetochores. J Cell Biol, 130, 941-948.

Rieder, C. L. and Salmon, E. D. (1998) The vertebrate cell kinetochore and its roles during mitosis. Trends Cell Biol, 8, 310-318.

Riento, K. and Ridley, A. J. (2003) Rocks: multifunctional kinases in cell behaviour. Nat Rev Mol Cell Biol, 4, 446-456.

Rodriguez, O. C., Schaefer, A. W., Mandato, C. A., Forscher, P., Bement, W. M. and Waterman-Storer, C. M. (2003) Conserved microtubule-actin interactions in cell movement and morphogenesis. Nat Cell Biol, 5, 599-609.

Rogers, S. L., Wiedemann, U., Hacker, U., Turck, C. and Vale, R. D. (2004) Drosophila RhoGEF2 associates with microtubule plus ends in an EB1-dependent manner. Curr Biol, 14, 1827-1833.

Salmon, W. C., Adams, M. C. and Waterman-Storer, C. M. (2002) Dual-wavelength fluorescent speckle microscopy reveals coupling of microtubule and actin movements in migrating cells. J Cell Biol, 158, 31-37.

Sanz-Moreno, V., Gadea, G., Ahn, J., Paterson, H., Marra, P., Pinner, S., Sahai, E. and Marshall, C. J. (2008) Rac activation and inactivation control plasticity of tumor cell movement. Cell, 135, 510-523.

Sastry, S. K. and Burridge, K. (2000) Focal adhesions: a nexus for intracellular signaling and cytoskeletal dynamics. Exp Cell Res, 261, 25-36.

Saurin, A. T., van der Waal, M. S., Medema, R. H., Lens, S. M. and Kops, G. J. (2011) Aurora B potentiates Mps1 activation to ensure rapid checkpoint establishment at the onset of mitosis. Nat Commun, 2.

Schafer-Hales, K., Iaconelli, J., Snyder, J. P., Prussia, A., Nettles, J. H., El-Naggar, A., Khuri, F. R., Giannakakou, P. and Marcus, A. I. (2007) Farnesyl transferase inhibitors impair chromosomal maintenance in cell lines and human tumors by compromising CENP-E and CENP-F function. Mol Cancer Ther, 6, 1317-1328.

Schlager, M. A., Hoang, H. T., Urnavicius, L., Bullock, S. L. and Carter, A. P. (2014) In vitro reconstitution of a highly processive recombinant human dynein complex. Embo J, 33, 1855-1868.

Schmoranzer, J., Kreitzer, G. and Simon, S. M. (2003) Migrating fibroblasts perform polarized, microtubule-dependent exocytosis towards the leading edge. J Cell Sci, 116, 4513-4519.

Schroer, T. A. (2004) Dynactin. Annu Rev Cell Dev Biol, 20, 759-779.

Schuyler, S. C. and Pellman, D. (2001) Microtubule "plus-end-tracking proteins": The end is just the beginning. Cell, 105, 421-424.

Screpanti, E., De Antoni, A., Alushin, G. M., Petrovic, A., Melis, T., Nogales, E. and Musacchio, A. (2011) Direct binding of Cenp-C to the Mis12 complex joins the inner and outer kinetochore. Curr Biol, 21, 391-398.

Sharp-Baker, H. and Chen, R. H. (2001) Spindle checkpoint protein Bub1 is required for kinetochore localization of Mad1, Mad2, Bub3, and CENP-E, independently of its kinase activity. J Cell Biol, 153, 1239-1250.

Sharp, D. J., Rogers, G. C. and Scholey, J. M. (2000) Microtubule motors in mitosis. Nature, 407, 41-47.

Silva, P. M. A., Reis, R. M., Bolanos-Garcia, V. M., Florindo, C., Tavares, Á. A. and Bousbaa, H. (2014) Dynein-dependent transport of spindle assembly checkpoint proteins off kinetochores toward spindle poles. FEBS Lett, 588, 3265-3273.

Sivakumar, S. and Gorbsky, G. J. (2015) Spatiotemporal regulation of the anaphase-promoting complex in mitosis. Nat Rev Mol Cell Biol, 16, 82-94.

Skoble, J., Portnoy, D. A. and Welch, M. D. (2000) Three regions within ActA promote Arp2/3 complex-mediated actin nucleation and Listeria monocytogenes motility. J Cell Biol, 150, 527-538.

Skoufias, D. A., DeBonis, S., Saoudi, Y., Lebeau, L., Crevel, I., Cross, R., Wade, R. H., Hackney, D. and Kozielski, F. (2006) S-trityl-L-cysteine is a reversible, tight binding inhibitor of the human kinesin Eg5 that specifically blocks mitotic progression. J Biol Chem, 281, 17559-17569.

Smith, D. S., Niethammer, M., Ayala, R., Zhou, Y., Gambello, M. J., Wynshaw-Boris, A. and Tsai, L. H. (2000) Regulation of cytoplasmic dynein behaviour and microtubule organization by mammalian Lis1. Nat Cell Biol, 2, 767-775.

Somsel Rodman, J. and Wandinger-Ness, A. (2000) Rab GTPases coordinate endocytosis. J Cell Sci, 2, 183-192.

Splinter, D., Razafsky, D. S., Schlager, M. A., Serra-Marques, A., Grigoriev, I., Demmers, J., Keijzer, N., Jiang, K., Poser, I., Hyman, A. A., Hoogenraad, C. C., King, S. J. and Akhmanova, A. (2012) BICD2, dynactin, and LIS1 cooperate in regulating dynein recruitment to cellular structures. Mol Biol Cell, 23, 4226-4241.

Splinter, D., Tanenbaum, M. E., Lindqvist, A., Jaarsma, D., Flotho, A., Yu, K. L., Grigoriev, I., Engelsma, D., Haasdijk, E. D., Keijzer, N., Demmers, J., Fornerod, M., Melchior, F., Hoogenraad, C. C., Medema, R. H. and Akhmanova, A. (2010) Bicaudal D2, dynein, and kinesin-1 associate with nuclear pore complexes and regulate centrosome and nuclear positioning during mitotic entry. PLoS Biol, 8, 1000350.

Spurck, T. P., Pickett-Heaps, J. D. and Klymkowsky, M. W. (1986) Metabolic inhibitors and mitosis: I. Effects of dinitrophenol/deoxyglucose and nocodazole on the live spindle. Protoplasma, 131, 47-59.

Starr, D. A., Saffery, R., Li, Z., Simpson, A. E., Choo, K. H., Yen, T. J. and Goldberg, M. L. (2000) HZwint-1, a novel human kinetochore component that interacts with HZW10. J Cell Sci, 113, 1939-1950.

Starr, D. A., Williams, B. C., Hays, T. S. and Goldberg, M. L. (1998) ZW10 helps recruit dynactin and dynein to the kinetochore. J Cell Biol, 142, 763-774.

Stehbens, S. and Wittmann, T. (2012) Targeting and transport: how microtubules control focal adhesion dynamics. J Cell Biol, 198, 481-489.

Stehman, S. A., Chen, Y., McKenney, R. J. and Vallee, R. B. (2007) NudE and NudEL are required for mitotic progression and are involved in dynein recruitment to kinetochores. J Cell Biol, 178, 583-594.

Stevenson, R. P., Veltman, D. and Machesky, L. M. (2012) Actin-bundling proteins in cancer progression at a glance. J Cell Sci, 125, 1073-1079.

Sudakin, V., Chan, G. K. and Yen, T. J. (2001) Checkpoint inhibition of the APC/C in HeLa cells is mediated by a complex of BUBR1, BUB3, CDC20, and MAD2. J Cell Biol, 154, 925-936.

Suzuki, A., Badger, B. L. and Salmon, E. D. (2015) A quantitative description of Ndc80 complex linkage to human kinetochores. Nat Commun, 6.

Swan, A. and Suter, B. (1996) Role of Bicaudal-D in patterning the Drosophila egg chamber in mid-oogenesis. Development, 122, 3577-3586.

Takenaka, K., Moriguchi, T. and Nishida, E. (1998) Activation of the protein kinase p38 in the spindle assembly checkpoint and mitotic arrest. Science, 280, 599-602.

Tanaka, T. U. (2008) Bi-orienting chromosomes: acrobatics on the mitotic spindle. Chromosoma, 117, 521-533.

Taylor, E. W. (1965) The Mechanism of Colchicine Inhibition of Mitosis. I. Kinetics of Inhibition and the Binding of H3-Colchicine. J Cell Biol, 25, 145-160.

Taylor, S. S., Ha, E. and McKeon, F. (1998) The human homologue of Bub3 is required for kinetochore localization of Bub1 and a Mad3/Bub1-related protein kinase. J Cell Biol, 142, 1-11.

Teichner, A., Eytan, E., Sitry-Shevah, D., Miniowitz-Shemtov, S., Dumin, E., Gromis, J. and Hershko, A. (2011) p31comet Promotes disassembly of the mitotic checkpoint complex in an ATP-dependent process. Proc Natl Acad Sci U S A, 108, 3187-3192.

Thomas, D. B. and Lingwood, C. A. (1975) A model of cell cycle control: effects of thymidine on synchronous cell cultures. Cell, 5, 37-42.

Tian, D., Diao, M., Jiang, Y., Sun, L., Zhang, Y., Chen, Z., Huang, S. and Ou, G. (2015) Anillin Regulates Neuronal Migration and Neurite Growth by Linking RhoG to the Actin Cytoskeleton. Curr Biol, 25, 1135-1145.

Tirnauer, J. S., Canman, J. C., Salmon, E. D. and Mitchison, T. J. (2002) EB1 targets to kinetochores with attached, polymerizing microtubules. Mol Biol Cell, 13, 4308-4316.

Toba, S., Watanabe, T. M., Yamaguchi-Okimoto, L., Toyoshima, Y. Y. and Higuchi, H. (2006) Overlapping hand-over-hand mechanism of single molecular motility of cytoplasmic dynein. Proc Natl Acad Sci U S A, 103, 5741-5745.

Tomishige, M., Klopfenstein, D. R. and Vale, R. D. (2002) Conversion of Unc104/KIF1A kinesin into a processive motor after dimerization. Science, 297, 2263-2267.

Toomre, D. and Manstein, D. J. (2001) Lighting up the cell surface with evanescent wave microscopy. Trends Cell Biol, 11, 298-303.

Totsukawa, G., Wu, Y., Sasaki, Y., Hartshorne, D. J., Yamakita, Y., Yamashiro, S. and Matsumura, F. (2004) Distinct roles of MLCK and ROCK in the regulation of membrane protrusions and focal adhesion dynamics during cell migration of fibroblasts. J Cell Biol, 164, 427-439.

Trokter, M., Mucke, N. and Surrey, T. (2012) Reconstitution of the human cytoplasmic dynein complex. Proc Natl Acad Sci U S A, 109, 20895-20900.

Tynan, S. H., Purohit, A., Doxsey, S. J. and Vallee, R. B. (2000) Light intermediate chain 1 defines a functional subfraction of cytoplasmic dynein which binds to pericentrin. J Biol Chem, 275, 32763-32768.

Uchida, K. S., Takagaki, K., Kumada, K., Hirayama, Y., Noda, T. and Hirota, T. (2009) Kinetochore stretching inactivates the spindle assembly checkpoint. J Cell Biol, 184, 383-390.

Urnavicius, L., Zhang, K., Diamant, A. G., Motz, C., Schlager, M. A., Yu, M., Patel, N. A., Robinson, C. V. and Carter, A. P. (2015) The structure of the dynactin complex and its interaction with dynein. Science, 347, 1441-1446.

Vale, R. D. (2000) AAA proteins. Lords of the ring. J Cell Biol, 150, F13-19.

Vallee, R. B., McKenney, R. J. and Ori-McKenney, K. M. (2012) Multiple modes of cytoplasmic dynein regulation. Nat Cell Biol, 14, 224-230.

van Vlijmen, T., Vleugel, M., Evers, M., Mohammed, S., Wulf, P. S., Heck, A. J., Hoogenraad, C. C. and van der Sluijs, P. (2008) A unique residue in rab3c determines the interaction with novel binding protein Zwint-1. FEBS Lett, 582, 2838-2842.

Varma, D., Dujardin, D. L., Stehman, S. A. and Vallee, R. B. (2006) Role of the kinetochore/cell cycle checkpoint protein ZW10 in interphase cytoplasmic dynein function. J Cell Biol, 172, 655-662.

Varma, D., Monzo, P., Stehman, S. A. and Vallee, R. B. (2008) Direct role of dynein motor in stable kinetochore-microtubule attachment, orientation, and alignment. J Cell Biol, 182, 1045-1054.

Varma, D., Wan, X., Cheerambathur, D., Gassmann, R., Suzuki, A., Lawrimore, J., Desai, A. and Salmon, E. D. (2013) Spindle assembly checkpoint proteins are positioned close to core microtubule attachment sites at kinetochores. J Cell Biol, 202, 735-746.

Vasiliev, J. M., Gelfand, I. M., Domnina, L. V., Ivanova, O. Y., Komm, S. G. and Olshevskaja, L. V. (1970) Effect of colcemid on the locomotory behaviour of fibroblasts. J Embryol Exp Morphol, 24, 625-640.

Vaughan, K. T., Tynan, S. H., Faulkner, N. E., Echeverri, C. J. and Vallee, R. B. (1999) Colocalization of cytoplasmic dynein with dynactin and CLIP-170 at microtubule distal ends. J Cell Sci, 112, 1437-1447.

Vaughan, K. T. and Vallee, R. B. (1995) Cytoplasmic dynein binds dynactin through a direct interaction between the intermediate chains and p150Glued. J Cell Biol, 131, 1507-1516.

Vaughan, P. S., Miura, P., Henderson, M., Byrne, B. and Vaughan, K. T. (2002) A role for regulated binding of p150(Glued) to microtubule plus ends in organelle transport. J Cell Biol, 158, 305-319.

Vicente-Manzanares, M., Ma, X., Adelstein, R. S. and Horwitz, A. R. (2009) Non-muscle myosin II takes centre stage in cell adhesion and migration. Nat Rev Mol Cell Biol, 10, 778-790.

Vicente-Manzanares, M., Zareno, J., Whitmore, L., Choi, C. K. and Horwitz, A. F. (2007) Regulation of protrusion, adhesion dynamics, and polarity by myosins IIA and IIB in migrating cells. J Cell Biol, 176, 573-580.

Vink, M., Simonetta, M., Transidico, P., Ferrari, K., Mapelli, M., De Antoni, A., Massimiliano, L., Ciliberto, A., Faretta, M., Salmon, E. D. and Musacchio, A. (2006) In vitro FRAP identifies the minimal requirements for Mad2 kinetochore dynamics. Curr Biol, 16, 755-766.

Vleugel, M., Hoek, T. A., Tromer, E., Sliedrecht, T., Groenewold, V., Omerzu, M. and Kops, G. J. (2015) Dissecting the roles of human BUB1 in the spindle assembly checkpoint. J Cell Sci, 128, 2975-2982.

Vleugel, M., Tromer, E., Omerzu, M., Groenewold, V., Nijenhuis, W., Snel, B. and Kops, G. J. (2013) Arrayed BUB recruitment modules in the kinetochore scaffold KNL1 promote accurate chromosome segregation. J Cell Biol, 203, 943-955.

Vos, L. J., Famulski, J. K. and Chan, G. K. (2011) hZwint-1 bridges the inner and outer kinetochore: identification of the kinetochore localization domain and the hZw10-interaction domain. Biochem J, 436, 157-168.

Wadsworth, P. and Khodjakov, A. (2004) E pluribus unum: towards a universal mechanism for spindle assembly. Trends Cell Biol, 14, 413-419.

Wan, J., Zhu, F., Zasadil, L. M., Yu, J., Wang, L., Johnson, A., Berthier, E., Beebe, D. J., Audhya, A. and Weaver, B. A. (2014) A Golgi-localized pool of the mitotic checkpoint component Mad1 controls integrin secretion and cell migration. Curr Biol, 24, 2687-2692.

Wang, L., Yin, F., Du, Y., Chen, B., Liang, S., Zhang, Y., Du, W., Wu, K., Ding, J. and Fan, D. (2010) Depression of MAD2 inhibits apoptosis and increases proliferation and multidrug resistance in gastric cancer cells by regulating the activation of phosphorylated survivin. Tumour Biol, 31, 225-232.

Wang, Y., Jin, F., Higgins, R. and McKnight, K. (2014) The current view for the silencing of the spindle assembly checkpoint. Cell Cycle, 13, 1694-1701.

Watanabe, T., Noritake, J. and Kaibuchi, K. (2005) Regulation of microtubules in cell migration. Trends Cell Biol, 15, 76-83.

Waterman-Storer, C. M., Worthylake, R. A., Liu, B. P., Burridge, K. and Salmon, E. D. (1999) Microtubule growth activates Rac1 to promote lamellipodial protrusion in fibroblasts. Nat Cell Biol, 1, 45-50.

Weaver, B. A. and Cleveland, D. W. (2005) Decoding the links between mitosis, cancer, and chemotherapy: The mitotic checkpoint, adaptation, and cell death. Cancer Cell, 8, 7-12.

Webb, D. J., Parsons, J. T. and Horwitz, A. F. (2002) Adhesion assembly, disassembly and turnover in migrating cells -- over and over and over again. Nat Cell Biol, 4, E97-100.

Weiss, E. and Winey, M. (1996) The Saccharomyces cerevisiae spindle pole body duplication gene MPS1 is part of a mitotic checkpoint. J Cell Biol, 132, 111-123.

Whyte, J., Bader, J. R., Tauhata, S. B. F., Raycroft, M., Hornick, J., Pfister, K. K., Lane, W. S., Chan, G. K., Hinchcliffe, E. H., Vaughan, P. S. and Vaughan, K. T. (2008) Phosphorylation regulates targeting of cytoplasmic dynein to kinetochores during mitosis. J Cell Biol, 183, 819-834.

Wickstead, B. and Gull, K. (2011) The evolution of the cytoskeleton. J Cell Biol, 194, 513-525.

Wollman, R., Cytrynbaum, E. N., Jones, J. T., Meyer, T., Scholey, J. M. and Mogilner, A. (2005) Efficient chromosome capture requires a bias in the 'search-and-capture' process during mitotic-spindle assembly. Curr Biol, 15, 828-832.

Woodruff, J. B., Wueseke, O. and Hyman, A. A. (2014) Pericentriolar material structure and dynamics. Philos Trans R Soc Lond B Biol Sci, 369.

Worthylake, R. A., Lemoine, S., Watson, J. M. and Burridge, K. (2001) RhoA is required for monocyte tail retraction during transendothelial migration. J Cell Biol, 154, 147-160.

Yamagishi, Y., Yang, C. H., Tanno, Y. and Watanabe, Y. (2012) MPS1/Mph1 phosphorylates the kinetochore protein KNL1/Spc7 to recruit SAC components. Nat Cell Biol, 14, 746-752.

Yamaguchi, H. and Condeelis, J. (2007) Regulation of the actin cytoskeleton in cancer cell migration and invasion. Biochim Biophys Acta, 1773, 642-652.

Yamamoto, T. G., Watanabe, S., Essex, A. and Kitagawa, R. (2008) SPDL-1 functions as a kinetochore receptor for MDF-1 in Caenorhabditis elegans. J Cell Biol, 183, 187-194.

Yang, Z., Tulu, U. S., Wadsworth, P. and Rieder, C. L. (2007) Kinetochore dynein is required for chromosome motion and congression independent of the spindle checkpoint. Curr Biol, 17, 973-980.

Yao, X., Abrieu, A., Zheng, Y., Sullivan, K. F. and Cleveland, D. W. (2000) CENP-E forms a link between attachment of spindle microtubules to kinetochores and the mitotic checkpoint. Nat Cell Biol, 2, 484-491.

Zhang, F. L. and Casey, P. J. (1996) Protein prenylation: molecular mechanisms and functional consequences. Annu Rev Biochem, 65, 241-269.

Zhang, G., Lischetti, T., Hayward, D. G. and Nilsson, J. (2015) Distinct domains in Bub1 localize RZZ and BubR1 to kinetochores to regulate the checkpoint. Nat Commun, 6.

Zhang, J., Yao, X., Fischer, L., Abenza, J. F., Penalva, M. A. and Xiang, X. (2011) The p25 subunit of the dynactin complex is required for dynein-early endosome interaction. J Cell Biol, 193, 1245-1255.

Zhang, Q. H., Wei, L., Tong, J. S., Qi, S. T., Li, S., Ou, X. H., Ouyang, Y. C., Hou, Y., An, L. G., Schatten, H. and Sun, Q. Y. (2010) Localization and function of mSpindly during mouse oocyte meiotic maturation. Cell Cycle, 9, 2230-2236.

Zhu, T., Dou, Z., Qin, B., Jin, C., Wang, X., Xu, L., Wang, Z., Zhu, L., Liu, F., Gao, X., Ke, Y., Aikhionbare, F., Fu, C., Ding, X. and Yao, X. (2013) Phosphorylation of microtubule-binding protein Hec1 by mitotic kinase Aurora B specifies spindle checkpoint kinase Mps1 signaling at the kinetochore. J Biol Chem, 288, 36149-36159.

Zhu, X., Chang, K. H., He, D., Mancini, M. A., Brinkley, W. R. and Lee, W. H. (1995) The C terminus of mitosin is essential for its nuclear localization, centromere/kinetochore targeting, and dimerization. J Biol Chem, 270, 19545-19550.

# 8 . Appendix

## 8.1 Generation of stable cell lines expressing GFP Spindly

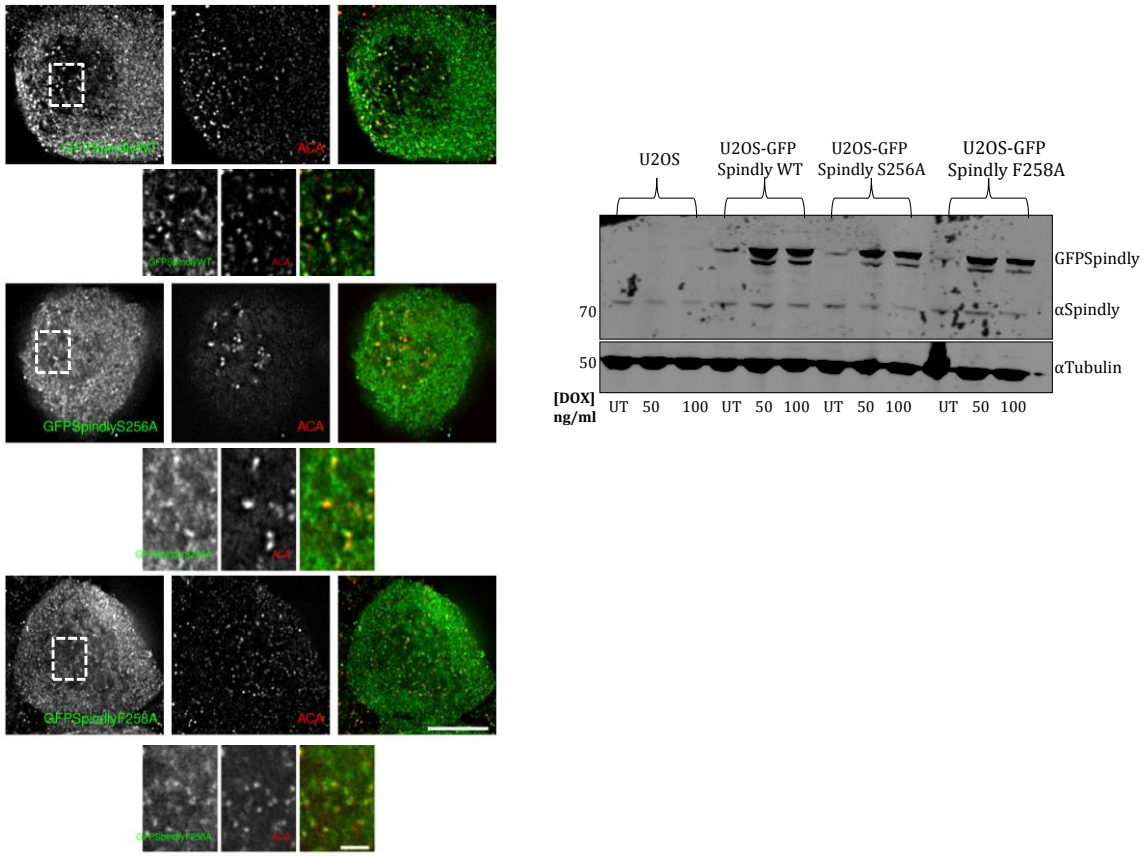


(a) (b)

**Figure 8. 1. U2OS cells express correctly GFP Spindly.**
U2OS cells stably expressing GFP Spindly WT, S256A mutant or F258A mutant. (a) Fluorescence images showing correct kinetochore localisation of all three constructs expressing GFP Spindly (green), co-localising with the kinetochore marker ACA (red). Details underneath each single GFP panel show correct KT localisation of GFP Spindly constructs (dashed white box). Scale bar 10 μm (or 2 μm for details). (b) Western blot experiment of U2OS cells expressing GFP Spindly constructs upon administration of Doxycycline (either 50 or 100 ng/mL for 24 hours). Tubulin was used as loading control.

## 8.2 Localisation of Spindly in mitosis

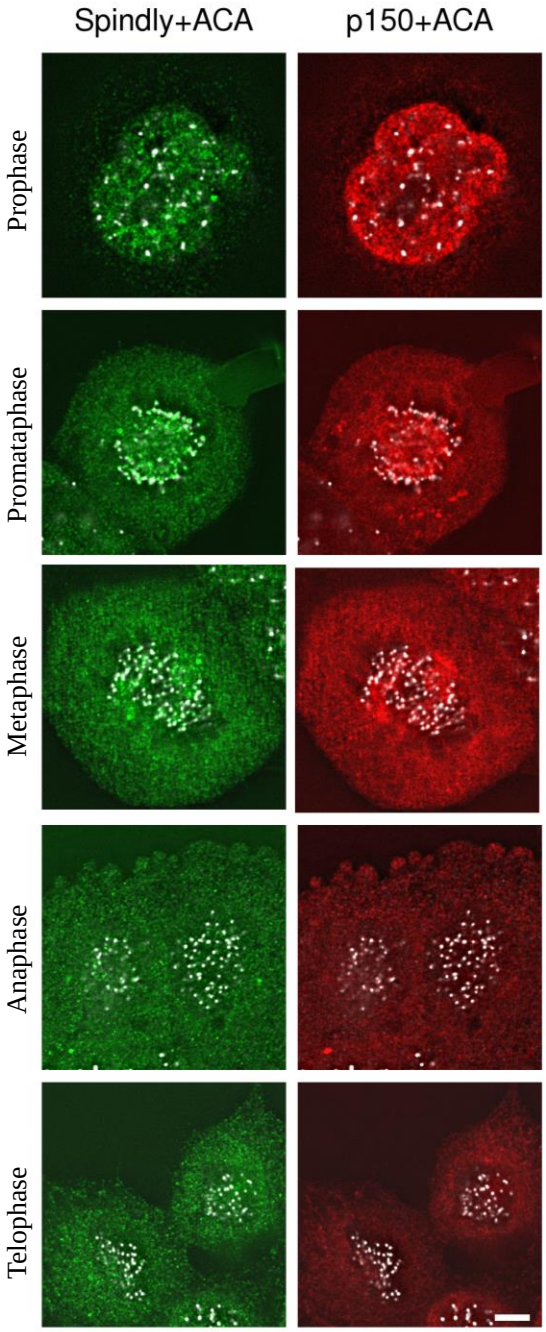


**Figure 8. 2. Spindly localises at kinetochores in mitosis.**
U2OS cells were stained with anti-Spindly (green) or anti-p150 (red) and anti-ACA (kinetochore marker, white) antibodies. Spindly and p150 co-localise with ACA at KTs mainly during prometaphase. Scale bar 5 μm.

## 8.3 Rapamycin mis-localisation experiment measurments

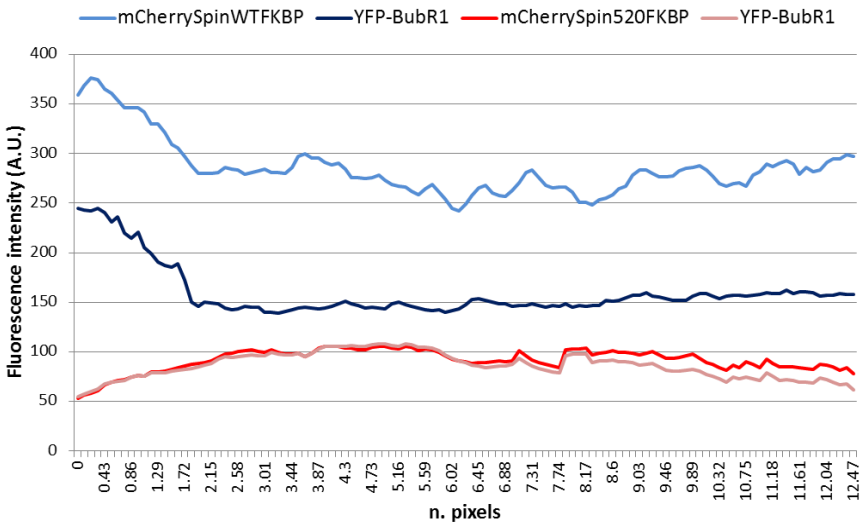


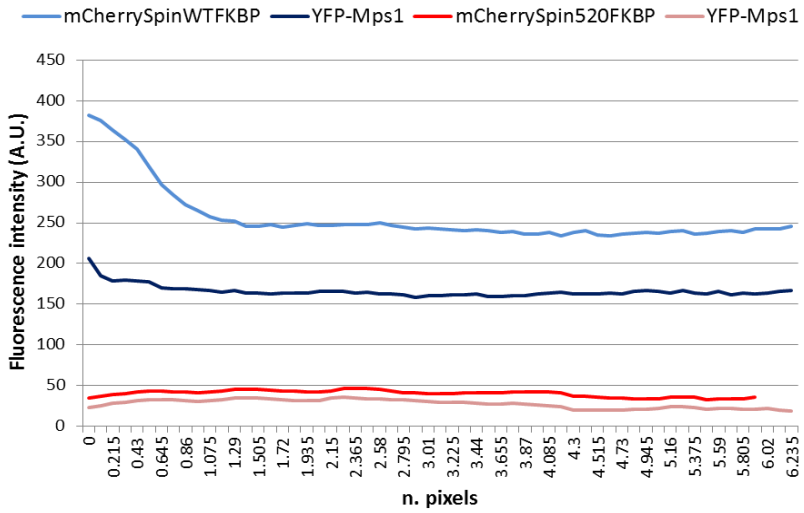

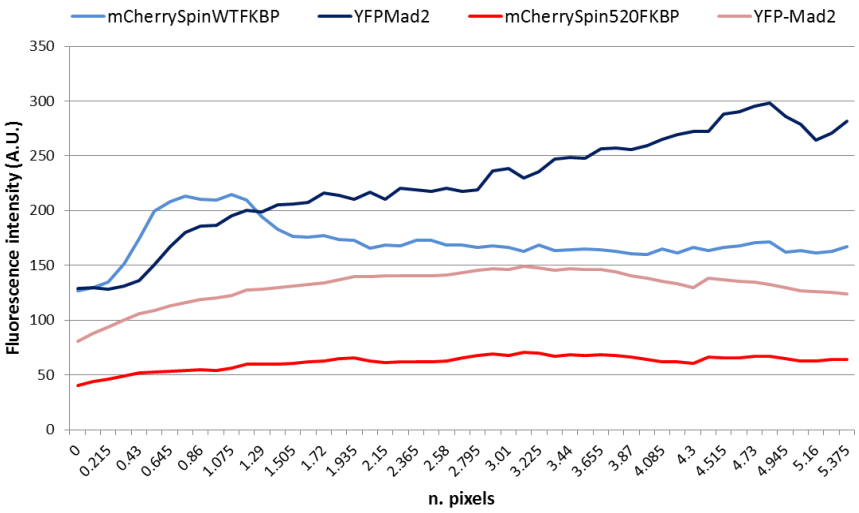


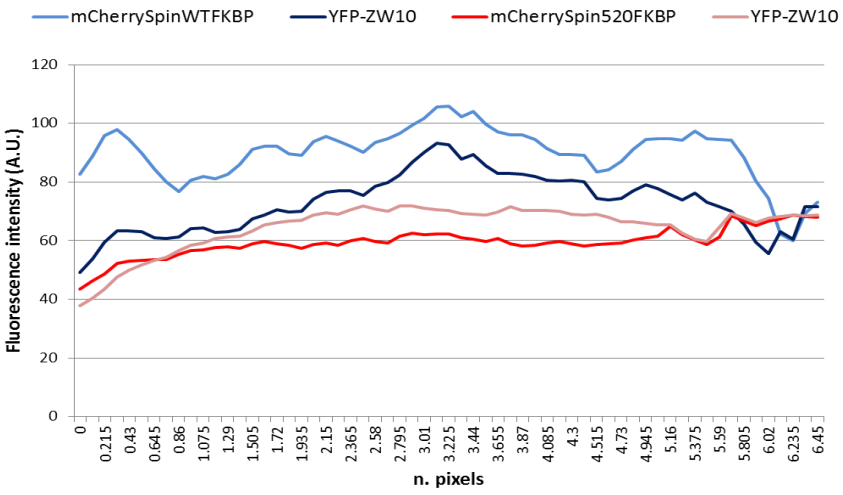


(b)

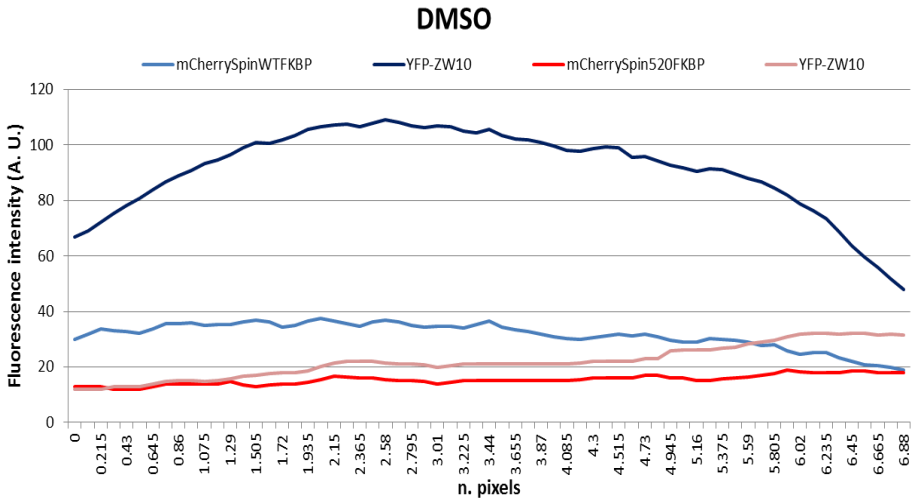


**Figure 8. 3. Expression of Spindly 1-520 does not affect interaction with SAC components.** HeLa cells transfected with mCherry-SpindlyFKBP WT or 1-520, Lin11FRB, YFP-SAC component tested. Images were collected upon staining under fluorescence microscopy (see Chapter 4, Fig. 4.6 and 4.7) and measurements were carried out by drawing a line between the two edges of the cell (n= 30). Comparison between

expressions of mCherrySpinWT-FKBP or mCherrySpin520-FKBP reveal similar capacities of the two constructs to interact with the different SAC component tested upon administration of Rapamycin (4μM) (a). In (b) is shown representative values obtained upon administration of DMSO. Here is reported the graph obtained for YFP-ZW10 to confirm lack of recruitment without addition of Rapamycin (for the other proteins tested similar negative results were obtained, data not shown).

## 8.4 Spindly is not only a nuclear protein

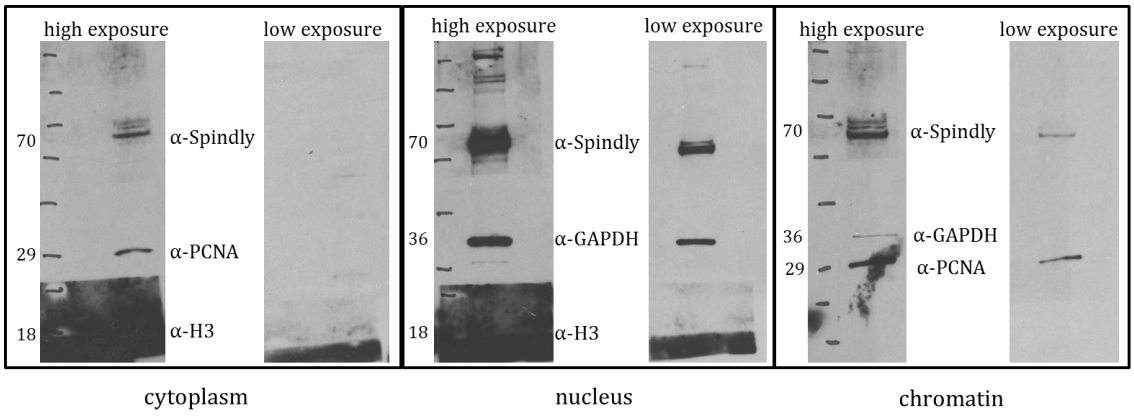


**Figure 8. 4. Spindly is not exclusively a nuclear protein.**
Fractionation experiment of U2OS cell lysate performed to analyse the expression of Spindly in different cellular compartments. Here is reported a western blotting analysis to cross check the isolation of the different fractions; positive isolation is reported in chapter 5, fig. 5.1. Antibodies tested as indicated. Anti-PCNA was used as nuclear marker; anti-H3 (anti-histone 3) was used as chromatin marker; anti-GAPDH was used as cytoplasm marker. This result suggests the presence of Spindly in all the fractions; however validation of the fractions with more stringent markers would be needed.

# 8.5 Mass spectrometry analysis of Spindly interacting proteins in mitosis

| Protein IDs | Peptides | Q-value | Noc IP Sum | Noc IgG Sum | STLC IP Sum | STLC IgG Sum | UT IP Sum | UT IgG Sum |
|---|---|---|---|---|---|---|---|---|
| sp\|Q14204\|DYHC1_HUMAN;tr\|H0YJ21\| | 215 | 0 | 528168900 | 92346940 | 257703500 | 159281070 | 781034600 | 135430070 |
| sp\|Q09666\|AHNK_HUMAN;tr\|Q6ZQN2 | 201 | 0 | 433201460 | 79022340 | 169055240 | 96483000 | 1278503200 | 54104830 |
| sp\|P78527\|PRKDC_HUMAN;sp\|P78527- | 163 | 0 | 330012800 | 43917790 | 165526680 | 54963120 | 1067001600 | 76804910 |
| sp\|P15924\|DESP_HUMAN;sp\|P15924-3 | 126 | 0 | 324473000 | 103972000 | 127217000 | 123059000 | 131292000 | 105272400 |
| sp\|P21333-2\|FLNA_HUMAN;sp\|P21333 | 111 | 0 | 243425630 | 72122500 | 140002020 | 71577750 | 184456790 | 79397900 |
| sp\|P49327\|FAS_HUMAN;tr\|Q6PJJ3\|Q6 | 107 | 0 | 301770100 | 51971460 | 184568742 | 90015300 | 605831550 | 51773500 |
| tr\|A0A024R1N1\|A0A024R1N1_HUMAN; | 106 | 0 | 132215096 | 50180010 | 143137050 | 29035765 | 1258123900 | 87227694 |
| sp\|Q9Y490\|TLN1_HUMAN;sp\|Q9Y4G6\| | 102 | 0 | 102428289 | 24554119 | 70755350 | 53836396 | 569220070 | 42596308 |
| sp\|Q15149-7\|PLEC_HUMAN;sp\|Q15149 | 102 | 0 | 83572302 | 7845233 | 41085310 | 9090485 | 61530530 | 8300600 |
| tr\|E1NZA1\|E1NZA1_HUMAN;sp\|Q9261 | 91 | 0 | 81628000 | 9560500 | 40015170 | 12054000 | 172988900 | 9482870 |
| sp\|P35580\|MYH10_HUMAN;sp\|P35580- | 91 | 0 | 69568510 | 23748000 | 71454000 | 20400607 | 512159725 | 53693120 |
| sp\|Q14008\|CKAP5_HUMAN;sp\|Q14008 | 83 | 0 | 157530714 | 37099830 | 86857620 | 32304410 | 193533550 | 10886000 |
| tr\|A0A087X1U6\|A0A087X1U6_HUMAN; | 81 | 0 | 137759700 | 21027380 | 44927790 | 35799026 | 210681900 | 26783630 |
| sp\|P49454\|CENPF_HUMAN;tr\|A0A087V | 81 | 0 | 81830590 | 0 | 16028542 | 0 | 12206621 | 0 |
| sp\|P58107\|EPIPL_HUMAN | 79 | 0 | 3357400 | 353460 | 1422300 | 217940 | 822750 | 417090 |
| sp\|Q6P2Q9\|PRP8_HUMAN;tr\|I3L0J9\|I3 | 78 | 0 | 22920500 | 4948800 | 27457217 | 5309803 | 150393300 | 9645700 |
| sp\|Q00610-2\|CLH1_HUMAN;sp\|Q0061( | 76 | 0 | 205622100 | 27204497 | 92999640 | 51295644 | 299444370 | 21604020 |
| sp\|O75643\|U520_HUMAN;tr\|A4FU77\|A | 76 | 0 | 68292700 | 12518000 | 45539683 | 13953000 | 284230650 | 14433412 |
| tr\|F8VPD4\|F8VPD4_HUMAN;sp\|P2770 | 71 | 0 | 117154520 | 12823000 | 72360500 | 22257000 | 315567560 | 21177300 |
| sp\|P35908\|K22E_HUMAN | 71 | 0 | 34077040 | 14776100 | 12355800 | 34741100 | 22306600 | 17050200 |
| sp\|P04259\|K2C6B_HUMAN | 61 | 0 | 48265500 | 23237400 | 19150300 | 24509000 | 18913200 | 21980400 |
| tr\|A0A024R9Y3\|A0A024R9Y3_HUMAN;t | 61 | 0 | 25657000 | 2316560 | 9387320 | 2818400 | 53810910 | 5241688 |
| sp\|P07814\|SYEP_HUMAN;tr\|Q3KQZ8\|C | 59 | 0 | 93166230 | 20675909 | 39208200 | 22423869 | 257429600 | 36766460 |
| tr\|B2R853\|B2R853_HUMAN;tr\|B4DXK4 | 59 | 0 | 10805070 | 7390400 | 4767110 | 11709100 | 8129400 | 10436300 |
| sp\|O75369-2\|FLNB_HUMAN;sp\|O7536 | 58 | 0 | 12650777 | 2964792 | 6294369 | 2204756 | 7520170 | 5800400 |
| sp\|P13639\|EF2_HUMAN;tr\|Q8TA90\|Q8 | 54 | 0 | 443794680 | 136084700 | 304680760 | 130504870 | 982477900 | 251745000 |
| tr\|A0A024R3T8\|A0A024R3T8_HUMAN;s | 54 | 0 | 163483500 | 54091264 | 106764390 | 40571410 | 537016190 | 90618890 |
| sp\|P55060-3\|XPO2_HUMAN;sp\|P55060 | 51 | 0 | 381581980 | 64661091 | 164130100 | 55287740 | 661848660 | 44056970 |
| tr\|A0A024R652\|A0A024R652_HUMAN;s | 51 | 0 | 301874690 | 101742710 | 253822400 | 77069210 | 1133105000 | 123454640 |
| tr\|E7EUU4\|E7EUU4_HUMAN;sp\|Q0463 | 51 | 0 | 135607135 | 27276960 | 71118470 | 29886214 | 348068350 | 28149686 |
| sp\|Q04637-3\|IF4G1_HUMAN;tr\|B4DGF | 51 | 1 | 1854300 | 0 | 1168800 | 242520 | 2807146 | 415780 |
| tr\|A0A024R1Y2\|A0A024R1Y2_HUMAN;s | 50 | 0 | 146042690 | 17710920 | 49655030 | 11282190 | 216243700 | 28301667 |
| sp\|Q9Y520-4\|PRC2C_HUMAN;tr\|E7EPN | 50 | 0 | 32112000 | 5362849 | 17583120 | 4589100 | 93520530 | 3654400 |
| sp\|P41252\|SYIC_HUMAN;tr\|Q59G75\|Q | 49 | 0 | 92430900 | 17332520 | 44353457 | 18403069 | 269842530 | 40242739 |
| tr\|F1T0J2\|F1T0J2_HUMAN;sp\|Q14789\|( | 49 | 0 | 13878910 | 5623097 | 15755060 | 6749400 | 10764800 | 1809210 |
| sp\|Q08211\|DHX9_HUMAN;tr\|Q58F26\|( | 48 | 0 | 74236530 | 12533300 | 42501771 | 11185740 | 351794940 | 27509328 |
| tr\|V9HWB8\|V9HWB8_HUMAN;sp\|P146 | 46 | 0 | 440740300 | 123027100 | 788513300 | 160118700 | 1568318000 | 220544500 |
| sp\|P22102\|PUR2_HUMAN;tr\|Q59HH3\|( | 46 | 0 | 153532578 | 35647160 | 95177720 | 40936600 | 477814000 | 56037900 |
| tr\|B2RCM2\|B2RCM2_HUMAN;sp\|Q9P2 | 46 | 0 | 75910570 | 16585900 | 56500470 | 18656380 | 354385000 | 35680130 |
| sp\|P51610-4\|HCFC1_HUMAN;tr\|A6NEN | 46 | 0 | 62500000 | 16861680 | 77459800 | 15613833 | 104375200 | 12549950 |
| sp\|O75533\|SF3B1_HUMAN;tr\|Q7Z497\| | 46 | 0 | 56275180 | 9187000 | 25002340 | 5597179 | 133598799 | 9941834 |
| tr\|V9HW29\|V9HW29_HUMAN;sp\|P331 | 45 | 0 | 47679000 | 10077220 | 28609340 | 6492103 | 118534030 | 11967585 |
| sp\|P49792\|RBP2_HUMAN;tr\|D3DX73\|D | 45 | 0 | 24866210 | 2011090 | 10220030 | 3021100 | 8347660 | 763398 |
| sp\|A5YKK6\|CNOT1_HUMAN;sp\|A5YKK6 | 45 | 0 | 23120000 | 3630200 | 13555380 | 4846814 | 104104000 | 3318000 |
| tr\|F5GWX5\|F5GWX5_HUMAN;sp\|Q148 | 45 | 0 | 20865130 | 3053900 | 17571300 | 2193600 | 92144947 | 3824200 |
| sp\|Q9NU22\|MDN1_HUMAN;tr\|Q6AI22 | 45 | 0 | 12782000 | 564690 | 4084200 | 797000 | 33351611 | 1050700 |
| sp\|P51610\|HCFC1_HUMAN;sp\|P51610- | 45 | 0.000358 | 3552100 | 1233400 | 3734700 | 1056100 | 5837500 | 1211310 |
| tr\|A0A024RDY0\|A0A024RDY0_HUMAN; | 44 | 0 | 115950500 | 19952620 | 65231200 | 17074910 | 262382100 | 23328860 |
| tr\|A0A024R4E5\|A0A024R4E5_HUMAN;s | 44 | 0 | 63558300 | 17718519 | 46996680 | 19273982 | 329368400 | 19804420 |
| sp\|P48634\|PRC2A_HUMAN;sp\|P48634- | 44 | 0 | 60149000 | 1380000 | 31129000 | 1643400 | 164703950 | 3213400 |
| tr\|Q24JU4\|Q24JU4_HUMAN;tr\|J9R021\| | 44 | 0 | 47399700 | 6749340 | 20964880 | 7476500 | 94518659 | 11075630 |
| sp\|Q5VYK3\|ECM29_HUMAN;tr\|J3KN16 | 44 | 0 | 41104000 | 3111400 | 12021620 | 4271900 | 82322700 | 4941604 |
| sp\|Q16531\|DDB1_HUMAN;tr\|F5GY55\|F | 44 | 0 | 31155350 | 6159100 | 15372550 | 6792300 | 51495000 | 9188693 |
| sp\|Q7KZF4\|SND1_HUMAN;tr\|B2R5U1\|I | 43 | 0 | 90937400 | 23458989 | 56565938 | 18983180 | 108176700 | 39066390 |
| sp\|P52732\|KIF11_HUMAN;tr\|B2RAM6\| | 43 | 0 | 62652408 | 11175000 | 53239209 | 9320800 | 168457610 | 9489800 |
| tr\|C1PHA2\|C1PHA2_HUMAN;tr\|M1V48 | 43 | 1 | 0 | 1293056 | 0 | 1062400 | 0 | 0 |
| sp\|P12270\|TPR_HUMAN;tr\|Q15624\|Q1 | 42 | 0 | 22054360 | 83693 | 14641420 | 0 | 23072000 | 1608480 |
| sp\|Q9BQG0\|MBB1A_HUMAN;sp\|Q9BQ | 42 | 0 | 14782000 | 343160 | 3779900 | 0 | 100699494 | 1050600 |
| sp\|Q5T4S7-3\|UBR4_HUMAN;sp\|Q5T4S7 | 42 | 0 | 5600200 | 0 | 3521960 | 518950 | 27864000 | 562960 |
| sp\|O75694-2\|NU155_HUMAN;tr\|B4DLT | 41 | 0 | 130305800 | 24210890 | 76356300 | 21939390 | 253052990 | 42336507 |
| sp\|P11717\|MPRI_HUMAN;tr\|Q59EZ3\|C | 41 | 0 | 24668000 | 79314 | 12890700 | 282960 | 5908100 | 133580 |
| sp\|P29144\|TPP2_HUMAN;tr\|Q5VZU9\|C | 41 | 0 | 24567900 | 3220800 | 15131000 | 2705400 | 106461130 | 7570720 |
| sp\|Q93008-1\|USP9X_HUMAN;sp\|Q930( | 41 | 0 | 17866000 | 2226619 | 13182630 | 2361200 | 60696490 | 2633440 |
| tr\|A0A024RD80\|A0A024RD80_HUMAN; | 40 | 0 | 356569620 | 168655300 | 569651500 | 184666500 | 671376600 | 240059000 |
| tr\|A8K8U1\|A8K8U1_HUMAN;sp\|Q86VP | 40 | 0 | 84462600 | 13931369 | 60075420 | 17472660 | 272799480 | 24726920 |
| sp\|Q709C8-3\|VP13C_HUMAN;sp\|Q709( | 40 | 0 | 42056300 | 1157274 | 9339710 | 139220 | 57476790 | 0 |
| sp\|Q15643\|TRIPB_HUMAN;tr\|A0A087W | 40 | 0 | 14119000 | 4376680 | 12172630 | 2777200 | 6966480 | 3323110 |
| sp\|O14980\|XPO1_HUMAN;tr\|B7ZB16\|E | 39 | 0 | 123485900 | 22168830 | 55852380 | 21393700 | 319223900 | 34266830 |
| tr\|K9JA46\|K9JA46_HUMAN;sp\|P07900\| | 39 | 0 | 103072290 | 62687048 | 170329110 | 60250938 | 154359300 | 68759300 |
| tr\|B3KMX0\|B3KMX0_HUMAN;tr\|A0A02 | 39 | 0 | 48796860 | 8956466 | 31155300 | 7117600 | 191082520 | 16143259 |
| sp\|P53621\|COPA_HUMAN;sp\|P53621-2 | 39 | 0 | 28630320 | 2630800 | 14939928 | 3310000 | 48105000 | 3961140 |
| tr\|Q86VX4\|Q86VX4_HUMAN;tr\|B0AZQ | 39 | 0 | 20131000 | 5461700 | 10641000 | 2433400 | 65723100 | 3984210 |
| sp\|P52701\|MSH6_HUMAN;sp\|P52701-3 | 39 | 0 | 19806000 | 3404098 | 4545850 | 1987200 | 78852760 | 5049900 |
| tr\|A8K5I0\|A8K5I0_HUMAN;sp\|P08107\| | 38 | 0 | 320189900 | 197561300 | 430216600 | 183972200 | 162203300 | 93576300 |

| | | | | | | | | |
|---|---|---|---|---|---|---|---|---|
| tr\|Q53HJ4\|Q53HJ4_HUMAN;tr\|B2R7C5 | 38 | 0 | 52707500 | 11337673 | 36234950 | 6738050 | 159714010 | 18625730 |
| tr\|G1UI16\|G1UI16_HUMAN;sp\|Q29RF7 | 38 | 0 | 20000420 | 3064900 | 11327150 | 3150300 | 79761013 | 3122000 |
| sp\|Q92621\|NU205_HUMAN;tr\|B4DE72\| | 38 | 0 | 19255430 | 7545191 | 25398000 | 3905431 | 104344800 | 8208210 |
| tr\|A0A024RAM4\|A0A024RAM4_HUMAN | 38 | 0 | 9082000 | 1314600 | 6973230 | 671730 | 69037690 | 4971550 |
| sp\|Q13813-3\|SPTN1_HUMAN;sp\|Q1383 | 38 | 0 | 4654800 | 0 | 1946500 | 0 | 477250 | 530370 |
| sp\|P07197\|NFM_HUMAN;tr\|E7ESP9\|E7 | 37 | 0 | 166559000 | 12007200 | 80508000 | 6580200 | 12667000 | 1002220 |
| tr\|V9HW96\|V9HW96_HUMAN;sp\|P783 | 37 | 0 | 139182147 | 60569550 | 355170020 | 73806130 | 433010100 | 111062300 |
| sp\|P49588\|SYAC_HUMAN;sp\|P49588-2 | 37 | 0 | 57332700 | 16672010 | 35006377 | 13413310 | 148381382 | 36538470 |
| sp\|Q99460\|PSMD1_HUMAN;sp\|Q9946( | 37 | 0 | 56263670 | 14620000 | 26611690 | 13795020 | 135785910 | 25670180 |
| tr\|A0A024RCN6\|A0A024RCN6_HUMAN | 37 | 0 | 40397840 | 8273500 | 29976177 | 9193234 | 144519130 | 12525000 |
| sp\|P50851\|LRBA_HUMAN | 37 | 0 | 9244800 | 1435980 | 7312770 | 2030400 | 42369000 | 2247500 |
| sp\|P50851-2\|LRBA_HUMAN;tr\|E9PEM5 | 37 | 0.006311 | 454740 | 0 | 449460 | 0 | 1742100 | 0 |
| tr\|A0A024R1N4\|A0A024R1N4_HUMAN; | 36 | 0 | 127645502 | 70031460 | 205347383 | 45201420 | 284589200 | 50559300 |
| tr\|A3RJH1\|A3RJH1_HUMAN;sp\|Q92499 | 36 | 0 | 78446370 | 38155971 | 140453070 | 29992000 | 124270320 | 31241060 |
| sp\|O95613-2\|PCNT_HUMAN;sp\|O9561 | 36 | 0 | 15200000 | 0 | 6738100 | 0 | 6929300 | 0 |
| sp\|A6NHR9-2\|SMHD1_HUMAN;sp\|A6N | 36 | 0 | 8115190 | 792119 | 5496405 | 892984 | 54166610 | 2026700 |
| sp\|P35658-2\|NU214_HUMAN;sp\|P3565 | 36 | 0 | 7692300 | 1375600 | 9707900 | 1298700 | 88374039 | 4232300 |
| tr\|V9HWE1\|V9HWE1_HUMAN;sp\|P086 | 35 | 0 | 103134100 | 8396900 | 78299070 | 3145630 | 4966950 | 58616 |
| tr\|V9HW37\|V9HW37_HUMAN;sp\|P486 | 35 | 0 | 78039400 | 19427200 | 136065560 | 29672470 | 225254670 | 44264450 |
| sp\|Q14683\|SMC1A_HUMAN;tr\|G8JLG1 | 35 | 0 | 42202000 | 4566723 | 11185560 | 9892510 | 90684300 | 12356780 |
| sp\|Q15029-2\|U5S1_HUMAN;tr\|Q6IBM8 | 35 | 0 | 26614000 | 4097700 | 17405880 | 2264700 | 97873190 | 7228700 |
| sp\|Q02224-3\|CENPE_HUMAN;tr\|A0A08 | 35 | 0 | 16080000 | 0 | 4829500 | 0 | 12052000 | 218510 |
| tr\|Q5CAQ5\|Q5CAQ5_HUMAN;tr\|V9HW | 35 | 0 | 10475410 | 7338680 | 8938820 | 4415490 | 14888040 | 11454300 |
| sp\|Q8N3C0\|ASCC3_HUMAN;tr\|B4DR60 | 35 | 0 | 6667300 | 0 | 4974760 | 394120 | 31978100 | 0 |
| sp\|P50990\|TCPQ_HUMAN;sp\|P50990-2 | 34 | 0 | 123239940 | 30712900 | 219449350 | 47037240 | 321011200 | 63834600 |
| tr\|A0A024R4F1\|A0A024R4F1_HUMAN;s | 34 | 0 | 76416100 | 55742200 | 58238500 | 36283800 | 54468700 | 120410000 |
| sp\|P22314-2\|UBA1_HUMAN;tr\|A0A024 | 34 | 0 | 56543704 | 26457400 | 32519560 | 17250300 | 106883950 | 53134900 |
| tr\|V9HW22\|V9HW22_HUMAN;sp\|P111 | 34 | 0 | 50618760 | 25164960 | 56264280 | 26229360 | 66583800 | 24357400 |
| tr\|Q4W4Y1\|Q4W4Y1_HUMAN | 34 | 0 | 37270500 | 10449000 | 31316300 | 10606831 | 113633100 | 21493080 |
| sp\|Q6P2E9\|EDC4_HUMAN;sp\|Q6P2E9-3 | 34 | 0 | 34733000 | 3964500 | 19300000 | 9167000 | 45857000 | 2726022 |
| tr\|A8K6X3\|A8K6X3_HUMAN;sp\|Q7L014 | 34 | 0 | 31076780 | 3300800 | 21547257 | 2402908 | 102114600 | 3801022 |
| sp\|Q9Y5B9\|SP16H_HUMAN;tr\|Q0VGA3 | 34 | 0 | 29446918 | 17617670 | 19926500 | 18547630 | 199456150 | 13495804 |
| tr\|Q53HS0\|Q53HS0_HUMAN;sp\|P4789 | 34 | 0 | 28004400 | 9607855 | 45289455 | 16156490 | 117408940 | 18169850 |
| sp\|Q14203-3\|DCTN1_HUMAN;sp\|Q142 | 34 | 0 | 20991000 | 3781417 | 14370024 | 8994400 | 45904270 | 6210100 |
| tr\|A0A024R7L5\|A0A024R7L5_HUMAN;s | 34 | 0 | 16979100 | 4319307 | 17861400 | 3265490 | 65170700 | 6116477 |
| tr\|B7ZMF2\|B7ZMF2_HUMAN;sp\|Q9NV | 34 | 0 | 12003410 | 353930 | 4011100 | 336800 | 30015000 | 204240 |
| sp\|P55196\|AFAD_HUMAN;tr\|J3KN01\|J | 34 | 0 | 11389789 | 1102255 | 8922007 | 2141576 | 53719756 | 1846127 |
| sp\|Q13428-8\|TCOF_HUMAN;sp\|Q1342 | 34 | 0 | 1831200 | 675600 | 1251000 | 455800 | 35948480 | 3553195 |
| sp\|Q8WUM4\|PDC6I_HUMAN;sp\|Q8WU | 34 | 1 | 1078600 | 0 | 0 | 0 | 2643400 | 0 |
| tr\|B3KX11\|B3KX11_HUMAN;sp\|P4936 | 33 | 0 | 156225280 | 38147550 | 220600460 | 50524760 | 309240600 | 58841400 |
| tr\|A0A024R1X8\|A0A024R1X8_HUMAN;s | 33 | 0 | 143388000 | 54668000 | 61797000 | 66071000 | 71139000 | 51665700 |
| sp\|P13010\|XRCC5_HUMAN;tr\|Q53T09\| | 33 | 0 | 117265320 | 52825270 | 164008680 | 43670240 | 277893900 | 63528000 |
| sp\|Q00839\|HNRPU_HUMAN;tr\|B3KX72 | 33 | 0 | 115841000 | 25776120 | 62048670 | 11747480 | 442974100 | 42853090 |
| sp\|Q13263\|TIF1B_HUMAN;tr\|B2R8R5\|E | 33 | 0 | 115522100 | 31030310 | 78792470 | 30337340 | 330238110 | 38371050 |
| tr\|X5D2J9\|X5D2J9_HUMAN;sp\|P78347- | 33 | 0 | 44949900 | 11211000 | 29074180 | 8629084 | 141347846 | 17458325 |
| tr\|A8K492\|A8K492_HUMAN;sp\|P56192 | 33 | 0 | 42469970 | 6048800 | 20548500 | 3788800 | 193133800 | 15033770 |
| sp\|Q9NR30\|DDX21_HUMAN;sp\|Q9NR3 | 33 | 0 | 25568900 | 6999690 | 20607949 | 3530790 | 144546294 | 8576110 |
| tr\|B1AHB0\|B1AHB0_HUMAN;sp\|P3399 | 33 | 0 | 16515200 | 3842700 | 28110300 | 6956900 | 96884200 | 10774490 |
| sp\|Q14697-2\|GANAB_HUMAN;tr\|V9HV | 33 | 0 | 10509540 | 4485705 | 5894186 | 3582156 | 16873118 | 14941500 |
| sp\|P52948-6\|NUP98_HUMAN;sp\|P5294 | 33 | 0 | 6255600 | 1297400 | 4766674 | 855920 | 59205000 | 2932300 |
| sp\|Q14974\|IMB1_HUMAN;tr\|B2RBR9\|E | 32 | 0 | 149174685 | 43261170 | 91952280 | 39186695 | 443427860 | 54341300 |
| tr\|Q53HV2\|Q53HV2_HUMAN;sp\|Q9983 | 32 | 0 | 74587336 | 17170950 | 159322140 | 28069400 | 269826130 | 36083960 |
| tr\|B5BTY4\|B5BTY4_HUMAN;sp\|O00571 | 32 | 0 | 52813945 | 16297316 | 69045318 | 16522382 | 139271390 | 13677920 |
| sp\|Q14566\|MCM6_HUMAN;tr\|Q4ZG57 | 32 | 0 | 52051440 | 13118070 | 34608800 | 7422650 | 164866400 | 17981980 |
| tr\|F4ZW66\|F4ZW66_HUMAN;sp\|Q1290 | 32 | 0 | 33547700 | 10759045 | 44180270 | 12184570 | 271581000 | 22848510 |
| tr\|Q53GX7\|Q53GX7_HUMAN;sp\|P2663 | 32 | 0 | 32303966 | 10808352 | 74833300 | 10103377 | 165069500 | 24032290 |
| tr\|A0A024RDG1\|A0A024RDG1_HUMAN | 32 | 0 | 22802000 | 6652700 | 21265000 | 5486800 | 180654160 | 15507003 |
| tr\|H3BPE1\|H3BPE1_HUMAN;tr\|H3BQK9 | 32 | 0 | 2568700 | 0 | 1349700 | 0 | 21004000 | 237860 |
| sp\|P55196-3\|AFAD_HUMAN;tr\|H0Y8U8 | 32 | 0 | 737200 | 284240 | 534200 | 0 | 0 | 206460 |
| sp\|Q9UPN3-3\|MACF1_HUMAN;sp\|Q9U | 32 | 1 | 0 | 0 | 0 | 0 | 1045200 | 0 |
| tr\|B3KMS0\|B3KMS0_HUMAN;sp\|Q1502 | 31 | 0 | 13254000 | 1478500 | 1830000 | 1839600 | 53191000 | 2758003 |
| sp\|Q15075\|EEA1_HUMAN;tr\|A8K7J3\|A | 31 | 0 | 9669600 | 520780 | 2526300 | 733800 | 38365000 | 1739660 |
| tr\|V9HWF4\|V9HWF4_HUMAN;sp\|P005 | 30 | 0 | 511032500 | 203926300 | 860284200 | 151211700 | 1453560500 | 165358900 |
| sp\|P17987\|TCPA_HUMAN;tr\|E7ERF2\|E7 | 30 | 0 | 173151540 | 44137990 | 322780200 | 55538910 | 385475800 | 74688700 |
| sp\|P50991\|TCPD_HUMAN;tr\|A8K3C3\|A | 30 | 0 | 133179186 | 39256280 | 212914000 | 48074210 | 328119560 | 61018400 |
| tr\|A8K8N7\|A8K8N7_HUMAN;tr\|A8K9T9 | 30 | 0 | 33313620 | 5679400 | 13202000 | 8633170 | 142567660 | 12486504 |
| sp\|P54136\|SYRC_HUMAN;sp\|P54136-2 | 30 | 0 | 31752063 | 7973707 | 53852160 | 9353820 | 108638270 | 9450229 |
| sp\|P06737-2\|PYGL_HUMAN;sp\|P06737 | 30 | 0 | 27910600 | 7407679 | 20592000 | 8485158 | 38098490 | 9340913 |
| sp\|Q14C86-5\|GAPD1_HUMAN;tr\|A0A0 | 30 | 0 | 23150000 | 2828660 | 8766490 | 5609600 | 54645120 | 4975600 |
| tr\|B2ZZ90\|B2ZZ90_HUMAN;sp\|Q13085 | 30 | 0 | 5056800 | 422740 | 3496600 | 1135600 | 29415000 | 1233200 |
| tr\|A0A0A0MSW3\|A0A0A0MSW3_HUMA | 30 | 1 | 0 | 0 | 0 | 0 | 0 | 0 |
| sp\|P29508\|SPB3_HUMAN;tr\|Q5K684\|Q | 29 | 0 | 127713440 | 3338120 | 7262210 | 11266630 | 26023100 | 5278230 |
| tr\|V9HWN7\|V9HWN7_HUMAN;sp\|P04( | 29 | 0 | 72576270 | 16914720 | 66796400 | 20708650 | 59198620 | 38196700 |
| tr\|B2RBA6\|B2RBA6_HUMAN;sp\|P3399 | 29 | 0 | 39416900 | 10847000 | 66738671 | 7923190 | 150251570 | 19636570 |
| sp\|Q8TEX9\|IPO4_HUMAN;sp\|Q8TEX9-2 | 29 | 0 | 34357750 | 4569000 | 16109060 | 4220600 | 55230310 | 5128380 |
| sp\|P52272-2\|HNRPM_HUMAN;sp\|P522 | 29 | 0 | 28126063 | 12403570 | 36501241 | 9158744 | 176694300 | 24996550 |

| | | | | | | | | |
|---|---|---|---|---|---|---|---|---|
| tr\|A0A024R4A0\|A0A024R4A0_HUMAN; | 29 | 0 | 23841350 | 14286110 | 19939360 | 9204550 | 111871570 | 31231300 |
| sp\|P49736\|MCM2_HUMAN;tr\|B3KXZ4\| | 29 | 0 | 20255390 | 3019600 | 8352280 | 1694700 | 40296200 | 7868160 |
| tr\|A8K6V3\|A8K6V3_HUMAN;sp\|Q1539 | 29 | 0 | 16257487 | 2909469 | 9048200 | 574671 | 81417271 | 5294900 |
| tr\|A0A024QZW7\|A0A024QZW7_HUMAI | 29 | 0 | 7598700 | 440950 | 2857200 | 931877 | 43642000 | 2329293 |
| tr\|Q8N516\|Q8N516_HUMAN;sp\|O9516 | 29 | 0 | 7587200 | 1758260 | 6649600 | 2856300 | 76912990 | 2448000 |
| tr\|B2R9K8\|B2R9K8_HUMAN;tr\|A0A024 | 28 | 0 | 115574360 | 32785690 | 198874190 | 39594230 | 301670300 | 61973500 |
| tr\|Q53YD7\|Q53YD7_HUMAN;sp\|P2664 | 28 | 0 | 81412070 | 44434960 | 187532970 | 42321890 | 334649800 | 86498700 |
| tr\|A4D210\|A4D210_HUMAN;tr\|A0A024 | 28 | 0 | 43240010 | 8116100 | 21630840 | 5001431 | 78415480 | 11788035 |
| sp\|P49915\|GUAA_HUMAN;sp\|P49915-2 | 28 | 0 | 27120780 | 6990800 | 35125980 | 7195078 | 88980880 | 14390660 |
| sp\|P31939-2\|PUR9_HUMAN;tr\|V9HWH | 28 | 0 | 18410847 | 7037687 | 23087000 | 6378875 | 11801000 | 5402750 |
| sp\|P43246\|MSH2_HUMAN;sp\|P43246-2 | 28 | 0 | 16325490 | 2306700 | 8846861 | 843629 | 64453400 | 6720500 |
| tr\|A0A0A0MRM8\|A0A0A0MRM8_HUMA | 28 | 0 | 9136700 | 1115375 | 6135160 | 1033200 | 53294000 | 2821820 |
| tr\|B2ZZ89\|B2ZZ89_HUMAN;sp\|Q01082 | 28 | 0 | 1813600 | 123400 | 3425780 | 0 | 0 | 175330 |
| sp\|Q96N67-4\|DOCK7_HUMAN;sp\|Q96N | 28 | 0 | 876640 | 144180 | 5739950 | 0 | 23163500 | 1064700 |
| tr\|Q6IPT9\|Q6IPT9_HUMAN;tr\|Q6IPS9\| | 27 | 0 | 1339230500 | 536482100 | 2209603000 | 580905100 | 2887259000 | 694210000 |
| sp\|P43243\|MATR3_HUMAN;tr\|A8MXP9 | 27 | 0 | 98480324 | 21118980 | 78085870 | 22386855 | 329156700 | 47107430 |
| tr\|J3KTA4\|J3KTA4_HUMAN;sp\|P17844\| | 27 | 0 | 69398000 | 21278260 | 114242480 | 20378186 | 185286450 | 16514330 |
| sp\|O95373\|IPO7_HUMAN;tr\|B3KQG6\|E | 27 | 0 | 68718250 | 12421000 | 37203497 | 9216800 | 123750000 | 14553220 |
| sp\|Q9Y230\|RUVB2_HUMAN;sp\|Q9Y230 | 27 | 0 | 64999531 | 25131400 | 119850920 | 25552217 | 253747680 | 46501510 |
| sp\|P42166\|LAP2A_HUMAN;sp\|P42167- | 27 | 0 | 53432700 | 17236810 | 121929870 | 13066980 | 266613290 | 28090937 |
| tr\|B3KTJ9\|B3KTJ9_HUMAN;sp\|Q8N163 | 27 | 0 | 27945000 | 6048440 | 18166600 | 5113800 | 95722996 | 7620770 |
| tr\|V9HWB4\|V9HWB4_HUMAN;sp\|P110 | 27 | 0 | 17328900 | 6285170 | 10311090 | 5996820 | 28939200 | 10879400 |
| sp\|Q08J23\|NSUN2_HUMAN;sp\|Q08J23 | 27 | 0 | 14199480 | 2135082 | 7844010 | 1367200 | 61438400 | 2170100 |
| sp\|O43143\|DHX15_HUMAN;tr\|B4E0S6\| | 27 | 0 | 13857700 | 5265720 | 23454340 | 5924090 | 25614500 | 7398660 |
| sp\|P42285\|SK2L2_HUMAN;tr\|A8K6I4\|A | 27 | 0 | 12059000 | 2438080 | 10623340 | 3226500 | 51328350 | 4850900 |
| sp\|O00203-3\|AP3B1_HUMAN;sp\|O002 | 27 | 0 | 9380900 | 526830 | 6136940 | 2025190 | 76888810 | 3765628 |
| sp\|Q8NI27\|THOC2_HUMAN;tr\|B4DKZ6 | 27 | 0 | 7584240 | 1352890 | 4444330 | 1413165 | 37353160 | 894660 |
| tr\|B4DM67\|B4DM67_HUMAN | 27 | 1 | 0 | 0 | 0 | 0 | 1763700 | 0 |
| tr\|V9HWB9\|V9HWB9_HUMAN;sp\|P003 | 26 | 0 | 165579400 | 159731100 | 229950000 | 136657700 | 480148300 | 182728500 |
| sp\|Q02413\|DSG1_HUMAN;sp\|Q02413-2 | 26 | 0 | 65225000 | 44126000 | 45136200 | 57818000 | 44251000 | 43756600 |
| sp\|Q16658\|FSCN1_HUMAN;tr\|B3KTA3\| | 26 | 0 | 61479197 | 20595904 | 99073836 | 21997216 | 210441800 | 40301560 |
| sp\|Q92945\|FUBP2_HUMAN;tr\|A0A087V | 26 | 0 | 36108600 | 77410027 | 101472974 | 102664530 | 63375000 | 68464700 |
| sp\|P63010-3\|AP2B1_HUMAN;tr\|H0UID4 | 26 | 0 | 27133000 | 6724400 | 17663960 | 5375600 | 77681000 | 4701400 |
| sp\|Q9BPX3\|CND3_HUMAN;tr\|Q6NUR1 | 26 | 0 | 25444000 | 2706100 | 8266000 | 2067000 | 57593933 | 2277600 |
| tr\|A0A087WZ13\|A0A087WZ13_HUMAN | 26 | 0 | 25358210 | 11652510 | 61693000 | 9062020 | 92170450 | 21640710 |
| sp\|P14868\|SYDC_HUMAN;tr\|D3DP78\|D | 26 | 0 | 24952500 | 6796000 | 28038000 | 6174190 | 91753080 | 10383430 |
| sp\|Q9UPN6\|SCAF8_HUMAN;tr\|B7Z876 | 26 | 0 | 24618550 | 3441100 | 9982220 | 3313200 | 60413750 | 1792570 |
| tr\|Q86VG2\|Q86VG2_HUMAN;sp\|P2324 | 26 | 0 | 23718219 | 13104810 | 29646488 | 8287900 | 281677930 | 26808100 |
| tr\|A8K607\|A8K607_HUMAN;sp\|Q9UIA9 | 26 | 0 | 16223000 | 2650000 | 9454710 | 217736 | 24324000 | 2618600 |
| tr\|V9HW80\|V9HW80_HUMAN;sp\|P550 | 26 | 0 | 12784000 | 2804100 | 3806400 | 1121300 | 16701500 | 5744730 |
| sp\|O94979-3\|SC31A_HUMAN;sp\|O9497 | 26 | 0 | 10756000 | 1924600 | 3546100 | 1217217 | 34940900 | 2962798 |
| tr\|E9PLK3\|E9PLK3_HUMAN;tr\|B7Z899\|I | 26 | 0 | 9832570 | 2748400 | 4154000 | 748810 | 850910 | 3596600 |
| tr\|Q5K634\|Q5K634_HUMAN;tr\|Q86W05 | 26 | 0 | 6598465 | 0 | 0 | 473720 | 2583800 | 0 |
| tr\|A0A087X0H9\|A0A087X0H9_HUMAN; | 26 | 0 | 5520400 | 5055300 | 21419710 | 4214200 | 59591010 | 21366420 |
| tr\|Q59GJ0\|Q59GJ0_HUMAN;sp\|O43432 | 26 | 0 | 3904200 | 986640 | 3522300 | 697950 | 19723000 | 598790 |
| tr\|B4DP06\|B4DP06_HUMAN;tr\|H7C1S2 | 26 | 0 | 2870200 | 1354200 | 5063400 | 801030 | 1935900 | 957800 |
| tr\|B3KWD0\|B3KWD0_HUMAN | 26 | 0 | 536350 | 0 | 0 | 0 | 2370600 | 0 |
| tr\|B3KPS3\|B3KPS3_HUMAN;sp\|P68363 | 25 | 0 | 852260000 | 339838100 | 1722802500 | 360276100 | 3385555000 | 568599000 |
| tr\|Q8IZ29\|Q8IZ29_HUMAN;sp\|P68371\| | 25 | 0 | 505369370 | 151583900 | 1007816200 | 196518000 | 1894110000 | 292897600 |
| tr\|A8K7F6\|A8K7F6_HUMAN;sp\|P60842 | 25 | 0 | 254899650 | 100679450 | 411240700 | 95148600 | 722942500 | 139249100 |
| sp\|Q92841\|DDX17_HUMAN;tr\|H3BLZ8\| | 25 | 0 | 27830783 | 9969240 | 50080118 | 7686811 | 143448530 | 14114590 |
| sp\|Q9Y678\|COPG1_HUMAN;tr\|B3KW21 | 25 | 0 | 26147000 | 3949200 | 13267870 | 3215380 | 76485500 | 7092810 |
| tr\|V9HW65\|V9HW65_HUMAN;tr\|A0A0 | 25 | 0 | 25402500 | 13739500 | 10626600 | 13773600 | 41156800 | 22060000 |
| sp\|Q13200\|PSMD2_HUMAN;tr\|Q59EG8 | 25 | 0 | 20719000 | 5018163 | 12559010 | 5250680 | 77079750 | 16550460 |
| sp\|Q71U36-2\|TBA1A_HUMAN;sp\|Q71U | 25 | 0 | 15757890 | 4436988 | 37816000 | 2552310 | 35931390 | 7455804 |
| sp\|Q9H3S7\|PTN23_HUMAN;tr\|B4DJ12\| | 25 | 0 | 14969000 | 805880 | 4281800 | 1288700 | 39603410 | 960020 |
| sp\|Q9Y262\|EIF3L_HUMAN;tr\|B0QY89\|E | 25 | 0 | 14479099 | 1834700 | 27937940 | 2051720 | 38446000 | 5466551 |
| sp\|Q96QK1\|VPS35_HUMAN;tr\|Q53FR4 | 25 | 0 | 12423210 | 5104870 | 28980132 | 5041126 | 52272910 | 8906291 |
| tr\|A0A024R4F4\|A0A024R4F4_HUMAN;s | 25 | 0 | 10500000 | 723030 | 8228500 | 411740 | 36654000 | 704920 |
| sp\|P34932\|HSP74_HUMAN;tr\|V9HW33 | 25 | 0 | 10096000 | 2625400 | 5326600 | 2512993 | 4076700 | 6741090 |
| tr\|K7EIG1\|K7EIG1_HUMAN;sp\|O75153\| | 25 | 0 | 9287300 | 685700 | 4576200 | 1308700 | 18490090 | 1126600 |
| sp\|Q9UPU5\|UBP24_HUMAN | 25 | 0 | 6638600 | 182400 | 4030600 | 433720 | 18350000 | 602200 |
| sp\|Q7LBC6\|KDM3B_HUMAN;sp\|Q7LBC | 25 | 0 | 5956180 | 1054701 | 2931300 | 606990 | 44391930 | 4116782 |
| sp\|O95239\|KIF4A_HUMAN;tr\|Q59HG1\| | 25 | 0 | 5698000 | 228260 | 4239970 | 1025200 | 34423000 | 989580 |
| sp\|Q9H0A0\|NAT10_HUMAN;sp\|Q9H0A | 25 | 0 | 3689900 | 114400 | 2867500 | 185680 | 17843600 | 341920 |
| tr\|Q53GA7\|Q53GA7_HUMAN;sp\|Q9BQ | 25 | 0 | 2303900 | 1244100 | 6387500 | 422190 | 10278000 | 1235700 |
| tr\|V9HWD9\|V9HWD9_HUMAN;tr\|Q53E | 25 | 0 | 1247720 | 1836800 | 614900 | 680060 | 0 | 4857030 |
| tr\|B3KUD7\|B3KUD7_HUMAN | 25 | 1 | 0 | 0 | 0 | 0 | 1271000 | 0 |
| sp\|Q5T8P6\|RBM26_HUMAN;sp\|Q5T8P6 | 25 | 0 | 0 | 0 | 344010 | 304360 | 2539500 | 1479700 |
| sp\|P61978-3\|HNRPK_HUMAN;tr\|B4DU0 | 24 | 0 | 193875310 | 55376820 | 265959100 | 61099050 | 677014000 | 111298400 |
| tr\|B5BUB1\|B5BUB1_HUMAN;sp\|Q9Y26 | 24 | 0 | 162275870 | 57464510 | 248808930 | 47212020 | 304973800 | 52846300 |
| tr\|B4DDF7\|B4DDF7_HUMAN;tr\|A8K7B7 | 24 | 0 | 59449090 | 11997355 | 108627310 | 15776780 | 151149920 | 23674100 |
| tr\|Q6NTA2\|Q6NTA2_HUMAN;sp\|P148 | 24 | 0 | 57483610 | 10801610 | 94082850 | 14688080 | 224096300 | 18008240 |
| tr\|Q58EY4\|Q58EY4_HUMAN;sp\|Q92922 | 24 | 0 | 30907590 | 1238700 | 10456350 | 695613 | 30468180 | 1675223 |
| sp\|O00231\|PSD11_HUMAN;sp\|O00231 | 24 | 0 | 27674180 | 4701250 | 36216940 | 7587350 | 72897630 | 25652220 |

| | | | | | | | | |
|---|---|---|---|---|---|---|---|---|
| tr\|A0A024RCR6\|A0A024RCR6_HUMAN; | 24 | 0 | 27411110 | 4025700 | 12020000 | 7107000 | 26232000 | 5647000 |
| sp\|Q96P70\|IPO9_HUMAN | 24 | 0 | 24438000 | 5610040 | 13915342 | 5553700 | 64762000 | 7291500 |
| sp\|P53618\|COPB_HUMAN;tr\|E9PP73\|E | 24 | 0 | 23541210 | 2718800 | 11390510 | 3172600 | 43796900 | 4262120 |
| sp\|P27694\|RFA1_HUMAN;tr\|I3L4R8\|I3 | 24 | 0 | 18796430 | 11422900 | 38142000 | 6264700 | 54194950 | 4958200 |
| tr\|A0A024R6M3\|A0A024R6M3_HUMAN | 24 | 0 | 18319668 | 3785900 | 17026800 | 3329240 | 64693600 | 1844200 |
| sp\|Q9BXJ9\|NAA15_HUMAN;tr\|B2RBE5 | 24 | 0 | 17516950 | 1888900 | 8128450 | 1712500 | 25228590 | 3374555 |
| sp\|P08243-2\|ASNS_HUMAN;sp\|P08243 | 24 | 0 | 16449490 | 3381358 | 25488020 | 3110560 | 102490450 | 17152290 |
| sp\|Q10567-2\|AP1B1_HUMAN;sp\|Q1056 | 24 | 0 | 15826000 | 3742500 | 12901000 | 3320500 | 40720000 | 4690000 |
| tr\|A8KA19\|A8KA19_HUMAN;sp\|O4359 | 24 | 0 | 14553000 | 2175150 | 7018900 | 2121900 | 56975480 | 5305090 |
| sp\|Q96RL7-4\|VP13A_HUMAN;sp\|Q96R | 24 | 0 | 14423000 | 0 | 3503610 | 0 | 1880320 | 0 |
| tr\|Q6IBN1\|Q6IBN1_HUMAN;sp\|P61978 | 24 | 1 | 10434000 | 2242100 | 25235000 | 0 | 0 | 0 |
| sp\|Q9UHB9\|SRP68_HUMAN;sp\|Q9UHB | 24 | 0 | 10151000 | 2116650 | 20073000 | 1845389 | 46548440 | 1029940 |
| sp\|Q01780-2\|EXOSX_HUMAN;sp\|Q017 | 24 | 0 | 8415253 | 997022 | 3448300 | 335560 | 47238510 | 6033780 |
| sp\|O95602\|RPA1_HUMAN;tr\|B7ZKR9\|E | 24 | 0 | 8217100 | 409280 | 2808000 | 404760 | 25575000 | 823060 |
| sp\|Q13045-2\|FLII_HUMAN;sp\|Q13045\| | 24 | 0 | 6601100 | 607300 | 3068200 | 582570 | 54116000 | 1273900 |
| sp\|O43390\|HNRPR_HUMAN;tr\|Q0VGD | 24 | 0 | 6488142 | 2310730 | 12500100 | 2376420 | 63769770 | 6298300 |
| sp\|O94906-2\|PRP6_HUMAN;sp\|O9490 | 24 | 0 | 4413100 | 603070 | 5109900 | 0 | 35110230 | 1520700 |
| sp\|O60610-2\|DIAP1_HUMAN;tr\|E9PHQ | 24 | 0 | 3525600 | 871990 | 936230 | 871880 | 26000000 | 1235400 |
| tr\|A0A024QZ63\|A0A024QZ63_HUMAN; | 24 | 0 | 2954000 | 548010 | 2929200 | 90051 | 19575000 | 689660 |
| tr\|A0A024QZN4\|A0A024QZN4_HUMAN | 24 | 0 | 933700 | 499810 | 660150 | 858860 | 0 | 2526390 |
| tr\|B2R959\|B2R959_HUMAN;tr\|B4DPK8 | 24 | 1 | 0 | 0 | 0 | 0 | 1168500 | 0 |
| tr\|B4DVK5\|B4DVK5_HUMAN | 24 | 0.000356 | 0 | 0 | 1075500 | 0 | 2055700 | 0 |
| tr\|D3DS63\|D3DS63_HUMAN;tr\|B3KTB3 | 24 | 1 | 0 | 0 | 0 | 0 | 0 | 0 |
| tr\|Q8IWP6\|Q8IWP6_HUMAN;tr\|B4DFH | 24 | 0.003325 | 0 | 192200 | 0 | 134800 | 0 | 696260 |
| tr\|A0A024RCM3\|A0A024RCM3_HUMAN | 23 | 0 | 143691440 | 63720590 | 285487080 | 56877130 | 793454700 | 102259800 |
| sp\|Q9BVA1\|TBB2B_HUMAN;tr\|A0A024 | 23 | 0 | 72112730 | 26658000 | 133817550 | 34232460 | 264509200 | 57605330 |
| sp\|Q14157\|UBP2L_HUMAN;sp\|Q14157 | 23 | 0 | 35122630 | 6232300 | 22382300 | 8189700 | 145858330 | 10513145 |
| sp\|P07384\|CAN1_HUMAN;tr\|A0A024R5 | 23 | 0 | 22340560 | 12635319 | 46234770 | 8979460 | 40701530 | 8911030 |
| sp\|P35606-2\|COPB2_HUMAN;sp\|P3560 | 23 | 0 | 17216670 | 3041328 | 11058080 | 2016890 | 33933440 | 2403472 |
| sp\|P45974-2\|UBP5_HUMAN;sp\|P45974 | 23 | 0 | 16367720 | 5278700 | 12363000 | 4521698 | 68831760 | 8062921 |
| sp\|P50570-2\|DYN2_HUMAN;sp\|P50570 | 23 | 0 | 15995420 | 4819200 | 14748470 | 4862700 | 86663740 | 9294000 |
| sp\|P17858\|PFKAL_HUMAN;sp\|P17858- | 23 | 0 | 13614970 | 4618070 | 29235540 | 3117440 | 56494470 | 8301575 |
| sp\|Q8N1F7\|NUP93_HUMAN;tr\|A8K897 | 23 | 0 | 11711780 | 1851700 | 21774000 | 3775800 | 58590600 | 3012910 |
| sp\|P51532-5\|SMCA4_HUMAN;sp\|P515 | 23 | 0 | 11166650 | 1259160 | 5009270 | 997980 | 35227690 | 1256800 |
| sp\|O00159-2\|MYO1C_HUMAN;tr\|F5H6 | 23 | 0 | 10436338 | 842630 | 3691480 | 531990 | 10025000 | 185230 |
| sp\|Q01813\|PFKAP_HUMAN;sp\|Q01813 | 23 | 0 | 8140100 | 2911958 | 18594910 | 3221480 | 54127030 | 4139960 |
| tr\|B2R8Z8\|B2R8Z8_HUMAN;sp\|O60506 | 23 | 0 | 7601260 | 2175800 | 11879661 | 742010 | 30652950 | 5102490 |
| tr\|B7ZLC9\|B7ZLC9_HUMAN;sp\|Q8TEQ6 | 23 | 0 | 7455850 | 605070 | 3799800 | 1254900 | 24361000 | 706268 |
| tr\|X5D2F4\|X5D2F4_HUMAN;sp\|Q7L576 | 23 | 0 | 7369300 | 586690 | 3552900 | 578010 | 25119000 | 1211100 |
| sp\|O00232\|PSD12_HUMAN;sp\|O00232 | 23 | 0 | 7215800 | 3703600 | 20664844 | 4092000 | 49511130 | 12079181 |
| tr\|B7ZLZ7\|B7ZLZ7_HUMAN;tr\|B3KMB1\| | 23 | 0 | 6355600 | 3041580 | 3800500 | 531010 | 34889300 | 2020900 |
| sp\|Q9UQ35\|SRRM2_HUMAN;tr\|O60382 | 23 | 0 | 4412500 | 0 | 2423800 | 547180 | 68284000 | 1526241 |
| sp\|Q14690\|RRP5_HUMAN;tr\|B4DH82\|E | 23 | 0 | 2664000 | 0 | 1670310 | 105280 | 15208000 | 0 |
| sp\|P27816-6\|MAP4_HUMAN;sp\|P27816 | 23 | 0 | 2269700 | 206459 | 989410 | 0 | 6444800 | 3657260 |
| sp\|Q13885\|TBB2A_HUMAN;tr\|B2R6L0\| | 23 | 1 | 767260 | 0 | 0 | 0 | 3502700 | 0 |
| tr\|Q8IUB0\|Q8IUB0_HUMAN | 23 | 0 | 711450 | 0 | 1876100 | 0 | 0 | 933400 |
| sp\|P50570-3\|DYN2_HUMAN;sp\|P50570 | 23 | 1 | 0 | 0 | 0 | 0 | 0 | 232030 |
| sp\|Q14157-4\|UBP2L_HUMAN;sp\|Q1415 | 23 | 1 | 0 | 0 | 0 | 312010 | 3878500 | 0 |
| tr\|B4DY32\|B4DY32_HUMAN | 23 | 0.002678 | 0 | 438520 | 0 | 393470 | 7754100 | 623260 |
| tr\|V9HVZ4\|V9HVZ4_HUMAN;sp\|P0440 | 22 | 0 | 357187000 | 420744000 | 413976100 | 341832000 | 902478000 | 414182000 |
| tr\|Q5JP53\|Q5JP53_HUMAN;tr\|Q5SU16 | 22 | 0 | 165984010 | 57581350 | 322979330 | 68880210 | 667659000 | 104927600 |
| sp\|O43175\|SERA_HUMAN;tr\|V9HW79\| | 22 | 0 | 161911760 | 65297380 | 295976000 | 60087880 | 747130900 | 115705400 |
| sp\|P23526\|SAHH_HUMAN;sp\|P23526-2 | 22 | 0 | 52093660 | 21997460 | 136209090 | 34419920 | 237532890 | 41088100 |
| sp\|P17812\|PYRG1_HUMAN;tr\|B4E1E0\| | 22 | 0 | 33230600 | 13093550 | 57879204 | 9627439 | 142521890 | 14758710 |
| tr\|A0A024R718\|A0A024R718_HUMAN;s | 22 | 0 | 25367900 | 4533900 | 53198039 | 6653510 | 72689000 | 12286640 |
| sp\|Q02790\|FKBP4_HUMAN;tr\|B2R9U2\| | 22 | 0 | 20015310 | 5926372 | 36074970 | 6029791 | 93222730 | 11812113 |
| sp\|Q9BXP5-4\|SRRT_HUMAN;sp\|Q9BXP | 22 | 0 | 19325000 | 4824600 | 11227000 | 1609000 | 40739639 | 7146040 |
| sp\|P09960\|LKHA4_HUMAN;sp\|P09960- | 22 | 0 | 15382000 | 8299643 | 42347928 | 6809549 | 77306240 | 8494586 |
| sp\|Q9H9A6\|LRC40_HUMAN | 22 | 0 | 14844420 | 3418100 | 34405050 | 704870 | 57830400 | 1613000 |
| tr\|B4DSH1\|B4DSH1_HUMAN;tr\|B3KY60 | 22 | 0 | 12281000 | 1770600 | 5906540 | 665340 | 52358540 | 2249500 |
| sp\|Q93009\|UBP7_HUMAN;sp\|Q93009-3 | 22 | 0 | 11469000 | 1563300 | 3337900 | 0 | 12282400 | 1870100 |
| tr\|B7Z6F7\|B7Z6F7_HUMAN;tr\|A0A024R | 22 | 0 | 11378000 | 1054700 | 2623226 | 1755600 | 36202040 | 1686700 |
| tr\|H0YM23\|H0YM23_HUMAN;sp\|O7517 | 22 | 0 | 10808700 | 1584055 | 7144200 | 1324600 | 40025910 | 713880 |
| tr\|A8QI98\|A8QI98_HUMAN;sp\|Q9Y2L1 | 22 | 0 | 10254000 | 1576700 | 5213000 | 1140700 | 50051200 | 4804800 |
| sp\|Q8WUM0\|NU133_HUMAN;tr\|B4E20 | 22 | 0 | 7140800 | 652520 | 4286700 | 219410 | 39848000 | 2327000 |
| tr\|E9PD53\|E9PD53_HUMAN;tr\|B3KXX5 | 22 | 0 | 6891600 | 1105800 | 1511900 | 940860 | 12564000 | 1464900 |
| sp\|Q13620-1\|CUL4B_HUMAN;tr\|K4DI93 | 22 | 0 | 5353800 | 2002310 | 4845600 | 791780 | 22119165 | 1621310 |
| sp\|P35573\|GDE_HUMAN;sp\|P35573-2\| | 22 | 0 | 4119100 | 590480 | 2700600 | 658130 | 20647000 | 1953700 |
| sp\|P54577\|SYYC_HUMAN | 22 | 0 | 2186510 | 0 | 1384400 | 782296 | 402850 | 6398900 |
| tr\|I3L2B0\|I3L2B0_HUMAN;tr\|I3L318\|I3 | 22 | 0.006554 | 830020 | 292770 | 655130 | 0 | 1694000 | 0 |
| tr\|Q5U077\|Q5U077_HUMAN;sp\|P0719 | 21 | 0 | 126152800 | 131659600 | 242003300 | 92546500 | 282464900 | 161244100 |
| sp\|Q7Z3B4-3\|NUP54_HUMAN;sp\|Q7Z3 | 21 | 0 | 53217590 | 20860000 | 145862257 | 16949530 | 110534930 | 9989200 |
| sp\|P23396\|RS3_HUMAN;tr\|Q53G83\|Q5 | 21 | 0 | 49880700 | 39915100 | 103964700 | 26372300 | 488561900 | 60387600 |
| tr\|A0A024RB85\|A0A024RB85_HUMAN;s | 21 | 0 | 47083590 | 20916400 | 83058000 | 15147300 | 198369800 | 38177400 |
| tr\|E9KL35\|E9KL35_HUMAN;sp\|P63244\| | 21 | 0 | 21664550 | 18059900 | 35566760 | 11617490 | 48769010 | 19191870 |

| | | | | | | | | | |
|---|---|---|---|---|---|---|---|---|---|
| sp\|P42566\|EPS15_HUMAN;tr\|Q7Z5V0\| | 21 | 0 | 15915000 | 1922200 | 8894000 | 4364400 | 11991000 | 5403750 |
| sp\|P35998\|PRS7_HUMAN;tr\|Q75L23\|Q | 21 | 0 | 12279020 | 5981100 | 17730605 | 5409500 | 51363789 | 11001100 |
| tr\|Q6IBR0\|Q6IBR0_HUMAN;sp\|P04843\| | 21 | 0 | 11907000 | 2681500 | 20249000 | 1077600 | 5659700 | 0 |
| tr\|B7Z5S9\|B7Z5S9_HUMAN;sp\|O94973\| | 21 | 0 | 11830730 | 964650 | 8054400 | 1363300 | 25557000 | 1735200 |
| sp\|Q7Z3K3-5\|POGZ_HUMAN;sp\|Q7Z3K | 21 | 0 | 11364000 | 1294500 | 4062347 | 754690 | 45122000 | 1920800 |
| sp\|P78344\|IF4G2_HUMAN;sp\|P78344-2 | 21 | 0 | 10327000 | 1402700 | 7944100 | 914740 | 29224000 | 1889400 |
| tr\|A0A024R8A7\|A0A024R8A7_HUMAN;\| | 21 | 0 | 9895900 | 2018496 | 9334400 | 2041200 | 41586135 | 979720 |
| tr\|Q6IAX5\|Q6IAX5_HUMAN;sp\|P60228\| | 21 | 0 | 9715230 | 5477519 | 18011182 | 3455498 | 25236000 | 3839963 |
| sp\|Q8WWM7\|ATX2L_HUMAN;sp\|Q8W | 21 | 0 | 9528800 | 3381800 | 10180207 | 2484200 | 64544000 | 4948575 |
| sp\|O43707\|ACTN4_HUMAN;tr\|Q96BG6\| | 21 | 0 | 9277200 | 141600 | 862140 | 0 | 1182790 | 310360 |
| sp\|P11388\|TOP2A_HUMAN;sp\|P11388- | 21 | 0 | 8210100 | 734450 | 3526600 | 923700 | 19023822 | 698450 |
| tr\|Q6IBN0\|Q6IBN0_HUMAN;sp\|O43242\| | 21 | 0 | 7625900 | 2112300 | 12614810 | 2413387 | 40634000 | 4675285 |
| sp\|O14617\|AP3D1_HUMAN;sp\|O14617\| | 21 | 0 | 6683600 | 0 | 4993750 | 0 | 37124890 | 376450 |
| sp\|P17655\|CAN2_HUMAN;tr\|Q59EF6\|C | 21 | 0 | 5279200 | 2786920 | 12236000 | 2469050 | 46532000 | 22290000 |
| tr\|E9PKG1\|E9PKG1_HUMAN;sp\|Q99873\| | 21 | 0 | 3065000 | 343620 | 7841280 | 953680 | 13544780 | 3300350 |
| tr\|B3KQT9\|B3KQT9_HUMAN;tr\|V9HVY3\| | 21 | 0 | 1474770 | 2454100 | 5312500 | 2070898 | 820450 | 6769970 |
| sp\|Q14966\|ZN638_HUMAN;sp\|Q14966\| | 21 | 0 | 1442100 | 431920 | 2977700 | 880480 | 25506000 | 1262800 |
| sp\|P68366-2\|TBA4A_HUMAN;sp\|P6836\| | 21 | 0.001715 | 1381500 | 0 | 0 | 0 | 0 | 0 |
| tr\|D3DTH7\|D3DTH7_HUMAN;tr\|A1L180\| | 21 | 0.006563 | 718060 | 237960 | 504740 | 0 | 1787900 | 0 |
| tr\|B4DE59\|B4DE59_HUMAN;tr\|C9JTX4\| | 21 | 1 | 0 | 601620 | 0 | 745473 | 258880 | 724000 |
| sp\|P63261\|ACTG_HUMAN;tr\|B4E3A4\|B | 20 | 0 | 531882200 | 144523000 | 583207600 | 239965600 | 192862000 | 191495000 |
| sp\|P07196\|NFL_HUMAN;tr\|B3KQI5\|B3 | 20 | 0 | 41790720 | 3243200 | 38647200 | 1672400 | 0 | 0 |
| tr\|B2CIS9\|B2CIS9_HUMAN;sp\|P31944\|( | 20 | 0 | 36765300 | 4746100 | 6159600 | 4229330 | 5990100 | 5824700 |
| tr\|Q96IR1\|Q96IR1_HUMAN;tr\|B2R491\| | 20 | 0 | 30083620 | 13506700 | 55750700 | 9939160 | 389158250 | 21718030 |
| sp\|Q92973-2\|TNPO1_HUMAN;tr\|A0A02\| | 20 | 0 | 29591200 | 6550090 | 16090500 | 4305397 | 79241906 | 8414870 |
| tr\|B4DVQ5\|B4DVQ5_HUMAN;tr\|A1KYC\| | 20 | 0 | 25132160 | 5209400 | 14636920 | 4484261 | 36316000 | 7535602 |
| tr\|A0A024R1U0\|A0A024R1U0_HUMAN;\| | 20 | 0 | 23173280 | 8180205 | 30424710 | 9023048 | 24825000 | 3421671 |
| tr\|Q9BR63\|Q9BR63_HUMAN;sp\|Q9NSD\| | 20 | 0 | 22886930 | 8552700 | 46816300 | 5731900 | 86923800 | 5468160 |
| tr\|A0A087WTT1\|A0A087WTT1_HUMAN\| | 20 | 0 | 21898590 | 4736492 | 37146700 | 4790687 | 130467890 | 7274500 |
| sp\|P61221\|ABCE1_HUMAN;tr\|D6R9I9\|D | 20 | 0 | 19383870 | 10650330 | 36466580 | 5408225 | 88524590 | 5058188 |
| tr\|B2RBI2\|B2RBI2_HUMAN;sp\|Q96A49\| | 20 | 0 | 15476250 | 16571232.8 | 75704520 | 22467090 | 61205870 | 53883000 |
| sp\|P39023\|RL3_HUMAN;tr\|Q8TBW1\|Q\| | 20 | 0 | 14370500 | 3805700 | 33793790 | 1698037.4 | 150584520 | 8459740 |
| sp\|P55265-5\|DSRAD_HUMAN;tr\|A0A02\| | 20 | 0 | 13739820 | 2559300 | 6830000 | 2205800 | 56215070 | 3987400 |
| sp\|Q15233\|NONO_HUMAN;tr\|A8K525\| | 20 | 0 | 13501530 | 5717740 | 28656150 | 4112040 | 125870246 | 17180580 |
| sp\|Q96KG9-3\|NTKL_HUMAN;tr\|E9PS17\| | 20 | 0 | 10929470 | 2447900 | 7312282 | 0 | 52426310 | 4908200 |
| tr\|A8K2M0\|A8K2M0_HUMAN;sp\|P4368\| | 20 | 0 | 10859976 | 2853100 | 17291000 | 3513600 | 54595750 | 11372580 |
| tr\|B2R8Y6\|B2R8Y6_HUMAN;tr\|Q6MZM\| | 20 | 0 | 10109910 | 243140 | 2276500 | 345900 | 28935000 | 547940 |
| tr\|A5PLK7\|A5PLK7_HUMAN;tr\|A0A024\| | 20 | 0 | 10036870 | 2927278 | 14241870 | 1822167 | 22927290 | 7883790 |
| tr\|B4DLG2\|B4DLG2_HUMAN;sp\|O75152\| | 20 | 0 | 9478600 | 1993600 | 4130782 | 878130 | 40020320 | 3062173 |
| tr\|B4DNN4\|B4DNN4_HUMAN;sp\|P2392\| | 20 | 0 | 9026730 | 5652440 | 17976290 | 5192305 | 13770100 | 3453180 |
| sp\|Q6Y7W6-4\|PERQ2_HUMAN;sp\|Q6Y7\| | 20 | 0 | 8732800 | 2583700 | 8288400 | 3006400 | 26909000 | 4381612 |
| tr\|A0A024R8W0\|A0A024R8W0_HUMAN\| | 20 | 0 | 7953800 | 3591960 | 11783460 | 2236400 | 30164620 | 5828890 |
| sp\|Q9Y5L0-3\|TNPO3_HUMAN;tr\|B2R6H\| | 20 | 0 | 7225620 | 668250 | 5343500 | 719688 | 29616790 | 1280980 |
| sp\|Q02952-3\|AKA12_HUMAN;sp\|Q029\| | 20 | 0 | 7175500 | 1463863 | 3407700 | 2864600 | 14460000 | 3452500 |
| tr\|A0A024RA61\|A0A024RA61_HUMAN;\| | 20 | 0 | 7011800 | 11545100 | 11357210 | 2797933 | 128944950 | 18259610 |
| sp\|P15170-2\|ERF3A_HUMAN;sp\|P1517\| | 20 | 0 | 6619010 | 1955300 | 15867029 | 924780 | 36086780 | 2533654 |
| tr\|Q53GK6\|Q53GK6_HUMAN;tr\|Q53G9\| | 20 | 0 | 6470000 | 2312100 | 5284800 | 3190700 | 4347500 | 1391404 |
| tr\|A0A024R6M2\|A0A024R6M2_HUMAN\| | 20 | 0 | 6210940 | 598083.9 | 1444200 | 261410 | 21685160 | 1162300 |
| sp\|Q9BTC0\|DIDO1_HUMAN;sp\|Q9BTC0\| | 20 | 0 | 5960200 | 1155000 | 3025100 | 314070 | 18487000 | 324770 |
| sp\|Q92576-2\|PHF3_HUMAN;sp\|Q92576\| | 20 | 0 | 5822500 | 262120 | 1551600 | 1544600 | 13594000 | 927270 |
| sp\|Q16513-2\|PKN2_HUMAN;sp\|Q1651\| | 20 | 0 | 5616000 | 1221190 | 5074710 | 886740 | 41250560 | 2880050 |
| tr\|A0A0A0MSQ0\|A0A0A0MSQ0_HUMA\| | 20 | 0 | 5345430 | 4194169 | 7526900 | 1985130 | 2035400 | 3166190 |
| sp\|O94832\|MYO1D_HUMAN;tr\|J3QRN6\| | 20 | 0 | 5226021 | 149830 | 3450800 | 73484 | 14511000 | 693150 |
| sp\|O60271-4\|JIP4_HUMAN;sp\|O60271-\| | 20 | 0 | 3693200 | 646640 | 796470 | 644980 | 11925000 | 815160 |
| sp\|P57740\|NU107_HUMAN;sp\|P57740-\| | 20 | 0 | 3285340 | 441040 | 3421400 | 220470 | 24733500 | 2133100 |
| sp\|Q12789-3\|TF3C1_HUMAN;tr\|Q6AHZ\| | 20 | 0 | 2348800 | 0 | 911480 | 232080 | 13024000 | 0 |
| tr\|B7ZME8\|B7ZME8_HUMAN;sp\|Q641C\| | 20 | 0 | 2324900 | 138900 | 393520 | 413610 | 45728220 | 1679200 |
| tr\|Q6IAT1\|Q6IAT1_HUMAN;sp\|P50395\| | 20 | 0 | 1883500 | 955200 | 1731000 | 576220 | 0 | 2402210 |
| tr\|A0A087X054\|A0A087X054_HUMAN;t\| | 20 | 0 | 936080 | 0 | 590080 | 0 | 0 | 488790 |
| sp\|P04350\|TBB4A_HUMAN;tr\|B4DJ43\|( | 20 | 0 | 870940 | 225570 | 2337600 | 0 | 3982200 | 618200 |
| tr\|Q59EC0\|Q59EC0_HUMAN;tr\|B7Z8Y3\| | 20 | 0.002729 | 634690 | 166340 | 650710 | 0 | 2229600 | 281690 |
| sp\|Q14315-2\|FLNC_HUMAN;sp\|Q1431\| | 20 | 0 | 355520 | 0 | 0 | 0 | 2277000 | 1686300 |
| tr\|V9HW72\|V9HW72_HUMAN;tr\|A8K69\| | 20 | 0 | 61899 | 169440 | 1011200 | 0 | 3107100 | 771350 |
| sp\|Q9Y4E1-2\|FA21C_HUMAN;sp\|Q9Y4E\| | 20 | 0 | 0 | 0 | 0 | 0 | 2979900 | 0 |
| sp\|Q15366-6\|PCBP2_HUMAN;sp\|Q153\| | 19 | 0 | 77699400 | 25108360 | 167697700 | 28450750 | 383846600 | 56520280 |
| tr\|F4ZW62\|F4ZW62_HUMAN;sp\|Q1290\| | 19 | 0 | 77154443 | 23050600 | 165898630 | 22203680 | 346922100 | 51582860 |
| tr\|V9HWH2\|V9HWH2_HUMAN;sp\|P122\| | 19 | 0 | 69768150 | 20835300 | 142690640 | 30433840 | 289822400 | 116346800 |
| tr\|A0A024RD93\|A0A024RD93_HUMAN;\| | 19 | 0 | 54521824 | 54765120 | 88269260 | 26882670 | 80147410 | 42292870 |
| tr\|A0A024R3X4\|A0A024R3X4_HUMAN;s\| | 19 | 0 | 38604520 | 13989854 | 71279133 | 11857713 | 13374000 | 2806521 |
| tr\|A0A024RBY4\|A0A024RBY4_HUMAN;s\| | 19 | 0 | 33742424 | 10643880 | 64485110 | 9915210 | 153727500 | 19905310 |
| tr\|R4GNH3\|R4GNH3_HUMAN;tr\|A8K78\| | 19 | 0 | 12400927 | 6840400 | 19686000 | 4520800 | 46215360 | 10546448 |
| sp\|O00148\|DX39A_HUMAN;tr\|B4DX78\| | 19 | 0 | 12116610 | 2618900 | 22049000 | 2044556 | 44342060 | 2758400 |
| tr\|A0A024R201\|A0A024R201_HUMAN;s\| | 19 | 0 | 11777891 | 0 | 31775880 | 5519100 | 56919400 | 13659518 |
| tr\|Q53H17\|Q53H17_HUMAN;tr\|Q53GN\| | 19 | 0 | 11624420 | 314400 | 11813480 | 490746 | 36322340 | 4427290 |
| sp\|P09651-3\|ROA1_HUMAN;tr\|F8W6I7\| | 19 | 0 | 11310310 | 8680550 | 21337828 | 3708487 | 130012440 | 17989790 |
| sp\|Q9Y2W1\|TR150_HUMAN;tr\|Q7Z5U1\| | 19 | 0 | 10866450 | 1314500 | 5748660 | 1106600 | 31909000 | 3623670 |

| | | | | | | | | |
|---|---|---|---|---|---|---|---|---|
| sp\|P24928\|RPB1_HUMAN;tr\|A0A087W | 19 | 0 | 10279480 | 0 | 3964400 | 0 | 14127000 | 171750 |
| tr\|D3DUP2\|D3DUP2_HUMAN;tr\|F5GW1 | 19 | 0 | 10108000 | 1841700 | 5624300 | 3059300 | 13455000 | 615490 |
| sp\|P16615-5\|AT2A2_HUMAN;sp\|P1661 | 19 | 0 | 8816440 | 1486500 | 6399790 | 1001400 | 4083450 | 0 |
| sp\|Q15020\|SART3_HUMAN;sp\|Q15020- | 19 | 0 | 8286300 | 630240 | 2666600 | 469440 | 37431000 | 2004100 |
| tr\|B4E0X8\|B4E0X8_HUMAN;sp\|Q96AE4 | 19 | 0 | 7354130 | 11125670 | 9297981 | 7190680 | 15323000 | 11581590 |
| sp\|Q15008\|PSMD6_HUMAN;sp\|Q1500 | 19 | 0 | 7162700 | 636610 | 8562400 | 735860 | 20182000 | 2549814 |
| sp\|Q14240\|IF4A2_HUMAN;sp\|Q14240- | 19 | 0 | 6356300 | 2419600 | 10997000 | 2445800 | 17877000 | 4693892 |
| sp\|Q9H4A4\|AMPB_HUMAN;tr\|A6NKB | 19 | 0 | 6112700 | 1873700 | 13580000 | 2165500 | 13914000 | 1386375 |
| sp\|Q86UK7-2\|ZN598_HUMAN;sp\|Q86U | 19 | 0 | 6092900 | 1532550 | 5179200 | 1436050 | 23526190 | 3865040 |
| tr\|E7EMW7\|E7EMW7_HUMAN;sp\|O95 | 19 | 0 | 5984100 | 236230 | 1638200 | 545510 | 16416050 | 394500 |
| tr\|V9HWK0\|V9HWK0_HUMAN;sp\|O76 | 19 | 0 | 5716100 | 217040 | 6533600 | 366970 | 36530000 | 1032000 |
| tr\|A0A090N8G0\|A0A090N8G0_HUMAN | 19 | 0 | 5607190 | 2865303 | 9917130 | 1416060 | 21378040 | 3307140 |
| sp\|Q9HCE1\|MOV10_HUMAN;tr\|Q5JR0 | 19 | 0 | 3298400 | 237737 | 2124000 | 0 | 19593540 | 689860 |
| sp\|P49321\|NASP_HUMAN;tr\|Q53H03\| | 19 | 0 | 2233298 | 1285758 | 1013350 | 846205 | 6481800 | 6898830 |
| tr\|A0A024R1K8\|A0A024R1K8_HUMAN;s | 19 | 0 | 1953825 | 758140 | 2658300 | 1140100 | 11019530 | 3126043 |
| tr\|Q8N5A0\|Q8N5A0_HUMAN;tr\|A0A08 | 19 | 0 | 1916600 | 713090 | 0 | 709270 | 7667000 | 1444900 |
| sp\|P49750\|YLPM1_HUMAN;sp\|P49750- | 19 | 0 | 1655100 | 171430 | 1636600 | 0 | 19657000 | 229940 |
| tr\|Q6FIC5\|Q6FIC5_HUMAN;sp\|Q9Y696 | 19 | 0 | 1347092 | 864952 | 4384740 | 2072000 | 63349600 | 4831190 |
| tr\|D3DPU2\|D3DPU2_HUMAN;tr\|B2RDY | 19 | 0 | 361290 | 286300 | 811910 | 0 | 3828200 | 2656490 |
| sp\|Q15366-3\|PCBP2_HUMAN;sp\|Q153 | 19 | 1 | 0 | 0 | 1091400 | 0 | 0 | 0 |
| sp\|Q8IWZ3-6\|ANKH1_HUMAN;sp\|Q8IV | 19 | 0 | 0 | 0 | 0 | 0 | 3675300 | 0 |
| sp\|P37802\|TAGL2_HUMAN;tr\|X6RJP6\|X | 18 | 0 | 100919970 | 75145970 | 254754660 | 73336430 | 467942970 | 143316710 |
| tr\|V9HWI5\|V9HWI5_HUMAN;sp\|P2352 | 18 | 0 | 40598100 | 27599850 | 64147850 | 21071600 | 329901300 | 53755590 |
| sp\|P52209-2\|6PGD_HUMAN;sp\|P52209 | 18 | 0 | 40107888 | 13642156 | 80092730 | 12290000 | 126186060 | 22227380 |
| sp\|Q06830\|PRDX1_HUMAN;tr\|A0A0A0 | 18 | 0 | 27511600 | 22009200 | 26481700 | 20588600 | 62100700 | 62800800 |
| tr\|A8K548\|A8K548_HUMAN;sp\|Q8IZL8 | 18 | 0 | 26042580 | 1722464 | 6641830 | 7566600 | 75283760 | 3822930 |
| sp\|O43776\|SYNC_HUMAN;tr\|B4DN60\| | 18 | 0 | 23016470 | 4941210 | 36266000 | 6104925 | 91325840 | 8701212 |
| sp\|Q9NZI8\|IF2B1_HUMAN;sp\|Q9NZI8- | 18 | 0 | 22652040 | 6277300 | 36099270 | 5532240 | 147103370 | 9409550 |
| tr\|D0PNI1\|D0PNI1_HUMAN;sp\|P63104 | 18 | 0 | 14802700 | 7666680 | 17193820 | 5393200 | 38625020 | 23459490 |
| sp\|P62195-2\|PRS8_HUMAN;sp\|P62195 | 18 | 0 | 13018865 | 5813120 | 24577460 | 7834714 | 63240780 | 12953569 |
| sp\|P36578\|RL4_HUMAN;tr\|Q59GY2\|Q5 | 18 | 0 | 11904700 | 2397140 | 37946460 | 1380980 | 328615200 | 6125300 |
| tr\|B7ZAX9\|B7ZAX9_HUMAN;tr\|B4DZC0 | 18 | 0 | 7999500 | 1950900 | 8058059 | 667216 | 20729660 | 1933480 |
| tr\|B4DSQ5\|B4DSQ5_HUMAN;tr\|F5H365 | 18 | 0 | 7827293 | 2016960 | 11548000 | 1093850 | 31993000 | 3093180 |
| tr\|I3L0N3\|I3L0N3_HUMAN;tr\|B7Z5J7\|B | 18 | 0 | 7656900 | 3045826 | 17497000 | 2966260 | 51361430 | 3695800 |
| sp\|Q9H2G2-2\|SLK_HUMAN;sp\|Q9H2G2 | 18 | 0 | 7583600 | 1257300 | 3806300 | 1462400 | 36937000 | 2281500 |
| tr\|Q59GB4\|Q59GB4_HUMAN;sp\|Q1655 | 18 | 0 | 7186200 | 2094000 | 22980731 | 2475800 | 38126430 | 3415777 |
| sp\|O00425\|IF2B3_HUMAN;sp\|O00425- | 18 | 0 | 7167000 | 3952600 | 13001735 | 2448200 | 72658801 | 4392960 |
| tr\|Q53GV6\|Q53GV6_HUMAN;tr\|B2R79 | 18 | 0 | 7060950 | 4327630 | 13395140 | 4264710 | 61172610 | 13503318 |
| tr\|A0A024RCR5\|A0A024RCR5_HUMAN; | 18 | 0 | 6040140 | 1125000 | 4123670 | 923410 | 44568000 | 3835810 |
| tr\|Q53XC0\|Q53XC0_HUMAN;sp\|P0519 | 18 | 0 | 5943100 | 3801026 | 13409470 | 2718957 | 114624640 | 9501920 |
| sp\|P57737-2\|CORO7_HUMAN;sp\|P573 | 18 | 0 | 5769500 | 417020 | 3734800 | 597260 | 34468710 | 1566900 |
| sp\|Q9Y2A7\|NCKP1_HUMAN;sp\|Q9Y2A | 18 | 0 | 5570200 | 184140 | 3308920 | 704490 | 19012000 | 1472600 |
| sp\|O15042-2\|SR140_HUMAN;sp\|O1504 | 18 | 0 | 5570000 | 991292 | 5305060 | 1352300 | 41708000 | 1588400 |
| sp\|P62424\|RL7A_HUMAN;tr\|Q9BY74\|Q | 18 | 0 | 5444580 | 2554500 | 13713840 | 979360 | 238211600 | 6534780 |
| sp\|Q7Z460-2\|CLAP1_HUMAN;sp\|Q7Z46 | 18 | 0 | 5006500 | 0 | 1018300 | 228270 | 13888000 | 0 |
| sp\|Q8NC51-3\|PAIRB_HUMAN;tr\|Q63HI | 18 | 0 | 4300515.3 | 3254862 | 8268251.7 | 1639417 | 17628640 | 7016684 |
| sp\|Q9NTI5-2\|PDS5B_HUMAN;sp\|Q9NT | 18 | 0 | 4234112 | 561320 | 1514800 | 268130 | 22141760 | 581820 |
| tr\|A0A024R179\|A0A024R179_HUMAN;s | 18 | 0 | 4147427 | 606830 | 11489000 | 601587 | 30386000 | 970380 |
| sp\|Q9Y6Y8\|S23IP_HUMAN;tr\|B4DWG1\| | 18 | 0 | 4125000 | 968750 | 3616300 | 666720 | 37177920 | 1694600 |
| tr\|A0A090N7U0\|A0A090N7U0_HUMAN | 18 | 0 | 4086140 | 1254329 | 8606070 | 840594 | 17651955 | 1270523 |
| sp\|Q9H2M9\|RBGPR_HUMAN;tr\|B3KNG | 18 | 0 | 3872200 | 166720 | 2431100 | 0 | 20353743 | 1315300 |
| tr\|Q2NKY5\|Q2NKY5_HUMAN;sp\|Q9H4 | 18 | 0 | 3094520 | 430179 | 5066290 | 0 | 13809820 | 323460 |
| sp\|Q12996\|CSTF3_HUMAN;tr\|B4DFQ5\| | 18 | 0 | 2625500 | 1546687 | 10038000 | 2348320 | 20531330 | 5377400 |
| tr\|A0A024RAV2\|A0A024RAV2_HUMAN | 18 | 0 | 2310870 | 432090 | 6037400 | 0 | 24742830 | 545210 |
| sp\|Q9H1A4\|APC1_HUMAN;tr\|H0Y564\| | 18 | 0 | 2024800 | 245707 | 881620 | 269870 | 11392250 | 530710 |
| sp\|Q12768\|STRUM_HUMAN;tr\|Q53EL1 | 18 | 0 | 1615300 | 213900 | 2384100 | 0 | 24549000 | 368590 |
| tr\|B1ANR0\|B1ANR0_HUMAN;sp\|Q1331 | 18 | 0 | 1109800 | 469430 | 3832400 | 0 | 24039000 | 479754 |
| sp\|Q9BUF5\|TBB6_HUMAN;tr\|B4DP54\|B | 18 | 0 | 760520 | 0 | 1373000 | 0 | 5856100 | 0 |
| sp\|O14776-2\|TCRG1_HUMAN;sp\|O147 | 18 | 0 | 641020 | 0 | 0 | 0 | 6587600 | 470940 |
| tr\|B4E0Q4\|B4E0Q4_HUMAN;tr\|B4DZJ7 | 18 | 0 | 409190 | 0 | 0 | 0 | 0 | 55850 |
| tr\|B5BUB5\|B5BUB5_HUMAN;sp\|P0545 | 18 | 0 | 207480 | 1159720 | 385450 | 157920 | 344960 | 3360130 |
| tr\|A0A024R643\|A0A024R643_HUMAN | 18 | 1 | 0 | 0 | 413570 | 0 | 699790 | 0 |
| tr\|Q9UQM3\|Q9UQM3_HUMAN | 18 | 0 | 0 | 0 | 0 | 0 | 699650 | 0 |
| sp\|P26599\|PTBP1_HUMAN;sp\|P26599- | 17 | 0 | 93496200 | 23624640 | 165240510 | 24153859 | 255150110 | 61736350 |
| tr\|Q7Z726\|Q7Z726_HUMAN;tr\|Q6NVW | 17 | 0 | 61514530 | 19856870 | 114698322 | 18971050 | 69473380 | 12272820 |
| tr\|V9HW24\|V9HW24_HUMAN;sp\|P623 | 17 | 0 | 23247000 | 2213800 | 42282000 | 7795100 | 57700960 | 11917535 |
| tr\|A0A024R5Q7\|A0A024R5Q7_HUMAN; | 17 | 0 | 21639000 | 6457000 | 41734000 | 6601300 | 64538910 | 7409128 |
| tr\|A0A024R0R4\|A0A024R0R4_HUMAN;s | 17 | 0 | 15961870 | 493740 | 22563000 | 2101200 | 58728880 | 11478791 |
| tr\|A0A024R4G1\|A0A024R4G1_HUMAN; | 17 | 0 | 10621190 | 3358500 | 22069000 | 2181000 | 50058000 | 1656667 |
| sp\|Q9Y3F4\|STRAP_HUMAN;sp\|Q9Y3F4 | 17 | 0 | 8789336 | 402610 | 18232000 | 2693660 | 34086100 | 11634080 |
| sp\|Q8WX92\|NELFB_HUMAN | 17 | 0 | 8596982 | 2341500 | 11282000 | 1723100 | 37902590 | 977524 |
| sp\|Q13435\|SF3B2_HUMAN;tr\|E9PPJ0\|E | 17 | 0 | 7278300 | 903340 | 2639305 | 362660 | 25827000 | 2648000 |
| tr\|G5EA31\|G5EA31_HUMAN;tr\|A0A024 | 17 | 0 | 6836869 | 1444200 | 4431000 | 1121400 | 37407080 | 3236500 |
| tr\|X5D2E5\|X5D2E5_HUMAN;sp\|Q86WJ | 17 | 0 | 5932400 | 930190 | 2956400 | 1012620 | 45411060 | 2471300 |
| tr\|A0A024R8V0\|A0A024R8V0_HUMAN; | 17 | 0 | 3844900 | 6279700 | 10099850 | 10267200 | 49397300 | 19231600 |
| tr\|Q3BDU5\|Q3BDU5_HUMAN;sp\|P0254 | 17 | 0 | 3676445 | 0 | 0 | 745050 | 551920 | 1485601 |
| tr\|A0A024RCS7\|A0A024RCS7_HUMAN;s | 17 | 0 | 3143000 | 1407200 | 7316100 | 1257800 | 30868200 | 1005200 |
| tr\|E7ERI8\|E7ERI8_HUMAN;tr\|E7EW49\|E | 17 | 0 | 3041900 | 344520 | 1766300 | 193490 | 17862000 | 350750 |

| | | | | | | | | | |
|---|---|---|---|---|---|---|---|---|---|
| tr\|A8K3W4\|A8K3W4_HUMAN;tr\|A0A02 | 17 | 0 | 2931960 | 221970 | 1265843 | 156330 | 24964300 | 875450 |
| tr\|D9YZV0\|D9YZV0_HUMAN;tr\|B3KNB9 | 17 | 0 | 2473210 | 24798000 | 15789500 | 23284600 | 29227500 | 27873600 |
| tr\|Q53EQ3\|Q53EQ3_HUMAN;sp\|Q9BSJ | 17 | 0 | 2422580 | 356480 | 3150104 | 509010 | 15319000 | 544950 |
| sp\|Q6PGP7\|TTC37_HUMAN;tr\|D6RCE2 | 17 | 0 | 2421890 | 100310 | 1409400 | 238930 | 13136070 | 210490 |
| sp\|P62136\|PP1A_HUMAN;sp\|P62136-2 | 17 | 0 | 2274810 | 4765010 | 18128000 | 1816100 | 95684000 | 13949390 |
| sp\|Q96JM3\|CHAP1_HUMAN;tr\|S4R3K0 | 17 | 0 | 2178600 | 816040 | 1140800 | 491710 | 20743000 | 1889000 |
| sp\|Q5SRE5-2\|NU188_HUMAN;sp\|Q5SR | 17 | 0 | 2173700 | 0 | 2877220 | 157700 | 9366900 | 120290 |
| tr\|A0A024R542\|A0A024R542_HUMAN;s | 17 | 0 | 1783900 | 120060 | 384730 | 154840 | 10966000 | 266810 |
| tr\|H0Y4W2\|H0Y4W2_HUMAN;tr\|F2Z2U | 17 | 0 | 1628200 | 0 | 482023 | 0 | 12352000 | 0 |
| tr\|V9HWC0\|V9HWC0_HUMAN;sp\|P260 | 17 | 0 | 520370 | 342720 | 0 | 393180 | 0 | 2343850 |
| tr\|V9HWE0\|V9HWE0_HUMAN;sp\|P087 | 17 | 0 | 0 | 1801780 | 0 | 592140 | 791300 | 6239540 |
| sp\|P31943\|HNRH1_HUMAN;tr\|G8JLB6\| | 16 | 0 | 72014980 | 21712793 | 122936960 | 25528850 | 248630800 | 46411510 |
| tr\|Q53SS8\|Q53SS8_HUMAN;sp\|Q15365 | 16 | 0 | 56519850 | 8100510 | 102627070 | 16513690 | 208985580 | 41823520 |
| sp\|Q9BZZ5-2\|API5_HUMAN;sp\|Q9BZZ5 | 16 | 0 | 51188860 | 8170320 | 62802249 | 9883830 | 216828650 | 24511190 |
| sp\|Q9UMS4\|PRP19_HUMAN;tr\|F5GY56 | 16 | 0 | 17669882 | 2849830 | 38465274 | 2436700 | 84298520 | 10069232 |
| sp\|Q9Y3I0\|RTCB_HUMAN;tr\|B4DNA0\|E | 16 | 0 | 17068998 | 3372051 | 20627380 | 2911000 | 80388860 | 5394070 |
| tr\|A0A087WUA5\|A0A087WUA5_HUMA | 16 | 0 | 14327087 | 6457030 | 34280860 | 5092100 | 3037300 | 2181334 |
| tr\|B5BU72\|B5BU72_HUMAN;tr\|A0A024 | 16 | 0 | 14320030 | 4213300 | 32549000 | 3287807 | 47532600 | 1121092 |
| sp\|P06748-2\|NPM_HUMAN;sp\|P06748 | 16 | 0 | 11695710 | 11123700 | 25011420 | 3388890 | 203632680 | 28953570 |
| tr\|Q0VGA5\|Q0VGA5_HUMAN;tr\|Q53HA | 16 | 0 | 11506770 | 2321900 | 21783000 | 5319890 | 62906000 | 10641620 |
| tr\|A0A024R4Z6\|A0A024R4Z6_HUMAN;s | 16 | 0 | 10764470 | 6625837 | 27831330 | 1844900 | 129131580 | 10956320 |
| sp\|Q6UWP8\|SBSN_HUMAN;sp\|Q6UWP | 16 | 0 | 9950500 | 6096200 | 7385700 | 8960900 | 6714800 | 7583100 |
| sp\|P51659\|DHB4_HUMAN;tr\|E7ER27\|E | 16 | 0 | 9654190 | 5315370 | 20603000 | 4471700 | 20890990 | 3400130 |
| sp\|Q96T58\|MINT_HUMAN;tr\|H0Y5U7\|H | 16 | 0 | 9403690 | 1184840 | 2261800 | 584670 | 5967400 | 0 |
| tr\|C9J2Y9\|C9J2Y9_HUMAN;tr\|B4DHJ3\|E | 16 | 0 | 8192600 | 558520 | 2909100 | 361580 | 16511000 | 1009900 |
| sp\|O60701\|UGDH_HUMAN;sp\|O60701- | 16 | 0 | 7466040 | 2266800 | 14282000 | 2363220 | 40127390 | 2799165 |
| tr\|V9HW98\|V9HW98_HUMAN;sp\|P622 | 16 | 0 | 7009650 | 6165570 | 26639009 | 3071250 | 29188800 | 17974020 |
| sp\|O43290\|SNUT1_HUMAN;tr\|B4DDH9 | 16 | 0 | 6722800 | 1496866 | 5518220 | 904660 | 36551720 | 2736738 |
| tr\|B2RNR6\|B2RNR6_HUMAN;sp\|Q96KR | 16 | 0 | 6528700 | 1593300 | 5882500 | 430230 | 39371680 | 3055700 |
| sp\|Q06210-2\|GFPT1_HUMAN;sp\|Q0621 | 16 | 0 | 5908200 | 2669400 | 4571600 | 1691628 | 31256000 | 2671992 |
| sp\|P14735\|IDE_HUMAN;tr\|Q59GA5\|Q5 | 16 | 0 | 5885472 | 357610 | 522620 | 442410 | 15262140 | 1126400 |
| sp\|Q05639\|EF1A2_HUMAN;tr\|Q59GP5\| | 16 | 0 | 5451022 | 922950 | 6854800 | 901460 | 8835900 | 2708100 |
| tr\|A8K9U6\|A8K9U6_HUMAN;sp\|Q7Z2W | 16 | 0 | 5438550 | 1611530 | 4254520 | 352718 | 17861900 | 904504 |
| sp\|Q15046\|SYK_HUMAN;sp\|Q15046-2\| | 16 | 0 | 5419900 | 2326193 | 7038900 | 1826064 | 22675450 | 3211210 |
| sp\|Q96T88\|UHRF1_HUMAN;tr\|A0A087 | 16 | 0 | 5403770 | 1532900 | 4556990 | 545625 | 17388540 | 1879770 |
| sp\|P26358\|DNMT1_HUMAN;tr\|A0A024 | 16 | 0 | 4513500 | 2721290 | 2693300 | 1839470 | 22550020 | 2578870 |
| sp\|Q9H2U1-2\|DHX36_HUMAN;sp\|Q9H2 | 16 | 0 | 4295900 | 266110 | 1723900 | 370290 | 16279545 | 0 |
| tr\|E5KLB5\|E5KLB5_HUMAN;sp\|P49916\| | 16 | 0 | 4226800 | 462090 | 2107406 | 128570 | 16853000 | 715948 |
| sp\|Q9H3U1-2\|UN45A_HUMAN;sp\|Q9H | 16 | 0 | 4042340 | 855740 | 3836300 | 620780 | 11423900 | 927760 |
| tr\|Q2M1V9\|Q2M1V9_HUMAN;tr\|A0A0 | 16 | 0 | 4006730 | 0 | 1239900 | 0 | 14778190 | 62408 |
| tr\|B2RDD7\|B2RDD7_HUMAN;sp\|O1474 | 16 | 0 | 3680800 | 2321600 | 6638000 | 2618837 | 5897000 | 2222170 |
| tr\|Q53FI7\|Q53FI7_HUMAN;sp\|Q13642- | 16 | 0 | 3413390 | 3389000 | 8297600 | 430960 | 80531600 | 3072080 |
| sp\|P18858\|DNLI1_HUMAN;tr\|F5GZ28\|F | 16 | 0 | 3369300 | 739120 | 2525200 | 521570 | 24259940 | 466990 |
| tr\|A0A024R0Y5\|A0A024R0Y5_HUMAN;s | 16 | 0 | 3340700 | 1178900 | 9077400 | 1125400 | 17448000 | 2797600 |
| sp\|Q27J81-2\|INF2_HUMAN;sp\|Q27J81\| | 16 | 0 | 1969100 | 208520 | 2614200 | 272170 | 24105000 | 379180 |
| tr\|A0A024R8S5\|A0A024R8S5_HUMAN;s | 16 | 0 | 1644837 | 0 | 395740 | 220540 | 0 | 0 |
| sp\|P35249\|RFC4_HUMAN;sp\|P35249-2 | 16 | 0 | 1612300 | 1171630 | 7797300 | 1009600 | 38471200 | 1367542 |
| tr\|Q53ZP9\|Q53ZP9_HUMAN;sp\|O9575 | 16 | 0 | 1544300 | 820440 | 1046500 | 429350 | 0 | 1144600 |
| sp\|Q13619\|CUL4A_HUMAN;sp\|Q13619 | 16 | 0 | 1523800 | 485940 | 4411000 | 582720 | 6854600 | 0 |
| tr\|V9HW04\|V9HW04_HUMAN;sp\|P621 | 16 | 0 | 1127100 | 1313100 | 3781500 | 922750 | 32072000 | 2186600 |
| sp\|A6NKT7\|RGPD3_HUMAN;tr\|J3KNE0 | 16 | 0.002691 | 831370 | 0 | 1143500 | 0 | 1710800 | 161920 |
| tr\|A0A024R222\|A0A024R222_HUMAN;s | 16 | 0 | 541320 | 435931 | 0 | 534825 | 4913200 | 4602720 |
| tr\|H0Y4R1\|H0Y4R1_HUMAN;sp\|P12268 | 16 | 0 | 272250 | 405145 | 694710 | 221072 | 0 | 2348210 |
| sp\|P26358-2\|DNMT1_HUMAN;tr\|I6L9H | 16 | 1 | 0 | 0 | 0 | 0 | 435740 | 0 |
| sp\|Q9BZZ5\|API5_HUMAN;tr\|G3V1C3\|G | 16 | 0.00363 | 0 | 0 | 0 | 0 | 513320 | 0 |
| tr\|B4DNH2\|B4DNH2_HUMAN;tr\|J3KTN | 16 | 1 | 0 | 0 | 388480 | 0 | 0 | 0 |
| tr\|Q6NUR7\|Q6NUR7_HUMAN;tr\|E7EQF | 16 | 0 | 0 | 0 | 0 | 0 | 0 | 840460 |
| sp\|Q9NZT1\|CALL5_HUMAN;tr\|Q53H37\| | 15 | 0 | 118812000 | 53358000 | 35790000 | 26915700 | 50570000 | 31410000 |
| tr\|E7DVW5\|E7DVW5_HUMAN;sp\|Q014 | 15 | 0 | 114243600 | 19735000 | 31803400 | 20002000 | 82614200 | 32940100 |
| sp\|Q08188\|TGM3_HUMAN | 15 | 0 | 27387810 | 6286900 | 5433370 | 10216250 | 3480810 | 9153930 |
| sp\|Q96EA4\|SPDLY_HUMAN;sp\|Q96EA4 | 15 | 0 | 25628357 | 0 | 15846150 | 0 | 9765700 | 0 |
| sp\|Q8WVV4\|POF1B_HUMAN;sp\|Q8WV | 15 | 0 | 21586190 | 694760 | 252050 | 1425830 | 104910 | 892222 |
| sp\|P16152\|CBR1_HUMAN;sp\|P16152-2 | 15 | 0 | 17471110 | 16397720 | 36161130 | 8524556 | 258198610 | 23926470 |
| tr\|B4DRA0\|B4DRA0_HUMAN;sp\|Q1449 | 15 | 0 | 17286550 | 9167570 | 47700812 | 3998619 | 126188940 | 6545080 |
| tr\|V9HW89\|V9HW89_HUMAN;sp\|Q007 | 15 | 0 | 13736310 | 1080510 | 4430231 | 3441679 | 55692000 | 8822280 |
| tr\|A0A024R4U3\|A0A024R4U3_HUMAN; | 15 | 0 | 13260000 | 4197761 | 15745160 | 4552766 | 52694000 | 7439970 |
| sp\|P13489\|RINI_HUMAN;tr\|A0A024RC8 | 15 | 0 | 13217000 | 4321600 | 24105835 | 4260540 | 49937020 | 6979460 |
| sp\|P15880\|RS2_HUMAN;tr\|Q8N5L9\|Q8 | 15 | 0 | 13176140 | 2791224 | 27589810 | 1705780 | 372108040 | 10704270 |
| tr\|A0A024RDV7\|A0A024RDV7_HUMAN | 15 | 0 | 12786476 | 5070530 | 33390500 | 3950700 | 78333259 | 8505910 |
| sp\|P49419-2\|AL7A1_HUMAN;sp\|P4941 | 15 | 0 | 12211000 | 4166763 | 18193580 | 2460340 | 41475000 | 3979960 |
| sp\|Q14677-3\|EPN4_HUMAN;sp\|Q1467 | 15 | 0 | 12126250 | 7557031 | 20748273 | 6277500 | 35134920 | 8078500 |
| sp\|Q5T749\|KPRP_HUMAN | 15 | 0 | 12071740 | 8000700 | 4196450 | 7186700 | 12056080 | 17611380 |
| tr\|Q5SRT3\|Q5SRT3_HUMAN;tr\|Q53FB0 | 15 | 0 | 11371500 | 18784468 | 27912993 | 10087550 | 212339140 | 39679160 |
| tr\|E9PIR7\|E9PIR7_HUMAN;tr\|B2R5P6\|E | 15 | 0 | 9806570 | 1917900 | 16835340 | 1338000 | 45458460 | 3275399 |
| tr\|V9HWK1\|V9HWK1_HUMAN;sp\|P601 | 15 | 0 | 9053820 | 7868670 | 5415500 | 5666900 | 9391100 | 20146000 |
| tr\|Q9BV28\|Q9BV28_HUMAN;tr\|B2RBD | 15 | 0.000369 | 8707000 | 0 | 0 | 0 | 0 | 0 |

| | | | | | | | | | |
|---|---|---|---|---|---|---|---|---|---|
| sp\|P50995-2\|ANX11_HUMAN;tr\|Q5T0G | 15 | 0 | 8307823 | 5818450 | 16979000 | 7209000 | 21823900 | 11400960 |
| sp\|Q9UBT2\|SAE2_HUMAN;tr\|B2RDF5\|E | 15 | 0 | 7916290 | 3846483 | 16020380 | 1880907 | 17460560 | 4600100 |
| sp\|O14497\|ARI1A_HUMAN;sp\|O14497- | 15 | 0 | 6936000 | 618350 | 2983000 | 542070 | 9343720 | 157530 |
| tr\|A0A0A0MTB8\|A0A0A0MTB8_HUMAN | 15 | 0 | 6547500 | 1741860 | 5804900 | 1741780 | 5441300 | 0 |
| sp\|P23258\|TBG1_HUMAN;sp\|Q9NRH3\| | 15 | 0 | 6136400 | 925750 | 14024472 | 906270 | 32351000 | 3448098 |
| sp\|P18124\|RL7_HUMAN;tr\|A0A024R81 | 15 | 0 | 6103140 | 3190890 | 19266550 | 1608840 | 301182460 | 3846120 |
| sp\|Q99615\|DNJC7_HUMAN;tr\|Q59EH7 | 15 | 0 | 5451900 | 2099700 | 10789660 | 3639677 | 14646000 | 1965784 |
| tr\|Q6IBR2\|Q6IBR2_HUMAN;sp\|Q9Y285 | 15 | 0 | 5282260 | 3741886 | 14867812 | 4051600 | 28282100 | 5785400 |
| tr\|H7BXH2\|H7BXH2_HUMAN;tr\|E9PKF6 | 15 | 0 | 5276000 | 102780 | 2627000 | 307290 | 21922000 | 1031800 |
| sp\|P39880-2\|CUX1_HUMAN;sp\|P39880 | 15 | 0 | 4962430 | 539870 | 2802000 | 147150 | 3179120 | 200500 |
| sp\|P04040\|CATA_HUMAN;tr\|B4DWK8\| | 15 | 0 | 4884540 | 3933830 | 3594550 | 5853010 | 2158310 | 3959830 |
| tr\|B4DYP7\|B4DYP7_HUMAN;sp\|Q96CW | 15 | 0 | 4813100 | 727370 | 3629300 | 231390 | 23380270 | 605930 |
| tr\|Q9HC39\|Q9HC39_HUMAN;tr\|Q9HBB | 15 | 0 | 4588600 | 357910 | 2321200 | 495960 | 13450000 | 818490 |
| sp\|P36871\|PGM1_HUMAN;tr\|B4DFP1\|I | 15 | 0 | 4563100 | 1446200 | 15598454 | 726801 | 31200370 | 3831470 |
| sp\|Q96ST3\|SIN3A_HUMAN;tr\|B3KQE3\| | 15 | 0 | 4258000 | 344410 | 1567300 | 196150 | 9877600 | 681980 |
| tr\|J3KNL6\|J3KNL6_HUMAN;sp\|O15027\| | 15 | 0 | 4210375 | 632660 | 4706610 | 831710 | 12912890 | 679790 |
| tr\|A0A024R2G2\|A0A024R2G2_HUMAN;\| | 15 | 0 | 4065900 | 100070 | 1028000 | 0 | 8225800 | 142160 |
| sp\|Q6PKG0\|LARP1_HUMAN;sp\|Q6PKG | 15 | 0 | 4005800 | 270550 | 974338 | 487080 | 12670640 | 2022660 |
| sp\|Q9NZB2\|F120A_HUMAN;sp\|Q9NZB2 | 15 | 0 | 3983400 | 903890 | 5107490 | 61333 | 20090620 | 1640300 |
| sp\|P09884\|DPOLA_HUMAN;tr\|A6NMQ | 15 | 0 | 3744200 | 186850 | 1279100 | 399960 | 13542000 | 747740 |
| tr\|Q6IB98\|Q6IB98_HUMAN;sp\|O15372 | 15 | 0 | 3594600 | 108680 | 15848700 | 785599 | 14011900 | 1395214 |
| sp\|Q9Y295\|DRG1_HUMAN;tr\|Q9UFA5\| | 15 | 0 | 3411600 | 479640 | 10207610 | 256440 | 21372000 | 2734933 |
| sp\|Q9UNE7\|CHIP_HUMAN;sp\|Q9UNE7 | 15 | 0 | 3375270 | 3306145 | 7598250 | 1807586 | 41727000 | 3410400 |
| tr\|Q6ZMY0\|Q6ZMY0_HUMAN | 15 | 0 | 2923532 | 0 | 470140 | 0 | 15090000 | 0 |
| sp\|Q9UK61-3\|F208A_HUMAN;sp\|Q9UK | 15 | 0 | 2740500 | 138470 | 462980 | 343720 | 12545780 | 137540 |
| sp\|Q8WUA4\|TF3C2_HUMAN;tr\|Q53QN | 15 | 0 | 2480800 | 74060 | 668620 | 0 | 16785320 | 756990 |
| tr\|A0A024R475\|A0A024R475_HUMAN;s | 15 | 0 | 2328580 | 363440 | 5794200 | 355680 | 12776800 | 1563570 |
| sp\|Q96L91-3\|EP400_HUMAN;sp\|Q96L9 | 15 | 0 | 2197400 | 0 | 1229200 | 44571 | 7511700 | 0 |
| sp\|Q9BY44-3\|EIF2A_HUMAN;sp\|Q9BY4 | 15 | 0 | 2160100 | 255700 | 4889600 | 693560 | 19679000 | 750110 |
| sp\|Q10570\|CPSF1_HUMAN;tr\|D3DWL9 | 15 | 0 | 2098600 | 350170 | 1399600 | 463560 | 12005240 | 573510 |
| tr\|Q6IAP9\|Q6IAP9_HUMAN;tr\|Q5T1M7 | 15 | 0 | 1459600 | 3357659 | 14677000 | 4529700 | 35035961 | 6173900 |
| sp\|Q9HC35\|EMAL4_HUMAN;tr\|B5MBZ0 | 15 | 0 | 1424800 | 165470 | 632860 | 0 | 12252360 | 626570 |
| tr\|A0A024R2Z6\|A0A024R2Z6_HUMAN;s | 15 | 0 | 1213300 | 198760 | 3881900 | 0 | 23881000 | 55333 |
| sp\|Q6P1N0\|C2D1A_HUMAN;sp\|Q6P1N | 15 | 0 | 1051000 | 793517 | 1569393 | 3351800 | 6820400 | 1022800 |
| sp\|Q8TAQ2-2\|SMRC2_HUMAN;sp\|Q8T | 15 | 0 | 968120 | 165420 | 544060 | 246790 | 12923406.6 | 233860 |
| tr\|B9A6J2\|B9A6J2_HUMAN;sp\|Q15042 | 15 | 0 | 963900 | 111930 | 1122500 | 294690 | 13311000 | 201400 |
| tr\|Q9UPN1\|Q9UPN1_HUMAN;tr\|F8VYE | 15 | 0 | 769310 | 840900 | 3075310 | 767080 | 18524000 | 312581 |
| tr\|V9HWH6\|V9HWH6_HUMAN;sp\|P004 | 15 | 0 | 541100 | 64278 | 0 | 229700 | 563180 | 1026174 |
| sp\|P63241\|IF5A1_HUMAN;tr\|I3L397\|I3 | 14 | 0 | 72448590 | 55798109 | 45385610 | 27433950 | 340028430 | 38916080 |
| sp\|P07737\|PROF1_HUMAN;tr\|K7EJ44\|K | 14 | 0 | 66733470 | 36016190 | 139953572 | 29617750 | 718661140 | 77883290 |
| sp\|P62826\|RAN_HUMAN;tr\|B5MDF5\|B | 14 | 0 | 51150400 | 47619960 | 83915500 | 35318610 | 39487250 | 17626290 |
| sp\|P27348\|1433T_HUMAN;tr\|B4DMT8\| | 14 | 0 | 18921000 | 2568484 | 15606000 | 649520 | 20238670 | 6911220 |
| tr\|Q53XL8\|Q53XL8_HUMAN;tr\|Q53HB3 | 14 | 0 | 18358580 | 2632900 | 37337000 | 6655788 | 68150790 | 16865340 |
| tr\|B4DWI8\|B4DWI8_HUMAN;sp\|Q8WX | 14 | 0 | 16226000 | 4873200 | 27342000 | 4052076 | 107553220 | 5850364 |
| tr\|C9J9K3\|C9J9K3_HUMAN;tr\|A0A024R | 14 | 0 | 15861630 | 1028790 | 7217860 | 1604400 | 21777760 | 15351620 |
| sp\|P62269\|RS18_HUMAN;tr\|Q5GGW2\| | 14 | 0 | 14371680 | 9212829 | 35563040 | 7281876 | 229374540 | 24140910 |
| sp\|Q7L2H7\|EIF3M_HUMAN;sp\|Q7L2H7 | 14 | 0 | 13422000 | 791230 | 20549000 | 2041400 | 34813380 | 6229050 |
| tr\|Q4VB24\|Q4VB24_HUMAN;tr\|A3R0T8 | 14 | 0 | 12981300 | 8628300 | 20966800 | 3965500 | 245119500 | 13411400 |
| tr\|Q6NXR8\|Q6NXR8_HUMAN;sp\|P6124 | 14 | 0 | 10496510 | 8287449 | 25724960 | 5903870 | 223190000 | 10606310 |
| sp\|Q86TB9\|PATL1_HUMAN;sp\|Q86TB9 | 14 | 0 | 10434300 | 990720 | 5780760 | 286880 | 12322120 | 0 |
| sp\|Q15645\|PCH2_HUMAN;tr\|H0YAL2\|H | 14 | 0 | 8430570 | 3391900 | 18217000 | 3853710 | 34593500 | 5125180 |
| sp\|P49756\|RBM25_HUMAN;sp\|P49756- | 14 | 0 | 8392100 | 915090 | 5802800 | 294480 | 40875000 | 2550500 |
| sp\|Q9UBB4\|ATX10_HUMAN;sp\|Q9UBB | 14 | 0 | 8107530 | 2008500 | 9614100 | 2802700 | 30288000 | 4464500 |
| sp\|P61011\|SRP54_HUMAN;tr\|G3V480\| | 14 | 0 | 7973200 | 1982300 | 14606000 | 1823500 | 25504000 | 4454800 |
| tr\|B2R858\|B2R858_HUMAN;sp\|P26196 | 14 | 0 | 7237080 | 3115400 | 16102000 | 2825400 | 30263730 | 3632700 |
| sp\|P04844-2\|RPN2_HUMAN;tr\|B2RE46 | 14 | 0 | 7043980 | 1094800 | 11515000 | 279140 | 3901100 | 0 |
| sp\|Q92878-3\|RAD50_HUMAN;sp\|Q928 | 14 | 0 | 5067500 | 2730210 | 1922300 | 628760 | 21318600 | 1469300 |
| tr\|A0A024R395\|A0A024R395_HUMAN;s | 14 | 0 | 4979703 | 618820 | 8104756 | 413548 | 19511480 | 1527590 |
| tr\|Q53FW2\|Q53FW2_HUMAN;sp\|P608 | 14 | 0 | 4537816 | 8229090 | 20572445 | 3586624 | 105780000 | 13228610 |
| sp\|Q86Y56\|DAAF5_HUMAN;sp\|Q86Y56 | 14 | 0 | 4387980 | 1221100 | 6678000 | 2130900 | 12710700 | 1057700 |
| sp\|O15397\|IPO8_HUMAN;sp\|O15397-2 | 14 | 0 | 4246400 | 456110 | 2279310 | 0 | 17987000 | 716550 |
| sp\|Q9BTW9\|TBCD_HUMAN;tr\|J3KR97\|. | 14 | 0 | 3962700 | 153620 | 2555500 | 286560 | 12421000 | 698410 |
| sp\|P46087\|NOP2_HUMAN;sp\|P46087-4 | 14 | 0 | 3883100 | 407560 | 1327500 | 49122 | 20064000 | 700140 |
| sp\|P42858\|HD_HUMAN;tr\|D3DVR8\|D3 | 14 | 0 | 3741900 | 0 | 289410 | 0 | 6382100 | 86558 |
| sp\|Q9BQ52-4\|RNZ2_HUMAN;tr\|B4DT15 | 14 | 0 | 3631900 | 352996 | 1008900 | 0 | 19587260 | 861810 |
| sp\|P19623\|SPEE_HUMAN;tr\|K7ESL0\|K7 | 14 | 0 | 3539300 | 4110700 | 8452800 | 2601090 | 60387000 | 6482970 |
| tr\|A1L3A9\|A1L3A9_HUMAN;sp\|Q66K14 | 14 | 0 | 3456700 | 261121 | 2126400 | 475010 | 12401000 | 443670 |
| tr\|A0MNN4\|A0MNN4_HUMAN;sp\|Q2T | 14 | 0 | 3169140 | 565350 | 4283300 | 175300 | 24437060 | 928885 |
| tr\|Q7RTQ9\|Q7RTQ9_HUMAN;tr\|Q7RTQ | 14 | 0 | 3004700 | 195250 | 3114400 | 124010 | 14616000 | 755498 |
| sp\|Q9UHX1-4\|PUF60_HUMAN;sp\|Q9UH | 14 | 0 | 2919800 | 2509600 | 28645000 | 1318900 | 42483000 | 6086612 |
| tr\|B3KY11\|B3KY11_HUMAN;tr\|A0A024R | 14 | 0 | 2914800 | 507550 | 3966100 | 0 | 31957400 | 505300 |
| tr\|A0A024R6D1\|A0A024R6D1_HUMAN;\| | 14 | 0 | 2837500 | 677021 | 1111400 | 577640 | 25675680 | 2125800 |
| tr\|A0A024R2Q4\|A0A024R2Q4_HUMAN;\| | 14 | 0 | 2823770 | 2376720 | 7602230 | 1095970 | 100303350 | 3597760 |
| sp\|O95782-2\|AP2A1_HUMAN;sp\|O957 | 14 | 0 | 2822695 | 558350 | 2438151 | 19985 | 3621200 | 0 |
| sp\|Q9Y371\|SHLB1_HUMAN;sp\|Q9Y371- | 14 | 0 | 2448400 | 3516100 | 31267000 | 8960900 | 67216910 | 46414310 |

| | | | | | | | | | |
|---|---|---|---|---|---|---|---|---|---|
| sp\|P62495-2\|ERF1_HUMAN;tr\|B7Z7P8\| | 14 | 0 | 2382800 | 1089000 | 3574800 | 144112 | 3878400 | 1327300 |
| sp\|O43795-2\|MYO1B_HUMAN;tr\|E9PDI | 14 | 0 | 2345500 | 247480 | 2170300 | 0 | 8950070 | 0 |
| tr\|Q6FHU2\|Q6FHU2_HUMAN;sp\|P1866 | 14 | 0 | 2176188 | 1282374 | 147610 | 660410 | 2456200 | 3798970 |
| sp\|P19367-4\|HXK1_HUMAN;tr\|B4DG62 | 14 | 0 | 2082100 | 718740 | 1834700 | 0 | 10394000 | 131940 |
| tr\|B2RTX8\|B2RTX8_HUMAN;sp\|Q7Z5K2 | 14 | 0 | 1949600 | 0 | 1616343 | 0 | 12995100 | 268430 |
| tr\|Q9NPK3\|Q9NPK3_HUMAN;tr\|O7604 | 14 | 0 | 1439800 | 0 | 543770 | 460330 | 10375000 | 0 |
| tr\|B3KUN1\|B3KUN1_HUMAN;sp\|P6777 | 14 | 0 | 1268580 | 2796200 | 5614279 | 1368400 | 64312000 | 4078400 |
| sp\|Q9Y4B6-2\|VPRBP_HUMAN;sp\|Q9Y4 | 14 | 0 | 1080000 | 121860 | 715690 | 110950 | 13142000 | 235650 |
| sp\|Q15785\|TOM34_HUMAN;tr\|B4DXU3 | 14 | 0 | 1050400 | 669150 | 6856300 | 856990 | 30081000 | 714700 |
| tr\|A8K2R3\|A8K2R3_HUMAN;sp\|O60341 | 14 | 0 | 941220 | 111020 | 0 | 0 | 6277800 | 277950 |
| tr\|Q5U0F4\|Q5U0F4_HUMAN;tr\|Q53HU | 14 | 0 | 869380 | 1206800 | 4025600 | 478630 | 23264090 | 1973280 |
| tr\|V9HW21\|V9HW21_HUMAN;sp\|P009 | 14 | 0 | 806270 | 5499340 | 1623000 | 2826080 | 3160090 | 18327460 |
| sp\|P40937-2\|RFC5_HUMAN;tr\|Q6LES9\| | 14 | 0 | 780460 | 0 | 1257360 | 217471 | 19960400 | 1734800 |
| sp\|Q9P265\|DIP2B_HUMAN;tr\|Q96IB4\| | 14 | 0 | 689030 | 195210 | 2463900 | 139310 | 13376000 | 333330 |
| tr\|Q5SQH4\|Q5SQH4_HUMAN;sp\|O6023 | 14 | 0 | 637670 | 645340 | 2394600 | 829350 | 16895000 | 2881800 |
| sp\|Q7Z406\|MYH14_HUMAN;sp\|Q7Z406 | 14 | 0 | 216736 | 1173800 | 0 | 892980 | 28715000 | 1941300 |
| sp\|Q14232\|EI2BA_HUMAN;sp\|Q14232- | 14 | 0 | 144820 | 311257 | 1359800 | 81643 | 17175000 | 1756758 |
| tr\|A8KAK1\|A8KAK1_HUMAN;sp\|Q9NYU | 14 | 0 | 0 | 0 | 0 | 0 | 0 | 460500 |
| sp\|P37837\|TALDO_HUMAN;tr\|F2Z393\| | 14 | 0 | 0 | 836760 | 369800 | 80307 | 579200 | 1724570 |
| tr\|V9HW63\|V9HW63_HUMAN;sp\|Q131 | 14 | 0 | 0 | 229510 | 121120 | 62111 | 1401600 | 1355100 |
| tr\|Q9UM02\|Q9UM02_HUMAN;tr\|B2RAI | 14 | 0 | 0 | 0 | 0 | 4057000 | 0 | 8496500 |
| tr\|M0R0F0\|M0R0F0_HUMAN;tr\|A0A024 | 13 | 0 | 62008630 | 15703662 | 74616120 | 13447110 | 304420660 | 30063370 |
| tr\|A0A024RDF4\|A0A024RDF4_HUMAN; | 13 | 0 | 45384300 | 14524730 | 80339320 | 16286150 | 173063200 | 33496290 |
| sp\|P25311\|ZA2G_HUMAN;tr\|C9JEV0\|C | 13 | 0 | 41092600 | 19371200 | 20236800 | 23095300 | 22253000 | 19424900 |
| tr\|V9HWF5\|V9HWF5_HUMAN;tr\|A8K48 | 13 | 0 | 38869330 | 22981870 | 61449060 | 11864430 | 211078080 | 61731930 |
| sp\|P27824\|CALX_HUMAN;sp\|P27824-2 | 13 | 0 | 28686420 | 7555800 | 40289910 | 8988320 | 17519000 | 1951994 |
| tr\|Q53FC7\|Q53FC7_HUMAN;tr\|B3KSM6 | 13 | 0 | 24510660 | 21047720 | 53781700 | 20700500 | 22015100 | 9962290 |
| tr\|A0A024R7T3\|A0A024R7T3_HUMAN;s | 13 | 0 | 23327000 | 6814800 | 22993109 | 3471500 | 37729970 | 7144190 |
| sp\|P55036\|PSMD4_HUMAN;tr\|Q5VWC | 13 | 0 | 19560188 | 4029200 | 28506000 | 5103500 | 59372870 | 8619950 |
| tr\|Q5VVD0\|Q5VVD0_HUMAN;sp\|P629 | 13 | 0 | 16079750 | 11671400 | 28544960 | 9947540 | 158972010 | 25190600 |
| tr\|Q6FHF5\|Q6FHF5_HUMAN;sp\|P1200 | 13 | 0 | 12282740 | 11169130 | 33052200 | 8148860 | 229922200 | 21886349 |
| sp\|P62906\|RL10A_HUMAN;tr\|Q1JQ76\| | 13 | 0 | 11386890 | 8999100 | 24832122 | 5664350 | 284420654 | 17681590 |
| tr\|B0YIW5\|B0YIW5_HUMAN;sp\|P48444 | 13 | 0 | 11318750 | 2023200 | 22837000 | 2790749 | 50892680 | 4616276 |
| sp\|O15371-2\|EIF3D_HUMAN;sp\|O1537 | 13 | 0 | 11205320 | 2333190 | 19383750 | 1777740 | 38215290 | 2426068 |
| sp\|P23381-2\|SYWC_HUMAN;tr\|A0A024 | 13 | 0 | 10571450 | 5790600 | 19421000 | 2568500 | 32384000 | 8823906 |
| sp\|P11387\|TOP1_HUMAN;tr\|B9EG90\|B | 13 | 0 | 9216700 | 1292723 | 1066500 | 0 | 38688260 | 1380600 |
| tr\|A0A024RAI1\|A0A024RAI1_HUMAN;s | 13 | 0 | 8636400 | 4325000 | 14111000 | 3179000 | 36944280 | 3099460 |
| tr\|V9HWE7\|V9HWE7_HUMAN;sp\|P515 | 13 | 0 | 8621400 | 1216000 | 19345000 | 3514600 | 37653000 | 5291090 |
| tr\|G3V4W0\|G3V4W0_HUMAN;tr\|B4DY0 | 13 | 0 | 8437530 | 2062570 | 10025958 | 2542420 | 96472320 | 14995300 |
| sp\|Q13363-2\|CTBP1_HUMAN;tr\|X5D8Y | 13 | 0 | 8184540 | 1787670 | 17449640 | 2380759 | 36462400 | 4373025 |
| sp\|P51114\|FXR1_HUMAN;sp\|P51114-2 | 13 | 0 | 7183680 | 3228840 | 10760000 | 346580 | 27501700 | 1093750 |
| sp\|Q12904\|AIMP1_HUMAN;sp\|Q12904 | 13 | 0 | 6225660 | 0 | 848510 | 1448600 | 61722663 | 3507700 |
| sp\|P16403\|H12_HUMAN;sp\|P16402\|H1 | 13 | 0 | 5769000 | 635980 | 1159563 | 1320502 | 10379460 | 8715590 |
| tr\|B3KMV5\|B3KMV5_HUMAN;tr\|A0A02 | 13 | 0 | 3644300 | 521300 | 2392800 | 565720 | 2160190 | 55047 |
| sp\|P20700\|LMNB1_HUMAN;tr\|Q6DC98 | 13 | 0 | 3559000 | 1982900 | 4161800 | 1496000 | 0 | 0 |
| sp\|Q99567\|NUP88_HUMAN;tr\|B7Z5I6\| | 13 | 0 | 3360500 | 809930 | 11012600 | 876310 | 31402000 | 1608695 |
| sp\|Q86X55-1\|CARM1_HUMAN;sp\|Q86X | 13 | 0 | 3319230 | 1988693 | 8816100 | 911930 | 17183890 | 3278100 |
| tr\|A0A024R4M0\|A0A024R4M0_HUMAN | 13 | 0 | 3133360 | 523776 | 7220250 | 516820 | 123022640 | 3904350 |
| sp\|O75400-2\|PR40A_HUMAN;sp\|O754( | 13 | 0 | 3109900 | 357530 | 3528704 | 59582 | 34593690 | 2106000 |
| sp\|Q15717\|ELAV1_HUMAN;sp\|Q15717 | 13 | 0 | 3066520 | 2537546 | 7410750 | 1559742 | 44241630 | 1747689 |
| sp\|O75475\|PSIP1_HUMAN;sp\|O75475- | 13 | 0 | 2887600 | 1988867 | 4938552 | 2523600 | 17412800 | 2437735 |
| sp\|P17480-2\|UBF1_HUMAN;tr\|E9PKP7 | 13 | 0 | 2783910 | 402300 | 0 | 145280 | 24761100 | 1535600 |
| sp\|O75717\|WDHD1_HUMAN;tr\|A8KAE( | 13 | 0 | 2718700 | 133680 | 1282104 | 0 | 10826000 | 855120 |
| sp\|Q9P2R3\|ANFY1_HUMAN;sp\|Q9P2R3 | 13 | 0 | 2710900 | 369680 | 2552800 | 204280 | 13418000 | 522880 |
| tr\|A0A024R0A8\|A0A024R0A8_HUMAN; | 13 | 0 | 2487390 | 507720 | 3508800 | 483390 | 16125800 | 1398500 |
| sp\|Q9Y6M1-1\|IF2B2_HUMAN;sp\|Q9Y6M | 13 | 0 | 2320100 | 717170 | 1353800 | 752462 | 18928000 | 3309681 |
| sp\|Q8NE71\|ABCF1_HUMAN;tr\|Q2L6I2\| | 13 | 0 | 2230950 | 206550 | 458580 | 240970 | 3548500 | 565850 |
| tr\|Q53FV3\|Q53FV3_HUMAN;tr\|B3KM4 | 13 | 0 | 2085100 | 894030 | 6389700 | 1607865 | 21531000 | 4779420 |
| tr\|A0A024R6Q1\|A0A024R6Q1_HUMAN; | 13 | 0 | 1893884 | 511980 | 4025800 | 417900 | 22602658 | 2473700 |
| tr\|E9PCY5\|E9PCY5_HUMAN;tr\|B4DKD0 | 13 | 0 | 1868500 | 0 | 1458400 | 571120 | 4217800 | 116830 |
| sp\|Q96F86\|EDC3_HUMAN;tr\|H3BPW9\| | 13 | 0 | 1768000 | 317280 | 4549000 | 799260 | 12931000 | 265780 |
| sp\|Q6KC79-2\|NIPBL_HUMAN;tr\|Q6IEH8 | 13 | 0 | 1749900 | 0 | 893110 | 0 | 9727700 | 0 |
| sp\|Q86U86-8\|PB1_HUMAN;sp\|Q86U86 | 13 | 0 | 1729500 | 3950130 | 764540 | 4603140 | 7481844 | 5869970 |
| tr\|Q5TZP7\|Q5TZP7_HUMAN;sp\|P27695 | 13 | 0 | 1616380 | 2994050 | 8184200 | 1673636 | 18544090 | 6586790 |
| tr\|A8K5T7\|A8K5T7_HUMAN;sp\|Q9Y2Z0 | 13 | 0 | 1471420 | 586826 | 7982300 | 1767653 | 23628000 | 4738815 |
| sp\|Q8N6T3\|ARFG1_HUMAN;tr\|Q53F62 | 13 | 0 | 1347100 | 3083123 | 17726600 | 5130346 | 55239720 | 22521913 |
| sp\|P06493\|CDK1_HUMAN;tr\|A0A024Q2 | 13 | 0 | 1163180 | 2326230 | 3925310 | 1693980 | 11757900 | 2613150 |
| tr\|E9PHA2\|E9PHA2_HUMAN;tr\|A8K4T8 | 13 | 0 | 1020300 | 46819 | 1936360 | 304740 | 19659110 | 2262000 |
| tr\|Q6DEN2\|Q6DEN2_HUMAN;sp\|Q141 | 13 | 0 | 1017400 | 312990 | 2747300 | 698460 | 15046000 | 1625900 |
| tr\|A0A024R7A8\|A0A024R7A8_HUMAN; | 13 | 0 | 878090 | 2147500 | 3164130 | 1001513 | 11747900 | 5631120 |
| tr\|A0PJ92\|A0PJ92_HUMAN;tr\|A8K9K6\| | 13 | 0 | 650450 | 0 | 736630 | 0 | 14328000 | 0 |
| tr\|A0A024R0R9\|A0A024R0R9_HUMAN;s | 13 | 0 | 610950 | 1064500 | 2297300 | 0 | 20063000 | 1566800 |
| tr\|A0A024RC67\|A0A024RC67_HUMAN;s | 13 | 0 | 602380 | 571420 | 4306540 | 541050 | 12779390 | 0 |
| tr\|Q9HBB3\|Q9HBB3_HUMAN;tr\|Q8TBK | 13 | 0 | 580620 | 1079530 | 684170 | 1001436 | 97757600 | 3439190 |
| sp\|Q12788\|TBL3_HUMAN;tr\|J3KNP2\|J3 | 13 | 0 | 537780 | 195970 | 4632428 | 539050 | 4500300 | 90362 |

| | | | | | | | | |
|---|---|---|---|---|---|---|---|---|
| tr\|B3KTM6\|B3KTM6_HUMAN;tr\|A2RUN | 13 | 0 | 253042 | 369220 | 696200 | 0 | 34397000 | 750313 |
| tr\|Q6IRT1\|Q6IRT1_HUMAN;tr\|Q6FI45\| | 13 | 0 | 239450 | 512560 | 2738800 | 0 | 4402500 | 0 |
| tr\|Q9GZV0\|Q9GZV0_HUMAN;tr\|A0A02 | 13 | 0 | 175456 | 731140 | 753440 | 0 | 3890050 | 485100 |
| sp\|P61011-2\|SRP54_HUMAN;tr\|G3V4F | 13 | 1 | 0 | 0 | 0 | 0 | 646830 | 0 |
| tr\|Q8WZ56\|Q8WZ56_HUMAN;tr\|Q5U0 | 13 | 1 | 0 | 0 | 0 | 0 | 406210 | 82752 |
| tr\|V9HWC7\|V9HWC7_HUMAN;sp\|P300 | 13 | 0 | 0 | 531140 | 458580 | 516572 | 2565300 | 2902310 |
| sp\|P06702\|S10A9_HUMAN;tr\|B2R4M6\| | 12 | 0 | 450728100 | 11618800 | 30893100 | 32009600 | 78376600 | 10658500 |
| sp\|P35251-2\|RFC1_HUMAN;sp\|P35251 | 12 | 0 | 93934000 | 2641569 | 28389800 | 711416 | 37522600 | 678430 |
| tr\|F8VY35\|F8VY35_HUMAN;sp\|P55209- | 12 | 0 | 37118170 | 8694776 | 63837221 | 13570959 | 78842290 | 26806787 |
| tr\|B7Z6P1\|B7Z6P1_HUMAN;tr\|A8K3K1\| | 12 | 0 | 30985780 | 10858300 | 35127250 | 14484840 | 13603890 | 4022580 |
| tr\|Q9HB00\|Q9HB00_HUMAN;sp\|Q0855 | 12 | 0 | 30366600 | 23926800 | 21073500 | 25087200 | 18519600 | 21864000 |
| tr\|A8K4Z4\|A8K4Z4_HUMAN;tr\|A0A024 | 12 | 0 | 25988500 | 34303290 | 61111760 | 19551200 | 468044600 | 74615100 |
| tr\|Q53G58\|Q53G58_HUMAN;tr\|B3KN0 | 12 | 0 | 12938006 | 2559500 | 18248904 | 2409200 | 35538010 | 5112899 |
| tr\|A0A024QYY3\|A0A024QYY3_HUMAN; | 12 | 0 | 12478000 | 669210 | 23715440 | 3928595 | 47724950 | 6408495 |
| tr\|B0ZBD0\|B0ZBD0_HUMAN;sp\|P39019 | 12 | 0 | 11876137 | 14064230 | 26662255 | 10262820 | 124281940 | 19511620 |
| tr\|Q53GS8\|Q53GS8_HUMAN;sp\|Q9H3P | 12 | 0 | 11566000 | 2583338 | 25481000 | 2831500 | 38509290 | 162470 |
| sp\|P29692-3\|EF1D_HUMAN;tr\|Q9BW34 | 12 | 0 | 10787110 | 8991120 | 21760170 | 6887230 | 83413130 | 14918507 |
| tr\|J3QT28\|J3QT28_HUMAN;sp\|O43684- | 12 | 0 | 10249190 | 1229400 | 15985160 | 4632174 | 49818400 | 9866158 |
| sp\|Q15084-3\|PDIA6_HUMAN;sp\|Q1508 | 12 | 0 | 9405700 | 6098224 | 21272720 | 5479374 | 8602360 | 8388000 |
| tr\|A0A087WYY6\|A0A087WYY6_HUMAN | 12 | 0 | 8621900 | 3748280 | 3376880 | 4105340 | 4609600 | 4841620 |
| tr\|A0A024R845\|A0A024R845_HUMAN;s | 12 | 0 | 8367390 | 8259525 | 16982952 | 5862638 | 24570000 | 2220352 |
| tr\|A0A024R994\|A0A024R994_HUMAN;s | 12 | 0 | 8127180 | 1468525 | 13331192 | 2704542 | 25934317 | 3464370 |
| tr\|Q6FHX6\|Q6FHX6_HUMAN;sp\|P3974 | 12 | 0 | 7700372 | 2214500 | 14722284 | 2086900 | 71183930 | 5077150 |
| sp\|Q0VDF9\|HSP7E_HUMAN;tr\|H7C2A1 | 12 | 0 | 7154900 | 1402100 | 8665900 | 699980 | 24004000 | 1977700 |
| sp\|P29692\|EF1D_HUMAN;tr\|D3DWK1\| | 12 | 0 | 6116890 | 5941821 | 12113180 | 4281440 | 31573440 | 7348881 |
| tr\|B4DE91\|B4DE91_HUMAN;sp\|P49189 | 12 | 0 | 5823030 | 239670 | 12860388 | 1296080 | 23654000 | 1382200 |
| sp\|O00629\|IMA3_HUMAN;tr\|H7C4F6\|H | 12 | 0 | 5129800 | 1155200 | 4238400 | 2006100 | 26668950 | 5501900 |
| tr\|B4DQ50\|B4DQ50_HUMAN;tr\|B4DRV | 12 | 0 | 5118880 | 2544650 | 2945260 | 3543130 | 3307100 | 2334210 |
| tr\|A0A024R2M7\|A0A024R2M7_HUMAN | 12 | 0 | 5019477 | 1225400 | 13077000 | 1693100 | 9515800 | 1371400 |
| sp\|P10155-3\|RO60_HUMAN;sp\|P10155 | 12 | 0 | 4847160 | 0 | 8926210 | 359150 | 17863680 | 1130700 |
| sp\|Q68E01-2\|INT3_HUMAN;sp\|Q68E01 | 12 | 0 | 4808940 | 0 | 1566500 | 340680 | 12990000 | 121120 |
| tr\|Q53GW1\|Q53GW1_HUMAN;sp\|Q8W | 12 | 0 | 4594200 | 779850 | 12453000 | 1003300 | 22247000 | 0 |
| sp\|P62917\|RL8_HUMAN;tr\|E9PKZ0\|E9P | 12 | 0 | 4587410 | 4312570 | 14084060 | 1744020 | 118600790 | 11889190 |
| tr\|V9HWC2\|V9HWC2_HUMAN;sp\|Q994 | 12 | 0 | 4557380 | 3328101 | 4714410 | 2648760 | 27579850 | 16775120 |
| sp\|O60343-2\|TBCD4_HUMAN;sp\|O6034 | 12 | 0 | 4538292 | 546080 | 1786700 | 528280 | 7537700 | 629830 |
| tr\|A0A087WTA5\|A0A087WTA5_HUMAN | 12 | 0 | 4403999 | 155470 | 2197600 | 0 | 23933000 | 622790 |
| sp\|Q9Y6G9\|DC1L1_HUMAN;tr\|Q6MZE7 | 12 | 0 | 4375200 | 737040 | 11148090 | 3684000 | 12096000 | 4280777 |
| sp\|Q96T76-9\|MMS19_HUMAN;sp\|Q96T | 12 | 0 | 4302900 | 302520 | 3440300 | 253410 | 11209000 | 774250 |
| tr\|U3KQC1\|U3KQC1_HUMAN;sp\|Q9BV | 12 | 0 | 4177800 | 247940 | 6968200 | 1108300 | 22393000 | 1797800 |
| sp\|P21281\|VATB2_HUMAN;tr\|Q59HF3\| | 12 | 0 | 4066050 | 2206100 | 8002200 | 1241800 | 4375000 | 639912 |
| sp\|P10768\|ESTD_HUMAN;tr\|X6RA14\|X | 12 | 0 | 4046140 | 5666100 | 7169592 | 3422400 | 87496000 | 4630197 |
| sp\|O00116\|ADAS_HUMAN;tr\|B7Z3Q4\|I | 12 | 0 | 3938800 | 1403000 | 13697000 | 1291500 | 7314600 | 0 |
| tr\|V9HWG9\|V9HWG9_HUMAN;tr\|B2R9 | 12 | 0 | 3870690 | 4682287 | 10046040 | 3395442 | 49078341 | 8752510 |
| sp\|Q9H0D6-2\|XRN2_HUMAN;tr\|B4DZC | 12 | 0 | 3848000 | 1311300 | 2638500 | 508860 | 11622940 | 1475100 |
| sp\|Q8NFD5\|ARI1B_HUMAN;sp\|Q8NFD | 12 | 0 | 3677400 | 87509 | 2237774 | 45285 | 6734100 | 168150 |
| sp\|Q86UP2-2\|KTN1_HUMAN;sp\|Q86UP | 12 | 0 | 3659900 | 0 | 767450 | 0 | 0 | 0 |
| tr\|Q75MT5\|Q75MT5_HUMAN;sp\|P3525 | 12 | 0 | 3640958 | 213760 | 8422150 | 760470 | 22148820 | 1697300 |
| tr\|Q05DH1\|Q05DH1_HUMAN;sp\|O1481 | 12 | 0 | 3561430 | 1205590 | 2296700 | 1051382 | 21311000 | 3709080 |
| tr\|Q0P607\|Q0P607_HUMAN;sp\|O9510 | 12 | 0 | 3405900 | 55459 | 1140000 | 860090 | 20576000 | 499910 |
| sp\|Q96T37-4\|RBM15_HUMAN;tr\|A0A08 | 12 | 0 | 3373400 | 583610 | 2007800 | 0 | 16864000 | 257700 |
| sp\|Q13136-2\|LIPA1_HUMAN;sp\|Q1313 | 12 | 0 | 3262600 | 406950 | 338500 | 87785 | 21354520 | 159590 |
| sp\|Q96PK6\|RBM14_HUMAN;tr\|B4DNG | 12 | 0 | 3238992 | 1406800 | 7560600 | 1287900 | 20818000 | 946100 |
| sp\|Q86XP3\|DDX42_HUMAN;tr\|A0A0A0 | 12 | 0 | 3014900 | 279540 | 712480 | 0 | 6978000 | 770080 |
| sp\|P22392-2\|NDKB_HUMAN;tr\|Q32Q1 | 12 | 0 | 2917710 | 7250260 | 5678260 | 4376770 | 14820000 | 35208910 |
| sp\|Q13617\|CUL2_HUMAN;tr\|A0A0A0M | 12 | 0 | 2663600 | 270280 | 5563299 | 354980 | 13938110 | 673830 |
| sp\|P49643\|PRI2_HUMAN;tr\|A8K7A0\|A | 12 | 0 | 2622700 | 0 | 2900600 | 291930 | 11723000 | 1419070 |
| tr\|A0A024R482\|A0A024R482_HUMAN;s | 12 | 0 | 2451100 | 2560000 | 9813000 | 2943600 | 13438000 | 4587900 |
| sp\|Q02543\|RL18A_HUMAN;tr\|M0R3D6 | 12 | 0 | 2310100 | 2749174 | 8955910 | 1119659 | 100621220 | 5947144 |
| sp\|O60664-4\|PLIN3_HUMAN;sp\|O6066 | 12 | 0 | 2261200 | 685390 | 1052800 | 0 | 17683000 | 7006100 |
| sp\|Q6P1J9\|CDC73_HUMAN;tr\|B4DV47\| | 12 | 0 | 2125520 | 301000 | 582610 | 314270 | 10431300 | 245390 |
| tr\|Q5RLJ0\|Q5RLJ0_HUMAN;tr\|Q549M8 | 12 | 0 | 2030750 | 3364100 | 4012590 | 2641000 | 59354500 | 5481600 |
| tr\|B4DS37\|B4DS37_HUMAN;sp\|O14976 | 12 | 0 | 2003600 | 267380 | 745350 | 688700 | 19255000 | 1851730 |
| tr\|Q6NX51\|Q6NX51_HUMAN;sp\|Q96A0 | 12 | 0 | 1960100 | 525870 | 1278100 | 103580 | 8945700 | 209655 |
| tr\|Q6DHZ8\|Q6DHZ8_HUMAN;tr\|B2RBM | 12 | 0 | 1946700 | 97795 | 1225000 | 302480 | 11789000 | 315140 |
| tr\|Q96FS1\|Q96FS1_HUMAN;sp\|O60716 | 12 | 0 | 1934100 | 0 | 1640200 | 0 | 8818424 | 381720 |
| sp\|Q96FW1\|OTUB1_HUMAN;tr\|J3KR44 | 12 | 0 | 1876200 | 3084600 | 9900200 | 3054566 | 53222000 | 4946500 |
| sp\|Q14671-2\|PUM1_HUMAN;sp\|Q1467 | 12 | 0 | 1817960 | 87854 | 2594790 | 0 | 19573290 | 441060 |
| sp\|Q12873-2\|CHD3_HUMAN;sp\|Q1287 | 12 | 0.000699 | 1797490 | 1511510 | 175500 | 964940 | 0 | 548689 |
| sp\|Q1KMD3\|HNRL2_HUMAN;tr\|H3BQZ | 12 | 0 | 1762800 | 0 | 1097100 | 0 | 6714400 | 721060 |
| sp\|P11908\|PRPS2_HUMAN;sp\|P11908- | 12 | 0 | 1691800 | 2335300 | 4101610 | 913890 | 29326000 | 1801760 |
| tr\|G3XAM7\|G3XAM7_HUMAN;tr\|B4E2C | 12 | 0 | 1488876 | 350750 | 3014500 | 132460 | 12438720 | 861930 |
| tr\|Q96F88\|Q96F88_HUMAN;sp\|Q99575 | 12 | 0 | 1465100 | 0 | 924700 | 0 | 4774530 | 549390 |
| sp\|Q9H0B6\|KLC2_HUMAN;sp\|Q9H0B6- | 12 | 0 | 1236000 | 165540 | 1457000 | 91759 | 7630060 | 202820 |
| sp\|Q9H9Y6\|RPA2_HUMAN;sp\|Q9H9Y6- | 12 | 0 | 1113300 | 86867 | 1045200 | 0 | 9890595 | 457320 |
| sp\|P07741\|APT_HUMAN;sp\|P07741-2\| | 12 | 0 | 1096870 | 1791100 | 1788600 | 742894 | 3163000 | 8309900 |

| | | | | | | | | | |
|---|---|---|---|---|---|---|---|---|---|
| tr\|V9HWF2\|V9HWF2_HUMAN;sp\|P409 | 12 | 0 | 1059217 | 803020 | 335350 | 0 | 794790 | 2419571 |
| tr\|B7ZKT9\|B7ZKT9_HUMAN;sp\|Q2M38 | 12 | 0 | 989340 | 0 | 734960 | 0 | 16828000 | 0 |
| tr\|E7EQ69\|E7EQ69_HUMAN;sp\|Q9GZZ | 12 | 0 | 906480 | 645620 | 2948700 | 460830 | 23506000 | 1500200 |
| tr\|Q6UQL6\|Q6UQL6_HUMAN;sp\|O757 | 12 | 0 | 731330 | 601890 | 960450 | 0 | 21966000 | 377740 |
| tr\|Q53HG7\|Q53HG7_HUMAN;sp\|Q142 | 12 | 0 | 635160 | 0 | 930900 | 0 | 1433700 | 151210 |
| tr\|Q9UNF3\|Q9UNF3_HUMAN;tr\|F5H1D | 12 | 0 | 559860 | 0 | 214360 | 0 | 4294100 | 0 |
| tr\|E7EVJ5\|E7EVJ5_HUMAN;sp\|Q96F07- | 12 | 0 | 559490 | 0 | 0 | 0 | 2314200 | 0 |
| tr\|Q53G71\|Q53G71_HUMAN;tr\|V9HW8 | 12 | 0 | 467080 | 84584 | 0 | 0 | 313600 | 1170680 |
| tr\|A0A024R5M9\|A0A024R5M9_HUMAN | 12 | 0 | 419420 | 0 | 737414 | 0 | 2083500 | 0 |
| tr\|A0A024RAE1\|A0A024RAE1_HUMAN; | 12 | 0 | 232331 | 479050 | 864120 | 165699 | 16543000 | 265030 |
| sp\|Q92974-3\|ARHG2_HUMAN;sp\|Q929 | 12 | 0 | 184370 | 0 | 483110 | 0 | 10532720 | 112610 |
| sp\|Q07955\|SRSF1_HUMAN;tr\|J3KTL2\|J | 12 | 0 | 0 | 0 | 271120 | 0 | 12129000 | 1573900 |
| tr\|A0A024RDQ0\|A0A024RDQ0_HUMAN | 12 | 0 | 0 | 0 | 0 | 0 | 0 | 521800 |
| tr\|H9KV75\|H9KV75_HUMAN;tr\|B7Z565 | 12 | 0 | 0 | 0 | 0 | 0 | 0 | 48229 |
| sp\|P31946-2\|1433B_HUMAN;tr\|V9HWD | 12 | 0 | 0 | 261270 | 518780 | 0 | 4315500 | 1209900 |
| tr\|V9HWB5\|V9HWB5_HUMAN;sp\|Q151 | 12 | 0 | 0 | 140900 | 140280 | 150130 | 0 | 2059107 |
| sp\|P12081-4\|SYHC_HUMAN;sp\|P12081 | 12 | 0 | 0 | 0 | 0 | 177033 | 0 | 388504 |
| tr\|Q5T081\|Q5T081_HUMAN;sp\|P18754 | 11 | 0 | 34673180 | 16691795 | 63887000 | 10334500 | 80713440 | 12733075 |
| tr\|A8K4W5\|A8K4W5_HUMAN;sp\|Q9BV | 11 | 0 | 26556380 | 70142 | 45675355 | 5664600 | 55250100 | 5887500 |
| sp\|P26368-2\|U2AF2_HUMAN;sp\|P2636 | 11 | 0 | 21508000 | 3227400 | 38151000 | 6482900 | 71456000 | 8669939 |
| tr\|Q6LET3\|Q6LET3_HUMAN;sp\|P00492 | 11 | 0 | 21480220 | 11716450 | 50343570 | 8243830 | 60750570 | 14071681 |
| sp\|P05089\|ARGI1_HUMAN;sp\|P05089-2 | 11 | 0 | 17645980 | 5140280 | 4464280 | 7657900 | 2281370 | 3032400 |
| tr\|A0A024QZF1\|A0A024QZF1_HUMAN; | 11 | 0 | 13022210 | 5602220 | 32039100 | 6844994 | 52888000 | 4484600 |
| tr\|V9HW12\|V9HW12_HUMAN;sp\|P321 | 11 | 0 | 11131900 | 6395610 | 26046360 | 5777830 | 22003530 | 9820700 |
| tr\|A0A024R9D2\|A0A024R9D2_HUMAN; | 11 | 0 | 10016072 | 3774665 | 6882200 | 1408608 | 725880 | 0 |
| tr\|B4DM97\|B4DM97_HUMAN;sp\|P611 | 11 | 0 | 8962600 | 2540300 | 16659000 | 4172800 | 27001000 | 9711000 |
| sp\|Q9UKX7-2\|NUP50_HUMAN;tr\|A0A0 | 11 | 0 | 8097100 | 2202500 | 23618915 | 3666100 | 37669132 | 4662500 |
| sp\|P38159\|RBMX_HUMAN;sp\|P38159-2 | 11 | 0 | 7966919 | 1378900 | 19098160 | 592920 | 61683900 | 3629105 |
| tr\|A0A024R6S1\|A0A024R6S1_HUMAN;s | 11 | 0 | 7113000 | 3349400 | 14835000 | 1752200 | 27982000 | 9292230 |
| tr\|Q8NCK5\|Q8NCK5_HUMAN;tr\|A0MN | 11 | 0 | 6657200 | 1740500 | 10672000 | 1419600 | 33291000 | 4453710 |
| sp\|P40429\|RL13A_HUMAN;tr\|Q9BSQ6\| | 11 | 0 | 6580700 | 1911780 | 11984760 | 1438190 | 176494600 | 10681660 |
| sp\|Q68EM7-6\|RHG17_HUMAN;sp\|Q68 | 11 | 0 | 6175600 | 410380 | 2172400 | 0 | 7753540 | 0 |
| sp\|O95336\|6PGL_HUMAN;tr\|M0R261\|M | 11 | 0 | 5987140 | 1411700 | 10191000 | 1340178 | 60211000 | 2868556 |
| tr\|E7EN20\|E7EN20_HUMAN;tr\|A0A024 | 11 | 0 | 5894700 | 736570 | 3703319 | 375180 | 19087000 | 1685100 |
| tr\|Q53Z07\|Q53Z07_HUMAN;sp\|P32969 | 11 | 0 | 5487520 | 5672800 | 12547000 | 3029810 | 250807290 | 11709750 |
| tr\|B4E1E2\|B4E1E2_HUMAN;sp\|O14964 | 11 | 0 | 5255100 | 673820 | 2891500 | 113300 | 15255220 | 694700 |
| tr\|B7Z4K8\|B7Z4K8_HUMAN;tr\|E7ETZ4\| | 11 | 0 | 5148200 | 1491500 | 8481800 | 982060 | 28522000 | 1002528 |
| sp\|Q15813\|TBCE_HUMAN;sp\|Q15813-2 | 11 | 0 | 5089200 | 0 | 8261250 | 1700700 | 18306580 | 952280 |
| sp\|Q9BY77\|PDIP3_HUMAN;tr\|F6VRR5\| | 11 | 0 | 4636300 | 1192200 | 7133100 | 1098000 | 27772000 | 2563640 |
| tr\|A0A087WUK2\|A0A087WUK2_HUMAN | 11 | 0 | 4475550 | 4238173 | 11017230 | 2812540 | 86388238 | 7523770 |
| tr\|B4DQT0\|B4DQT0_HUMAN;tr\|B4E1J2 | 11 | 0 | 4311000 | 606360 | 7380800 | 267600 | 24863000 | 1480600 |
| sp\|P56545\|CTBP2_HUMAN;tr\|Q5SQP8\| | 11 | 0 | 4168300 | 1441392 | 8899470 | 601920 | 21164150 | 1743500 |
| sp\|P98175-2\|RBM10_HUMAN;sp\|P9817 | 11 | 0 | 4015300 | 634820 | 1810800 | 141760 | 11788000 | 1664100 |
| sp\|O15294\|OGT1_HUMAN;sp\|O15294-3 | 11 | 0 | 3932288 | 538710 | 2897800 | 516320 | 5100370 | 539690 |
| sp\|P55263-2\|ADK_HUMAN;sp\|P55263\| | 11 | 0 | 3910000 | 731940 | 5299300 | 1384368 | 7095200 | 1951700 |
| tr\|Q2L6I0\|Q2L6I0_HUMAN;sp\|Q96QC0 | 11 | 0 | 3880200 | 1546200 | 1861700 | 878610 | 17395200 | 700190 |
| sp\|P62750\|RL23A_HUMAN;tr\|H7BY10\| | 11 | 0 | 3507490 | 280400 | 9634010 | 2123310 | 126858500 | 6240030 |
| sp\|P62280\|RS11_HUMAN;tr\|M0QZC5\|M | 11 | 0 | 3506110 | 2012000 | 13506211 | 618860 | 110338160 | 5173568 |
| sp\|Q15907\|RB11B_HUMAN;tr\|H3BMH2 | 11 | 0 | 3376370 | 5005100 | 11860200 | 4061500 | 8614870 | 3204300 |
| tr\|A8K5D9\|A8K5D9_HUMAN;sp\|Q9NQV | 11 | 0 | 3316900 | 82122 | 1269300 | 0 | 3305500 | 0 |
| sp\|Q52LJ0-2\|FA98B_HUMAN;sp\|Q52LJ0 | 11 | 0 | 3314220 | 1832844 | 10345860 | 1432103 | 28839100 | 4869560 |
| sp\|P31947\|1433S_HUMAN;sp\|P31947-2 | 11 | 0 | 3086069 | 1690640 | 0 | 0 | 9762890 | 3974400 |
| sp\|Q9Y383\|LC7L2_HUMAN;sp\|Q9Y383- | 11 | 0 | 3024800 | 356820 | 5541800 | 156160 | 10276000 | 2064700 |
| tr\|B4E3E6\|B4E3E6_HUMAN;tr\|B4DDB6\| | 11 | 0 | 2859614 | 585994 | 4637008 | 592848 | 36396000 | 4568770 |
| tr\|Q6IAU5\|Q6IAU5_HUMAN;tr\|B2R665 | 11 | 0 | 2840382 | 3076834 | 18215000 | 678820 | 16195000 | 604420 |
| sp\|Q99661\|KIF2C_HUMAN;sp\|Q99661- | 11 | 0 | 2583500 | 1254951 | 5151052 | 4072110 | 15276730 | 5983401 |
| sp\|Q9Y5K5-2\|UCHL5_HUMAN;sp\|Q9Y5U | 11 | 0 | 2562980 | 0 | 3563200 | 2106700 | 29953000 | 5591780 |
| sp\|O43491\|E41L2_HUMAN;sp\|O43491- | 11 | 0 | 2560100 | 185434 | 1133700 | 0 | 4731000 | 156650 |
| sp\|Q96EV2\|RBM33_HUMAN;sp\|Q96EV | 11 | 0 | 2375700 | 0 | 2755150 | 0 | 12879000 | 208850 |
| tr\|Q53HS1\|Q53HS1_HUMAN;sp\|Q9NRC | 11 | 0 | 2331300 | 0 | 5560570 | 0 | 3447200 | 0 |
| tr\|A0A087X0Q1\|A0A087X0Q1_HUMAN; | 11 | 0 | 2277400 | 2780900 | 4306700 | 2808400 | 20775000 | 2330100 |
| sp\|Q5T6F2\|UBAP2_HUMAN;tr\|B4DRB6 | 11 | 0 | 2185900 | 304508 | 1839600 | 405160 | 12207000 | 0 |
| sp\|Q9NRY5\|F1142_HUMAN;tr\|E7ESJ7\|E | 11 | 0.00037 | 2135600 | 0 | 0 | 327270 | 4749100 | 1270300 |
| tr\|B2R7T8\|B2R7T8_HUMAN;sp\|P47756- | 11 | 0 | 2126130 | 7428454 | 3853990 | 1536336 | 30193770 | 6206430 |
| tr\|Q4ZG72\|Q4ZG72_HUMAN;tr\|A0A024 | 11 | 0 | 2074300 | 217920 | 3826400 | 0 | 22444000 | 366121 |
| tr\|A0A024R534\|A0A024R534_HUMAN;s | 11 | 0 | 1704136 | 0 | 1133100 | 0 | 6428160 | 801924 |
| sp\|Q15654\|TRIP6_HUMAN;tr\|F2ZC06\|F | 11 | 0 | 1643500 | 299330 | 6057200 | 284710 | 12073610 | 480655 |
| tr\|V9HWI0\|V9HWI0_HUMAN;sp\|P1455 | 11 | 0 | 1443210 | 316980 | 983880 | 0 | 7738920 | 2814360 |
| sp\|Q13561\|DCTN2_HUMAN;sp\|Q13561 | 11 | 0 | 1270800 | 214580 | 7059700 | 352900 | 20992000 | 5790800 |
| tr\|Q5TZZ9\|Q5TZZ9_HUMAN;sp\|P04083 | 11 | 0 | 1236180 | 1606150 | 1902520 | 2146760 | 21625520 | 5343860 |
| sp\|P48382-2\|RFX5_HUMAN;tr\|F8W689 | 11 | 0 | 1117000 | 506930 | 2059100 | 0 | 16271395 | 0 |
| tr\|A0A087WW77\|A0A087WW77_HUMA | 11 | 0 | 1101800 | 201300 | 1485620 | 0 | 11378360 | 0 |
| sp\|P60900\|PSA6_HUMAN;tr\|G3V5Z7\|G | 11 | 0 | 1011770 | 644260 | 714500 | 680130 | 3600970 | 2956170 |
| tr\|B4DYK6\|B4DYK6_HUMAN;tr\|A0A024 | 11 | 0 | 949940 | 0 | 0 | 312340 | 4961000 | 0 |
| sp\|O43660\|PLRG1_HUMAN;sp\|O43660- | 11 | 0 | 918390 | 305180 | 3502900 | 331010 | 12106000 | 265930 |

| | | | | | | | | | |
|---|---|---|---|---|---|---|---|---|---|
| sp\|Q6NZY4\|ZCHC8_HUMAN;tr\|A8K559 | 11 | 0 | 901500 | 0 | 774210 | 0 | 20024000 | 641950 |
| tr\|B4DS79\|B4DS79_HUMAN;tr\|B4DKH5 | 11 | 0.000364 | 862540 | 0 | 0 | 234050 | 0 | 0 |
| tr\|A0A024R9G4\|A0A024R9G4_HUMAN; | 11 | 0 | 719290 | 1151300 | 2762170 | 1386300 | 32409000 | 2550800 |
| tr\|A1L3A7\|A1L3A7_HUMAN;sp\|Q7Z417 | 11 | 0 | 660182 | 0 | 11465154 | 176000 | 20594370 | 915810 |
| tr\|D5MQE1\|D5MQE1_HUMAN;tr\|B2RE5 | 11 | 0 | 633300 | 148020 | 1534900 | 178700 | 17737000 | 1015000 |
| sp\|Q9NXF1-2\|TEX10_HUMAN;tr\|A0A02 | 11 | 0 | 591240 | 0 | 688570 | 0 | 13251000 | 0 |
| sp\|Q9HCK8\|CHD8_HUMAN;sp\|Q9HCK8 | 11 | 0 | 468850 | 0 | 233530 | 0 | 9851100 | 0 |
| sp\|Q9NYV4-2\|CDK12_HUMAN;sp\|Q9N | 11 | 0 | 428350 | 0 | 573360 | 0 | 10713000 | 0 |
| sp\|Q86W42\|THOC6_HUMAN;sp\|Q86W | 11 | 0 | 421500 | 178360 | 696480 | 0 | 18361000 | 1065450 |
| sp\|Q13257\|MD2L1_HUMAN;sp\|Q13257 | 11 | 0 | 411520 | 0 | 791470 | 375570 | 30210990 | 369360 |
| tr\|E9PC74\|E9PC74_HUMAN;sp\|Q13144 | 11 | 0 | 384950 | 458430 | 703190 | 0 | 18523650 | 2381540 |
| tr\|Q6FGU2\|Q6FGU2_HUMAN;sp\|P2391 | 11 | 0 | 263660 | 1896100 | 1643930 | 756590 | 21740270 | 913150 |
| tr\|Q6FGS1\|Q6FGS1_HUMAN;sp\|O4339 | 11 | 0 | 238840 | 242240 | 712800 | 0 | 3542200 | 489670 |
| sp\|P61981\|1433G_HUMAN;tr\|B3KNB4\| | 11 | 0 | 225980 | 0 | 1834783 | 7288050 | 2962100 | 24357100 |
| tr\|D9IAI1\|D9IAI1_HUMAN;sp\|P30086\|F | 11 | 0 | 204070 | 618340 | 118750 | 177490 | 732570 | 1649382 |
| sp\|Q9GZS3\|WDR61_HUMAN;tr\|H0YN8 | 11 | 0 | 187330 | 408180 | 1809800 | 0 | 22715560 | 1472200 |
| tr\|B4DHS5\|B4DHS5_HUMAN;sp\|Q9NXH | 11 | 0 | 167170 | 0 | 1541400 | 0 | 12189000 | 306680 |
| sp\|Q96EE3\|SEH1_HUMAN;sp\|Q96EE3-1 | 11 | 0 | 158820 | 111040 | 1167300 | 146630 | 14172930 | 314780 |
| sp\|Q04760-2\|LGUL_HUMAN;tr\|X5DNM | 11 | 0 | 65656 | 175980 | 676610 | 115420 | 4964400 | 3469579 |
| sp\|O14979-3\|HNRDL_HUMAN;sp\|O149 | 11 | 0.000693 | 0 | 0 | 199200 | 0 | 1607200 | 0 |
| sp\|Q92625\|ANS1A_HUMAN;tr\|Q49AR9 | 11 | 0 | 0 | 0 | 287010 | 0 | 9597800 | 0 |
| sp\|Q9UPN9-2\|TRI33_HUMAN | 11 | 0.000355 | 0 | 0 | 0 | 0 | 365430 | 0 |
| tr\|B4DHY7\|B4DHY7_HUMAN | 11 | 1 | 0 | 0 | 0 | 0 | 3492700 | 0 |
| tr\|B4DI68\|B4DI68_HUMAN;tr\|G5E9S2\|( | 11 | 1 | 0 | 0 | 0 | 0 | 541700 | 0 |
| tr\|Q68E05\|Q68E05_HUMAN;sp\|O43399 | 11 | 1 | 0 | 0 | 0 | 0 | 0 | 0 |
| tr\|Q86U75\|Q86U75_HUMAN;tr\|A9CQZ | 11 | 1 | 0 | 0 | 0 | 0 | 0 | 0 |
| tr\|J3QSV6\|J3QSV6_HUMAN;tr\|A0PJ61\| | 11 | 0 | 0 | 0 | 1108500 | 0 | 18626460 | 421071 |
| sp\|Q15019\|SEPT2_HUMAN;sp\|Q15019- | 11 | 0 | 0 | 0 | 0 | 0 | 0 | 686620 |
| sp\|O00429-4\|DNM1L_HUMAN;sp\|O004 | 11 | 0 | 0 | 94268 | 1040900 | 0 | 1203500 | 318200 |
| tr\|B2R6U8\|B2R6U8_HUMAN;tr\|A0A024 | 11 | 0 | 0 | 381230 | 525030 | 0 | 4956100 | 1659900 |
| sp\|Q5SSJ5\|HP1B3_HUMAN;tr\|X6RGJ2\| | 11 | 0 | 0 | 294930 | 2441770 | 162680 | 25345300 | 1445270 |
| tr\|Q05CN7\|Q05CN7_HUMAN;sp\|Q9UK | 11 | 0 | 0 | 910420 | 2294540 | 1066100 | 10266100 | 1571800 |
| sp\|P28074\|PSB5_HUMAN;sp\|P28074-3 | 11 | 0 | 0 | 0 | 122620 | 141740 | 522530 | 672150 |
| tr\|F8W543\|F8W543_HUMAN | 11 | 1 | 0 | 0 | 0 | 153680 | 0 | 0 |
| tr\|B4DVJ0\|B4DVJ0_HUMAN;tr\|K7EQ48 | 11 | 0 | 0 | 140830 | 0 | 145630 | 0 | 2648210 |
| sp\|P05109\|S10A8_HUMAN | 10 | 0 | 292375100 | 13296300 | 28627600 | 34376900 | 47099600 | 15969200 |
| sp\|P04632\|CPNS1_HUMAN;tr\|K7ELJ7\|K | 10 | 0 | 45288340 | 10646830 | 78166000 | 6810900 | 57251000 | 15659376 |
| tr\|Q96HT3\|Q96HT3_HUMAN;sp\|O1516 | 10 | 0 | 41290900 | 125930 | 33595500 | 16735700 | 47467000 | 50980000 |
| tr\|A0A024R3Q3\|A0A024R3Q3_HUMAN; | 10 | 0 | 29106820 | 41876370 | 73948710 | 21673918 | 169311550 | 35314410 |
| sp\|P62249\|RS16_HUMAN;tr\|M0R210\|M | 10 | 0 | 26782870 | 11893570 | 40191890 | 9130680 | 292052500 | 19417610 |
| sp\|P61160\|ARP2_HUMAN;sp\|P61160-2 | 10 | 0 | 9953806 | 0 | 20234280 | 3599800 | 24946520 | 2604084 |
| sp\|Q96P63\|SPB12_HUMAN;sp\|Q96P63 | 10 | 0 | 8467900 | 7142200 | 7084500 | 10292900 | 5541500 | 5757010 |
| sp\|Q8IWX8\|CHERP_HUMAN;tr\|J3QK89 | 10 | 0 | 8318100 | 1287800 | 4307500 | 541870 | 27433240 | 1878500 |
| tr\|F2Z2V0\|F2Z2V0_HUMAN;sp\|Q99829 | 10 | 0 | 7588700 | 839749 | 13687000 | 2665180 | 42234830 | 7175330 |
| tr\|A8K5J1\|A8K5J1_HUMAN;sp\|P11172\| | 10 | 0 | 7460100 | 1851100 | 17354000 | 2051600 | 24876000 | 4842799 |
| tr\|Q5JR94\|Q5JR94_HUMAN;sp\|P62241\| | 10 | 0 | 7270860 | 4771020 | 18445090 | 3302100 | 252955000 | 12329270 |
| sp\|P35659\|DEK_HUMAN;sp\|P35659-2\| | 10 | 0 | 6824800 | 4116951 | 12684000 | 2943700 | 20804140 | 7048610 |
| sp\|P11216\|PYGB_HUMAN;tr\|Q59GM9\| | 10 | 0 | 6316600 | 2095600 | 8044600 | 816990 | 24166200 | 253550 |
| tr\|Q6NZ55\|Q6NZ55_HUMAN;tr\|A8K4C8 | 10 | 0 | 5950750 | 3718710 | 17443970 | 1159890 | 200841550 | 4658020 |
| sp\|Q09028-3\|RBBP4_HUMAN;sp\|Q0902 | 10 | 0 | 5857700 | 2117500 | 6787500 | 538870 | 18789480 | 3839950 |
| sp\|P18085\|ARF4_HUMAN;tr\|C9JPM4\|C | 10 | 0 | 5750810 | 8550300 | 9328600 | 4869200 | 28111000 | 7419700 |
| sp\|P51149\|RAB7A_HUMAN;tr\|C9J592\|( | 10 | 0 | 5397040 | 6415100 | 8486740 | 2817780 | 12918000 | 2457080 |
| sp\|Q96SN8-3\|CK5P2_HUMAN;tr\|B9EG7 | 10 | 0 | 5260400 | 0 | 2225577 | 0 | 1418200 | 0 |
| tr\|A6NJA2\|A6NJA2_HUMAN;sp\|P54578 | 10 | 0 | 5217700 | 829510 | 2155700 | 1603300 | 15532000 | 3855714 |
| tr\|A0A024R9J0\|A0A024R9J0_HUMAN;sp | 10 | 0 | 5120500 | 146206 | 2295200 | 0 | 16549000 | 1373100 |
| tr\|A0A087WSW7\|A0A087WSW7_HUMA | 10 | 0 | 5031600 | 920660 | 3543750 | 485540 | 13355010 | 390990 |
| sp\|P52306\|GDS1_HUMAN;sp\|P52306-5 | 10 | 0 | 4814680 | 1554762 | 11621000 | 2120176 | 14218200 | 1663966 |
| tr\|A0A024RAD5\|A0A024RAD5_HUMAN | 10 | 0 | 4686200 | 164620 | 8475600 | 199760 | 1063400 | 0 |
| tr\|D6W625\|D6W625_HUMAN;sp\|Q131 | 10 | 0 | 4278800 | 762150 | 771310 | 423870 | 7821500 | 218740 |
| tr\|B2RCJ6\|B2RCJ6_HUMAN;sp\|Q9BZH6 | 10 | 0 | 4046170 | 118740 | 3208520 | 0 | 6276510 | 497570 |
| tr\|A0A024R1U4\|A0A024R1U4_HUMAN; | 10 | 0 | 3925856 | 7219680 | 15932587 | 5939750 | 9084700 | 3887780 |
| sp\|P43034\|LIS1_HUMAN;tr\|B4DF38\|B4 | 10 | 0 | 3836170 | 1068873 | 6811800 | 960310 | 29462250 | 3468901 |
| sp\|Q7Z3U7-2\|MON2_HUMAN;tr\|B7ZM | 10 | 0 | 3811200 | 0 | 1071300 | 741730 | 4892100 | 0 |
| tr\|E7EVX8\|E7EVX8_HUMAN;tr\|F1T0A5\| | 10 | 0 | 3626000 | 361610 | 8870800 | 859950 | 28272540 | 347760 |
| sp\|Q9UI26\|IPO11_HUMAN;sp\|Q9UI26- | 10 | 0 | 3530700 | 0 | 3043830 | 0 | 12384000 | 406110 |
| tr\|Q5BKZ2\|Q5BKZ2_HUMAN;sp\|P5229 | 10 | 0 | 3312100 | 257570 | 8681100 | 663980 | 19665000 | 1880900 |
| sp\|P05023-3\|AT1A1_HUMAN;tr\|B7Z3V | 10 | 0 | 3177820 | 127310 | 1413220 | 0 | 0 | 0 |
| tr\|B1AKK2\|B1AKK2_HUMAN;sp\|O9476 | 10 | 0 | 3133000 | 2087600 | 3719100 | 737180 | 60967000 | 2914800 |
| sp\|Q99729-3\|ROAA_HUMAN;tr\|D6R9P3 | 10 | 0 | 3113190 | 1057888 | 4959610 | 1041710 | 11291350 | 4195520 |
| sp\|Q6P4R8-3\|NFRKB_HUMAN;tr\|A0A0 | 10 | 0 | 3091400 | 254530 | 682420 | 0 | 4121102 | 0 |
| sp\|O00268\|TAF4_HUMAN;tr\|V9GY14\|V | 10 | 0 | 2886200 | 206660 | 2059600 | 0 | 9941100 | 274810 |
| tr\|I3L0H8\|I3L0H8_HUMAN;tr\|B4DS24\|B | 10 | 0 | 2801103 | 1222670 | 4091900 | 1037300 | 15021740 | 1510000 |
| tr\|F6T1Q0\|F6T1Q0_HUMAN;sp\|Q6L8Q7 | 10 | 0 | 2676300 | 0 | 3870000 | 254430 | 12746000 | 0 |
| tr\|Q8TDR3\|Q8TDR3_HUMAN;tr\|Q8NEH | 10 | 0 | 2632400 | 0 | 2305400 | 0 | 11865970 | 452930 |
| tr\|F8W8R3\|F8W8R3_HUMAN;sp\|P4900 | 10 | 0 | 2391040 | 1059752 | 1713400 | 299060 | 12641000 | 1434900 |

| | | | | | | | | |
|---|---|---|---|---|---|---|---|---|
| tr\|B4DJU4\|B4DJU4_HUMAN;tr\|A0A024 | 10 | 0 | 2322410 | 1886233 | 4075400 | 1163600 | 17165340 | 2484966 |
| sp\|O95394\|AGM1_HUMAN;sp\|O95394- | 10 | 0 | 2288145 | 0 | 5654959 | 0 | 18371220 | 0 |
| sp\|Q9NR09\|BIRC6_HUMAN;tr\|Q9H8B7 | 10 | 0 | 2276300 | 0 | 68790 | 92529 | 4564500 | 0 |
| tr\|M0R3F6\|M0R3F6_HUMAN;sp\|Q8IX0 | 10 | 0 | 2270000 | 0 | 792160 | 0 | 9937000 | 0 |
| sp\|Q14684\|RRP1B_HUMAN;sp\|Q14684 | 10 | 0 | 2227030 | 1069600 | 1557190 | 597040 | 18321700 | 1207350 |
| tr\|Q5TDG3\|Q5TDG3_HUMAN;sp\|Q9UN | 10 | 0 | 2196720 | 0 | 604670 | 0 | 4388760 | 0 |
| sp\|P42345\|MTOR_HUMAN;tr\|B3KX59\| | 10 | 0 | 2172400 | 432450 | 356650 | 0 | 8517500 | 0 |
| sp\|Q99996-5\|AKAP9_HUMAN;sp\|Q999 | 10 | 0 | 2149300 | 0 | 661120 | 0 | 1462100 | 0 |
| sp\|Q66K74-2\|MAP1S_HUMAN;tr\|A8K9 | 10 | 0 | 1847900 | 462907 | 1162000 | 0 | 11888000 | 520950 |
| tr\|C9JFE4\|C9JFE4_HUMAN;tr\|A0A096LF | 10 | 0 | 1834400 | 349050 | 6914400 | 618170 | 22124100 | 648880 |
| sp\|O43324\|MCA3_HUMAN;sp\|O43324- | 10 | 0 | 1695008 | 3012100 | 4374338 | 1334700 | 30896580 | 5352881 |
| sp\|Q9NZJ4\|SACS_HUMAN;sp\|Q9NZJ4- | 10 | 0 | 1653900 | 0 | 356110 | 0 | 2815900 | 0 |
| tr\|B7ZM87\|B7ZM87_HUMAN;tr\|A2RUF | 10 | 0 | 1630700 | 296200 | 1225110 | 0 | 5804100 | 145400 |
| tr\|B4DL80\|B4DL80_HUMAN;tr\|G5EA36\| | 10 | 0 | 1556400 | 191330 | 2491600 | 0 | 11362000 | 614360 |
| sp\|O43747\|AP1G1_HUMAN;tr\|Q8IY97\| | 10 | 0 | 1540990 | 440590 | 3840190 | 579680 | 18107800 | 977840 |
| tr\|B1AJY7\|B1AJY7_HUMAN;sp\|O75832 | 10 | 0 | 1516100 | 1964835 | 5214612 | 1496300 | 38922220 | 1307100 |
| sp\|Q8IZH2-2\|XRN1_HUMAN;sp\|Q8IZH2 | 10 | 0 | 1306600 | 0 | 277380 | 0 | 7451000 | 0 |
| sp\|Q9UBQ5\|EIF3K_HUMAN;sp\|Q9UBQ | 10 | 0 | 1074600 | 1568500 | 3040800 | 977370 | 4683500 | 1996400 |
| tr\|Q5JW30\|Q5JW30_HUMAN;sp\|O9579 | 10 | 0 | 1044900 | 429320 | 1057300 | 215810 | 7641000 | 139000 |
| sp\|P42025\|ACTY_HUMAN;tr\|Q13841\|C | 10 | 0 | 1033800 | 0 | 4385200 | 0 | 8199000 | 1050700 |
| sp\|Q8TBC4-2\|UBA3_HUMAN;tr\|B2RBP3 | 10 | 0 | 935460 | 3205630 | 2045600 | 3939490 | 5873370 | 1413766 |
| tr\|B4DWS6\|B4DWS6_HUMAN;sp\|Q53G | 10 | 0 | 839060 | 641830 | 2949200 | 505810 | 467510 | 0 |
| tr\|B4E074\|B4E074_HUMAN;tr\|B4E303\| | 10 | 0 | 805330 | 0 | 2749700 | 0 | 6848700 | 331060 |
| sp\|Q9Y5Q8-2\|TF3C5_HUMAN;sp\|Q9Y5( | 10 | 0 | 801210 | 0 | 1084700 | 182270 | 10895000 | 85070 |
| tr\|D6W646\|D6W646_HUMAN;sp\|Q6ZS2 | 10 | 0 | 777850 | 0 | 251250 | 0 | 10908000 | 0 |
| sp\|Q9Y6D9\|MD1L1_HUMAN;tr\|A4D218 | 10 | 0 | 710580 | 135420 | 2084200 | 295240 | 18550000 | 6757000 |
| sp\|Q9NYF8-2\|BCLF1_HUMAN;sp\|Q9NY | 10 | 0 | 701070 | 770240 | 155520 | 127990 | 12799000 | 707740 |
| tr\|A0A024R6H0\|A0A024R6H0_HUMAN; | 10 | 0 | 699580 | 263240 | 391650 | 281040 | 11053000 | 124350 |
| tr\|A0A024R7F7\|A0A024R7F7_HUMAN;s | 10 | 0 | 655725 | 236560 | 237190 | 0 | 5107700 | 109310 |
| tr\|A0A024RCC9\|A0A024RCC9_HUMAN; | 10 | 0 | 541250 | 700440 | 2864900 | 405700 | 2664100 | 1764600 |
| tr\|H0YMZ1\|H0YMZ1_HUMAN;tr\|H0YL69 | 10 | 0 | 531100 | 458071 | 1220160 | 1057907 | 4501800 | 1993540 |
| sp\|Q9UJX2\|CDC23_HUMAN;sp\|Q9UJX2 | 10 | 0 | 438930 | 0 | 1700900 | 0 | 3002890 | 0 |
| sp\|P25786\|PSA1_HUMAN;sp\|P25786-2 | 10 | 0 | 385420 | 0 | 0 | 0 | 12912000 | 136940 |
| sp\|Q9NTK5\|OLA1_HUMAN;tr\|J3KQ32\| | 10 | 0 | 379180 | 0 | 0 | 0 | 0 | 406520 |
| tr\|Q0QF37\|Q0QF37_HUMAN;tr\|Q75MT | 10 | 0 | 373120 | 140060 | 0 | 0 | 0 | 0 |
| tr\|A0A087WWU8\|A0A087WWU8_HUM | 10 | 0 | 338200 | 196570 | 161690 | 153910 | 0 | 849130 |
| tr\|A0A087X0I4\|A0A087X0I4_HUMAN;sp | 10 | 0 | 335460 | 370340 | 404350 | 0 | 22729000 | 566020 |
| tr\|A0A024R0F1\|A0A024R0F1_HUMAN;s | 10 | 0 | 283580 | 0 | 747310 | 0 | 9896000 | 0 |
| sp\|Q9NQG5\|RPR1B_HUMAN;tr\|E9PIQ9 | 10 | 0 | 272970 | 710760 | 626334 | 282990 | 11960000 | 1149370 |
| tr\|B3KY04\|B3KY04_HUMAN;sp\|Q96CX2 | 10 | 0 | 269780 | 209160 | 5669900 | 0 | 11518010 | 811960 |
| tr\|A0A024R896\|A0A024R896_HUMAN;s | 10 | 0 | 259880 | 201940 | 1750700 | 1205700 | 15815000 | 16584000 |
| tr\|B3KXN0\|B3KXN0_HUMAN | 10 | 1 | 242440 | 0 | 623260 | 0 | 389453 | 0 |
| sp\|Q16222-2\|UAP1_HUMAN;sp\|Q1622 | 10 | 0 | 0 | 0 | 0 | 0 | 867610 | 0 |
| sp\|Q5T5Y3-2\|CAMP1_HUMAN;sp\|Q5T5 | 10 | 0 | 0 | 0 | 217640 | 0 | 10470000 | 0 |
| sp\|Q9UMR2-2\|DD19B_HUMAN;tr\|Q53C | 10 | 0 | 0 | 0 | 1155500 | 0 | 2609400 | 0 |
| tr\|A0A024R753\|A0A024R753_HUMAN;s | 10 | 0 | 0 | 0 | 95389 | 0 | 12495000 | 0 |
| tr\|B4DM78\|B4DM78_HUMAN;tr\|Q1434 | 10 | 0 | 0 | 0 | 266300 | 0 | 553270 | 0 |
| tr\|H0Y3K4\|H0Y3K4_HUMAN;tr\|B4DVQ2 | 10 | 1 | 0 | 0 | 0 | 0 | 1188800 | 0 |
| sp\|Q92888-2\|ARHG1_HUMAN;tr\|A0A02 | 10 | 0 | 0 | 0 | 0 | 0 | 7581000 | 168440 |
| tr\|A8K8X0\|A8K8X0_HUMAN;sp\|Q14CX | 10 | 0 | 0 | 0 | 0 | 0 | 0 | 161230 |
| tr\|A0A024RBE7\|A0A024RBE7_HUMAN;s | 10 | 0.005178 | 0 | 106010 | 160250 | 0 | 0 | 0 |
| sp\|Q96AC1-2\|FERM2_HUMAN;tr\|H0YJ3 | 10 | 0 | 0 | 163930 | 0 | 0 | 4721500 | 282100 |
| tr\|A8K3D0\|A8K3D0_HUMAN;tr\|B4DUD | 10 | 0 | 0 | 125340 | 362619 | 64356 | 324440 | 668679 |
| tr\|Q53T99\|Q53T99_HUMAN;sp\|Q9GZL7 | 10 | 0 | 0 | 160530 | 1395300 | 250890 | 8475500 | 204500 |
| sp\|P01857\|IGHG1_HUMAN;tr\|Q6PYX1\| | 9 | 0 | 345194000 | 305691000 | 356642900 | 291049000 | 298365000 | 459413000 |
| tr\|V9HW43\|V9HW43_HUMAN;sp\|P047 | 9 | 0 | 62132000 | 3402120 | 5122800 | 5710370 | 16264000 | 4247900 |
| tr\|Q5U0I6\|Q5U0I6_HUMAN;sp\|P62820 | 9 | 0 | 23949570 | 6690178 | 43212760 | 3745730 | 24861320 | 4099883 |
| tr\|B2R4R0\|B2R4R0_HUMAN;sp\|P62805 | 9 | 0 | 18786530 | 8181711 | 23778280 | 2842941 | 66231210 | 15882550 |
| tr\|B4E0K0\|B4E0K0_HUMAN;tr\|Q5JRG1\| | 9 | 0 | 17968593 | 10121863 | 48073240 | 6563000 | 38429000 | 1799900 |
| tr\|V9HWE9\|V9HWE9_HUMAN;sp\|P092 | 9 | 0 | 13532270 | 7518862 | 18792720 | 4055850 | 80146270 | 13825320 |
| sp\|Q58FF8\|H90B2_HUMAN | 9 | 0 | 12005840 | 4549400 | 21521150 | 5923100 | 18960640 | 4563860 |
| sp\|P0CW22\|RS17L_HUMAN;sp\|P08708 | 9 | 0 | 11561890 | 4525790 | 24901800 | 3552870 | 154351206 | 15897140 |
| tr\|X5D8S6\|X5D8S6_HUMAN;tr\|Q71UA4 | 9 | 0 | 9395650 | 1888000 | 10577569 | 1568500 | 34966657 | 2943627 |
| tr\|H9ZYJ2\|H9ZYJ2_HUMAN;sp\|P10599\| | 9 | 0 | 8393900 | 7196100 | 4784730 | 4642230 | 12220200 | 40153100 |
| tr\|Q96DV6\|Q96DV6_HUMAN;tr\|A2A3R | 9 | 0 | 8314050 | 337380 | 21152830 | 421661 | 166110000 | 3118850 |
| tr\|A0A087WXS7\|A0A087WXS7_HUMAN | 9 | 0 | 7814900 | 0 | 25354000 | 4184085 | 18281000 | 3910400 |
| tr\|B2RD27\|B2RD27_HUMAN;sp\|P51665 | 9 | 0 | 7775657 | 0 | 7778100 | 1995400 | 31386291 | 10380620 |
| sp\|O00154-4\|BACH_HUMAN;sp\|O0015 | 9 | 0 | 7050790 | 487610 | 11837932 | 1003462 | 29468670 | 2284863 |
| tr\|B2R7X3\|B2R7X3_HUMAN;sp\|Q13112 | 9 | 0 | 6914200 | 11243520 | 10422900 | 96466 | 8328820 | 139860 |
| tr\|F5GX71\|F5GX71_HUMAN;tr\|H3BPB8 | 9 | 0 | 6725500 | 2223600 | 12434000 | 953860 | 33538330 | 3383200 |

| | | | | | | | | | |
|---|---|---|---|---|---|---|---|---|---|
| sp\|Q96PU8-9\|QKI_HUMAN;sp\|Q96PU8 | 9 | 0 | 5993410 | 1878360 | 21541080 | 3820600 | 66828600 | 7143276 |
| tr\|V9HW39\|V9HW39_HUMAN;sp\|Q9N | 9 | 0 | 5027000 | 303990 | 10152720 | 1299800 | 29955870 | 1283200 |
| tr\|A8K8N3\|A8K8N3_HUMAN;sp\|Q96R0 | 9 | 0 | 4958500 | 262370 | 2508400 | 0 | 3813900 | 104340 |
| sp\|Q3ZCM7\|TBB8_HUMAN;tr\|A0A075B | 9 | 0 | 4049600 | 0 | 0 | 1276300 | 16939000 | 0 |
| sp\|P24666\|PPAC_HUMAN;tr\|Q59EH3\| | 9 | 0 | 3925470 | 1478200 | 7831850 | 1127500 | 47354000 | 3342800 |
| sp\|O76003\|GLRX3_HUMAN | 9 | 0 | 3701406 | 480400 | 5281860 | 664480 | 9263530 | 3328740 |
| tr\|A0A024R4T4\|A0A024R4T4_HUMAN;s | 9 | 0 | 3539378 | 2470700 | 12432000 | 1375088 | 78528600 | 7070900 |
| tr\|Q6FHH6\|Q6FHH6_HUMAN;tr\|Q53TN | 9 | 0 | 3381548 | 0 | 4039600 | 690280 | 17674450 | 1498570 |
| tr\|A0A024R0E5\|A0A024R0E5_HUMAN;s | 9 | 0 | 3300250 | 3216858 | 6725490 | 1953170 | 29093000 | 6350070 |
| sp\|Q9Y613\|FHOD1_HUMAN;tr\|A0A068 | 9 | 0 | 3274900 | 0 | 1541600 | 0 | 6285000 | 0 |
| tr\|A0A087WXZ3\|A0A087WXZ3_HUMAN | 9 | 0 | 3240820 | 0 | 6886200 | 1323253 | 20299090 | 799291 |
| sp\|Q9ULT8\|HECD1_HUMAN;tr\|A0A087 | 9 | 0 | 3015900 | 0 | 1108000 | 543950 | 1785200 | 0 |
| sp\|P35611-2\|ADDA_HUMAN;tr\|E7EV99 | 9 | 0 | 2919485 | 507430 | 2156689 | 0 | 9594830 | 1738290 |
| sp\|Q9UJY4\|GGA2_HUMAN;tr\|B0QYR9\| | 9 | 0 | 2810700 | 244370 | 10445450 | 1012100 | 11805180 | 0 |
| sp\|Q9H0C8\|ILKAP_HUMAN;tr\|F8SNU7\| | 9 | 0 | 2803600 | 205530 | 4695100 | 0 | 9504800 | 951430 |
| sp\|Q9P2N5\|RBM27_HUMAN;tr\|U3KPZ7 | 9 | 0 | 2726100 | 1204700 | 1812700 | 178540 | 10923000 | 3193700 |
| tr\|B4DKX4\|B4DKX4_HUMAN;sp\|Q53EL6 | 9 | 0 | 2722000 | 401150 | 3515000 | 295640 | 4686600 | 2494100 |
| tr\|B7Z8A2\|B7Z8A2_HUMAN;sp\|Q9UHG | 9 | 0 | 2564200 | 275330 | 0 | 0 | 0 | 0 |
| sp\|Q96AG4\|LRC59_HUMAN;tr\|I3L223\|I | 9 | 0 | 2542380 | 3803050 | 10267411 | 1733734 | 4793400 | 0 |
| sp\|O95487-2\|SC24B_HUMAN;sp\|O9548 | 9 | 0 | 2430900 | 284880 | 1230300 | 107200 | 8636932 | 304923 |
| tr\|A0A024QZD1\|A0A024QZD1_HUMAN | 9 | 0 | 2349400 | 428340 | 3425270 | 144911 | 148255280 | 4501990 |
| sp\|Q13151\|ROA0_HUMAN | 9 | 0 | 2202774 | 2832760 | 6935500 | 1121866 | 86599370 | 9382748 |
| tr\|A0A087WYU1\|A0A087WYU1_HUMAN | 9 | 0 | 2180700 | 267870 | 3024700 | 0 | 12630000 | 0 |
| sp\|O75150-4\|BRE1B_HUMAN;tr\|H3BP7 | 9 | 0 | 2124800 | 175630 | 1199900 | 0 | 8325500 | 367350 |
| tr\|B4DKE6\|B4DKE6_HUMAN;sp\|P40938 | 9 | 0 | 2096207 | 93608 | 1619700 | 805956 | 13731590 | 1586068 |
| sp\|Q92769-3\|HDAC2_HUMAN;sp\|Q927 | 9 | 0 | 1868200 | 0 | 952700 | 191850 | 3052700 | 916227 |
| tr\|A0A024RCU9\|A0A024RCU9_HUMAN; | 9 | 0 | 1794570 | 221834 | 5735620 | 183343 | 15699770 | 451213 |
| sp\|Q9Y3Z3-4\|SAMH1_HUMAN;sp\|Q9Y3 | 9 | 0 | 1791800 | 215190 | 1151600 | 331572 | 9786300 | 188670 |
| tr\|B4DII5\|B4DII5_HUMAN;sp\|O60684\|I | 9 | 0 | 1789500 | 0 | 1681600 | 398450 | 5582800 | 504700 |
| tr\|Q0QER2\|Q0QER2_HUMAN;tr\|V9HW | 9 | 0 | 1667451 | 1543500 | 4021600 | 1106900 | 4878560 | 3162038 |
| tr\|B2RAU8\|B2RAU8_HUMAN;sp\|Q1497 | 9 | 0 | 1643700 | 849224 | 319020 | 130889 | 12324200 | 347255 |
| tr\|E9PGT1\|E9PGT1_HUMAN;sp\|Q15631 | 9 | 0 | 1636880 | 1499710 | 3685180 | 1184550 | 11125960 | 2562250 |
| tr\|B4DT77\|B4DT77_HUMAN;tr\|B4DWU | 9 | 0 | 1618200 | 546784 | 3179100 | 237430 | 11606690 | 1026050 |
| tr\|A0A087WUY3\|A0A087WUY3_HUMAN | 9 | 0 | 1592000 | 298750 | 2178600 | 305230 | 16915440 | 543110 |
| tr\|C9J2Z4\|C9J2Z4_HUMAN;tr\|B4DZH9\|I | 9 | 0 | 1560000 | 313000 | 3797277 | 628007 | 525440 | 360210 |
| sp\|Q9UQ13\|SHOC2_HUMAN;sp\|Q9UQ1 | 9 | 0 | 1522100 | 379610 | 4059200 | 287720 | 18603000 | 0 |
| sp\|A3KN83-3\|SBNO1_HUMAN;sp\|A3KN | 9 | 0 | 1499700 | 515580 | 618030 | 197430 | 3351700 | 118780 |
| sp\|P62633-2\|CNBP_HUMAN;sp\|P62633 | 9 | 0 | 1441613 | 511620 | 1341200 | 382930 | 20291000 | 1879200 |
| tr\|A4QPB0\|A4QPB0_HUMAN;tr\|A0A02 | 9 | 0 | 1321400 | 0 | 503750 | 0 | 3549200 | 0 |
| sp\|Q92879-5\|CELF1_HUMAN;sp\|Q9287 | 9 | 0 | 1308600 | 1090800 | 7193600 | 1163100 | 18901940 | 2119500 |
| tr\|Q59GW5\|Q59GW5_HUMAN | 9 | 0 | 1294930 | 0 | 2381050 | 0 | 13261500 | 0 |
| sp\|P49721\|PSB2_HUMAN;tr\|B7Z478\|B7 | 9 | 0 | 1258960 | 0 | 0 | 243677 | 1133700 | 1167700 |
| sp\|Q6UVJ0\|SAS6_HUMAN;tr\|B4DYM7\| | 9 | 0 | 1244000 | 1344700 | 5563000 | 207850 | 6287300 | 184420 |
| tr\|C9JNW5\|C9JNW5_HUMAN;tr\|V9HW | 9 | 0 | 1239500 | 1436283 | 5790348 | 793650 | 84989700 | 3198650 |
| tr\|B7Z6H4\|B7Z6H4_HUMAN;sp\|O14802 | 9 | 0 | 1221700 | 0 | 323200 | 0 | 1336300 | 0 |
| sp\|Q9NR50\|EI2BG_HUMAN;sp\|Q9NR50 | 9 | 0 | 1192900 | 132410 | 2617100 | 591960 | 11700000 | 339980 |
| tr\|H0YH87\|H0YH87_HUMAN;sp\|Q9970 | 9 | 0 | 1187300 | 187020 | 680020 | 0 | 10616000 | 288860 |
| sp\|O60566-2\|BUB1B_HUMAN;sp\|O605 | 9 | 0 | 1185600 | 0 | 1547600 | 0 | 1931000 | 0 |
| sp\|O15357\|SHIP2_HUMAN;tr\|A0A0A0M | 9 | 0 | 1107700 | 0 | 1101500 | 154520 | 7431700 | 76688 |
| tr\|B2RAG9\|B2RAG9_HUMAN;sp\|Q1564 | 9 | 0 | 1083700 | 157100 | 327410 | 157020 | 9038000 | 298580 |
| sp\|Q8WXI9\|P66B_HUMAN;tr\|B3KSZ4\|B | 9 | 0 | 1072382 | 990900 | 5205100 | 1205500 | 10035490 | 424160 |
| sp\|P46779-3\|RL28_HUMAN;sp\|P46779\| | 9 | 0 | 1033500 | 374730 | 3579600 | 212300 | 48049000 | 3338743 |
| sp\|Q99543\|DNJC2_HUMAN;sp\|Q99543 | 9 | 0 | 857680 | 1893900 | 1847700 | 1655900 | 16732780 | 3911500 |
| sp\|Q9Y5Q9\|TF3C3_HUMAN;tr\|H7BZV8 | 9 | 0 | 855670 | 146330 | 373950 | 158250 | 7713100 | 313630 |
| tr\|B7WPG3\|B7WPG3_HUMAN;sp\|Q8W | 9 | 0 | 837140 | 0 | 513660 | 115750 | 4132000 | 468230 |
| sp\|O60502-4\|OGA_HUMAN;sp\|O60502 | 9 | 0 | 794420 | 0 | 0 | 0 | 7637000 | 0 |
| tr\|A0A087X020\|A0A087X020_HUMAN;s | 9 | 0 | 786640 | 1864754 | 5336760 | 991910 | 42617620 | 3034800 |
| sp\|Q92522\|H1X_HUMAN | 9 | 0 | 781273 | 1007380 | 4860850 | 225102 | 95582510 | 3962690 |
| tr\|Q9BPW0\|Q9BPW0_HUMAN;tr\|H0YD | 9 | 0 | 742240 | 0 | 160290 | 0 | 2541400 | 770490 |
| sp\|Q6ZRS2-3\|SRCAP_HUMAN;sp\|Q6ZR | 9 | 0 | 649970 | 0 | 184500 | 0 | 4564400 | 0 |
| sp\|P35520\|CBS_HUMAN;sp\|P35520-2\| | 9 | 0 | 638130 | 0 | 2401000 | 0 | 2935800 | 3483820 |
| sp\|P19105\|ML12A_HUMAN;sp\|O14950 | 9 | 0 | 586940 | 1575545 | 5586600 | 1478900 | 76784000 | 4631383 |
| tr\|Q6FGJ9\|Q6FGJ9_HUMAN;sp\|P21266 | 9 | 0 | 441430 | 710650 | 2853530 | 250540 | 8283820 | 1857800 |
| sp\|Q99426\|TBCB_HUMAN;tr\|K7EK42\|K | 9 | 0 | 431970 | 1104000 | 1930400 | 742619 | 16287000 | 1462400 |
| sp\|P23193\|TCEA1_HUMAN;tr\|B7Z4W0\| | 9 | 0 | 419123 | 173610 | 1285505 | 0 | 8898600 | 160130 |
| tr\|A4D0Z3\|A4D0Z3_HUMAN;sp\|P84085 | 9 | 0 | 382890 | 632849 | 1427470 | 673080 | 3652900 | 748060 |
| sp\|Q9BZK7\|TBL1R_HUMAN;tr\|B7Z475\| | 9 | 0 | 375270 | 0 | 3279100 | 0 | 17761000 | 0 |
| tr\|Q53GG3\|Q53GG3_HUMAN;tr\|B3KN5 | 9 | 0 | 357410 | 194990 | 0 | 0 | 0 | 0 |
| sp\|P09525\|ANXA4_HUMAN;tr\|V9HW5 | 9 | 0 | 334720 | 659550 | 5680000 | 575590 | 4378080 | 365180 |
| tr\|B4DWN1\|B4DWN1_HUMAN;tr\|A8K7 | 9 | 0 | 330350 | 0 | 0 | 0 | 13727700 | 150360 |
| sp\|A1L0T0\|ILVBL_HUMAN;tr\|M0R026\|I | 9 | 0 | 262410 | 0 | 103920 | 0 | 0 | 0 |
| sp\|O95861-4\|BPNT1_HUMAN;tr\|V9HW | 9 | 0 | 244220 | 0 | 313191 | 162244 | 6976000 | 2380640 |
| tr\|Q6IAX1\|Q6IAX1_HUMAN;sp\|P37268 | 9 | 0 | 234180 | 0 | 2493200 | 202350 | 0 | 0 |
| sp\|Q9UGI8-2\|TES_HUMAN;tr\|B2RDR4\| | 9 | 0 | 225410 | 120086 | 839850 | 0 | 9025700 | 602687 |
| sp\|Q8N766-4\|EMC1_HUMAN;sp\|Q8N7 | 9 | 0 | 208910 | 0 | 0 | 0 | 0 | 232310 |

| | | | | | | | | |
|---|---|---|---|---|---|---|---|---|
| tr\|B7Z592\|B7Z592_HUMAN;sp\|Q8WU9 | 9 | 0 | 136510 | 0 | 1359600 | 0 | 11635000 | 959290 |
| sp\|P61086\|UBE2K_HUMAN;tr\|B4DIZ2\| | 9 | 0 | 123120 | 918110 | 407340 | 163920 | 2639800 | 1140000 |
| sp\|P15531\|NDKA_HUMAN;sp\|P15531-2 | 9 | 0 | 91906 | 1608800 | 953760 | 654410 | 2306300 | 2656500 |
| tr\|Q53GE2\|Q53GE2_HUMAN;tr\|Q53GC7 | 9 | 0 | 84163 | 116630 | 679440 | 0 | 9250300 | 1142730 |
| sp\|O60502\|OGA_HUMAN;sp\|O60502-3 | 9 | 0.005168 | 0 | 0 | 0 | 0 | 0 | 0 |
| sp\|O60832\|DKC1_HUMAN;sp\|O60832-2 | 9 | 0 | 0 | 0 | 0 | 0 | 7161500 | 0 |
| tr\|Q4KMR3\|Q4KMR3_HUMAN;sp\|Q129 | 9 | 0 | 0 | 0 | 921080 | 0 | 7350700 | 155630 |
| sp\|P14314-2\|GLU2B_HUMAN;tr\|A0A02 | 9 | 0 | 0 | 0 | 0 | 0 | 2572790 | 496169 |
| sp\|P22061\|PIMT_HUMAN;sp\|P22061-2 | 9 | 0 | 0 | 0 | 110930 | 0 | 631060 | 1560400 |
| sp\|P51116\|FXR2_HUMAN;tr\|I3L1Z2\|I3L | 9 | 0 | 0 | 282330 | 532850 | 0 | 4686700 | 259350 |
| tr\|F8W1A4\|F8W1A4_HUMAN;sp\|P5481 | 9 | 0 | 0 | 197590 | 0 | 0 | 0 | 784420 |
| tr\|B4DRA5\|B4DRA5_HUMAN;tr\|B4DJW | 9 | 0 | 0 | 471290 | 1615700 | 303840 | 5995000 | 962420 |
| tr\|A0A024R1K7\|A0A024R1K7_HUMAN;s | 9 | 0 | 0 | 312300 | 285190 | 169690 | 1978900 | 1550000 |
| sp\|Q69YN2\|C19L1_HUMAN;sp\|Q69YN2 | 9 | 0 | 0 | 98572 | 467080 | 388070 | 8505278 | 0 |
| tr\|B4DV28\|B4DV28_HUMAN;tr\|V9HWE | 9 | 0 | 0 | 365240 | 0 | 486340 | 4382700 | 477890 |
| sp\|P12273\|PIP_HUMAN | 8 | 0 | 30819300 | 20347800 | 22355600 | 24738200 | 27335700 | 31651800 |
| tr\|V9HWI3\|V9HWI3_HUMAN;sp\|P0733 | 8 | 0 | 29773560 | 1310840 | 1603220 | 3130210 | 1132570 | 1567530 |
| tr\|Q5SQT9\|Q5SQT9_HUMAN;tr\|B2R679 | 8 | 0 | 28614700 | 16315000 | 69308000 | 11355690 | 79246000 | 27063300 |
| sp\|P62263\|RS14_HUMAN;tr\|E5RH77\|E5 | 8 | 0 | 19216930 | 13030180 | 40230410 | 12606110 | 206833790 | 26222580 |
| tr\|Q59H57\|Q59H57_HUMAN;tr\|B4DR70 | 8 | 0 | 12685770 | 3793913 | 20442636 | 2356959 | 122591000 | 2720940 |
| tr\|B2R4W8\|B2R4W8_HUMAN;sp\|P6224 | 8 | 0 | 11418860 | 7790608 | 20367398 | 10157740 | 182022150 | 19975400 |
| sp\|P62081\|RS7_HUMAN;tr\|B5MCP9\|B5 | 8 | 0 | 10720100 | 8720006 | 20357600 | 2648310 | 107949430 | 8984770 |
| tr\|B4DMT5\|B4DMT5_HUMAN;sp\|O0030 | 8 | 0 | 10301000 | 4005400 | 15218000 | 2799000 | 19335000 | 5332180 |
| tr\|B7Z2Z1\|B7Z2Z1_HUMAN;sp\|Q15424- | 8 | 0 | 9606100 | 1360900 | 3576300 | 640860 | 8444800 | 1140900 |
| tr\|A8YXX4\|A8YXX4_HUMAN;sp\|P15104 | 8 | 0 | 9133948 | 257172 | 738054 | 381056 | 1046560 | 421314 |
| sp\|Q15185-4\|TEBP_HUMAN;tr\|A0A024 | 8 | 0 | 7811000 | 2233850 | 9425880 | 3251800 | 82507000 | 6370600 |
| tr\|Q6IBR8\|Q6IBR8_HUMAN;sp\|P20042 | 8 | 0 | 7650700 | 2246000 | 11763770 | 2301800 | 47381000 | 6348180 |
| tr\|B2R7B5\|B2R7B5_HUMAN;sp\|Q07666 | 8 | 0 | 7189989 | 1125067 | 15410334 | 1570240 | 62263310 | 6264570 |
| tr\|Q6IAM0\|Q6IAM0_HUMAN;sp\|O7582 | 8 | 0 | 7072800 | 1458680 | 10807000 | 1980700 | 11757000 | 3845500 |
| sp\|O43852-9\|CALU_HUMAN;sp\|O43852 | 8 | 0 | 5929700 | 2375810 | 4756000 | 1839110 | 2610800 | 1829720 |
| sp\|Q9ULH7-4\|MKL2_HUMAN;sp\|Q9ULH | 8 | 0 | 5929300 | 0 | 1533300 | 0 | 9667400 | 0 |
| sp\|Q9ULC4\|MCTS1_HUMAN;sp\|Q9ULC4 | 8 | 0 | 5784500 | 3863500 | 18980857 | 898770 | 58754000 | 1178400 |
| sp\|P18583-6\|SON_HUMAN;sp\|P18583- | 8 | 0 | 5595300 | 79908 | 1326600 | 863952 | 6585600 | 128190 |
| tr\|E9PC52\|E9PC52_HUMAN;tr\|Q6FHQ0 | 8 | 0 | 4981800 | 182470 | 6708700 | 1510000 | 0 | 1048300 |
| sp\|P06132\|DCUP_HUMAN;tr\|B4DEM5\| | 8 | 0 | 4785990 | 0 | 738410 | 3283900 | 11707200 | 1681800 |
| tr\|Q53HJ0\|Q53HJ0_HUMAN;sp\|P61201 | 8 | 0 | 4686600 | 1386300 | 12197000 | 433870 | 25174000 | 1747390 |
| sp\|P25398\|RS12_HUMAN | 8 | 0 | 4558149 | 12128691 | 14994013 | 9825470 | 220254710 | 30183340 |
| tr\|B3KUH0\|B3KUH0_HUMAN;sp\|Q8WU | 8 | 0 | 4171600 | 489910 | 9975700 | 249960 | 0 | 0 |
| tr\|A0A024R3W7\|A0A024R3W7_HUMAN | 8 | 0 | 3844890 | 2479200 | 8410660 | 1937885 | 66393480 | 4368160 |
| sp\|P38606-2\|VATA_HUMAN;sp\|P38606 | 8 | 0 | 3823900 | 1916900 | 6355400 | 1471700 | 3530500 | 593760 |
| sp\|Q5TDH0\|DDI2_HUMAN;sp\|Q5TDH0- | 8 | 0 | 3641848 | 1162100 | 2500984 | 733330 | 11598919 | 2413200 |
| tr\|F8W1R7\|F8W1R7_HUMAN;sp\|P6066 | 8 | 0 | 3542330 | 3469400 | 17024000 | 3268289 | 141850000 | 10982000 |
| sp\|Q16186\|ADRM1_HUMAN;tr\|B4DMP | 8 | 0 | 3483441 | 2112200 | 12043607 | 2082800 | 11340220 | 12714667 |
| tr\|A8K6Q8\|A8K6Q8_HUMAN;sp\|P0278 | 8 | 0 | 3298330 | 0 | 1899522 | 476530 | 180860 | 132410 |
| sp\|Q13564-3\|ULA1_HUMAN;sp\|Q13564 | 8 | 0 | 3291800 | 1240000 | 2383126 | 1192400 | 5076380 | 1966320 |
| sp\|P56537\|IF6_HUMAN;sp\|P56537-2\|IF | 8 | 0 | 3207020 | 3010580 | 4652200 | 2340920 | 61249000 | 5813090 |
| sp\|P31350\|RIR2_HUMAN;tr\|D6W4Z6\|D | 8 | 0 | 3145100 | 0 | 3533800 | 967470 | 13340100 | 748350 |
| sp\|Q96BY7\|ATG2B_HUMAN;tr\|B4DYX0 | 8 | 0 | 3082580 | 0 | 792920 | 0 | 4056200 | 0 |
| sp\|Q9HD26-2\|GOPC_HUMAN;sp\|Q9HD | 8 | 0 | 2934400 | 0 | 2144700 | 0 | 896300 | 0 |
| tr\|Q8TB01\|Q8TB01_HUMAN;tr\|Q6NWZ | 8 | 0 | 2843480 | 598014 | 1698200 | 1328720 | 0 | 58146 |
| tr\|V9HVZ6\|V9HVZ6_HUMAN;sp\|Q9274 | 8 | 0 | 2808650 | 0 | 1385791 | 299580 | 17888300 | 0 |
| sp\|Q92917\|GPKOW_HUMAN | 8 | 0 | 2787137 | 311270 | 6530900 | 303900 | 3506300 | 0 |
| tr\|Q8IVQ8\|Q8IVQ8_HUMAN;tr\|Q0VG7 | 8 | 0 | 2661300 | 0 | 834160 | 0 | 5333610 | 268570 |
| tr\|A0A024R0H7\|A0A024R0H7_HUMAN; | 8 | 0 | 2580000 | 452040 | 6312600 | 1656400 | 3832050 | 3023000 |
| sp\|Q53GS9\|SNUT2_HUMAN;sp\|Q53GS9 | 8 | 0 | 2404160 | 1489500 | 6820300 | 253100 | 12022000 | 927170 |
| tr\|J3QR09\|J3QR09_HUMAN;tr\|J3KTE4\|J | 8 | 0 | 2383970 | 710770 | 5602000 | 302107 | 85403620 | 1254570 |
| tr\|Q6FI03\|Q6FI03_HUMAN;tr\|Q5U0Q1\| | 8 | 0 | 2278500 | 538460 | 4696600 | 1345600 | 10441000 | 2082140 |
| sp\|Q9BTE3-2\|MCMBP_HUMAN;sp\|Q9B | 8 | 0 | 2144800 | 668380 | 4478300 | 644490 | 528610 | 0 |
| tr\|A0A024R3R7\|A0A024R3R7_HUMAN;t | 8 | 0 | 2029300 | 0 | 1081300 | 0 | 818350 | 0 |
| tr\|A2RUU9\|A2RUU9_HUMAN;tr\|A6NNM | 8 | 0 | 1932900 | 0 | 898080 | 0 | 0 | 0 |
| tr\|A8K964\|A8K964_HUMAN;sp\|Q9H307 | 8 | 0 | 1885800 | 490510 | 741120 | 319040 | 21822000 | 928240 |
| sp\|P31153\|METK2_HUMAN;tr\|B4DEX8\| | 8 | 0 | 1799400 | 1029300 | 3380600 | 441870 | 0 | 976787 |
| sp\|P30154-4\|2AAB_HUMAN;sp\|P30154 | 8 | 1 | 1578500 | 4027920 | 2137715 | 0 | 1581914 | 0 |
| sp\|Q5TFE4\|NT5D1_HUMAN;sp\|Q5TFE4 | 8 | 0 | 1568100 | 366800 | 3253700 | 0 | 11999680 | 974580 |
| sp\|Q5RKV6\|EXOS6_HUMAN | 8 | 0 | 1510762 | 1082100 | 3638661 | 1227571 | 20085000 | 2150500 |
| tr\|M0QY97\|M0QY97_HUMAN;sp\|Q9UP | 8 | 0 | 1430300 | 0 | 252820 | 0 | 14100000 | 0 |
| tr\|B7ZKR8\|B7ZKR8_HUMAN;sp\|Q86UV5 | 8 | 0 | 1382500 | 0 | 0 | 0 | 9613600 | 395260 |
| sp\|O75116\|ROCK2_HUMAN;tr\|E9PF63\| | 8 | 0 | 1349600 | 91266 | 234120 | 0 | 644230 | 500720 |
| tr\|Q53GF5\|Q53GF5_HUMAN;tr\|A0A024 | 8 | 0 | 1234190 | 0 | 0 | 0 | 516760 | 1688990 |
| tr\|B5BU08\|B5BU08_HUMAN;sp\|Q01081 | 8 | 0 | 1231630 | 1040000 | 2139096 | 488940 | 26667240 | 1297030 |
| sp\|Q04726-2\|TLE3_HUMAN;sp\|Q04726 | 8 | 0 | 1195200 | 280220 | 2266490 | 1155270 | 10686100 | 963220 |
| sp\|Q96JB5\|CK5P3_HUMAN;sp\|Q96JB5- | 8 | 0 | 1174800 | 0 | 2430000 | 185510 | 6999700 | 0 |
| tr\|A0A024R830\|A0A024R830_HUMAN;s | 8 | 0 | 1157033 | 1457800 | 4213600 | 1070800 | 16879000 | 2108600 |
| sp\|Q15269\|PWP2_HUMAN;tr\|C9J544\|C | 8 | 0 | 1154300 | 0 | 773660 | 0 | 10576600 | 168550 |
| tr\|A0A024R7V6\|A0A024R7V6_HUMAN; | 8 | 0 | 1139200 | 723330 | 3112200 | 274980 | 2195700 | 546430 |

| | | | | | | | | | |
|---|---|---|---|---|---|---|---|---|---|
| sp\|P49720\|PSB3_HUMAN;tr\|A0A087W | 8 | 0 | 1111420 | 214280 | 0 | 200700 | 493050 | 2050520 |
| tr\|A0A024R3J7\|A0A024R3J7_HUMAN;sp | 8 | 0 | 1107300 | 0 | 1391410 | 0 | 0 | 0 |
| sp\|Q92793-2\|CBP_HUMAN;sp\|Q92793\| | 8 | 0 | 1083900 | 0 | 308700 | 73249 | 5349900 | 0 |
| sp\|Q15723-4\|ELF2_HUMAN;tr\|B7Z720\| | 8 | 0 | 1083700 | 164850 | 2894100 | 0 | 4412700 | 0 |
| tr\|B3KNH5\|B3KNH5_HUMAN;tr\|A0A02 | 8 | 0 | 1081800 | 0 | 2833400 | 0 | 10080000 | 704630 |
| sp\|Q99549\|MPP8_HUMAN;sp\|Q99549- | 8 | 0 | 1051800 | 0 | 346880 | 0 | 7662440 | 0 |
| sp\|O75396\|SC22B_HUMAN;tr\|I1VE16\|I | 8 | 0 | 1051170 | 632660 | 2495588 | 254460 | 7772000 | 585310 |
| tr\|A0A0A0MSK6\|A0A0A0MSK6_HUMAN | 8 | 0 | 1020100 | 77102.2 | 981270 | 30037.7 | 2000400 | 35702.4 |
| tr\|I6L9E8\|I6L9E8_HUMAN;sp\|Q8NCA5- | 8 | 0 | 1007500 | 0 | 2460900 | 367770 | 9511400 | 0 |
| tr\|Q2TAM5\|Q2TAM5_HUMAN;tr\|E9PKH | 8 | 0 | 998960 | 0 | 2202100 | 395000 | 10410000 | 848900 |
| tr\|Q5T6L4\|Q5T6L4_HUMAN;tr\|A8KAP9 | 8 | 0 | 960860 | 686340 | 1605950 | 0 | 2826570 | 1291000 |
| tr\|Q53EL3\|Q53EL3_HUMAN;tr\|B5BU52\| | 8 | 0 | 914450 | 262910 | 1107500 | 489330 | 6925200 | 0 |
| sp\|Q9UBQ7\|GRHPR_HUMAN;tr\|Q5M7Z | 8 | 0 | 901960 | 1667780 | 3037800 | 1164070 | 45297870 | 3145380 |
| tr\|J3KMX2\|J3KMX2_HUMAN;sp\|Q9292 | 8 | 0 | 858820 | 0 | 1214000 | 55368 | 2637200 | 0 |
| tr\|Q53F98\|Q53F98_HUMAN;tr\|B2RBY4 | 8 | 0 | 836900 | 126250 | 1629700 | 0 | 8064800 | 224920 |
| tr\|Q6IT96\|Q6IT96_HUMAN;sp\|Q13547\| | 8 | 0 | 815340 | 167540 | 1545700 | 42058 | 2914500 | 53500 |
| tr\|Q5JRC6\|Q5JRC6_HUMAN;sp\|Q8IWS0 | 8 | 0 | 807190 | 80436 | 1506900 | 199800 | 7670900 | 69644 |
| sp\|P53582\|MAP11_HUMAN;tr\|Q5CZ91 | 8 | 0 | 805920 | 568070 | 3461400 | 0 | 6664600 | 774880 |
| tr\|H0YN26\|H0YN26_HUMAN;tr\|Q6PKH8 | 8 | 0 | 788640 | 3716627 | 4663290 | 1217909 | 50933000 | 7118720 |
| sp\|P55735\|SEC13_HUMAN;sp\|P55735-2 | 8 | 0 | 772270 | 1062400 | 2417401 | 317480 | 36362840 | 432720 |
| tr\|A8K6G9\|A8K6G9_HUMAN;sp\|Q9262 | 8 | 0 | 710640 | 0 | 639060 | 0 | 6511500 | 0 |
| tr\|Q149P1\|Q149P1_HUMAN;tr\|Q149P0 | 8 | 0 | 685620 | 117180 | 553850 | 437200 | 5397200 | 72979 |
| tr\|Q53HN4\|Q53HN4_HUMAN;sp\|O002 | 8 | 0 | 668514 | 194350 | 2970800 | 340407 | 20563500 | 5677400 |
| tr\|A0A024R5K8\|A0A024R5K8_HUMAN;s | 8 | 0 | 652970 | 1014700 | 3897900 | 510890 | 2063300 | 0 |
| sp\|Q7Z478\|DHX29_HUMAN;tr\|A0A087 | 8 | 0 | 648880 | 113190 | 1118060 | 0 | 5567508 | 107460 |
| tr\|E7EU96\|E7EU96_HUMAN;tr\|B5BUH5 | 8 | 0 | 644980 | 0 | 0 | 0 | 4782700 | 441330 |
| tr\|G5E9A6\|G5E9A6_HUMAN;tr\|Q6P453 | 8 | 0 | 596590 | 0 | 707440 | 0 | 5625700 | 600585 |
| sp\|Q8NFH5-2\|NUP53_HUMAN;tr\|A8K3 | 8 | 0 | 577210 | 1349500 | 2982400 | 1769111 | 57815070 | 8302400 |
| tr\|A0A024QZM5\|A0A024QZM5_HUMAN | 8 | 0 | 520670 | 0 | 544300 | 0 | 48940000 | 39764 |
| sp\|Q8N201\|INT1_HUMAN;tr\|A4D212\|A | 8 | 0 | 479370 | 0 | 590500 | 0 | 4978820 | 0 |
| sp\|P62316\|SMD2_HUMAN;sp\|P62316-2 | 8 | 0 | 468520 | 805150 | 1579300 | 423630 | 27033000 | 4183700 |
| tr\|Q5U0A0\|Q5U0A0_HUMAN;sp\|P2806 | 8 | 0 | 453923 | 1238640 | 610989 | 1061110 | 11924110 | 4359720 |
| sp\|Q5JPE7-2\|NOMO2_HUMAN;sp\|Q15 | 8 | 0 | 429190 | 79389 | 162410 | 0 | 321130 | 0 |
| sp\|Q9UHB7\|AFF4_HUMAN;sp\|Q9UHB7 | 8 | 0 | 391410 | 0 | 0 | 0 | 6303100 | 0 |
| tr\|A0A024R496\|A0A024R496_HUMAN;s | 8 | 0 | 369070 | 151440 | 875860 | 87402 | 2374800 | 0 |
| tr\|A0A024R1I3\|A0A024R1I3_HUMAN;sp | 8 | 0 | 346320 | 202250 | 821070 | 233710 | 12622000 | 525740 |
| tr\|A8K1E1\|A8K1E1_HUMAN;sp\|P20585 | 8 | 0 | 322420 | 0 | 667270 | 0 | 5514000 | 0 |
| tr\|B7Z7P2\|B7Z7P2_HUMAN;tr\|Q59EA0 | 8 | 0.003 | 309230 | 0 | 0 | 0 | 0 | 0 |
| tr\|Q5U071\|Q5U071_HUMAN;sp\|P26583 | 8 | 0 | 283845 | 371196 | 131330 | 156766 | 550550 | 2554191 |
| tr\|A0A0A0MSW4\|A0A0A0MSW4_HUMA | 8 | 0 | 249110 | 270290 | 355060 | 0 | 6041420 | 0 |
| sp\|P53004\|BIEA_HUMAN;tr\|C9J1E1\|C9 | 8 | 0 | 246680 | 416880 | 966530 | 129370 | 6698900 | 0 |
| sp\|Q5T1M5\|FKB15_HUMAN;tr\|A0A0A0 | 8 | 0 | 212240 | 111250 | 0 | 0 | 4075200 | 89481 |
| sp\|Q96H79\|ZCCHL_HUMAN;sp\|Q96H79 | 8 | 0 | 201130 | 209770 | 1069220 | 1134050 | 12980000 | 229230 |
| tr\|B4DZQ5\|B4DZQ5_HUMAN;tr\|A0A024 | 8 | 0 | 192080 | 0 | 0 | 0 | 8037200 | 0 |
| tr\|Q53G61\|Q53G61_HUMAN;tr\|Q53G21 | 8 | 0 | 175280 | 0 | 566560 | 0 | 9851800 | 1398100 |
| sp\|Q9BTA9-2\|WAC_HUMAN;sp\|Q9BTA | 8 | 0 | 126520 | 517750 | 2701400 | 653890 | 5505500 | 660670 |
| sp\|Q86V81\|THOC4_HUMAN;tr\|E9PB61 | 8 | 0 | 124750 | 0 | 1687400 | 0 | 37541000 | 725630 |
| tr\|Q86SZ7\|Q86SZ7_HUMAN;tr\|Q6FHK9 | 8 | 0 | 112080 | 711630 | 976400 | 0 | 729170 | 101590 |
| tr\|A8K9K8\|A8K9K8_HUMAN;sp\|Q9UNC | 8 | 0 | 75843 | 64586 | 799879.7 | 0 | 14297000 | 0 |
| sp\|P08579\|RU2B_HUMAN;tr\|B5BTZ8\|B | 8 | 0 | 74457 | 0 | 231400 | 0 | 4780270 | 0 |
| tr\|A0A024R333\|A0A024R333_HUMAN;s | 8 | 0 | 59259 | 43752 | 531700 | 0 | 16331000 | 253390 |
| sp\|O75155-2\|CAND2_HUMAN;sp\|O751 | 8 | 0 | 0 | 0 | 0 | 0 | 5924940 | 0 |
| sp\|O95834\|EMAL2_HUMAN;tr\|K7EIK7\| | 8 | 0 | 0 | 0 | 0 | 0 | 1597200 | 0 |
| sp\|P56270-2\|MAZ_HUMAN;sp\|P56270- | 8 | 0 | 0 | 0 | 0 | 0 | 4482450 | 0 |
| sp\|Q6P158\|DHX57_HUMAN;sp\|Q6P158 | 8 | 0 | 0 | 0 | 0 | 0 | 3485400 | 0 |
| sp\|Q6S8J3\|POTEE_HUMAN;sp\|A5A3E0 | 8 | 1 | 0 | 0 | 2251600 | 0 | 4109800 | 0 |
| sp\|Q96CN7\|ISOC1_HUMAN;tr\|D6RGE2 | 8 | 0 | 0 | 0 | 0 | 0 | 402680 | 0 |
| tr\|A0A024R1Z6\|A0A024R1Z6_HUMAN;s | 8 | 0 | 0 | 0 | 727870 | 0 | 0 | 0 |
| tr\|B2R7G4\|B2R7G4_HUMAN;sp\|P32780 | 8 | 0 | 0 | 0 | 0 | 0 | 7036400 | 0 |
| tr\|B2R9I9\|B2R9I9_HUMAN;tr\|A0MNP2 | 8 | 0 | 0 | 0 | 0 | 0 | 18434600 | 0 |
| tr\|B4DG22\|B4DG22_HUMAN;tr\|B7ZB17 | 8 | 0 | 0 | 0 | 0 | 0 | 1764700 | 0 |
| tr\|B4DWB1\|B4DWB1_HUMAN;sp\|O606 | 8 | 0 | 0 | 0 | 1622400 | 0 | 4768600 | 0 |
| tr\|S4R3H4\|S4R3H4_HUMAN;tr\|Q69YJ6\| | 8 | 0 | 0 | 0 | 0 | 0 | 5210200 | 58792 |
| sp\|Q9Y315\|DEOC_HUMAN;tr\|G3V158\| | 8 | 0 | 0 | 0 | 386950 | 0 | 6176900 | 232540 |
| tr\|Q9NX34\|Q9NX34_HUMAN | 8 | 0 | 0 | 0 | 0 | 0 | 2110700 | 583160 |
| tr\|Q5T7C4\|Q5T7C4_HUMAN;tr\|Q5T7C6 | 8 | 0 | 0 | 0 | 0 | 0 | 418090 | 1289110 |
| sp\|P22059\|OSBP1_HUMAN;tr\|B4DR25\| | 8 | 0 | 0 | 0 | 0 | 0 | 0 | 188310 |
| tr\|A8K067\|A8K067_HUMAN;tr\|B4DI19\| | 8 | 0 | 0 | 0 | 558170 | 0 | 0 | 356446 |
| tr\|A8KAQ5\|A8KAQ5_HUMAN;tr\|A0A02 | 8 | 0 | 0 | 0 | 0 | 0 | 0 | 29021 |
| tr\|B4E2H2\|B4E2H2_HUMAN;tr\|B4DZD5 | 8 | 1 | 0 | 0 | 0 | 0 | 0 | 514110 |
| tr\|J3KN67\|J3KN67_HUMAN;sp\|P06753 | 8 | 0.006803 | 0 | 0 | 0 | 0 | 0 | 251980 |
| tr\|Q6NVY0\|Q6NVY0_HUMAN;tr\|A0A02 | 8 | 0 | 0 | 0 | 0 | 0 | 0 | 1018200 |
| tr\|Q5W009\|Q5W009_HUMAN;sp\|Q96I2 | 8 | 0 | 0 | 0 | 967100 | 99786 | 10325000 | 204160 |
| sp\|Q9NPI6-2\|DCP1A_HUMAN;tr\|Q3LIB | 8 | 0 | 0 | 0 | 1173800 | 129280 | 9420100 | 0 |
| sp\|Q8N335\|GPD1L_HUMAN;tr\|C9JM46 | 8 | 0 | 0 | 408170 | 933820 | 166590 | 9860600 | 0 |

| | | | | | | | | | |
|---|---|---|---|---|---|---|---|---|---|
| tr\|Q96CV8\|Q96CV8_HUMAN;sp\|P5288 | 8 | 0 | 0 | 367820 | 1299800 | 387580 | 1342700 | 1500000 |
| sp\|Q8N7H5-3\|PAF1_HUMAN;tr\|A0A02 | 8 | 0 | 0 | 0 | 730350 | 236500 | 10749000 | 624200 |
| tr\|V9HW41\|V9HW41_HUMAN;sp\|P610 | 8 | 0 | 0 | 308330 | 99889 | 55365 | 1770700 | 5270700 |
| tr\|B2R514\|B2R514_HUMAN;tr\|E7EM64 | 8 | 0 | 0 | 0 | 1800600 | 1038500 | 14573000 | 1501990 |
| sp\|P17174\|AATC_HUMAN;tr\|B7Z1I2\|B7 | 8 | 0 | 0 | 0 | 0 | 276865 | 0 | 367240 |
| tr\|Q5RKT7\|Q5RKT7_HUMAN;tr\|B2RDW | 7 | 0 | 99724000 | 48617000 | 85700000 | 41241700 | 230828000 | 134368000 |
| sp\|P47929\|LEG7_HUMAN | 7 | 0 | 47520060 | 516540 | 1903750 | 2015990 | 11467750 | 2219680 |
| sp\|P46783\|RS10_HUMAN;tr\|Q59GE4\|Q | 7 | 0 | 31117680 | 6201390 | 31002950 | 3285690 | 79371090 | 9470910 |
| sp\|P30050\|RL12_HUMAN;tr\|Q59FI9\|Q5 | 7 | 0 | 19995400 | 27390580 | 49191870 | 19613420 | 293008940 | 33797170 |
| tr\|Q53F20\|Q53F20_HUMAN;sp\|Q9BTT0 | 7 | 0 | 17339000 | 4480900 | 22754000 | 5736527 | 185540000 | 26117983 |
| sp\|Q13867\|BLMH_HUMAN;tr\|K7ESE8\|K | 7 | 0 | 15333330 | 1205420 | 1740580 | 2508710 | 1901270 | 1638360 |
| sp\|P62277\|RS13_HUMAN;tr\|J3KMX5\|J3 | 7 | 0 | 12146840 | 6116870 | 17016860 | 6499480 | 191287420 | 23802460 |
| tr\|E5RI99\|E5RI99_HUMAN;tr\|A0A024R9 | 7 | 0 | 11878200 | 33551500 | 24733070 | 23979210 | 213130000 | 46806000 |
| tr\|Q9BTQ7\|Q9BTQ7_HUMAN;tr\|A0A02 | 7 | 0 | 11734770 | 5812340 | 28355490 | 2982068 | 192509070 | 11893065 |
| tr\|A0A024R4E2\|A0A024R4E2_HUMAN;s | 7 | 0 | 10476300 | 3856941 | 21995780 | 3260400 | 38419370 | 6234654 |
| sp\|P31151\|S10A7_HUMAN;sp\|Q86SG5\| | 7 | 0 | 9452320 | 2136620 | 2276000 | 3443180 | 2662520 | 3371400 |
| tr\|Q6MZW0\|Q6MZW0_HUMAN;sp\|P01 | 7 | 0 | 9381580 | 2663640 | 2752000 | 4605610 | 6905550 | 5388900 |
| tr\|A0A090N7V5\|A0A090N7V5_HUMAN | 7 | 0 | 7857130 | 2168660 | 1585910 | 967390 | 637510 | 1310940 |
| sp\|P61026\|RAB10_HUMAN;tr\|Q53T70\| | 7 | 0 | 7634270 | 190390 | 5678600 | 91529 | 3007090 | 216540 |
| tr\|B7Z1N6\|B7Z1N6_HUMAN;tr\|B7Z1Y2 | 7 | 0 | 6647600 | 0 | 20529000 | 0 | 12453870 | 1069878 |
| tr\|Q6FGX3\|Q6FGX3_HUMAN;tr\|A0A02 | 7 | 0 | 5758010 | 4839382 | 11422110 | 2367300 | 17651000 | 2592600 |
| tr\|A0A024QZY1\|A0A024QZY1_HUMAN;\| | 7 | 0 | 5153700 | 2189800 | 9480200 | 1609100 | 42779000 | 4023400 |
| tr\|A8K517\|A8K517_HUMAN;sp\|P62266 | 7 | 0 | 5122500 | 3508300 | 5656570 | 2229220 | 127187150 | 4270870 |
| sp\|Q8IXH7-4\|NELFD_HUMAN;sp\|Q8IXH | 7 | 0 | 4498516 | 754020 | 5899200 | 819832 | 8507100 | 438240 |
| sp\|Q9UNS2\|CSN3_HUMAN;sp\|Q9UNS2 | 7 | 0 | 4452360 | 397830 | 10221000 | 846470 | 15725000 | 2601288 |
| sp\|P13807-2\|GYS1_HUMAN;tr\|Q53ER0 | 7 | 0 | 4359710 | 0 | 1935000 | 0 | 8547510 | 629760 |
| sp\|A8K2U0\|A2ML1_HUMAN;tr\|Q6ZWK | 7 | 0 | 4329490 | 0 | 0 | 0 | 0 | 0 |
| sp\|Q9BV20\|MTNA_HUMAN;sp\|Q9BV20 | 7 | 0 | 4107100 | 0 | 4536014 | 966049 | 13576610 | 2646567 |
| tr\|Q5U0E4\|Q5U0E4_HUMAN;tr\|B6E4X6 | 7 | 0 | 3373300 | 864930 | 6539900 | 1322400 | 7336700 | 811430 |
| tr\|Q6PKC2\|Q6PKC2_HUMAN;tr\|Q86Y74 | 7 | 0 | 3369500 | 1976901 | 8280500 | 2319100 | 20541000 | 4621066 |
| tr\|Q5H909\|Q5H909_HUMAN;sp\|Q9UNF | 7 | 0 | 3365700 | 950780 | 2915900 | 937020 | 7472800 | 434820 |
| tr\|K7EJR3\|K7EJR3_HUMAN;tr\|Q5U0B3\| | 7 | 0 | 2881301 | 2501100 | 13966000 | 1468900 | 64546000 | 2748900 |
| tr\|B4DEN6\|B4DEN6_HUMAN;tr\|A0A02 | 7 | 0 | 2821200 | 0 | 10015000 | 338020 | 6164000 | 0 |
| sp\|Q5JRA6-2\|MIA3_HUMAN;sp\|Q5JRA | 7 | 0 | 2723800 | 330900 | 2395530 | 0 | 0 | 0 |
| tr\|B4DLT1\|B4DLT1_HUMAN;sp\|O75436 | 7 | 0 | 2575395 | 0 | 360550 | 421740 | 11308510 | 1607250 |
| tr\|V9HW95\|V9HW95_HUMAN;sp\|Q152 | 7 | 0 | 2565700 | 238510 | 3772433 | 909670 | 1963300 | 1343140 |
| sp\|Q5VUA4\|ZN318_HUMAN;sp\|Q5VUA | 7 | 0 | 2490120 | 0 | 219300 | 0 | 1664400 | 0 |
| sp\|Q9H3N1\|TMX1_HUMAN;tr\|B4DZX7\| | 7 | 0 | 2462600 | 2008300 | 3803700 | 542800 | 1156800 | 299450 |
| sp\|Q5JVF3-3\|PCID2_HUMAN;tr\|A8K097 | 7 | 0 | 2417900 | 0 | 2487700 | 369050 | 9120500 | 510920 |
| tr\|B3KU09\|B3KU09_HUMAN;sp\|Q5XPI4 | 7 | 0 | 2331000 | 0 | 1782600 | 412510 | 2179900 | 212140 |
| sp\|O00139-2\|KIF2A_HUMAN;tr\|B0AZS5 | 7 | 0 | 2109070 | 387360 | 3616480 | 219110 | 5472700 | 494620 |
| sp\|O60885\|BRD4_HUMAN;sp\|O60885-2 | 7 | 0 | 2004300 | 387970 | 1268500 | 384940 | 13386000 | 783770 |
| sp\|Q9UPN7\|PP6R1_HUMAN;tr\|B4DLT9 | 7 | 0 | 1867500 | 311670 | 1190700 | 73710 | 5547500 | 412900 |
| tr\|A0A024R411\|A0A024R411_HUMAN;s | 7 | 0 | 1821000 | 225470 | 2482140 | 478910 | 12934150 | 0 |
| sp\|Q6UN15-3\|FIP1_HUMAN;sp\|Q6UN1 | 7 | 0 | 1744700 | 216550 | 2669600 | 384410 | 10359000 | 714340 |
| sp\|Q5VTR2\|BRE1A_HUMAN;tr\|Q05DC0 | 7 | 0 | 1683000 | 0 | 500970 | 0 | 4025800 | 0 |
| tr\|B7Z341\|B7Z341_HUMAN;tr\|F8WBF9 | 7 | 0 | 1661500 | 397847 | 4321780 | 433765 | 10535090 | 487550 |
| tr\|B2RCD8\|B2RCD8_HUMAN;sp\|Q8IU83 | 7 | 0 | 1629200 | 1138200 | 4351200 | 1488200 | 4943700 | 0 |
| tr\|Q6IPN0\|Q6IPN0_HUMAN;tr\|F8W914 | 7 | 0 | 1623210 | 565422 | 2307100 | 581768 | 413410 | 477026 |
| tr\|D3DXC9\|D3DXC9_HUMAN;sp\|P3489 | 7 | 0 | 1580294 | 330010 | 2835900 | 268860 | 7828600 | 779560 |
| sp\|Q9UBW8\|CSN7A_HUMAN;tr\|Q567U | 7 | 0 | 1532320 | 936510 | 3482900 | 0 | 32195000 | 1762500 |
| tr\|A1L3Z9\|A1L3Z9_HUMAN;sp\|Q2TAL8 | 7 | 0 | 1462180 | 323010 | 646790 | 369560 | 9786435 | 238210 |
| sp\|Q9H0S4-2\|DDX47_HUMAN;tr\|Q53G3 | 7 | 0 | 1423200 | 169930 | 2446600 | 337160 | 6959200 | 0 |
| sp\|Q14694\|UBP10_HUMAN;sp\|Q14694 | 7 | 0 | 1419200 | 0 | 319000 | 0 | 0 | 209040 |
| tr\|B2RAH5\|B2RAH5_HUMAN;sp\|O1497 | 7 | 0 | 1393539 | 0 | 1036300 | 0 | 7470600 | 253510 |
| sp\|Q96RN5-3\|MED15_HUMAN;tr\|G3V1 | 7 | 0 | 1382000 | 608730 | 2480000 | 695995 | 6163455 | 1204500 |
| sp\|Q7L1Q6-2\|BZW1_HUMAN;tr\|A0A02 | 7 | 0 | 1356400 | 572510 | 2811900 | 624860 | 15866330 | 722100 |
| tr\|B5BU53\|B5BU53_HUMAN;tr\|B2R9L6 | 7 | 0 | 1348300 | 141310 | 2140200 | 345580 | 4544500 | 535430 |
| tr\|Q59GQ7\|Q59GQ7_HUMAN;tr\|A8K5B | 7 | 0 | 1348200 | 132030 | 690140 | 164580 | 6749900 | 0 |
| sp\|Q9NQW7-4\|XPP1_HUMAN;sp\|Q9N0 | 7 | 0 | 1341715 | 328840 | 574560 | 259840 | 1166800 | 472840 |
| tr\|Q6I9S2\|Q6I9S2_HUMAN;sp\|Q13573\| | 7 | 0 | 1336800 | 437210 | 1674200 | 733550 | 4972000 | 201890 |
| sp\|O43237-2\|DC1L2_HUMAN;tr\|A0A02 | 7 | 0 | 1292400 | 765140 | 7620300 | 860080 | 7019780 | 3011400 |
| tr\|E9PB90\|E9PB90_HUMAN;tr\|A8K2U2 | 7 | 0 | 1251100 | 0 | 550540 | 0 | 1684700 | 0 |
| tr\|H0Y2Y8\|H0Y2Y8_HUMAN;sp\|Q15942 | 7 | 0 | 1214500 | 386803 | 5456300 | 604660 | 13956000 | 582440 |
| tr\|E9PQP3\|E9PQP3_HUMAN;tr\|G5E9L0 | 7 | 0 | 1212600 | 1195568 | 9642159 | 1460300 | 17255650 | 2317942 |
| tr\|A8K6X9\|A8K6X9_HUMAN;sp\|Q6PD6 | 7 | 0 | 1195000 | 0 | 422640 | 0 | 10367000 | 187200 |
| tr\|A0A024RAC6\|A0A024RAC6_HUMAN;\| | 7 | 0 | 1179100 | 66003 | 306600 | 0 | 4740000 | 369950 |
| sp\|Q96SI9-2\|STRBP_HUMAN;tr\|V9HWH | 7 | 0.000357 | 1137790 | 0 | 0 | 0 | 6023900 | 0 |
| sp\|Q6XQN6-3\|PNCB_HUMAN;sp\|Q6XC | 7 | 0 | 1123500 | 0 | 3040800 | 0 | 8839300 | 1151800 |
| sp\|Q7Z4H3-2\|HDDC2_HUMAN;sp\|Q7Z4 | 7 | 0 | 1066400 | 516390 | 2008900 | 612130 | 15453000 | 1948400 |
| tr\|F8W7C6\|F8W7C6_HUMAN;tr\|A0A08 | 7 | 0 | 1032092 | 407070 | 4657620 | 0 | 29375000 | 2550600 |
| sp\|Q92572\|AP3S1_HUMAN;tr\|B2R4I8\|B | 7 | 0 | 1015600 | 3901022 | 6049840 | 1239700 | 16691000 | 255140 |
| sp\|Q7Z7L1\|SLN11_HUMAN;tr\|K7ER38\|I | 7 | 0 | 1009700 | 0 | 916170 | 0 | 6029500 | 0 |
| sp\|Q9NX46\|ARHL2_HUMAN;tr\|B4DHV5 | 7 | 0 | 964760 | 0 | 2186500 | 0 | 947450 | 1076249 |
| tr\|V9HWA6\|V9HWA6_HUMAN;sp\|P609 | 7 | 0 | 915110 | 665940 | 3629700 | 461140 | 9024500 | 1040767 |

| | | | | | | | | |
|---|---|---|---|---|---|---|---|---|
| tr\|Q8IW76\|Q8IW76_HUMAN;tr\|B7ZKK7 | 7 | 0 | 861110 | 0 | 2985100 | 0 | 11303000 | 0 |
| sp\|P14324-2\|FPPS_HUMAN;sp\|P14324 | 7 | 0 | 859400 | 1237300 | 1633100 | 0 | 17157000 | 4065730 |
| tr\|Q53GF0\|Q53GF0_HUMAN;sp\|Q8NFV | 7 | 0 | 854080 | 0 | 2601500 | 111820 | 10213540 | 544850 |
| tr\|A0PJ47\|A0PJ47_HUMAN;sp\|Q14151 | 7 | 0.00036 | 845750 | 0 | 0 | 0 | 0 | 0 |
| sp\|Q9BS26\|ERP44_HUMAN | 7 | 0 | 844580 | 308690 | 1375910 | 0 | 9480800 | 0 |
| sp\|Q9Y266\|NUDC_HUMAN;tr\|Q9H2R7 | 7 | 0 | 837350 | 1260180 | 1771000 | 310220 | 2077900 | 1864106 |
| sp\|O95758-1\|PTBP3_HUMAN;sp\|O9575 | 7 | 0 | 820750 | 0 | 3172200 | 0 | 8544500 | 0 |
| tr\|Q6FH36\|Q6FH36_HUMAN;sp\|O4344 | 7 | 0 | 820670 | 935140 | 1695880 | 716300 | 31196000 | 1954248 |
| tr\|V9HW40\|V9HW40_HUMAN;sp\|O758 | 7 | 0 | 797300 | 0 | 1647600 | 46899 | 14645000 | 1393200 |
| tr\|B2R8A2\|B2R8A2_HUMAN;tr\|A0A024 | 7 | 0 | 770820 | 0 | 1221060 | 0 | 11909000 | 1676290 |
| sp\|Q96L92-3\|SNX27_HUMAN;sp\|Q96L9 | 7 | 0 | 767310 | 0 | 832760 | 0 | 7341000 | 216820 |
| sp\|P48449-3\|ERG7_HUMAN;sp\|P48449 | 7 | 0 | 763490 | 378240 | 1251600 | 0 | 339390 | 0 |
| sp\|Q12802-4\|AKP13_HUMAN;sp\|Q128 | 7 | 0 | 738400 | 0 | 250280 | 228710 | 13350300 | 112720 |
| tr\|Q9UHT7\|Q9UHT7_HUMAN | 7 | 0.00682 | 737830 | 0 | 0 | 0 | 0 | 0 |
| tr\|Q05BW9\|Q05BW9_HUMAN;tr\|Q6IA | 7 | 0 | 718760 | 0 | 3146200 | 0 | 2688040 | 0 |
| tr\|Q53F37\|Q53F37_HUMAN;sp\|Q9Y6B6 | 7 | 0 | 703210 | 0 | 8058600 | 0 | 8984480 | 1488100 |
| sp\|Q5SW79\|CE170_HUMAN;tr\|A6H8X9 | 7 | 0 | 630880 | 0 | 631660 | 0 | 4402700 | 251120 |
| tr\|B3KR89\|B3KR89_HUMAN;sp\|O95785 | 7 | 0 | 629681 | 130000 | 433100 | 0 | 3324800 | 90226 |
| sp\|P46939\|UTRO_HUMAN;sp\|P46939-2 | 7 | 0 | 622250 | 0 | 444840 | 0 | 1805940 | 0 |
| tr\|V9HW74\|V9HW74_HUMAN;sp\|P099 | 7 | 0 | 621390 | 484190 | 1995137 | 200530 | 8972800 | 2133900 |
| sp\|P22307-7\|NLTP_HUMAN;sp\|P22307 | 7 | 0 | 517048 | 2071500 | 4349140 | 643130 | 9003070 | 1536400 |
| tr\|Q53R19\|Q53R19_HUMAN;sp\|O15144 | 7 | 0 | 484260 | 298090 | 1550900 | 720290 | 2337800 | 1103000 |
| tr\|B2RAJ6\|B2RAJ6_HUMAN;tr\|A0JP11 | 7 | 0 | 473610 | 0 | 686980 | 0 | 9027500 | 355152 |
| tr\|B7ZAC0\|B7ZAC0_HUMAN;tr\|B4DK06 | 7 | 0 | 440970 | 0 | 326830 | 0 | 4811800 | 437150 |
| tr\|Q5TDE9\|Q5TDE9_HUMAN;sp\|Q9BSD | 7 | 0 | 440680 | 0 | 1395100 | 0 | 18392000 | 1436900 |
| sp\|Q92995-2\|UBP13_HUMAN;sp\|Q929 | 7 | 0 | 440550 | 0 | 320480 | 0 | 2438200 | 204830 |
| sp\|Q9C0J8\|WDR33_HUMAN;tr\|C9J8B4 | 7 | 0 | 424630 | 0 | 173470 | 0 | 4721700 | 0 |
| tr\|B2R7E8\|B2R7E8_HUMAN;sp\|P15927 | 7 | 0 | 418991 | 437090 | 1825400 | 251610 | 10950000 | 1127900 |
| sp\|Q9NPQ8-4\|RIC8A_HUMAN;sp\|Q9NI | 7 | 0 | 401360 | 0 | 398570 | 268719 | 1761400 | 0 |
| tr\|E5KT65\|E5KT65_HUMAN;sp\|P19388 | 7 | 0 | 399930 | 0 | 797879 | 19671 | 18900000 | 711880 |
| tr\|A8MZF9\|A8MZF9_HUMAN;sp\|P5503 | 7 | 0 | 394010 | 0 | 3793600 | 0 | 5172400 | 234430 |
| sp\|Q86VM9\|ZCH18_HUMAN;tr\|E7ERS3 | 7 | 0 | 392530 | 2729115 | 0 | 1032190 | 6136400 | 374940 |
| tr\|Q549N5\|Q549N5_HUMAN;sp\|Q9Y5M | 7 | 0 | 374970 | 508160 | 1237800 | 200120 | 648680 | 0 |
| tr\|V9HWJ8\|V9HWJ8_HUMAN;sp\|P6128 | 7 | 0 | 361720 | 99505 | 3156900 | 235860 | 12411890 | 1112300 |
| tr\|B2RDN3\|B2RDN3_HUMAN;sp\|Q9Y5Y | 7 | 0 | 319360 | 502360 | 1539600 | 483030 | 14790000 | 966910 |
| sp\|Q08379\|GOGA2_HUMAN;sp\|Q0837 | 7 | 0 | 318870 | 0 | 238740 | 0 | 4956600 | 0 |
| tr\|Q53SW3\|Q53SW3_HUMAN;sp\|Q9BP | 7 | 0 | 297170 | 372610 | 8356100 | 265630 | 20815000 | 0 |
| tr\|A0A024R4U0\|A0A024R4U0_HUMAN; | 7 | 0 | 276110 | 0 | 911800 | 319840 | 6426100 | 685100 |
| sp\|P25490\|TYY1_HUMAN;tr\|H0YJV7\|H0 | 7 | 0 | 268340 | 153320 | 2320200 | 153300 | 8932175 | 627450 |
| tr\|D3YTB1\|D3YTB1_HUMAN;tr\|A0A024 | 7 | 0 | 246180 | 0 | 1929570 | 52987 | 33288000 | 1861120 |
| tr\|Q6FHF7\|Q6FHF7_HUMAN;sp\|Q9269 | 7 | 0 | 234610 | 0 | 1965900 | 0 | 2540270 | 0 |
| sp\|Q9BZV1-2\|UBXN6_HUMAN;sp\|Q9B2 | 7 | 0 | 231050 | 0 | 1978900 | 0 | 6885800 | 0 |
| tr\|A0A024RB09\|A0A024RB09_HUMAN;s | 7 | 0 | 221560 | 313430 | 56285 | 420760 | 0 | 0 |
| sp\|P55795\|HNRH2_HUMAN;tr\|B4DFK9 | 7 | 0 | 218440 | 0 | 548320 | 0 | 968150 | 0 |
| sp\|Q9NPF4\|OSGEP_HUMAN;tr\|G3V4G4 | 7 | 0 | 217100 | 858050 | 1162300 | 0 | 12812000 | 1209500 |
| sp\|Q9H0U4\|RAB1B_HUMAN;tr\|E9PLD0 | 7 | 0 | 212680 | 332340 | 876820 | 188870 | 933990 | 332220 |
| sp\|Q8TC07-2\|TBC15_HUMAN;sp\|Q8TC0 | 7 | 0 | 171750 | 0 | 971200 | 0 | 4721400 | 0 |
| tr\|C9JFR7\|C9JFR7_HUMAN;tr\|G4XXL9 | 7 | 0 | 149800 | 107850 | 0 | 57785 | 372240 | 3469300 |
| tr\|Q5VXV3\|Q5VXV3_HUMAN;sp\|Q011 | 7 | 0 | 149010 | 1304590 | 1393330 | 821000 | 871480 | 5315490 |
| tr\|Q9H2G0\|Q9H2G0_HUMAN;tr\|Q5W7 | 7 | 0 | 136710 | 0 | 958390 | 0 | 3306200 | 0 |
| sp\|Q15018\|F175B_HUMAN | 7 | 0 | 128150 | 0 | 613160 | 0 | 4643700 | 81704 |
| sp\|P53384-2\|NUBP1_HUMAN;sp\|P5338 | 7 | 0 | 122400 | 0 | 1337400 | 0 | 10813210 | 980690 |
| tr\|Q6PKD2\|Q6PKD2_HUMAN;sp\|P0DM | 7 | 0.003002 | 104720 | 0 | 0 | 0 | 0 | 0 |
| sp\|Q14019\|COTL1_HUMAN;tr\|H3BT58 | 7 | 0 | 76352 | 1105700 | 614040 | 1937000 | 6499600 | 754500 |
| sp\|Q9BUH6\|CI142_HUMAN;sp\|Q9BUH6 | 7 | 0 | 76070 | 0 | 133640 | 0 | 4500200 | 463990 |
| tr\|F5GXF5\|F5GXF5_HUMAN;sp\|Q12830 | 7 | 0 | 52883 | 13211 | 0 | 0 | 4706100 | 40085 |
| sp\|P14635-2\|CCNB1_HUMAN;tr\|E9PC9 | 7 | 0 | 0 | 0 | 1049800 | 0 | 1293800 | 0 |
| sp\|P36507\|MP2K2_HUMAN;tr\|G5E9C7 | 7 | 0 | 0 | 0 | 973660 | 0 | 4818530 | 0 |
| sp\|P54619-2\|AAKG1_HUMAN;tr\|A0A02 | 7 | 0 | 0 | 0 | 468500 | 0 | 4021120 | 0 |
| sp\|Q01804\|OTUD4_HUMAN;sp\|Q01804 | 7 | 0 | 0 | 0 | 172600 | 0 | 4021600 | 0 |
| sp\|Q13330-3\|MTA1_HUMAN;tr\|E7ESY4 | 7 | 0 | 0 | 0 | 489510 | 0 | 1144600 | 0 |
| sp\|Q5MIZ7-3\|P4R3B_HUMAN;sp\|Q5MI | 7 | 0.009394 | 0 | 0 | 0 | 0 | 816640 | 0 |
| sp\|Q9NTX5-6\|ECHD1_HUMAN;sp\|Q9N | 7 | 0 | 0 | 0 | 480710 | 0 | 4090000 | 0 |
| sp\|Q9UBD5-3\|ORC3_HUMAN;tr\|B4E014 | 7 | 0 | 0 | 0 | 0 | 0 | 4926200 | 0 |
| sp\|Q9Y2X3\|NOP58_HUMAN;tr\|B3KN82 | 7 | 0 | 0 | 0 | 1016000 | 0 | 9622500 | 0 |
| tr\|A0A024RCZ8\|A0A024RCZ8_HUMAN;s | 7 | 0 | 0 | 0 | 0 | 0 | 2928170 | 0 |
| tr\|F8W950\|F8W950_HUMAN;tr\|A8MU5 | 7 | 1 | 0 | 0 | 0 | 0 | 930010 | 0 |
| tr\|Q1W6G4\|Q1W6G4_HUMAN;sp\|Q9N | 7 | 0.006548 | 0 | 0 | 0 | 0 | 733060 | 0 |
| tr\|Q53FR9\|Q53FR9_HUMAN;sp\|Q9P00 | 7 | 0 | 0 | 0 | 112030 | 0 | 5486500 | 0 |
| tr\|V9HWG0\|V9HWG0_HUMAN;sp\|P459 | 7 | 0 | 0 | 0 | 1889600 | 0 | 3337600 | 86830 |
| tr\|X1WI28\|X1WI28_HUMAN;tr\|X5D2T3 | 7 | 0 | 0 | 0 | 3266200 | 0 | 9784700 | 479590 |
| sp\|O95983-2\|MBD3_HUMAN;sp\|O9598 | 7 | 0 | 0 | 0 | 0 | 0 | 5177800 | 269850 |
| tr\|A0A023T6R1\|A0A023T6R1_HUMAN;s | 7 | 0 | 0 | 0 | 0 | 0 | 5620260 | 1074100 |
| tr\|V9HW92\|V9HW92_HUMAN;sp\|O001 | 7 | 0 | 0 | 0 | 392900 | 0 | 3545060 | 1270900 |
| sp\|P33316-2\|DUT_HUMAN;tr\|H0YNW5 | 7 | 0 | 0 | 0 | 0 | 0 | 0 | 1314767 |

| | | | | | | | | |
|---|---|---|---|---|---|---|---|---|
| tr\|A0A024R2U9\|A0A024R2U9_HUMAN; | 7 | 0 | 0 | 0 | 0 | 0 | 0 | 502160 |
| tr\|A0A024RDB0\|A0A024RDB0_HUMAN; | 7 | 0 | 0 | 0 | 0 | 0 | 0 | 249630 |
| tr\|B4DEA3\|B4DEA3_HUMAN;tr\|Q53F10 | 7 | 0 | 0 | 0 | 0 | 0 | 0 | 243230 |
| tr\|D6RGI3\|D6RGI3_HUMAN;sp\|Q9NVA | 7 | 0 | 0 | 0 | 0 | 0 | 0 | 303120 |
| sp\|Q86U44\|MTA70_HUMAN;tr\|B4E2F6 | 7 | 0 | 0 | 262960 | 3219000 | 0 | 8711880 | 0 |
| sp\|Q8TDD1\|DDX54_HUMAN;sp\|Q8TDD | 7 | 0 | 0 | 97676 | 0 | 0 | 8213600 | 0 |
| tr\|Q96BS4\|Q96BS4_HUMAN;sp\|P22087 | 7 | 0 | 0 | 268440 | 402550 | 0 | 8318700 | 0 |
| tr\|Q6FHU3\|Q6FHU3_HUMAN;sp\|Q0632 | 7 | 0 | 0 | 87745 | 137320 | 0 | 750200 | 506380 |
| sp\|Q9NRN7\|ADPPT_HUMAN;sp\|Q9NRI | 7 | 0 | 0 | 60615 | 30054 | 0 | 41704 | 353780 |
| sp\|A6NDG6\|PGP_HUMAN;tr\|H3BV17\|H | 7 | 0 | 0 | 137230 | 817860 | 90115 | 7509000 | 0 |
| tr\|B4DRN6\|B4DRN6_HUMAN;tr\|A0A02 | 7 | 0 | 0 | 434990 | 3017700 | 357210 | 17406000 | 711240 |
| tr\|B7Z4Q0\|B7Z4Q0_HUMAN;tr\|H0Y6A0 | 7 | 0.001036 | 0 | 0 | 681900 | 86276 | 765220 | 0 |
| tr\|A0A024R471\|A0A024R471_HUMAN;s | 7 | 0 | 0 | 223180 | 951210 | 322800 | 15021000 | 710040 |
| sp\|Q9BTT0-3\|AN32E_HUMAN | 7 | 0 | 0 | 248630 | 544670 | 321390 | 2465000 | 0 |
| tr\|J3QLE5\|J3QLE5_HUMAN;tr\|Q66K91\| | 7 | 0 | 0 | 216455 | 186120 | 204747 | 8234000 | 870880 |
| tr\|F8VR84\|F8VR84_HUMAN;tr\|Q8WYI2 | 7 | 0 | 0 | 0 | 0 | 305021 | 0 | 274380 |
| sp\|P14859-4\|PO2F1_HUMAN;sp\|P1485 | 7 | 0 | 0 | 397030 | 0 | 180090 | 14724300 | 2536600 |
| tr\|Q53FT8\|Q53FT8_HUMAN;sp\|P20618 | 7 | 0 | 0 | 632625 | 0 | 67090 | 486460 | 962220 |
| sp\|P81605\|DCD_HUMAN | 6 | 0 | 161153000 | 142438000 | 117114000 | 150502000 | 117449000 | 178818000 |
| tr\|Q53FU3\|Q53FU3_HUMAN;tr\|A0A024 | 6 | 0 | 19683000 | 13877000 | 76857000 | 7440378 | 124500000 | 6126500 |
| sp\|P01040\|CYTA_HUMAN;tr\|C9J0E4\|C9 | 6 | 0 | 13585300 | 9799200 | 10506500 | 10817900 | 12214900 | 11597000 |
| tr\|V9HW34\|V9HW34_HUMAN | 6 | 0 | 9804900 | 4941800 | 2847370 | 5775000 | 7193670 | 6676720 |
| tr\|A0A024RCA7\|A0A024RCA7_HUMAN; | 6 | 0 | 9058040 | 11053020 | 33744220 | 10505100 | 136780000 | 41028020 |
| tr\|Q6NZ52\|Q6NZ52_HUMAN;sp\|P4677 | 6 | 0 | 8457690 | 3867850 | 13015800 | 2554290 | 140372000 | 13995140 |
| sp\|P62847-2\|RS24_HUMAN;tr\|E7ETK0\| | 6 | 0 | 7528200 | 790720 | 12129000 | 255280 | 41975960 | 2789660 |
| tr\|V9HWH9\|V9HWH9_HUMAN;sp\|P319 | 6 | 0 | 7468320 | 3057800 | 541320 | 0 | 194790 | 4681360 |
| tr\|Q7RTM4\|Q7RTM4_HUMAN | 6 | 0 | 7016070 | 2773573 | 11311975 | 2519400 | 33974450 | 6455190 |
| tr\|E5RGR0\|E5RGR0_HUMAN;sp\|O7560 | 6 | 0 | 6749110 | 2804200 | 12407000 | 1795807 | 53327000 | 2586200 |
| tr\|B4DUS0\|B4DUS0_HUMAN;sp\|Q9P28 | 6 | 0 | 5961800 | 353580 | 9456700 | 1065600 | 14247000 | 1366700 |
| tr\|B0AZN7\|B0AZN7_HUMAN;tr\|A8K5N | 6 | 0 | 5898750 | 679270 | 683110 | 2047830 | 225180 | 0 |
| sp\|P42357\|HUTH_HUMAN;sp\|P42357-2 | 6 | 0 | 5494020 | 0 | 0 | 167170 | 0 | 0 |
| sp\|Q58FF6\|H90B4_HUMAN | 6 | 0 | 5280600 | 3356413 | 9172834 | 3030435 | 9170880 | 4943190 |
| tr\|Q59GU5\|Q59GU5_HUMAN;sp\|Q1340 | 6 | 0 | 4489300 | 2301921 | 9263630 | 2024784 | 14974980 | 3482500 |
| tr\|A8K7N0\|A8K7N0_HUMAN | 6 | 0 | 4480250 | 3804275 | 10204540 | 1969600 | 146085704 | 6968020 |
| sp\|P40616-2\|ARL1_HUMAN;sp\|P40616 | 6 | 0 | 4427700 | 2396000 | 8477200 | 1497500 | 30745100 | 12069241 |
| tr\|B2R4S9\|B2R4S9_HUMAN;tr\|A8K9J7\| | 6 | 0 | 4378910 | 3793396 | 6152370 | 248483 | 28749100 | 2181050 |
| tr\|Q8N355\|Q8N355_HUMAN;tr\|Q6GMV | 6 | 0 | 4292500 | 1996000 | 3116060 | 1113490 | 4573850 | 2698240 |
| tr\|K7EQ02\|K7EQ02_HUMAN;sp\|Q96EP5 | 6 | 0 | 4149442 | 1082000 | 13779666 | 1184600 | 29123000 | 5677563 |
| tr\|B7Z5J4\|B7Z5J4_HUMAN;sp\|Q9UI42-2 | 6 | 0 | 4057045 | 65017 | 0 | 0 | 50154 | 0 |
| tr\|B4DHC5\|B4DHC5_HUMAN;tr\|A0A024 | 6 | 0 | 4037200 | 743250 | 10640320 | 779990 | 12726460 | 1054300 |
| tr\|C9JGI3\|C9JGI3_HUMAN;tr\|E5KRG5\|E | 6 | 0 | 4000400 | 0 | 0 | 0 | 0 | 0 |
| sp\|Q02241-2\|KIF23_HUMAN;tr\|H7BYN4 | 6 | 0 | 3793000 | 168350 | 1463500 | 0 | 2673300 | 0 |
| sp\|Q9P035\|HACD3_HUMAN;tr\|H3BS72 | 6 | 0 | 3739340 | 322140 | 1583080 | 633940 | 2087590 | 0 |
| sp\|P61224-2\|RAP1B_HUMAN;sp\|P6122 | 6 | 0 | 3560900 | 1076182 | 14010000 | 5170625 | 5882800 | 2873400 |
| sp\|Q8WYA6-4\|CTBL1_HUMAN;sp\|Q8W | 6 | 0 | 3450100 | 624750 | 6066300 | 245500 | 14072000 | 0 |
| tr\|A0A024R8P8\|A0A024R8P8_HUMAN;s | 6 | 0 | 3202370 | 4069100 | 8658500 | 2469666 | 80123460 | 17875000 |
| sp\|Q05048\|CSTF1_HUMAN;tr\|B4DDG3\| | 6 | 0 | 3173300 | 158690 | 2393800 | 399340 | 13742000 | 1492600 |
| sp\|Q14257\|RCN2_HUMAN;sp\|Q14257-2 | 6 | 0 | 3126900 | 0 | 5010600 | 218340 | 7265500 | 1424700 |
| sp\|Q9H6R4-4\|NOL6_HUMAN;sp\|Q9H6R | 6 | 0 | 2898900 | 274790 | 787850 | 0 | 4482500 | 423880 |
| tr\|Q5JR08\|Q5JR08_HUMAN;tr\|A0A024R | 6 | 0 | 2875300 | 2835800 | 6984800 | 2068320 | 24472000 | 7552100 |
| sp\|P49903\|SPS1_HUMAN;sp\|P49903-2 | 6 | 0 | 2678800 | 2105900 | 6988300 | 862758 | 11642000 | 1512100 |
| tr\|B7Z7Z8\|B7Z7Z8_HUMAN;tr\|B7Z8G2\| | 6 | 0 | 2668700 | 568530 | 4311800 | 623190 | 13356000 | 1755100 |
| tr\|E9PG22\|E9PG22_HUMAN;sp\|Q8IW35 | 6 | 0 | 2640800 | 107210 | 781160 | 148660 | 1591500 | 109840 |
| sp\|P59998\|ARPC4_HUMAN;tr\|F8WCF6 | 6 | 0 | 2588720 | 2600600 | 3721400 | 1249407 | 6229100 | 3941300 |
| tr\|B4DXG8\|B4DXG8_HUMAN;tr\|D6RIY6 | 6 | 0 | 2565000 | 198290 | 5860900 | 315850 | 9189560 | 0 |
| sp\|Q6PJT7-10\|ZC3HE_HUMAN;sp\|Q6PJ | 6 | 0 | 2528000 | 228153 | 1223870 | 280290 | 6011800 | 715520 |
| sp\|Q2TAZ0\|ATG2A_HUMAN;sp\|Q2TAZ0 | 6 | 0 | 2475200 | 0 | 570060 | 0 | 4176000 | 0 |
| tr\|Q6PKI6\|Q6PKI6_HUMAN;tr\|Q05D43 | 6 | 0 | 2440931 | 600406 | 3482600 | 425640 | 8967000 | 1520150 |
| tr\|A0A024R8M4\|A0A024R8M4_HUMAN | 6 | 0 | 2419100 | 0 | 1900600 | 644280 | 8587490 | 1031800 |
| sp\|P31942-3\|HNRH3_HUMAN;sp\|P3194 | 6 | 0 | 2381640 | 621300 | 5055500 | 355770 | 14915000 | 2568080 |
| sp\|O95155-2\|UBE4B_HUMAN;sp\|O9515 | 6 | 0 | 2280000 | 0 | 0 | 0 | 4858680 | 0 |
| sp\|Q8TCG1\|CIP2A_HUMAN;tr\|A0A087X | 6 | 0 | 2088920 | 0 | 190890 | 0 | 1191800 | 0 |
| sp\|Q8WWH5\|TRUB1_HUMAN;tr\|B4DZ9 | 6 | 0 | 1989120 | 0 | 1479130 | 132680 | 1719700 | 529090 |
| sp\|Q5UIP0-2\|RIF1_HUMAN;sp\|Q5UIP0 | 6 | 0 | 1886300 | 0 | 285710 | 0 | 1504940 | 0 |
| sp\|P12532\|KCRU_HUMAN;sp\|P12532-2 | 6 | 0 | 1883200 | 0 | 3123100 | 0 | 4849000 | 2321300 |
| tr\|B0AZM4\|B0AZM4_HUMAN;tr\|A8K6F | 6 | 0 | 1865500 | 97746 | 663840 | 0 | 3357300 | 50897 |
| tr\|Q71UA6\|Q71UA6_HUMAN;sp\|Q1575 | 6 | 0 | 1829000 | 0 | 1993200 | 0 | 0 | 0 |
| sp\|O00487\|PSDE_HUMAN;tr\|Q53TH1\|Q | 6 | 0 | 1758620 | 1981866 | 5947100 | 1483505 | 27175000 | 5906939 |
| tr\|E9PRQ7\|E9PRQ7_HUMAN;tr\|A0A024 | 6 | 0 | 1690679 | 269330 | 0 | 1225070 | 13072400 | 2263700 |
| tr\|E9PIN3\|E9PIN3_HUMAN;sp\|Q9UBU9 | 6 | 0 | 1684430 | 222030 | 2048310 | 0 | 5443530 | 0 |
| tr\|A0A087WXM6\|A0A087WXM6_HUMA | 6 | 0 | 1664890 | 2612100 | 7410288 | 0 | 96602040 | 5901210 |
| tr\|B4E054\|B4E054_HUMAN;tr\|A0A024R | 6 | 0 | 1494400 | 113860 | 2874700 | 121560 | 1776600 | 157620 |
| tr\|B2R7C2\|B2R7C2_HUMAN;sp\|O43264 | 6 | 0 | 1490700 | 328200 | 3397200 | 107720 | 4501600 | 0 |
| sp\|Q9UFC0\|LRWD1_HUMAN;tr\|H7C5S6 | 6 | 0 | 1484040 | 0 | 2328300 | 0 | 8859300 | 0 |
| sp\|Q96G03\|PGM2_HUMAN;tr\|B4DN40 | 6 | 0 | 1418500 | 143567000 | 4270000 | 143932000 | 19448900 | 197262000 |

| | | | | | | | | | |
|---|---|---|---|---|---|---|---|---|---|
| sp\|Q9BW27-3\|NUP85_HUMAN;sp\|Q9B | 6 | 0 | 1402200 | 0 | 2930400 | 498580 | 10741851 | 0 |
| tr\|Q68CN2\|Q68CN2_HUMAN;tr\|Q71SV | 6 | 0 | 1347800 | 0 | 0 | 0 | 4247100 | 167030 |
| sp\|Q68CP9-3\|ARID2_HUMAN;sp\|Q68CI | 6 | 0 | 1328400 | 0 | 926410 | 229120 | 4301100 | 0 |
| tr\|A0A024R388\|A0A024R388_HUMAN;s | 6 | 0 | 1262800 | 426560 | 3173500 | 421610 | 8787200 | 1044300 |
| sp\|O15400-2\|STX7_HUMAN;sp\|O15400 | 6 | 0 | 1204470 | 175880 | 2206460 | 0 | 5136300 | 0 |
| tr\|B7Z9T5\|B7Z9T5_HUMAN;tr\|A0A024R | 6 | 0 | 1195100 | 1375000 | 2753800 | 251510 | 4460300 | 0 |
| sp\|Q9C0C9\|UBE2O_HUMAN;tr\|K7ES11\| | 6 | 0 | 1176100 | 0 | 0 | 0 | 1912900 | 0 |
| sp\|Q15056-2\|IF4H_HUMAN;sp\|Q15056 | 6 | 0 | 1146920 | 1330500 | 3195100 | 1077100 | 31913180 | 1575400 |
| sp\|O75376-2\|NCOR1_HUMAN;tr\|A0A0 | 6 | 0 | 1128200 | 96204 | 374370 | 187910 | 5354800 | 0 |
| tr\|Q8N959\|Q8N959_HUMAN;tr\|B3KU6 | 6 | 0 | 1068000 | 1601600 | 3369800 | 908910 | 10487559 | 267410 |
| sp\|P13861-2\|KAP2_HUMAN;tr\|A8KAH7 | 6 | 0 | 1053900 | 422180 | 3354300 | 0 | 4626000 | 532170 |
| tr\|E5RHW4\|E5RHW4_HUMAN;sp\|O949 | 6 | 0 | 994810 | 0 | 2607200 | 0 | 0 | 0 |
| sp\|P20339-2\|RAB5A_HUMAN;tr\|A0A02 | 6 | 0 | 969910 | 982220 | 1595700 | 680960 | 994420 | 705040 |
| tr\|F8VSC5\|F8VSC5_HUMAN;sp\|Q6P3W | 6 | 0 | 944310 | 181300 | 338690 | 0 | 3128500 | 537860 |
| sp\|Q92783-2\|STAM1_HUMAN;tr\|B2RA | 6 | 0 | 926160 | 0 | 2051500 | 0 | 6094600 | 0 |
| sp\|Q14574-2\|DSC3_HUMAN;tr\|A8K6T3 | 6 | 0 | 900810 | 3052660 | 1153020 | 4786830 | 4082050 | 1177910 |
| sp\|Q8IZ83-3\|A16A1_HUMAN;sp\|Q8IZ8 | 6 | 0 | 888610 | 0 | 1866200 | 0 | 6355600 | 141210 |
| tr\|Q0IJ56\|Q0IJ56_HUMAN;tr\|B4E0U6\|B | 6 | 0 | 878100 | 772030 | 800650 | 360310 | 3024200 | 2579508 |
| sp\|Q9NZL4\|HPBP1_HUMAN;sp\|Q9NZL4 | 6 | 0 | 872590 | 0 | 2329900 | 199840 | 9521000 | 0 |
| sp\|P06730\|IF4E_HUMAN;sp\|P06730-2\| | 6 | 0 | 814059 | 818790 | 2357770 | 594090 | 32192656 | 1043800 |
| sp\|Q14444-2\|CAPR1_HUMAN;sp\|Q144 | 6 | 0 | 770350 | 0 | 1263140 | 0 | 4431880 | 1283900 |
| sp\|Q01433-5\|AMPD2_HUMAN;sp\|Q014 | 6 | 0 | 769920 | 133370 | 516310 | 0 | 4325900 | 1688800 |
| tr\|E9PID8\|E9PID8_HUMAN;tr\|B4DUD5\| | 6 | 0 | 761010 | 400340 | 1395000 | 489480 | 4909500 | 0 |
| sp\|Q96P48-3\|ARAP1_HUMAN;sp\|Q96P | 6 | 0 | 675960 | 0 | 330470 | 0 | 1891200 | 195060 |
| tr\|H7BZJ3\|H7BZJ3_HUMAN | 6 | 0 | 665730 | 511630 | 707290 | 358610 | 892260 | 440070 |
| tr\|A8K9U0\|A8K9U0_HUMAN;sp\|Q9BWI | 6 | 0 | 655800 | 0 | 1406100 | 251760 | 4153960 | 391420 |
| sp\|Q16629-3\|SRSF7_HUMAN;sp\|Q1662 | 6 | 0 | 644360 | 674800 | 876430 | 478340 | 6642700 | 4604220 |
| sp\|O43719\|HTSF1_HUMAN;tr\|B4DRS4\| | 6 | 0 | 629930 | 0 | 132050 | 0 | 5961200 | 54779 |
| sp\|Q9UJU6\|DBNL_HUMAN;sp\|Q9UJU6- | 6 | 0 | 600350 | 127130 | 1025000 | 0 | 6117300 | 274750 |
| sp\|P50748\|KNTC1_HUMAN;sp\|P50748- | 6 | 0 | 600330 | 0 | 519620 | 117950 | 3418200 | 0 |
| tr\|B4DYG5\|B4DYG5_HUMAN;sp\|P4235E | 6 | 0 | 572030 | 0 | 467900 | 0 | 3179000 | 0 |
| tr\|A0A024R9B5\|A0A024R9B5_HUMAN;s | 6 | 0 | 558820 | 282360 | 3324400 | 0 | 9327100 | 162830 |
| tr\|Q5U025\|Q5U025_HUMAN;sp\|P62330 | 6 | 0 | 558430 | 4134500 | 1393300 | 997060 | 10928000 | 2236300 |
| sp\|O95433\|AHSA1_HUMAN;tr\|H0YJG7\| | 6 | 0 | 552950 | 0 | 1596200 | 0 | 0 | 89607 |
| sp\|Q14738-3\|2A5D_HUMAN;tr\|B4DSD7 | 6 | 0 | 524270 | 0 | 299880 | 0 | 1171100 | 0 |
| sp\|Q13724-2\|MOGS_HUMAN;tr\|Q58F0 | 6 | 0 | 523960 | 126710 | 0 | 312220 | 0 | 0 |
| tr\|A0A024R582\|A0A024R582_HUMAN;s | 6 | 0 | 517530 | 181390 | 1851840 | 0 | 6526700 | 208460 |
| sp\|Q9UIG0-2\|BAZ1B_HUMAN;sp\|Q9UI | 6 | 0 | 497250 | 0 | 0 | 0 | 4103200 | 0 |
| sp\|P42574\|CASP3_HUMAN;tr\|C9JXR7\| | 6 | 0 | 494820 | 0 | 1425000 | 0 | 5464100 | 453730 |
| tr\|B4E205\|B4E205_HUMAN;sp\|O95486 | 6 | 0 | 435410 | 0 | 1645130 | 0 | 0 | 112540 |
| sp\|P62873-2\|GBB1_HUMAN;tr\|B2R6K4 | 6 | 0 | 430980 | 198171 | 2065500 | 361117 | 2207041 | 350050 |
| tr\|H3BLU7\|H3BLU7_HUMAN;tr\|V9HWA | 6 | 0 | 418000 | 1139700 | 2605300 | 824030 | 7273900 | 1527900 |
| sp\|Q3YEC7\|RABL6_HUMAN;sp\|Q3YEC7 | 6 | 0 | 416150 | 563700 | 1051700 | 219420 | 2283400 | 298110 |
| sp\|Q15750-2\|TAB1_HUMAN;tr\|A8K6K3 | 6 | 0 | 399130 | 0 | 2786100 | 0 | 4445200 | 0 |
| tr\|B4DZF1\|B4DZF1_HUMAN;sp\|Q9UHD | 6 | 0 | 393750 | 1409800 | 1555200 | 676970 | 3256500 | 3791205 |
| sp\|P26232-3\|CTNA2_HUMAN;sp\|P2623 | 6 | 0.004246 | 384990 | 0 | 0 | 0 | 0 | 0 |
| tr\|B5MCF9\|B5MCF9_HUMAN;sp\|O0054 | 6 | 0 | 384910 | 76239 | 312207 | 0 | 1985410 | 148260 |
| sp\|Q9H1B7\|I2BPL_HUMAN | 6 | 0 | 382020 | 0 | 328320 | 0 | 5512120 | 140350 |
| tr\|H7BXY3\|H7BXY3_HUMAN;sp\|Q7L2E3 | 6 | 0 | 381170 | 0 | 651920 | 0 | 3936200 | 100210 |
| sp\|Q96B26\|EXOS8_HUMAN;tr\|Q5JXM0 | 6 | 0 | 375990 | 295690 | 1009400 | 227980 | 6252400 | 356320 |
| sp\|Q6PJ69\|TRI65_HUMAN;tr\|H0YGS7\|H | 6 | 0 | 373650 | 0 | 172930 | 0 | 4924300 | 0 |
| tr\|A0A024R3P9\|A0A024R3P9_HUMAN;s | 6 | 0 | 342740 | 536010 | 1606500 | 477340 | 7099500 | 276660 |
| sp\|P82979\|SARNP_HUMAN;tr\|Q567R9 | 6 | 0 | 336000 | 831280 | 2905100 | 904770 | 12695375 | 3015000 |
| sp\|Q12792\|TWF1_HUMAN;sp\|Q12792- | 6 | 0 | 333590 | 95497 | 502980 | 81355 | 1094400 | 151180 |
| sp\|Q86TP1\|PRUNE_HUMAN;sp\|Q86TP1 | 6 | 0 | 326350 | 611620 | 2519700 | 825770 | 5937260 | 937724 |
| tr\|A0A024R565\|A0A024R565_HUMAN;s | 6 | 0 | 316970 | 1056600 | 2223860 | 376880 | 9940480 | 2275400 |
| sp\|Q7Z5L9-2\|I2BP2_HUMAN;sp\|Q7Z5L9 | 6 | 0 | 316768 | 369390 | 3705700 | 824940 | 2620900 | 0 |
| sp\|Q9NT62\|ATG3_HUMAN;sp\|Q9NT62- | 6 | 0 | 308395 | 0 | 0 | 166610 | 9225300 | 366620 |
| sp\|Q06124-2\|PTN11_HUMAN;sp\|Q0612 | 6 | 0 | 305810 | 173850 | 1057991 | 0 | 2415900 | 0 |
| sp\|Q8NB90\|SPAT5_HUMAN;sp\|Q8NB9 | 6 | 0 | 299400 | 0 | 470670 | 0 | 4989614 | 0 |
| sp\|Q8TC12\|RDH11_HUMAN;tr\|G3V2G6 | 6 | 0 | 296760 | 382990 | 522230 | 145650 | 485080 | 0 |
| sp\|P83881\|RL36A_HUMAN;tr\|H0Y5B4\|H | 6 | 0 | 290010 | 325051 | 672070 | 323430 | 19126550 | 224850 |
| tr\|Q6IPH7\|Q6IPH7_HUMAN;tr\|E7EPB3\| | 6 | 0 | 272650 | 261150 | 1368400 | 160460 | 15418000 | 625220 |
| tr\|A0A024R784\|A0A024R784_HUMAN;s | 6 | 0 | 271580 | 0 | 216880 | 0 | 3316000 | 0 |
| sp\|O14686\|KMT2D_HUMAN;sp\|O14686 | 6 | 0 | 243020 | 0 | 0 | 0 | 3093000 | 1072200 |
| tr\|Q9UES0\|Q9UES0_HUMAN;tr\|A4D2J0 | 6 | 0 | 224827 | 192090 | 369530 | 0 | 1107170 | 224420 |
| sp\|O00560-3\|SDCB1_HUMAN;tr\|A0A02 | 6 | 0 | 222710 | 397800 | 1393100 | 254030 | 25158950 | 551000 |
| tr\|B2RCM6\|B2RCM6_HUMAN;sp\|Q96S4 | 6 | 0 | 212330 | 287490 | 1065200 | 157380 | 10306200 | 243139 |
| tr\|B4DJ39\|B4DJ39_HUMAN;sp\|O94842- | 6 | 0 | 209130 | 66336 | 548990 | 440110 | 9872800 | 332230 |
| tr\|B2R802\|B2R802_HUMAN;sp\|P09012 | 6 | 0 | 184830 | 327140 | 379080 | 0 | 1587300 | 317480 |
| tr\|A2VCR0\|A2VCR0_HUMAN;sp\|Q1569 | 6 | 0 | 175470 | 507590 | 1676370 | 262810 | 8568000 | 3045190 |
| sp\|Q8IYS1\|P20D2_HUMAN | 6 | 0 | 174190 | 0 | 414420 | 0 | 0 | 541620 |
| tr\|A0A024R7W9\|A0A024R7W9_HUMAN | 6 | 0 | 174170 | 648330 | 1237710 | 366260 | 5705400 | 388080 |
| tr\|A0A024R7I3\|A0A024R7I3_HUMAN;sp | 6 | 0 | 156980 | 0 | 193890 | 593330 | 1184100 | 514130 |
| tr\|Q53YD8\|Q53YD8_HUMAN;sp\|P3640 | 6 | 0 | 138270 | 342640 | 2006300 | 558100 | 8695400 | 0 |

| | | | | | | | | |
|---|---|---|---|---|---|---|---|---|
| tr\|J3KTF8\|J3KTF8_HUMAN;tr\|V9HWE8\| | 6 | 0 | 118880 | 131790 | 506260 | 524300 | 0 | 1777960 |
| tr\|X6RJS7\|X6RJS7_HUMAN;sp\|P46736-2 | 6 | 0 | 117450 | 0 | 613520 | 0 | 7270200 | 195870 |
| tr\|F5H5V4\|F5H5V4_HUMAN;tr\|F5GX23 | 6 | 0 | 109060 | 0 | 34425 | 0 | 2471400 | 0 |
| tr\|Q53HT6\|Q53HT6_HUMAN;tr\|Q53G72 | 6 | 0 | 41999 | 453750 | 1221400 | 409870 | 147730 | 0 |
| sp\|A2RTX5-2\|SYTC2_HUMAN;sp\|A2RTX | 6 | 0.002737 | 0 | 0 | 0 | 0 | 1912200 | 0 |
| sp\|O00560-2\|SDCB1_HUMAN;tr\|G5EAC | 6 | 0 | 0 | 0 | 0 | 0 | 2945500 | 0 |
| sp\|P15374\|UCHL3_HUMAN;tr\|A0A087V | 6 | 0 | 0 | 0 | 0 | 0 | 1658000 | 0 |
| sp\|P51617-4\|IRAK1_HUMAN;sp\|P51617 | 6 | 0 | 0 | 0 | 1381200 | 0 | 4426600 | 0 |
| sp\|Q08AD1-2\|CAMP2_HUMAN;sp\|Q08 | 6 | 0 | 0 | 0 | 0 | 0 | 6184100 | 0 |
| sp\|Q5TBB1-2\|RNH2B_HUMAN;sp\|Q5TB | 6 | 0 | 0 | 0 | 0 | 0 | 3934600 | 0 |
| sp\|Q7KZ85\|SPT6H_HUMAN;sp\|Q7KZ85 | 6 | 0 | 0 | 0 | 0 | 0 | 510960 | 0 |
| sp\|Q8TDN6\|BRX1_HUMAN;tr\|A0JLQ5\| | 6 | 0 | 0 | 0 | 2737100 | 0 | 9346100 | 0 |
| sp\|Q9HAU5\|RENT2_HUMAN;sp\|Q9HAU | 6 | 0 | 0 | 0 | 0 | 0 | 3964990 | 0 |
| sp\|Q9NZN3\|EHD3_HUMAN | 6 | 1 | 0 | 0 | 1959500 | 0 | 0 | 0 |
| sp\|Q9P1Y5\|CAMP3_HUMAN;tr\|D6W64 | 6 | 0 | 0 | 0 | 0 | 0 | 3194100 | 0 |
| tr\|A0A024QZ77\|A0A024QZ77_HUMAN; | 6 | 0 | 0 | 0 | 0 | 0 | 204340 | 0 |
| tr\|A0A024R861\|A0A024R861_HUMAN;s | 6 | 0 | 0 | 0 | 0 | 0 | 3841500 | 0 |
| tr\|A0A024R9E6\|A0A024R9E6_HUMAN;s | 6 | 0 | 0 | 0 | 0 | 0 | 4782300 | 0 |
| tr\|B3KPR5\|B3KPR5_HUMAN;sp\|Q7Z2Z2 | 6 | 0 | 0 | 0 | 0 | 0 | 5411400 | 0 |
| tr\|E7EVE9\|E7EVE9_HUMAN;tr\|A8MX75 | 6 | 0 | 0 | 0 | 0 | 0 | 2804080 | 0 |
| tr\|H0Y990\|H0Y990_HUMAN | 6 | 0.006526 | 0 | 0 | 1064100 | 0 | 2776300 | 0 |
| tr\|K7EM56\|K7EM56_HUMAN;tr\|S4R417 | 6 | 0 | 0 | 0 | 176290 | 0 | 4970900 | 0 |
| tr\|Q56VW8\|Q56VW8_HUMAN;sp\|P631 | 6 | 0 | 0 | 0 | 381080 | 0 | 0 | 0 |
| tr\|Q59GC1\|Q59GC1_HUMAN;sp\|Q0678 | 6 | 0 | 0 | 0 | 0 | 0 | 2748365 | 0 |
| tr\|Q6IB29\|Q6IB29_HUMAN;sp\|Q99848 | 6 | 0 | 0 | 0 | 0 | 0 | 6695100 | 0 |
| tr\|Q6UUU9\|Q6UUU9_HUMAN;tr\|G3V1F | 6 | 0 | 0 | 0 | 276900 | 0 | 0 | 0 |
| tr\|C9JQV0\|C9JQV0_HUMAN;sp\|Q9BRJ6 | 6 | 0 | 0 | 0 | 524670 | 0 | 14124000 | 598970 |
| tr\|Q53F02\|Q53F02_HUMAN;sp\|Q9UKF6 | 6 | 0 | 0 | 0 | 504190 | 0 | 6686800 | 318780 |
| sp\|Q9UBF2-2\|COPG2_HUMAN;sp\|Q9UI | 6 | 0.000361 | 0 | 0 | 0 | 0 | 1089500 | 52243 |
| tr\|A0A087WWS1\|A0A087WWS1_HUMA | 6 | 0 | 0 | 0 | 761560 | 0 | 5966400 | 301060 |
| tr\|A0A024R3L9\|A0A024R3L9_HUMAN;s | 6 | 0 | 0 | 0 | 1445800 | 0 | 1166800 | 85179 |
| tr\|B4DW90\|B4DW90_HUMAN;tr\|Q53HI | 6 | 0 | 0 | 0 | 0 | 0 | 3305700 | 443580 |
| tr\|B4DDL4\|B4DDL4_HUMAN;sp\|P30085 | 6 | 0 | 0 | 0 | 0 | 0 | 2806700 | 408780 |
| tr\|B4E345\|B4E345_HUMAN;tr\|Q5T7A9\| | 6 | 0 | 0 | 0 | 235170 | 0 | 512910 | 163870 |
| tr\|Q6FHM2\|Q6FHM2_HUMAN;sp\|P628 | 6 | 0.000356 | 0 | 0 | 0 | 0 | 336870 | 134930 |
| sp\|Q9Y281-3\|COF2_HUMAN;tr\|Q549N0 | 6 | 0.000368 | 0 | 0 | 0 | 0 | 895660 | 375790 |
| tr\|Q59GY3\|Q59GY3_HUMAN;sp\|Q1324 | 6 | 0 | 0 | 0 | 935570 | 0 | 2664870 | 1736120 |
| sp\|P30044\|PRDX5_HUMAN;tr\|V9HW35 | 6 | 0 | 0 | 0 | 0 | 0 | 771860 | 607260 |
| sp\|O60361\|NDK8_HUMAN | 6 | 1 | 0 | 0 | 109220 | 0 | 0 | 303380 |
| sp\|Q969Q0\|RL36L_HUMAN;tr\|B2R4V2\| | 6 | 0 | 0 | 67874 | 88407 | 0 | 1686900 | 0 |
| sp\|Q9NP55-2\|BPIA1_HUMAN;sp\|Q9NP | 6 | 0 | 0 | 85819 | 0 | 0 | 9701000 | 0 |
| sp\|Q9Y570\|PPME1_HUMAN;sp\|Q9Y570 | 6 | 0 | 0 | 147810 | 992550 | 0 | 0 | 0 |
| tr\|A4D275\|A4D275_HUMAN;sp\|O15143 | 6 | 0 | 0 | 54378 | 58553 | 0 | 6866880 | 0 |
| tr\|A0A024R649\|A0A024R649_HUMAN;s | 6 | 0 | 0 | 141460 | 724530 | 0 | 19914300 | 359630 |
| tr\|F5H669\|F5H669_HUMAN;tr\|B4DGF8 | 6 | 0 | 0 | 179690 | 830490 | 0 | 2072800 | 311070 |
| tr\|A0A024R324\|A0A024R324_HUMAN;s | 6 | 1 | 0 | 158530 | 433520 | 0 | 1651000 | 328000 |
| tr\|B2RD36\|B2RD36_HUMAN;sp\|Q96DG | 6 | 0 | 0 | 48255 | 0 | 0 | 1228900 | 244900 |
| sp\|Q9UBQ0\|VPS29_HUMAN;sp\|Q9UBC | 6 | 0 | 0 | 245490 | 1512060 | 0 | 1603900 | 506410 |
| tr\|A0A024QZN2\|A0A024QZN2_HUMAN | 6 | 0 | 0 | 228150 | 0 | 0 | 2182200 | 1258780 |
| tr\|Q9NWX4\|Q9NWX4_HUMAN;sp\|Q9P | 6 | 0 | 0 | 294578 | 697620 | 0 | 435510 | 256940 |
| tr\|J3KP15\|J3KP15_HUMAN;tr\|Q53FN0\| | 6 | 0 | 0 | 130560 | 0 | 0 | 281680 | 407422 |
| tr\|A0A024QZV0\|A0A024QZV0_HUMAN | 6 | 0 | 0 | 88937 | 0 | 0 | 0 | 187131 |
| tr\|Q6IBA2\|Q6IBA2_HUMAN;sp\|P53999 | 6 | 0 | 0 | 260740 | 0 | 0 | 0 | 1504000 |
| sp\|Q9BUL8\|PDC10_HUMAN;tr\|C9J5C3\| | 6 | 0 | 0 | 165140 | 612650 | 196630 | 3361400 | 311220 |
| tr\|Q6FI51\|Q6FI51_HUMAN;tr\|Q6FHS4\| | 6 | 0 | 0 | 0 | 1312290 | 640670 | 5630200 | 1629400 |
| tr\|B8ZZU8\|B8ZZU8_HUMAN;sp\|Q15370 | 6 | 0 | 0 | 136700 | 403560 | 273320 | 4339500 | 479710 |
| sp\|Q96M27\|PRRC1_HUMAN;sp\|Q96M2 | 6 | 0 | 0 | 1007574 | 4314400 | 3135088 | 1041700 | 12989580 |
| tr\|Q69YJ7\|Q69YJ7_HUMAN;tr\|B3KQH4 | 6 | 0 | 0 | 169640 | 151650 | 331270 | 2602600 | 734890 |
| sp\|P28838-2\|AMPL_HUMAN;tr\|V9HW3 | 6 | 0 | 0 | 0 | 0 | 162500 | 944670 | 0 |
| tr\|Q6N093\|Q6N093_HUMAN;sp\|P0185 | 6 | 0 | 0 | 284370 | 0 | 857670 | 4094100 | 1176350 |
| tr\|A0A087WYL9\|A0A087WYL9_HUMAN | 6 | 0.009094 | 0 | 4802810 | 0 | 3695650 | 1391700 | 7278220 |
| sp\|P28070\|PSB4_HUMAN;tr\|B4DFL3\|B4 | 6 | 0 | 0 | 382306 | 0 | 274312 | 117200 | 1033257 |
| sp\|Q562R1\|ACTBL_HUMAN | 5 | 0.005475 | 135348459 | 3946500 | 171760000 | 0 | 81121000 | 12743500 |
| tr\|Q7Z4W8\|Q7Z4W8_HUMAN;sp\|P352 | 5 | 0 | 16750140 | 13681020 | 28466070 | 8813110 | 180270000 | 25332550 |
| sp\|P47813\|IF1AX_HUMAN;sp\|O14602\| | 5 | 0 | 7188150 | 1602300 | 11502000 | 1540700 | 48224000 | 3756000 |
| sp\|P17900\|SAP3_HUMAN;tr\|Q14427\|Q | 5 | 0 | 6522502 | 372503 | 0 | 359557 | 360270 | 401800 |
| sp\|Q9GZZ9\|UBA5_HUMAN;sp\|Q9GZZ9- | 5 | 0 | 5760270 | 967520 | 3669585.3 | 186460 | 6399723 | 353562 |
| sp\|Q01844-6\|EWS_HUMAN;tr\|B0QYK0 | 5 | 0 | 5617380 | 1540050 | 8902540 | 1164180 | 52153530 | 2634550 |
| sp\|Q12824-2\|SNF5_HUMAN;sp\|Q12824 | 5 | 0 | 4950900 | 683960 | 4903100 | 0 | 11355660 | 1131500 |
| sp\|P31689-2\|DNJA1_HUMAN;sp\|P3168 | 5 | 0 | 4905900 | 2084600 | 11491000 | 2954100 | 13856000 | 4914640 |
| tr\|J3QKS7\|J3QKS7_HUMAN;sp\|Q969G3 | 5 | 0 | 3420800 | 0 | 1723900 | 0 | 4113800 | 251540 |
| sp\|O14929\|HAT1_HUMAN;sp\|O14929-2 | 5 | 0 | 3413000 | 1231200 | 4936800 | 854640 | 1363000 | 948015 |
| sp\|P21964-2\|COMT_HUMAN;sp\|P2196 | 5 | 0 | 2788100 | 234410 | 177120 | 0 | 4802800 | 264660 |
| sp\|P24752\|THIL_HUMAN;tr\|E9PRQ6\|E9 | 5 | 0 | 2602400 | 276930 | 3168600 | 349270 | 0 | 0 |
| tr\|A8K8K1\|A8K8K1_HUMAN;sp\|O00442 | 5 | 0 | 2524100 | 243720 | 5711033 | 520790 | 9030500 | 1754488 |
| tr\|A0A024RDH8\|A0A024RDH8_HUMAN | 5 | 0 | 2406442 | 490710 | 3327880 | 573709 | 37178547 | 3007180 |

| | | | | | | | | |
|---|---|---|---|---|---|---|---|---|
| tr\|H0YE97\|H0YE97_HUMAN;tr\|H0YEY8\| | 5 | 0 | 2400400 | 620520 | 5935600 | 0 | 7766500 | 0 |
| tr\|Q53EY9\|Q53EY9_HUMAN;sp\|Q8NEZ5 | 5 | 0 | 2322900 | 0 | 2835200 | 268480 | 8973900 | 1572900 |
| sp\|P35613-3\|BASI_HUMAN;tr\|A0A087V | 5 | 0 | 2294700 | 0 | 3408810 | 0 | 751170 | 0 |
| tr\|B4DWR5\|B4DWR5_HUMAN;sp\|P074 | 5 | 0 | 2266520 | 0 | 0 | 0 | 1493070 | 0 |
| tr\|A8K5M4\|A8K5M4_HUMAN;sp\|Q131 | 5 | 0 | 2137770 | 0 | 0 | 0 | 0 | 0 |
| sp\|Q96J01\|THOC3_HUMAN;sp\|Q96J01- | 5 | 0 | 1992000 | 0 | 4474100 | 0 | 6267670 | 0 |
| tr\|K7EK77\|K7EK77_HUMAN;sp\|P25705- | 5 | 0 | 1936200 | 980040 | 2065070 | 441667 | 2723540 | 0 |
| tr\|A0A024RAE4\|A0A024RAE4_HUMAN; | 5 | 0 | 1933097 | 1704600 | 34478000 | 883370 | 10143000 | 757410 |
| tr\|B3KRC6\|B3KRC6_HUMAN;sp\|Q1685 | 5 | 0 | 1886700 | 263370 | 391140 | 0 | 0 | 0 |
| sp\|Q9NXR7-4\|BRE_HUMAN;sp\|Q9NXR | 5 | 0 | 1867300 | 0 | 5630300 | 0 | 14592000 | 0 |
| tr\|K7EQ03\|K7EQ03_HUMAN;sp\|Q9BTD | 5 | 0 | 1852400 | 229780 | 3402300 | 686260 | 17374000 | 2095800 |
| tr\|Q1ET65\|Q1ET65_HUMAN;tr\|Q1ET64 | 5 | 0 | 1823360 | 4982700 | 1852550 | 1661630 | 5760410 | 3561160 |
| sp\|Q9HDC9-2\|APMAP_HUMAN;sp\|Q9H | 5 | 0 | 1783600 | 2003800 | 97133 | 118450 | 0 | 389670 |
| tr\|E5RHG8\|E5RHG8_HUMAN;tr\|A0A024 | 5 | 0 | 1708110 | 3213140 | 1275540 | 5441100 | 2858800 | 1632790 |
| tr\|A8MYT4\|A8MYT4_HUMAN;sp\|Q8NEI | 5 | 0 | 1617000 | 275200 | 1107600 | 262070 | 6502300 | 228600 |
| sp\|Q6NUQ4-2\|TM214_HUMAN;tr\|B3LE | 5 | 0 | 1575120 | 332190 | 864120 | 401760 | 0 | 0 |
| tr\|Q53FS4\|Q53FS4_HUMAN;tr\|B2R774\| | 5 | 0 | 1557800 | 474990 | 2824800 | 0 | 7390500 | 658910 |
| tr\|Q96RG4\|Q96RG4_HUMAN;sp\|Q9Y4H | 5 | 0 | 1533600 | 176460 | 1658800 | 0 | 5136500 | 137540 |
| sp\|P81605-2\|DCD_HUMAN | 5 | 0.002677 | 1521030 | 159680 | 1344420 | 1887930 | 0 | 1095500 |
| sp\|O95235-2\|KI20A_HUMAN;sp\|O9523 | 5 | 0 | 1519300 | 325920 | 1127700 | 88132 | 0 | 0 |
| sp\|Q9Y5K6\|CD2AP_HUMAN | 5 | 0 | 1493800 | 0 | 3019900 | 0 | 1578500 | 0 |
| tr\|B3KN05\|B3KN05_HUMAN;tr\|B2RBE0 | 5 | 0 | 1473500 | 0 | 2413200 | 136860 | 0 | 0 |
| sp\|Q96EK5\|KBP_HUMAN | 5 | 0 | 1468300 | 309460 | 955320 | 968360 | 6152900 | 962390 |
| sp\|Q08378-2\|GOGA3_HUMAN;sp\|Q083 | 5 | 0 | 1458600 | 0 | 1792930 | 0 | 733010 | 0 |
| sp\|Q9UNS1-2\|TIM_HUMAN;sp\|Q9UNS | 5 | 0 | 1401300 | 0 | 0 | 0 | 2579100 | 0 |
| sp\|Q9BQC3\|DPH2_HUMAN;sp\|Q9BQC3 | 5 | 0 | 1399800 | 0 | 2526300 | 0 | 2960800 | 0 |
| tr\|F8VQE1\|F8VQE1_HUMAN;sp\|Q9UHE | 5 | 0 | 1335310 | 0 | 3013040 | 0 | 5998100 | 291550 |
| sp\|Q9NQT5\|EXOS3_HUMAN;sp\|Q9NQT | 5 | 0 | 1316580 | 770930 | 2022000 | 406380 | 26442750 | 1602200 |
| sp\|P25788-2\|PSA3_HUMAN;tr\|Q6IB71\| | 5 | 0 | 1242260 | 638864 | 0 | 315350 | 2033800 | 910970 |
| sp\|Q3MHD2\|LSM12_HUMAN;sp\|Q3MH | 5 | 0 | 1178200 | 1357900 | 3515700 | 959420 | 24072000 | 1167500 |
| sp\|Q9BVI4\|NOC4L_HUMAN;tr\|F5H303\| | 5 | 0 | 1176000 | 0 | 0 | 0 | 816340 | 0 |
| tr\|Q6FGM6\|Q6FGM6_HUMAN;tr\|E5KN5 | 5 | 0 | 1026400 | 0 | 2696200 | 754660 | 2696500 | 1405775 |
| tr\|B3KUR4\|B3KUR4_HUMAN;tr\|A4D299 | 5 | 0 | 997790 | 153650 | 0 | 125050 | 2777500 | 173160 |
| sp\|Q03252\|LMNB2_HUMAN;tr\|J9JID7\|. | 5 | 0 | 969250 | 0 | 1060300 | 0 | 0 | 0 |
| tr\|E7EX83\|E7EX83_HUMAN;tr\|E7ENQ1\| | 5 | 0 | 951940 | 0 | 382190 | 0 | 3367000 | 0 |
| sp\|O60784-4\|TOM1_HUMAN;sp\|O6078 | 5 | 0 | 937050 | 0 | 3038800 | 316260 | 5523300 | 418700 |
| tr\|A0A024RC00\|A0A024RC00_HUMAN;s | 5 | 0 | 922180 | 292710 | 0 | 0 | 2518900 | 382040 |
| tr\|Q6IAX2\|Q6IAX2_HUMAN;sp\|P46778 | 5 | 0 | 920990 | 1127900 | 3866295 | 635200 | 54491380 | 1946180 |
| tr\|H7BYG8\|H7BYG8_HUMAN;sp\|O9482 | 5 | 0 | 908470 | 0 | 337110 | 0 | 3380330 | 0 |
| sp\|Q9UBB6-2\|NCDN_HUMAN;sp\|Q9UB | 5 | 0 | 881510 | 326290 | 1456200 | 348030 | 4389300 | 361090 |
| tr\|A0A024R6I3\|A0A024R6I3_HUMAN;sp | 5 | 0 | 862167 | 614210 | 997830 | 277790 | 14654240 | 508920 |
| sp\|P00387\|NB5R3_HUMAN;sp\|P00387- | 5 | 0 | 856460 | 727290 | 924610 | 0 | 1051100 | 277810 |
| tr\|Q6IBH6\|Q6IBH6_HUMAN;sp\|P61254 | 5 | 0 | 851170 | 367650 | 2314000 | 568610 | 31350100 | 1517300 |
| tr\|Q53FG6\|Q53FG6_HUMAN;sp\|Q1542 | 5 | 0 | 844050 | 298378 | 1045250 | 0 | 5461500 | 1453300 |
| sp\|Q9UK59\|DBR1_HUMAN;tr\|B3KSR5\|I | 5 | 0 | 837920 | 291050 | 4684300 | 377160 | 15486350 | 307310 |
| sp\|Q9Y4C2-2\|F115A_HUMAN;sp\|Q9Y4( | 5 | 0 | 836070 | 0 | 161070 | 0 | 1546300 | 0 |
| sp\|Q96I15\|SCLY_HUMAN;tr\|A0A0A0M( | 5 | 0 | 790080 | 0 | 0 | 0 | 1355000 | 0 |
| tr\|A4D2P2\|A4D2P2_HUMAN;tr\|A4D2P1 | 5 | 0 | 788050 | 1584400 | 938670 | 344010 | 1896540 | 918455 |
| tr\|C9J4Z3\|C9J4Z3_HUMAN;sp\|P61513\| | 5 | 0 | 775020 | 450660 | 3022130 | 145520 | 22982000 | 1569900 |
| sp\|Q12800-2\|TFCP2_HUMAN;sp\|Q1280 | 5 | 0 | 732000 | 440350 | 4310400 | 647940 | 11702800 | 490780 |
| sp\|Q9H974-3\|QTRD1_HUMAN;sp\|Q9H9 | 5 | 0 | 730060 | 0 | 3582700 | 967220 | 2638600 | 476210 |
| sp\|Q9UPY3-2\|DICER_HUMAN;sp\|Q9UP | 5 | 0 | 723300 | 59681 | 155100 | 0 | 5189400 | 0 |
| tr\|C9J0K6\|C9J0K6_HUMAN;sp\|P30626-2 | 5 | 0 | 712308 | 390870 | 1192600 | 559150 | 4507800 | 5222640 |
| tr\|A0A087WY55\|A0A087WY55_HUMAN | 5 | 0 | 698353 | 1012770 | 1948700 | 720759 | 14073000 | 3756618 |
| sp\|Q99961-3\|SH3G1_HUMAN;tr\|Q9UQI | 5 | 0 | 681060 | 0 | 3471400 | 550629 | 4800500 | 1856039 |
| tr\|F8WCX2\|F8WCX2_HUMAN;sp\|Q8N1 | 5 | 0 | 679710 | 0 | 270220 | 103250 | 1710600 | 0 |
| tr\|A0A024R912\|A0A024R912_HUMAN;s | 5 | 0 | 649520 | 66616 | 846900 | 187040 | 6515700 | 902380 |
| tr\|B3KPP7\|B3KPP7_HUMAN;tr\|A8K140 | 5 | 0 | 572190 | 0 | 849850 | 0 | 1336300 | 0 |
| sp\|Q15386\|UBE3C_HUMAN;tr\|B4DHJ9\| | 5 | 0 | 545680 | 0 | 0 | 0 | 5022400 | 0 |
| tr\|A0A024RBA9\|A0A024RBA9_HUMAN; | 5 | 0 | 524980 | 337000 | 1038800 | 196570 | 3101100 | 266880 |
| tr\|I3L2K5\|I3L2K5_HUMAN;sp\|Q8IWR0\| | 5 | 0 | 524380 | 0 | 158950 | 0 | 3574500 | 0 |
| tr\|B2R7D3\|B2R7D3_HUMAN;sp\|Q96D7 | 5 | 0 | 516780 | 0 | 95725 | 0 | 4709800 | 0 |
| sp\|P51571\|SSRD_HUMAN;tr\|A6NLM8\|A | 5 | 0 | 505150 | 104630 | 240760 | 97464 | 1649900 | 0 |
| sp\|P37108\|SRP14_HUMAN;tr\|H0YLA2\|I | 5 | 0 | 495390 | 681240 | 3813700 | 1761429 | 14804000 | 5243450 |
| tr\|A0A024R1T5\|A0A024R1T5_HUMAN;s | 5 | 0 | 478710 | 296410 | 2669900 | 215670 | 3921700 | 179140 |
| sp\|Q9H7D7-2\|WDR26_HUMAN;sp\|Q9H | 5 | 0 | 431290 | 0 | 41434 | 0 | 1402400 | 119040 |
| tr\|Q53FL4\|Q53FL4_HUMAN;tr\|A0A087V | 5 | 0 | 424750 | 0 | 0 | 0 | 3545400 | 0 |
| tr\|Q6IB11\|Q6IB11_HUMAN;sp\|O00264 | 5 | 0 | 424650 | 246800 | 742730 | 0 | 6330100 | 0 |
| sp\|P53990-2\|IST1_HUMAN;tr\|A8K5S3\|A | 5 | 0 | 424220 | 212450 | 2949500 | 232720 | 9242700 | 208850 |
| tr\|Q5T8C6\|Q5T8C6_HUMAN;sp\|Q13042 | 5 | 0 | 407640 | 0 | 0 | 0 | 3429220 | 0 |
| tr\|A0A0A0MR59\|A0A0A0MR59_HUMAN | 5 | 0.006544 | 400630 | 0 | 0 | 0 | 496880 | 0 |
| sp\|O95219\|SNX4_HUMAN;sp\|O95219-2 | 5 | 0 | 399070 | 261270 | 406790 | 0 | 772850 | 0 |
| sp\|Q9H444\|CHM4B_HUMAN;sp\|Q96CF | 5 | 0 | 398450 | 0 | 453580 | 0 | 258960 | 83268 |
| sp\|O75569-3\|PRKRA_HUMAN;sp\|O755 | 5 | 0 | 373490 | 0 | 714850 | 64244 | 17023000 | 756330 |
| tr\|A8K7H4\|A8K7H4_HUMAN;sp\|O4392 | 5 | 0 | 368420 | 0 | 2987690 | 129150 | 7502700 | 1015800 |

| | | | | | | | | |
|---|---|---|---|---|---|---|---|---|
| tr\|B3KY28\|B3KY28_HUMAN;tr\|A8K968\| | 5 | 0 | 362480 | 0 | 466010 | 0 | 0 | 0 |
| tr\|Q53HI2\|Q53HI2_HUMAN;sp\|Q9UJV9 | 5 | 0 | 346240 | 81487000 | 652430 | 0 | 4263800 | 0 |
| sp\|Q9BRP1\|PDD2L_HUMAN;tr\|U3KQA4 | 5 | 0 | 331400 | 0 | 2037200 | 108070 | 6066186 | 321220 |
| sp\|Q9UID3\|VPS51_HUMAN;sp\|Q9UID3 | 5 | 0 | 307460 | 0 | 1568400 | 0 | 3105400 | 0 |
| sp\|Q9NXV6\|CARF_HUMAN;tr\|B3KTW3 | 5 | 0 | 300760 | 0 | 371610 | 0 | 877660 | 84895 |
| sp\|Q5VIR6-4\|VPS53_HUMAN;tr\|B3KS0 | 5 | 0 | 249790 | 0 | 219250 | 0 | 4090212 | 0 |
| sp\|Q13526\|PIN1_HUMAN;tr\|K7EN45\|K | 5 | 0 | 235270 | 0 | 422600 | 231760 | 8921900 | 544250 |
| tr\|Q5T321\|Q5T321_HUMAN;sp\|Q8NFP9 | 5 | 0.003308 | 220020 | 0 | 152270 | 0 | 304290 | 0 |
| tr\|A0A024R4X1\|A0A024R4X1_HUMAN;t | 5 | 0 | 213190 | 0 | 872870 | 0 | 2522300 | 19536 |
| tr\|C9J9W2\|C9J9W2_HUMAN;tr\|A0A024 | 5 | 0 | 190320 | 195320 | 774660 | 159610 | 5645900 | 309910 |
| tr\|X5D7P8\|X5D7P8_HUMAN;tr\|Q6E0B2 | 5 | 0 | 181600 | 0 | 1683200 | 0 | 4484000 | 0 |
| tr\|C9JEL3\|C9JEL3_HUMAN;tr\|B9A044\|B | 5 | 0 | 180650 | 0 | 1377050 | 0 | 7878900 | 0 |
| tr\|A0A024R1Q3\|A0A024R1Q3_HUMAN; | 5 | 0 | 171990 | 759340 | 1659070 | 0 | 4587700 | 0 |
| tr\|F5CTF3\|F5CTF3_HUMAN;sp\|P27707\| | 5 | 0 | 167230 | 0 | 440090 | 0 | 5296100 | 234240 |
| sp\|Q13242\|SRSF9_HUMAN;tr\|A8K3M9\| | 5 | 0 | 150090 | 0 | 0 | 0 | 4813900 | 261310 |
| tr\|H9A532\|H9A532_HUMAN;sp\|Q6W2J | 5 | 0 | 149290 | 0 | 105460 | 0 | 1001600 | 0 |
| sp\|Q9H7Z7\|PGES2_HUMAN;tr\|B3KPZ2\| | 5 | 0 | 140150 | 267270 | 573890 | 0 | 4844100 | 120590 |
| tr\|Q5QPL9\|Q5QPL9_HUMAN;sp\|Q9UKM | 5 | 0 | 129540 | 178000 | 145140 | 0 | 4289200 | 0 |
| sp\|Q6ZN17\|LN28B_HUMAN;sp\|Q6ZN17 | 5 | 0 | 83911 | 0 | 476240 | 0 | 5166000 | 69419 |
| tr\|J3KRC4\|J3KRC4_HUMAN;tr\|V9HWF3 | 5 | 0 | 70310 | 0 | 0 | 0 | 9623100 | 0 |
| sp\|O60493\|SNX3_HUMAN;sp\|O60493-4 | 5 | 0 | 70308 | 0 | 78575 | 0 | 251260 | 0 |
| tr\|B2R823\|B2R823_HUMAN;sp\|Q9NRX3 | 5 | 0 | 52023 | 0 | 0 | 0 | 2293400 | 0 |
| sp\|O00287\|RFXAP_HUMAN | 5 | 0 | 0 | 0 | 0 | 0 | 2450300 | 0 |
| sp\|O75113\|N4BP1_HUMAN;tr\|B3KMA4 | 5 | 0 | 0 | 0 | 0 | 0 | 4339100 | 0 |
| sp\|P32929-3\|CGL_HUMAN;sp\|P32929\| | 5 | 0 | 0 | 0 | 456570 | 0 | 0 | 0 |
| sp\|P41227\|NAA10_HUMAN;sp\|P41227-2 | 5 | 0 | 0 | 0 | 0 | 0 | 659690 | 0 |
| sp\|P62314\|SMD1_HUMAN;tr\|Q7Z5A3\| | 5 | 0 | 0 | 0 | 166030 | 0 | 13565000 | 0 |
| sp\|Q12872\|SFSWA_HUMAN;sp\|Q12872 | 5 | 0 | 0 | 0 | 265690 | 0 | 3603960 | 0 |
| sp\|Q15417-2\|CNN3_HUMAN;tr\|E9PDU0 | 5 | 0 | 0 | 0 | 122400 | 0 | 1012200 | 0 |
| sp\|Q15650\|TRIP4_HUMAN;tr\|H0YL91\|H | 5 | 0 | 0 | 0 | 0 | 0 | 4878300 | 0 |
| sp\|Q86U06-5\|RBM23_HUMAN;tr\|Q6IAS9 | 5 | 0 | 0 | 0 | 0 | 0 | 1066900 | 0 |
| sp\|Q8NFH4\|NUP37_HUMAN;tr\|B4DKV8 | 5 | 0 | 0 | 0 | 359940 | 0 | 2738200 | 0 |
| sp\|Q93034\|CUL5_HUMAN;tr\|L0L6C1\|L0 | 5 | 0 | 0 | 0 | 883590 | 0 | 3691360 | 0 |
| sp\|Q96CW1-2\|AP2M1_HUMAN;tr\|A0A0 | 5 | 0 | 0 | 0 | 1234195 | 0 | 4741500 | 0 |
| sp\|Q9NR12-2\|PDLI7_HUMAN;sp\|Q9NR | 5 | 0 | 0 | 0 | 1122900 | 0 | 5120400 | 0 |
| sp\|Q9NSI2-2\|F207A_HUMAN;sp\|Q9NSI | 5 | 0 | 0 | 0 | 105730 | 0 | 1720100 | 0 |
| sp\|Q9NTJ5\|SAC1_HUMAN;tr\|E9PGZ4\|E | 5 | 0 | 0 | 0 | 348550 | 0 | 0 | 0 |
| sp\|Q9UGJ1-2\|GCP4_HUMAN;sp\|Q9UGJ | 5 | 0 | 0 | 0 | 1050300 | 0 | 2477000 | 0 |
| sp\|Q9UNH7-2\|SNX6_HUMAN;tr\|B4DJS7 | 5 | 0 | 0 | 0 | 0 | 0 | 0 | 0 |
| sp\|Q9UNX3\|RL26L_HUMAN;tr\|E5RIT6\|I | 5 | 0 | 0 | 0 | 0 | 0 | 403860 | 0 |
| sp\|Q9Y316-2\|MEMO1_HUMAN;sp\|Q9Y | 5 | 0 | 0 | 0 | 189470 | 0 | 2823700 | 0 |
| sp\|Q9Y4W2-2\|LAS1L_HUMAN;sp\|Q9Y4 | 5 | 0 | 0 | 0 | 0 | 0 | 5205780 | 0 |
| tr\|A0A024R294\|A0A024R294_HUMAN;s | 5 | 0 | 0 | 0 | 245050 | 0 | 3963200 | 0 |
| tr\|A0A024R3A2\|A0A024R3A2_HUMAN; | 5 | 0 | 0 | 0 | 0 | 0 | 2925100 | 0 |
| tr\|A0A024R8R4\|A0A024R8R4_HUMAN;s | 5 | 0 | 0 | 0 | 0 | 0 | 4377000 | 0 |
| tr\|A0A024RAL3\|A0A024RAL3_HUMAN;s | 5 | 0 | 0 | 0 | 0 | 0 | 5116500 | 0 |
| tr\|A4FU51\|A4FU51_HUMAN;sp\|Q6N06 | 5 | 1 | 0 | 0 | 174650 | 0 | 777880 | 0 |
| tr\|B2R5U7\|B2R5U7_HUMAN;tr\|A0A087 | 5 | 0 | 0 | 0 | 0 | 0 | 3035500 | 0 |
| tr\|B3KM97\|B3KM97_HUMAN;sp\|Q9NZI | 5 | 0 | 0 | 0 | 227010 | 0 | 337410 | 0 |
| tr\|B3KMP2\|B3KMP2_HUMAN;sp\|Q9UJX | 5 | 0 | 0 | 0 | 944390 | 0 | 5599100 | 0 |
| tr\|B3KQF0\|B3KQF0_HUMAN;sp\|Q9UGF | 5 | 0 | 0 | 0 | 1764000 | 0 | 0 | 0 |
| tr\|B3KRJ9\|B3KRJ9_HUMAN;sp\|Q8WXA | 5 | 0 | 0 | 0 | 629020 | 0 | 11048990 | 0 |
| tr\|B4DNR3\|B4DNR3_HUMAN;tr\|V9HW8 | 5 | 0 | 0 | 0 | 0 | 0 | 6570600 | 0 |
| tr\|B4DXV1\|B4DXV1_HUMAN;sp\|Q9H9T | 5 | 0 | 0 | 0 | 1286500 | 0 | 7479100 | 0 |
| tr\|B7ZA76\|B7ZA76_HUMAN;tr\|B4DIA9\| | 5 | 0 | 0 | 0 | 900600 | 0 | 1922000 | 0 |
| tr\|C9IYN7\|C9IYN7_HUMAN;tr\|B4DP60\| | 5 | 0 | 0 | 0 | 0 | 0 | 1924400 | 0 |
| tr\|D6RHE1\|D6RHE1_HUMAN;tr\|I6L894\| | 5 | 0 | 0 | 0 | 0 | 0 | 3802500 | 0 |
| tr\|E7ER60\|E7ER60_HUMAN;tr\|B4DLC4\| | 5 | 0 | 0 | 0 | 0 | 0 | 3692300 | 0 |
| tr\|E9PGC0\|E9PGC0_HUMAN;tr\|B4DTX4 | 5 | 0 | 0 | 0 | 345310 | 0 | 2504100 | 0 |
| tr\|F5H3Y4\|F5H3Y4_HUMAN;sp\|Q8IY37\| | 5 | 0 | 0 | 0 | 0 | 0 | 2243500 | 0 |
| tr\|F6WIT2\|F6WIT2_HUMAN;sp\|Q15257 | 5 | 0 | 0 | 0 | 0 | 0 | 231840 | 0 |
| tr\|G3V1S1\|G3V1S1_HUMAN;tr\|B3KTH1 | 5 | 0 | 0 | 0 | 0 | 0 | 2095000 | 0 |
| tr\|I3L412\|I3L412_HUMAN;tr\|K7ENA6\|K | 5 | 0 | 0 | 0 | 0 | 0 | 3353030 | 0 |
| tr\|I7GPQ7\|I7GPQ7_HUMAN;sp\|Q92541 | 5 | 0 | 0 | 0 | 0 | 0 | 1877400 | 0 |
| tr\|J3KPD3\|J3KPD3_HUMAN;tr\|I3L521\|I | 5 | 0 | 0 | 0 | 0 | 0 | 3191000 | 0 |
| tr\|M0R088\|M0R088_HUMAN;tr\|E9PCT1 | 5 | 0 | 0 | 0 | 0 | 0 | 963910 | 0 |
| tr\|Q1W6H1\|Q1W6H1_HUMAN;sp\|P293 | 5 | 0 | 0 | 0 | 0 | 0 | 1464000 | 0 |
| tr\|Q5T0F3\|Q5T0F3_HUMAN;sp\|Q13823 | 5 | 0 | 0 | 0 | 0 | 0 | 3742800 | 0 |
| tr\|Q5VU11\|Q5VU11_HUMAN;sp\|P7834 | 5 | 0 | 0 | 0 | 0 | 0 | 1105100 | 0 |
| tr\|Q6FGR6\|Q6FGR6_HUMAN;sp\|P1938 | 5 | 0 | 0 | 0 | 102650 | 0 | 5114500 | 0 |
| tr\|Q8NI62\|Q8NI62_HUMAN | 5 | 1 | 0 | 0 | 0 | 0 | 2705500 | 0 |
| tr\|V9HWC5\|V9HWC5_HUMAN;tr\|F5GW | 5 | 0 | 0 | 0 | 0 | 0 | 3219000 | 0 |
| sp\|Q9UQR0\|SCML2_HUMAN;tr\|B4DZR9 | 5 | 0 | 0 | 0 | 619050 | 0 | 4343800 | 55666 |
| tr\|A0A024RDY9\|A0A024RDY9_HUMAN; | 5 | 0 | 0 | 0 | 1316300 | 0 | 3782600 | 187830 |

| | | | | | | | | |
|---|---|---|---|---|---|---|---|---|
| tr\|B4DEQ6\|B4DEQ6_HUMAN;sp\|Q6ZW | 5 | 0 | 0 | 0 | 0 | 0 | 3083300 | 174180 |
| sp\|Q9UJW0\|DCTN4_HUMAN;sp\|Q9UJV | 5 | 0 | 0 | 0 | 823920 | 0 | 4665300 | 382310 |
| tr\|B4DQC7\|B4DQC7_HUMAN;tr\|A8K6D | 5 | 0 | 0 | 0 | 186570 | 0 | 1541400 | 133010 |
| tr\|A0A024R1X3\|A0A024R1X3_HUMAN;s | 5 | 0 | 0 | 0 | 133990 | 0 | 4582900 | 509240 |
| tr\|A0A024R2X1\|A0A024R2X1_HUMAN;s | 5 | 0 | 0 | 0 | 1131400 | 0 | 2309800 | 387840 |
| sp\|Q9Y5S9-2\|RBM8A_HUMAN;tr\|A0A0 | 5 | 0 | 0 | 0 | 245420 | 0 | 5765600 | 1066400 |
| sp\|Q9NPD3\|EXOS4_HUMAN;tr\|E9PI41\| | 5 | 0 | 0 | 0 | 0 | 0 | 893240 | 394140 |
| sp\|P20290\|BTF3_HUMAN;sp\|P20290-2 | 5 | 0 | 0 | 0 | 0 | 0 | 711120 | 822270 |
| tr\|A4D177\|A4D177_HUMAN;sp\|Q1318 | 5 | 0 | 0 | 0 | 104050 | 0 | 627770 | 1261700 |
| sp\|Q13404\|UB2V1_HUMAN;sp\|Q13404 | 5 | 0 | 0 | 0 | 0 | 0 | 404590 | 830790 |
| sp\|O43598\|DNPH1_HUMAN;tr\|H0Y8X4 | 5 | 0 | 0 | 0 | 0 | 0 | 518330 | 1258000 |
| sp\|Q9H3K6\|BOLA2_HUMAN;sp\|Q9H3K | 5 | 0 | 0 | 0 | 0 | 0 | 322230 | 5224800 |
| tr\|B4DR80\|B4DR80_HUMAN;tr\|Q6P0Y1 | 5 | 0.002718 | 0 | 0 | 198590 | 0 | 0 | 226590 |
| tr\|D6RG15\|D6RG15_HUMAN;sp\|Q6IBS0 | 5 | 0 | 0 | 0 | 451710 | 0 | 0 | 334560 |
| sp\|Q5T200\|ZC3HD_HUMAN;sp\|Q5T200 | 5 | 0 | 0 | 725290 | 0 | 0 | 777000 | 0 |
| sp\|Q709F0\|ACD11_HUMAN;tr\|D6RDI8\| | 5 | 0 | 0 | 269660 | 555740 | 0 | 3111300 | 0 |
| sp\|Q86YR5-4\|GPSM1_HUMAN;tr\|A0A0 | 5 | 0 | 0 | 46255 | 186830 | 0 | 2941613 | 0 |
| tr\|B7Z3B5\|B7Z3B5_HUMAN;sp\|Q15349 | 5 | 0.006579 | 0 | 74830 | 0 | 0 | 1063000 | 0 |
| tr\|Q3SYF1\|Q3SYF1_HUMAN;sp\|Q9UMY | 5 | 0 | 0 | 49220 | 0 | 0 | 0 | 0 |
| tr\|Q59H56\|Q59H56_HUMAN;tr\|Q5SRN | 5 | 0 | 0 | 698810 | 292180 | 0 | 3620700 | 0 |
| tr\|A0A024R3V8\|A0A024R3V8_HUMAN; | 5 | 0 | 0 | 125460 | 0 | 0 | 3413900 | 58696 |
| sp\|Q9Y3B2\|EXOS1_HUMAN;tr\|R4GMQ7 | 5 | 0 | 0 | 106330 | 797200 | 0 | 8179000 | 152970 |
| sp\|Q9H2P9-3\|DPH5_HUMAN;sp\|Q9H2P | 5 | 0 | 0 | 367820 | 1035600 | 0 | 7522100 | 199270 |
| tr\|B7Z1J9\|B7Z1J9_HUMAN;tr\|B7ZKW4\| | 5 | 0 | 0 | 368190 | 295420 | 0 | 9096600 | 297830 |
| sp\|Q9Y3B3-2\|TMED7_HUMAN;sp\|Q9Y3 | 5 | 0 | 0 | 106620 | 0 | 0 | 6681800 | 243960 |
| sp\|P11441\|UBL4A_HUMAN;tr\|Q5HY81\| | 5 | 0 | 0 | 248670 | 508590 | 0 | 3431800 | 436340 |
| sp\|Q92688-2\|AN32B_HUMAN;tr\|Q53F3 | 5 | 0 | 0 | 250680 | 0 | 0 | 8584400 | 1955500 |
| sp\|P49458\|SRP09_HUMAN;tr\|Q6P2S0\| | 5 | 0 | 0 | 30745 | 0 | 0 | 2553638 | 1624700 |
| tr\|B4DMK6\|B4DMK6_HUMAN;sp\|Q9NP | 5 | 0 | 0 | 116030 | 1380300 | 111410 | 4909800 | 0 |
| tr\|B4DXX1\|B4DXX1_HUMAN;tr\|B2R713 | 5 | 0 | 0 | 0 | 759720 | 86730 | 1566990 | 467950 |
| sp\|Q08209-3\|PP2BA_HUMAN;sp\|Q082( | 5 | 0 | 0 | 886490 | 2674760 | 547850 | 8682040 | 969160 |
| tr\|Q6FI97\|Q6FI97_HUMAN;tr\|Q53FS0\|( | 5 | 0 | 0 | 243560 | 955940 | 226530 | 2696700 | 300590 |
| tr\|A8K4M5\|A8K4M5_HUMAN;sp\|O605( | 5 | 0 | 0 | 0 | 111490 | 36322 | 2010000 | 0 |
| tr\|Q6FGV9\|Q6FGV9_HUMAN;sp\|Q1512 | 5 | 0 | 0 | 162840 | 406860 | 140170 | 5126300 | 566390 |
| sp\|Q5VWZ2\|LYPL1_HUMAN;sp\|Q5VWZ | 5 | 0 | 0 | 195380 | 422500 | 157780 | 3623400 | 230580 |
| tr\|B2R9D9\|B2R9D9_HUMAN;sp\|Q96EK9 | 5 | 0 | 0 | 0 | 527150 | 214500 | 3841700 | 0 |
| tr\|H6V745\|H6V745_HUMAN;tr\|F5ATB8 | 5 | 0 | 0 | 0 | 158990 | 444480 | 1816190 | 0 |
| tr\|A0A024R258\|A0A024R258_HUMAN;s | 5 | 0 | 0 | 0 | 0 | 689600 | 2747900 | 1690300 |
| tr\|B4DEA6\|B4DEA6_HUMAN;sp\|O4376 | 5 | 0 | 0 | 0 | 0 | 923810 | 0 | 1979460 |
| tr\|Q502X2\|Q502X2_HUMAN;sp\|Q9NR2 | 5 | 0 | 0 | 0 | 0 | 334040 | 0 | 570610 |
| tr\|Q6NS95\|Q6NS95_HUMAN;tr\|A0M8C | 5 | 0.0007 | 0 | 414770 | 0 | 689000 | 59202 | 595501 |
| tr\|A3KPC7\|A3KPC7_HUMAN;sp\|Q9987 | 4 | 0 | 32146500 | 6046110 | 51236880 | 2474674 | 71762780 | 11824260 |
| sp\|P60866\|RS20_HUMAN;sp\|P60866-2 | 4 | 0 | 16619840 | 14213108 | 34961760 | 10491680 | 160110480 | 22249760 |
| tr\|Q9BRL5\|Q9BRL5_HUMAN;tr\|B4DJ51 | 4 | 0 | 14019900 | 1574540 | 3999300 | 1048100 | 11387620 | 3510700 |
| sp\|P27482\|CALL3_HUMAN | 4 | 0 | 13751140 | 291500 | 508460 | 251950 | 1476800 | 575200 |
| tr\|I4AY87\|I4AY87_HUMAN;sp\|P14174\| | 4 | 0 | 10185450 | 9585060 | 18677890 | 7261070 | 68936810 | 23623960 |
| tr\|B2R4C5\|B2R4C5_HUMAN;sp\|P61626 | 4 | 0 | 9453400 | 1613130 | 2217910 | 3680430 | 4581800 | 4248910 |
| sp\|Q5VW32-2\|BROX_HUMAN;sp\|Q5VV | 4 | 0 | 5621400 | 2888800 | 8728503 | 2237400 | 3254200 | 1580600 |
| sp\|A6NHL2-2\|TBAL3_HUMAN;sp\|A6NH | 4 | 0 | 5365100 | 1303000 | 7626700 | 2211500 | 27583000 | 5600040 |
| sp\|P62851\|RS25_HUMAN | 4 | 0 | 4790230 | 5696980 | 19619340 | 3920814 | 65443940 | 15921130 |
| sp\|Q5TAX3\|TUT4_HUMAN;tr\|H0YDJ1\|H | 4 | 0 | 4777400 | 0 | 5231400 | 0 | 10387000 | 0 |
| sp\|Q9NZH8-2\|IL36G_HUMAN;sp\|Q9NZ | 4 | 0 | 4689370 | 622670 | 761810 | 730220 | 269130 | 98307 |
| sp\|P42677\|RS27_HUMAN;tr\|Q5T4L4\|Q | 4 | 0 | 4056860 | 2807100 | 6954528 | 763696 | 64255000 | 2745539 |
| tr\|E4W6B6\|E4W6B6_HUMAN;tr\|B2R4D | 4 | 0 | 3453630 | 1247985 | 11832570 | 2010398 | 112101380 | 7692010 |
| tr\|A0A024R7B7\|A0A024R7B7_HUMAN;s | 4 | 0 | 3206307 | 2148158 | 8971224 | 1298300 | 12081590 | 4743765 |
| tr\|Q8WUB5\|Q8WUB5_HUMAN;tr\|Q96J | 4 | 0 | 2895400 | 318540 | 4377960 | 497690 | 1644530 | 806060 |
| tr\|J3KRG2\|J3KRG2_HUMAN;sp\|Q96QA5 | 4 | 0 | 2518380 | 0 | 0 | 270930 | 0 | 0 |
| tr\|B2R4C1\|B2R4C1_HUMAN;sp\|P62899 | 4 | 0 | 2347770 | 1444065 | 5431010 | 907693 | 51462310 | 5176010 |
| sp\|Q6ZVX7\|FBX50_HUMAN | 4 | 0 | 2271720 | 1280100 | 698460 | 2427220 | 1187550 | 0 |
| sp\|P42766\|RL35_HUMAN;tr\|F2Z388\|F2 | 4 | 0 | 2265420 | 955467 | 4576180 | 365240 | 43998900 | 3620660 |
| tr\|A8K6V7\|A8K6V7_HUMAN;tr\|A0A024 | 4 | 0 | 2118600 | 576680 | 4173344 | 311910 | 11066807 | 62543 |
| tr\|A8K9V9\|A8K9V9_HUMAN;sp\|Q96KN | 4 | 0 | 2099700 | 283050 | 3353100 | 611830 | 109240 | 0 |
| sp\|P21796\|VDAC1_HUMAN;tr\|B4DEI3\| | 4 | 0 | 1995740 | 121960 | 717630 | 0 | 476560 | 0 |
| tr\|A0A024RB14\|A0A024RB14_HUMAN;s | 4 | 0 | 1985040 | 2235326 | 5869700 | 1619930 | 82863560 | 12662400 |
| sp\|P49411\|EFTU_HUMAN | 4 | 0 | 1822000 | 241710 | 585400 | 0 | 0 | 0 |
| sp\|Q9NWV4\|CA123_HUMAN;tr\|D3DQ3 | 4 | 0 | 1795630 | 1651400 | 3200800 | 1057800 | 38446000 | 1217600 |
| tr\|A0A024QZX3\|A0A024QZX3_HUMAN; | 4 | 0 | 1775100 | 265489000 | 4826220 | 304747000 | 5007920 | 448075000 |
| tr\|B4DYH4\|B4DYH4_HUMAN;sp\|Q1467( | 4 | 0 | 1691000 | 0 | 0 | 0 | 526350 | 0 |
| tr\|A0A087WZH7\|A0A087WZH7_HUMAN | 4 | 0 | 1551700 | 1551200 | 2867500 | 840640 | 599910 | 1283680 |
| tr\|B0I1S0\|B0I1S0_HUMAN;sp\|Q8NCM8 | 4 | 0 | 1421100 | 0 | 3356541 | 0 | 1241200 | 0 |
| sp\|Q6NXE6-2\|ARMC6_HUMAN;sp\|Q6N | 4 | 0 | 1385900 | 0 | 2239800 | 0 | 8462400 | 0 |
| tr\|V9HW44\|V9HW44_HUMAN;sp\|P684 | 4 | 0 | 1353000 | 194740 | 531850 | 411100 | 2723500 | 2327900 |
| sp\|Q86TG7-2\|PEG10_HUMAN;tr\|A0A08 | 4 | 0 | 1346200 | 295700 | 1643334 | 291510 | 897630 | 0 |
| sp\|P16383-2\|GCFC2_HUMAN;sp\|P1638 | 4 | 0 | 1274900 | 129640 | 210120 | 0 | 2107700 | 206350 |
| tr\|Q6FHM6\|Q6FHM6_HUMAN;sp\|P557 | 4 | 0 | 1215000 | 2446800 | 3522900 | 1888700 | 21444000 | 3683300 |
| tr\|Q569I7\|Q569I7_HUMAN;tr\|S6AWF4\| | 4 | 0.004257 | 1210600 | 0 | 1317700 | 0 | 2748200 | 0 |

| | | | | | | | | | |
|---|---|---|---|---|---|---|---|---|---|
| sp\|Q9H501\|ESF1_HUMAN;tr\|A0JLU5\|A | 4 | 0 | 1098670 | 0 | 0 | 0 | 576230 | 0 |
| sp\|P22528\|SPR1B_HUMAN;tr\|Q2I377\|( | 4 | 0 | 1096160 | 741520 | 734230 | 738512 | 1041200 | 1554770 |
| tr\|Q4W5L2\|Q4W5L2_HUMAN;tr\|H6UYS | 4 | 0 | 1092100 | 163990 | 1524200 | 0 | 503120 | 0 |
| sp\|P49815-7\|TSC2_HUMAN;sp\|P49815- | 4 | 0 | 1089300 | 0 | 0 | 0 | 2896300 | 0 |
| sp\|Q8N4C6-6\|NIN_HUMAN;sp\|Q8N4C6 | 4 | 0 | 1079800 | 0 | 429830 | 0 | 0 | 0 |
| tr\|C7DJS2\|C7DJS2_HUMAN | 4 | 0 | 1079400 | 4818340 | 1651200 | 2859460 | 3263000 | 1002319 |
| sp\|P19174\|PLCG1_HUMAN;sp\|P19174- | 4 | 0 | 995330 | 0 | 344600 | 0 | 0 | 291090 |
| tr\|B4DQG8\|B4DQG8_HUMAN;sp\|Q9NP | 4 | 0 | 958200 | 0 | 1267900 | 0 | 1944700 | 0 |
| sp\|P43487-2\|RANG_HUMAN;sp\|P4348 | 4 | 0 | 932440 | 964950 | 3085600 | 873010 | 9822200 | 909169 |
| tr\|B4DJV5\|B4DJV5_HUMAN;tr\|Q9BV37 | 4 | 0 | 929160 | 0 | 1444200 | 0 | 3843400 | 0 |
| tr\|Q561W4\|Q561W4_HUMAN;sp\|Q129 | 4 | 0 | 919300 | 0 | 2551900 | 0 | 4113800 | 806900 |
| tr\|A7E2Y5\|A7E2Y5_HUMAN;sp\|O75165 | 4 | 0 | 878790 | 0 | 0 | 0 | 1470300 | 0 |
| sp\|O14578\|CTRO_HUMAN;sp\|O14578- | 4 | 0 | 812090 | 0 | 410810 | 0 | 0 | 0 |
| sp\|Q6VMQ6-2\|MCAF1_HUMAN;sp\|Q6V | 4 | 0 | 787770 | 237610 | 317540 | 153270 | 3403000 | 366850 |
| sp\|P63092-3\|GNAS2_HUMAN;tr\|Q5FW | 4 | 0 | 772840 | 0 | 2446400 | 322833 | 1875020 | 0 |
| sp\|Q14181\|DPOA2_HUMAN;tr\|B3KSX6 | 4 | 0 | 747330 | 0 | 1190090 | 0 | 5018590 | 60629 |
| sp\|Q9UKJ3-2\|GPTC8_HUMAN;sp\|Q9UK | 4 | 0 | 740200 | 0 | 418610 | 0 | 3733900 | 0 |
| tr\|B4DJ85\|B4DJ85_HUMAN;sp\|Q92990 | 4 | 0 | 718460 | 226220 | 3337100 | 250720 | 6961300 | 307214 |
| tr\|Q6IAT9\|Q6IAT9_HUMAN;sp\|P28072 | 4 | 0 | 706593 | 696050 | 695256 | 489230 | 1347540 | 1493390 |
| tr\|H7C1I7\|H7C1I7_HUMAN;sp\|Q5VZL5- | 4 | 0 | 703290 | 0 | 578530 | 0 | 1721800 | 0 |
| tr\|A8K6Q9\|A8K6Q9_HUMAN;tr\|A0A024 | 4 | 0 | 684170 | 0 | 2712900 | 179270 | 0 | 0 |
| tr\|A0A024R9M3\|A0A024R9M3_HUMAN | 4 | 0 | 676860 | 267740 | 625350 | 0 | 4959700 | 0 |
| sp\|O75175-2\|CNOT3_HUMAN;tr\|B7Z6J | 4 | 0 | 651260 | 0 | 512420 | 0 | 6028400 | 23114 |
| tr\|B4DZM3\|B4DZM3_HUMAN;tr\|Q53FR | 4 | 0 | 633870 | 144850 | 1004800 | 136400 | 8934100 | 534440 |
| sp\|Q86W56-5\|PARG_HUMAN;tr\|B4DX7 | 4 | 0 | 624380 | 0 | 0 | 0 | 1282700 | 98789 |
| sp\|Q16512-3\|PKN1_HUMAN;sp\|Q1651 | 4 | 0 | 610050 | 0 | 591520 | 0 | 3294600 | 0 |
| sp\|Q16637-4\|SMN_HUMAN;sp\|Q16637 | 4 | 0 | 604690 | 625290 | 797300 | 141150 | 13299000 | 0 |
| tr\|Q4G0D9\|Q4G0D9_HUMAN;tr\|B4DEN | 4 | 0 | 598230 | 0 | 180450 | 0 | 0 | 0 |
| sp\|Q96GM8\|TOE1_HUMAN;tr\|B3KSC7\| | 4 | 0 | 594970 | 0 | 1582630 | 0 | 4283700 | 0 |
| tr\|Q504W7\|Q504W7_HUMAN;sp\|Q019 | 4 | 0 | 575730 | 76189 | 858890 | 0 | 1030098 | 46159 |
| tr\|A0A024R3R5\|A0A024R3R5_HUMAN;s | 4 | 0 | 559600 | 0 | 261581 | 0 | 0 | 0 |
| tr\|A0A024RDE8\|A0A024RDE8_HUMAN; | 4 | 0 | 555090 | 0 | 439720 | 0 | 2958200 | 0 |
| tr\|C9K025\|C9K025_HUMAN;sp\|P18077 | 4 | 0 | 551389 | 1161468 | 3710510 | 651790 | 52779000 | 4274700 |
| sp\|Q8WVB6-3\|CTF18_HUMAN;tr\|E7EX/ | 4 | 0 | 546740 | 0 | 0 | 0 | 2164800 | 0 |
| tr\|Q32Q83\|Q32Q83_HUMAN;tr\|Q6P39 | 4 | 0 | 540980 | 237370 | 732300 | 190780 | 5040200 | 416090 |
| sp\|Q9NY33-4\|DPP3_HUMAN;tr\|Q5JPB8 | 4 | 0 | 527490 | 0 | 1441948 | 200210 | 585710 | 423786 |
| tr\|E5KLK1\|E5KLK1_HUMAN;tr\|E5KLJ9\|E | 4 | 0 | 489360 | 97344 | 0 | 0 | 0 | 0 |
| sp\|Q96DH6-2\|MSI2H_HUMAN;tr\|B4DH | 4 | 0 | 463030 | 0 | 0 | 0 | 10307600 | 495259 |
| tr\|C9JLU1\|C9JLU1_HUMAN;sp\|P52434\| | 4 | 0 | 445780 | 0 | 476530 | 0 | 215490 | 255640 |
| sp\|Q53LP3\|SWAHC_HUMAN | 4 | 0 | 434480 | 169850 | 1252700 | 204080 | 1285000 | 0 |
| sp\|Q99504-5\|EYA3_HUMAN;sp\|Q99504 | 4 | 0 | 424980 | 159350 | 1581700 | 201640 | 3114100 | 0 |
| tr\|A0A024R3X7\|A0A024R3X7_HUMAN;t | 4 | 0.000363 | 412540 | 0 | 0 | 0 | 0 | 0 |
| tr\|A0A090N7X1\|A0A090N7X1_HUMAN; | 4 | 0 | 409960 | 270330 | 274980 | 256950 | 4248000 | 0 |
| sp\|Q92615\|LAR4B_HUMAN;tr\|H0Y641\| | 4 | 0 | 409210 | 0 | 471820 | 0 | 5483700 | 169240 |
| tr\|H3BV55\|H3BV55_HUMAN;tr\|B2R6D4 | 4 | 0 | 403860 | 0 | 811670 | 416690 | 11942000 | 715320 |
| sp\|O00291-3\|HIP1_HUMAN;tr\|V5LU97\| | 4 | 0 | 396490 | 145807 | 87403 | 0 | 2532000 | 0 |
| tr\|A0A075B785\|A0A075B785_HUMAN;s | 4 | 0 | 395430 | 0 | 0 | 0 | 1689900 | 0 |
| sp\|Q92896\|GSLG1_HUMAN;sp\|Q92896- | 4 | 0 | 382250 | 0 | 552760 | 0 | 522670 | 0 |
| tr\|A8KA83\|A8KA83_HUMAN;sp\|Q9P0L( | 4 | 0 | 376410 | 0 | 606380 | 0 | 0 | 175220 |
| tr\|Q05DK5\|Q05DK5_HUMAN;sp\|P3561 | 4 | 0 | 363360 | 0 | 0 | 0 | 3397610 | 0 |
| tr\|Q5J8M4\|Q5J8M4_HUMAN;sp\|P7840 | 4 | 0 | 350550 | 0 | 888180 | 0 | 6032000 | 618790 |
| sp\|O95372\|LYPA2_HUMAN;tr\|Q5QPQ1 | 4 | 0 | 349031 | 0 | 47901 | 71490 | 4936870 | 0 |
| sp\|P01877\|IGHA2_HUMAN;tr\|Q9NPP6\| | 4 | 0.003634 | 342170 | 0 | 0 | 371160 | 0 | 332590 |
| sp\|Q8N573-5\|OXR1_HUMAN;sp\|Q8N57 | 4 | 0 | 339930 | 0 | 341100 | 0 | 2217600 | 0 |
| tr\|A8K3Y5\|A8K3Y5_HUMAN;sp\|Q9NX5 | 4 | 0 | 331960 | 0 | 922560 | 0 | 2225200 | 428410 |
| sp\|P22681\|CBL_HUMAN | 4 | 0 | 330740 | 0 | 0 | 0 | 2321600 | 0 |
| tr\|F8VZJ2\|F8VZJ2_HUMAN;tr\|F8W0W4 | 4 | 0 | 305050 | 1186570 | 453210 | 1106250 | 3147020 | 2560750 |
| tr\|B3KPN7\|B3KPN7_HUMAN;tr\|A0A024 | 4 | 0 | 304670 | 0 | 0 | 0 | 1018300 | 163690 |
| tr\|E5RIM3\|E5RIM3_HUMAN;sp\|Q9Y263 | 4 | 0 | 298176 | 99780 | 2410900 | 237741 | 2796428 | 115940 |
| tr\|A0A024R3Z2\|A0A024R3Z2_HUMAN;s | 4 | 0 | 296490 | 185223 | 611000 | 377200 | 1627580 | 878926 |
| tr\|C9J0J7\|C9J0J7_HUMAN;sp\|P35080-2 | 4 | 0 | 292670 | 0 | 469810 | 0 | 1863400 | 1372500 |
| sp\|Q9Y3U8\|RL36_HUMAN;tr\|J3QSB5\|J3 | 4 | 0 | 288890 | 248750 | 1060790 | 266780 | 58083000 | 5986020 |
| sp\|Q99627-2\|CSN8_HUMAN;tr\|E9PGT6 | 4 | 0 | 285860 | 451020 | 1022600 | 521360 | 19230000 | 352840 |
| sp\|Q70CQ2-3\|UBP34_HUMAN;sp\|Q70C | 4 | 0.000362 | 284430 | 0 | 0 | 0 | 1649500 | 0 |
| tr\|H3BTA2\|H3BTA2_HUMAN;tr\|A0A024 | 4 | 0 | 279490 | 217020 | 589690 | 157830 | 3882400 | 510470 |
| sp\|P49023-2\|PAXI_HUMAN;tr\|F5GZ78\| | 4 | 0 | 271640 | 164640 | 721940 | 280700 | 3162600 | 408370 |
| sp\|O95251-2\|KAT7_HUMAN;sp\|O95251 | 4 | 0 | 267450 | 0 | 0 | 0 | 2285040 | 0 |
| tr\|Q8IX26\|Q8IX26_HUMAN;tr\|F5GZI3\|F | 4 | 0 | 262840 | 0 | 291950 | 0 | 3100700 | 0 |
| tr\|F5H8F7\|F5H8F7_HUMAN;tr\|B4DPT1\| | 4 | 0 | 255560 | 0 | 0 | 0 | 4567200 | 0 |
| tr\|V9HW51\|V9HW51_HUMAN;tr\|B2R96 | 4 | 0 | 250623 | 192080 | 703930 | 147590 | 7763000 | 512550 |
| tr\|Q5TZN3\|Q5TZN3_HUMAN;tr\|B2R4U3 | 4 | 0 | 237786 | 1810800 | 482090 | 287430 | 433450 | 215890 |
| sp\|O15173\|PGRC2_HUMAN;sp\|O15173 | 4 | 0 | 237320 | 235020 | 640690 | 0 | 710600 | 0 |
| sp\|Q9Y3D0\|MIP18_HUMAN;tr\|H3BNV7 | 4 | 0 | 231760 | 205570 | 430410 | 109070 | 9184300 | 294280 |
| tr\|F5H8D7\|F5H8D7_HUMAN;tr\|A0A024 | 4 | 0 | 230040 | 0 | 445270 | 0 | 1043200 | 23293 |
| sp\|Q8WWK9-6\|CKAP2_HUMAN;tr\|B2R | 4 | 0 | 229160 | 45278 | 1322100 | 0 | 3105948 | 0 |
| tr\|A0A024RAS8\|A0A024RAS8_HUMAN; | 4 | 0 | 209970 | 1720800 | 2259520 | 2130300 | 5450100 | 1099700 |

| | | | | | | | | |
|---|---|---|---|---|---|---|---|---|
| tr\|B2RAR2\|B2RAR2_HUMAN;sp\|Q9ULX | 4 | 0 | 209430 | 0 | 330570 | 0 | 1971300 | 0 |
| sp\|P80723\|BASP1_HUMAN;sp\|P80723- | 4 | 0 | 201420 | 89159 | 151090 | 0 | 0 | 0 |
| sp\|O95456-2\|PSMG1_HUMAN;tr\|B2RD | 4 | 0 | 184540 | 258950 | 763410 | 0 | 11054000 | 1231400 |
| tr\|A0A024QZB1\|A0A024QZB1_HUMAN; | 4 | 0 | 183680 | 0 | 162740 | 0 | 4026760 | 0 |
| sp\|Q9BW83-2\|IFT27_HUMAN;sp\|Q9BW | 4 | 0 | 175570 | 262350 | 0 | 0 | 3466800 | 502490 |
| tr\|Q2LE71\|Q2LE71_HUMAN;tr\|B2R4D5\| | 4 | 0 | 159660 | 268720 | 806180 | 207090 | 8839500 | 395100 |
| sp\|Q5JSZ5-5\|PRC2B_HUMAN;sp\|Q5JSZ | 4 | 0 | 155190 | 0 | 144190 | 0 | 1269100 | 0 |
| tr\|B7WP74\|B7WP74_HUMAN;sp\|Q9HC | 4 | 0 | 142800 | 0 | 0 | 0 | 2299100 | 0 |
| tr\|C9J2P0\|C9J2P0_HUMAN;tr\|H7C061\| | 4 | 0.00269 | 138040 | 147980 | 353180 | 0 | 1452100 | 0 |
| tr\|A9QQ22\|A9QQ22_HUMAN;tr\|A9QQ | 4 | 0 | 136120 | 0 | 623900 | 74204 | 2046200 | 173340 |
| sp\|Q9Y394-2\|DHRS7_HUMAN;sp\|Q9Y3 | 4 | 0 | 135750 | 155360 | 674430 | 93647 | 0 | 0 |
| sp\|Q9BY32\|ITPA_HUMAN;sp\|Q9BY32-2 | 4 | 0 | 128520 | 209680 | 829490 | 222510 | 6913800 | 348220 |
| tr\|C9J384\|C9J384_HUMAN;tr\|D3DN44\| | 4 | 0 | 126700 | 0 | 292630 | 0 | 1620300 | 0 |
| sp\|Q9Y5B6-2\|PAXB1_HUMAN;sp\|Q9Y5 | 4 | 0.00037 | 123230 | 0 | 0 | 0 | 2897550 | 35671 |
| tr\|Q6FHJ5\|Q6FHJ5_HUMAN;sp\|O14828 | 4 | 0 | 119460 | 146300 | 664630 | 0 | 937160 | 0 |
| sp\|O75935-3\|DCTN3_HUMAN;sp\|O759 | 4 | 0 | 118410 | 0 | 0 | 0 | 2616000 | 810000 |
| sp\|Q15051\|IQCB1_HUMAN;sp\|Q15051- | 4 | 0 | 100110 | 0 | 0 | 0 | 1571400 | 0 |
| tr\|D3DR37\|D3DR37_HUMAN;sp\|Q53EZ | 4 | 0 | 95773 | 0 | 785160 | 0 | 963990 | 0 |
| sp\|Q71UM5\|RS27L_HUMAN;tr\|H0YMV | 4 | 0.000703 | 93193 | 147610 | 1220800 | 0 | 3187700 | 456320 |
| sp\|Q96DB5-2\|RMD1_HUMAN;sp\|Q96D | 4 | 0 | 71838 | 0 | 315830 | 0 | 2404600 | 126690 |
| tr\|B4E312\|B4E312_HUMAN;sp\|Q92804 | 4 | 0.005197 | 70581 | 0 | 211333 | 0 | 0 | 0 |
| sp\|Q9NZL9-4\|MAT2B_HUMAN;tr\|A8K7 | 4 | 0 | 58158 | 0 | 0 | 0 | 565280 | 856640 |
| sp\|O00469\|PLOD2_HUMAN;sp\|O00469 | 4 | 0 | 0 | 0 | 520080 | 0 | 0 | 0 |
| sp\|O14727-3\|APAF_HUMAN;tr\|A5YM4 | 4 | 0 | 0 | 0 | 0 | 0 | 1436300 | 0 |
| sp\|O15260-2\|SURF4_HUMAN;tr\|Q5T8U | 4 | 0 | 0 | 0 | 0 | 0 | 4188750 | 0 |
| sp\|O75419-2\|CDC45_HUMAN;sp\|O754 | 4 | 0 | 0 | 0 | 0 | 0 | 7965000 | 0 |
| sp\|P35270\|SPRE_HUMAN;tr\|Q9UEC5\|C | 4 | 0 | 0 | 0 | 321370 | 0 | 1741100 | 0 |
| sp\|P38432\|COIL_HUMAN;tr\|I3L369\|I3L | 4 | 0 | 0 | 0 | 541400 | 0 | 3419700 | 0 |
| sp\|P41223\|BUD31_HUMAN;sp\|P41223- | 4 | 0 | 0 | 0 | 0 | 0 | 1884600 | 0 |
| sp\|P42695\|CNDD3_HUMAN;tr\|Q96FA6 | 4 | 0 | 0 | 0 | 0 | 0 | 2693700 | 0 |
| sp\|P54687-4\|BCAT1_HUMAN;tr\|A0A02 | 4 | 0 | 0 | 0 | 295640 | 0 | 509240 | 0 |
| sp\|P61964\|WDR5_HUMAN | 4 | 0 | 0 | 0 | 0 | 0 | 1335810 | 0 |
| sp\|Q00403\|TF2B_HUMAN;tr\|B1APE1\|B | 4 | 0 | 0 | 0 | 323340 | 0 | 1871400 | 0 |
| sp\|Q3ZCW2\|LEGL_HUMAN;tr\|U3KQ88\| | 4 | 0 | 0 | 0 | 0 | 0 | 1363210 | 0 |
| sp\|Q5SY16\|NOL9_HUMAN | 4 | 0 | 0 | 0 | 0 | 0 | 1699000 | 0 |
| sp\|Q6ZU65\|UBN2_HUMAN;sp\|Q6ZU65- | 4 | 0 | 0 | 0 | 121890 | 0 | 436530 | 0 |
| sp\|Q7Z7H5-3\|TMED4_HUMAN;sp\|Q7Z7 | 4 | 0 | 0 | 0 | 0 | 0 | 4425900 | 0 |
| sp\|Q86V48-2\|LUZP1_HUMAN;sp\|Q86V | 4 | 0 | 0 | 0 | 0 | 0 | 1383600 | 0 |
| sp\|Q86X76-2\|NIT1_HUMAN;tr\|B7Z410\| | 4 | 0 | 0 | 0 | 0 | 0 | 1143200 | 0 |
| sp\|Q8IUF8-4\|MINA_HUMAN;sp\|Q8IUF8 | 4 | 0 | 0 | 0 | 407150 | 0 | 1628200 | 0 |
| sp\|Q8WX93-7\|PALLD_HUMAN;sp\|Q8W | 4 | 0 | 0 | 0 | 1666980 | 0 | 2581600 | 0 |
| sp\|Q8WZA9\|IRGQ_HUMAN;tr\|B7ZMD6 | 4 | 0 | 0 | 0 | 427070 | 0 | 0 | 0 |
| sp\|Q92889\|XPF_HUMAN;tr\|A0PJA9\|A0 | 4 | 0 | 0 | 0 | 486570 | 0 | 1888100 | 0 |
| sp\|Q96GM5-2\|SMRD1_HUMAN;sp\|Q96 | 4 | 0 | 0 | 0 | 259360 | 0 | 1089300 | 0 |
| sp\|Q96JB1-2\|DYH8_HUMAN;sp\|Q96JB1 | 4 | 0.000358 | 0 | 0 | 0 | 0 | 2753200 | 0 |
| sp\|Q96P16-3\|RPR1A_HUMAN;tr\|A0A02 | 4 | 0.000368 | 0 | 0 | 0 | 0 | 579700 | 0 |
| sp\|Q96Q15-4\|SMG1_HUMAN;sp\|Q96Q | 4 | 0.000354 | 0 | 0 | 106560 | 0 | 1017300 | 0 |
| sp\|Q9BWT3-2\|PAPOG_HUMAN;sp\|Q9B | 4 | 0.005393 | 0 | 0 | 0 | 0 | 472480 | 0 |
| sp\|Q9BYJ9\|YTHD1_HUMAN;tr\|B4DT65\| | 4 | 0.000371 | 0 | 0 | 553900 | 0 | 2017400 | 0 |
| sp\|Q9H6T3-3\|RPAP3_HUMAN;sp\|Q9H6 | 4 | 0 | 0 | 0 | 0 | 0 | 1766200 | 0 |
| sp\|Q9H8S9\|MOB1A_HUMAN;sp\|Q7L9L | 4 | 0 | 0 | 0 | 0 | 0 | 332840 | 0 |
| sp\|Q9NUQ6-2\|SPS2L_HUMAN;tr\|A0A0 | 4 | 0 | 0 | 0 | 1066290 | 0 | 6335200 | 0 |
| sp\|Q9NVE7\|PANK4_HUMAN;tr\|B4DHW | 4 | 0 | 0 | 0 | 0 | 0 | 2901700 | 0 |
| sp\|Q9UL40-3\|ZN346_HUMAN;sp\|Q9UL | 4 | 0 | 0 | 0 | 0 | 0 | 1359600 | 0 |
| sp\|Q9ULK4-2\|MED23_HUMAN;sp\|Q9UL | 4 | 0 | 0 | 0 | 290170 | 0 | 1739400 | 0 |
| sp\|Q9Y6W5\|WASF2_HUMAN;tr\|Q05BU | 4 | 0 | 0 | 0 | 0 | 0 | 4947400 | 0 |
| tr\|A0A024QZH6\|A0A024QZH6_HUMAN | 4 | 0 | 0 | 0 | 0 | 0 | 1691700 | 0 |
| tr\|A0A024RB31\|A0A024RB31_HUMAN;s | 4 | 0.000369 | 0 | 0 | 0 | 0 | 1678600 | 0 |
| tr\|A0A087WV25\|A0A087WV25_HUMAN | 4 | 0 | 0 | 0 | 778090 | 0 | 8625700 | 0 |
| tr\|A0A090N7W4\|A0A090N7W4_HUMAI | 4 | 0 | 0 | 0 | 0 | 0 | 1457600 | 0 |
| tr\|A6QKW0\|A6QKW0_HUMAN;tr\|A0A0 | 4 | 0 | 0 | 0 | 0 | 0 | 1329200 | 0 |
| tr\|A8MTY9\|A8MTY9_HUMAN;sp\|O1497 | 4 | 0 | 0 | 0 | 0 | 0 | 787690 | 0 |
| tr\|B2RDJ6\|B2RDJ6_HUMAN;sp\|O76071 | 4 | 0 | 0 | 0 | 0 | 0 | 1972000 | 0 |
| tr\|B3KNC3\|B3KNC3_HUMAN;sp\|Q9Y3T | 4 | 0 | 0 | 0 | 0 | 0 | 1165490 | 0 |
| tr\|B3KPC1\|B3KPC1_HUMAN;tr\|A0A024 | 4 | 0 | 0 | 0 | 638370 | 0 | 1314200 | 0 |
| tr\|B3KS28\|B3KS28_HUMAN;sp\|Q147X3 | 4 | 0 | 0 | 0 | 0 | 0 | 1455300 | 0 |
| tr\|B3KT11\|B3KT11_HUMAN;sp\|Q96D46 | 4 | 0 | 0 | 0 | 0 | 0 | 3628400 | 0 |
| tr\|B3KW08\|B3KW08_HUMAN;sp\|Q96Q | 4 | 0 | 0 | 0 | 400010 | 0 | 2834800 | 0 |
| tr\|B4DFV1\|B4DFV1_HUMAN;tr\|A0A024 | 4 | 0 | 0 | 0 | 0 | 0 | 3597500 | 0 |
| tr\|B4DNU0\|B4DNU0_HUMAN;tr\|Q53HH | 4 | 0 | 0 | 0 | 281040 | 0 | 2961700 | 0 |
| tr\|B4DW97\|B4DW97_HUMAN;tr\|A0A08 | 4 | 0.000355 | 0 | 0 | 0 | 0 | 2085400 | 0 |
| tr\|B4DZ22\|B4DZ22_HUMAN;sp\|P28288 | 4 | 0 | 0 | 0 | 355200 | 0 | 0 | 0 |
| tr\|B4E086\|B4E086_HUMAN;tr\|K7EJH0\| | 4 | 0 | 0 | 0 | 0 | 0 | 2650000 | 0 |
| tr\|B4E253\|B4E253_HUMAN;tr\|F5H5V6\| | 4 | 0 | 0 | 0 | 132730 | 0 | 1111700 | 0 |
| tr\|B7Z2V7\|B7Z2V7_HUMAN;tr\|B7Z1V5\| | 4 | 0 | 0 | 0 | 302830 | 0 | 4865400 | 0 |
| tr\|B7ZA10\|B7ZA10_HUMAN;tr\|B4E273\| | 4 | 0 | 0 | 0 | 0 | 0 | 610950 | 0 |
| tr\|C9J177\|C9J177_HUMAN;sp\|Q15435- | 4 | 0 | 0 | 0 | 0 | 0 | 0 | 0 |
| tr\|C9JRJ5\|C9JRJ5_HUMAN;sp\|Q9UGP4\| | 4 | 0 | 0 | 0 | 0 | 0 | 4628400 | 0 |

| | | | | | | | | |
|---|---|---|---|---|---|---|---|---|
| tr\|E7EPJ7\|E7EPJ7_HUMAN;sp\|O75962- | 4 | 0 | 0 | 0 | 0 | 0 | 1858100 | 0 |
| tr\|E7ERH2\|E7ERH2_HUMAN;tr\|F8W8N3 | 4 | 0 | 0 | 0 | 0 | 0 | 2013040 | 0 |
| tr\|E9PCN5\|E9PCN5_HUMAN;sp\|Q9H9A | 4 | 0 | 0 | 0 | 1049100 | 0 | 2955790 | 0 |
| tr\|H0YEF3\|H0YEF3_HUMAN;sp\|Q8TDP1 | 4 | 0 | 0 | 0 | 0 | 0 | 1657400 | 0 |
| tr\|J3QR55\|J3QR55_HUMAN | 4 | 1 | 0 | 0 | 0 | 0 | 353810 | 0 |
| tr\|M0R3B2\|M0R3B2_HUMAN;tr\|A8K67 | 4 | 0 | 0 | 0 | 1082800 | 0 | 7110800 | 0 |
| tr\|Q5TB52\|Q5TB52_HUMAN;sp\|O9534 | 4 | 0 | 0 | 0 | 769920 | 0 | 0 | 0 |
| tr\|Q63HP7\|Q63HP7_HUMAN;tr\|Q5G0E | 4 | 0 | 0 | 0 | 550950 | 0 | 2372100 | 0 |
| tr\|Q86TY2\|Q86TY2_HUMAN;tr\|V9GYX7 | 4 | 0 | 0 | 0 | 343710 | 0 | 1929000 | 0 |
| tr\|Q9BS45\|Q9BS45_HUMAN;tr\|A0A024 | 4 | 0 | 0 | 0 | 466970 | 0 | 4906400 | 0 |
| tr\|Q9UK43\|Q9UK43_HUMAN;tr\|Q95HA | 4 | 0 | 0 | 0 | 397300 | 0 | 2189600 | 0 |
| tr\|X6RAL5\|X6RAL5_HUMAN;tr\|H7BZW6 | 4 | 0 | 0 | 0 | 0 | 0 | 2555500 | 0 |
| tr\|A0A024R1F9\|A0A024R1F9_HUMAN;s | 4 | 0 | 0 | 0 | 0 | 0 | 2925540 | 162790 |
| sp\|Q9BWJ5\|SF3B5_HUMAN | 4 | 0 | 0 | 0 | 29406 | 0 | 2030000 | 140680 |
| tr\|N0E4C7\|N0E4C7_HUMAN;sp\|P67870 | 4 | 0 | 0 | 0 | 208320 | 0 | 3301000 | 235210 |
| tr\|B5BUI8\|B5BUI8_HUMAN;sp\|P51452\| | 4 | 0 | 0 | 0 | 197150 | 0 | 4647100 | 332320 |
| tr\|Q8IYS3\|Q8IYS3_HUMAN;tr\|Q53FW7 | 4 | 0 | 0 | 0 | 0 | 0 | 3214800 | 253740 |
| tr\|F5GYK2\|F5GYK2_HUMAN;tr\|B4DMU7 | 4 | 0 | 0 | 0 | 191770 | 0 | 2103180 | 178050 |
| tr\|Q05BU6\|Q05BU6_HUMAN;tr\|Q6PJY9 | 4 | 0 | 0 | 0 | 1593600 | 0 | 18821920 | 1758169 |
| sp\|P61962\|DCAF7_HUMAN;tr\|B4DH46\| | 4 | 0 | 0 | 0 | 0 | 0 | 5030800 | 470940 |
| sp\|P46020-3\|KPB1_HUMAN;tr\|A6NIT2\| | 4 | 0 | 0 | 0 | 0 | 0 | 2654460 | 286390 |
| tr\|A0A024R7G6\|A0A024R7G6_HUMAN; | 4 | 0 | 0 | 0 | 0 | 0 | 1416100 | 203330 |
| tr\|B4DRU9\|B4DRU9_HUMAN;sp\|Q9NU | 4 | 0 | 0 | 0 | 0 | 0 | 1610400 | 274410 |
| tr\|Q6IAV3\|Q6IAV3_HUMAN;sp\|P41567 | 4 | 0 | 0 | 0 | 0 | 0 | 4838300 | 947610 |
| sp\|O75340-2\|PDCD6_HUMAN;tr\|Q53F0 | 4 | 0 | 0 | 0 | 0 | 0 | 2183400 | 698180 |
| tr\|Q53H22\|Q53H22_HUMAN;tr\|A8K4H7 | 4 | 0 | 0 | 0 | 1788743 | 0 | 1014100 | 386570 |
| sp\|Q7L5D6\|GET4_HUMAN;sp\|Q7L5D6-2 | 4 | 0 | 0 | 0 | 147280 | 0 | 1272500 | 542270 |
| tr\|Q6FGX9\|Q6FGX9_HUMAN;tr\|Q53EY8 | 4 | 0 | 0 | 0 | 0 | 0 | 512210 | 377520 |
| tr\|S4R3N1\|S4R3N1_HUMAN;tr\|A8K012 | 4 | 0 | 0 | 0 | 422740 | 0 | 522410 | 514580 |
| sp\|Q9Y237\|PIN4_HUMAN;sp\|Q9Y237-2 | 4 | 0 | 0 | 0 | 109270 | 0 | 268790 | 421630 |
| sp\|Q9BTZ2-8\|DHRS4_HUMAN;sp\|Q9BT | 4 | 0 | 0 | 1146800 | 172380 | 0 | 622500 | 0 |
| tr\|A2I829\|A2I829_HUMAN;tr\|Q6NUN2 | 4 | 0 | 0 | 148100 | 0 | 0 | 2815840 | 0 |
| tr\|B4DKV5\|B4DKV5_HUMAN;sp\|Q96EK | 4 | 0 | 0 | 114540 | 169750 | 0 | 1550600 | 0 |
| tr\|B7Z5N6\|B7Z5N6_HUMAN;sp\|Q5T1V | 4 | 0 | 0 | 150580 | 350370 | 0 | 4412200 | 0 |
| tr\|R4GND1\|R4GND1_HUMAN;tr\|A0A02 | 4 | 0 | 0 | 148430 | 337530 | 0 | 7203400 | 160340 |
| sp\|O75607\|NPM3_HUMAN | 4 | 0 | 0 | 337960 | 384290 | 0 | 20681000 | 891750 |
| sp\|O94888\|UBXN7_HUMAN;tr\|C9JAT7\| | 4 | 0 | 0 | 274120 | 908427 | 0 | 2790600 | 531882 |
| tr\|V9HWC9\|V9HWC9_HUMAN;sp\|P004 | 4 | 0 | 0 | 577800 | 0 | 0 | 0 | 1535910 |
| sp\|Q9Y547\|IFT25_HUMAN;tr\|A6NIR2\|A | 4 | 0 | 0 | 259920 | 588160 | 74696 | 10500000 | 658740 |
| tr\|C9JG97\|C9JG97_HUMAN;tr\|A0A024R | 4 | 0 | 0 | 161580 | 1292500 | 316400 | 3006700 | 0 |
| tr\|A8K6I6\|A8K6I6_HUMAN;sp\|Q9NZ52 | 4 | 0 | 0 | 166750 | 820650 | 231640 | 2595400 | 494990 |
| sp\|P62995-3\|TRA2B_HUMAN;tr\|Q8N1H | 4 | 0 | 0 | 0 | 654870 | 218106 | 1836820 | 820301 |
| sp\|Q53GG5-2\|PDLI3_HUMAN;sp\|Q53G | 4 | 0 | 0 | 269990 | 319110 | 119630 | 10410000 | 1233007 |
| tr\|B5MC59\|B5MC59_HUMAN;tr\|A4D10 | 4 | 0 | 0 | 455860 | 639460 | 246300 | 18602000 | 4082500 |
| sp\|Q9NQT4\|EXOS5_HUMAN;tr\|M0R05 | 4 | 0 | 0 | 252390 | 314760 | 148790 | 11199000 | 928210 |
| tr\|B2R5I8\|B2R5I8_HUMAN;sp\|Q13637\| | 4 | 0 | 0 | 0 | 288660 | 141670 | 0 | 0 |
| sp\|Q9UJ70\|NAGK_HUMAN;sp\|Q9UJ70- | 4 | 0 | 0 | 0 | 0 | 44573 | 2003200 | 109330 |
| tr\|H3BRV9\|H3BRV9_HUMAN;tr\|A0A02 | 4 | 0 | 0 | 0 | 0 | 65972 | 0 | 1042000 |
| tr\|Q7Z612\|Q7Z612_HUMAN;tr\|A0A024 | 3 | 0 | 29833000 | 3508000 | 60867000 | 5914700 | 148340000 | 15003000 |
| tr\|S6AWD6\|S6AWD6_HUMAN | 3 | 0 | 23449010 | 33362540 | 30749068 | 27900360 | 70141900 | 48302050 |
| sp\|P0CG22\|DR4L1_HUMAN | 3 | 1 | 15799860 | 0 | 0 | 0 | 0 | 0 |
| tr\|B4DKW4\|B4DKW4_HUMAN;sp\|Q8TE | 3 | 0.000359 | 13666300 | 9663400 | 9288400 | 11306300 | 11449600 | 1760370 |
| tr\|Q0EFA5\|Q0EFA5_HUMAN;tr\|A8K9C1 | 3 | 0 | 7045000 | 6024300 | 4903160 | 6783900 | 4310280 | 3520070 |
| sp\|Q9Y3D6\|FIS1_HUMAN | 3 | 0 | 2427000 | 990480 | 6179600 | 590630 | 4575300 | 830970 |
| sp\|Q53RT3\|APRV1_HUMAN | 3 | 0 | 2338740 | 594350 | 845034 | 0 | 4547900 | 603259 |
| tr\|A0A024R5H0\|A0A024R5H0_HUMAN; | 3 | 0 | 2182610 | 790290 | 3726800 | 302200 | 20794020 | 1656200 |
| tr\|B3KRY3\|B3KRY3_HUMAN;tr\|A0A024 | 3 | 0 | 2121228 | 0 | 486920 | 0 | 0 | 167680 |
| tr\|A0A024R6D4\|A0A024R6D4_HUMAN; | 3 | 0 | 1973400 | 1172062 | 4735800 | 1285111 | 21572250 | 10383941 |
| tr\|B4DK32\|B4DK32_HUMAN;sp\|Q14139 | 3 | 0 | 1817200 | 92459 | 609760 | 0 | 0 | 0 |
| sp\|Q15738\|NSDHL_HUMAN;tr\|C9JDR0\| | 3 | 0 | 1796500 | 0 | 0 | 0 | 0 | 0 |
| sp\|P63172\|DYLT1_HUMAN;tr\|Q5VTU3\| | 3 | 0 | 1738900 | 344750 | 2190800 | 0 | 7032000 | 664550 |
| sp\|P62318-2\|SMD3_HUMAN;sp\|P6231 | 3 | 0 | 1599300 | 2003610 | 4654560 | 1596420 | 30821000 | 9581875 |
| tr\|B4E240\|B4E240_HUMAN;sp\|Q92575 | 3 | 0 | 1418200 | 0 | 839790 | 0 | 0 | 0 |
| tr\|Q6FGG2\|Q6FGG2_HUMAN;sp\|Q1583 | 3 | 0 | 1397400 | 441740 | 1870500 | 167680 | 3697500 | 689830 |
| tr\|Q4G1A8\|Q4G1A8_HUMAN;sp\|Q1355 | 3 | 0 | 1313800 | 0 | 1673800 | 0 | 1555400 | 0 |
| sp\|Q86X10-3\|RLGPB_HUMAN;sp\|Q86X | 3 | 0 | 1201300 | 0 | 0 | 48685 | 2513300 | 0 |
| tr\|B4DHS3\|B4DHS3_HUMAN;tr\|Q59G4 | 3 | 0 | 1158120 | 0 | 1336400 | 0 | 4482700 | 0 |
| tr\|C9JP00\|C9JP00_HUMAN;sp\|Q9NR56 | 3 | 0 | 1080100 | 0 | 1781459 | 0 | 7173463 | 583020 |
| sp\|Q32MZ4-3\|LRRF1_HUMAN;sp\|Q32M | 3 | 0 | 1053300 | 67582 | 210080 | 0 | 0 | 87870 |
| tr\|B7ZKN7\|B7ZKN7_HUMAN;tr\|B7Z2X2 | 3 | 0 | 1024600 | 0 | 15727921 | 224490 | 294230 | 0 |
| tr\|R4SBI6\|R4SBI6_HUMAN;tr\|Q6FGZ3\| | 3 | 0 | 1002100 | 387540 | 0 | 0 | 0 | 0 |
| tr\|Q59HA2\|Q59HA2_HUMAN;tr\|Q6IBL8 | 3 | 0 | 946590 | 342700 | 1815200 | 171560 | 7354300 | 322870 |
| tr\|Q53RZ9\|Q53RZ9_HUMAN;sp\|Q9HCN | 3 | 0 | 937070 | 0 | 2683700 | 0 | 0 | 897620 |
| tr\|B2RE34\|B2RE34_HUMAN;tr\|A0A024F | 3 | 0 | 906100 | 247530 | 1001800 | 151120 | 2301100 | 0 |
| sp\|O00461\|GOLI4_HUMAN;tr\|F8W785\| | 3 | 0 | 879030 | 434910 | 960260 | 241160 | 1708600 | 196880 |

| | | | | | | | | |
|---|---|---|---|---|---|---|---|---|
| tr\|I3L2R3\|I3L2R3_HUMAN;tr\|I3L533\|I3L | 3 | 0 | 771520 | 96498 | 1483200 | 360430 | 977160 | 204760 |
| tr\|Q96J85\|Q96J85_HUMAN;sp\|Q71RC2 | 3 | 0 | 760984 | 0 | 972290 | 0 | 2890330 | 0 |
| tr\|A0A024QZC1\|A0A024QZC1_HUMAN; | 3 | 0 | 744000 | 0 | 0 | 0 | 2694700 | 230810 |
| sp\|Q8WZA0-2\|LZIC_HUMAN;tr\|A0A024 | 3 | 0 | 727560 | 0 | 533770 | 164990 | 0 | 331887 |
| sp\|Q96DT7-3\|ZBT10_HUMAN;tr\|A8E4L4 | 3 | 0 | 696960 | 0 | 166750 | 0 | 1295300 | 0 |
| sp\|O94874-2\|UFL1_HUMAN;sp\|O94874 | 3 | 0 | 693890 | 0 | 0 | 0 | 0 | 32691 |
| sp\|Q5VVQ6-2\|OTU1_HUMAN;sp\|Q5VV | 3 | 0 | 659440 | 0 | 0 | 0 | 6256000 | 0 |
| sp\|P42684-7\|ABL2_HUMAN;sp\|P42684 | 3 | 0 | 655150 | 323960 | 692100 | 250230 | 4297800 | 970950 |
| tr\|A6NML8\|A6NML8_HUMAN;sp\|O608 | 3 | 0 | 650070 | 0 | 410700 | 0 | 1676000 | 0 |
| tr\|X6R9L0\|X6R9L0_HUMAN;tr\|A8KA82\| | 3 | 0 | 638650 | 0 | 885540 | 0 | 3371800 | 0 |
| sp\|Q4KMP7\|TB10B_HUMAN | 3 | 0 | 633340 | 162400 | 0 | 0 | 0 | 0 |
| tr\|B4DNM0\|B4DNM0_HUMAN;sp\|Q8W | 3 | 0 | 624410 | 0 | 380740 | 0 | 5799600 | 0 |
| tr\|B4DQJ4\|B4DQJ4_HUMAN;sp\|O15381 | 3 | 0 | 611260 | 0 | 549590 | 0 | 2798300 | 0 |
| sp\|Q9UPP1-4\|PHF8_HUMAN;tr\|H0Y3N9 | 3 | 0 | 594220 | 165430 | 232920 | 118930 | 1499100 | 0 |
| sp\|Q9BRA2\|TXD17_HUMAN;tr\|I3L0K2\| | 3 | 0 | 593680 | 449770 | 1358300 | 0 | 9488600 | 1848500 |
| sp\|Q9Y6H1\|CHCH2_HUMAN;sp\|Q5T1J5 | 3 | 0 | 570350 | 1470700 | 1419100 | 565500 | 663590 | 0 |
| tr\|E5RHD8\|E5RHD8_HUMAN;sp\|Q0539 | 3 | 0 | 563140 | 0 | 0 | 0 | 4026500 | 0 |
| tr\|B4DG55\|B4DG55_HUMAN;tr\|L7RRS0 | 3 | 0 | 545920 | 0 | 0 | 0 | 4953800 | 0 |
| tr\|A0A024QYV8\|A0A024QYV8_HUMAN | 3 | 0 | 509440 | 0 | 312960 | 0 | 460930 | 0 |
| sp\|Q8ND04\|SMG8_HUMAN;sp\|Q8ND04 | 3 | 0.000373 | 499820 | 0 | 0 | 0 | 2983640 | 0 |
| sp\|O75420\|PERQ1_HUMAN;tr\|A2VDH9 | 3 | 0 | 492680 | 135540 | 215180 | 0 | 1690200 | 0 |
| sp\|Q13131\|AAPK1_HUMAN;sp\|Q13131 | 3 | 0.00273 | 489090 | 0 | 0 | 0 | 0 | 0 |
| tr\|A0A024R1S5\|A0A024R1S5_HUMAN;s | 3 | 0 | 487470 | 0 | 0 | 0 | 1581800 | 0 |
| tr\|C9J8T0\|C9J8T0_HUMAN;sp\|P57772\|S | 3 | 0 | 469620 | 0 | 963680 | 0 | 1552290 | 0 |
| tr\|B2R9T9\|B2R9T9_HUMAN;sp\|Q9BVC6 | 3 | 0 | 454520 | 1301100 | 681674 | 0 | 100780 | 637880 |
| sp\|Q6YP21-3\|KAT3_HUMAN;tr\|B4DW1 | 3 | 0 | 452330 | 0 | 703790 | 0 | 2355200 | 0 |
| tr\|B7Z3S8\|B7Z3S8_HUMAN;sp\|Q8N122 | 3 | 0 | 451480 | 0 | 0 | 0 | 2846600 | 0 |
| sp\|Q03164-2\|KMT2A_HUMAN;sp\|Q031 | 3 | 0 | 448060 | 0 | 0 | 0 | 0 | 0 |
| tr\|A0A024R7W0\|A0A024R7W0_HUMAN | 3 | 0 | 444480 | 0 | 2497800 | 194230 | 595890 | 0 |
| tr\|A0A024RDA1\|A0A024RDA1_HUMAN | 3 | 0 | 435760 | 272736 | 542590 | 0 | 2490240 | 0 |
| sp\|P11171-6\|41_HUMAN;sp\|P11171-4\| | 3 | 0.000363 | 420570 | 0 | 0 | 0 | 472770 | 0 |
| sp\|Q9HBK9-2\|AS3MT_HUMAN;tr\|A0A0 | 3 | 0 | 399060 | 0 | 1279500 | 0 | 1993800 | 227580 |
| tr\|A0A024R6N2\|A0A024R6N2_HUMAN; | 3 | 0 | 397120 | 161077 | 0 | 0 | 1253700 | 0 |
| sp\|Q4J6C6-4\|PPCEL_HUMAN;sp\|Q4J6C | 3 | 0 | 391370 | 0 | 0 | 0 | 0 | 0 |
| tr\|H0YE29\|H0YE29_HUMAN;sp\|Q07960 | 3 | 0 | 387810 | 0 | 1205400 | 0 | 0 | 0 |
| tr\|Q6FGH9\|Q6FGH9_HUMAN;sp\|P6316 | 3 | 0 | 384240 | 386101 | 1231300 | 664030 | 4028800 | 1902020 |
| sp\|Q96RU2-2\|UBP28_HUMAN;sp\|Q96R | 3 | 0.000356 | 383310 | 0 | 228460 | 0 | 0 | 0 |
| sp\|Q15542\|TAF5_HUMAN;sp\|Q15542-2 | 3 | 0 | 371900 | 0 | 0 | 0 | 3092400 | 0 |
| sp\|Q7Z589-2\|EMSY_HUMAN;sp\|Q7Z58 | 3 | 0 | 362690 | 0 | 59819 | 0 | 980810 | 0 |
| tr\|B7ZMB3\|B7ZMB3_HUMAN;sp\|Q5TC8 | 3 | 0.000369 | 355700 | 0 | 0 | 0 | 510300 | 0 |
| tr\|E7ER32\|E7ER32_HUMAN;tr\|A4FUJ8\| | 3 | 0 | 355340 | 0 | 651620 | 0 | 708610 | 0 |
| sp\|P60468\|SC61B_HUMAN;tr\|Q53FA5\| | 3 | 0.000703 | 347110 | 0 | 795680 | 167850 | 0 | 825480 |
| tr\|C9JP85\|C9JP85_HUMAN;sp\|Q16656- | 3 | 0.002699 | 341430 | 0 | 680320 | 0 | 1112900 | 0 |
| sp\|Q69YN4-2\|VIR_HUMAN;sp\|Q69YN4 | 3 | 0 | 336000 | 0 | 0 | 0 | 4341900 | 0 |
| tr\|H0Y8L0\|H0Y8L0_HUMAN | 3 | 1 | 329960 | 0 | 0 | 0 | 0 | 0 |
| tr\|B7Z361\|B7Z361_HUMAN;tr\|A0A024R | 3 | 0 | 318390 | 415660 | 963150 | 293030 | 1694600 | 327920 |
| tr\|A8K7B1\|A8K7B1_HUMAN;sp\|Q96T51 | 3 | 0.000367 | 301920 | 0 | 237830 | 0 | 566800 | 0 |
| tr\|A0A024R094\|A0A024R094_HUMAN;t | 3 | 0 | 301870 | 0 | 501130 | 0 | 1766900 | 188140 |
| tr\|A0A0A0MRX2\|A0A0A0MRX2_HUMAN | 3 | 0 | 298640 | 0 | 993990 | 0 | 0 | 0 |
| sp\|Q6BDS2\|URFB1_HUMAN;tr\|H7C1J4\| | 3 | 0 | 292530 | 226140 | 412170 | 0 | 1146700 | 0 |
| tr\|H1UBN3\|H1UBN3_HUMAN;tr\|Q5U0M | 3 | 0 | 288280 | 0 | 587070 | 0 | 685420 | 0 |
| tr\|B4E2V7\|B4E2V7_HUMAN;tr\|A0A087 | 3 | 0 | 285430 | 0 | 144200 | 0 | 1525900 | 0 |
| tr\|A0A024RBR4\|A0A024RBR4_HUMAN; | 3 | 0 | 283780 | 0 | 354790 | 0 | 552910 | 0 |
| tr\|A0A024R2G8\|A0A024R2G8_HUMAN; | 3 | 0 | 282510 | 0 | 213400 | 0 | 873290 | 0 |
| tr\|J3QRD1\|J3QRD1_HUMAN;sp\|P51648 | 3 | 0 | 279020 | 0 | 0 | 0 | 0 | 35626 |
| sp\|Q96JH7\|VCIP1_HUMAN;tr\|B4DM84 | 3 | 0 | 268940 | 537350 | 380840 | 0 | 1499900 | 0 |
| sp\|Q5BKZ1\|ZN326_HUMAN | 3 | 0 | 267400 | 0 | 0 | 0 | 3021800 | 0 |
| tr\|Q6I9V5\|Q6I9V5_HUMAN;tr\|A8K787\| | 3 | 0.006571 | 262020 | 0 | 0 | 0 | 0 | 0 |
| tr\|B2R841\|B2R841_HUMAN;sp\|P53350 | 3 | 0 | 257170 | 340130 | 835290 | 0 | 0 | 0 |
| tr\|B4DV85\|B4DV85_HUMAN;tr\|A0A024 | 3 | 0 | 250170 | 0 | 236750 | 0 | 1343500 | 0 |
| sp\|P52630-4\|STAT2_HUMAN;tr\|R9QGC | 3 | 0 | 238780 | 0 | 0 | 0 | 2377900 | 0 |
| tr\|A0A087X0M4\|A0A087X0M4_HUMAN | 3 | 0 | 231670 | 0 | 0 | 0 | 0 | 71342 |
| tr\|Q2NLC8\|Q2NLC8_HUMAN;tr\|E9PFN5 | 3 | 0 | 229741 | 0 | 0 | 106943 | 576400 | 36082 |
| sp\|Q9NVH2-4\|INT7_HUMAN;sp\|Q9NVI | 3 | 0 | 223810 | 111750 | 301520 | 54940 | 712960 | 0 |
| tr\|A0A024R1D6\|A0A024R1D6_HUMAN; | 3 | 0 | 221520 | 0 | 862280 | 93961 | 2104500 | 0 |
| sp\|Q969U7-2\|PSMG2_HUMAN;tr\|K7EN | 3 | 0 | 215890 | 0 | 546030 | 0 | 5627900 | 57276 |
| sp\|P48507\|GSH0_HUMAN;sp\|P48507-2 | 3 | 0 | 213110 | 181270 | 704470 | 0 | 1086500 | 328170 |
| sp\|Q9BTY7\|HGH1_HUMAN;tr\|Q9P0T5\| | 3 | 0.00332 | 202810 | 0 | 502470 | 0 | 0 | 0 |
| tr\|B4DEZ8\|B4DEZ8_HUMAN;tr\|B2RCG9 | 3 | 0 | 202510 | 0 | 175810 | 0 | 1782100 | 75029 |
| tr\|D6RBS5\|D6RBS5_HUMAN;sp\|Q8IZ81 | 3 | 0.000358 | 200037 | 0 | 259230 | 0 | 0 | 0 |
| sp\|Q14686\|NCOA6_HUMAN;tr\|F6M2K3 | 3 | 0 | 174620 | 0 | 208800 | 0 | 3190300 | 73459 |
| tr\|F5GXX5\|F5GXX5_HUMAN;sp\|P61803 | 3 | 0 | 171930 | 0 | 277260 | 0 | 0 | 0 |
| sp\|P0CJ79\|ZN888_HUMAN | 3 | 0 | 164580 | 0 | 0 | 0 | 1463090 | 0 |
| sp\|O14893-2\|GEMI2_HUMAN;sp\|O148 | 3 | 0 | 162170 | 318140 | 579330 | 142690 | 2066300 | 138930 |
| sp\|O95248\|MTMR5_HUMAN;tr\|G5E933 | 3 | 0 | 156600 | 0 | 358010 | 0 | 1634300 | 371690 |

| | | | | | | | | |
|---|---|---|---|---|---|---|---|---|
| sp\|Q7KZI7-10\|MARK2_HUMAN;tr\|A0A( | 3 | 0 | 155230 | 0 | 633610 | 0 | 399620 | 0 |
| tr\|B2R4R9\|B2R4R9_HUMAN;sp\|P62857 | 3 | 0 | 154250 | 55076 | 251360 | 0 | 1366400 | 6820955 |
| tr\|Q53XM7\|Q53XM7_HUMAN;sp\|O952 | 3 | 0 | 149650 | 126380 | 1103200 | 180130 | 578020 | 0 |
| sp\|O75170-6\|PP6R2_HUMAN;sp\|O7517 | 3 | 0 | 146860 | 0 | 0 | 0 | 568050 | 0 |
| sp\|Q86W92\|LIPB1_HUMAN;tr\|F5GZP6\| | 3 | 0 | 142730 | 0 | 0 | 0 | 738820 | 0 |
| tr\|A8CDT9\|A8CDT9_HUMAN;tr\|A0A087 | 3 | 0.002055 | 142240 | 0 | 0 | 0 | 422600 | 0 |
| tr\|B7Z6B3\|B7Z6B3_HUMAN;tr\|B7Z2A3\| | 3 | 0 | 137860 | 79791 | 123090 | 0 | 393390 | 301850 |
| tr\|V9HW53\|V9HW53_HUMAN;sp\|O958 | 3 | 0 | 132330 | 191690 | 281770 | 0 | 1049700 | 0 |
| tr\|Q6IN90\|Q6IN90_HUMAN;tr\|E5RJV1\| | 3 | 1 | 126810 | 0 | 0 | 0 | 0 | 0 |
| tr\|I3L3Q7\|I3L3Q7_HUMAN;tr\|I3L3B0\|I3 | 3 | 0.00037 | 124190 | 1093700 | 0 | 0 | 0 | 0 |
| tr\|G8JLI5\|G8JLI5_HUMAN;tr\|A0A024QY | 3 | 0 | 116790 | 0 | 138700 | 0 | 545910 | 0 |
| sp\|Q9H7E9\|CH033_HUMAN;sp\|Q9H7E9 | 3 | 0 | 115310 | 123540 | 375430 | 78725 | 668040 | 146100 |
| sp\|Q96H20-2\|SNF8_HUMAN;sp\|Q96H2 | 3 | 0 | 112560 | 539260 | 1342630 | 432560 | 7114100 | 677500 |
| tr\|D3DWK4\|D3DWK4_HUMAN;tr\|B4DG | 3 | 0 | 110360 | 0 | 247520 | 0 | 587770 | 0 |
| tr\|Q549M9\|Q549M9_HUMAN;sp\|P5637 | 3 | 0 | 107900 | 152270 | 813560 | 143270 | 8690600 | 171880 |
| tr\|A0A024R1T1\|A0A024R1T1_HUMAN;s | 3 | 0 | 104610 | 0 | 382510 | 0 | 4111200 | 0 |
| sp\|P60983\|GMFB_HUMAN;tr\|G3V4P8\| | 3 | 0 | 98777 | 155890 | 0 | 0 | 8746900 | 0 |
| sp\|Q9ULL5-3\|PRR12_HUMAN;sp\|Q9ULI | 3 | 0.00037 | 94693 | 0 | 0 | 0 | 908860 | 0 |
| tr\|Q49AG2\|Q49AG2_HUMAN;tr\|B4DDR | 3 | 0 | 91011 | 0 | 145460 | 0 | 3270500 | 186410 |
| tr\|V9HW91\|V9HW91_HUMAN;sp\|Q9N( | 3 | 0 | 90003 | 152550 | 198970 | 125720 | 0 | 430130 |
| tr\|A8K7A1\|A8K7A1_HUMAN;sp\|Q9Y6V | 3 | 0.0007 | 84111 | 0 | 692770 | 0 | 2224100 | 0 |
| tr\|B4DHX2\|B4DHX2_HUMAN;tr\|A0A02 | 3 | 0 | 79610 | 0 | 47899 | 0 | 1371700 | 0 |
| sp\|Q9Y3Y2-4\|CHTOP_HUMAN;tr\|X6R7( | 3 | 0 | 51565 | 0 | 150170 | 0 | 9797500 | 53213 |
| tr\|E7EQ72\|E7EQ72_HUMAN;tr\|B4DP27 | 3 | 0 | 47365 | 0 | 92038 | 78019 | 2735800 | 0 |
| tr\|A8K724\|A8K724_HUMAN;tr\|A0A024 | 3 | 0 | 43945 | 0 | 401430 | 0 | 1736200 | 0 |
| sp\|Q0VF96\|CGNL1_HUMAN;tr\|Q6P5Q2 | 3 | 0.000355 | 24815 | 379782 | 2328519 | 256087 | 148039 | 1460671 |
| sp\|A6NKF9\|GPHRC_HUMAN;sp\|B7ZAQ | 3 | 0.000365 | 0 | 0 | 0 | 0 | 0 | 0 |
| sp\|O60293-2\|ZC3H1_HUMAN;sp\|O6029 | 3 | 0 | 0 | 0 | 0 | 0 | 1495200 | 0 |
| sp\|O60645-2\|EXOC3_HUMAN;tr\|Q69YP | 3 | 0 | 0 | 0 | 588860 | 0 | 1397000 | 0 |
| sp\|O76041\|NEBL_HUMAN;tr\|F6TRT2\|F | 3 | 0.003316 | 0 | 0 | 0 | 0 | 139270 | 0 |
| sp\|O76075-2\|DFFB_HUMAN;tr\|A0A024 | 3 | 0 | 0 | 0 | 0 | 0 | 1935800 | 0 |
| sp\|O95425-2\|SVIL_HUMAN;sp\|O95425- | 3 | 0 | 0 | 0 | 0 | 0 | 445870 | 0 |
| sp\|P04818-2\|TYSY_HUMAN;tr\|Q53Y97\| | 3 | 0 | 0 | 0 | 0 | 0 | 0 | 0 |
| sp\|P07305\|H10_HUMAN;sp\|P07305-2\| | 3 | 0 | 0 | 0 | 0 | 0 | 1795600 | 0 |
| sp\|P07954-2\|FUMH_HUMAN;sp\|P0795 | 3 | 0 | 0 | 0 | 0 | 0 | 0 | 0 |
| sp\|P25325\|THTM_HUMAN;sp\|P25325-2 | 3 | 0 | 0 | 0 | 0 | 0 | 2806800 | 0 |
| sp\|P41214\|EIF2D_HUMAN;tr\|Q5SY38\|C | 3 | 0 | 0 | 0 | 0 | 0 | 3242700 | 0 |
| sp\|P46013-2\|KI67_HUMAN;tr\|A0A087V | 3 | 0.000703 | 0 | 0 | 0 | 0 | 1190300 | 0 |
| sp\|P46109\|CRKL_HUMAN | 3 | 0 | 0 | 0 | 0 | 0 | 0 | 0 |
| sp\|P46734-2\|MP2K3_HUMAN;tr\|C7DUV | 3 | 0 | 0 | 0 | 0 | 0 | 965070 | 0 |
| sp\|P48729\|KC1A_HUMAN;tr\|V9HW00\| | 3 | 0 | 0 | 0 | 0 | 0 | 532810 | 0 |
| sp\|P53680-2\|AP2S1_HUMAN;sp\|P5368 | 3 | 0.000697 | 0 | 0 | 654940 | 0 | 3171500 | 0 |
| sp\|P54198-2\|HIRA_HUMAN;sp\|P54198 | 3 | 0 | 0 | 0 | 0 | 0 | 1260300 | 0 |
| sp\|P55145\|MANF_HUMAN;tr\|A8K878\| | 3 | 0 | 0 | 0 | 0 | 0 | 0 | 0 |
| sp\|P55210-4\|CASP7_HUMAN;sp\|P5521 | 3 | 0.000361 | 0 | 0 | 280180 | 0 | 2418500 | 0 |
| sp\|P62487\|RPB7_HUMAN;tr\|E9PIU7\|E9 | 3 | 0 | 0 | 0 | 170810 | 0 | 988430 | 0 |
| sp\|P78524\|ST5_HUMAN;tr\|E9PPL2\|E9P | 3 | 0.000368 | 0 | 0 | 0 | 0 | 0 | 0 |
| sp\|Q05682-5\|CALD1_HUMAN;tr\|E9PGZ | 3 | 0 | 0 | 0 | 0 | 0 | 0 | 0 |
| sp\|Q13445\|TMED1_HUMAN;tr\|K7EIN4\| | 3 | 0.00037 | 0 | 0 | 0 | 0 | 1164600 | 0 |
| sp\|Q15139\|KPCD1_HUMAN;tr\|Q1KKQ2 | 3 | 0 | 0 | 0 | 282660 | 0 | 475420 | 0 |
| sp\|Q5C9Z4\|NOM1_HUMAN | 3 | 0 | 0 | 0 | 0 | 0 | 1468000 | 0 |
| sp\|Q5JSL3\|DOC11_HUMAN;tr\|A6NIW2 | 3 | 0 | 0 | 0 | 0 | 0 | 1744300 | 0 |
| sp\|Q5JTH9-2\|RRP12_HUMAN;sp\|Q5JTH | 3 | 0 | 0 | 0 | 0 | 0 | 971180 | 0 |
| sp\|Q6IA86-4\|ELP2_HUMAN;sp\|Q6IA86- | 3 | 0.000702 | 0 | 0 | 0 | 0 | 0 | 0 |
| sp\|Q6P2H3-2\|CEP85_HUMAN;sp\|Q6P2 | 3 | 0 | 0 | 0 | 0 | 0 | 2672400 | 0 |
| sp\|Q86U38-2\|NOP9_HUMAN;tr\|Q5HYL | 3 | 0 | 0 | 0 | 0 | 0 | 1086600 | 0 |
| sp\|Q86VS8\|HOOK3_HUMAN;tr\|H0YE69 | 3 | 0 | 0 | 0 | 0 | 0 | 1070200 | 0 |
| sp\|Q8ND24-2\|RN214_HUMAN;tr\|A0A0 | 3 | 0 | 0 | 0 | 337400 | 0 | 2781600 | 0 |
| sp\|Q8WXE0-2\|CSKI2_HUMAN;sp\|Q8W2 | 3 | 0 | 0 | 0 | 0 | 0 | 2164800 | 0 |
| sp\|Q93100-4\|KPBB_HUMAN;sp\|Q9310( | 3 | 0 | 0 | 0 | 0 | 0 | 2762800 | 0 |
| sp\|Q96BD5-2\|PF21A_HUMAN;sp\|Q96B | 3 | 0 | 0 | 0 | 1726500 | 0 | 2651900 | 0 |
| sp\|Q96GX9\|MTNB_HUMAN;tr\|B4DY17\| | 3 | 0 | 0 | 0 | 0 | 0 | 29719 | 0 |
| sp\|Q96KQ7-2\|EHMT2_HUMAN;tr\|A0A0 | 3 | 0.000372 | 0 | 0 | 0 | 0 | 669490 | 0 |
| sp\|Q9BXS6-7\|NUSAP_HUMAN;sp\|Q9B) | 3 | 0 | 0 | 0 | 0 | 0 | 1303500 | 0 |
| sp\|Q9BYG3\|MK67I_HUMAN;tr\|B4DSM4 | 3 | 0 | 0 | 0 | 0 | 0 | 622420 | 0 |
| sp\|Q9H0A8-2\|COMD4_HUMAN;tr\|H3B( | 3 | 0.001375 | 0 | 0 | 0 | 0 | 1051600 | 0 |
| sp\|Q9H0L4\|CSTFT_HUMAN | 3 | 0.005392 | 0 | 0 | 0 | 0 | 1558700 | 0 |
| sp\|Q9H840\|GEMI7_HUMAN | 3 | 0 | 0 | 0 | 0 | 0 | 4362300 | 0 |
| sp\|Q9HBM1\|SPC25_HUMAN;tr\|C9JW9 | 3 | 0 | 0 | 0 | 50755 | 0 | 1023200 | 0 |
| sp\|Q9NRY4\|RHG35_HUMAN;tr\|A2RRE5 | 3 | 0 | 0 | 0 | 0 | 0 | 1746700 | 0 |
| sp\|Q9NUD5\|ZCHC3_HUMAN;sp\|Q9NU( | 3 | 0 | 0 | 0 | 0 | 0 | 2065300 | 0 |
| sp\|Q9NW08-2\|RPC2_HUMAN;tr\|Q7Z3F | 3 | 0 | 0 | 0 | 0 | 0 | 1885900 | 0 |
| sp\|Q9NW64-2\|RBM22_HUMAN;sp\|Q9N | 3 | 0 | 0 | 0 | 0 | 0 | 3233200 | 0 |
| sp\|Q9P031\|TAP26_HUMAN;tr\|F8VNY5\| | 3 | 0 | 0 | 0 | 0 | 0 | 938050 | 0 |
| sp\|Q9UBS4\|DJB11_HUMAN;tr\|B3KW63 | 3 | 0 | 0 | 0 | 477820 | 0 | 0 | 0 |
| sp\|Q9UEG4\|ZN629_HUMAN;sp\|Q8N8L2 | 3 | 0 | 0 | 0 | 0 | 0 | 1186680 | 0 |

| | | | | | | | | |
|---|---|---|---|---|---|---|---|---|
| sp\|Q9UNP9-2\|PPIE_HUMAN;tr\|A8KAM | 3 | 0 | 0 | 0 | 168440 | 0 | 2036200 | 0 |
| sp\|Q9Y2L5-2\|TPPC8_HUMAN;tr\|J3QQJ5 | 3 | 0 | 0 | 0 | 0 | 0 | 746490 | 0 |
| sp\|Q9Y3P9\|RBGP1_HUMAN;sp\|Q9Y3P9 | 3 | 0 | 0 | 0 | 317510 | 0 | 2278500 | 0 |
| sp\|Q9Y608-2\|LRRF2_HUMAN;sp\|Q9Y60 | 3 | 0 | 0 | 0 | 0 | 0 | 1129400 | 0 |
| tr\|A0A024QYR8\|A0A024QYR8_HUMAN; | 3 | 0 | 0 | 0 | 617320 | 0 | 0 | 0 |
| tr\|A0A024QZE9\|A0A024QZE9_HUMAN; | 3 | 0 | 0 | 0 | 0 | 0 | 2629900 | 0 |
| tr\|A0A024R0V9\|A0A024R0V9_HUMAN; | 3 | 0.000362 | 0 | 0 | 180600 | 0 | 1155800 | 0 |
| tr\|A0A024R1U2\|A0A024R1U2_HUMAN; | 3 | 0 | 0 | 0 | 0 | 0 | 1885300 | 0 |
| tr\|A0A024R4M8\|A0A024R4M8_HUMAN | 3 | 0 | 0 | 0 | 34921 | 0 | 1456100 | 0 |
| tr\|A0A024R8K8\|A0A024R8K8_HUMAN;s | 3 | 0 | 0 | 0 | 0 | 0 | 1982300 | 0 |
| tr\|A0A024R9K4\|A0A024R9K4_HUMAN;s | 3 | 0 | 0 | 0 | 0 | 0 | 3041100 | 0 |
| tr\|A0A024R9R3\|A0A024R9R3_HUMAN;s | 3 | 0 | 0 | 0 | 0 | 0 | 1452600 | 0 |
| tr\|A0A024RD28\|A0A024RD28_HUMAN; | 3 | 0 | 0 | 0 | 0 | 0 | 1731800 | 0 |
| tr\|A0A024RE27\|A0A024RE27_HUMAN;s | 3 | 0 | 0 | 0 | 0 | 0 | 4638100 | 0 |
| tr\|A0A0A0MR02\|A0A0A0MR02_HUMAN | 3 | 0.000353 | 0 | 0 | 201560 | 0 | 0 | 0 |
| tr\|A0PJK4\|A0PJK4_HUMAN;tr\|B3KTT0\| | 3 | 0 | 0 | 0 | 0 | 0 | 5040440 | 0 |
| tr\|A4UCU2\|A4UCU2_HUMAN | 3 | 0 | 0 | 0 | 905250 | 0 | 1151200 | 0 |
| tr\|A8K2F9\|A8K2F9_HUMAN;sp\|Q9BWH | 3 | 0.000357 | 0 | 0 | 294350 | 0 | 860880 | 0 |
| tr\|A8K330\|A8K330_HUMAN;sp\|Q8IWA | 3 | 0 | 0 | 0 | 387731 | 0 | 0 | 0 |
| tr\|A8K4A1\|A8K4A1_HUMAN;sp\|Q96HV | 3 | 0 | 0 | 0 | 228390 | 0 | 1548500 | 0 |
| tr\|B1AJQ6\|B1AJQ6_HUMAN;tr\|Q6LEU0 | 3 | 0.005208 | 0 | 0 | 985850 | 0 | 0 | 0 |
| tr\|B2R6H6\|B2R6H6_HUMAN;sp\|Q9HBM | 3 | 0 | 0 | 0 | 0 | 0 | 2243300 | 0 |
| tr\|B3KM65\|B3KM65_HUMAN;tr\|Q59H2 | 3 | 0 | 0 | 0 | 1467890 | 0 | 907300 | 0 |
| tr\|B4DH39\|B4DH39_HUMAN;tr\|Q8TAF6 | 3 | 0.000356 | 0 | 0 | 1534100 | 0 | 945690 | 0 |
| tr\|B4DSN8\|B4DSN8_HUMAN | 3 | 0 | 0 | 0 | 0 | 0 | 738510 | 0 |
| tr\|B4DUJ0\|B4DUJ0_HUMAN;tr\|Q5QPM | 3 | 0 | 0 | 0 | 0 | 0 | 1481200 | 0 |
| tr\|B4DX46\|B4DX46_HUMAN;sp\|Q6GMV | 3 | 0 | 0 | 0 | 677410 | 0 | 4156000 | 0 |
| tr\|B4DZF6\|B4DZF6_HUMAN;tr\|Q59F94\| | 3 | 0.003327 | 0 | 0 | 0 | 0 | 756470 | 0 |
| tr\|B5BUF9\|B5BUF9_HUMAN;tr\|B5BU32 | 3 | 0 | 0 | 0 | 155540 | 0 | 3077400 | 0 |
| tr\|B5BUK7\|B5BUK7_HUMAN;tr\|B2RCZ4 | 3 | 0 | 0 | 0 | 0 | 0 | 1565490 | 0 |
| tr\|B7SBB1\|B7SBB1_HUMAN;tr\|G9I2H4\| | 3 | 0 | 0 | 0 | 514690 | 0 | 586150 | 0 |
| tr\|B9A6K1\|B9A6K1_HUMAN;tr\|A0A024 | 3 | 0 | 0 | 0 | 0 | 0 | 3022490 | 0 |
| tr\|C9JJ54\|C9JJ54_HUMAN;tr\|Q9H8N9\| | 3 | 0 | 0 | 0 | 671290 | 0 | 1504000 | 0 |
| tr\|C9JXC3\|C9JXC3_HUMAN;tr\|C9JNE2\| | 3 | 0 | 0 | 0 | 0 | 0 | 1252600 | 0 |
| tr\|E5RIS3\|E5RIS3_HUMAN;sp\|Q8TCF1-4 | 3 | 0.005405 | 0 | 0 | 0 | 0 | 1019900 | 0 |
| tr\|E7EW84\|E7EW84_HUMAN;tr\|B4DEZ1 | 3 | 0 | 0 | 0 | 0 | 0 | 1635500 | 0 |
| tr\|F5H442\|F5H442_HUMAN;sp\|Q99816 | 3 | 0.000371 | 0 | 0 | 659600 | 0 | 2004900 | 0 |
| tr\|H0YI09\|H0YI09_HUMAN;tr\|A0A024R | 3 | 0 | 0 | 0 | 188560 | 0 | 0 | 0 |
| tr\|I6L969\|I6L969_HUMAN;sp\|Q8TES7-5 | 3 | 0.000364 | 0 | 0 | 487400 | 0 | 106300 | 0 |
| tr\|J3KS22\|J3KS22_HUMAN;tr\|J3QS36\|J | 3 | 0 | 0 | 0 | 0 | 0 | 429020 | 0 |
| tr\|Q5U5Z3\|Q5U5Z3_HUMAN;sp\|Q9UL4 | 3 | 0.000359 | 0 | 0 | 812340 | 0 | 4110890 | 0 |
| tr\|Q643R0\|Q643R0_HUMAN;sp\|Q9ULW | 3 | 0.000692 | 0 | 0 | 150520 | 0 | 0 | 0 |
| tr\|Q69YG1\|Q69YG1_HUMAN;sp\|P58546 | 3 | 0 | 0 | 0 | 0 | 0 | 0 | 0 |
| tr\|Q6FG85\|Q6FG85_HUMAN;tr\|Q53F41 | 3 | 0.005998 | 0 | 0 | 0 | 0 | 0 | 0 |
| tr\|Q6IBK3\|Q6IBK3_HUMAN;tr\|A8K769\| | 3 | 0 | 0 | 0 | 193090 | 0 | 214500 | 0 |
| tr\|Q6ICQ8\|Q6ICQ8_HUMAN;sp\|P84095 | 3 | 0 | 0 | 0 | 0 | 0 | 1476000 | 0 |
| tr\|Q8N523\|Q8N523_HUMAN;tr\|A0A024 | 3 | 0 | 0 | 0 | 342100 | 0 | 3808400 | 0 |
| sp\|Q9NY12-2\|GAR1_HUMAN;tr\|A0A024 | 3 | 0 | 0 | 0 | 0 | 0 | 5238700 | 149960 |
| tr\|H7C5L6\|H7C5L6_HUMAN;tr\|A0A024R | 3 | 0.0052 | 0 | 0 | 0 | 0 | 2551800 | 74204 |
| sp\|O75494-5\|SRS10_HUMAN;tr\|Q5JRI1 | 3 | 0 | 0 | 0 | 255340 | 0 | 5252240 | 166630 |
| tr\|Q7Z6U0\|Q7Z6U0_HUMAN;tr\|Q7Z6U1 | 3 | 0 | 0 | 0 | 143690 | 0 | 1765400 | 75554 |
| tr\|K7ENX8\|K7ENX8_HUMAN;tr\|K7ELV6 | 3 | 0 | 0 | 0 | 241030 | 0 | 4868400 | 238280 |
| tr\|Q5SYZ4\|Q5SYZ4_HUMAN;sp\|P29373 | 3 | 0 | 0 | 0 | 0 | 0 | 3224000 | 171690 |
| tr\|B8ZZS4\|B8ZZS4_HUMAN;tr\|A0A024R | 3 | 0 | 0 | 0 | 0 | 0 | 2222400 | 129830 |
| sp\|Q9UQ88-5\|CD11A_HUMAN;sp\|Q9U | 3 | 0 | 0 | 0 | 0 | 0 | 1842900 | 122610 |
| tr\|B2R7W3\|B2R7W3_HUMAN;sp\|O759 | 3 | 0 | 0 | 0 | 416080 | 0 | 3658500 | 249670 |
| tr\|Q9NUF9\|Q9NUF9_HUMAN;sp\|Q132 | 3 | 0 | 0 | 0 | 234170 | 0 | 1499100 | 184310 |
| sp\|Q16890-4\|TPD53_HUMAN;sp\|Q168 | 3 | 0 | 0 | 0 | 0 | 0 | 848230 | 107520 |
| tr\|A8K646\|A8K646_HUMAN;sp\|Q92882 | 3 | 0 | 0 | 0 | 0 | 0 | 7557770 | 980170 |
| tr\|Q5QPP3\|Q5QPP3_HUMAN;tr\|Q5QPI | 3 | 0 | 0 | 0 | 835310 | 0 | 1539300 | 320590 |
| tr\|A9CQZ4\|A9CQZ4_HUMAN | 3 | 0.006606 | 0 | 0 | 0 | 0 | 1865200 | 397772 |
| sp\|Q96T60-2\|PNKP_HUMAN;sp\|Q96T6 | 3 | 0 | 0 | 0 | 235110 | 0 | 394890 | 98399 |
| sp\|Q9BTE6\|AASD1_HUMAN;tr\|C9J5N1 | 3 | 0.000362 | 0 | 0 | 0 | 0 | 2387700 | 603370 |
| sp\|O15530-4\|PDPK1_HUMAN;tr\|E9PER | 3 | 0.004274 | 0 | 0 | 142420 | 0 | 682720 | 205960 |
| sp\|Q9BYB4\|GNB1L_HUMAN;sp\|Q9BYB4 | 3 | 0.000356 | 0 | 0 | 0 | 0 | 1051600 | 341330 |
| sp\|Q9NP97\|DLRB1_HUMAN;tr\|B4DFR2 | 3 | 0 | 0 | 0 | 252760 | 0 | 4413900 | 1488300 |
| sp\|Q9Y333\|LSM2_HUMAN | 3 | 0 | 0 | 0 | 0 | 0 | 3254500 | 2228700 |
| tr\|E9PNC7\|E9PNC7_HUMAN;sp\|Q1491 | 3 | 0 | 0 | 0 | 0 | 0 | 424660 | 858050 |
| sp\|A6ZKI3\|F127A_HUMAN;sp\|Q9BWD3 | 3 | 0.000364 | 0 | 0 | 176610 | 0 | 0 | 353660 |
| tr\|Q8WVC2\|Q8WVC2_HUMAN;tr\|Q6FG | 3 | 0 | 0 | 0 | 146650 | 0 | 0 | 3184100 |
| sp\|O14757-2\|CHK1_HUMAN;tr\|J3KN87 | 3 | 0 | 0 | 32129 | 632380 | 0 | 428380 | 0 |
| sp\|O60921-2\|HUS1_HUMAN;tr\|A4D2F2 | 3 | 0 | 0 | 65703 | 159510 | 0 | 1784700 | 0 |
| sp\|Q7Z6E9-2\|RBBP6_HUMAN;sp\|Q7Z6I | 3 | 0 | 0 | 264387 | 388130 | 0 | 3007000 | 0 |
| sp\|Q9Y4Z0\|LSM4_HUMAN;tr\|V9GZ56\|V | 3 | 0 | 0 | 151430 | 593493 | 0 | 4067400 | 0 |
| tr\|A0A024R688\|A0A024R688_HUMAN;s | 3 | 0 | 0 | 1375000 | 2741700 | 0 | 5553800 | 0 |

| | | | | | | | | |
|---|---|---|---|---|---|---|---|---|
| tr\|B7Z7C0\|B7Z7C0_HUMAN;sp\|Q16537 | 3 | 0 | 0 | 138000 | 0 | 0 | 525460 | 0 |
| tr\|C9JUT4\|C9JUT4_HUMAN;tr\|B7ZLW0\| | 3 | 0 | 0 | 83534 | 0 | 0 | 2893100 | 0 |
| sp\|Q96AT9-2\|RPE_HUMAN;sp\|Q96AT9 | 3 | 0 | 0 | 602950 | 0 | 0 | 15506000 | 304380 |
| sp\|Q9BXK1\|KLF16_HUMAN;tr\|D6W5Z8 | 3 | 0 | 0 | 93849 | 112570 | 0 | 1830600 | 67313 |
| sp\|Q8NCW5-2\|NNRE_HUMAN;sp\|Q8N | 3 | 0 | 0 | 167830 | 317600 | 0 | 2257500 | 747520 |
| sp\|Q8IUR0\|TPPC5_HUMAN;tr\|M0QZQ8 | 3 | 0.000703 | 0 | 0 | 1565400 | 112390 | 0 | 0 |
| sp\|Q9H8Y8-2\|GORS2_HUMAN;tr\|B4DEI | 3 | 0 | 0 | 0 | 1397400 | 149070 | 1107300 | 373360 |
| tr\|B9EGR5\|B9EGR5_HUMAN;sp\|Q8IWI9 | 3 | 0 | 0 | 0 | 302890 | 58108 | 568130 | 0 |
| sp\|Q9UFW8\|CGBP1_HUMAN;tr\|C9JUJ0 | 3 | 0 | 0 | 0 | 955870 | 186150 | 1190300 | 312450 |
| tr\|B3KQC8\|B3KQC8_HUMAN;tr\|Q4G10 | 3 | 0 | 0 | 0 | 1239210 | 274660 | 0 | 0 |
| sp\|Q9Y3B4\|SF3B6_HUMAN | 3 | 0 | 0 | 0 | 519130 | 137350 | 5394600 | 603690 |
| tr\|F8VP97\|F8VP97_HUMAN;sp\|Q9NZN | 3 | 0 | 0 | 0 | 1692100 | 453070 | 499680 | 878080 |
| tr\|B3KQ71\|B3KQ71_HUMAN;tr\|B4DWL | 3 | 0 | 0 | 228430 | 634610 | 186040 | 1132500 | 0 |
| tr\|B4E0Q6\|B4E0Q6_HUMAN;tr\|B4DKZ7 | 3 | 0 | 0 | 134010 | 413470 | 128080 | 2256700 | 145440 |
| tr\|E7EQL8\|E7EQL8_HUMAN;tr\|A7E2V7\| | 3 | 0 | 0 | 0 | 298360 | 117780 | 2628200 | 0 |
| sp\|Q8TBA6-2\|GOGA5_HUMAN;tr\|A8KA | 3 | 0 | 0 | 0 | 1586800 | 645125 | 925850 | 854320 |
| tr\|Q7Z508\|Q7Z508_HUMAN;tr\|A0A087 | 3 | 0 | 0 | 206280 | 243720 | 163840 | 0 | 218780 |
| sp\|P62273\|RS29_HUMAN;tr\|A0A087W | 3 | 0 | 0 | 0 | 134120 | 113070 | 6022300 | 397920 |
| tr\|Q53GC2\|Q53GC2_HUMAN;tr\|A0A02 | 3 | 0 | 0 | 155120 | 181800 | 158000 | 133330 | 0 |
| tr\|A0A087WYR0\|A0A087WYR0_HUMAN | 3 | 0 | 0 | 0 | 0 | 49668 | 2548500 | 89493 |
| sp\|Q15843\|NEDD8_HUMAN;tr\|F8VSA6 | 3 | 0 | 0 | 0 | 0 | 318930 | 2480340 | 3414600 |
| sp\|Q8IW75\|SPA12_HUMAN | 3 | 0.000693 | 0 | 376196 | 0 | 559972 | 0 | 0 |
| tr\|B3KPA1\|B3KPA1_HUMAN;sp\|O1465 | 3 | 0 | 0 | 629770 | 0 | 253100 | 1316600 | 0 |
| tr\|H3BRS3\|H3BRS3_HUMAN;tr\|B4DXS2 | 3 | 0 | 0 | 70828 | 0 | 125390 | 0 | 0 |
| sp\|P62304\|RUXE_HUMAN;tr\|A6NHK2\| | 3 | 0 | 0 | 674550 | 0 | 473530 | 23667000 | 6852600 |
| sp\|Q5T750\|XP32_HUMAN | 3 | 0.002673 | 0 | 437100 | 0 | 437736 | 864110 | 714270 |
| sp\|P11532-3\|DMD_HUMAN;sp\|P11532 | 2 | 0 | 134101000 | 44785000 | 5656600 | 81339000 | 20305000 | 18501500 |
| tr\|Q6FHL9\|Q6FHL9_HUMAN;tr\|B1AKZ5 | 2 | 0.001378 | 9865900 | 6263350 | 0 | 7759600 | 0 | 8933400 |
| sp\|P80188-2\|NGAL_HUMAN;sp\|P80188 | 2 | 0 | 7523200 | 0 | 0 | 0 | 1152500 | 0 |
| tr\|K7EMV3\|K7EMV3_HUMAN;tr\|K7EP0 | 2 | 0 | 6185830 | 2635313 | 8098370 | 271780 | 20307620 | 2373230 |
| sp\|Q66GS9\|CP135_HUMAN | 2 | 0.000693 | 3312290 | 0 | 0 | 0 | 715290 | 0 |
| sp\|Q9GZZ8\|LACRT_HUMAN;tr\|F8W0V3 | 2 | 0 | 2371500 | 90026 | 765060 | 1469120 | 0 | 300069 |
| tr\|A0A024R326\|A0A024R326_HUMAN;s | 2 | 0 | 2255430 | 988780 | 5313800 | 825810 | 39899620 | 2717740 |
| sp\|O95969\|SG1D2_HUMAN | 2 | 0 | 2080950 | 1120220 | 1131440 | 1485740 | 1558110 | 1921040 |
| sp\|P35813-2\|PPM1A_HUMAN;tr\|B5BU | 2 | 0 | 1933400 | 532350 | 1744900 | 490840 | 2641860 | 810310 |
| sp\|P62877\|RBX1_HUMAN | 2 | 0 | 1686500 | 2103410 | 4663800 | 1233900 | 15210000 | 1926300 |
| sp\|P25815\|S100P_HUMAN | 2 | 0 | 1651983 | 174466 | 198225 | 159767 | 300560 | 168501 |
| tr\|B4DMY4\|B4DMY4_HUMAN;tr\|B4DL4 | 2 | 0.000367 | 1571640 | 0 | 0 | 0 | 0 | 0 |
| sp\|P08047-2\|SP1_HUMAN;sp\|P08047\|S | 2 | 0 | 1536200 | 644960 | 402040 | 697870 | 8418800 | 0 |
| tr\|G3V1B8\|G3V1B8_HUMAN;tr\|H0YEB6 | 2 | 0.000354 | 1516500 | 174390 | 190020 | 0 | 1135000 | 116840 |
| tr\|Q76LA1\|Q76LA1_HUMAN;sp\|P04080 | 2 | 0 | 1472347 | 0 | 161250 | 0 | 1116200 | 3191600 |
| tr\|F5H3C5\|F5H3C5_HUMAN;sp\|P04179 | 2 | 0 | 1371900 | 0 | 0 | 0 | 0 | 0 |
| tr\|B4E2S7\|B4E2S7_HUMAN;sp\|P13473- | 2 | 0 | 1332110 | 471340 | 0 | 348960 | 280040 | 159082 |
| tr\|M0R132\|M0R132_HUMAN;tr\|W8GIV | 2 | 0.000354 | 1313660 | 0 | 0 | 0 | 0 | 0 |
| sp\|P04062-4\|GLCM_HUMAN;tr\|A0A068 | 2 | 0 | 1212000 | 0 | 0 | 0 | 0 | 0 |
| tr\|A8K6H9\|A8K6H9_HUMAN;tr\|A0A024 | 2 | 0 | 1197020 | 229348 | 0 | 334719 | 0 | 0 |
| tr\|K7EIY6\|K7EIY6_HUMAN;tr\|A8K0Q1\| | 2 | 0.000693 | 1172600 | 147910 | 2061690 | 0 | 1354741 | 0 |
| tr\|F5H0V4\|F5H0V4_HUMAN;sp\|Q9HAP | 2 | 0 | 1162200 | 0 | 476490 | 0 | 0 | 0 |
| tr\|C9JYN0\|C9JYN0_HUMAN;sp\|Q16563 | 2 | 0 | 969020 | 0 | 0 | 0 | 217150 | 101390 |
| tr\|Q5T085\|Q5T085_HUMAN;tr\|Q6NSB3 | 2 | 0 | 929010 | 712930 | 0 | 621190 | 0 | 927120 |
| tr\|B2RAR3\|B2RAR3_HUMAN;sp\|Q9BXR | 2 | 0 | 925700 | 0 | 0 | 0 | 1356000 | 939230 |
| sp\|Q16610-2\|ECM1_HUMAN;sp\|Q1661 | 2 | 0 | 896010 | 542800 | 453260 | 620230 | 545730 | 0 |
| tr\|A0A024R4V8\|A0A024R4V8_HUMAN;\| | 2 | 0 | 891470 | 0 | 607620 | 0 | 2918450 | 0 |
| tr\|Q5JVD1\|Q5JVD1_HUMAN;sp\|Q7Z7A | 2 | 0 | 861430 | 0 | 0 | 0 | 0 | 0 |
| tr\|Q6FG99\|Q6FG99_HUMAN | 2 | 0.000372 | 850350 | 516210 | 2255000 | 1151200 | 14686290 | 0 |
| tr\|A0A024R8T9\|A0A024R8T9_HUMAN;s | 2 | 0.000363 | 830290 | 0 | 748220 | 0 | 1720700 | 341150 |
| sp\|Q8NBX0\|SCPDL_HUMAN | 2 | 0.000372 | 805790 | 320590 | 499710 | 0 | 0 | 0 |
| sp\|P35326\|SPR2A_HUMAN;sp\|P35325\| | 2 | 0 | 785150 | 571140 | 872110 | 770496 | 2140140 | 2364390 |
| sp\|Q96A33\|CCD47_HUMAN;tr\|A0A087 | 2 | 0 | 779880 | 0 | 1569800 | 0 | 0 | 0 |
| sp\|Q6GTS8\|P20D1_HUMAN | 2 | 0.002689 | 716540 | 0 | 0 | 0 | 0 | 0 |
| tr\|A0A024R277\|A0A024R277_HUMAN;s | 2 | 0 | 703180 | 0 | 110470 | 0 | 0 | 0 |
| tr\|H0YH81\|H0YH81_HUMAN;tr\|Q0QEN | 2 | 0 | 695680 | 0 | 1676500 | 207960 | 0 | 0 |
| tr\|B3KM89\|B3KM89_HUMAN;tr\|A8K6V | 2 | 0 | 659020 | 0 | 202355 | 0 | 1269700 | 0 |
| tr\|E7EWM1\|E7EWM1_HUMAN;sp\|Q15 | 2 | 0 | 646530 | 142760 | 277640 | 0 | 983910 | 0 |
| tr\|Q5H9S0\|Q5H9S0_HUMAN;tr\|B4DTN | 2 | 0 | 641810 | 0 | 0 | 0 | 769430 | 0 |
| tr\|B4DVB5\|B4DVB5_HUMAN;tr\|A0A02 | 2 | 0 | 631190 | 0 | 1080400 | 235450 | 2912200 | 0 |
| tr\|Q05BV7\|Q05BV7_HUMAN;tr\|B4DYZ | 2 | 0 | 626010 | 0 | 0 | 0 | 528060 | 0 |
| tr\|A0A024R8D7\|A0A024R8D7_HUMAN;\| | 2 | 0 | 621620 | 672940 | 0 | 994520 | 634470 | 1024650 |
| tr\|Q59G54\|Q59G54_HUMAN;sp\|Q9NRL | 2 | 0 | 610190 | 0 | 0 | 0 | 0 | 0 |

| | | | | | | | | |
|---|---|---|---|---|---|---|---|---|
| tr\|G1UCX3\|G1UCX3_HUMAN;sp\|Q96ER | 2 | 0 | 598420 | 0 | 714100 | 0 | 1441100 | 0 |
| tr\|Q5SYF9\|Q5SYF9_HUMAN;sp\|Q7Z4H7 | 2 | 0 | 596470 | 79153 | 489260 | 0 | 750080 | 0 |
| tr\|E5RIF2\|E5RIF2_HUMAN;tr\|Q59FY5\|C | 2 | 0.003624 | 562840 | 0 | 350900 | 0 | 0 | 0 |
| sp\|Q9NS87-2\|KIF15_HUMAN;sp\|Q9NS8 | 2 | 0 | 549740 | 0 | 0 | 0 | 0 | 0 |
| tr\|Q5HY57\|Q5HY57_HUMAN;sp\|P5040 | 2 | 0 | 543900 | 104420 | 634210 | 0 | 555000 | 0 |
| tr\|B4DZG6\|B4DZG6_HUMAN;sp\|Q9BTX | 2 | 0.000359 | 508360 | 0 | 0 | 0 | 0 | 0 |
| tr\|E9PP67\|E9PP67_HUMAN;tr\|E9PQ25\| | 2 | 0.000364 | 471290 | 0 | 0 | 0 | 0 | 0 |
| sp\|Q49A26-5\|GLYR1_HUMAN;sp\|Q49A | 2 | 0 | 471000 | 67537 | 0 | 0 | 393470 | 0 |
| sp\|O75592-2\|MYCB2_HUMAN;sp\|O755 | 2 | 0.004271 | 469270 | 0 | 0 | 0 | 820550 | 0 |
| sp\|P01622\|KV304_HUMAN;tr\|G3GAU4 | 2 | 0 | 464860 | 0 | 125520 | 0 | 878270 | 0 |
| tr\|A4D110\|A4D110_HUMAN | 2 | 0 | 463400 | 1041100 | 20768000 | 7426700 | 0 | 0 |
| tr\|H7C1T3\|H7C1T3_HUMAN;tr\|D3DXB2 | 2 | 0.0027 | 459930 | 0 | 0 | 193180 | 3236000 | 787020 |
| sp\|P41229-4\|KDM5C_HUMAN;tr\|A6N6 | 2 | 0 | 456360 | 0 | 234950 | 0 | 0 | 0 |
| sp\|Q96PY6-4\|NEK1_HUMAN;sp\|Q96PY | 2 | 0.001373 | 452130 | 0 | 159340 | 0 | 253150 | 0 |
| tr\|Q05CT8\|Q05CT8_HUMAN;sp\|Q8NHV | 2 | 0 | 445000 | 146910 | 708250 | 178500 | 2361000 | 272190 |
| tr\|B2RAN2\|B2RAN2_HUMAN;sp\|O9549 | 2 | 0.002999 | 424555 | 0 | 15800 | 0 | 0 | 0 |
| tr\|A8KAK5\|A8KAK5_HUMAN;sp\|O6024 | 2 | 0.005418 | 412550 | 0 | 0 | 0 | 0 | 0 |
| sp\|Q9ULU4-4\|PKCB1_HUMAN;sp\|Q9UL | 2 | 0 | 405010 | 0 | 0 | 0 | 1851800 | 0 |
| tr\|E7ETU5\|E7ETU5_HUMAN;tr\|F6Y5H0\| | 2 | 0 | 397580 | 0 | 0 | 0 | 2317400 | 0 |
| tr\|C9J2I1\|C9J2I1_HUMAN;tr\|G5E9V6\|G | 2 | 0 | 395530 | 0 | 0 | 0 | 1091700 | 0 |
| sp\|P48163-2\|MAOX_HUMAN;tr\|A8K16 | 2 | 0 | 394682 | 0 | 457080 | 153190 | 0 | 120920 |
| tr\|B4DWZ7\|B4DWZ7_HUMAN;tr\|B3KTN | 2 | 0 | 388840 | 204550 | 483860 | 159030 | 1631300 | 247990 |
| sp\|P62861\|RS30_HUMAN;tr\|E9PR30\|E9 | 2 | 0.006805 | 383780 | 0 | 0 | 142690 | 20927000 | 4413690 |
| tr\|Q5T093\|Q5T093_HUMAN;tr\|Q5T092 | 2 | 0 | 375200 | 0 | 246770 | 0 | 1453110 | 0 |
| sp\|O00186\|STXB3_HUMAN | 2 | 0 | 368090 | 112630 | 747770 | 0 | 0 | 0 |
| sp\|O43913-2\|ORC5_HUMAN;tr\|Q9UDM | 2 | 0 | 363290 | 0 | 1379400 | 0 | 1713900 | 0 |
| sp\|Q9H4L7-3\|SMRCD_HUMAN;sp\|Q9H4 | 2 | 0.005397 | 360900 | 0 | 0 | 0 | 0 | 57990 |
| sp\|Q8N1G2\|CMTR1_HUMAN | 2 | 0 | 345800 | 0 | 0 | 0 | 0 | 0 |
| sp\|O43156\|TTI1_HUMAN;tr\|Q3B768\|Q | 2 | 0 | 343450 | 0 | 245980 | 0 | 1450600 | 0 |
| sp\|Q9BRP4-3\|PAAF1_HUMAN;tr\|A0A0 | 2 | 0 | 340320 | 0 | 420230 | 0 | 1077200 | 0 |
| sp\|Q7Z4L5\|TT21B_HUMAN;sp\|Q7Z4L5- | 2 | 0.006604 | 334280 | 0 | 0 | 0 | 3470500 | 0 |
| sp\|Q9UIQ6-3\|LCAP_HUMAN;sp\|Q9UIQ | 2 | 0.002674 | 329960 | 0 | 0 | 0 | 0 | 0 |
| sp\|Q86WB0-3\|NIPA_HUMAN;tr\|C9J0I9 | 2 | 0 | 328450 | 0 | 0 | 145140 | 1048800 | 0 |
| tr\|S5DU05\|S5DU05_HUMAN;tr\|F6IQK6 | 2 | 0 | 313640 | 227650 | 0 | 230690 | 0 | 0 |
| tr\|B4DR88\|B4DR88_HUMAN;sp\|Q8IX18 | 2 | 0 | 313020 | 0 | 464560 | 0 | 1642400 | 0 |
| tr\|A0A024R8B1\|A0A024R8B1_HUMAN;s | 2 | 0.000692 | 307540 | 275970 | 0 | 0 | 0 | 0 |
| sp\|Q96JG6-3\|CC132_HUMAN;tr\|A7MD0 | 2 | 0 | 296090 | 0 | 412700 | 0 | 1748800 | 0 |
| tr\|B7Z4K5\|B7Z4K5_HUMAN;tr\|A8MT72 | 2 | 0.003622 | 292350 | 84084 | 70360 | 0 | 1005900 | 23427 |
| tr\|B4DY59\|B4DY59_HUMAN;tr\|E9PF19\| | 2 | 0 | 285480 | 0 | 554530 | 0 | 0 | 0 |
| sp\|Q9H4L4\|SENP3_HUMAN;tr\|J3QL36\| | 2 | 0 | 282870 | 0 | 417580 | 0 | 1470200 | 0 |
| tr\|Q15203\|Q15203_HUMAN;tr\|Q7KZ52 | 2 | 0 | 274740 | 1257141 | 735750 | 653186 | 0 | 7909100 |
| sp\|P33981-2\|TTK_HUMAN;sp\|P33981\|T | 2 | 0 | 269030 | 0 | 0 | 0 | 1086300 | 0 |
| sp\|Q9H9B1-4\|EHMT1_HUMAN;sp\|Q9H9 | 2 | 0.000358 | 264210 | 0 | 233110 | 0 | 734760 | 0 |
| tr\|A8K335\|A8K335_HUMAN;sp\|Q92820 | 2 | 0.007367 | 224837 | 0 | 0 | 0 | 0 | 49220 |
| tr\|A8K1V4\|A8K1V4_HUMAN;sp\|Q1578 | 2 | 0.000362 | 199750 | 0 | 475980 | 0 | 457370 | 0 |
| sp\|Q6P1Q9\|MET2B_HUMAN;tr\|F8WAS | 2 | 0.00426 | 197710 | 0 | 294990 | 0 | 566600 | 0 |
| tr\|D3DSB5\|D3DSB5_HUMAN;tr\|B2R928 | 2 | 0.002707 | 197650 | 0 | 0 | 0 | 0 | 0 |
| tr\|A0A024QYW3\|A0A024QYW3_HUMAI | 2 | 0 | 196531 | 21552 | 1674800 | 263590 | 728800 | 0 |
| tr\|H0YFD2\|H0YFD2_HUMAN;tr\|F8WFC1 | 2 | 0 | 181350 | 0 | 0 | 0 | 1018300 | 0 |
| sp\|Q14669-4\|TRIPC_HUMAN;sp\|Q1466 | 2 | 0 | 179500 | 0 | 170710 | 0 | 1381500 | 0 |
| tr\|F8VUA7\|F8VUA7_HUMAN;tr\|F8VQX | 2 | 0.009691 | 173860 | 0 | 0 | 0 | 0 | 0 |
| tr\|D3DR32\|D3DR32_HUMAN;sp\|Q96Q8 | 2 | 0.005431 | 173310 | 0 | 142170 | 0 | 0 | 0 |
| tr\|E9PRF4\|E9PRF4_HUMAN;sp\|Q15047 | 2 | 0.003003 | 163630 | 0 | 0 | 0 | 849880 | 0 |
| tr\|Q53HG5\|Q53HG5_HUMAN;tr\|A8K4K | 2 | 0 | 134110 | 0 | 448590 | 0 | 499480 | 0 |
| sp\|Q9BVC4\|LST8_HUMAN;tr\|H3BR38\|H | 2 | 0.002703 | 123290 | 0 | 0 | 0 | 1532700 | 0 |
| tr\|E9PIY1\|E9PIY1_HUMAN;tr\|B4DUI2\|B | 2 | 0.006776 | 118480 | 0 | 0 | 0 | 0 | 0 |
| sp\|Q8IXW5\|RPAP2_HUMAN;sp\|Q8IXW | 2 | 0 | 114830 | 0 | 0 | 0 | 387220 | 0 |
| tr\|D3VVC3\|D3VVC3_HUMAN | 2 | 0.00652 | 112080 | 0 | 0 | 0 | 579040 | 0 |
| tr\|H0Y4F4\|H0Y4F4_HUMAN;tr\|F8W6D9 | 2 | 0.002727 | 109350 | 0 | 0 | 0 | 428640 | 0 |
| sp\|Q9UQN3-2\|CHM2B_HUMAN;tr\|A0A | 2 | 0 | 101880 | 115910 | 460110 | 106620 | 465630 | 0 |
| tr\|A0A024QYT6\|A0A024QYT6_HUMAN; | 2 | 0 | 100890 | 171030 | 320350 | 0 | 2809700 | 242680 |
| sp\|Q15652-2\|JHD2C_HUMAN;tr\|B7ZLC8 | 2 | 0 | 100780 | 0 | 0 | 0 | 765990 | 0 |
| sp\|Q9NP72\|RAB18_HUMAN;tr\|Q59EW3 | 2 | 0.000372 | 91285 | 281790 | 153600 | 0 | 669170 | 0 |
| tr\|A6NGW1\|A6NGW1_HUMAN;tr\|A8K5 | 2 | 0 | 90459 | 0 | 173230 | 0 | 848730 | 0 |
| sp\|Q9H6V9\|CB043_HUMAN;sp\|Q9H6V9 | 2 | 0 | 90361 | 97669 | 161210 | 0 | 655590 | 0 |
| tr\|A0A024QYX0\|A0A024QYX0_HUMAN; | 2 | 0 | 90032 | 0 | 139220 | 0 | 0 | 0 |
| sp\|Q9BT22\|ALG1_HUMAN;tr\|K7EID2\|K | 2 | 0 | 85190 | 0 | 0 | 0 | 0 | 0 |
| tr\|F5H1S8\|F5H1S8_HUMAN;tr\|F5GX14\| | 2 | 0 | 84776 | 0 | 234590 | 0 | 345910 | 0 |
| sp\|Q96HR3-2\|MED30_HUMAN;sp\|Q96H | 2 | 0 | 79812 | 0 | 216630 | 0 | 1624540 | 0 |
| sp\|Q9BXB4\|OSB11_HUMAN;tr\|Q9GZM0 | 2 | 0.006591 | 55082 | 0 | 0 | 0 | 0 | 0 |
| tr\|Q6ZS01\|Q6ZS01_HUMAN;sp\|O60281 | 2 | 1 | 45252 | 0 | 1966100 | 0 | 0 | 0 |
| tr\|C9JDZ2\|C9JDZ2_HUMAN;sp\|Q9NVQ4 | 2 | 0 | 44138 | 0 | 60425 | 0 | 2264870 | 0 |
| sp\|A6NDU8\|CE051_HUMAN | 2 | 0 | 0 | 0 | 0 | 0 | 1831800 | 0 |
| sp\|O14646-2\|CHD1_HUMAN;sp\|O1464 | 2 | 0.001375 | 0 | 0 | 0 | 0 | 1033200 | 0 |
| sp\|O15116\|LSM1_HUMAN | 2 | 0 | 0 | 0 | 0 | 0 | 809990 | 0 |

| | | | | | | | | |
|---|---|---|---|---|---|---|---|---|
| sp\|O43301\|HS12A_HUMAN;tr\|B7Z2M8 | 2 | 0.004255 | 0 | 0 | 0 | 0 | 532710 | 0 |
| sp\|O43414-3\|ERI3_HUMAN;tr\|B4DEX5\| | 2 | 0.0007 | 0 | 0 | 0 | 0 | 2835700 | 0 |
| sp\|O43474-4\|KLF4_HUMAN;sp\|O43474 | 2 | 0 | 0 | 0 | 368820 | 0 | 3207700 | 0 |
| sp\|O75182-2\|SIN3B_HUMAN;sp\|O7518 | 2 | 0 | 0 | 0 | 56249 | 0 | 636800 | 0 |
| sp\|O75191-2\|XYLB_HUMAN;sp\|O75191 | 2 | 0 | 0 | 0 | 286400 | 0 | 137280 | 0 |
| sp\|O95721\|SNP29_HUMAN;tr\|C9JAF7\| | 2 | 0 | 0 | 0 | 282490 | 0 | 485950 | 0 |
| sp\|P05412\|JUN_HUMAN;tr\|Q6FHK0\|Q | 2 | 0 | 0 | 0 | 2355400 | 0 | 4888800 | 0 |
| sp\|P10746\|HEM4_HUMAN;tr\|Q5T3L7\|C | 2 | 0.005202 | 0 | 0 | 0 | 0 | 1906000 | 0 |
| sp\|P21359-2\|NF1_HUMAN;sp\|P21359-( | 2 | 0.000365 | 0 | 0 | 0 | 0 | 926430 | 0 |
| sp\|P55201-4\|BRPF1_HUMAN;sp\|P5520 | 2 | 0.00517 | 0 | 0 | 0 | 0 | 1050200 | 0 |
| sp\|P58004\|SESN2_HUMAN | 2 | 0.000361 | 0 | 0 | 341590 | 0 | 1420500 | 0 |
| sp\|Q02040-2\|AK17A_HUMAN;sp\|Q020 | 2 | 0 | 0 | 0 | 0 | 0 | 1544900 | 0 |
| sp\|Q12974-3\|TP4A2_HUMAN;sp\|Q1297 | 2 | 0 | 0 | 0 | 538260 | 0 | 1319159 | 0 |
| sp\|Q13427-2\|PPIG_HUMAN;tr\|Q6GMS9 | 2 | 0 | 0 | 0 | 0 | 0 | 259820 | 0 |
| sp\|Q15475\|SIX1_HUMAN;sp\|Q9NPC8\|S | 2 | 0 | 0 | 0 | 0 | 0 | 1195300 | 0 |
| sp\|Q1ED39\|KNOP1_HUMAN;tr\|H3BNU | 2 | 0 | 0 | 0 | 0 | 0 | 2825200 | 0 |
| sp\|Q3B726\|RPA43_HUMAN | 2 | 0.003629 | 0 | 0 | 0 | 0 | 1246300 | 0 |
| sp\|Q3KQU3-2\|MA7D1_HUMAN;sp\|Q3K | 2 | 0.005444 | 0 | 0 | 0 | 0 | 752780 | 0 |
| sp\|Q5JTV8-3\|TOIP1_HUMAN;tr\|J3KN66 | 2 | 0 | 0 | 0 | 697480 | 0 | 0 | 0 |
| sp\|Q5T0B9\|ZN362_HUMAN;tr\|F5H055\| | 2 | 0.002736 | 0 | 0 | 0 | 0 | 82820 | 0 |
| sp\|Q5THR3-5\|EFCB6_HUMAN;sp\|Q5TH | 2 | 0.005387 | 0 | 0 | 3601140 | 0 | 0 | 0 |
| sp\|Q6IBW4-2\|CNDH2_HUMAN;sp\|Q6IB | 2 | 0 | 0 | 0 | 493810 | 0 | 0 | 0 |
| sp\|Q6P582\|MZT2A_HUMAN;sp\|Q6NZ6 | 2 | 0.000366 | 0 | 0 | 0 | 0 | 1541000 | 0 |
| sp\|Q6PK04\|CC137_HUMAN;tr\|I3L0U5\|I | 2 | 0 | 0 | 0 | 0 | 0 | 686810 | 0 |
| sp\|Q6SPF0\|SAMD1_HUMAN;tr\|E9PIW9 | 2 | 0.002706 | 0 | 0 | 0 | 0 | 230010 | 0 |
| sp\|Q71F23-2\|CENPU_HUMAN;tr\|Q09GI | 2 | 0.00736 | 0 | 0 | 0 | 0 | 130910 | 0 |
| sp\|Q7Z4Q2\|HEAT3_HUMAN;sp\|Q7Z4Q2 | 2 | 0.000368 | 0 | 0 | 0 | 0 | 2600600 | 0 |
| sp\|Q8IWV7\|UBR1_HUMAN;sp\|Q8IWV7 | 2 | 0.009949 | 0 | 0 | 0 | 0 | 567590 | 0 |
| sp\|Q8N6M0\|OTU6B_HUMAN;tr\|A0A08 | 2 | 0 | 0 | 0 | 0 | 0 | 1556200 | 0 |
| sp\|Q8N954\|GPT11_HUMAN;tr\|A0A0A0 | 2 | 0.003627 | 0 | 0 | 0 | 0 | 700950 | 0 |
| sp\|Q8NAV1\|PR38A_HUMAN;tr\|B2RDP2 | 2 | 0 | 0 | 0 | 574460 | 0 | 2460400 | 0 |
| sp\|Q8NEY1-7\|NAV1_HUMAN;sp\|Q8NE | 2 | 0.001374 | 0 | 0 | 0 | 0 | 848700 | 0 |
| sp\|Q8TEU7-5\|RPGF6_HUMAN;sp\|Q8TE | 2 | 0.000353 | 0 | 0 | 0 | 0 | 601850 | 0 |
| sp\|Q8WW12-2\|PCNP_HUMAN;sp\|Q8W | 2 | 0 | 0 | 0 | 0 | 0 | 395930 | 0 |
| sp\|Q92520\|FAM3C_HUMAN;tr\|C9JP35\| | 2 | 0.000364 | 0 | 0 | 146755 | 0 | 884340 | 0 |
| sp\|Q92558\|WASF1_HUMAN;tr\|Q5SZK4 | 2 | 0.009685 | 0 | 0 | 475330 | 0 | 1247630 | 0 |
| sp\|Q96MG7\|MAGG1_HUMAN | 2 | 0 | 0 | 0 | 0 | 0 | 270990 | 0 |
| sp\|Q96MU7-2\|YTDC1_HUMAN;sp\|Q96M | 2 | 0.003623 | 0 | 0 | 0 | 0 | 2254840 | 0 |
| sp\|Q96MW1\|CCD43_HUMAN;tr\|Q86W | 2 | 0.006309 | 0 | 0 | 0 | 0 | 598930 | 0 |
| sp\|Q96P11-5\|NSUN5_HUMAN;sp\|Q96P | 2 | 0 | 0 | 0 | 0 | 0 | 1734800 | 0 |
| sp\|Q96PV6\|LENG8_HUMAN;tr\|A0A087 | 2 | 0.00425 | 0 | 0 | 0 | 0 | 1265900 | 0 |
| sp\|Q99747-2\|SNAG_HUMAN;tr\|Q6FHY4 | 2 | 0.000704 | 0 | 0 | 0 | 0 | 1996100 | 0 |
| sp\|Q9BU89\|DOHH_HUMAN;tr\|K7ERU8 | 2 | 0 | 0 | 0 | 0 | 0 | 1423100 | 0 |
| sp\|Q9GZR2\|REXO4_HUMAN;tr\|B4E331\| | 2 | 0.005445 | 0 | 0 | 0 | 0 | 1349100 | 0 |
| sp\|Q9GZS1-2\|RPA49_HUMAN;sp\|Q9GZ | 2 | 0.000368 | 0 | 0 | 0 | 0 | 3965400 | 0 |
| sp\|Q9GZT4\|SRR_HUMAN;tr\|Q3ZK31\|Q | 2 | 0 | 0 | 0 | 0 | 0 | 1287400 | 0 |
| sp\|Q9H7S9\|ZN703_HUMAN;tr\|A0A0A0 | 2 | 0.000359 | 0 | 0 | 656670 | 0 | 307700 | 0 |
| sp\|Q9H832-2\|UBE2Z_HUMAN;tr\|B4DL6 | 2 | 0.000356 | 0 | 0 | 264770 | 0 | 2952500 | 0 |
| sp\|Q9HCE5\|MET14_HUMAN;tr\|B4DJF7 | 2 | 0 | 0 | 0 | 0 | 0 | 2280100 | 0 |
| sp\|Q9HD40\|SPCS_HUMAN;sp\|Q9HD40- | 2 | 0.003636 | 0 | 0 | 51008 | 0 | 0 | 0 |
| sp\|Q9NQE9\|HINT3_HUMAN | 2 | 0.002731 | 0 | 0 | 0 | 0 | 287930 | 0 |
| sp\|Q9NRH1\|YAED1_HUMAN;tr\|C9IZ57\| | 2 | 0 | 0 | 0 | 0 | 0 | 1294300 | 0 |
| sp\|Q9NV56\|MRGBP_HUMAN | 2 | 0 | 0 | 0 | 111330 | 0 | 1298200 | 0 |
| sp\|Q9NW82\|WDR70_HUMAN;tr\|D6RIW | 2 | 0 | 0 | 0 | 1021300 | 0 | 3012300 | 0 |
| sp\|Q9NYJ8-2\|TAB2_HUMAN;tr\|B4DIR9 | 2 | 0 | 0 | 0 | 335590 | 0 | 430070 | 0 |
| sp\|Q9NZQ3-3\|SPN90_HUMAN;sp\|Q9N | 2 | 0.002717 | 0 | 0 | 1067200 | 0 | 0 | 0 |
| sp\|Q9P2D3-3\|HTR5B_HUMAN;tr\|B9EK4 | 2 | 0 | 0 | 0 | 0 | 0 | 1037400 | 0 |
| sp\|Q9UHD2\|TBK1_HUMAN;tr\|B4E164\|B | 2 | 0.005395 | 0 | 0 | 0 | 0 | 595870 | 0 |
| sp\|Q9UIV1-2\|CNOT7_HUMAN;tr\|Q96IC | 2 | 0 | 0 | 0 | 258070 | 0 | 3445900 | 0 |
| sp\|Q9UK99-3\|FBX3_HUMAN;sp\|Q9UK9 | 2 | 0 | 0 | 0 | 0 | 0 | 748120 | 0 |
| sp\|Q9UKB1-2\|FBW1B_HUMAN;tr\|B4DH | 2 | 0.000354 | 0 | 0 | 269750 | 0 | 0 | 0 |
| sp\|Q9UKL0\|RCOR1_HUMAN;tr\|J3KN32 | 2 | 0.000369 | 0 | 0 | 503950 | 0 | 1966920 | 0 |
| sp\|Q9Y3A4\|RRP7A_HUMAN | 2 | 0 | 0 | 0 | 0 | 0 | 1889000 | 0 |
| sp\|Q9Y6A4\|CFA20_HUMAN;tr\|B4DN94 | 2 | 0.000367 | 0 | 0 | 60256 | 0 | 851570 | 0 |
| sp\|Q9Y6X8\|ZHX2_HUMAN | 2 | 0.006794 | 0 | 0 | 0 | 0 | 1354680 | 0 |
| tr\|A0A024R029\|A0A024R029_HUMAN;s | 2 | 0.007941 | 0 | 0 | 0 | 0 | 1071100 | 0 |
| tr\|A0A024R5K1\|A0A024R5K1_HUMAN;s | 2 | 0.002696 | 0 | 0 | 608660 | 0 | 1301400 | 0 |
| tr\|A0A024R611\|A0A024R611_HUMAN;s | 2 | 0.000363 | 0 | 0 | 148560 | 0 | 463250 | 0 |
| tr\|A0A024R806\|A0A024R806_HUMAN;s | 2 | 0.000705 | 0 | 0 | 120170 | 0 | 0 | 0 |
| tr\|A0A024R8G1\|A0A024R8G1_HUMAN; | 2 | 0.000361 | 0 | 0 | 0 | 0 | 1333600 | 0 |
| tr\|A0A024RDS3\|A0A024RDS3_HUMAN; | 2 | 0.002712 | 0 | 0 | 0 | 0 | 968840 | 0 |
| tr\|A0A087WYQ5\|A0A087WYQ5_HUMAI | 2 | 0.003307 | 0 | 0 | 0 | 0 | 352250 | 0 |
| tr\|A0A087X0S7\|A0A087X0S7_HUMAN;t | 2 | 0 | 0 | 0 | 152580 | 0 | 212800 | 0 |
| tr\|A0A087X271\|A0A087X271_HUMAN;t | 2 | 0 | 0 | 0 | 0 | 0 | 419100 | 0 |
| tr\|A0A090N7U2\|A0A090N7U2_HUMAN | 2 | 0 | 0 | 0 | 491010 | 0 | 867330 | 0 |

| | | | | | | | | |
|---|---|---|---|---|---|---|---|---|
| tr\|A0A0A0MQR4\|A0A0A0MQR4_HUMA | 2 | 0.00653 | 0 | 0 | 0 | 0 | 1280500 | 0 |
| tr\|A0PJ71\|A0PJ71_HUMAN;tr\|A8K1D3\| | 2 | 0.000361 | 0 | 0 | 187590 | 0 | 1164150 | 0 |
| tr\|A6PVP4\|A6PVP4_HUMAN;tr\|B7ZBQ3 | 2 | 0.00654 | 0 | 0 | 346092 | 0 | 1065200 | 0 |
| tr\|A8K719\|A8K719_HUMAN;sp\|Q13951 | 2 | 0 | 0 | 0 | 0 | 0 | 899340 | 0 |
| tr\|A8K874\|A8K874_HUMAN;sp\|Q5VZE5 | 2 | 0.006583 | 0 | 0 | 0 | 0 | 565570 | 0 |
| tr\|B1AMY1\|B1AMY1_HUMAN;tr\|B1AM1 | 2 | 0.006792 | 0 | 0 | 0 | 0 | 1836400 | 0 |
| tr\|B2RDG4\|B2RDG4_HUMAN;sp\|Q1539 | 2 | 0.000697 | 0 | 0 | 0 | 0 | 541050 | 0 |
| tr\|B2RUU3\|B2RUU3_HUMAN;sp\|Q1418 | 2 | 0 | 0 | 0 | 287950 | 0 | 2432800 | 0 |
| tr\|B3KNS8\|B3KNS8_HUMAN;sp\|O7568 | 2 | 0 | 0 | 0 | 0 | 0 | 695680 | 0 |
| tr\|B3KPC7\|B3KPC7_HUMAN;tr\|A0A024 | 2 | 0.000357 | 0 | 0 | 228560 | 0 | 561970 | 0 |
| tr\|B4DDR0\|B4DDR0_HUMAN;sp\|Q9NV | 2 | 0.000369 | 0 | 0 | 98142 | 0 | 579871 | 0 |
| tr\|B4DE40\|B4DE40_HUMAN;sp\|P52788 | 2 | 0 | 0 | 0 | 1111100 | 0 | 1293500 | 0 |
| tr\|B4DFD7\|B4DFD7_HUMAN;tr\|F5H658 | 2 | 0.005438 | 0 | 0 | 0 | 0 | 2037400 | 0 |
| tr\|B4DFU6\|B4DFU6_HUMAN;sp\|Q6IPR3 | 2 | 0.000695 | 0 | 0 | 0 | 0 | 533600 | 0 |
| tr\|B4DKR0\|B4DKR0_HUMAN;sp\|Q1319 | 2 | 0 | 0 | 0 | 0 | 0 | 1694500 | 0 |
| tr\|B4DLW5\|B4DLW5_HUMAN;tr\|A0A09 | 2 | 0 | 0 | 0 | 0 | 0 | 2309900 | 0 |
| tr\|B4DNS2\|B4DNS2_HUMAN;tr\|Q5D1D | 2 | 0.000701 | 0 | 0 | 0 | 0 | 1189700 | 0 |
| tr\|B4DQ03\|B4DQ03_HUMAN;tr\|A0A087 | 2 | 0.005183 | 0 | 0 | 98091 | 0 | 213590 | 0 |
| tr\|B4DQX8\|B4DQX8_HUMAN;sp\|Q9UK | 2 | 0.00036 | 0 | 0 | 0 | 0 | 472430 | 0 |
| tr\|B4DTZ4\|B4DTZ4_HUMAN;tr\|A0A024 | 2 | 0 | 0 | 0 | 0 | 0 | 1137400 | 0 |
| tr\|B4DZX4\|B4DZX4_HUMAN | 2 | 1 | 0 | 0 | 88403 | 0 | 0 | 0 |
| tr\|B4E2T4\|B4E2T4_HUMAN;tr\|E9PS42\| | 2 | 0.002681 | 0 | 0 | 0 | 0 | 751680 | 0 |
| tr\|B4E308\|B4E308_HUMAN;tr\|B4DI83\| | 2 | 0 | 0 | 0 | 0 | 0 | 1009900 | 0 |
| tr\|B5BU41\|B5BU41_HUMAN;tr\|B0YIY3\| | 2 | 0 | 0 | 0 | 0 | 0 | 468730 | 0 |
| tr\|B5MDQ0\|B5MDQ0_HUMAN;sp\|Q2N | 2 | 0 | 0 | 0 | 0 | 0 | 915000 | 0 |
| tr\|B7Z3Z9\|B7Z3Z9_HUMAN;tr\|E7EPM6\| | 2 | 0.006796 | 0 | 0 | 0 | 0 | 1331200 | 0 |
| tr\|B8ZZP4\|B8ZZP4_HUMAN;tr\|C9J7U9\| | 2 | 0.003946 | 0 | 0 | 512370 | 0 | 1044600 | 0 |
| tr\|C9J3L8\|C9J3L8_HUMAN;tr\|C9J5W0\|C | 2 | 0 | 0 | 0 | 1618500 | 0 | 484890 | 0 |
| tr\|C9J979\|C9J979_HUMAN;tr\|A0A024R | 2 | 0.002725 | 0 | 0 | 0 | 0 | 863080 | 0 |
| tr\|C9JB42\|C9JB42_HUMAN;tr\|C9JDR7\|C | 2 | 0.007353 | 0 | 0 | 0 | 0 | 729090 | 0 |
| tr\|C9JDF5\|C9JDF5_HUMAN;sp\|Q9NP71 | 2 | 0 | 0 | 0 | 0 | 0 | 657760 | 0 |
| tr\|C9JEV9\|C9JEV9_HUMAN;sp\|O95639- | 2 | 0.006809 | 0 | 0 | 0 | 0 | 1597400 | 0 |
| tr\|C9JVP0\|C9JVP0_HUMAN;sp\|Q9UPW | 2 | 0 | 0 | 0 | 0 | 0 | 851090 | 0 |
| tr\|D3DQS4\|D3DQS4_HUMAN;sp\|Q8N3 | 2 | 0.005383 | 0 | 0 | 0 | 0 | 1368800 | 0 |
| tr\|D3VVJ8\|D3VVJ8_HUMAN;tr\|G3V4U9 | 2 | 0.000353 | 0 | 0 | 88076 | 0 | 239930 | 0 |
| tr\|D6R9R7\|D6R9R7_HUMAN;tr\|B4DHK6 | 2 | 0 | 0 | 0 | 0 | 0 | 608920 | 0 |
| tr\|D6RAD4\|D6RAD4_HUMAN;sp\|P5061 | 2 | 0.005473 | 0 | 0 | 0 | 0 | 857290 | 0 |
| tr\|D6W5D1\|D6W5D1_HUMAN;sp\|Q3V6 | 2 | 0.004253 | 0 | 0 | 0 | 0 | 630480 | 0 |
| tr\|E7EN32\|E7EN32_HUMAN;tr\|A0A024 | 2 | 0 | 0 | 0 | 0 | 0 | 1806900 | 0 |
| tr\|E7EVL6\|E7EVL6_HUMAN;tr\|C9JZE3\|C | 2 | 0 | 0 | 0 | 0 | 0 | 725460 | 0 |
| tr\|E9PDR5\|E9PDR5_HUMAN;tr\|B7ZLD4 | 2 | 0.009099 | 0 | 0 | 0 | 0 | 513220 | 0 |
| tr\|E9PKG6\|E9PKG6_HUMAN;tr\|V9HW7 | 2 | 0.002714 | 0 | 0 | 0 | 0 | 491600 | 0 |
| tr\|E9PKN0\|E9PKN0_HUMAN;tr\|B7Z7X4 | 2 | 0 | 0 | 0 | 0 | 0 | 2067200 | 0 |
| tr\|E9PL47\|E9PL47_HUMAN;tr\|F8W860\| | 2 | 0.005402 | 0 | 0 | 0 | 0 | 578410 | 0 |
| tr\|E9PMI6\|E9PMI6_HUMAN;tr\|E9PJF4\| | 2 | 0 | 0 | 0 | 0 | 0 | 1348000 | 0 |
| tr\|E9PMS6\|E9PMS6_HUMAN;tr\|B7Z8W | 2 | 0.007362 | 0 | 0 | 0 | 0 | 1132700 | 0 |
| tr\|E9PPY3\|E9PPY3_HUMAN;sp\|O43159 | 2 | 0 | 0 | 0 | 0 | 0 | 1140500 | 0 |
| tr\|F5GZF0\|F5GZF0_HUMAN;sp\|O14519 | 2 | 0.000365 | 0 | 0 | 0 | 0 | 145820 | 0 |
| tr\|F5H0U5\|F5H0U5_HUMAN;tr\|A0A024 | 2 | 0.000706 | 0 | 0 | 168550 | 0 | 19621600 | 0 |
| tr\|F5H452\|F5H452_HUMAN;tr\|Q5JSB6\| | 2 | 0.002734 | 0 | 0 | 681140 | 0 | 2535600 | 0 |
| tr\|F8VQR7\|F8VQR7_HUMAN;tr\|A0A02 | 2 | 0.000363 | 0 | 0 | 0 | 0 | 763440 | 0 |
| tr\|F8VVY2\|F8VVY2_HUMAN;tr\|F8VNZ6 | 2 | 0.009976 | 0 | 0 | 0 | 0 | 57707 | 0 |
| tr\|F8W0J4\|F8W0J4_HUMAN;sp\|O9561 | 2 | 0.000363 | 0 | 0 | 0 | 0 | 348030 | 0 |
| tr\|F8W8I6\|F8W8I6_HUMAN;sp\|P31483 | 2 | 0 | 0 | 0 | 0 | 0 | 691120 | 0 |
| tr\|F8WBV5\|F8WBV5_HUMAN;tr\|G3XAJ | 2 | 0.005215 | 0 | 0 | 111380 | 0 | 1890700 | 0 |
| tr\|G3V195\|G3V195_HUMAN;sp\|Q32P4 | 2 | 0.000358 | 0 | 0 | 0 | 0 | 511990 | 0 |
| tr\|G3V2H7\|G3V2H7_HUMAN;sp\|Q86SZ | 2 | 0.00656 | 0 | 0 | 0 | 0 | 319040 | 0 |
| tr\|G3V2N2\|G3V2N2_HUMAN;sp\|Q9UIL | 2 | 0 | 0 | 0 | 373280 | 0 | 1230400 | 0 |
| tr\|H0Y565\|H0Y565_HUMAN;tr\|D3DW07 | 2 | 0.006799 | 0 | 0 | 0 | 0 | 591190 | 0 |
| tr\|H0Y5S9\|H0Y5S9_HUMAN;tr\|H0Y682\| | 2 | 0.000355 | 0 | 0 | 0 | 0 | 1200000 | 0 |
| tr\|H0Y6B5\|H0Y6B5_HUMAN;tr\|Q53SH3 | 2 | 0 | 0 | 0 | 105060 | 0 | 1945300 | 0 |
| tr\|H3BQ06\|H3BQ06_HUMAN;sp\|Q9ULP | 2 | 0.003628 | 0 | 0 | 0 | 0 | 604130 | 0 |
| tr\|H3BRL9\|H3BRL9_HUMAN;sp\|P78549 | 2 | 0 | 0 | 0 | 0 | 0 | 1721200 | 0 |
| tr\|H3BS42\|H3BS42_HUMAN;tr\|B2RD90 | 2 | 0.002695 | 0 | 0 | 0 | 0 | 12388800 | 0 |
| tr\|H7C2A6\|H7C2A6_HUMAN;tr\|C9JIK8\| | 2 | 0.000357 | 0 | 0 | 402680 | 0 | 0 | 0 |
| tr\|I3L252\|I3L252_HUMAN;tr\|H0YCY6\|H | 2 | 0 | 0 | 0 | 0 | 0 | 928590 | 0 |
| tr\|I3L2W9\|I3L2W9_HUMAN;tr\|B4E2D6\| | 2 | 0.000359 | 0 | 0 | 87743 | 0 | 1673270 | 0 |
| tr\|J3QLW7\|J3QLW7_HUMAN;tr\|B3KM4 | 2 | 0.001034 | 0 | 0 | 0 | 0 | 1554700 | 0 |
| tr\|K7ERP4\|K7ERP4_HUMAN;sp\|P36969 | 2 | 0.001715 | 0 | 0 | 0 | 0 | 405080 | 0 |
| tr\|Q05DB8\|Q05DB8_HUMAN;tr\|Q53FI8 | 2 | 0.000369 | 0 | 0 | 0 | 0 | 995910 | 0 |
| tr\|Q2NLD4\|Q2NLD4_HUMAN;tr\|Q2NLC | 2 | 0 | 0 | 0 | 0 | 0 | 911150 | 0 |
| tr\|Q32MN6\|Q32MN6_HUMAN;tr\|B4DP | 2 | 0.002682 | 0 | 0 | 0 | 0 | 1344400 | 0 |
| tr\|Q53G15\|Q53G15_HUMAN;tr\|B7Z6D5 | 2 | 0.002716 | 0 | 0 | 0 | 0 | 2192200 | 0 |
| tr\|Q53RX3\|Q53RX3_HUMAN;sp\|Q9HBH | 2 | 0 | 0 | 0 | 112100 | 0 | 912180 | 0 |
| tr\|Q541A5\|Q541A5_HUMAN;sp\|Q9289 | 2 | 0 | 0 | 0 | 0 | 0 | 1202300 | 0 |
| tr\|Q59G93\|Q59G93_HUMAN;tr\|J3KQ61 | 2 | 0.00036 | 0 | 0 | 115630 | 0 | 299600 | 0 |

| | | | | | | | | |
|---|---|---|---|---|---|---|---|---|
| tr\|Q59HE6\|Q59HE6_HUMAN;tr\|A0A024 | 2 | 0 | 0 | 0 | 0 | 0 | 689550 | 0 |
| tr\|Q5JWM4\|Q5JWM4_HUMAN;sp\|Q9H | 2 | 0.002722 | 0 | 0 | 0 | 0 | 2231800 | 0 |
| tr\|Q5VVL2\|Q5VVL2_HUMAN;tr\|B4DIY2 | 2 | 0.000372 | 0 | 0 | 0 | 0 | 392730 | 0 |
| tr\|Q6FI27\|Q6FI27_HUMAN;tr\|B5BUC0\| | 2 | 0.006516 | 0 | 0 | 682980 | 0 | 589150 | 0 |
| tr\|Q6GMQ7\|Q6GMQ7_HUMAN;tr\|Q5JU | 2 | 0.001378 | 0 | 0 | 0 | 0 | 1062900 | 0 |
| tr\|Q6I9T1\|Q6I9T1_HUMAN;tr\|Q68DB7\| | 2 | 0 | 0 | 0 | 420810 | 0 | 1010500 | 0 |
| tr\|Q6P9C2\|Q6P9C2_HUMAN;tr\|B2RAL9 | 2 | 0 | 0 | 0 | 0 | 0 | 1513600 | 0 |
| tr\|Q8N8L9\|Q8N8L9_HUMAN;tr\|Q6PIW | 2 | 0.000692 | 0 | 0 | 0 | 0 | 324500 | 0 |
| tr\|Q96KB7\|Q96KB7_HUMAN;sp\|Q9ULV | 2 | 0.000701 | 0 | 0 | 440310 | 0 | 0 | 0 |
| tr\|Q9NXD3\|Q9NXD3_HUMAN;tr\|H0Y6U | 2 | 0.005193 | 0 | 0 | 0 | 0 | 859130 | 0 |
| tr\|Q9Y5Q4\|Q9Y5Q4_HUMAN;sp\|A8MW | 2 | 0.000697 | 0 | 0 | 179620 | 0 | 0 | 0 |
| tr\|R4GMU7\|R4GMU7_HUMAN;sp\|Q6DK | 2 | 0 | 0 | 0 | 106200 | 0 | 2288300 | 0 |
| tr\|R4GN54\|R4GN54_HUMAN;tr\|B3KY73 | 2 | 0.000358 | 0 | 0 | 0 | 0 | 2166800 | 0 |
| tr\|S4R3K7\|S4R3K7_HUMAN;tr\|S4R469\| | 2 | 0.002683 | 0 | 0 | 661050 | 0 | 2047200 | 0 |
| tr\|A0A024R6Q2\|A0A024R6Q2_HUMAN; | 2 | 0 | 0 | 0 | 0 | 0 | 2246700 | 151150 |
| sp\|P24390-2\|ERD21_HUMAN;sp\|P2439 | 2 | 0 | 0 | 0 | 0 | 0 | 2868500 | 240000 |
| tr\|H3BV23\|H3BV23_HUMAN;tr\|H3BUV | 2 | 0.00037 | 0 | 0 | 0 | 0 | 2731800 | 308030 |
| tr\|H3BPK3\|H3BPK3_HUMAN;tr\|H3BPQ | 2 | 0.005477 | 0 | 0 | 90950 | 0 | 821250 | 95720 |
| tr\|Q75M98\|Q75M98_HUMAN;tr\|Q75M | 2 | 0 | 0 | 0 | 343440 | 0 | 2568600 | 302060 |
| sp\|Q9NRA8-2\|4ET_HUMAN;tr\|A0A024F | 2 | 0 | 0 | 0 | 129410 | 0 | 1042900 | 126060 |
| tr\|Q49AN9\|Q49AN9_HUMAN;tr\|F5H01 | 2 | 0 | 0 | 0 | 0 | 0 | 2803200 | 387400 |
| sp\|Q6PCE3\|PGM2L_HUMAN | 2 | 0.005459 | 0 | 0 | 0 | 0 | 877540 | 152470 |
| tr\|E9PQR7\|E9PQR7_HUMAN;tr\|Q548N1 | 2 | 0.000366 | 0 | 0 | 0 | 0 | 1124700 | 199100 |
| sp\|Q6UB99\|ANR11_HUMAN;tr\|Q9UHR | 2 | 0.002693 | 0 | 0 | 0 | 0 | 460810 | 83493 |
| sp\|Q96CP2\|FWCH2_HUMAN;tr\|I3L1Y9\| | 2 | 0.001374 | 0 | 0 | 0 | 0 | 387900 | 71631 |
| sp\|Q9NXF7\|DCA16_HUMAN | 2 | 0.002708 | 0 | 0 | 0 | 0 | 1475500 | 349100 |
| tr\|H7C218\|H7C218_HUMAN;tr\|H7C0X5 | 2 | 0.002396 | 0 | 0 | 0 | 0 | 849080 | 255450 |
| tr\|Q6IB68\|Q6IB68_HUMAN;sp\|Q99417 | 2 | 0 | 0 | 0 | 183510 | 0 | 520900 | 182450 |
| tr\|B2R7U5\|B2R7U5_HUMAN;tr\|A0A024 | 2 | 0.003322 | 0 | 0 | 0 | 0 | 283230 | 128370 |
| sp\|O95295\|SNAPN_HUMAN | 2 | 0 | 0 | 0 | 239130 | 0 | 543300 | 437820 |
| sp\|O15511\|ARPC5_HUMAN;sp\|O15511 | 2 | 0 | 0 | 0 | 0 | 0 | 235470 | 781870 |
| sp\|Q9H0F7\|ARL6_HUMAN;sp\|Q9H0F7- | 2 | 0.003001 | 0 | 0 | 160950 | 0 | 0 | 158350 |
| tr\|R4GMS9\|R4GMS9_HUMAN;tr\|Q86U8 | 2 | 0.000368 | 0 | 0 | 311710 | 0 | 0 | 290658 |
| sp\|P48059\|LIMS1_HUMAN;sp\|P48059-4 | 2 | 0 | 0 | 207080 | 0 | 0 | 7366500 | 0 |
| sp\|P63218\|GBG5_HUMAN | 2 | 0 | 0 | 83713 | 165190 | 0 | 2798620 | 0 |
| sp\|Q7L4I2-2\|RSRC2_HUMAN;sp\|Q7L4I2 | 2 | 0 | 0 | 182630 | 144830 | 0 | 0 | 0 |
| sp\|Q9BQ69\|MACD1_HUMAN | 2 | 0 | 0 | 150410 | 0 | 0 | 2607400 | 0 |
| tr\|B3KNA1\|B3KNA1_HUMAN;tr\|B3KT7 | 2 | 0 | 0 | 844404 | 0 | 0 | 977630 | 0 |
| tr\|B4DDC2\|B4DDC2_HUMAN;sp\|P3232 | 2 | 0 | 0 | 155840 | 278650 | 0 | 922390 | 0 |
| tr\|G3V2Y4\|G3V2Y4_HUMAN;tr\|H0YIZ0\| | 2 | 0 | 0 | 150110 | 239690 | 0 | 0 | 0 |
| tr\|H7C0G7\|H7C0G7_HUMAN;sp\|Q9H9C | 2 | 0 | 0 | 155590 | 0 | 0 | 1142600 | 0 |
| tr\|U3KQU7\|U3KQU7_HUMAN;sp\|Q9UP | 2 | 0.009952 | 0 | 164310 | 389430 | 0 | 0 | 0 |
| tr\|E9PRR7\|E9PRR7_HUMAN;sp\|Q14331 | 2 | 0 | 0 | 108120 | 207460 | 0 | 3113600 | 183300 |
| sp\|Q5HYI8\|RABL3_HUMAN;tr\|H7C533\| | 2 | 0 | 0 | 136680 | 0 | 0 | 4083100 | 294380 |
| sp\|Q8IYI6\|EXOC8_HUMAN | 2 | 0 | 0 | 106380 | 453100 | 0 | 1919000 | 232120 |
| sp\|Q8WZ42-5\|TITIN_HUMAN;tr\|C0JYZ2 | 2 | 0.004261 | 0 | 263420 | 0 | 0 | 1036500 | 694810 |
| sp\|Q8IZP0-2\|ABI1_HUMAN;sp\|Q8IZP0- | 2 | 0 | 0 | 186450 | 1001400 | 209140 | 3180600 | 345920 |
| tr\|A0A024RBV5\|A0A024RBV5_HUMAN; | 2 | 0 | 0 | 277320 | 697630 | 163730 | 0 | 0 |
| sp\|Q9Y4X5\|ARI1_HUMAN;tr\|H3BSK4\|H | 2 | 0 | 0 | 567390 | 1305500 | 331060 | 794120 | 0 |
| sp\|Q6IQ49-2\|SDE2_HUMAN;sp\|Q6IQ49 | 2 | 0.000702 | 0 | 0 | 565560 | 170000 | 1182600 | 319100 |
| sp\|P33908\|MA1A1_HUMAN;sp\|P33908 | 2 | 0.000366 | 0 | 180190 | 575310 | 182130 | 0 | 0 |
| tr\|D3DSR2\|D3DSR2_HUMAN;sp\|P05423 | 2 | 0 | 0 | 0 | 449120 | 154850 | 1037000 | 0 |
| sp\|Q9BU76-4\|MMTA2_HUMAN;sp\|Q9B | 2 | 0 | 0 | 98469 | 133690 | 46501 | 735350 | 143013 |
| sp\|P61956-2\|SUMO2_HUMAN;tr\|A0A0 | 2 | 0 | 0 | 2684220 | 7379060 | 3018060 | 31712280 | 6472810 |
| tr\|A8K818\|A8K818_HUMAN;sp\|O15446 | 2 | 0 | 0 | 321330 | 664860 | 283620 | 5219000 | 0 |
| sp\|Q9HC07\|TM165_HUMAN;tr\|V9GYC8 | 2 | 0 | 0 | 335120 | 1409110 | 654560 | 0 | 0 |
| tr\|A6NKE1\|A6NKE1_HUMAN;sp\|O4361 | 2 | 0.002717 | 0 | 203490 | 170120 | 133840 | 1125600 | 321000 |
| sp\|Q9UBI6\|GBG12_HUMAN;tr\|Q53GD1 | 2 | 0.000367 | 0 | 109600 | 264400 | 275860 | 310720 | 0 |
| tr\|Q9BX72\|Q9BX72_HUMAN | 2 | 1 | 0 | 1923720 | 1324900 | 2046160 | 4755070 | 4650800 |
| tr\|Q69YR1\|Q69YR1_HUMAN;sp\|Q9BRR | 2 | 0.005382 | 0 | 0 | 307160 | 586480 | 0 | 0 |
| sp\|O15068-3\|MCF2L_HUMAN;sp\|O150 | 2 | 0.006801 | 0 | 0 | 0 | 225600 | 5781800 | 0 |
| tr\|C3PTT6\|C3PTT6_HUMAN;tr\|G8H6I3\| | 2 | 0.000694 | 0 | 0 | 0 | 642848 | 1237300 | 155230 |
| tr\|D6RFM0\|D6RFM0_HUMAN;tr\|D6RAH | 2 | 0 | 0 | 0 | 0 | 112390 | 1050500 | 1650600 |
| sp\|Q7Z3Z4\|PIWL4_HUMAN;tr\|F5H116\| | 2 | 0.003311 | 0 | 197514 | 0 | 468570 | 3650100 | 56450 |
| tr\|H3BRR0\|H3BRR0_HUMAN;sp\|Q9NZD | 1 | 0 | 18583530 | 2127920 | 2059540 | 2871140 | 4170310 | 5098050 |
| tr\|Q5VXJ5\|Q5VXJ5_HUMAN;tr\|Q9H2G7 | 1 | 0.003321 | 14147700 | 16407000 | 11194500 | 9280700 | 26565000 | 19056500 |
| tr\|B4DGK9\|B4DGK9_HUMAN;sp\|Q9UHV | 1 | 0 | 5230770 | 6697000 | 4285430 | 3850470 | 5628230 | 4112800 |
| tr\|O15310\|O15310_HUMAN;tr\|O15313 | 1 | 1 | 4207000 | 3296060 | 2768000 | 8616600 | 15988400 | 8623900 |
| tr\|L0R6T2\|L0R6T2_HUMAN | 1 | 1 | 3424760 | 2216850 | 2441910 | 2412140 | 1492510 | 3531570 |
| tr\|Q6ZP92\|Q6ZP92_HUMAN | 1 | 0.005198 | 3135400 | 1417740 | 530380 | 2610600 | 2300340 | 2755210 |
| tr\|H3BS88\|H3BS88_HUMAN;sp\|Q8N6V | 1 | 1 | 3023640 | 6436900 | 5524900 | 4255490 | 9886100 | 8688240 |
| tr\|C9J7L5\|C9J7L5_HUMAN;tr\|C9JY31\|C | 1 | 0.008239 | 2942240 | 21917000 | 16947430 | 10615130 | 33042000 | 4307460 |
| tr\|B4DJY8\|B4DJY8_HUMAN | 1 | 0.004248 | 2737000 | 0 | 3532000 | 1717800 | 0 | 0 |
| tr\|Q499Z6\|Q499Z6_HUMAN | 1 | 1 | 1813100 | 693160 | 0 | 2141300 | 0 | 3275050 |
| tr\|A0A024R2D7\|A0A024R2D7_HUMAN; | 1 | 0.005195 | 1289830 | 236960 | 818670 | 0 | 1518610 | 0 |

| | | | | | | | | |
|---|---|---|---|---|---|---|---|---|
| sp\|P01609\|KV117_HUMAN | 1 | 0 | 1273140 | 1721800 | 6388800 | 2447000 | 14126000 | 1614500 |
| sp\|Q9UGI0\|ZRAN1_HUMAN | 1 | 0.006567 | 1208200 | 0 | 0 | 0 | 3005700 | 0 |
| tr\|B7ZMF1\|B7ZMF1_HUMAN;tr\|B2RTQ | 1 | 0.003317 | 1038000 | 0 | 0 | 0 | 0 | 984160 |
| tr\|B9TX32\|B9TX32_HUMAN;tr\|B9TX33\| | 1 | 0.004569 | 971930 | 385550 | 0 | 506090 | 2401030 | 0 |
| tr\|B4DJB3\|B4DJB3_HUMAN;sp\|Q8IUX7 | 1 | 1 | 952380 | 0 | 0 | 322930 | 0 | 0 |
| tr\|H3BPG5\|H3BPG5_HUMAN;tr\|H3BV8 | 1 | 0 | 948070 | 268090 | 1529300 | 0 | 6639100 | 571986 |
| sp\|Q9BZG9-3\|LYNX1_HUMAN;sp\|Q9BZ | 1 | 0.000354 | 912420 | 854280 | 919540 | 723710 | 0 | 629250 |
| tr\|Q8TEP9\|Q8TEP9_HUMAN;tr\|A0A024 | 1 | 0.001036 | 901960 | 0 | 0 | 0 | 0 | 0 |
| tr\|B4DR67\|B4DR67_HUMAN;sp\|Q9Y673 | 1 | 0.006524 | 859775 | 0 | 123920 | 0 | 0 | 0 |
| tr\|Q5T8R3\|Q5T8R3_HUMAN;sp\|P53985 | 1 | 0.003309 | 823230 | 0 | 0 | 0 | 0 | 0 |
| sp\|Q8WWL2-3\|SPIR2_HUMAN;sp\|Q8W | 1 | 1 | 813310 | 479870 | 1877400 | 439860 | 4083300 | 744130 |
| tr\|B4DYH6\|B4DYH6_HUMAN;tr\|B4DH8 | 1 | 0 | 803220 | 0 | 0 | 0 | 2079860 | 0 |
| sp\|Q5SY68\|S1A7B_HUMAN | 1 | 0.009964 | 732650 | 0 | 224320 | 0 | 0 | 0 |
| tr\|Q9P0G0\|Q9P0G0_HUMAN;tr\|H0YI36 | 1 | 0.005435 | 704880 | 0 | 0 | 0 | 1217300 | 159190 |
| sp\|P23610\|F8I2_HUMAN | 1 | 0 | 682220 | 0 | 0 | 377910 | 1990300 | 0 |
| tr\|B3KNQ9\|B3KNQ9_HUMAN;tr\|B3KW | 1 | 0 | 673290 | 0 | 0 | 0 | 1037700 | 0 |
| tr\|H0YFX4\|H0YFX4_HUMAN;tr\|A0A024 | 1 | 0.000706 | 595220 | 0 | 462760 | 0 | 0 | 0 |
| tr\|B4DH44\|B4DH44_HUMAN;sp\|P4598 | 1 | 0.004571 | 594730 | 213870 | 822320 | 0 | 1555200 | 0 |
| tr\|L0R5C7\|L0R5C7_HUMAN | 1 | 0.005404 | 586090 | 1776750 | 0 | 1020750 | 0 | 4679010 |
| sp\|Q86XI8\|CS068_HUMAN;tr\|A0A087W | 1 | 0.006818 | 576230 | 1011800 | 722940 | 934430 | 1049600 | 1338220 |
| tr\|H0YLW7\|H0YLW7_HUMAN;tr\|H0YMV | 1 | 0 | 574860 | 150890 | 514610 | 0 | 1782300 | 222420 |
| tr\|F6RY50\|F6RY50_HUMAN;tr\|B4E0W3 | 1 | 0.009979 | 510990 | 0 | 39593 | 0 | 0 | 0 |
| sp\|Q9Y3R4\|NEUR2_HUMAN | 1 | 0 | 500460 | 0 | 0 | 0 | 0 | 0 |
| sp\|P42224-2\|STAT1_HUMAN;tr\|J3KPM | 1 | 0.002697 | 435560 | 0 | 0 | 0 | 0 | 0 |
| tr\|B4DMS9\|B4DMS9_HUMAN;sp\|Q9H0 | 1 | 0 | 435350 | 0 | 0 | 0 | 1309600 | 0 |
| sp\|Q9BQ50-2\|TREX2_HUMAN;tr\|Q06S7 | 1 | 0 | 432810 | 0 | 0 | 0 | 0 | 0 |
| tr\|B2R717\|B2R717_HUMAN;tr\|A0A024F | 1 | 0.003626 | 429530 | 0 | 0 | 0 | 0 | 0 |
| sp\|Q9HCD5\|NCOA5_HUMAN | 1 | 0.000355 | 412730 | 0 | 0 | 0 | 777790 | 0 |
| tr\|B7Z1C2\|B7Z1C2_HUMAN;tr\|F5H8H2\| | 1 | 0 | 405350 | 0 | 0 | 0 | 1221400 | 0 |
| tr\|F8VVM2\|F8VVM2_HUMAN;tr\|Q8NC | 1 | 0.005451 | 364510 | 0 | 262680 | 0 | 510740 | 0 |
| tr\|J3KSK6\|J3KSK6_HUMAN;sp\|Q7RTP6- | 1 | 0.00547 | 355780 | 0 | 0 | 0 | 0 | 0 |
| tr\|F8WE41\|F8WE41_HUMAN;sp\|P5229 | 1 | 0.009105 | 355700 | 0 | 0 | 0 | 0 | 537680 |
| tr\|H0YMP2\|H0YMP2_HUMAN;tr\|H0YL7 | 1 | 0.002684 | 346710 | 0 | 1004800 | 0 | 2218000 | 0 |
| tr\|Q9H984\|Q9H984_HUMAN;tr\|A0PJ59 | 1 | 0.000694 | 342990 | 0 | 0 | 0 | 945440 | 0 |
| sp\|Q9Y5T5-5\|UBP16_HUMAN;sp\|Q9Y5 | 1 | 0.000371 | 336180 | 146230 | 315230 | 0 | 1348900 | 146070 |
| tr\|H3BTI5\|H3BTI5_HUMAN;tr\|H3BVG8\| | 1 | 0 | 330600 | 0 | 0 | 0 | 796410 | 0 |
| tr\|B4DS19\|B4DS19_HUMAN;tr\|B4DWW | 1 | 0.000372 | 316350 | 0 | 0 | 0 | 754170 | 0 |
| tr\|Q5HYD9\|Q5HYD9_HUMAN;tr\|D6RFH | 1 | 0.001035 | 306540 | 278600 | 389350 | 127170 | 0 | 0 |
| tr\|A0A024R8L8\|A0A024R8L8_HUMAN;s | 1 | 0.002702 | 303910 | 0 | 0 | 0 | 0 | 0 |
| tr\|H3BRX7\|H3BRX7_HUMAN;sp\|Q1467 | 1 | 0.000371 | 290000 | 0 | 267810 | 0 | 0 | 0 |
| tr\|B4DGH7\|B4DGH7_HUMAN;sp\|Q9UJX | 1 | 0.002719 | 288630 | 0 | 141230 | 0 | 647080 | 0 |
| tr\|Q8N2P4\|Q8N2P4_HUMAN;tr\|B3KXZ | 1 | 0 | 264810 | 0 | 556000 | 192790 | 300710 | 0 |
| tr\|F5GXG4\|F5GXG4_HUMAN;sp\|Q96HS | 1 | 0.00679 | 254820 | 0 | 401800 | 0 | 0 | 0 |
| tr\|K7EQ71\|K7EQ71_HUMAN;tr\|K7EKI8\| | 1 | 0.005399 | 246360 | 0 | 0 | 0 | 226090 | 0 |
| sp\|Q14657\|LAGE3_HUMAN | 1 | 0 | 239800 | 215090 | 597680 | 142070 | 3149800 | 312660 |
| tr\|A0PJ80\|A0PJ80_HUMAN;sp\|Q96K76 | 1 | 0.000362 | 232500 | 0 | 212750 | 0 | 507100 | 0 |
| sp\|Q8WY22\|BRI3B_HUMAN | 1 | 0 | 218840 | 156640 | 395960 | 102620 | 327590 | 59466 |
| tr\|B0QY86\|B0QY86_HUMAN;sp\|Q8N3F | 1 | 0.006552 | 218200 | 0 | 158770 | 0 | 0 | 0 |
| tr\|V9HWG2\|V9HWG2_HUMAN;sp\|Q9Y | 1 | 1 | 217270 | 0 | 0 | 0 | 0 | 0 |
| tr\|A8KAQ8\|A8KAQ8_HUMAN;sp\|O957 | 1 | 0.000699 | 208570 | 0 | 0 | 0 | 0 | 0 |
| sp\|Q9Y446\|PKP3_HUMAN;sp\|Q9Y446-2 | 1 | 0.005185 | 205740 | 0 | 0 | 0 | 0 | 0 |
| tr\|F8WC82\|F8WC82_HUMAN;tr\|C9J4N2 | 1 | 0.000704 | 197100 | 0 | 0 | 0 | 1080400 | 0 |
| sp\|Q9NVT9-2\|ARMC1_HUMAN;sp\|Q9N | 1 | 0.000354 | 183870 | 170270 | 383720 | 0 | 1246000 | 0 |
| tr\|C9JQG7\|C9JQG7_HUMAN;sp\|Q9Y232 | 1 | 0 | 176590 | 0 | 222420 | 0 | 682760 | 0 |
| tr\|B4DDM2\|B4DDM2_HUMAN;sp\|Q8TE | 1 | 0.009113 | 173040 | 89738 | 209000 | 0 | 189280 | 0 |
| sp\|Q9Y2S0\|RPAC2_HUMAN | 1 | 0 | 137000 | 0 | 362200 | 0 | 2642800 | 212880 |
| sp\|O60942-3\|MCE1_HUMAN;tr\|B4DSJ8 | 1 | 0.001376 | 134080 | 0 | 194680 | 0 | 472200 | 0 |
| tr\|C9J0T6\|C9J0T6_HUMAN;tr\|H7C1P7\|H | 1 | 0.005203 | 132160 | 174680 | 0 | 223970 | 380460 | 0 |
| tr\|B4DK86\|B4DK86_HUMAN;tr\|A0A0A0 | 1 | 0 | 128880 | 0 | 0 | 0 | 195990 | 0 |
| tr\|H7C3P7\|H7C3P7_HUMAN;sp\|P11233 | 1 | 0 | 126570 | 113770 | 220820 | 0 | 575750 | 0 |
| sp\|Q9P2X0\|DPM3_HUMAN;tr\|Q86TM7 | 1 | 0 | 114230 | 0 | 0 | 0 | 250430 | 279420 |
| sp\|Q7Z7F0-4\|K0907_HUMAN;tr\|D3DVA | 1 | 0.000363 | 72552 | 0 | 118090 | 0 | 190130 | 32844 |
| sp\|P0C2W1\|FBSP1_HUMAN | 1 | 0.005472 | 71195 | 0 | 113850 | 0 | 0 | 0 |
| tr\|A0A0A0MSU2\|A0A0A0MSU2_HUMAI | 1 | 0.000357 | 60850 | 0 | 0 | 0 | 156590 | 0 |
| tr\|H3BUD2\|H3BUD2_HUMAN;tr\|H3BS0 | 1 | 0.004251 | 52795 | 0 | 86369 | 0 | 568240 | 0 |
| tr\|K7EQT9\|K7EQT9_HUMAN;tr\|K7ES75 | 1 | 0.004254 | 34971 | 0 | 0 | 0 | 0 | 0 |
| sp\|Q9NPE3\|NOP10_HUMAN | 1 | 1 | 21204 | 0 | 54913 | 0 | 344070 | 0 |
| sp\|O15379\|HDAC3_HUMAN;sp\|O15379 | 1 | 0 | 0 | 0 | 0 | 0 | 613790 | 0 |
| sp\|P10767\|FGF6_HUMAN | 1 | 1 | 0 | 0 | 271920 | 0 | 0 | 0 |
| sp\|P16233\|LIPP_HUMAN | 1 | 1 | 0 | 0 | 158600 | 0 | 0 | 0 |
| sp\|P51808\|DYLT3_HUMAN;tr\|F2Z328\|F | 1 | 0.004892 | 0 | 0 | 0 | 0 | 540610 | 0 |
| sp\|P52735-3\|VAV2_HUMAN;sp\|P52735 | 1 | 0.006589 | 0 | 0 | 195330 | 0 | 505380 | 0 |
| sp\|P55081\|MFAP1_HUMAN | 1 | 0 | 0 | 0 | 0 | 0 | 1334500 | 0 |
| sp\|Q07889-2\|SOS1_HUMAN;tr\|Q8NIA3 | 1 | 0.005156 | 0 | 0 | 0 | 0 | 779570 | 0 |
| sp\|Q12962\|TAF10_HUMAN | 1 | 0.000361 | 0 | 0 | 0 | 0 | 341500 | 0 |
| sp\|Q15398-1\|DLGP5_HUMAN;tr\|B4DM | 1 | 0 | 0 | 0 | 0 | 0 | 772650 | 0 |
| sp\|Q5SYE7-2\|NHSL1_HUMAN;sp\|Q5SYE | 1 | 0.003326 | 0 | 0 | 0 | 0 | 2345770 | 0 |
| sp\|Q5T280\|CI114_HUMAN | 1 | 0.00036 | 0 | 0 | 0 | 0 | 1131200 | 0 |

| | | | | | | | | |
|---|---|---|---|---|---|---|---|---|
| sp\|Q5T2E6\|CJ076_HUMAN | 1 | 0.001716 | 0 | 0 | 0 | 0 | 2555200 | 0 |
| sp\|Q5T481\|RBM20_HUMAN | 1 | 0 | 0 | 0 | 114420 | 0 | 919260 | 0 |
| sp\|Q6P6C2\|ALKB5_HUMAN;sp\|Q6P6C2 | 1 | 0.005463 | 0 | 0 | 0 | 0 | 1091900 | 0 |
| sp\|Q6XZF7\|DNMBP_HUMAN | 1 | 0.001714 | 0 | 0 | 0 | 0 | 169750 | 0 |
| sp\|Q7RTS3\|PTF1A_HUMAN | 1 | 0.006575 | 0 | 0 | 635340 | 0 | 0 | 0 |
| sp\|Q7Z6V5-2\|ADAT2_HUMAN;sp\|Q7Z6 | 1 | 0.007073 | 0 | 0 | 0 | 0 | 1270300 | 0 |
| sp\|Q86U90\|YRDC_HUMAN | 1 | 0.000696 | 0 | 0 | 0 | 0 | 164980 | 0 |
| sp\|Q86UA6\|RIP_HUMAN;tr\|A0A0A0MS | 1 | 0 | 0 | 0 | 0 | 0 | 1220900 | 0 |
| sp\|Q86V85\|GP180_HUMAN | 1 | 0.006788 | 0 | 0 | 0 | 0 | 133910 | 0 |
| sp\|Q8IXM2-2\|BAP18_HUMAN;tr\|F8W0 | 1 | 0.006565 | 0 | 0 | 0 | 0 | 1061900 | 0 |
| sp\|Q8N5L8\|RP25L_HUMAN | 1 | 0.005161 | 0 | 0 | 0 | 0 | 368320 | 0 |
| sp\|Q8N9B5-2\|JMY_HUMAN;sp\|Q8N9B5 | 1 | 0.000362 | 0 | 0 | 150890 | 0 | 321150 | 0 |
| sp\|Q8N9N5-3\|BANP_HUMAN;tr\|B3KM | 1 | 0.007645 | 0 | 0 | 0 | 0 | 317750 | 0 |
| sp\|Q8NDX6\|ZN740_HUMAN | 1 | 0.000353 | 0 | 0 | 0 | 0 | 782150 | 0 |
| sp\|Q8NG68\|TTL_HUMAN | 1 | 0 | 0 | 0 | 791270 | 0 | 0 | 0 |
| sp\|Q8NH76\|O56B4_HUMAN | 1 | 1 | 0 | 0 | 0 | 0 | 0 | 0 |
| sp\|Q8NHU6\|TDRD7_HUMAN | 1 | 1 | 0 | 0 | 0 | 0 | 0 | 0 |
| sp\|Q8TB03-3\|CX038_HUMAN;tr\|B4E32 | 1 | 0.005419 | 0 | 0 | 0 | 0 | 407370 | 0 |
| sp\|Q8TB52\|FBX30_HUMAN | 1 | 0.005376 | 0 | 0 | 0 | 0 | 840350 | 0 |
| sp\|Q8TBK6-2\|ZCH10_HUMAN;tr\|B3KVL | 1 | 0 | 0 | 0 | 0 | 0 | 487610 | 0 |
| sp\|Q8TEQ8\|PIGO_HUMAN | 1 | 1 | 0 | 0 | 0 | 0 | 0 | 0 |
| sp\|Q8TF65\|GIPC2_HUMAN | 1 | 0.002692 | 0 | 0 | 0 | 0 | 0 | 0 |
| sp\|Q8WUX2\|CHAC2_HUMAN | 1 | 0.005165 | 0 | 0 | 0 | 0 | 0 | 0 |
| sp\|Q8WVH0\|CPLX3_HUMAN | 1 | 1 | 0 | 0 | 0 | 0 | 0 | 0 |
| sp\|Q8WVY7\|UBCP1_HUMAN | 1 | 0.009132 | 0 | 0 | 0 | 0 | 0 | 0 |
| sp\|Q8WXD5\|GEMI6_HUMAN | 1 | 0.00331 | 0 | 0 | 84293 | 0 | 667390 | 0 |
| sp\|Q96BK5\|PINX1_HUMAN | 1 | 0 | 0 | 0 | 0 | 0 | 723680 | 0 |
| sp\|Q96BN8\|OTUL_HUMAN | 1 | 0.003635 | 0 | 0 | 0 | 0 | 0 | 0 |
| sp\|Q96G25-3\|MED8_HUMAN;sp\|Q96G2 | 1 | 0.001376 | 0 | 0 | 0 | 0 | 410380 | 0 |
| sp\|Q96G46-2\|DUS3L_HUMAN;tr\|B2RDV | 1 | 0.000365 | 0 | 0 | 714800 | 0 | 1292000 | 0 |
| sp\|Q96GS4\|CQ059_HUMAN | 1 | 0.00518 | 0 | 0 | 0 | 0 | 1334800 | 0 |
| sp\|Q96JP5-2\|ZFP91_HUMAN;tr\|A0A024 | 1 | 0.000367 | 0 | 0 | 0 | 0 | 1508400 | 0 |
| sp\|Q96KM6\|Z512B_HUMAN | 1 | 0.000364 | 0 | 0 | 0 | 0 | 1322300 | 0 |
| sp\|Q9BQS8-3\|FYCO1_HUMAN;sp\|Q9B0 | 1 | 0 | 0 | 0 | 0 | 0 | 539120 | 0 |
| sp\|Q9BSM1-3\|PCGF1_HUMAN;tr\|A0A0 | 1 | 0.003618 | 0 | 0 | 0 | 0 | 676880 | 0 |
| sp\|Q9H8G2\|CAAP1_HUMAN | 1 | 0.005428 | 0 | 0 | 0 | 0 | 250680 | 0 |
| sp\|Q9NVU7-2\|SDA1_HUMAN;tr\|E7EW0 | 1 | 0.000695 | 0 | 0 | 0 | 0 | 1310321 | 0 |
| sp\|Q9NX07-2\|TSAP1_HUMAN;sp\|Q9NX | 1 | 0.006534 | 0 | 0 | 0 | 0 | 399310 | 0 |
| sp\|Q9NZM4-2\|GSCR1_HUMAN;tr\|A0A0 | 1 | 0.006577 | 0 | 0 | 0 | 0 | 505340 | 0 |
| sp\|Q9UBF6-4\|RBX2_HUMAN;tr\|B2R4X4 | 1 | 0 | 0 | 0 | 0 | 0 | 383740 | 0 |
| sp\|Q9UHR4\|BI2L1_HUMAN | 1 | 0.006556 | 0 | 0 | 0 | 0 | 151880 | 0 |
| sp\|Q9Y2P8\|RCL1_HUMAN | 1 | 0.00543 | 0 | 0 | 0 | 0 | 596390 | 0 |
| sp\|Q9Y4E5-2\|ZN451_HUMAN;tr\|Q4KM | 1 | 0.000698 | 0 | 0 | 0 | 0 | 103430 | 0 |
| sp\|Q9Y4U1\|MMAC_HUMAN | 1 | 0 | 0 | 0 | 0 | 0 | 1573100 | 0 |
| sp\|Q9Y5U9\|IR3IP_HUMAN | 1 | 0.005424 | 0 | 0 | 0 | 0 | 1405600 | 0 |
| sp\|Q9Y651\|SOX21_HUMAN | 1 | 0.001377 | 0 | 0 | 0 | 0 | 242360 | 0 |
| tr\|A0A024QYX3\|A0A024QYX3_HUMAN; | 1 | 0.007937 | 0 | 0 | 0 | 0 | 935570 | 0 |
| tr\|A0A024QZS1\|A0A024QZS1_HUMAN; | 1 | 0.006813 | 0 | 0 | 0 | 0 | 826230 | 0 |
| tr\|A0A024R7R3\|A0A024R7R3_HUMAN;t | 1 | 0.002695 | 0 | 0 | 328590 | 0 | 0 | 0 |
| tr\|A0A024R8N4\|A0A024R8N4_HUMAN; | 1 | 0.005454 | 0 | 0 | 322610 | 0 | 1338870 | 0 |
| tr\|A0A024R8Q8\|A0A024R8Q8_HUMAN; | 1 | 0.00678 | 0 | 0 | 205640 | 0 | 0 | 0 |
| tr\|A0A024R9N0\|A0A024R9N0_HUMAN; | 1 | 0 | 0 | 0 | 182640 | 0 | 578540 | 0 |
| tr\|A0A024RBB9\|A0A024RBB9_HUMAN; | 1 | 1 | 0 | 0 | 0 | 0 | 0 | 0 |
| tr\|A0A024RCX8\|A0A024RCX8_HUMAN; | 1 | 0 | 0 | 0 | 0 | 0 | 587480 | 0 |
| tr\|A0A087WTF1\|A0A087WTF1_HUMAN | 1 | 0.006528 | 0 | 0 | 0 | 0 | 1462260 | 0 |
| tr\|A0A087WUD3\|A0A087WUD3_HUMA | 1 | 0.000693 | 0 | 0 | 0 | 0 | 740060 | 0 |
| tr\|A0A087WUU7\|A0A087WUU7_HUMA | 1 | 0.007373 | 0 | 0 | 0 | 0 | 241500 | 0 |
| tr\|A0A087WVQ2\|A0A087WVQ2_HUMA | 1 | 0.007944 | 0 | 0 | 89772 | 0 | 326530 | 0 |
| tr\|A0A087WWQ9\|A0A087WWQ9_HUM | 1 | 1 | 0 | 0 | 0 | 0 | 0 | 0 |
| tr\|A0A087WXF7\|A0A087WXF7_HUMAN | 1 | 0 | 0 | 0 | 0 | 0 | 1194600 | 0 |
| tr\|A4D1W6\|A4D1W6_HUMAN;sp\|Q8TA | 1 | 0 | 0 | 0 | 0 | 0 | 376170 | 0 |
| tr\|A4IF61\|A4IF61_HUMAN;sp\|Q9P0W2 | 1 | 0.009958 | 0 | 0 | 28649 | 0 | 768230 | 0 |
| tr\|A6NLH6\|A6NLH6_HUMAN;tr\|Q53HE | 1 | 0.006782 | 0 | 0 | 282640 | 0 | 2016100 | 0 |
| tr\|A8K0F7\|A8K0F7_HUMAN;sp\|Q8N0U | 1 | 0.0007 | 0 | 0 | 0 | 0 | 0 | 0 |
| tr\|A8K0I0\|A8K0I0_HUMAN;tr\|A0A024R | 1 | 0.002694 | 0 | 0 | 0 | 0 | 433160 | 0 |
| tr\|B0V3J0\|B0V3J0_HUMAN;tr\|A9C4B9\| | 1 | 0 | 0 | 0 | 0 | 0 | 146210 | 0 |
| tr\|B1AK63\|B1AK63_HUMAN;sp\|Q9HAF | 1 | 0.005999 | 0 | 0 | 0 | 0 | 1348900 | 0 |
| tr\|B1B5T7\|B1B5T7_HUMAN;tr\|B1B5T0\| | 1 | 1 | 0 | 0 | 0 | 0 | 0 | 0 |
| tr\|B2RAX6\|B2RAX6_HUMAN;sp\|Q9Y5J1 | 1 | 0.009096 | 0 | 0 | 215840 | 0 | 276130 | 0 |
| tr\|B3KNV9\|B3KNV9_HUMAN;tr\|S4R400 | 1 | 0 | 0 | 0 | 0 | 0 | 387540 | 0 |
| tr\|B3KTC3\|B3KTC3_HUMAN;sp\|Q9H2C0 | 1 | 0 | 0 | 0 | 302950 | 0 | 817333 | 0 |
| tr\|B3KV54\|B3KV54_HUMAN;tr\|H0Y760 | 1 | 0 | 0 | 0 | 0 | 0 | 192440 | 0 |
| tr\|B4DDK7\|B4DDK7_HUMAN;tr\|B1AK66 | 1 | 0.000371 | 0 | 0 | 0 | 0 | 303350 | 0 |
| tr\|B4DFK0\|B4DFK0_HUMAN;tr\|E9PJK2\| | 1 | 0.005163 | 0 | 0 | 0 | 0 | 993360 | 0 |
| tr\|B4DGW0\|B4DGW0_HUMAN;sp\|O75 | 1 | 0.006538 | 0 | 0 | 0 | 0 | 706190 | 0 |
| tr\|B4DJU5\|B4DJU5_HUMAN;sp\|Q8IUI8 | 1 | 0.000365 | 0 | 0 | 0 | 0 | 448619 | 0 |

| | | | | | | | | |
|---|---|---|---|---|---|---|---|---|
| tr\|B4DLZ1\|B4DLZ1_HUMAN;sp\|Q9P107 | 1 | 0.006614 | 0 | 0 | 0 | 0 | 515310 | 0 |
| tr\|B4DRB3\|B4DRB3_HUMAN;tr\|B4DTN( | 1 | 0.005188 | 0 | 0 | 0 | 0 | 479500 | 0 |
| tr\|B4DSF4\|B4DSF4_HUMAN;tr\|B3KS94\| | 1 | 0 | 0 | 0 | 0 | 0 | 145510 | 0 |
| tr\|B4DSN5\|B4DSN5_HUMAN;tr\|A8K3M | 1 | 0 | 0 | 0 | 408320 | 0 | 0 | 0 |
| tr\|B4DSV2\|B4DSV2_HUMAN;tr\|B4DFD9 | 1 | 0.000362 | 0 | 0 | 97058 | 0 | 410230 | 0 |
| tr\|B4DU58\|B4DU58_HUMAN;sp\|P40121 | 1 | 0.005442 | 0 | 0 | 0 | 0 | 227930 | 0 |
| tr\|B7Z821\|B7Z821_HUMAN;tr\|A0A024R | 1 | 0.006602 | 0 | 0 | 0 | 0 | 330650 | 0 |
| tr\|B7Z9U0\|B7Z9U0_HUMAN;sp\|Q9UFF9 | 1 | 0.002688 | 0 | 0 | 0 | 0 | 621160 | 0 |
| tr\|C4TNW4\|C4TNW4_HUMAN;tr\|Q2VP | 1 | 0.006596 | 0 | 0 | 0 | 0 | 344340 | 0 |
| tr\|C9J5E0\|C9J5E0_HUMAN;tr\|C9JZW2\|( | 1 | 1 | 0 | 0 | 386280 | 0 | 0 | 0 |
| tr\|C9JIZ3\|C9JIZ3_HUMAN;tr\|H7C2Z6\|H | 1 | 0 | 0 | 0 | 0 | 0 | 518110 | 0 |
| tr\|C9JYM0\|C9JYM0_HUMAN;sp\|O75817 | 1 | 0.005212 | 0 | 0 | 0 | 0 | 891670 | 0 |
| tr\|C9K0U8\|C9K0U8_HUMAN;tr\|E7EUY5 | 1 | 0.006618 | 0 | 0 | 132060 | 0 | 0 | 0 |
| tr\|D6RBA9\|D6RBA9_HUMAN;sp\|Q1528 | 1 | 0 | 0 | 0 | 0 | 0 | 938070 | 0 |
| tr\|D6RC40\|D6RC40_HUMAN;tr\|D6RCQ3 | 1 | 0.002728 | 0 | 0 | 0 | 0 | 187420 | 0 |
| tr\|D6RGK9\|D6RGK9_HUMAN;tr\|B4E2S0 | 1 | 0.00036 | 0 | 0 | 517380 | 0 | 0 | 0 |
| tr\|D6RH30\|D6RH30_HUMAN;tr\|A0A024 | 1 | 0.00519 | 0 | 0 | 0 | 0 | 2237400 | 0 |
| tr\|E5RIV7\|E5RIV7_HUMAN;tr\|A0A024R | 1 | 0.00539 | 0 | 0 | 0 | 0 | 2098860 | 0 |
| tr\|E9PGE5\|E9PGE5_HUMAN;sp\|Q9NUY | 1 | 0.003006 | 0 | 0 | 0 | 0 | 913870 | 0 |
| tr\|E9PLD3\|E9PLD3_HUMAN;tr\|E9PRG8\| | 1 | 0.005466 | 0 | 0 | 0 | 0 | 1169600 | 0 |
| tr\|E9PLL0\|E9PLL0_HUMAN;tr\|M0QZK6\| | 1 | 1 | 0 | 0 | 111810 | 0 | 0 | 0 |
| tr\|E9PRK7\|E9PRK7_HUMAN;sp\|Q8N8R7 | 1 | 0.002705 | 0 | 0 | 0 | 0 | 716490 | 0 |
| tr\|F8W895\|F8W895_HUMAN;tr\|A0A0A | 1 | 0.008237 | 0 | 0 | 0 | 0 | 477770 | 0 |
| tr\|F8WBT6\|F8WBT6_HUMAN;sp\|Q8IXJ( | 1 | 0.002705 | 0 | 0 | 0 | 0 | 475770 | 0 |
| tr\|F8WDT8\|F8WDT8_HUMAN;tr\|G3V0( | 1 | 0.000364 | 0 | 0 | 0 | 0 | 705310 | 0 |
| tr\|F8WEI7\|F8WEI7_HUMAN;sp\|P09382 | 1 | 0.005423 | 0 | 0 | 609710 | 0 | 3181000 | 0 |
| tr\|H0Y720\|H0Y720_HUMAN;tr\|A0A024F | 1 | 0.002675 | 0 | 0 | 0 | 0 | 529710 | 0 |
| tr\|H0Y9G4\|H0Y9G4_HUMAN;tr\|H0Y9S6 | 1 | 0 | 0 | 0 | 0 | 0 | 420690 | 0 |
| tr\|H0YFG1\|H0YFG1_HUMAN;tr\|B4E3T6 | 1 | 0 | 0 | 0 | 0 | 0 | 1179300 | 0 |
| tr\|H0YGN0\|H0YGN0_HUMAN;tr\|F5GZ97 | 1 | 0.000696 | 0 | 0 | 0 | 0 | 659960 | 0 |
| tr\|H0YH35\|H0YH35_HUMAN | 1 | 1 | 0 | 0 | 358460 | 0 | 0 | 0 |
| tr\|H0YHB7\|H0YHB7_HUMAN;sp\|O4334 | 1 | 0.005171 | 0 | 0 | 0 | 0 | 915740 | 0 |
| tr\|H0YII3\|H0YII3_HUMAN;tr\|J3QK86\|J3 | 1 | 0 | 0 | 0 | 0 | 0 | 140240 | 0 |
| tr\|H0YJ08\|H0YJ08_HUMAN;tr\|B4E3E1\|E | 1 | 0.000359 | 0 | 0 | 0 | 0 | 111600 | 0 |
| tr\|H0YLM3\|H0YLM3_HUMAN;tr\|H0YLD4 | 1 | 0.000698 | 0 | 0 | 0 | 0 | 404450 | 0 |
| tr\|H0YMN5\|H0YMN5_HUMAN;tr\|A8K2Y | 1 | 0.006587 | 0 | 0 | 0 | 0 | 1003400 | 0 |
| tr\|H0YMR5\|H0YMR5_HUMAN;tr\|H0YLR | 1 | 0 | 0 | 0 | 0 | 0 | 713160 | 0 |
| tr\|H3BTU7\|H3BTU7_HUMAN;sp\|Q9BVA | 1 | 0.000365 | 0 | 0 | 0 | 0 | 471090 | 0 |
| tr\|H3BUU8\|H3BUU8_HUMAN;sp\|Q08AI | 1 | 0.00362 | 0 | 0 | 0 | 0 | 683430 | 0 |
| tr\|H7C170\|H7C170_HUMAN;tr\|Q75ME3 | 1 | 0.004258 | 0 | 0 | 0 | 0 | 1573400 | 0 |
| tr\|H7C1R0\|H7C1R0_HUMAN;tr\|B4E0G0 | 1 | 0.001037 | 0 | 0 | 0 | 0 | 1050000 | 0 |
| tr\|H7C528\|H7C528_HUMAN;sp\|Q8IXK0 | 1 | 0.006573 | 0 | 0 | 0 | 0 | 1635870 | 0 |
| tr\|I3L3E4\|I3L3E4_HUMAN;tr\|I3L4G8\|I3L | 1 | 0 | 0 | 0 | 140150 | 0 | 0 | 0 |
| tr\|J3KRR0\|J3KRR0_HUMAN;tr\|J3QQM5 | 1 | 0 | 0 | 0 | 0 | 0 | 198720 | 0 |
| tr\|J3KS14\|J3KS14_HUMAN;tr\|F5H478\|F | 1 | 0.005458 | 0 | 0 | 534920 | 0 | 0 | 0 |
| tr\|J3QKK8\|J3QKK8_HUMAN;sp\|Q8TBF2 | 1 | 0.008537 | 0 | 0 | 0 | 0 | 598350 | 0 |
| tr\|J3QQW9\|J3QQW9_HUMAN;tr\|A8K1U | 1 | 0.002713 | 0 | 0 | 278120 | 0 | 0 | 0 |
| tr\|J7Q2I4\|J7Q2I4_HUMAN;tr\|J7Q1C6\|J7 | 1 | 1 | 0 | 0 | 0 | 0 | 558470 | 0 |
| tr\|K7EJ58\|K7EJ58_HUMAN;tr\|K7EQU8\| | 1 | 0 | 0 | 0 | 0 | 0 | 252820 | 0 |
| tr\|K7EK72\|K7EK72_HUMAN;tr\|K7EJA9\| | 1 | 0.008531 | 0 | 0 | 0 | 0 | 441860 | 0 |
| tr\|K7EKS1\|K7EKS1_HUMAN;sp\|P36954 | 1 | 0.00544 | 0 | 0 | 0 | 0 | 1045700 | 0 |
| tr\|K7EKY2\|K7EKY2_HUMAN;tr\|C9JZ58\|( | 1 | 0 | 0 | 0 | 0 | 0 | 495240 | 0 |
| tr\|K7EN05\|K7EN05_HUMAN;sp\|P60002 | 1 | 1 | 0 | 0 | 0 | 0 | 733670 | 0 |
| tr\|L7N2F3\|L7N2F3_HUMAN;tr\|W4VSQ2 | 1 | 0.006773 | 0 | 0 | 0 | 0 | 100690 | 0 |
| tr\|Q05BS8\|Q05BS8_HUMAN;tr\|A0A0A0 | 1 | 0 | 0 | 0 | 0 | 0 | 742590 | 0 |
| tr\|Q53GY5\|Q53GY5_HUMAN;sp\|Q8WY( | 1 | 0.003314 | 0 | 0 | 0 | 0 | 673670 | 0 |
| tr\|Q53R15\|Q53R15_HUMAN;sp\|P05976 | 1 | 1 | 0 | 0 | 0 | 0 | 1383000 | 0 |
| tr\|Q53YM3\|Q53YM3_HUMAN;sp\|O754( | 1 | 1 | 0 | 0 | 0 | 0 | 630320 | 0 |
| tr\|Q5TBH0\|Q5TBH0_HUMAN;tr\|Q5TBG | 1 | 0.000357 | 0 | 0 | 0 | 0 | 1640400 | 0 |
| tr\|Q68DM7\|Q68DM7_HUMAN;tr\|B4E02 | 1 | 0.007939 | 0 | 0 | 0 | 0 | 415320 | 0 |
| tr\|Q96BL1\|Q96BL1_HUMAN;sp\|Q96PM | 1 | 0.000705 | 0 | 0 | 0 | 0 | 209610 | 0 |
| tr\|Q96FT4\|Q96FT4_HUMAN;sp\|Q92733 | 1 | 0.003331 | 0 | 0 | 131710 | 0 | 0 | 0 |
| tr\|Q9BRW5\|Q9BRW5_HUMAN;sp\|Q02( | 1 | 0.00913 | 0 | 0 | 0 | 0 | 516390 | 0 |
| tr\|Q9BUD9\|Q9BUD9_HUMAN;tr\|E9PG4 | 1 | 0.004247 | 0 | 0 | 0 | 0 | 1090800 | 0 |
| tr\|Q9UFV9\|Q9UFV9_HUMAN;sp\|O4337 | 1 | 0.000354 | 0 | 0 | 234930 | 0 | 485350 | 0 |
| tr\|Q9UHU9\|Q9UHU9_HUMAN | 1 | 1 | 0 | 0 | 0 | 0 | 1778100 | 0 |
| tr\|Q9UNU2\|Q9UNU2_HUMAN;tr\|F5GXS | 1 | 0 | 0 | 0 | 848340 | 0 | 542500 | 0 |
| tr\|U4PP31\|U4PP31_HUMAN;sp\|Q9P08( | 1 | 0.002679 | 0 | 0 | 107240 | 0 | 601020 | 0 |
| tr\|W0FSR8\|W0FSR8_HUMAN;tr\|F2Z2T2 | 1 | 0 | 0 | 0 | 0 | 0 | 715120 | 0 |
| tr\|H0YE68\|H0YE68_HUMAN;sp\|Q9BZ95 | 1 | 0.002726 | 0 | 0 | 211940 | 0 | 850250 | 80801 |
| tr\|B0I1S3\|B0I1S3_HUMAN;tr\|K7ELN3\|K | 1 | 0.006612 | 0 | 0 | 0 | 0 | 2042050 | 201690 |
| sp\|Q96EY9\|ADAT3_HUMAN;tr\|D6W601 | 1 | 0.009116 | 0 | 0 | 294930 | 0 | 605350 | 61309 |
| sp\|P18615-4\|NELFE_HUMAN;tr\|H9ZYJ1 | 1 | 0.006608 | 0 | 0 | 0 | 0 | 1271000 | 192760 |
| sp\|Q9H5X1\|FA96A_HUMAN | 1 | 1 | 0 | 0 | 121940 | 0 | 440660 | 75940 |
| sp\|Q9ULR0\|ISY1_HUMAN;sp\|Q9ULR0-2 | 1 | 0 | 0 | 0 | 0 | 0 | 487080 | 98602 |

| | | | | | | | | |
|---|---|---|---|---|---|---|---|---|
| tr\|B8ZZF8\|B8ZZF8_HUMAN;tr\|A0A090N | 1 | 0 | 0 | 0 | 0 | 0 | 1109000 | 286490 |
| tr\|Q6PKD4\|Q6PKD4_HUMAN;tr\|A8K2A | 1 | 0.000356 | 0 | 0 | 0 | 0 | 619900 | 175820 |
| tr\|M0QY17\|M0QY17_HUMAN;sp\|Q9NV | 1 | 0.009102 | 0 | 0 | 821480 | 0 | 837546 | 262430 |
| tr\|A0A024R829\|A0A024R829_HUMAN;s | 1 | 0 | 0 | 0 | 0 | 0 | 814390 | 255890 |
| tr\|B2R4N3\|B2R4N3_HUMAN;tr\|A0A024 | 1 | 0.000696 | 0 | 0 | 389910 | 0 | 1151000 | 464230 |
| tr\|E9PS71\|E9PS71_HUMAN;tr\|B7Z8B3\| | 1 | 0.002704 | 0 | 0 | 0 | 0 | 457790 | 200248 |
| tr\|B2R5H5\|B2R5H5_HUMAN;sp\|P62310 | 1 | 0.005465 | 0 | 0 | 0 | 0 | 1439500 | 776820 |
| tr\|F8W099\|F8W099_HUMAN;tr\|F8W60 | 1 | 0.002733 | 0 | 0 | 0 | 0 | 278440 | 219850 |
| sp\|P36406-3\|TRI23_HUMAN;sp\|P36406 | 1 | 0.002698 | 0 | 584670 | 0 | 0 | 1980400 | 0 |
| sp\|Q4G0P3-2\|HYDIN_HUMAN;sp\|Q4G0 | 1 | 1 | 0 | 37778 | 0 | 0 | 0 | 0 |
| tr\|A0A024R978\|A0A024R978_HUMAN;s | 1 | 1 | 0 | 318700 | 0 | 0 | 0 | 0 |
| tr\|F8VS92\|F8VS92_HUMAN;tr\|F5H023\| | 1 | 1 | 0 | 131430 | 0 | 0 | 0 | 0 |
| tr\|I7H6J7\|I7H6J7_HUMAN | 1 | 1 | 0 | 292300 | 0 | 0 | 0 | 0 |
| tr\|Q8N9Z3\|Q8N9Z3_HUMAN;sp\|Q1293 | 1 | 0.007369 | 0 | 189350 | 579380 | 0 | 0 | 0 |
| tr\|B3KN59\|B3KN59_HUMAN;tr\|B3KM3 | 1 | 0 | 0 | 256430 | 203140 | 0 | 1162400 | 378620 |
| tr\|S4R460\|S4R460_HUMAN;tr\|A0A087V | 1 | 0 | 0 | 0 | 872230 | 169240 | 0 | 425960 |
| sp\|Q9GZT9-2\|EGLN1_HUMAN;tr\|R4SCC | 1 | 0 | 0 | 144880 | 703870 | 153370 | 1044800 | 184630 |
| tr\|B4DEN5\|B4DEN5_HUMAN;tr\|B3KQQ | 1 | 0.000366 | 0 | 182920 | 355860 | 110140 | 0 | 0 |
| tr\|Q5T4U8\|Q5T4U8_HUMAN;tr\|Q59GT6 | 1 | 0.00036 | 0 | 0 | 790410 | 264080 | 1360800 | 253860 |
| tr\|B4DQC9\|B4DQC9_HUMAN;sp\|Q9BX4 | 1 | 0 | 0 | 0 | 506390 | 169440 | 1106600 | 0 |
| tr\|H0YL59\|H0YL59_HUMAN;sp\|Q9BYU1 | 1 | 0.009943 | 0 | 0 | 1205700 | 676880 | 665840 | 0 |
| tr\|M1FWY0\|M1FWY0_HUMAN | 1 | 0.00268 | 0 | 2780600 | 2963900 | 2238400 | 9965300 | 0 |
| sp\|P01602\|KV110_HUMAN | 1 | 0.002723 | 0 | 2878300 | 156510 | 438500 | 1021300 | 4401300 |
| sp\|Q5VTQ0-7\|TT39B_HUMAN;sp\|Q5VT | 1 | 0.001037 | 0 | 363692 | 0 | 813310 | 988580 | 761180 |
| tr\|A2J1N8\|A2J1N8_HUMAN | 1 | 0.006593 | 0 | 9039030 | 0 | 8768120 | 771020 | 13553650 |